PRINCIPLES OF
Jet Propulsion
and
Gas Turbines

M. J. ZUCROW

PRINCIPLES OF
Jet Propulsion
and
Gas Turbines

PRINCIPLES OF

Jet Propulsion
and
Gas Turbines

M. J. ZUCROW

Professor of Gas Turbines and
Jet Propulsion, Purdue University

Revised Printing

Dedicated

to my beloved but much-neglected wife

LILLIAN ZUCROW

whose patience made this book possible

Preface

This book is based on a lecture course entitled The Principles of Jet Propulsion given by the author in 1943 and 1944, under the sponsorship of the University of California ESMWT program, to graduate engineers working in the aircraft companies located in the Los Angeles area.

It was decided in preparing the original lecture notes to discuss basic principles only, and in order to conform with the wartime restrictions on security only unclassified material was included. Since the manuscript for this book was completed during the war years the same policy was observed in its preparation. This introduced certain difficulties, because it was necessary to omit certain data and useful information. It is felt, however, that because the discussions in this book are confined to basic principles the observance of the interests of military security has not impaired the attainment of the main objectives: the presentation of requisite fundamental theory pertinent to an intelligent understanding of jet-propulsion engines and gas-turbine power plants. Although the book is written primarily for the student, and not for the specialist, it is hoped that it will also be useful to those actively engaged in the aforementioned fields.

In preparing the manuscript the author was guided by the experience obtained in teaching the ESMWT course discussed above. He found that the interest in the subject cross-sectioned various branches of engineering. For that reason certain material which may not be necessary for instructing aeronautical engineering students has been included. The instructor must use his own judgment in the selection and order of the subject matter to be taught.

The author has drawn freely from the unclassified literature, and credit is due to those authors, professional societies, publishers, and manufacturers who were kind enough to permit the use of their material. In this connection the National Advisory Committee for Aeronautics deserves special mention. References to publications are given in the text, and those used in any chapter are collected at the end of that chapter. An earnest effort has been made to make

the acknowledgments complete, but some omissions may have been made inadvertently. The author hopes that the reader will take the charitable point of view, and call the omission to his attention.

The author realizes that despite all his efforts it is probable that some errors, and even mistakes, will be found in this book. He is hopeful that they are few and insignificant, but he will welcome all communications calling them to his attention.

Except for the last chapter, "Some Aspects of High-Temperature Metallurgy," the author takes full responsibility for the material presented. He regrets that, owing to the conditions existing when the manuscript was written, he was unable to avail himself of helpful criticisms as is possible under more normal conditions. He is happy, however, to share the responsibility for the last chapter with his co-author Mr. C. T. Evans, Jr., Chief Metallurgist, Elliott Company, Jeannette, Pennsylvania. The excellent cooperation received from Mr. Evans in preparing the aforementioned chapter is gratefully acknowledged.

It is with great pleasure that the author expresses his indebtedness to his colleague Dr. C. F. Warner, Assistant Professor of Mechanical Engineering, Purdue University, who gave unsparingly of his valuable time to the reading of proof. He also wishes to express his thanks to his former colleagues Mr. W. Murray, Mr. R. D. Geckler, and Mr. T. B. Swanson for valuable aid in connection with some of the charts and tables presented in Chapter 12. Finally, he feels it is fitting to express here his appreciation to his former colleagues Mr. B. L. Dorman and Mr. L. K. Petersen, and also to Mr. J. Dillon, University of California, for their helpfulness in connection with the ESMWT course mentioned above.

LAFAYETTE, INDIANA
October 1947

Contents

Chapter 1. Review of Fundamental Principles

Chapter 2. Momentum and Energy Relationships for Fluids

Chapter 3. Thermodynamics of Gas Flow

Chapter 4. Thermodynamic Properties of Air

Chapter 5. Airplane Performance Calculations

Chapter 6. The Airplane Propeller

Chapter 7. The Gas-Turbine Power Plant

Chapter 8. The Gas-Turbine Type of Thermal Jet Engine (The Turbojet Engine)

Chapter 9. Air Compressors

Chapter 10. Turbine Characteristics

Chapter 11. The Combustion Chamber

Chapter 12. The Rocket Motor

Chapter 13. Some Aspects of High-Temperature Metallurgy

REVIEW OF FUNDAMENTAL PRINCIPLES

1. Units and Dimensions

Two kinds of quantities enter quite generally into engineering measurements: *dimensional* quantities and *dimensionless* quantities. A dimensional quantity is one which has its magnitude expressed in terms of one or more fundamental units: for example, a velocity of so many *feet per second*, an area of so many *square feet*, a momentum of so many *slug-feet per second*, or the like.

A dimensionless quantity is one that has no dimensional category and is, therefore, a pure number. Furthermore, the numerical magnitude of a dimensionless quantity is independent of the size of the fundamental units used for evaluating it, provided that a *consistent set* of units is employed. A dimensionless quantity may be a coefficient, such as the discharge coefficient for an orifice, the ratio of two similar variables, or the product of several dimensional quantities so arranged that the result is dimensionless. A familiar example of the last is the Reynolds number, which is the product (velocity × length × density) *divided by* dynamic (absolute) viscosity.

The choice of either the size of the fundamental units or of the dimensions for expressing the magnitude of a physical measurement is arbitrary.[1] Experience has shown, however, that in the fields of mechanics three principal dimensions suffice. They are length $[L]$, time $[T]$, and either mass $[M]$ or force $[F]$. All other dimensions for expressing the magnitude of a physical measurement are derivable from these. Thus. the dimensions of area are $[L]^2$, of velocity $[L]/[T]$, and so forth.

It should be noted that, if mass $[M]$ is taken as a principal dimension, then force is a derived quantity, and vice versa. Mass and force are related by Newton's law of motion, *force* $[F] = mass$ $[M] \times acceleration$ $[A]$. Hence, if mass is a principal dimension, the dimensions of force are $[M][L][T]^{-2}$.

---

[1] Superior numbers refer to items in the bibliography at the end of the chapter.

1

Each of the principal dimensions $[L]$, $[T]$, and $[M]$ or $[F]$ can be expressed in terms of the others. Thus,

$$[F] = [M][L][T]^{-2}; \quad [L] = [F][T]^2[M]^{-1}; \quad [M] = [F][T]^2[L]^{-1}$$

and

$$[T]^2 = [M][L][F]^{-1}$$

Further:

$$[M][L][F]^{-1}[T]^{-2} = 1$$

It should not be implied from the foregoing that the principal dimensions $[L]$, $[T]$, $[M]$ or $[F]$ are basic. As pointed out above, their choice is arbitrary and is based on convenience. In general, the principal dimensions may be any mutually independent set which are convenient to use.

The selection of the size of the fundamental units is also arbitrary, but the demand that they be *consistent* requires that numerically they satisfy Newton's second law of motion. Thus the product *unit mass* $\times$ *unit acceleration* must equal *unit force*.

In the field of mechanics two basic systems of measurement are used: (1) the English gravitational system (EGS) and (2) the English absolute system (EAS). Confusion sometimes arises in evaluating the units of mass and weight (force) for these systems. This may be due to the use of the same word, *pound*, for the unit of *force* (weight) in the (EGS) and for the unit of *mass* in the (EAS). Another contributing factor may be the fact that the *mass* of a body is determined by measuring its *weight*, that is, the gravitational force exerted upon it.

The confusion is avoided by noting that *mass is a quantitative measure of matter*. It is characterized by possessing the property called *inertia*, the tendency of a lump of matter to remain at rest or in an existing state of motion unless acted upon by an external force. Furthermore, the mass of a substance is independent of its volume, its numerical value being the same when the body is heated (expanded) or cooled (contracted). Mass is a scalar quantity, while force is a vector quantity.

In the EGS of units, which is used in this book unless specifically stated to be otherwise, the unit of force F and the unit of acceleration a are chosen and the unit of mass m is calculated from $F = ma$. Thus the *pound* is the chosen unit for force, the *foot per second per second* is chosen as the unit for acceleration, and the unit of mass is derived from substituting $F = 1$ and $a = 1$ into $F = ma$. The unit of mass is a lump of matter which is given an acceleration of

1 *ft per sec per sec*, in a vacuum, when acted upon by a force of 1 *pound*.

The simplest way to measure the mass of a body is to weigh it. Hence, if a body weighs 1 *pound*, the gravitational attraction exerted upon it is a force of 1 *pound* and this attraction imparts an acceleration $a = g$ *ft per sec per sec*, the numerical value of g depending upon the location of the body on the surface of the earth. To satisfy the equation $F = ma$, the body should experience an acceleration of 1 *ft per sec per sec*. This means that $m = W/g$, where W is the weight, must be equal to unity. Hence, the unit mass weighs g-*pounds*. This unit is called 1 *slug*.

The standard acceleration is 32.1740 *ft per sec per sec*, and is assumed to be the value at 45 degrees latitude and sea level.[2] Its value in metric units is 980.665 *cm per sec per sec*.

In the EAS the units of *mass* and *acceleration* are chosen and the unit of *force* is the derived unit. The unit of *mass* is called the *pound*, and the unit of acceleration is 1 *ft per sec per sec*. The unit *force* imparts an acceleration of 1 *ft per sec per sec* to a 1-*pound* mass. To satisfy Newton's law, this unit of force must be 1/gth of the weight of the 1-*pound* mass, and is called the *poundal*.

For a more detailed discussion of units of measurement consult references 12 and 13.

Table 1·1 presents conversion factors for transferring measurements from one system to another.

TABLE 1·1

CONVERSION FACTORS FOR GRAVITATIONAL AND ABSOLUTE SYSTEMS
OF MEASUREMENT

Given	Multiply by	Result
Force in pounds	32.174	Force in poundals
	444,823	in dynes
Mass in pounds	0 0311	Mass in slugs
	454 0	in grams
	0.454	in kilograms
Length in feet	30.5	Length in centimeters
	0 305	in meters

Table 1·2 lists the units which must be used with their respective systems of measurement in order to satisfy the requirements of consistency.

TABLE 1·2

FUNDAMENTAL UNITS OF MEASUREMENT AND DIMENSIONS

Fundamental Quantity	Dimensional Symbol	Gravitational System English	Absolute System	
			English	Metric
Mass	$[M]$	1 slug	1 pound	1 gram
Length	$[L]$	1 foot	1 foot	1 centimeter
Time	$[T]$	1 second	1 second	1 second
Force	$[F]$	1 pound	1 poundal	1 dyne

Table 1·3 presents the dimensional formulas and units of those physical quantities pertinent to propulsion problems.

TABLE 1·3

DIMENSIONAL FORMULAS AND UNITS

Quantity	Unit English Gravitational System	Dimensional Formula	
		M, L, T	F, L, T
Acceleration	ft/sec^2	L/T^2	L/T^2
Angular velocity	rad/sec	$1/T$	$1/T$
Angular acceleration	rad/sec^2	$1/T^2$	$1/T^2$
Area	ft^2	L^2	L^2
Compressibility	ft^2/lb	LT^2/M	L^2/F
Density	slug/ft^3	M/L^3	FT^2/L^4
Dynamic viscosity	lb-sec/ft^2	M/LT	FT/L^2
Energy	ft-lb	ML^2/T^2	FL
Force	lb	ML/T^2	F
Gravity acceleration	ft/sec^2	L/T^2	L/T^2
Impulse	lb-sec	ML/T	FT
Kinematic viscosity	ft^2/sec	L^2/T	L^2/T
Length, linear dimension	1 ft	L	L
Mass	1 slug	M	FT^2/L
Mechanical equivalent of heat	ft-lb	ML^2/T^2	FL
Modulus of elasticity	lb/ft^2	M/LT^2	F/L^2
Moment	ft-lb	ML^2/T^2	FL
Momentum	slug-ft/sec	ML/T	FT
Peripheral velocity	ft/sec	L/T	L/T
Pressure	lb/ft^2	M/LT^2	F/L^2
Power	ft-lb/sec	ML^2/T^3	FL/T
Revolutions per time	rev/sec	$1/T$	$1/T$
Rigidity modulus	lb/ft^2	M/LT^2	F/L^2
Surface tension	lb/ft	M/T^2	F/L
Specific weight	lb/ft^3	M/L^2T^2	F/L^3
Time	1 sec	T	T
Torque	ft-lb	ML^2/T^2	FL
Weight	lb	ML/T^2	F
Work	ft-lb	ML^2/T^2	FL

2. Dimensional Analysis

Many problems in engineering involve comparing the behavior of two similar machines of widely different size or the prediction of the behavior of a prototype from the behavior of a model. For the comparisons to be accurate, it is essential that the prototype and its model be geometrically similar in all respects. When the study also involves the flow of a fluid, as in aerodynamics, it is also required that the ratio of the forces due to the inertia and viscosity of the fluid be in a constant ratio, if the flow patterns are to be similar. This means that in problems involving fluid flow there must be dynamic similarity as well as geometric similarity. The comparison of the behavior of machines and fluids utilizing the principle for geometric and dynamic similarity is based on *dimensional analysis*.

Principal Notation

a = acoustic velocity = $\sqrt{gkRT}$, fps.

B = mR = universal gas constant = 1.9864, Btu/lb mole F.

C_D = drag coefficient.

c_p = specific heat at constant pressure = $\dfrac{R}{J}\left(\dfrac{k}{k-1}\right)$, Btu/lb F.

c_v = specific heat at constant volume = $\dfrac{R}{J}\left(\dfrac{1}{k-1}\right)$, Btu/lb F.

D = drag.

g = acceleration due to gravity = 32.174 ft/sec^2.

g-mole = gram mole.

$h = u + \dfrac{1}{J}(pv)$ = enthalpy, Btu/lb.

$\Delta h' = h_1 - h_2'$ = isentropic enthalpy change, Btu/lb.

$\Delta h = h_1 - h_2$ = enthalpy change, Btu/lb.

$\Delta h_t' = c_p T_1 \dfrac{Z_t}{1+Z_t}$ = enthalpy change due to isentropic expansion, Btu/lb.

$\Delta h_c' = c_p T_1 Z_c$ = enthalpy change due to isentropic compression, Btu/lb.

J = mechanical equivalent of heat = $\frac{1}{778}$ Btu/ft-lb.

k = specific heat ratio, c_p/c_v.

k-cal = kilogram calorie.

k-mole = kilogram mole.

$$K = \text{bulk modulus} = \frac{dp}{(dv/v)}, \text{ psf.}$$

$(K)_T$ = isothermal bulk modulus for a perfect gas = p.

$(K)_{ad}$ = adiabatic bulk modulus for a perfect gas = kp.

m = molecular weight.

M = Mach's number.

p = pressure intensity, psfa.

dQ = heat added, Btu/lb.

$q = \frac{1}{2}\rho V^2$ = dynamic pressure, psf.

$_1Q_2$ = heat added during a change from state 1 to state 2, Btu/lb.

R = gas constant = $1545/m$, ft-lb/lb F.

$r_t = p_1/p_2$ = pressure ratio for an expansion process from p_1.

$r_c = p_2/p_1$ = pressure ratio for a compression process from p_1.

ds = entropy change = dQ/T, Btu/lb F.

T = absolute temperature in degrees Rankine ($460 + t^\circ$ F).

u = internal energy, Btu/lb.

$du = c_v dT$ = internal energy change for a perfect gas, Btu/lb.

v = specific volume, ft^3/lb.

$V_m = mv$ = molar volume, ft^3/lb-mole.

V = velocity of a body in a fluid medium, fps, or total volume as indicated in text.

W = weight, lb.

$Z_c = r_c^{\frac{k-1}{k}} - 1.$

$Z_t = r_t^{\frac{k-1}{k}} - 1.$

Greek Symbols

ρ = density, slug/ft^3.

ρ_0 = air density at sea level = 0.002378 slug/ft^3.

$\sigma = \rho/\rho_0$ = density ratio.

γ = specific weight, lb/ft^3.

γ_0 = specific weight of air at sea level = 0.07651 lb/ft^3.

μ = absolute or dynamic viscosity, slug/ft sec.

$\nu = \mu/\rho$ kinematic viscosity, ft^2/sec.

The importance of dimensional analysis to the engineer is that it permits arranging the variables of a physical problem in such a manner that the experimental work can be conducted without de-

stroying the generality of the physical relationship.[17] This is particularly true when a large number of variables are involved.[18,19]

The dimensions of a physical quantity stem from its definition; thus density is *mass per unit volume* and is accordingly expressed by the dimensional formula $[M]/[L]^3$. An important principle in analyzing physical phenomena by applying dimensional analysis is the principle of dimensional homogeneity.[1] This states that all the terms of an equation expressing an actual relationship between physical variables must have the same dimensions.

If a certain number of physical quantities enter into an equation, since the equation must be dimensionally homogeneous, the number of possible relationships is limited in a special manner.[3] Thus it can be shown that, if the functional relationship

$$F(Q_1, Q_2 \cdots Q_m) = 0 \tag{1}$$

is a complete equation describing the relationship between m different physical quantities $Q_1, Q_2 \cdots Q_m$, then, if there are n principal dimensions, the relationship may be put in the form [3]

$$f(\pi_1, \pi_2 \cdots \pi_{m-n}) = 0 \tag{2}$$

Relationship 1 is said to be a complete equation if it remains true regardless of the size of the consistent set of fundamental units used in evaluating it. In equation 2 the π's are $m - n$ independent *dimensionless quantities* formed from the original variables $Q_1, Q_2 \cdots Q_m$. In each π there will be $n + 1$ variables, and in each successive π only one variable changes.

It should be noted that if more than one of the same kind of quantity is involved in the relationship, such as several lengths, then all of the same kind of quantity can be represented by means of one of them and ratios of the others to it. In that case equation 2 becomes

$$f(\pi_1, \pi_2 \cdots \pi_{m-n}, \quad r_1, r_2 \cdots) = 0 \tag{3}$$

where $r_1, r_2 \cdots$ are ratios.

Each π represents a dimensionless product of the form

$$\pi = Q_1{}^a \cdot Q_2{}^b \cdots Q_m{}^m \tag{4}$$

where the $a, b, \cdots m$ are exponents.

To illustrate the method of analysis, consider the problem of determining the aerodynamic resistance of an airplane or an airfoil.

The resistance will depend upon those variables that affect the resistance of any body which is completely submerged in a large body of fluid. Owing to the great depth of the submergence of the

airfoil, no surface waves are formed in the free surface of the atmosphere so that gravity has no effect upon the resistance.

If it is assumed that the airfoil moves through the air at constant speed so that there are no acceleration forces, then the resistance force, or drag D, will depend upon the following variables: V, the relative velocity of the air and the airfoil; ρ, the density of the air; μ, the viscosity of the air; a, the acoustic velocity; and the size and shape of the body.

For a series of geometrically similar bodies, a single linear dimension l will define each of them. Hence

$$F(D, l, V, \rho, \mu, a) = 0 \qquad\qquad (a)$$

Since there are three principal dimensions, $[F]$, $[L]$, and $[T]$, and six variables, there must be three dimensionless ratios. Hence, the equation similar to equation 3 is

$$f(\pi_1, \pi_2, \pi_3) = 0 \qquad\qquad (b)$$

The π's are determined by selecting three variables raised to exponents and combining them with a fourth until all the variables have been used. Hence, selecting l, V, and ρ as the three variables,

$$\pi_1 = D l^{x_1} V^{y_1} \rho^{z_1}$$

$$\pi_2 = \mu l^{x_2} V^{y_2} \rho^{z_2}$$

$$\pi_3 = a l^{x_3} V^{y_3} \rho^{z_3}$$

To solve for the exponents of the variables in π_1, they are expressed in terms of their dimensions raised to the exponent of the variable for which they are substituted. Thus

$$\pi_1 = F \cdot L^{x_1} \cdot L^{y_1} T^{-y_1} \cdot F^{z_1} T^{2z_1} L^{-4z_1}$$

Writing an equation for the exponents of each dimension, thus

$$
\begin{array}{lll}
[F] & 1 + z_1 \hspace{2em} = 0 & z_1 = -1 \\
[L] & x_1 + y_1 - 4z_1 = 0 & x_1 = -2 \\
[T] & -y_1 + 2z_1 \hspace{1em} = 0 & y_1 = -2
\end{array}
$$

Hence

$$\pi_1 = \frac{D}{l^2 V^2 \rho}$$

Similarly, for π_2,

$$\pi_2 = FTL^{-2} \cdot L^{x_2} \cdot L^{y_2} T^{-y_2} \cdot F^{z_2} T^{2z_2} L^{-4z_2}$$

Solving for the exponents

$$[F] \quad y_2 + 1 \qquad\qquad = 0$$
$$[L] \quad x_2 - 4z_2 + y_2 - 2 = 0 \qquad y_2 = -1$$
$$[T] \quad 2z_2 - y_2 + 1 \qquad = 0 \qquad x_2 = -1$$
$$z_2 = 1$$

Hence

$$\pi_2 = \frac{\mu}{l\rho V}$$

Similarly, for π_3,

$$\pi_3 = LT^{-1} \cdot L^{x_3} \cdot L^{y_3} T^{-y_3} \cdot F^{z_3} T^{2z_3} L^{-4z_3}$$

Hence

$$[F] \quad z_3 \qquad\qquad = 0 \qquad z_3 = 0$$
$$[L] \quad 1 + x_3 + y_3 - 4z_3 = 0 \qquad x_3 = 0$$
$$[T] \quad -1 - y_3 \qquad = 0 \qquad y_3 = -1$$

Hence

$$\pi_3 = \frac{a}{V} = \frac{1}{\text{Mach number}}$$

The dimensionless ratios give the following functional relationship

$$f\left(\frac{D}{l^2 \rho V^2}, \frac{\mu}{l\rho V}, \frac{a}{V}\right) = 1$$

Or, since an expression for the drag D is desired,

$$D = l^2 \rho V^2 \phi\left(\frac{l\rho V}{\mu}, \frac{V}{a}\right) \qquad\qquad (5)$$

The values of the unknown function are determined by test. Measured values of $D/l^2\rho V^2$ are plotted against simultaneous values of $l\rho V/\mu$ for a constant value of V/a.

Similarly for a fixed value of $l\rho V/\mu$ (the Reynolds number) values of $D/l^2\rho V^2$ can be plotted against V/a.

It should be noted that, at the usual speeds of airplanes, the air can be assumed to be incompressible.[16] The effect of V/a can then be neglected, and the drag equation can be assumed to be given by

$$D = l^2 \rho V^2 \phi\left(\frac{l\rho V}{\mu}\right)$$

Experiments also indicate that the resistance of an airplane under the conditions where the compressibility of the air can be neglected is approximately proportional to the square of the relative velocity V

Then the function $\phi\left(\dfrac{l\rho V}{\mu}\right)$ reduces to a constant, the value of which depends upon the shape of the body. Hence

$$D = l^2 \rho V^2 \times \text{Constant}$$

If the projected area of the body S is used in place of l^2, since area has the same dimensional formula, then

$$D = K_D \rho V^2 S$$

Since the dynamic pressure of moving air is given by $q = \frac{1}{2}\rho V^2$, it is convenient to express the drag in terms of the dynamic pressure. Thus

$$D = C_D \tfrac{1}{2}\rho V^2 S = C_D q S \tag{6}$$

where C_D is called the drag coefficient.

From equation 6 it is seen that the drag of an airfoil or airplane depends upon the density of the air, the relative wind velocity, the wing area, and an experimentally determined drag coefficient.

For a more complete treatment of dimensional analysis and also dynamic similarity the reader is referred to the references at the end of this chapter.

3. Classification of Matter

Material substances can be segregated into two broad classifications: solids and fluids. Although the interest in this book is mainly in the phenomena associated with motions of fluids, it is instructive to focus the attention briefly upon the essential differences between these two subdivisions of matter before proceeding to the study of the pertinent properties of fluids.

To facilitate the manipulation of the mathematical relationships which arise, it is convenient to assume the existence of *ideal* substances. Consequently, it is the criteria distinguishing *ideal solids* from *ideal fluids* that are to be discussed. Although no such idealized substances occur in nature, their consideration yields important information which may be regarded as a first approximation to the behavior of real substances. Furthermore, the equations derived for an ideal substance can be made applicable to real substances by introducing experimental coefficients or other suitable modifications.[4]

A *fluid* is defined as a substance composed of particles which move with ease, change their relative positions without separation of mass, and yield readily to pressure. This definition places in the category

of fluids such substances as liquids, vapors, and gases or any substance which cannot be classified as a solid. There are borderline cases where the line of demarkation between a fluid and a solid is not clearly established by this definition. In by far the majority of cases, however, the basic differences between solids, liquids, and gases are sufficiently pronounced to distinguish them. This is most conveniently accomplished by comparing their elastic properties.[4,6]

4. Elastic Properties of Ideal Substances

An ideal substance is assumed to be homogeneous in composition and isotropic. It can be shown that an isotropic body has only two elastic constants: the *bulk modulus* K, and the *rigidity modulus* N. These assumptions greatly reduce the complexity of the study of elastic properties.[5]

(a) **Bulk Modulus** (K). Consider a cube having unit edges that is subjected to a uniform hydrostatic pressure p; see Fig. 1. Assume that the stresses due to the hydrostatic pressure are small so that Hooke's law, *the stress is proportional to the strain*, is applicable.

The volume of the cube, as the result of the compression, is reduced by the amount $\Delta v = v_0 - v_1$, where the subscripts 0 and 1 refer to the initial and final volumes of the cube. Since it was assumed that the cube had unit edges, the volume change Δv represents the change in volume for a unit volume

FIG. 1. Unit cube subjected to uniform hydrostatic pressure.

of the material composing the cube; it is the *strain*. The ratio of the stress acting on the cube to the strain is a measure of the *bulk modulus* K of the material.

Owing to the hydrostatic pressure p, each side of the cube experiences a reduction in length e. Hence, the compressed volume of the cube is

$$v_1 = (1 - e)^3 = 1 - 3e + 3e^2 - e^3 \approx 1 - 3e \qquad (7)$$

Since the deformation e is very small, all powers higher than the first may be neglected, so that the strain is given by

$$\Delta v = v_0 - v_1 = -3e \qquad (8)$$

Let it now be assumed that the hydrostatic pressure, stress per unit area, is changed by the infinitesimal amount dp. The corresponding

decrease in volume will be $-dv$. If the initial volume is denoted by v, then the strain is $-dv/v$. By definition

$$K = \text{Bulk modulus} = \frac{\text{Increment of stress per unit area}}{\text{Unit strain produced}}$$

or

$$K = -v\frac{dp}{dv} \tag{9}$$

(b) **Compressibility** (τ). The compressibility of a material is defined as the inverse of its *bulk modulus*. Since the compressibility of a substance varies with the predominating temperature, it and the bulk modulus must be defined at a particular temperature and the conditions under which the compression is conducted must be specified.

It should be noted that the dimensions of the bulk modulus are force/area $= [F]/[L]^2$. Its units are *pounds per square foot*, for which the abbreviation is psf.

(c) **Rigidity Modulus** (N). Consider the unit cube illustrated in Fig. 2a. The sides AD and BC are extended by the tension stress p, while the sides AB and DC are shortened by a compression stress p of the same magnitude. Let the increase in the length of the sides AD and BC be denoted by e, and let the sides AB and DC be reduced by this same amount. The type of strain produced by these stresses is a *shearing strain* or *shear*.
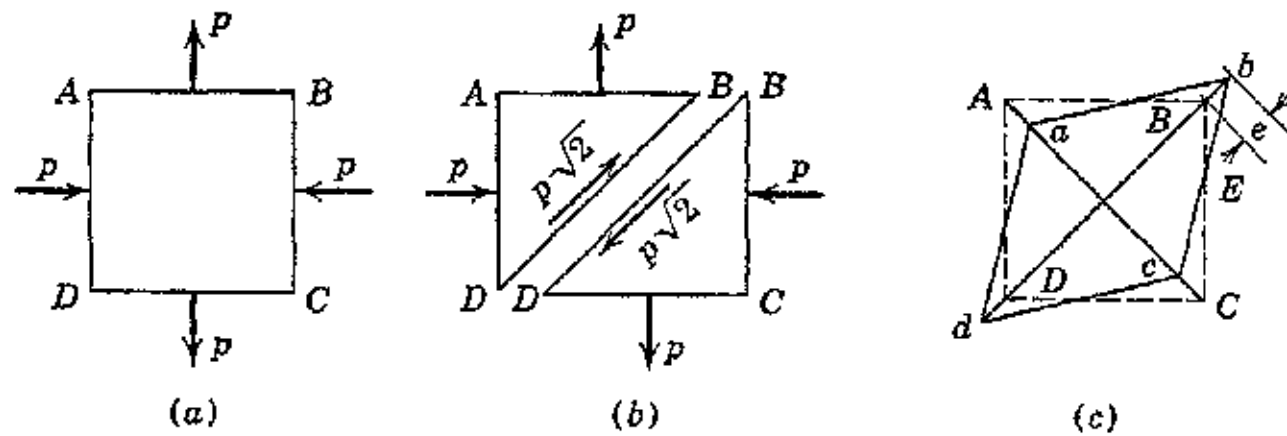
FIG. 2.   Unit cube subjected to a shearing strain.

Refer to Fig. 2b, and consider the rectangular prism BCD. The face BC is subjected to the hydrostatic pressure p, while the face DC is acted upon by the tension p of the same magnitude. The prism BCD is in equilibrium under the combined actions of these two normal stresses and the forces due to the action of ABD on BCD. The resultant of the two normal forces is the force $p\sqrt{2}$ acting along BD.

The action of ABD on BCD is equal to this force but oppositely directed as illustrated in the figure.

Since the cube was assumed to have unit edges, the area of the face BD is $\sqrt{2}$ units. Consequently, the tangential stress on this face has the same intensity p as the normal stresses acting on DC and BC. Hence, the shearing stress may be measured on the area subjected to either pure normal or pure tangential stress.

Refer to Fig. 2c. Assume that the directions of the principal axes of shear are along the diagonals AC and BD, and that these diagonals are contracted and elongated respectively by an amount e per unit length. It can be demonstrated that, when the strains are small, no change is produced in the sides of the cube, the area of its un-stressed face, and the perpendicular distance between the stressed faces if all powers of e above the first are neglected. The square of Fig. 2a merely distorts to form the rhombus, Fig. 2c. In other words, the material of the cube is distorted without expansion. The plane of the shear is the plane parallel to which all points are displaced. This type of strain is called a *pure shear*.[14]

If the rhombus of Fig. 2c is rotated so that dc coincides with a line through DC the result is that illustrated in Fig. 3. The shearing strain may be regarded as being produced by the material of the cube sliding along parallel planes through distances proportional to the perpendicular distances of these planes from the face DC, the sliding being caused by the tangential

FIG. 3. Deformation of unit cube due to tangential stress.

stress p acting along the upper face of the cube. The strain due to this tangential stress is measured by the angular displacement θ. The *rigidity modulus*, also called the *shear modulus*, is defined by

$$N = \frac{p}{\theta} = \frac{p}{\Delta L/L} \tag{10}$$

For small angles $\tan \theta = \theta$.

5. Definitions for Ideal Solids and Fluids

Ideal solids and ideal fluids can be defined in terms of their bulk and rigidity moduli.

(a) **Ideal Solid.** An ideal solid is a substance possessing bulk elasticity and rigidity. When it is stressed, the external forces are balanced by internal forces arising from the elastic strains, and in this manner equilibrium is maintained. It should be noted that the

stress on an element plane of an ideal solid may have any direction with respect to that plane.[4,6]

(b) **Ideal Fluid.** An ideal fluid is a substance possessing bulk elasticity but no rigidity. An ideal fluid cannot, therefore, permanently resist a tangential stress no matter how small the stress may be. Consequently, the stress on any element plane in an ideal fluid is always normal to that plane; the pressure is, therefore, independent of the orientation of the plane. Hence, *in an ideal fluid the pressure at any point is the same in every direction.*

From the foregoing, it is apparent that an ideal fluid has the following properties:[15]

1. It can transmit pressure only.
2. It cannot transmit a tangential stress, hence it is frictionless.
3. The pressure at any point in the fluid is the same in all directions.

Actual fluids differ from ideal fluids in that they are not frictionless. There arise tangential stresses whenever there is relative motion between the fluid particles. These tangential stresses tend to damp out the relative motion, and they exist as long as there is such motion. The fluid yields to these stresses, different fluids yielding at different rates depending upon their internal friction or their *dynamic or absolute viscosity.* It should be noted, however, that when a real fluid is at rest it behaves as an ideal fluid, for in that condition it cannot support a tangential stress.

(c) **Ideal Liquid.** An ideal liquid is defined as an incompressible ideal fluid. This means that the bulk modulus for an ideal liquid is infinite, or, conversely, the compressibility is zero. No real liquid is truly incompressible, but the numerical values of the bulk moduli for most real liquids are large enough to justify this assumption. This is particularly true when small pressure changes are involved.[15]

(d) **Ideal Gas.** The ideal gas is likewise defined in terms of the bulk modulus. Since the value of bulk modulus for a gas depends upon the type of compression process employed, the condition under which the compression takes place must be specified. Two principal compression processes are of particular interest: (a) isothermal and (b) adiabatic.

An *ideal or perfect gas* is defined as a perfect fluid for which the bulk modulus when determined by compressing it isothermally is numerically equal to the pressure.[4] Thus, the *isothermal bulk modulus* $(K)_T$ *for a perfect gas* is given by

$$(K)_T = -\frac{dp}{(dv/v)_T} = p \tag{11}$$

The subscript T indicates that the temperature is constant. Hence for the *isothermal compression of an ideal gas* the following equation applies

$$p\,dv + v\,dp = 0 \tag{12}$$

The integration of equation 12 yields

$$pv = \text{Constant} \tag{13}$$

Equation 13 states that, when an ideal gas is held at a constant temperature, the pressure on the gas varies inversely with its volume. This law was determined experimentally by Boyle and also by Mariotte.

If the compression of the gas is frictionless and is conducted under adiabatic conditions, no heat exchange between the gas and outside sources or sinks, then the equation for the compression process is $pv^k = \text{Constant}$. The exponent k represents the value of the ratio of the specific heat of the gas at constant pressure to its specific heat at constant volume and has different values for different gases. Differentiating $pv^k = \text{Constant}$ yields

$$v^k\,dp + kv^{k-1}p\,dv = 0$$

Dividing by pv^k

$$\frac{dp}{p} + k\frac{dv}{v} = 0$$

or

$$(K)_{ad} = -\frac{dp}{(dv/v)} = kp \tag{14}$$

Equation 14 states that the adiabatic bulk modulus of an ideal gas is equal to the product of its adiabatic exponent, k, and the absolute pressure.

Thus, assuming air to be an ideal gas for which $k = 1.4$, then its adiabatic bulk modulus is given by $(K)_{ad} = 1.4p$. Hence, at sea level, $(K)_{ad}$ for air is $1.4 \times 14.7 \times 144 = 2970$ psf.

6. Dynamic or Absolute Viscosity

It is this property of a real fluid, its viscosity, that is the source of all so-called fluid friction.[8] It is by virtue of this property that a real fluid in motion can sustain a shearing stress whereas an ideal fluid cannot. Consequently, in formulating the equations of motion for a real fluid, its dynamic viscosity, or more briefly its viscosity, should be considered.

The definition of the viscosity of a fluid is based upon the ability of the fluid to resist and distort when subjected to an external force causing a shear stress. Thus Maxwell defined viscosity as follows: The viscosity of a substance is measured by the tangential force per unit area on either of two horizontal planes at a unit distance apart required to move one plane with unit velocity in reference to the other plane, the space between being filled with the viscous fluid.
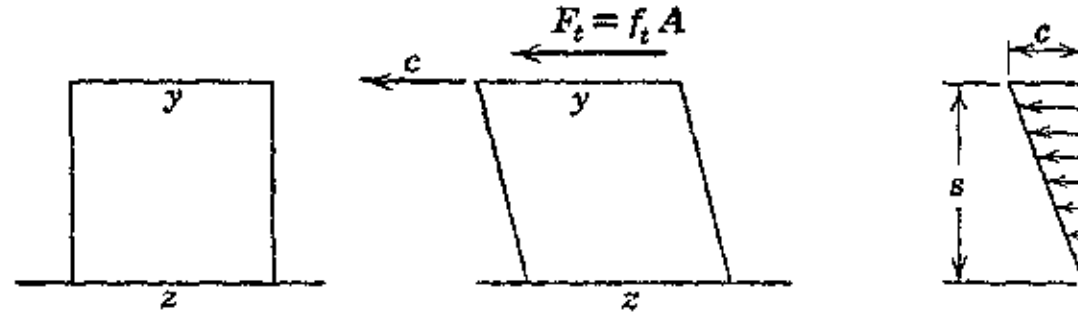
FIG. 4.   Distribution of shearing stress in a fluid.

Figure 4 illustrates two parallel planes Y and Z at a distance apart s. If the shearing stress f_t, force per unit area, gives plane Y the velocity V with respect to plane Z, then, as first pointed out by Newton, the velocity of each stratum of fluid between the planes Y and Z will be proportional to its perpendicular distance from plane Z.

The *rate of shear* is V/s and is, therefore, constant throughout a homogeneous fluid. The total shearing force is $F_t = f_t A$, where A is the area of plane Y.

To maintain constant velocity the tangential force F_t must be opposed by an equal force due to the internal resistance of the fluid. The ratio of this force to the rate of shear, called the *coefficient of viscosity*, is defined by

$$\mu = \frac{F_t}{A\,V/s} = \frac{f_t s}{V} \tag{15}$$

If $A = 1$, $s = 1$, and $V = 1$, then μ is the dynamic viscosity as defined by Maxwell. In general, therefore,

$$\mu = [M][L][T]^{-2} \times [L]^{-2} \times [L] \times [T][L]^{-1}$$

or

$$\mu = [M][L]^{-1}[T]^{-1} \quad \text{(slug/ft sec)}$$

If $[F]$, $[L]$, and $[T]$ are taken as the principal dimensions, then the unit of viscosity is

$$\mu = [F][T][L]^{-2} \quad \text{(lb sec/sq ft)}$$

Most physical data pertaining to the viscosity of fluids are ordinarily stated in metric units, usually *centipoises*, where 1 *poise* = 100 *centipoise*.

Table 1·4 presents the conversion factors for transferring the units of dynamic viscosity from one system of measurement to another.

TABLE 1·4

CONVERSION FACTORS FOR DYNAMIC VISCOSITY

$$[M][L]^{-1}[T]^{-1} \quad \text{or} \quad [F][T][L]^{-2}$$

μ Given in	Multiply by	Obtained in
poises	100	centipoises
(1 gram/cm sec	0.0672	lb/ft sec
or	0.0672	poundal sec/ft^2
dyne-sec/cm^2)	0.00209	slug/ft sec
	0.00209	lb sec/ft^2
	360	kg/meter hr
lb/ft sec	14.88	poise
or poundal sec/ft^2	1,488	centipoise
	0.03105	slug/ft sec
	0.03105	lb sec/ft^2
	5,356	kg/meter hr
slug/ft sec	478.5	poise
or lb sec/ft^2	47,850	centipoise
	32.174	lb/ft sec
	172,300	kg/meter hr
1 kg/meter hr	0.002778	poise
	0.2778	centipoise
	0.0001867	lb/ft sec
	0.000005804	lb sec/ft^2

In general, the viscosities of liquids decrease with increasing temperature whereas the viscosities of gases increase with the temperature.

The viscosity of air as a function of temperature in degrees centigrade is given by Holman's formula.[10] Thus

$$\mu = 1715.5(1 + 0.00275t - 0.00000034t^2) \times 10^{-7} \quad \text{(poises)} \quad (16)$$

where μ = viscosity, poises.
t = temperature, C.

To obtain the viscosity in slug/ft sec, the coefficient of the equation is multiplied by 2.09 $\times$ 10^{-3}. Thus

$$\mu = 3582.9(1 + 0.00275t - 0.00000034t^2) \times 10^{-10} \quad (17)$$

7. Kinematic Viscosity

Although the dynamic viscosity is a measure of the stresses in a fluid, in general it is the ratio of these stresses to the inertia of the fluid which has to be considered. The inertial forces in the fluid depend upon its density ρ. The ratio μ/ρ is called the kinematic viscosity and is denoted by ν. Its dimensions are ft^2/sec

$$\nu = \frac{\mu}{\rho} \frac{slug}{ft\ sec} \times \frac{ft^3}{slug} \tag{18}$$

The data pertaining to the viscosity of a fluid are often stated in terms other than its dynamic viscosity, such as (a) relative viscosity or (b) Saybolt seconds.

8. Relative Viscosity

This is the ratio of the dynamic viscosity of the fluid to that of water at a definite reference temperature. In this country relative viscosity is ordinarily referred to the dynamic viscosity of water at 20 C or 68 F. At this temperature, the viscosity of water is practically $\frac{1}{100}$ poise or 1 centipoise. With this reference base, the numerical value of the relative viscosity of a fluid is the same as its dynamic viscosity in the proper units. Sometimes water at 0 C or 32 F is taken as the base liquid. Since the dynamic viscosity of water at that temperature is 1.7921 centipoises, the dynamic viscosity in terms of relative viscosity is given by

Dynamic viscosity = Relative viscosity × 1.7921 (centipoise)

9. Saybolt Viscosity

This method of measuring and stating viscosity is very common. Since the rate of flow through the nozzle of the Saybolt viscometer depends on the dynamic viscosity and the pressure head, and since the pressure head is a function of the density of the fluid, Saybolt viscosity is a function of the kinematic viscosity. For the new Saybolt viscometer, Herschel gives

$$\nu = \text{Kinematic viscosity} = \frac{poises}{grams/cc}$$

or

$$\nu = 0.0022 \times t - \frac{1.8}{t} \tag{19}$$

where t is the time in Saybolt seconds.

Since the kinematic viscosity, ν, is the ratio of the dynamic viscosity of the fluid to its density, equation 19 can be transformed to give the dynamic viscosity μ. Thus

$$\mu = \rho \left(0.0022t - \frac{1.8}{t} \right) \tag{20}$$

where ρ is in grams per cubic centimeter.

In the metric system the density is equal to the specific gravity s, so that equation 20 can be written

$$\mu = s \left(0.0022t - \frac{1.8}{t} \right) \quad \text{poise} \tag{21}$$

Some commercial measurements of viscosity are made with the Engler viscometer and the results are stated in Engler seconds. The equation for this viscometer is

$$\nu = \frac{\mu}{\rho} = 0.00147t - \frac{3.74}{t} \quad \text{poise/gram} \tag{22}$$

Hence

$$\mu = 0.00147t\rho - 3.74\frac{\rho}{t} \quad \text{poise}$$

or

$$\mu = s \left(0.00147t - \frac{3.74}{t} \right) \quad \text{poise} \tag{23}$$

10. Ideal or Perfect Gases

The ideal or perfect gas is a fluid which cannot be liquefied by merely lowering its temperature. It is assumed that its structure is such that the individual gas molecules remain so far apart that they exert no attraction forces upon each other, and there is no internal friction. Real gases deviate from these assumptions, but the experimental results of the earlier scientists led to the belief that certain gases such as oxygen, nitrogen, hydrogen, and helium behaved as ideal gases because they had been unable to liquefy them. It has now been demonstrated that under suitable conditions all known gases can be liquefied.

Experiments indicate that the deviations in the behavior of a real gas from the perfect gas increase as the pressure acting upon the gas is raised or as the temperature is decreased. For many engineering calculations the error due to assuming ideal-gas behavior is relatively small and the results need not be corrected for deviations from the perfect gas laws. These laws will now be reviewed.[7]

(*a*) **Boyle's or Mariotte's Law.** This law has been discussed in Section 5(*d*) of this chapter. Its most usual statement is, *when the temperature of a given mass of gas is kept constant, the volume and pressure vary in inverse ratio.* The mathematical statement of this law is equation 13, which is also written in the form

$$p_1 v_1 = p_2 v_2 = pv = \text{Constant} \tag{24}$$

The numerical value of the constant depends upon the mass and kind of gas involved, and the temperature predominating during the isothermal change from state 1 to state 2. The graphical representation of this law, the plot of absolute pressure as a function of volume, is a rectangular hyperbola.

The product *pv* is a constant provided that the absolute temperature, *T*, is constant. Consequently, the numerical value of *pv* changes with *T*, or

$$pv = f(T) \tag{25}$$

In dealing with gases or vapors which do not follow the gas laws closely the specific volume of the fluid should be obtained from experimental data. Thus, for steam the tables of Keenan and Keyes, *Thermodynamic Properties of Steam*, John Wiley and Sons, should be used.

(*b*) **Charles' Law.** Charles' law may be stated as follows: *if the volume of a given mass of gas is kept constant and the temperature is changed, the accompanying change in pressure is proportional to the change in absolute temperature.* Mathematically,

$$\frac{p_1}{T_1} = \frac{p_2}{T_2} = \frac{p}{T} = \text{Constant} \tag{26}$$

where *p* is in pounds per square foot absolute and *T* in degrees Rankine.

(*c*) **Combination of Boyle's and Charles' Laws.** Boyle's and Charles' laws when combined yield the following equation

$$\frac{p_1 v_1}{T_1} = \frac{p_2 v_2}{T_2} = \frac{pv}{T} = \text{Constant} \tag{27}$$

(*d*) **Characteristic Equation.** If the volume and temperature of a confined gas are unchanged, then the pressure it exerts against the containing vessel is proportional to the weight of gas. Obviously, it requires five times as much pressure to force five times the weight of the same gas into the identical volume. Furthermore, if the pressure and volume are unaltered, then the temperature will vary inversely as the weight of gas.

From the foregoing, it follows that the constant in equation 27 must be proportional to the weight of gas. Replacing the constant by WR, where R depends only upon the kind of gas and W is its weight, then for a given volume of gas

$$\frac{pv}{T} = WR = \text{Constant}$$

or

$$pv = WRT \tag{28}$$

If a weight of 1 lb of gas is considered, then v is the specific volume of the gas in cubic feet per pound, and equation 28 becomes

$$pv = RT \tag{29}$$

Equation 29 is known as the *characteristic equation for perfect gases.* The differential forms of this equation are

$$p\,dv + v\,dp = R\,dT \tag{30}$$

or

$$p\,dv = R\,dT - v\,dp = R\,dT - RT\left(\frac{dp}{p}\right) \tag{31}$$

(e) Avogadro's Hypothesis. According to Avogadro's hypothesis, *equal volumes of all gases when at the same temperature and pressure contain an equal number of molecules.* This indicates that under the same conditions of pressure and temperature a molecule of any gas possesses a fixed volume. The specific weights of different gases must, therefore, be proportional to their molecular weights.

Let v denote the specific volume of a gas and γ its specific weight, and consider two different gases denoting them by the subscripts 1 and 2 respectively. Then, since $v = 1/\gamma$,

$$\frac{v_1}{v_2} = \frac{\gamma_2}{\gamma_1} = \frac{g\rho_2}{g\rho_1} = \frac{m_2}{m_1} \tag{32}$$

where m_1 and m_2 are the molecular weights of the gases and ρ denotes density.

In studies involving gases the calculations are frequently simplified by introducing the unit called the *mole*, which is defined as follows: let m denote the molecular weight of a gas; then 1 mole $= m$ lb (or m grams in the metric system). Thus 1 mole of oxygen, O_2, weighs $2 \times 16 = 32$ lb, and 1 mole of ammonia, NH_3, weighs $14 + 3 = 17$ lb.

Since, at the same T and p, the volume of one molecule is the same for all gases, it follows that the volume of 1 mole is the same for all

gases at identical values of p and T. Thus at $t = 32$ F and $p = 14.7$ psia, 1 cu ft of oxygen weighs 0.08922 lb. Hence the volume of 1 mole of oxygen under these conditions is $32 \times 1/0.08922 = 358.7$ cu ft. Thus 1 mole of any gas at 32 F and 14.7 psia occupies a volume of 358.7 cu ft. Similarly, at 14.7 psia and 60 F, the volume of 1 mole of any gas is 380.6 cu ft.

(f) **Relation between Gas Constant and Molecular Weight.** Multiply each side of equation 29 by the molecular weight m. Then

$$p \times vm = RT \times m \qquad (33)$$

Since v is the specific volume in cubic feet per pound and m is the weight of gas in 1 mole, the product vm is the volume of 1 mole of gas. For the conditions $p = 14.7 \times 144 = 2116.3$ psfa and $T = 32 + 460 = 492$ R, the product $vm = 358.7$ cu ft. Substituting for mv in equation 33 gives

$$R = \frac{2116.3 \times 358.7}{492 \times m} = \frac{1545}{m} \qquad (34)$$

The above relationship is not quite true for real gases but is sufficiently accurate for most purposes.

If the characteristic equation is applied to 1 mole of gas, that is m lb, then the volume term on the left-hand side is the same for all gases. Let $V_m = mv =$ the volume of 1 mole of gas, and let $mR = B$.

Then equation 33 becomes

$$pV_m = BT \qquad (35)$$

where $B =$ the universal gas constant and is independent of the kind of gas.

The values of the universal gas constant in different units of measurement are listed below

$$B = 1.9864 \text{ Btu/F lb-mole}$$

$$1.9864 \text{ k cal/K k-mole}$$

$$3.40709 \text{ ft lb/F g-mole}$$

$$847.81 \text{ m kg/K k-mole}$$

$$8311.5 \text{ int. joule/K k-mole}$$

$$8.3141 \times 10^{10} \text{ erg/K k-mole}$$

where K denotes degrees Kelvin.

In this book the value of B used will be $B = 1.986$ Btu/F lb mole.

The thermodynamic constants for certain common gases are presented in Table 1·5.

TABLE 1·5

THERMODYNAMIC CONSTANTS FOR COMMON GASES AND VAPORS

Gas or Vapor	Chemical Symbol	Molecular Weight	Gas Constant R (ft-lb/ lb F)	Specific Heat at 70 F c_p (Btu/ lb F)	$k = \frac{c_p}{c_v}$ at 70 F approx
Argon	Ar	39.90	38.70	0.124	1.66
Helium	He	4.00	386.00	1.25	1.66
Hydrogen	H_2	2.016	765.86	3 42	1.40
Nitrogen	N_2	28.02	54.99	0.246	1.40
Oxygen	O_2	32.00	48.25	0.217	1.40
Air		28.96	53.35	0.240	1.40
Carbon dioxide	CO_2	44.00	35.12	0.206	1.30
Carbon monoxide	CO	28.00	55.14	0.243	1.40
Methane	CH_4	16.03	96.31	0.528	1.31
Octane	C_8H_{18}	114.14	13.55	0.349	1.66
Propane	C_3H_8	44.06	35.04	0.473	1.15
Water vapor	H_2O	18.01	85.6	0.46	1.28

(*g*) **Dalton's Law.** This law states that, in a mixture of gases where the constituents do not react chemically with one another, each constituent behaves as if the others were absent.

From this law it follows that the pressure exerted by a mixture of gases upon the walls of the containing vessel is the sum of the pressures exerted by each gas in the mixture. The individual gas pressures are called *partial pressures*. If p_m is the total pressure of the gaseous mixture and p_1, p_2, p_3, etc., are the partial pressures of the constituents, then

$$p_m = p_1 + p_2 + \cdots p_n \tag{36}$$

or

$$p_m = \Sigma p = \frac{w_1 R_1 T_1 + w_2 R_2 T_2 + \cdots + w_n R_n T_n}{v_m} \tag{37}$$

where v_m is the volume of the gas mixture and w_1, $w_2 \cdots w_m$ are the weights of the individual constituents.

11. Principal Thermodynamic Properties of Perfect Gases

A perfect gas is a homogeneous substance, and its state is completely determined if two of the coordinates p, v, and T are given. Hence the following functional relationships can be written for a perfect gas or any homogeneous fluid. Thus

$$p = p(v, T), \quad v = v(p, T), \quad \text{and} \quad T = T(p, v) \tag{38}$$

The total differential dT is given by

$$dT = \left(\frac{\partial T}{\partial p}\right)_v dp + \left(\frac{\partial T}{\partial v}\right)_p dv \tag{39}$$

where the subscripts denote the coordinate that is held constant during the change.

The total differentials dp and dv are accordingly

$$dp = \left(\frac{\partial p}{\partial v}\right)_T dv + \left(\frac{\partial p}{\partial T}\right)_v dT \tag{40}$$

and

$$dv = \left(\frac{\partial v}{\partial p}\right)_T dp + \left(\frac{\partial v}{\partial T}\right)_p dT \tag{41}$$

In the thermodynamic discussions which follow the weight of gas considered is 1 lb unless specifically stated to be otherwise.

(a) **Specific Heats and Specific Heat Ratio.** The Regnault relationship between the specific heat at constant pressure c_p, and that at constant volume c_v, is given by

$$c_p - c_v = \frac{R}{J} = c_v(k - 1) \tag{42}$$

Hence

$$\frac{Jc_p}{R} = \frac{k}{k-1} \quad \text{or} \quad c_p = \frac{R}{J}\left(\frac{k}{k-1}\right) \tag{43}$$

and

$$\frac{Jc_v}{R} = \frac{1}{k-1} \quad \text{or} \quad c_v = \frac{R}{J}\left(\frac{1}{k-1}\right) \tag{43a}$$

According to the kinetic theory for gases the specific-heat ratio depends on the number of atoms in the gas molecule [6] Thus gases having the same atomic number should have approximately the same values for $k = c_p/c_v$. Thus according to that theory

For monatomic gases $k = 1.66$

For diatomic gases $k = 1.40$

For triatomic gases $k = 1.30$

The above conclusion is accurate for monatomic gases, less accurate for diatomic gases, and least accurate for triatomic gases

For *air* the value of k at ordinary conditions is taken as 1.40. At high temperatures and pressures this value will lead to substantial error, but at ordinary temperatures it is reasonably accurate. Its use simplifies the numerical values of the functions of k in flow equations. Thus

$$\frac{k+1}{2(k-1)} = 3, \quad \frac{2}{k-1} = 5, \quad \text{and} \quad \frac{2k}{k-1} = 7 \qquad (44)$$

(b) Internal Energy of a Perfect Gas. Joule's law shows that the internal energy of a perfect gas is a function only of its temperature. Thus for 1 lb of gas the internal energy u is given by

$$u = f(T) \quad \text{Btu/lb} \qquad (45)$$

According to the kinetic theory of gases the internal kinetic energy of a perfect gas depends only upon the velocities of translation and rotation of the gas molecules. These velocities and their associated kinetic energies are functions only of the gas temperature. Since the internal energy u is a direct function of the temperature T, this means that the internal potential energy of a gas is zero. Hence, the temperature of a gas is a direct measure of the random kinetic energy of its gas molecules.

A differential change in the internal energy of 1 lb of gas is

$$du = c_v \, dT \quad \text{Btu/lb} \qquad (46)$$

For a perfect gas the specific heat c_v is assumed to be a constant. Hence

$$u = \int c_v \, dT = c_v T + u_0 \qquad (47)$$

where u_0 is a constant of integration. Hence the change in internal energy in passing from state 1 to state 2 is

$$u_2 - u_1 = c_v(T_2 - T_1) \quad \text{Btu/lb} \qquad (48)$$

If the internal energy is measured above some arbitrary datum for which $u_1 = 0$, then at this datum $c_v T_1 = 0$ and $u_2 = c_v T_2$. Dropping the subscripts, the internal energy can be expressed above the datum $T_1 = 0$ by the equation

$$u = f(T) = c_v T = c_v \frac{pv}{R} \quad \text{Btu/lb} \qquad (49)$$

EXAMPLE. The internal energy of air is measured above 520 R as the datum If its molar internal energy at 1000 R is 2431 Btu per lb mole F, what is its specific heat at constant pressure? The molecular weight of air is 28.96.

Solution.

$$m(u_2 - u_1) = 2431 = mc_v(1000 - 520) = 480mc_v$$

Hence

$$mc_v = \frac{2431}{480} = 5.06 \quad \text{Btu/lb mole F}$$

$$c_v = \frac{5.06}{28.96} = 0.1745 \quad \text{Btu/lb F}$$

For air

$$R = \frac{1545}{m} = \frac{1545}{28.96} = 53.35 \quad \text{ft-lb/lb F}$$

$$c_p = 0.1745 + \frac{53.35}{778} = 0.2430 \quad \text{Btu/lb F}$$

The internal energy when measured from the base $T_1 = 0$ can be expressed in terms of the gas constant R. Thus, substituting for c_v from equation 43a into equation 49,

$$u = \frac{pv}{J(k-1)} = \frac{RT}{J(k-1)} \tag{50}$$

EXAMPLE. Calculate the molar internal energy of air at 1000 R, assuming it to be a perfect gas, $k = 1.4$, and the base temperature is 520 R.

Solution.

$$mu = \frac{mR(T_1 - T_0)}{J(k-1)}$$

$$= \frac{28.96 \times 53.35 \times 480}{778 \times 0.4} = 2383 \quad \text{Btu/lb mole F}$$

(c) **Enthalpy of Perfect Gas.** The thermodynamic property called *enthalpy* (also *heat content* and *total heat*) is defined by

$$h = u + \frac{pv}{J} \quad \text{Btu/lb} \tag{51}$$

The enthalpy of a gas is, therefore, the sum of its internal energy and the compression work pv/J done on the moving boundary of the fluid. The compression work, also a state property, is the work required to compress a gas volume v into a space which is at the pressure p. Differentiating equation 51 gives the equation for an infinitesimal change in enthalpy. Thus

$$dh = du + \frac{1}{J}(p\,dv + v\,dp) \tag{52}$$

But from the first law of thermodynamics

$$du = dQ - \frac{1}{J} p \, dv \tag{53}$$

where dQ is the heat added to the fluid from external sources in Btu per pound. Hence the heat added during a change from state 1 to state 2 is given by

$$_1Q_2 = h_2 - h_1 - \frac{1}{J} \int_1^2 v \, dp \tag{54}$$

or

$$h_1 - h_2 = -_1Q_2 - \frac{1}{J} \int_1^2 v \, dp \tag{55}$$

The enthalpy, and also the internal energy, are state properties. The value of the enthalpy at a given state is independent of the path or process employed in bringing a substance to that state. For this reason, the analysis of *steady-flow* processes for gases is greatly simplified by using this thermodynamic property. Any convenient datum may be used for calculating differences in enthalpy.

Substituting for u from equation 49 in equation 51 and for pv

$$h = c_v T + \frac{RT}{J} \quad \text{Btu/lb} \tag{56}$$

Substituting for $c_v T$ from equation 50 and introducing $k = c_p/c_v$ gives the following

$$h = \frac{k}{k-1} \frac{pv}{J} = \frac{k}{k-1} \frac{RT}{J} = c_p T \tag{57}$$

Hence for perfect gases, since $c_p = (R/J)(k/k - 1)$, the enthalpy above any datum is the product of the specific heat and the temperature rise above the datum.

Let Δh denote a finite change in the enthalpy of a perfect gas accompanying a change from state 1 to state 2; then

$$\Delta h = h_1 - h_2 = \frac{k}{k-1} (p_1 v_1 - p_2 v_2) \frac{1}{J} = c_p(T_1 - T_2) \tag{58}$$

(*d*) **Entropy Change for Perfect Gas.** If dQ is the heat added from external sources, then the entropy change for a pure fluid which undergoes a *reversible* change of state is defined by

$$ds = \frac{dQ}{T} \tag{59}$$

According to the first law

$$dQ = du + \frac{1}{J} p \, dv \tag{60}$$

or

$$dQ = dh - \frac{1}{J} v \, dp \tag{61}$$

Hence

$$ds = \frac{du}{T} + \frac{1}{J}\frac{p \, dv}{T} = c_v \frac{dT}{T} + \frac{1}{J}\frac{p \, dv}{T} \tag{62}$$

or

$$ds = \frac{dh}{T} - \frac{1}{J}\frac{v \, dp}{T} = c_p \frac{dT}{T} - \frac{1}{J} v \frac{dp}{T} \tag{63}$$

These equations cannot be applied without modification to irreversible processes. (See Chapter 3.) To integrate these equations the characteristic equation $pv = RT$ is used to give the following expressions

$$ds = c_v \frac{dT}{T} + \frac{R}{J}\frac{dv}{v} = c_v \left[\frac{dT}{T} + (k-1)\frac{dv}{v} \right] \tag{64a}$$

$$= c_p \frac{dT}{T} - \frac{R}{J}\frac{dp}{p} \tag{64b}$$

Hence

$$s_1 - s_2 = c_v \log_e \frac{T_2}{T_1} + \frac{R}{J} \log_e \frac{v_2}{v_1} \tag{65a}$$

$$= c_p \log_e \frac{T_2}{T_1} - \frac{R}{J} \log_e \frac{p_2}{p_1} \tag{65b}$$

If the entropy at some arbitrary selected base is $s_1 = 0$, then the value of s at any other state is

$$s = c_v \log_e \frac{T}{T_0} + \frac{R}{J} \log_e \frac{v}{v_0} \tag{66a}$$

$$= c_p \log_e \frac{T}{T_0} - \frac{R}{J} \log_e \frac{p}{p_0} \tag{66b}$$

The entropy is constant for a reversible adiabatic process for which $pv^k = $ Constant. Hence, a reversible adiabatic process is an *isentropic process*. An irreversible adiabatic is not given by $pv^k = $ Constant and is not isentropic.

(f) **Changes of State.**   Processes by which a gas can pass from state 1 to state 2 are, in the abstract at least, infinite in number. In general, the following particular types of processes are of greatest significance:

1. The isothermal change of state ($dT = 0$).
2. The adiabatic change of state ($dQ = 0$).
3. The polytropic change of state ($pv^n = $ Constant).
4. The isentropic change of state ($ds = 0$).

It will be recalled from elementary thermodynamics that all the above changes of state can be regarded as special cases of the polytropic change:

$$n = 0 \quad \text{corresponds to } dp = 0$$

$$n = 1 \quad \text{corresponds to } dT = 0$$

$$n = k \quad \text{corresponds to } dQ = 0; \quad ds = 0$$

$$n = \infty \quad \text{corresponds to } dV = 0$$

Flow processes which take place rapidly, such as the flow of gases through the nozzle of a rocket motor or a thermal jet engine, the blade passages of turbines and compressors, ducts and diffusers, and the like, are substantially adiabatic ($dQ = 0$) owing to the extremely short time interval available for heat transfer.   These processes, however, are never isentropic ($ds = 0$) because they are invariably accompanied by internal friction, turbulence, wall friction, and eddies, all of which increase the entropy of the fluid stream.   Consequently, when discussing the flow of gases through an ideal nozzle, turbine, or compressor, it is tacitly assumed as a first approximation that the changes of state are *reversible and adiabatic,* that is, *isentropic.*

From elementary thermodynamics a change of state under isentropic conditions is given by

$$p_1 v_1{}^k = p_2 v_2{}^k \quad \text{so that} \quad v_2 = v_1 \left(\frac{p_1}{p_2}\right)^{\frac{1}{k}} \tag{67}$$

Substituting equation 67 into equation 58 gives the following expression for an isentropic decrease in enthalpy

$$\Delta h_t' = \frac{k}{J(k-1)} p_1 v_1 \left[1 - \frac{p_2}{p_1}\left(\frac{p_2}{p_1}\right)^{-\frac{1}{k}}\right]$$

which can be transformed to read

$$\Delta h_t' = c_p T_1 \left[1 - \frac{p_2}{p_1}\left(\frac{p_2}{p_1}\right)^{-\frac{1}{k}}\right] \tag{68}$$

or

$$\Delta h_t' = c_p T_1 \left[1 - \left(\frac{p_2}{p_1}\right)^{\frac{k-1}{k}} \right] \quad \text{Btu/lb} \qquad (68a)$$

In the above equations the prime denotes that the change of state is brought about by an isentropic process. Since the final entropy h_2' is smaller than the initial entropy h_1, the final pressure p_2 is less than p_1. Equation 68a applies, therefore, to an isentropic expansion. The corresponding enthalpy change for an isentropic compression $(p_2 > p_1)$ will be denoted by $\Delta h_c'$, and it is given by

$$\Delta h_c' = h_2' - h_1 = \frac{k}{J(k-1)} p_1 v_1 \left[\left(\frac{p_2}{p_1}\right)^{\frac{k-1}{k}} - 1 \right] \qquad (69a)$$

or

$$\Delta h_c' = c_p T_1 \left[\left(\frac{p_2}{p_1}\right)^{\frac{k-1}{k}} - 1 \right] \quad \text{Btu/lb} \qquad (69b)$$

Let $r_t = p_1/p_2$ and $r_c = p_2/p_1$, and let

$$Z_t = r_t^{\frac{k-1}{k}} - 1 \qquad (70a)$$

and

$$Z_c = r_c^{\frac{k-1}{k}} - 1 \qquad (70b)$$

Then

$$\Delta h_t' = c_p T_1 \frac{Z_t}{1 + Z_t} \quad \text{Btu/lb} \qquad (71)$$

and

$$\Delta h_c' = c_p T_1 Z_c \quad \text{Btu/lb} \qquad (72)$$

EXAMPLE. Air at 60 F is compressed isentropically from a pressure of 1 atm. Calculate the enthalpy change in Btu per pound. Assume that $k = 1.395$ and $c_p = 0.24$ Btu/lb F.

Solution.

$$\frac{k-1}{k} = \frac{0.395}{1.395} = 0.283$$

$$r_c = 2$$

$$Z_c = 2^{0.283} - 1 = 0.21672$$

$$\Delta h_c' = c_p T_1 Z_c = 0.24 \times 520 \times 0.21672$$

$$= 27.0 \quad \text{Btu/lb}$$

EXAMPLE. An ideal air turbine receives air at 1600 R and 3 atm pressure. Calculate the ideal output in pound feet per pound of air. Assume that $c_p = 0.24$ Btu/lb F and $k = 1.395$.

Solution.

$$r_t = 3 \quad \text{and} \quad Z_t = 3^{0.283} - 1 = 0.3647$$

From equation 71

$$J\Delta h_t{}' = 0.24 \times 1600 \times \frac{0.3647}{1.3647} \times 778$$

$$= 80,000 \quad \text{ft-lb/lb}$$

12. Acoustic Velocity

The acoustic or sonic velocity is the speed with which sound and also small disturbances are propagated in a fluid medium. Its importance is due to its association with the phenomena encountered in the flow of gases at high speeds. It also enters into the resistance phenomena or drag encountered by high-speed aircraft.

From elementary physics the acoustic velocity for a fluid is the square root of the ratio of its bulk modulus K to its density ρ. Thus, let a denote the acoustic velocity, then

$$a = \sqrt{\frac{K}{\rho}} \tag{73}$$

Since a liquid has a large bulk modulus, and its value is practically constant, its acoustic velocity is large. To illustrate, consider the acoustic velocity for water. According to reference 8, for this liquid $K = 43,200,000$ lb/ft^2 and at ordinary temperatures $\gamma = \rho g$ $= 62.41$ lb/ft^3, so that

$$a = \sqrt{\frac{43.2 \times 10^6 \times 32.174}{62.41}} = 4700 \quad \text{fps}$$

As pointed out in Section 5d, the bulk modulus of a gas depends upon the thermodynamic process used to produce the relative change in volume. If the pressure change is rapid, as it usually is, then the assumption of adiabatic conditions is permissible, and from equation 14, $(K)_{ad} = kp$. Substituting the latter into equation 73, the following equation is obtained for the acoustic velocity

$$a = \sqrt{\frac{kp}{\rho}} = \sqrt{gkpv} = \sqrt{gkRT} \tag{74}$$

For standard air $k = 1.40$ and $R = 53.35$. Hence, at sea level where the standard temperature is 59 F, small pressure differences are propagated through the air with a velocity of 1120 fps.

The acoustic velocity for standard air at any absolute temperature T is accordingly

$$a = 1120 \sqrt{\frac{T}{519}} \tag{75}$$

Values of the acoustic velocity for standard air are presented in Table 1·6.

13. Mach Number

It was mentioned in Section 2, in discussing the resistance of a body in an infinite medium, that when the compressibility of the air affects the resistance the ratio of the local velocity V to the acoustic velocity a, called the Mach number M, is a dimensionless criterion of the flow phenomena. For a compressible fluid it follows from equation 74 that the Mach number is given by

$$M = \frac{V}{a} = \frac{V}{\sqrt{gkRT}} \tag{76}$$

or

$$M^2 = \frac{V^2}{a^2} = \frac{V^2}{gkRT} \tag{77}$$

As pointed out in reference 9, the physical significance of the Mach number can be readily grasped by considering equation 77. The ratio V^2/a^2 is a ratio of kinetic energies. Since V is the velocity of the directed motion of the gas particles, V^2 measures the kinetic energy of directed flow. The magnitude of the acoustic velocity a for a given gas depends upon the absolute temperature T, so that the kinetic energy corresponding to a^2 depends upon the thermal energy imparted to the gas. According to the kinetic theory of gases the thermal energy is utilized in increasing the random translation and random rotation of the gas molecules. Hence, a^2 is a measure of the kinetic energy associated with the random movements of the gas molecules. The value of M^2 for a given set of conditions, therefore, measures the ratio of the kinetic energy of directed flow to the kinetic energy of random motion. Since both thermal and directed kinetic energies appear in the flow equations for compressible fluids, the Mach number of the directed flow indicates the degree of controlled motion regardless of the cause producing the type of motion.

Taking the logarithms of both sides of equation 77 and differentiating gives the following relationship between changes in the Mach number, gas velocity, and gas temperature.

$$\frac{dM}{M} = \frac{dV}{V} - \frac{1}{2}\frac{dT}{T} \qquad (78)$$

EXAMPLE. A gas flows through a restricted passage with a speed of 2800 fps. Its local temperature is 3000 R; its specific heat ratio k and gas constant R are 1.25 and 60 respectively. Calculate the local sonic velocity and Mach number.

Solution.

$$a = \sqrt{1.25 \times 32.174 \times 60 \times 3000} = 2680 \text{ fps}$$

$$M = \frac{2800}{2680} = 1.045$$

It is shown in reference 11 that the pressure and density changes produced by a plane disturbance in a compressible fluid are related to the acoustic velocity by the relationship

$$\frac{dp}{d\rho} = a^2 \qquad (79)$$

As the speed of a body through a compressible fluid increases, the effect of the compressibility of the fluid is to distort the normal stream lines. When sonic and supersonic speeds are attained there is a change in the character of the flow patterns. The basic characteristics associated with high-speed air flow are discussed in later chapters.

14. Standard Atmosphere

The aerodynamic forces acting upon an airplane are dependent upon the physical properties of the atmospheric air at the flight altitude. Furthermore, the power output of any type of propulsion system utilizing air as one of its working fluids or the reactions of flowing air to produce a thrust for propulsion purposes are also affected by the properties of the atmosphere. The altitude of the airplane enters into performance problems because the following properties of the air change with altitude: air density ρ, air pressure p, and air temperature T.

Because these properties of the air change with the altitude, it has become the practice to express the performance characteristics of the airplane, or its components, as a function of altitude rather than by the specific variables ρ, p, and T. For the purpose of standardizing performance data, practically all the major countries have

TABLE 1·6

Properties of Standard Air

Altitude in 1000 ft	Temperature °R	Density Ratio $\sigma = \dfrac{\rho}{\rho_0}$	$\dfrac{1}{\sigma}$	$\sqrt{\dfrac{1}{\sigma}}$	Pressure Ratio $\dfrac{p}{p_0}$	Acoustic Velocity fps a
0	519.0	1.0000	1.000	1.000	1.0000	1120
1	515.4	0.9710	1.0299	1.015	0.9643	1116
2	511.8	.9428	1.0607	1.030	.9297	1112
3	508.4	.9151	1.0928	1.045	.8962	1109
4	504.8	.8881	1.1260	1.061	.8636	1105
5	501.2	.8616	1.1606	1.077	.8320	1101
6	497.6	.8358	1.1965	1.094	.8013	1097
7	494.0	.8106	1.2336	1.111	.7716	1093
8	490.6	.7859	1.2724	1.128	.7426	1089
9	487.0	.7618	1.3125	1.146	.7147	1085
10	483.4	.7384	1.3542	1.164	.6876	1081
11	479.8	.7154	1.3977	1.182	.6613	1077
12	476.2	.6931	1.4428	1.201	.6366	1073
13	472.6	.6712	1.4898	1.221	.6112	1069
14	469.1	.6499	1.5386	1.240	.5874	1065
15	465.5	.6291	1.5896	1.261	.5642	1061
16	461.9	.6088	1.6425	1.282	.5418	1057
17	458.3	.5891	1.6975	1.303	.5201	1053
18	454.7	.5698	1.7550	1.325	.4992	1048
19	451.3	.5509	1.8152	1.347	.4789	1044
20	447.7	.5327	1.8772	1.370	.4593	1040
21	444.1	.5148	1.9425	1.394	.4404	1036
22	440.5	.4974	2.0104	1.418	.4221	1032
23	436.9	.4805	2.0812	1.443	.4045	1028
24	433.5	.4640	2.1551	1.468	.3874	1023
25	429.9	.4480	2.2321	1.494	.3709	1019
26	426.3	.4323	2.3132	1.521	.3550	1015
27	422.7	.4171	2.3975	1.548	.3396	1011
28	419.1	.4023	2.4857	1.577	.3249	1007
29	415.5	.3879	2.5780	1.606	.3105	1002
30	412.1	.3740	2.6737	1.635	.2968	997.9
31	408.5	.3603	2.7755	1.666	.2836	993.5
32	404.9	.3472	2.8801	1.697	.2708	989.1
33	401.3	.3343	2.9913	1.730	.2584	984.7
34	397.7	.3218	3.1075	1.763	.2466	980.3
35	394.3	.3098	3.2279	1.797	.2351	976.1
36	393.0	.2962	3.3761	1.837	.2242	974.5
37	393.0	.2824	3.5411	1.882	.2137	974.5
38	393.0	.2692	3.7147	1.927	.2038	974.5
39	393.0	.2566	3.8971	1.974	.1942	974.5
40	393.0	.2447	4.0866	2.022	.1851	974.5

TABLE 1·6 (*Continued*)

PROPERTIES OF STANDARD AIR

Altitude in 1000 ft	Temperature °R	Density Ratio $\sigma = \dfrac{\rho}{\rho_0}$	$\dfrac{1}{\sigma}$	$\sqrt{\dfrac{1}{\sigma}}$	Pressure Ratio $\dfrac{p}{p_0}$	Acoustic Velocity fps a
41	393.0	0.2332	4.289	2.070	0.1761	974.5
42	393.0	.2224	4.497	2.120	.1683	974.5
43	393.0	.2120	4.717	2.171	.1605	974.5
44	393.0	.2021	4.949	2.224	.1530	974.5
45	393.0	.1926	5.192	2.278	.1458	974.5
46	393.0	.1837	5.444	2.333	.1391	974.5
47	393.0	.1751	5.711	2.390	.1325	974.5
48	393.0	.1669	5.992	2.447	.1264	974.5
49	393.0	.1591	6.285	2.507	.1205	974.5
50	393.0	.1517	6.592	2.567	.1149	974.5
51	393.0	.1446	6.916	2.630	.1095	974.5
52	393.0	.1379	7.252	2.693	.1044	974.5
53	393.0	.1315	7.605	2.758	.0995	974.5
54	393.0	.1254	7.974	2.824	.0949	974.5
55	393.0	.1195	8.368	2.892	.0905	974.5
56	393.0	.1139	8.780	2.963	.0863	974.5
57	393.0	.1086	9.208	3.034	.0822	974.5
58	393.0	.1036	9.653	3.107	.0784	974.5
59	393.0	.09872	10.13	3.183	.0747	974.5
60	393.0	.09412	10.63	3.261	.0713	974.5
61	393.0	.08974	11.15	3.340	.0679	974.5
62	393.0	.08555	11.70	3.421	.0648	974.5
63	393.0	.08155	12.26	3.502	.0617	974.5
64	393.0	.07775	12.86	3.586	.0589	974.5
65	393.0	.07413	13.49	3.687	.0561	974.5
66	393.0	.07067	14.15	3.761	.0535	974.5
67	393.0	.06737	14.85	3.853	.0510	974.5
68	393.0	.06422	15.58	3.947	.0486	974.5
69	393.0	.06123	16.30	4.037	.0464	974.5
70	393.0	.05838	17.13	4.139	.0442	974.5
75	393.0	.04597	21.76	4.665	.0348	974.5
80	393.0	.03621	27.54	5.248	.0274	974.5
85	393.0	.02852	35.07	5.922	.0216	974.5
90	393.0	.02246	44.52	6.673	.0170	974.5
95	393.0	.01769	56.53	7.519	.0134	974.5
100	393.0	.01393	71.79	8.472	.0106	974.5
105	393.0	.01097	90.99	9.538	.00831	974.5
110	393.0	.00864	115.7	10.75	.00654	974.5
115	393.0	.00681	146.8	12.11	.00515	974.5
120	393.0	.00536	186.6	13.66	.00406	974.5
125	393.0	.00422	237.0	15.39	.00320	974.5

adopted the so-called International Standard Atmosphere. This standard is based upon the assumptions presented below:

Sea-level temperature $t_0 = 15\ C = 59\ F = 519\ R$

Isothermal temperature $t_i = -55\ C = -67\ F = 393\ R$

Temperature gradient $0.0065\ C/m = 0.003566\ F/ft$

Linear lapse rate $59 - 0.003566\ F/ft$

Sea-level pressure $p_0 = 2116.4\ lb/ft^2$

A detailed discussion of the Standard Atmosphere is presented in *N.A.C.A. Technical Report* 218, 1925.

The ratio of the density ρ of the air at an altitude h to the sea-level density ρ_0 is denoted by σ, where $\sigma = \rho/\rho_0$. It is customary to express the air density at any altitude in terms of the density ratio. Thus

$$\rho = \sigma\rho_0 = \frac{\sigma\gamma_0}{g} \tag{80}$$

where ρ_0 = sea-level density = 0.002378 slug/ft^3.

γ_0 = sea-level specific weight = 0.07651 lb/ft^3.

Table 1·6 presents the characteristics of the standard atmosphere from sea level up to an altitude of 125,000 ft.

REFERENCES

1. P. W. BRIDGMAN, *Dimensional Analysis*, Yale University Press, 1922.
2. L. S. MARKS, *Mechanical Engineers' Handbook*, McGraw-Hill Book Co., 4th ed., 1941, p. 84.
3. E. BUCKINGHAM, "Model Experiments and the Forms of Empirical Equations," *Trans. A.S.M.E.*, Vol. 37, 1915.
4. ALLAN FERGUSON, *The Mechanical Properties of Fluids*, Blackie and Son, 1915, pp. 1 to 6.
5. A. G. WEBSTER, *The Dynamics of Particles and of Elastic and Fluid Bodies*, G. E. Stechert and Co., 1922.
6. P. P. EWALD, T. PÖSCHL, and L. PRANDTL, *The Physics of Solids and Fluids*, Blackie and Son, 1936.
7. J. A. MOYER, J. P. CALDERWOOD, and A. A. POTTER, *Elements of Engineering Thermodynamics*, John Wiley & Sons, 1931, pp. 15–17.
8. A. H. GIBSON, *Hydraulics and Its Applications*, D. Van Nostrand Co., 1925.
9. NEIL P. BAILEY, "The Thermodynamics of Air at High Velocities," *J. Aero. Sci.*, July, 1944, pp. 227–238.
10. W. S. DIEHL, *Engineering Aerodynamics*, Ronald Press, 1936.
11. G. I. TAYLOR and J. W. MOCCOLL, *The Mechanics of Compressible Fluids*, *Aerodynamic Theory*, Vol. III, Division H, pp. 210–222.
12. H. ROUSE, *Fluid Mechanics for Hydraulic Engineers*, McGraw-Hill Book Co., 1938, pp. 5–12.

13. F. B. SEELY and N. E. ENSIGN, *Analytical Mechanics for Engineers*, John Wiley & Sons.

14. G. F. SWAIN, *Structural Engineering*, McGraw-Hill Book Co., 1924, pp. 61–64.

15. W. SPANNHAKE, *Centrifugal Pumps, Turbines and Propellers*, The Technology Press, M.I.T., Cambridge, 1934, pp. 1–10.

16. C. B. MILLIKAN, *Aerodynamics of the Airplane*, John Wiley & Sons, 1941, p. 27.

17. L. PRANDTL and C. G. TIETJENS, *The Fundamentals of Hydro- and Aeromechanics*, McGraw-Hill Book Co., 1934, Chapter XIII.

18. E. R. VAN DRIEST, "On Dimensional Analysis and the Presentation of Data in Fluid-Flow Problems," Paper 45-A-7, Annual Meeting, A.S.M.E., New York, N. Y., Nov. 26–29, 1945.

19. MAX JAKOB, "A Survey of the Science of Heat Transmission," Engineering Experiment Station, *Research Series* 68, Purdue University, Lafayette, Ind.

20. E. SCHMIDT, *Einfuhrung in die technische Thermodynamik*, Julius Springer, Berlin, 1936.

MOMENTUM AND ENERGY RELATIONSHIPS FOR FLUIDS

1. The Reaction Principle

The fundamental operating principle of any jet-propulsion device is the *action-equals-reaction* principle formulated by Sir Isaac Newton in 1687. This principle, generally known as Newton's third law of motion, states that *to every action there is an equal and opposite reaction.* Examples of this principle are quite familiar. Thus if one throws a large stone away from him, a reaction is experienced by the thrower tending to move him backwards. Another familiar illustration is the recoil of a gun when the projectile leaves the barrel.

Where motion of a body through a fluid medium is concerned the reaction principle predominates.[1] Thus rowing a boat or swimming in water are methods for utilizing this principle. It is employed by the screw for propelling a ship, the propeller for moving an airplane, and for jet propulsion. In all these examples a fluid is accelerated in the direction opposite to that of the desired motion for the body, and the reaction due to its acceleration produces a propulsion force or thrust in the direction of motion. The magnitude of the propulsion force is determined by the application of the momentum principle.

2. Definition of Momentum

Newton termed the *momentum* of a body the *quantity of motion* and defined it as the product of the mass of the body and its velocity.[10] Thus, if $\mathbf{v}$ is the velocity of a body and m its mass, its momentum $\mathbf{M}$ is given by

$$\mathbf{M} = m\mathbf{v} = \frac{W}{g}\,\mathbf{v} \tag{1}$$

The symbols in bold-face type are vector quantities.

The direction of the momentum vector is identical with that of the velocity vector. The momentum vector can be resolved into

38

its components in any specified direction.[2] If the components are referred to three mutually perpendicular axes X, Y, and Z, then, denoting the direction of the components by the subscripts x, y, and z respectively, the following *vector equations* may be written

$$\mathbf{M} = M_x + M_y + M_z \tag{2}$$

and

$$\mathbf{v} = v_x + v_y + v_z$$

where $v_x = dx/dt$, $v_y = dy/dt$, and $v_z = dz/dt$.

If the mass of the body is constant, Newton's first law of motion can be applied to the force acting in any specified direction.[6] Thus, for the x direction

$$X = m \frac{d}{dt}(v_x) = ma_x \tag{3}$$

Similar expressions can be written for the y and z directions.

In general, the following expression can be written for each direction:

$$\mathbf{F} = \frac{d}{dt}(m\mathbf{v}) = \frac{d}{dt}(\mathbf{M}) \tag{4}$$

Equation 4 is the mathematical representation of Newton's second law, and it states that *the rate of change of momentum in any direction is equal to the force acting in that direction.*

Equation 4 can be rewritten in the form

$$\mathbf{F}\,dt = d(m\mathbf{v}) = d(\mathbf{M}) \tag{5}$$

This equation states that the change in momentum is equal to the time impulse ($\mathbf{F}\,dt$) of the force ($\mathbf{F}$). Figure 1 is a vector representation of a change in the momentum of a particle.
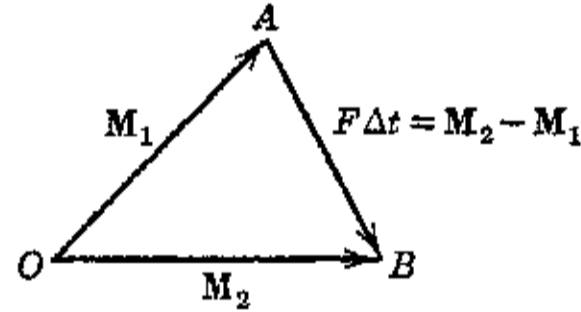
Fig. 1. Vector representation of momentum change.

3. Conservation of Momentum

This important principle may be stated as follows: *if the resultant of the external forces which act on a body has no component in a given direction, the linear momentum of the body in the given direction remains constant.* This means that, if any portion of a system experiences a momentum change in one direction, the rest of the system experiences a corresponding change in momentum in the opposite direction so that the resultant of all the momentum changes for the

complete system is zero. This principle can be represented by the vector equation

$$\mathbf{M}_1 + \mathbf{M}_2 = m_1\mathbf{v}_1 + m_2\mathbf{v}_2 = 0 \qquad (6)$$

where the subscripts 1 and 2 refer to the two portions of the material system under consideration.

Thus consider a projectile fired from a gun. Suppose that the projectile weighs 1000 lb and the gun is mounted on a ship weighing 2000 tons (4,000,000 lb). If the muzzle velocity of the projectile is 2500 fps, the conservation of momentum principle applied to the ship and projectile gives

$$m_1 v_1 = m_2 v_2 \qquad (7)$$

$$\frac{1000}{32.174} \times 2500 = \frac{4,000,000}{32.174} v_2$$

Hence the velocity imparted to the ship in the direction opposite to the motion of the projectile is 0.625 fps.

It is quite apparent from equation 7 that, the larger the difference in the masses of the bodies exchanging momentum, the greater is the difference in their velocities.

4. Momentum of a Continuum of Particles

The equations presented in the preceding sections are in a strict sense applicable only to an isolated particle. Consider now a mass of fluid; this may be regarded to be a system composed of a large number of discrete particles. It is possible to write an expression similar to equation 4 for each particle of the system.[2] The resultant force acting on the continuum of particles can then be obtained by taking the vector sum of the momenta of all the particles. This can be expressed mathematically by the equation

$$\frac{d}{dt}(m\mathbf{v}) = \frac{d}{dt}\Sigma(M) = \Sigma F \qquad (8)$$

The above equation states that the time rate of change of momentum for a system of discrete particles is equal to the total of all the forces acting on the particles comprising the system.

In general, the forces acting on any single particle of the fluid may be segregated into two groups:[3] (1) external forces, such as gravity, mass attraction, pressures acting on outer boundary, and friction forces on outer boundary; and (2) internal forces, pressure and friction, acting within the outer boundary surface and between adjacent particles.

The internal forces act in pairs. Thus consider any pair of particles, such as those illustrated in Fig. 2; for each of the internal forces P_{ab} or F_{ab} exercised by particle a on particle b there is an equivalent force exercised by particle b on particle a. Consequently, if the summation described by equation 8 is made for all the particles forming a bounded volume of fluid, the internal forces cancel out and only the external forces remain.[2][10] Hence, the momentum change of
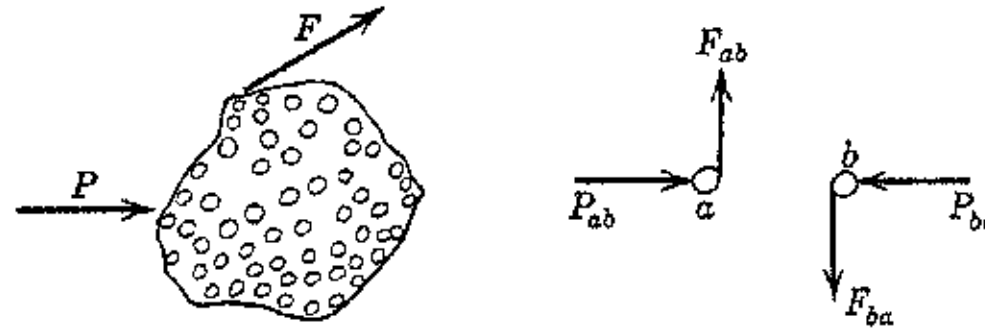
FIG. 2.   Internal forces acting on a continuum of particles.

a fluid depends only upon the external forces. The result of the summation equation 8 written for $n = i$ particles may be written in the form

$$\frac{d}{dt}\left(\sum_{n=1}^{n=i} m_i \mathbf{v}_i\right) = \Sigma \mathbf{F}_{ext} \qquad (9)$$

Equation 9 states that *the time rate of change of the total momentum of a bounded mass system of discrete particles is equal to the resultant of the external forces and is independent of the internal forces.*

Integrating 9 between the time limits t_1 and t_2, and letting Δ denote a finite change,

$$\Delta(\Sigma m \mathbf{v}) = \int_1^2 (\Sigma \mathbf{F}_{ext})\, dt \qquad (10)$$

Equation 10 states that *the change in momentum of a bounded system of particles during any period of time is equal to the integral of the time impulse of the sum of the external forces acting on the system over that period.*

In many engineering problems it is not the force acting on the fluid that is of interest, but the reaction exerted by the fluid on some body with which it is in contact.

5. External Forces Acting on a Flowing Fluid

Consider a fluid flowing through the passage illustrated in Fig. 3. From Section 4 it follows that the following kinds of external force can act upon the boundaries of the fluid.

(a) Pressures over the bounding surfaces at the cross sections A and B; both these forces are directed inward with respect to the fluid boundaries.

(b) Impressed forces, such as gravitational attraction.

(c) Pressures due to the inner surface of the conduit acting *upon* the boundary of the fluid.

In the majority of cases of fluid flow the effect of gravity is so small that it may be neglected, and the external forces then belong to categories (a) and (c) above.

$$R = M_b + (-M_a) + (-P_a) + (-P_b) =$$
Resultant force acting on fluid
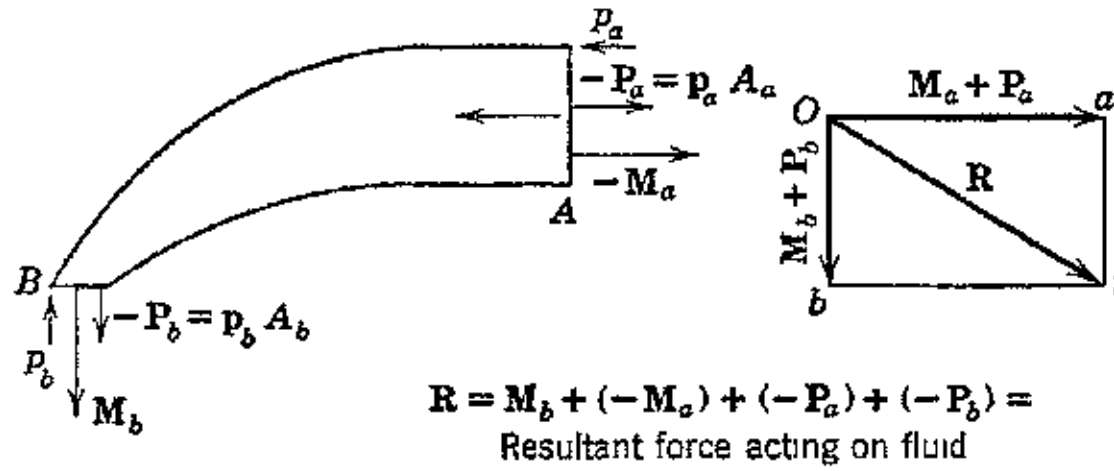
FIG. 3.　Determination of the resultant force exerted by the walls of a conduit on a fluid

Refer to Fig. 3, and let the subscripts a and b refer to cross sections A and B respectively.　Let

$P_a = A_a p_a =$ pressure force acting on a.

$P_b = A_b p_b =$ pressure force acting on b.

$R =$ resultant pressure force from the conduit acting on the fluid.

$M =$ momentum per second.

$p =$ pressure intensity.

$A =$ area.

The *vector* sum of the forces P_a, P_b, and R must be equal to the change in the momentum entering and leaving the conduit in 1 sec Thus

$$P_a + P_b + R = M_b - M_a$$

Hence

$$R = M_b - M_a - P_a - P_b \qquad (11)$$

This last equation may be rewritten as a sum of the vectors,[4] thus

$$R = M_b + (-M_a) + (-P_a) + (-P_b) \qquad (12)$$

Equation 12 gives the value of the force acting on the fluid. Reversing the direction of R gives the force exerted by the fluid on the conduit.

Refer to Fig. 3. The vector $Oa = \mathbf{M}_a + \mathbf{P}_a$, $Ob = \mathbf{M}_b + \mathbf{P}_b$, and the resultant $Or = \mathbf{R}$. Hence the vector $rO = -\mathbf{R}$ is the resultant force exerted by the fluid on the conduit.

6. Reaction of a Fluid upon a Body Immersed within It

Figure 4 illustrates schematically a body immersed in a stream of fluid. The force acting on the body in the direction of its motion can be calculated by applying the principles discussed in the preceding sections. In analyzing the problem two methods of approach
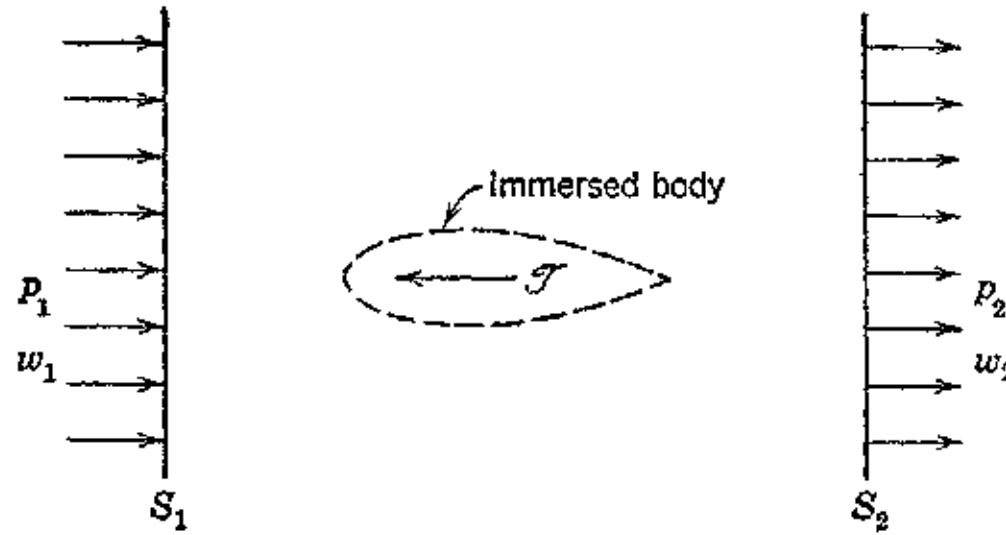
FIG. 4.   Momentum theorem applied to a body immersed in a fluid.

are possible: (a) the fluid may be considered to be at rest and the body to move through it; or (b) the body may be assumed to be stationary and the fluid to flow toward the body with the velocity which the body actually possesses.

In the first approach the problem is referred to an absolute system of coordinates, and in the second to a relative coordinate system. Since the reactions between the body and the fluid are independent of the coordinate system selected either approach may be employed to determine the magnitude of the force acting on the immersed body. This force is equal to the difference between the increase in the momentum of the fluid stream and the increase in the pressure force acting on the surfaces enclosing the body. These surfaces are the planes S_1 and S_2 which are perpendicular to the reaction force, called the thrust $\mathfrak{I}$, and they extend to infinity. The surfaces S_1 and S_2 are located far enough from the body so that the pressure intensities p_1 and p_2, acting over S_1 and S_2, are the same as the fluid pressures in the absence of the body; that is, p_1 and p_2 are the undisturbed pressures for the fluid. If m_1 and m_2 are the mass rates of flow per unit area crossing S_1 and S_2 respectively, the thrust $\mathfrak{I}$ is

$$\mathfrak{I} = \int_{S_2} mw_2 \, dS_2 - \int_{S_1} mw_1 \, dS_1 + \left[\int_{S_2} p_2 \, dS - \int_{S_2} p_1 \, dS \right] \quad (13)$$

It is apparent from equation 13 that only where $p_1 = p_2$ is the thrust given solely by the rate of change in the momentum of the fluid.

7. Moment of Momentum (Angular Momentum)

The moment of momentum of a particle about a fixed axis, most frequently called its *angular momentum*, is the product of the momentum of the particle and the distance perpendicular to the line drawn in the direction of the velocity of the particle; see Fig. 5.
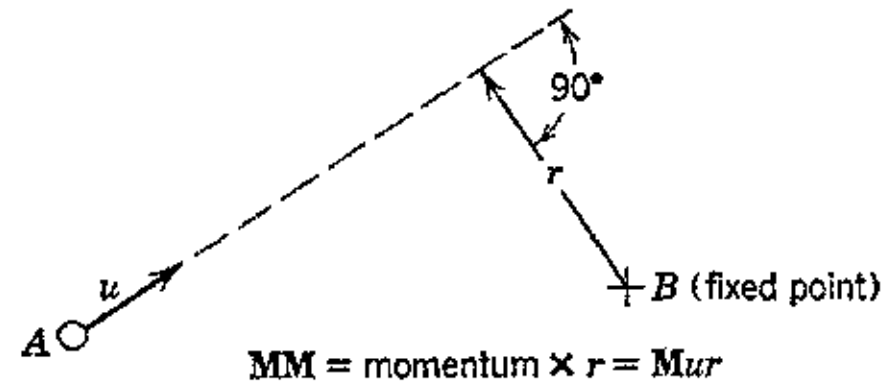
FIG. 5.   Moment of momentum (angular momentum) of a particle.

Since momentum is a vector quantity, angular momentum can also be represented by a vector.[2,6] The vector representing the angular momentum of a particle bears the same relation to the vector representing momentum that the vector representing the moment of a force bears to the vector representing the force.[6]

Since the momentum and time impulse of the external force **F** are equivalent vectors, moments may be taken about a selected axis. Let

r_m = radius to momentum vector

r_f = radius to force vector

Then for a system of particles

$$\frac{d}{dt} \Sigma(m\mathbf{v})r_m = \Sigma \mathbf{F} r_f \tag{14}$$

This last equation states that *the time rate of change of the resultant angular momentum of a system of particles is equal to the resultant moment of the external forces.*

From the preceding sections it is seen that for a body of flowing fluid the resultant momentum and the resultant moment of momentum depend on the external forces alone.

8. Energy Transfer between a Fluid and a Rotor

The gas-turbine type of power plant is an assembly of fluid dynamical machines which depend for their operation upon the energy

transfer between a working fluid and a rotor. In the case of turbine machines, the fluid transfers energy to the rotor, while in the case of pumps and compressors the rotor transfers energy to the fluid. In neither of these cases is the energy transfer complete because of losses, and the excellence of the energy transfer is expressed in terms of experimentally determined coefficients.

The mathematical development of the underlying principles of energy transfer is due to the German mathematician Euler, but the
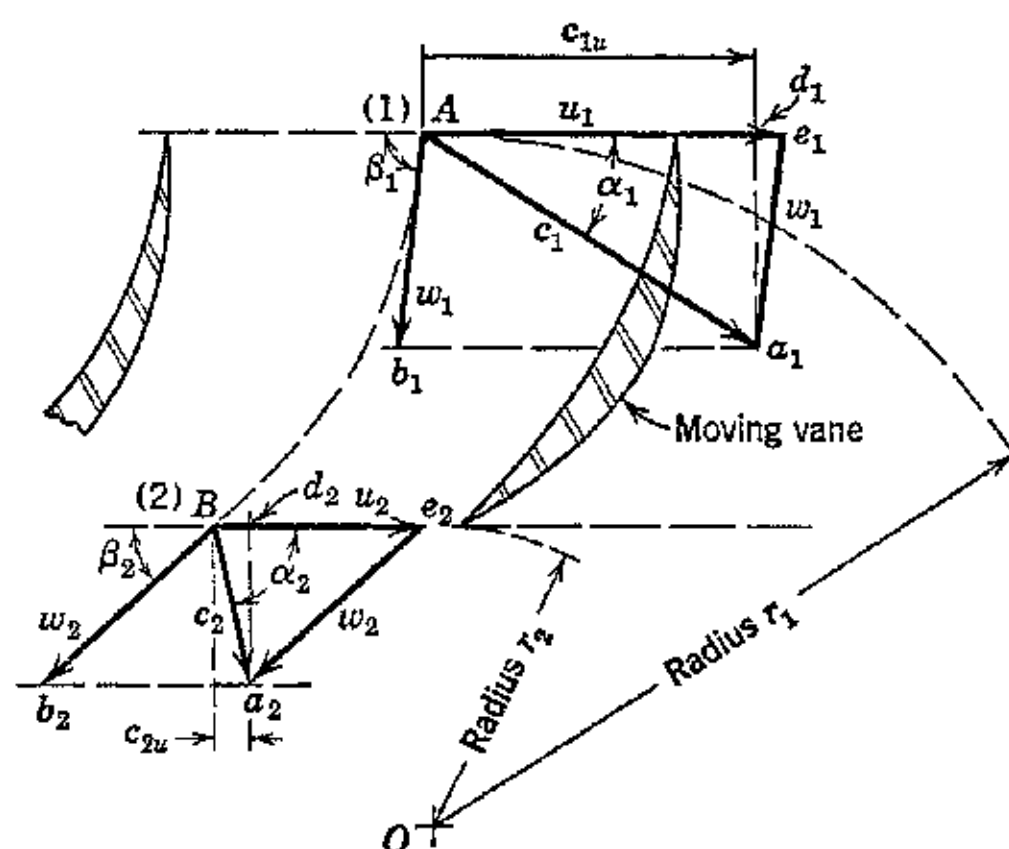
FIG. 6. General case of a moving blade passage.

first clear explanation of the application of these principles to turbines and compressors is due to G. Zeuner (*Theorien der Turbinen*, Leipzig, 1899). The analysis presented here is based on references 7 and 8.

The basis of the theory of energy transfer rests on the following simplifying assumptions: (a) the flow through the rotor is steady and uniform over the entrance and exit cross sections of the flow passage; (b) the rotor, to which the blades which form the flow passages are attached, rotates with a uniform angular velocity; (c) there are no losses due to fluid by-passing the flow passages formed by the blading; (d) there is no friction loss due to the sides of the rotor being in contact with the fluid; (e) the fluid completely fills the flow passages in the rotor.

It should be realized that no real machine behaves in accordance with the assumptions outlined in the preceding. Furthermore, the theory is incomplete since it neglects the effect of circulation by not

taking into consideration the actual velocity and pressure distributions around the rotor blades. Since the losses external to the rotor are neglected, and the fluid which by-passes the blading is not taken into account, the theory is concerned only with the fluid which actually flows through the blading. Nevertheless, the theory is instructive since it gives an understanding of the factors influencing the energy transfer.

Figure 6 illustrates a rotating blade passage. Since the velocity of flow over any cross section is uniform, all velocities are referred to points in the entrance and exit cross sections which are representative of the average fluid velocities.

Notation

c = absolute velocity.

$\Delta c_u = c_{1u} - c_{2u}$ = whirl velocity, fps.

w = relative velocity.

u = tangential velocity.

Subscripts

1 entrance.

2 exit.

a axial direction.

u direction of u.

Angles

α = angle between c and u.

β = angle between w and u.
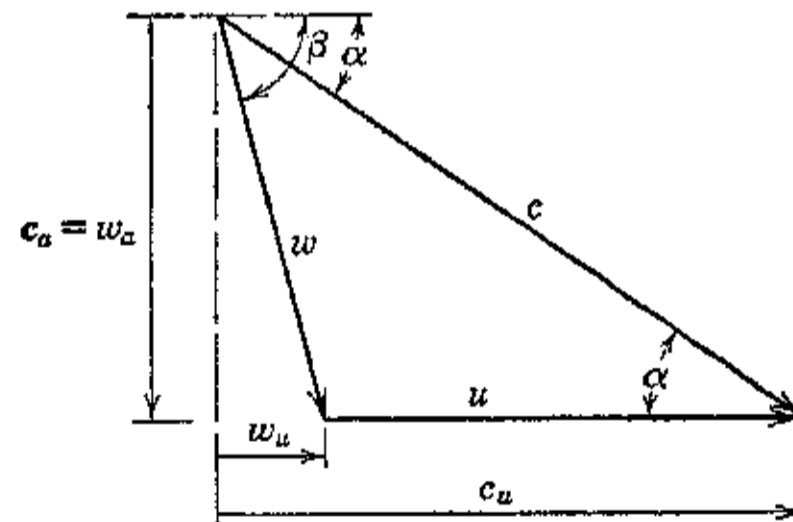
FIG. 7.   Velocity diagram for a fluid entering a moving blade passage.

Let the rotor have the uniform angular velocity ω rad/sec. The general forms of the velocity triangles for the fluid entering and leaving the blade passage are illustrated in Fig. 8.
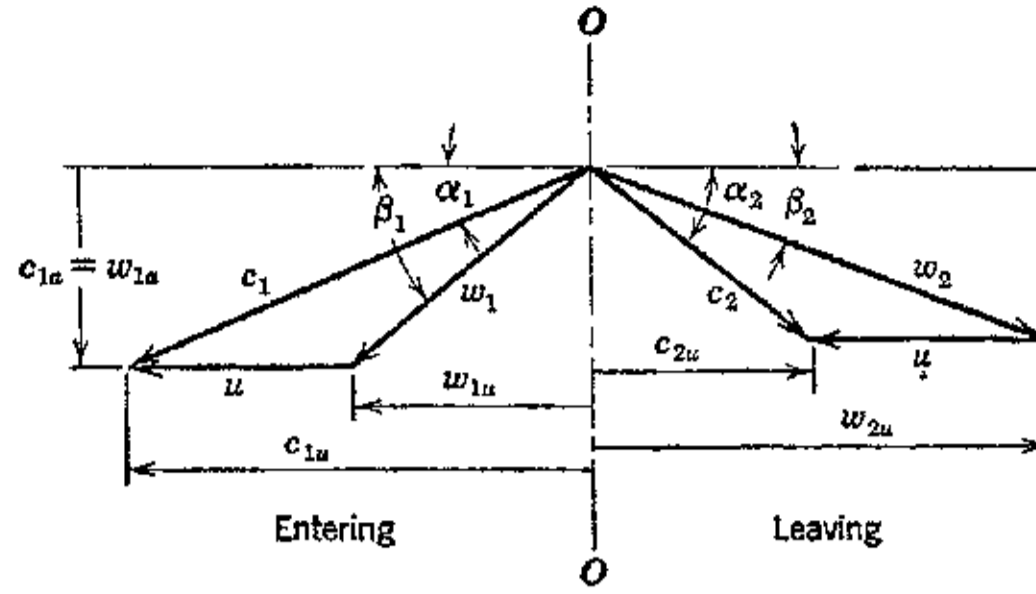
FIG. 8.   Velocity diagrams for a fluid entering and leaving a moving blade passage.

It is apparent from Figs. 7 and 8 that any axial component of either an absolute or a relative velocity is given by an equation of the form

$$c_a = w_a = c \sin \alpha = w \sin \beta \tag{15}$$

In general, a relative velocity is given by the vector equation

$$\mathbf{w} = \mathbf{c} - \mathbf{u} \tag{16}$$

and its tangential component w_u is given by

$$w_u = w \cos \beta \tag{17}$$

The tangential component of the entrance absolute velocity c_1 is given by

$$c_{1u} = w_{1u} + u_1 = c_1 \cos \alpha_1 = w_1 \cos \beta_1 + u_1 \tag{18}$$

The tangential component of the exit absolute velocity c_2 is given by

$$c_{2u} = w_{2u} - u_2 = c_2 \cos \alpha_2 = w_2 \cos \beta_2 - u_2 \tag{19}$$

The relationship between the velocity vectors c, w, and u is obtained by applying the law of cosines. Thus, in general, this gives

$$w^2 = c^2 + u^2 - 2uc \cos \alpha \tag{20}$$

Substituting c_u for $c \cos \alpha$, equation 20 becomes

$$w^2 = c^2 + u^2 - 2uc_u$$

Rearranging

$$c^2 + u^2 - w^2 = 2uc_u \tag{21}$$

An equation similar to equation 21 can be written for the entrance and exit velocity triangles. Thus for the entrance to the blade passage

$$c_1{}^2 + u_1{}^2 - w_1{}^2 = 2u_1c_{1u} \qquad (22a)$$

and for the exit section

$$c_2{}^2 + u_2{}^2 - w_2{}^2 = 2u_2c_{2u} \qquad (22b)$$

The velocity triangles are employed for calculating the tangential components c_{1u} and c_{2u}, while the absolute velocity c_2 and the relative velocity w_2 are determined by applying the energy and continuity equations. The absolute velocity c_1 is usually known or readily determined; for example, in a turbine c_1 would be the exit velocity of the fluid leaving the nozzle or stationary blades. The tangential velocities u_1 and u_2 are determined from the rotational speed of the rotor ω, and the radii R_1 and R_2 from the center of rotation to the inlet and exit reference points.

Subtracting equation 22b from 22a and rearranging the terms,

$$(u_1c_{1u} - u_2c_{2u})$$

$$= \tfrac{1}{2}[(c_1{}^2 - c_2{}^2) + (u_1{}^2 - u_2{}^2) + (w_2{}^2 - w_1{}^2)] \quad (23a)$$

When u_2c_{2u} is larger than u_1c_{1u}, equation 22a is subtracted from 22b, and

$$(u_2c_{2u} - u_1c_{1u})$$

$$= \tfrac{1}{2}[(c_2{}^2 - c_1{}^2) + (u_2{}^2 - u_1{}^2) + (w_1{}^2 - w_2{}^2)] \quad (23b)$$

Examination of equation 23a or 23b reveals that each term on the right-hand side has the form $\tfrac{1}{2}(\text{velocity})^2$. Hence, since the equation applies to a constant weight rate of flow of fluid, which is premised by the assumption of steady flow, it signifies that equations 23a and 23b are energy equations. Each term in parentheses corresponds to a change in the kinetic energy of the fluid. It is, therefore, concluded that equations 23a and 23b present the factors influencing the energy transfer, and if these equations are multiplied by $1/g$ they present the energy transfer relationship for 1 lb of fluid. Let L denote the energy transfer in foot-pounds per pound of fluid, the subscript t denoting that the fluid transfers energy to the rotor, and the subscript c that the energy transfer is from the rotor to the fluid.

As a consequence of the energy transfer there is a torque *interaction* between the rotor and fluid, or vice versa. In either event

the net effect is a tangential force acting on the fluid in a pump, and on the rotor in a turbine. The moment of this force around the axis of rotation is the torque due to the interaction of the fluid and rotor. The product of the torque and the angular velocity of the rotor give the rate of energy transfer, that is, the power absorbed or developed. The magnitude of the torque is equal to the rate of change in the angular momentum of the fluid between the entrance and exit sections. In a pump, the angular momentum is increased, while in a turbine it is decreased.

The angular momentum theorem applied to a flowing fluid states that the time rate of change of the resultant angular momentum of a system of discrete particles in a given direction is equal to the moment of the external forces acting in the same direction.

Let the symbol **MM** denote angular momentum and Φ denote torque.

If the torque is exerted by the fluid, it will be denoted by Φ_t; if the rotor exerts torque on the fluid the torque is denoted by Φ_c.

For a turbine c_{1u} is larger than c_{2u}, hence

$$\Phi_t = \mathbf{MM}_1 - \mathbf{MM}_2 = \frac{1}{g}(R_1 c_{1u} - R_2 c_{2u}) \qquad (24a)$$

whereas for a pump or compressor

$$\Phi_c = \mathbf{MM}_2 - \mathbf{MM}_1 = \frac{1}{g}(R_2 c_{2u} - R_1 c_{1u}) \qquad (24b)$$

The energy transfer per pound of fluid is accordingly

$$L_t = \Phi_t \omega = \frac{\omega}{g}(R_1 c_{1u} - R_2 c_{2u}) \qquad (25a)$$

and

$$L_c = \Phi_c \omega = \frac{\omega}{g}(R_2 c_{2u} - R_1 c_{1u}) \qquad (25b)$$

When the energy transfer is from the fluid to the rotor, as in a turbine, then $c_{1u} > c_{2u}$ so that equations 24a and 24b show that the energy transfer depends only upon the tangential components, c_{1u} and c_{2u}, and the tangential velocities u_1 and u_2. The axial components $c_{1a} = w_{1a}$ and $c_{2a} = w_{2a}$ do not enter into the energy transfer in any manner. The change in these components is effective only in producing axial thrust on the rotor.

Substituting for $(u_1 c_{1u} - u_2 c_{2u})$ and for $(u_2 c_{2u} - u_1 c_{1u})$ from equations 23a and 23b into the above equations gives

$$L_t = \frac{1}{2g} [(c_1{}^2 - c_2{}^2) + (u_1{}^2 - u_2{}^2) - (w_1{}^2 - w_2{}^2)] \quad (26a)$$

and

$$L_c = \frac{1}{2g} [(c_2{}^2 - c_1{}^2) + (u_2{}^2 - u_1{}^2) + (w_1{}^2 - w_2{}^2)] \quad (26b)$$

Equations 26a and 26b present the energy transfer in terms of kinetic-energy changes for the fluid.

In general, the energy transfer is independent of the path taken by the fluid in flowing through the rotor. The conditions at the entrance and exit sections determine the effectiveness of the energy transfer.

Equations 24a and 24b show that the basic requirement is that the flow passage be so arranged that a change in the direction of the flow is produced. In other words, the fluid-flow direction must be turned, and the net amount of this turning determines the energy transfer. Consequently, if the flow passage is so designed that the net amount of turning of the flow direction is zero, there can be no energy transfer.[7]

Equations 24a and 24b are applicable to any type of fluid and any rotor, since no assumptions were made concerning either of them. The only assumption that is implied, in addition to those made at the outset, is that it is possible to calculate the velocity terms involved. Until the magnitudes of c_{1u} and c_{2u} are established, the equations cannot be solved.

The magnitudes of the tangential components c_{1u} and c_{2u} are governed by the angles with which the fluid enters and leaves the flow passage. In a strict sense, the angles α and β are not the geometric angles of the blading, but those made by the absolute and relative velocities with the tangential velocities. Practically, they may be regarded as being the blade angles required to give the fluid *shockless* entrance and exit.

The derivation of the energy-transfer equation imposed no restrictions upon the magnitudes of the tangential velocities u_1 and u_2. They may be unequal as in radial-flow machines, or equal as in axial-flow machines.

In axial-flow machines, the entire flow is assumed to be concentrated at some circle which is representative of the average flow conditions. This circle is usually taken at the pitch diameter that divides

the flow area through the blades into two equal portions. This pitch diameter is generally taken to be the root mean square of the diameters based on the radii from the center of rotation to the blade root and blade tip. If the blade height is small enough, compared to the wheel diameter, no serious error is introduced by using the radius from the center of rotation to the mean height of the blade in calculating the pitch diameter.

Since equations 24a and 24b involved no assumptions regarding the characteristics of the fluid, they apply to both incompressible and compressible fluids. Although the equations contain no factors that are related explicitly to the characteristics of the working fluid, the fluid characteristics enter in an indirect manner since the magnitudes of w_2 and c_2 are affected by the properties of the fluid.

Similar comments are applicable to the losses in the flow passage due to heat transfer, fluid friction, and shock. Since the equation is concerned only with the inlet and exit conditions, it is independent of these losses. Though the losses, like the fluid characteristics, do not appear explicitly, they are incorporated in the equation by virtue of the effect these losses produce upon the exit velocities. This means that any improvement that reduces the losses in the blade passage will be indicated by the effect produced on the exit velocity.

It has been shown that the energy transfer equations for a turbine or a compressor in foot-pounds per pound are given by

$$L_t = \frac{1}{g}(u_1 c_{1u} - u_2 c_{2u}) \tag{26c}$$

and

$$L_c = \frac{1}{g}(u_2 c_{2u} - u_1 c_{1u}) \tag{26d}$$

Since the rotor turns with the uniform angular velocity ω rad/sec, then

$$u_1 = R_1\omega \quad \text{and} \quad u_2 = R_2\omega \tag{27}$$

Substituting for u_1 and u_2 in the above energy equations

$$L_t = \frac{\omega}{g}(R_1 c_{1u} - R_2 c_{2u}) \tag{28a}$$

and

$$L_c = \frac{\omega}{g}(R_2 c_{2u} - R_1 c_{1u}) \tag{28b}$$

A product of the form Rc_u is termed the *whirl* of the fluid, and the velocity change $\Delta c_u = c_{1u} - c_{2u}$ is called the whirl velocity. It is

seen from equations 28a and 28b that the energy transfer depends directly upon the change in whirl produced between entrance and exit sections of the flow passage. If the entrance whirl is the larger, the machine is a turbine; if it is the smaller, the machine is a pump or compressor.

The interpretation of equations 26a and 26b for a turbine and pump are as follows:

In a turbine the term $(c_1{}^2 - c_2{}^2)/2g$ represents the change in the kinetic energy of the fluid due to its change in absolute velocities. Since c_2 is smaller than c_1 the above term represents a removal of kinetic energy from the fluid by the rotor. The kinetic energy $(1/2g)c_2{}^2$ is called the leaving or exit loss.

The term $(u_1{}^2 - u_2{}^2)/2g$ is a change in kinetic energy in the turbine blades due to R_1 and R_2 being unequal. This indicates that, if this so-called "centrifugal effect" is to be utilized to transfer energy from the fluid to the rotor, then the flow through a radial turbine must be radially inward.

The term $(w_1{}^2 - w_2{}^2)/2g$ represents the conversion of pressure into kinetic energy in the flow passage through the turbine rotor. If the velocity of the fluid relative to the rotor is greater at exit than at entrance, this means that pressure energy has been converted into kinetic energy in the flow passages. This effect is termed the reaction effect.

For a pump or compressor, the above terms have similar significance. The term $(c_2{}^2 - c_1{}^2)/2g$ represents the change in kinetic energy of the fluid as it flows through the rotor. Since c_2 is greater than c_1 in this type of machine, the increase in kinetic energy is provided by the rotor. This increase in kinetic energy is available for conversion into pressure energy in the machine itself, and not in the rotor.

The term $(u_2{}^2 - u_1{}^2)/2g$ represents a change in static pressure accomplished within the rotor due to centrifugal force acting on the fluid. When u_2 and u_1 are unequal, as in a centrifugal compressor, the fluid flows radially and, as it flows to the impeller tip, it experiences an increasing centrifugal effect. Since a centripetal force is required at any radius to rotate the fluid about the axis of the impeller, all fluid at the greater radii exerts a force on the fluid at the smaller radii, indicating that the static pressure of the fluid increases from the impeller hub to its tip. This centrifugal effect exists in conjunction with other flow effects superposed upon it

The term $(w_1{}^2 - w_2{}^2)/2g$ is the change in kinetic energy due to the change in the relative velocity of the fluid relative to the rotor

flow passages. In a radial-flow pump or compressor, the fluid is retarded in its flow relative to the rotor, so that $w_1 > w_2$; this term, therefore, represents a conversion of kinetic energy into static pressure within the rotor itself. Consequently, the total increase in static pressure within the rotor or impeller is given by

$$\frac{1}{2g} [(u_2{}^2 - u_1{}^2) + (w_1{}^2 - w_2{}^2)]$$

This increase in static pressure is termed the *reaction effect* of the pump or compressor.

In *axial-flow* machines $R_1 = R_2 = R$ and $u_1 = u_2 = u$, so that the energy transfer equations differ from those for a radial-flow machine by the absence of the centrifugal-effect term. Hence for an axial-flow turbine

$$L_t = \frac{u}{g} (c_{1u} - c_{2u}) = \frac{u}{g} \Delta c_u \qquad (29)$$

or

$$L_t = \frac{1}{2g} [(c_1{}^2 - c_2{}^2) + (w_2{}^2 - w_1{}^2)] \qquad (30)$$

This work is available at the periphery of the turbine and is, of course, equal to the product of the tangential force $F_u \times u$. The equation gives the work transferred to the turbine rotor periphery.

In an *axial-flow fan*, compressor, or blower the energy transferred by the rotor to 1 lb of the fluid is

$$L_c = \frac{1}{2g} [(c_2{}^2 - c_1{}^2) + (w_1{}^2 - w_2{}^2)] \qquad (31)$$

Equation 31 gives the work done by the ideal compressor upon 1 lb of fluid.

It is instructive to consider the energy changes for a complete machine. Consider a centrifugal pump [7] such as that illustrated schematically in Fig. 9.

The fluid enters the pump with the absolute velocity c_0 and leaves with the absolute velocity c_3. If
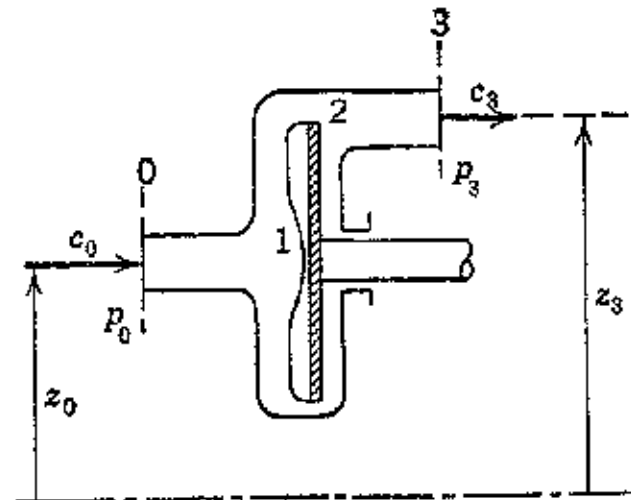
FIG. 9. Energy changes for a complete machine.

there is no friction in the inlet to the pump, then

$$\frac{p_0}{\gamma} + \frac{c_0^2}{2g} = \frac{p_{t1}}{\gamma} = \text{Total pressure} = \text{Constant} \qquad (32)$$

Since there are no losses, it follows from the Bernoulli theorem that

$$\frac{p_0}{\gamma} + \frac{c_0^2}{2g} = \frac{p_1}{\gamma} + \frac{c_1^2}{2g} \qquad (33)$$

or

$$p_{t0} = p_{t1} \qquad (34)$$

In this case the total pressure at the entrance to the impeller p_{t1} is equal to the total pressure at the entrance to the machine p_{t0}. If c_0 is small compared to c_1, so that it can be assumed that $c_0 = 0$, then the kinetic energy term is due to conversion of the static pressure p_1 into kinetic energy. Otherwise, it is due to the conversion of total pressure.

If the conversion of pressure into kinetic energy is accompanied by loss, this is indicated by the efficiency coefficient, less than unity, η_e. In that case, the kinetic energy of the fluid entering the impeller is reduced, and

$$\eta_e \frac{c_1^2}{2g} = \frac{p_{t0} - p_1}{\gamma} \qquad (35)$$

Equation 35 is quite general and is applicable to the passage leading from the entrance to the machine to the entrance of the rotor. As written, it applies to any incompressible fluid, but a similar expression can be written for a compressible fluid by replacing the Bernoulli equation by the energy equation for the stream lines taken with reference to the rotating axes. Thus for 1 lb of fluid

$$c_p T + \frac{1}{2g} w^2 - \frac{1}{2g} \omega^2 R^2 = \text{Constant} \qquad (36)$$

For simplicity, the discussion for the present will be confined to incompressible fluids.

The process of converting kinetic energy into static pressure within the rotor is also accompanied by losses. In an actual pump impeller the fluid motion is accompanied by turbulence and friction and the fluid does not move along stream lines as assumed by theory. The velocity distribution across the flow passage is non-uniform, being the resultant of a circulatory and a translatory flow. The fluid tends to

rotate in the direction opposite to that of the rotor. The extent of the circulatory flow depends upon the shape of the flow passage. Increasing the number of blades, which gives better guidance to the fluid, tends to reduce the circulatory flow.[15]

In impellers for compressible fluids such as air compressors, the conditions are generally worse. The fluid enters the impeller with large impact losses, if the speed of rotation deviates from the best operating speed. Flow separation generally begins at the inlet-vane tips, and, by the time the fluid reaches the impeller outlet, the passage is incompletely filled. The circumferential velocity traverse of the air in any one passage is very complicated. The fluid is generally flowing radially outward near the high-pressure side of the blade and radially inward near the low-pressure side of the adjacent blade. Besides all of this, most of the air crowds to the back wall of the impeller.

Because of the losses associated with the aforementioned phenomena, the reaction effect is smaller than in the ideal case. This can be expressed by means of the efficiency coefficient η_r.

It has already been pointed out that the transformation of the kinetic-energy term $(c_2{}^2 - c_1{}^2)/2g$ into pressure must be accomplished in the diffuser, which is generally not an efficient process. The fluid leaves the pump impeller with the large velocity c_2, and leaves the machine with the lower velocity c_3. Let

$$\frac{p_{t3}}{\gamma} = \frac{p_3}{\gamma} + \frac{c_3{}^2}{2g}$$

If there were no losses in the passage leading from the rotor exit to the machine exit (diffuser), then

$$\frac{p_2}{\gamma} + \frac{c_2{}^2}{2g} = \frac{p_3}{\gamma} + \frac{c_3{}^2}{2g} = \frac{p_{t3}}{\gamma}$$

or

$$\frac{c_2{}^2}{2g} = \frac{p_{t3} - p_2}{\gamma}$$

Owing to the aforementioned losses, the transformation of $c_2{}^2/2g$ into pressure is reduced. Let η_d be the efficiency coefficient for this process; then

$$\eta_d \frac{c_2{}^2}{2g} = \frac{p_{t3} - p_2}{\gamma}$$

Losses are encountered due to fluid friction in the flow passages. These friction losses increase practically proportional to the square of the velocity of the fluid and the wetted areas of the flow passages. Since the friction factor for a flow passage increases with its roughness, in the interest of reducing the friction losses, the surfaces of all the flow passages should be as smooth as is practicable. Energy must be expended to rotate a rotor surrounded by a body of fluid. This energy is dissipated in heating the fluid and is called the disk friction loss.

9. Characteristics of Hydraulic Jet Propulsion

Some of the earliest applications of jet propulsion were made by the British and Swedish governments to the propulsion of ships.[9] Water was inducted at the forward end of the vessel, it flowed through pumps which imparted energy to it, and it was then discharged at the rear through suitable nozzles. The complete flow path for the propulsive fluid, the water, comprises the entrance piping, the pump impeller passages, the outlet piping, and the discharge nozzle. These form the complete guide system acting on the fluid, and the fluid reacts upon the guide system.[8] For the purpose of propelling the ship, it is only the fore and aft component of the fluid reaction that is of interest. This component of force is denoted by $\mathfrak{I}$ and is termed the propulsion force or thrust. Let

V = absolute velocity of ship, fps.

c = absolute velocity of jet, fps.

w = relative velocity of the water discharged to the rear, taken with respect to the discharge nozzle, fps.

A = area of exit section of nozzle, sq ft

G = weight flow rate of water, lb/sec.

P = propulsion power, ft-lb/sec.

P_T = thrust power, ft-lb/sec.

P_L = leaving loss, ft-lb/sec.

$\mathbf{R}$ = resultant force acting on water in the fore and aft direction, lb.

$\mathfrak{I}$ = force or thrust propelling ship, lb.

$\mathbf{M}$ = momentum, slug-ft/sec.

γ = specific weight of propulsion fluid, lb/ft³.

ρ = density of propulsive fluid = γ/g, slug/ft³.

ν = V/w = speed ratio.

ω = angular velocity of pump impellers, rad/sec.

η = efficiency.

Subscripts

  1   at entrance
  2   at exit.
  h hydraulic.
  P propulsion.
  0   at time $t = 0$.
  m condition of maximum thrust power
  R required.
  a available.

The jet of water is discharged from the exhaust nozzle with the relative velocity w, while the ship moves in the opposite direction with the absolute velocity V. Hence, the absolute velocity of the jet is $c = (w - V)$.

For convenience the relative coordinate system will be used. The ship is assumed to be at rest, and the water approaches the ship with the actual velocity of the ship V. The velocity of the water entering the guide system is assumed to be so small that it may be neglected, which is substantially correct.[8][9,2] Its momentum at the entrance section is $M_1 = 0$. Let the weight flow of water be G lb/sec; then the change in momentum per second is given by

$$\mathbf{R} = \mathbf{M}_2 - \mathbf{M}_1 = \frac{G}{g} c = \frac{G}{g} (w - V) \quad \text{lb}$$

The external force $\mathbf{R}$ is the reaction of the guide system on the fluid and acts in the direction of increasing fluid velocity. The propulsion thrust $\mathfrak{I} = -\mathbf{R}$ acts in the direction of motion of the ship. Neglecting the minus sign, which denotes the direction of the thrust, the thrust equation becomes

$$\mathfrak{I} = \frac{G}{g} (w - V) = \frac{\gamma A w}{g} (w - V) \quad \text{lb} \tag{37}$$

since $G = \gamma A w$ lb/sec.

The net work done upon the water is utilized to increase its kinetic energy. This work is the energy transferred by the pump impeller and the reaction force of the guide system. The pump work in foot-pounds per second is the torque of the impeller M_t times its angular velocity ω and its hydraulic efficiency η_h. This work $M_t \omega \eta_h$ is called the *propulsion power* P and is equal to the useful work done by the propulsion jet $\mathfrak{I}V$, called the *thrust power* P_T, plus the kinetic energy lost with the ejected fluid $(G/2g)c^2$, called the *exit or leaving*

loss P_L. Hence, noting that $c = (w - V)$, the energy equation becomes

$$P = P_T + P_L \tag{38}$$

Substituting for P, P_T, and P_L

$$M_t \omega \eta_h = 5V + \frac{G}{2g} (w - V)^2 \tag{39}$$

Substituting for 5 from equation 37

$$M_t \omega \eta_h = \frac{G}{g} (w - V) V + \frac{G}{2g} (w - V)^2 \tag{40}$$

$$= \frac{G}{2g} (w^2 - V^2)$$

The ratio of the thrust power $5V$ to the propulsion power $M_t \omega \eta_h$ is a measure of the effectiveness with which the kinetic energy imparted to the fluid is transformed into useful work. This ratio is called the *propulsion efficiency* and is denoted by η_P. Thus

$$\eta_P = \frac{5V}{M_t \omega \eta_h} \tag{41}$$

Substituting for 5 from equation 37 and for $M_t \omega \eta_h$ from equation 40 gives the following equation for the propulsion efficiency

$$\eta_P = \frac{2(w - V)V}{w^2 - V^2} = \frac{2V}{V + w} = \frac{2\nu}{1 + \nu} \tag{42}$$

where $\nu = V/w$ is called the *speed ratio*.

The overall efficiency for the propulsion plant (the pumps and hydraulic system) is denoted by η and is given by

$$\eta = \eta_h \eta_P = \frac{5V}{M_t \omega} = \eta_h \left(\frac{2V}{V + w} \right) = \eta_h \left(\frac{2\nu}{1 + \nu} \right) \tag{43}$$

It is seen from equation 43 that to obtain a high propulsion efficiency the velocity ratio ν must be close to unity. This means that the exit relative velocity of the jet w should be of the same order of magnitude as the speed of the ship V. Equation 37 shows that, when V and w are of the same order of magnitude, the thrust developed per pound of water $5/G$ approaches zero. This means that if V and w are of the same order of magnitude the weight of water pumped per second, G, becomes extremely large. Further, when $V = w$ all thrust development ceases.

Equation 43 indicates why the early attempts to apply hydraulic jet propulsion to ships were unsuccessful. The plant efficiency η depends directly upon the hydraulic efficiency of the pump η_h, which had a low value. With a more efficient pump the possibilities of hydraulic jet propulsion became more favorable.

The thrust equation when expressed in terms of the jet area, speed ratio, and fluid density ρ is given by

$$\Im = \rho A w^2 (1 - \nu) \tag{44}$$

The corresponding equation for the thrust power P_T is

$$P_T = \Im V = \rho A w^3 (1 - \nu)\nu \tag{45}$$

From these equations it is apparent that, as w approaches the magnitude of V, to obtain a high value of propulsion efficiency, the area of the discharge nozzle A sq ft becomes exceedingly large.

If the rate of flow of water G is kept constant, the thrust power P_T is a parabolic function of the speed of the ship V, since for that condition the discharge velocity w is a constant. In that case the thrust power equation becomes

$$P_T = \Im V = \text{Constant}(\nu - \nu^2) \tag{46}$$

Differentiating equation 46 with respect to ν and setting the right-hand side equal to zero shows that the maximum thrust power occurs when the speed ratio is $\nu = 0.5$. The propulsion efficiency corresponding to the speed ratio for maximum thrust power is obtained by substituting $\nu = 0.5$ into equation 42.

Thus, when the thrust power attains its maximum value (G constant)

$$\eta_P = \frac{2\nu}{1 + \nu} = \frac{2}{3} = 0.667$$

The rate of flow of water through the propulsion system can be determined directly from equation 40. Thus

$$G = \frac{2g M_t \omega}{w^2 - V^2} \eta_h \tag{47}$$

The thrust can be expressed in terms of the pump power by combining equations 47 and 37. Thus

$$\Im = \frac{2 M_t \omega}{w^2 - V^2} \eta_h (w - V)$$

$$= \frac{2 M_t \omega}{w + V} \eta_h \tag{48}$$

Let $\mathfrak{I}_0$ be the thrust at starting up, that is, when the speed of the ship is $V = 0$. Then

$$\mathfrak{I}_0 = \frac{2M_t\omega}{w}\, \eta_h \tag{49}$$

Let $\mathfrak{I}_m$ denote the magnitude of the thrust when the thrust power is a maximum. It will be recalled that the thrust power is a maximum when $\nu = V/w = 0.5$, or when $V = w/2$. Then from equation 48

$$\mathfrak{I}_m = \left(\frac{2M_t\omega}{w+V}\right)\eta_h = \frac{4}{3}\left(\frac{M_t\omega}{w}\right)\eta_h \tag{50}$$

The ratio of the starting-up thrust $\mathfrak{I}_0$ to the thrust at maximum thrust power $\mathfrak{I}_m$ is seen to be $\mathfrak{I}_0/\mathfrak{I}_m = 1.5$. This thrust ratio is considerably smaller than that obtainable from a screw propeller. To increase this ratio during the start-up period additional power would have to be supplied.

In ship propulsion the required thrust power P_{TR} is given by an equation of the following form [9]

$$P_{TR} = bV^3 \quad \text{ft-lb/sec} \tag{51}$$

where b is a constant depending for its value on the characteristics of the ship in question.

When a ship propelled by a hydraulic jet is moving at constant speed, the required thrust power P_{TR} and the available thrust power $P_{Ta} = \mathfrak{I}V$ are equal. Hence

$$\mathfrak{I}V = bV^3 = \frac{\gamma Aw}{g}(w - V)V \tag{a}$$

Hence

$$V^2 + V\frac{\gamma Aw}{gb} - \frac{\gamma Aw^2}{gb} = 0 \tag{b}$$

Solving equation (b) for the speed of the ship

$$V = -\frac{\gamma Aw}{2gb}\left(1 - \sqrt{1 + \frac{4gb}{\gamma A}}\right) \tag{c}$$

The propulsion efficiency is

$$\eta_P = \frac{2V}{V + w} = \frac{2\left(1 - \sqrt{1 + \dfrac{4gb}{\gamma A}}\right)}{1 - \sqrt{1 + \dfrac{4gb}{\gamma A}} - \dfrac{2gb}{\gamma A}} \tag{52}$$

Multiply the numerator and the denominator of equation 52 by $[1 + \sqrt{1 + (4gb/\gamma A)}]$; then

$$\eta_P = \frac{4}{3 + \sqrt{1 + \dfrac{4gb}{\gamma A}}} \tag{53}$$

To compare the efficiency of the jet propulsion system with that of the screw propeller, the plant efficiency is required. Thus

$$\eta = \eta_h \eta_P = \frac{4\eta_h}{3 + \sqrt{1 + \dfrac{4gb}{\gamma A}}} \tag{54}$$

This last equation gives the combined efficiency of the hydraulic jet and its pump.

EXAMPLE. A ship is propelled at 20 mph by hydraulic jet propulsion. The resistance coefficient of the ship is $b = 2.5$; the area of the discharge nozzle opening is $A = 2.5$ sq ft; the hydraulic efficiency of the pumps is $\eta_h = 0.60$; and the specific weight of the water is $\gamma = 62.5$ lb/ft^3.

Calculate: (a) the propulsion efficiency η_P; (b) the volumetric rate of flow of water Q cfs; (c) the plant efficiency η.

Solution.

$$(a) \quad \eta_P = \frac{4}{3 + \sqrt{1 + \dfrac{4 \times 32.17 \times 2.5}{62.5 \times 2.5}}} = \frac{4}{4.75} = 0.842$$

(b) 20 mph $= \frac{20}{60} \times 88 = 29.3$ fps

From equation 42

$$\eta_P = 0.842 = \frac{2 \times 29.3}{29.3 + w}$$

Hence

$$w = 40.3 \quad \text{fps}$$

$$Q = Aw$$

$$= 2.5 \times 40.3 = 101 \quad \text{cfs}$$

(c) $\eta = \eta_P \cdot \eta_h = 0.842 \times 0.60 = 0.505$

10. Momentum and Circulation

When a moving body is completely submerged in a fluid the reaction of the fluid on the body is to produce a resistance force opposing the motion and a force normal to the direction of motion. The resistance force is termed the *drag*, and the normal force the *lift*. As pointed out in reference 14, if every detail of the flow conditions around the body were known then the velocities and pressures at all points in its surface could be evaluated by applying the

Bernoulli theorem to each point. By integrating the results the resultant pressure force would be obtained, and its components in the direction of motion and normal to that direction would be the drag and lift respectively. Since the foregoing procedure cannot be applied these force components are evaluated by applying the momentum principle to the flow.
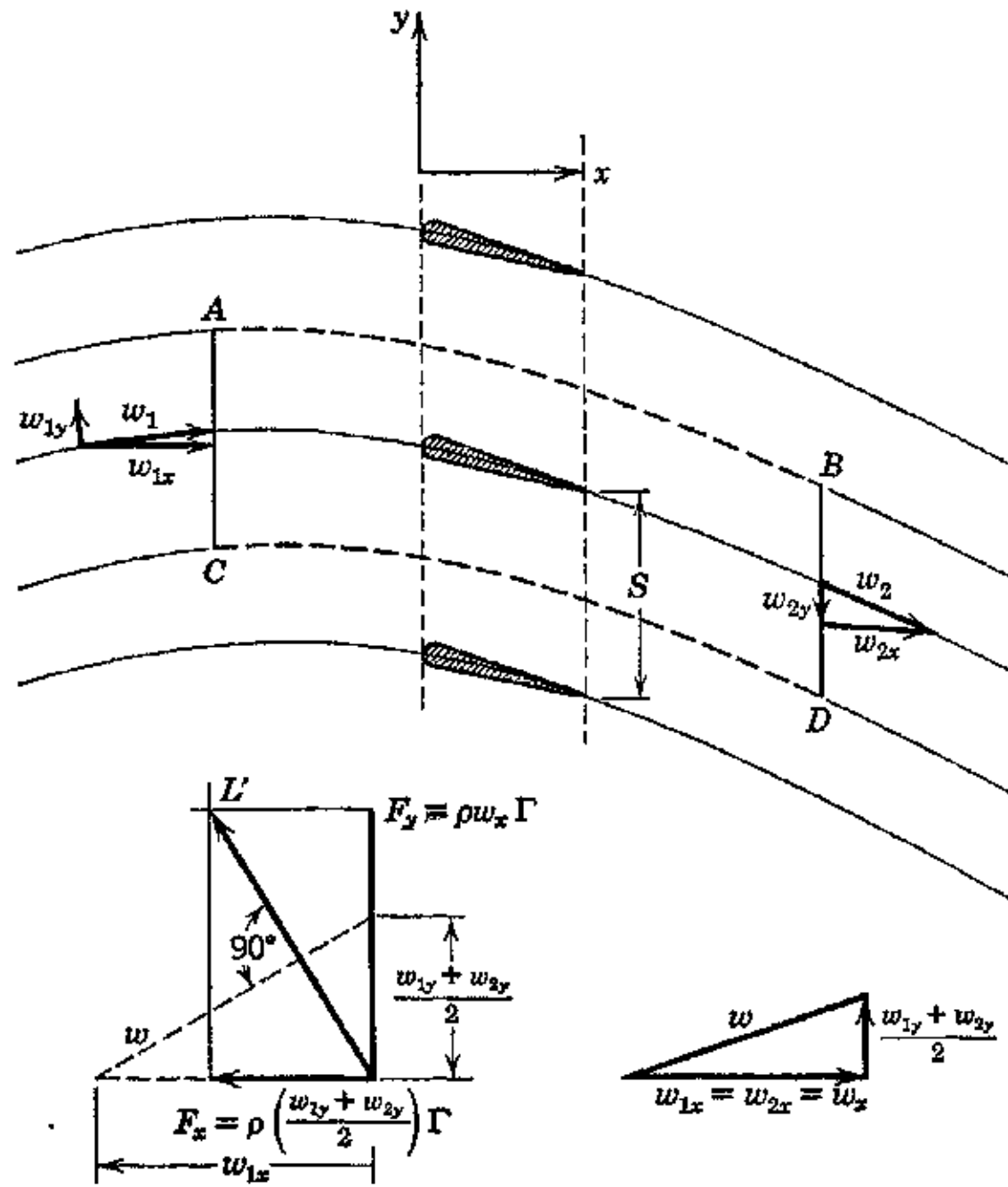
FIG. 10.   Flow through a blade grid.

Figure 10 illustrates schematically a portion of an infinite row of equally spaced identical blades. Since it is the relative motion between the blades and the fluid which gives rise to the hydrodynamic forces, the relative coordinate system can be used. This assumes that the blades are stationary and the fluid flows towards them. Further, let all the blades be placed at the same angle of attack with their leading edges on a line normal to the direction of the flow. Let the spacing between the blades be denoted by S, and consider unit length of blade perpendicular to the plane of the paper of an arbitrary blade. Owing to the geometrical arrangement the flow pattern around each blade is identical. The lines AB and CD

may be regarded as the typical stream lines or stream surfaces for each blade of the row.

Let $ABCD$ be a region between the two aforementioned stream lines that is bounded by the lines (surfaces) AC and BD drawn parallel to the y axis.

Let

w = velocity.

$\mathbf{M}$ = momentum.

F = force.

p = pressure.

G = weight rate of flow, lb/sec.

$m = G/g$ = mass rate of flow, slug/sec.

g = acceleration due to gravity = 32.174 ft/sec².

L = lift force, lb.

D = drag force, lb.

Subscripts

1   denotes at section AC.

2   denotes at section BD.

x in direction of x axis.

y in direction of y axis.

Greek

ρ = density, slug/ft³.

γ = specific weight, lb/ft³.

Γ = circulation.

Since the bounding surfaces AB and CD are tangent to the direction of flow at all points, no fluid can flow across these boundaries. Therefore, fluid can flow only across the surfaces AC and BD. The weight rates of flow across these two surfaces are

$$G_1 = w_{1x}S\gamma_1 \quad \text{and} \quad G_2 = w_{2x}S\gamma_2 \tag{55}$$

Since S has the same value at AC that it has at BD, and γ is assumed constant, then from continuity $G_1 = G_2$ and $w_{1x} = w_{2x} = w_x$.

Assume that there is no heat transfer, no losses due to friction, and no turbulence. The Bernoulli theorem applied to these two cross sections gives

$$\frac{p_1}{\gamma} + \frac{w_1^2}{2g} = \frac{p_2}{\gamma} + \frac{w_2^2}{2g}$$

or

$$p_1 - p_2 = \frac{\gamma}{2g}(w_2^2 - w_1^2) \tag{56}$$

Any forces acting upon the bounded mass of fluid bounded by the surface $ABCD$ will be transmitted to the blade. The total external force acting in any direction is the vector sum of that due to momentum change and that due to change in pressure forces. Since there is no velocity change in the x direction ($w_{1x} = w_{2x} = w_x$) the only forces acting on AC and BD in the x direction are those due to pressure difference; there can be no force in the x direction owing to momentum considerations. Let this pressure force component be denoted by $\mathbf{F}_x$. Hence

$$\mathbf{F}_x = S(p_1 - p_2) \tag{57}$$

Noting that

$$w_1{}^2 = w_{1x}{}^2 + w_{1y}{}^2 \tag{a}$$

and

$$w_2{}^2 = w_{2x}{}^2 + w_{2y}{}^2 \tag{b}$$

substitute (a) and (b) into equation 56 and then in equation 57. The result is

$$\mathbf{F}_x = \frac{\gamma S}{2g} (w_{2x}{}^2 + w_{2y}{}^2 - w_{1x}{}^2 - w_{1y}{}^2) \tag{58}$$

or since $w_{1x} = w_{2x} = w_x$

$$\mathbf{F}_x = \frac{\gamma S}{2g} (w_{2y}{}^2 - w_{1y}{}^2) = \frac{\gamma}{2g} S(w_{2y} + w_{1y})(w_{2y} - w_{1y}) \tag{59}$$

The surfaces AB and CD are located in the same relative positions with regard to adjacent blades; hence there is no unbalanced pressure force acting on those surfaces. The velocity component w_{1y} is *not* equal to w_{2y}; consequently there is a force acting in the y direction due to the rate of change in momentum.

The rate of change in momentum of the fluid is $\mathbf{M}_{2y} - \mathbf{M}_{1y}$, and the force required to produce this change is

$$\mathbf{M}_{2y} - \mathbf{M}_{1y} = \frac{G}{g} (w_{2y} - w_{1y})$$

The force acting on the blade is

$$\mathbf{F}_y = \frac{S\gamma}{g} w_x(w_{1y} - w_{2y}) \tag{60}$$

Let

$$\Gamma = S(w_{1y} - w_{2y}) = S \, \Delta w_y \tag{61}$$

Substituting equation 61 into equation 59 gives the following equation for the force $\mathbf{F}_x$. Since $\mathbf{F}_x = D$ the drag force acting on the blade

$$D = \mathbf{F}_x = -\rho\Gamma\frac{(w_{1y} + w_{2y})}{2} \tag{62}$$

The force $\mathbf{F}_y$ is a lift force acting on the blade. Let $L = \mathbf{F}_y$, then

$$L = \rho\Gamma w_x \tag{63}$$

In equation 62 the factor $(w_{1y} + w_{2y})/2$ is the average of the y components for the entrance and exit velocities. Consequently, the $\mathbf{F}_x$ is proportional to the average y component of the velocity of the fluid. Similarly, the force $L = \mathbf{F}_y$ is proportional to the average x component of the fluid velocity.

The physical significance of the factor Γ can be obtained in the following manner. Let the boundaries of the region enclosed by $CABDC$ be traversed in the order indicated, and the length of the boundary be multiplied by the velocity component parallel to the boundary. Thus

> For CA the result is Sw_{1y}
> For AB the result is $\mathbf{AB} \cdot w$
> For BD the result is $-Sw_{2y}$
> For DC the result is $-\mathbf{DB} \cdot w$

If the above products are summed up, taking cognizance of the signs, the clockwise direction being taken as positive, then, since $\mathbf{AB} = \mathbf{DB}$, the result of the summation is $S(w_{1y} - w_{2y})$ which from equation 61 is equal to Γ.

The value of Γ is called the circulation around the blade. It can be shown, by using the same argument as above, that the value of the circulation is the same for all closed regions enclosing the blade. Mathematically speaking, the summation procedure in the foregoing is equivalent to taking the line integral around the closed curve of the tangential velocity to the bounding surface. Thus

$$\Gamma = \oint w \cos\theta \cdot ds \tag{64}$$

where θ = angle between the velocity vector w, and a tangent to the closed curve.

ds = an elementary length of the closed curve.

Physically, the circulation Γ is a measure of the speed of rotation of the fluid as a solid body.

If the blade pitch S is made infinite the system illustrated in Fig. 9 reduces to a single blade (or airfoil) in an infinite fluid medium. If at the same time the bounding sections AC and BD are moved infinite distances to the left and right respectively the circulation is maintained constant, and the lifting force per unit length of blade, which is denoted by L', is given by

$$L' = \rho \Gamma V_0 \tag{65}$$

where V_0 is the velocity of the undisturbed stream.

Equation 65 is known as the Kutta-Joukowski theorem.

REFERENCES

1. E. Sänger, *Raketenflugtechnik*, Oldenbourg, Munich, 1933.
2. B. A. Bakmeteff, *Mechanics of Fluids, Compendium of Course C.E. 261*, Columbia University, Morningside Heights, New York.
3. L. Prandtl and O. G. Tietjens, *Fundamentals of Hydro- and Aeromechanics*, McGraw-Hill Book Co., New York, 1934.
4. W. F. Durand, *Aerodynamic Theory*, Vol. 1.
5. A. Stodola, *Steam and Gas Turbines*, McGraw-Hill Book Co., New York, 1927.
6. A. G. Webster, *The Dynamics of Particles*, G. E. Stechert & Co., New York.
7. S. A. Moss, C. W. Smith, and W. R. Foote, "Energy Transfer between a Fluid and a Rotor for Pump and Turbine Machinery," *Trans. A.S.M.E.*, August, 1942, pp. 567–596.
8. R. Eksergian, "On the Reactions of Fluids and Fluid Jets," *J. Franklin Institute*, May, 1944.
9. A. H. Gibson, *Hydraulics and Its Applications*, D. Van Nostrand Co., New York.
10. Th. von Kármán and M. A. Biot, *Mathematical Methods in Engineering*, McGraw-Hill Book Co., New York, 1940.
11. W. C. Johnson, *Mathematical and Physical Principles of Engineering Analysis*, McGraw-Hill Book Co., New York, 1944.
12. J. H. Keenan, *Thermodynamics*, John Wiley & Sons, New York, 1941.
13. H. Rouse, *Fluid Mechanics for Hydraulic Engineers*, McGraw-Hill Book Co., New York, 1938.
14. R. A. Dodge and M. J. Thompson, *Fluid Mechanics*, McGraw-Hill Book Co., New York, 1937, Chapter VII.
15. A. H. Church, *Centrifugal Pumps and Blowers*, John Wiley & Sons, New York, 1944.

THERMODYNAMICS OF GAS FLOW

1. Introduction

Turbojet engines and gas turbines utilize the thermodynamic processes of compressing atmospheric air, heating it to a high temperature by burning a fuel in it, and where auxiliary jet propulsion is utilized with the gas turbine then in both cases the gases are finally discharged through a suitably shaped exhaust nozzle. These processes are common regardless of the prime mover used for driving the air compressor. On the other hand, rocket motors generate high-pressure, high-temperature gases in a suitable combustion chamber and then exhaust the gases through some form of nozzle.

The purpose of this chapter is to review the thermodynamic principles upon which the processes mentioned above are based. As a first approximation it will be assumed that air or the propellant gases behave thermodynamically in accordance with the laws for perfect gases and the flow is one-dimensional. The basic relationships involved can be demonstrated by applying these laws. The results obtained in this manner can then be modified to take into account the deviations from the foregoing assumptions.

The equations derived in this chapter can be used with any consistent set of units (see page 2); those presented with the notation are for the English gravitational system.

Notation

$a = \sqrt{gkRT}$ = acoustic velocity, fps.

A = area, sq ft.

A_t = area of smallest cross section (throat), sq ft.

c = absolute velocity, fps.

$B = (h - T_0 s)$ = availability function, Btu/lb.

$c_p = \dfrac{R}{J}\left(\dfrac{k}{k-1}\right)$ = specific heat at constant pressure, Btu/lb F.

$c_v = \dfrac{R}{J}\left(\dfrac{1}{k-1}\right)$ = specific heat at constant volume, Btu/lb F.

C_c = contraction coefficient for a fluid jet.

$C_D = \varphi C_c$ = discharge coefficient for a nozzle or orifice.

D = diameter, ft.

E_k = kinetic energy, ft-lb/lb.

E_p = potential energy, ft-lb/lb.

E_F = heat energy due to friction, ft-lb/lb.

f = friction factor in the Fanning equation.

$f = A/G$ = area which passes a flow of 1 lb/sec.

g = acceleration due to gravity, 32.174 ft/sec².

G = weight flow rate, lb/sec.

$H = (h_1 - h_2')$ = available energy for an expansion, Btu/lb.

h = enthalpy of fluid $= u + \dfrac{1}{J}pv = \dfrac{k}{k-1}\left(\dfrac{RT}{J}\right)$ for a perfect gas, Btu/lb.

Δh = a finite charge in enthalpy, Btu/lb.

Δh_c = a finite increase in enthalpy (flow compression), Btu/lb.

Δh_t = a finite decrease in enthalpy (flow expansion), Btu/lb.

J = 778 ft-lb/Btu = mechanical equivalent of heat.

$k = c_p/c_v$ = specific heat ratio.

L = useful work done on or by a fluid, Btu/lb.

$_1L_2$ = useful work done on or by a fluid between sections 1 and 2.

m = molecular weight, mass rate of flow (slug/sec), or hydraulic radius (ft), as indicated in the text.

M = velocity/a = Mach number.

p = absolute static pressure, psf.

Q = heat flow, Btu/lb.

$_1Q_2$ = heat added between sections 1 and 2, Btu/lb.

$q = \frac{1}{2}\rho(\text{velocity})^2$ = dynamic pressure, psf.

R = gas constant = 1545/(molecular weight), ft-lb/lb F.

$\mathcal{R}$ = friction force, lb.

$r_c = p_2/p_1$ = pressure ratio for a compression process.

$r_t = p_1/p_2$ = pressure ratio for an expansion process.

$1/r_t = p_2/p_1$ = expansion ratio for an expansion process.

s = entropy, Btu/lb F.

Δs = a finite change in entropy, Btu/lb F.

T = absolute temperature (460 + t° F), ° R.

T_t = total temperature $= T_1\left[1 + \left(\dfrac{k-1}{2}\right)M^2\right].$

$\mathfrak{I}$ = thrust, lb.

$u = \dfrac{RT}{J}\left(\dfrac{1}{k-1}\right)$ = internal energy for a perfect gas, Btu/lb

$v = 1/\gamma = $ specific volume, cu ft/lb.

$w = $ relative velocity, fps.

$W = $ total weight, lb.

$x = $ distance in direction of x axis.

$X = $ force in direction of x axis.

$y = $ wetted perimeter, ft.

$z = $ elevation, ft.

$Z_c = (r_c^{\frac{k-1}{k}} - 1)$ for a compression process $= \dfrac{k-1}{2} M^2.$

$Z_t = (r_t^{\frac{k-1}{k}} - 1)$ for an expansion process.

Greek

$\alpha = $ divergence angle for a nozzle.

$\gamma = 1/v = \rho g = $ specific weight, lb/ft^3.

$\theta = \dfrac{T_2'}{T_1} = \left(\dfrac{p_2}{p_1}\right)^{\frac{k-1}{k}} = $ isentropic temperature ratio.

$\eta = $ efficiency.

$\rho = \gamma/g = 1/vg = $ density, slug/ft^3.

$\Sigma = $ summation.

$\tau = $ friction force per unit area, psf.

$\varphi = \sqrt{\eta} = $ velocity coefficient.

$\psi = \sqrt{\dfrac{k}{k-1}\left[\left(\dfrac{1}{r_t}\right)^{\frac{2}{k}} - \left(\dfrac{1}{r_t}\right)^{\frac{k+1}{k}}\right]}.$

$\Phi = \dfrac{T_t}{T_1} = \dfrac{\text{Total temperature}}{\text{Initial static temperature}} = 1 + \left(\dfrac{k-1}{2}\right) M^2.$

Subscripts

$1 = $ initial state (in general).

$2 = $ final state (in general).

$cr = $ critical.

$e = $ exit section.

$t = $ throat section of nozzle, or total, as indicated in text.

$c = $ combustion chamber, or compression, as indicated in text

$0 = $ initial or rest condition.

max. $= $ maximum.

$L = $ limiting value.

$F = $ friction.

Superscripts

Prime denotes isentropic process.

2. Dynamic Equations for the Steady Flow of Fluids

The discussions in this chapter assume that the fluid moves under the conditions for *steady flow*. This signifies that the static pressure p, the specific weight of the fluid γ and the velocity w are constant with respect to time at each cross section of the flow passage. Under these conditions the weight rate of flow G is the same at all cross sections and does not vary with time.

In reality, steady flow can exist only if the fluid particles move along stream lines. Consequently, the turbulent eddying flow which accompanies most of the practical examples of flow is not steady, even if no variations in the rate of flow can be detected with ordinary measuring instruments. However, under the conditions where the rate of discharge G is constant, it is possible to draw fixed lines in the fluid stream in such a manner that they are tangential to the average direction of the flow. The actual fluid motion can thereby be conceived as being composed of a steady motion along these stream lines, with irregular random disturbances of velocity superimposed upon them.[1]

Fig 1.   Fluid element flowing in a converging passage.

Figure 1 illustrates an arbitrary converging passage through which a fluid is flowing. Assume that the flow is steady, does not change its elevation, and is in the direction of the constriction, so that the velocity is increasing; that is, the fluid is being accelerated. To determine the magnitude of the force causing the acceleration consider an element of the fluid bounded by the two parallel surfaces 1-1 and 2-2 perpendicular to the direction of flow and the infinitesimal distance dx apart.[2]

The following forces act on the fluid element in the direction of the x axis:

(a) The pressure force pa on the left-hand face due to the pressure intensity p.

(b) The pressure force $-(p + dp)(A + dA)$ on the right-hand face, the negative sign indicating that it acts in the negative direction. It should be noted that for the configuration shown dp and dA are both negative since the pressure and area have decreased at section 2.

(c) On the bounding surface of the element of fluid there acts a force which has the component $[p + (dp/2)]\, dA$ acting in the x direction.

(d) The x component of the wall friction force which is denoted by $-d\mathcal{R}$.

The net force acting on the fluid element in the positive direction of the x axis is the vector sum of the aforementioned forces. Neglecting all differentials smaller than the first, the general equation for the sum of the external forces is

$$\Sigma X = pA - (p + dp)(A + dA) + \left(p + \frac{dp}{2}\right) dA - d\mathfrak{R}$$
$$= -A \, dp - d\mathfrak{R} \tag{1}$$

The resultant external force, $-A \, dp - d\mathfrak{R}$, imparts to the element the acceleration dw/dt. The mass of the element is $\rho A \, dx = (\gamma/g)A \, dx$. The equation for the acceleration of the element will now be determined.

Each particle of fluid moves along a certain stream line, and its instantaneous velocity w is a function of the time t and the distance x it moves along its stream line. Hence w is a function of both t and x. Thus $w = f(t, x)$, and its total differential dw is

$$dw = \frac{\partial w}{\partial x} dx + \frac{\partial w}{\partial t} dt \tag{2}$$

The acceleration equation for the particle is

$$\frac{dw}{dt} = \frac{\partial w}{\partial x}\frac{dx}{dt} + \frac{\partial w}{\partial t}\frac{dt}{dt} = w \frac{\partial w}{\partial x} + \frac{\partial w}{\partial t} \tag{3}$$

The term $\partial w/\partial t$ is the increase in velocity with respect to time at the same point on the stream line, while the term $w \, \partial w/\partial x$ is the increase in velocity due to the particle moving with the velocity w through a field of flow having the velocity gradient $\partial w/\partial x$.

In view of the assumption of steady flow, the velocity at a given point is invariant with time. Hence the term $\partial w/\partial t = 0$, and the term $w \, \partial w/\partial x$ is the only one that is significant. This means that the fluid particle acceleration in steady flow is a function of x alone, and the partial differential notation may be replaced by that for ordinary differentials. Thus

$$\frac{dw}{dt} = w \frac{dw}{dx} \tag{4}$$

The external force producing this acceleration is given by equation 1. Hence, using equation 4 for the acceleration, applying D'Alembert's principle, and dividing through by the area A, gives

$$dp + \rho w \, dw + \frac{d\mathfrak{R}}{A} = 0 \tag{5}$$

Multiplying through by $v = 1/\gamma = 1/\rho g$, where v is the specific volume

$$v \, dp + \frac{w}{g} dw + \frac{v \, d\mathfrak{R}}{A} = 0 \qquad (6)$$

If the fluid changes its elevation by the amount dz in the distance dx, equation 6 becomes

$$v \, dp + d\left(\frac{w^2}{2g}\right) + \frac{v \, d\mathfrak{R}}{A} + dz = 0 \qquad (7)$$

Equation 7 is the general form of the dynamic equation for the flow of any fluid in contact with solid boundaries. To integrate this equation the relationship between p and v, the flow area, and the friction force must be established as functions of the flow path.

In general, where the flow of a gas is under consideration the term dz is so small that it may be neglected. Further, if the friction coefficient for the passage is denoted by f, its hydraulic radius by m, and its length by dx, then, for perfect gases, the dynamic equation for flow with friction becomes

$$dp = -\frac{p}{gRT} f \frac{w^2}{2m} dx - \frac{p}{gRT} w \, dw \qquad (7a)$$

3. Energy Equation for the Flow of Gases

Refer to Fig. 2, which illustrates the general condition for the flow of a fluid. The energy relationships for the flow of a gas are
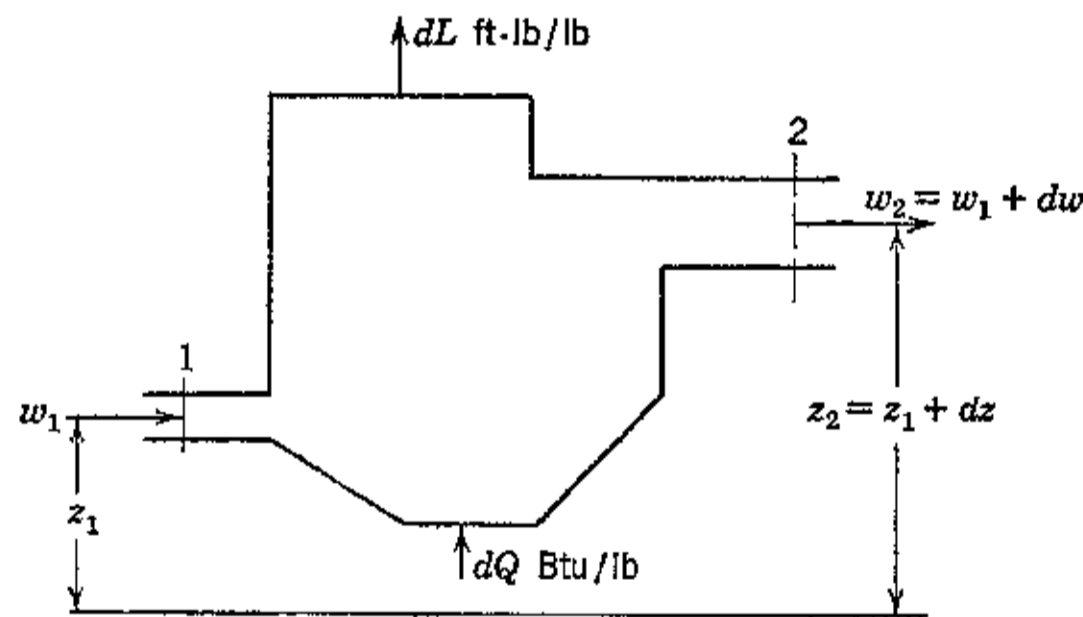
FIG. 2. Energy balance for steady flow of a fluid.

based on the conception that its motion is related to some process that involves heat exchange. Consequently, the macroscopic aspects of the flow process are amenable to analysis by the application of the law of the conservation of energy. Consider a flow of 1 lb of gas.

Then, if the quantity of heat dQ Btu/lb is added to the gas from all sources, and the external work $1/J \, dL$ Btu/lb is removed from the gas, it follows from the first law of thermodynamics that, in the absence of friction and changes in potential energy,

$$dQ = du + \frac{1}{J} v \, dp + \frac{1}{J} p \, dv + \frac{1}{Jg} w \, dw + \frac{1}{J} dL \quad \text{Btu/lb} \qquad (8)$$

Where the flow process involves energy losses such as friction, shock, and turbulence the energy expended in overcoming the resistances is converted into heat that remains in the gas. Its effect, as is shown later, is to raise the final enthalpy of the fluid above that which would have resulted if no friction or turbulence were associated with its motion. Let the energy loss per unit weight due to friction be denoted by $1/J \, dE_F$; then for *flow with friction* equation 8 becomes

$$dQ = du + \frac{1}{J} v \, dp + \frac{1}{J} p \, dv + \frac{1}{Jg} w \, dw + \frac{1}{J} dL + \frac{1}{J} dE_F \qquad (9)$$

If the fluid experiences a change in its potential energy by virtue of changing its elevation by the amount dE_p per unit weight, then equation 9 becomes

$$dQ = du + \frac{1}{J} \left(v \, dp + p \, dv + \frac{1}{g} w \, dw + dL + dE_F + dE_P \right) \quad \text{Btu/lb} \tag{10}$$

But, by definition, the enthalpy change dh is given by

$$dh = du + \frac{1}{J} d(pv) = du + \frac{1}{J} (p \, dv + v \, dp) \qquad (11)$$

Substituting in terms of dh into equation 10 from equation 11 and noting that $dh = c_p \, dT$ for gases

$$dQ = dh + \frac{1}{Jg} w \, dw + \frac{1}{J} (dE_F + dE_P) + \frac{1}{J} dL \qquad (12a)$$

For gases

$$dQ = c_p \, dT + \frac{1}{Jg} w \, dw + \frac{1}{J} (dE_F + dE_P) + \frac{1}{J} dL \qquad (12b)$$

or

$$dQ = \left(\frac{k}{k-1} \right) \frac{R}{J} dT + \frac{1}{Jg} w \, dw + \frac{1}{J} (dE_F + dE_P) + \frac{1}{J} dL \qquad (12c)$$

Referring to the flow passage illustrated in Fig. 2, denote the state coordinates of the fluid at section 1 by the subscript 1, and those at

section 2 by the subscript 2. Further, let $_1Q_2$ denote the heat added
to the gas from all sources during its movement from section 1 to sec-
tion 2, $1/J_1(E_P)_2$ denote the potential energy change, and $1/J_1(E_F)_2$
denote the heat energy due to frictional effects. Integrating equa-
tion 10 between the limits 1 and 2 gives

$$_1Q_2 = (u_2 - u_1) + \frac{1}{2gJ}(w_2{}^2 - w_1{}^2) + \frac{1}{J}(p_2v_2 - p_1v_1)$$

$$+ \frac{1}{J}{}_1(E_P)_2 + \frac{1}{J}{}_1L_2 + \frac{1}{J}{}_1(E_F)_2 \quad (13)$$

The above energy equation can be stated in terms of the enthalpy
changes for the fluid by integrating equation 12a. Thus

$$_1Q_2 = h_2 - h_1 + \frac{1}{2gJ}(w_2{}^2 - w_1{}^2) + \frac{1}{J}{}_1(E_P)_2 + \frac{1}{J}{}_1(E_F)_2 + \frac{1}{J}{}_1L_2 \quad (14)$$

Equations 10 and 14 are the most general forms of the energy
equation for the steady flow of a fluid. They are general statements
of the energy relationship for any flow passage and any fluid. The
only restriction imposed is that the passage cannot store energy.

4. Reversible Processes and Available Energy

A *reversible* process may be defined as one which is in such a state
of equilibrium at all points in its path that any small change in the
"driving force" will cause it to proceed in the direction corresponding
to the sign of the change. In a heat-flow process the driving force
is the temperature difference applied to the equilibrium state. Con-
sequently, if an arbitrarily small temperature difference will produce
either a compression or an expansion, depending upon its sign, and
the corresponding works are equal to the quantities of heat trans-
ferred, then the process is reversible. It is apparent from the fore-
going that heat-flow processes involving friction cannot be reversible
because an amount of heat equal to the friction must always be
supplied before the direction of the process can be reversed. This
heat of friction does not reappear as external work but is dissipated
within the system. Since friction invariably accompanies the flow
of real gases, *actual flow processes are irreversible.* As a matter of
fact all natural processes are irreversible; they tend to proceed in a
given direction and never reverse themselves unless work is done,
at the expense of some other system, to reverse them. *Ideal* flow

processes can be conceived, however, which are frictionless and reversible. They are of great importance because actual flow processes can be studied in terms of these ideal processes and the results corrected to take care of the departures from the ideal.

Even in reversible processes it is not possible to transform thermal energy completely from one form into another. Experience has demonstrated that the transformation is inevitably accompanied by a degradation of energy into a less useful form.[8] The thermal energy associated with a gas cannot, therefore, be converted entirely into mechanical work by permitting the fluid to expand. This is because the thermal energy is associated with the random movements of the gas molecules[4] and is not completely subject to control. It should be realized that the first law of thermodynamics is not concerned with this matter and gives no information regarding it. It is concerned only with that portion of the thermal energy that is converted into useful work and points out that each Btu of heat converted into work produces 778 ft-lb (the exact value is 778.2 ft-lb).[2] It is the second law that is concerned with the quantity of thermal energy that can be converted into useful work, and this law presents the basis for judging the performances of actual processes.[8]

The second law is based entirely on scientific experience[10] which has demonstrated, as stated by Stodola,[12] that "whereas work can always be transformed into heat (as, for example, through friction) the reverse process, transformation of heat into work, is neither unlimited nor can it be carried out at will." The transformation of heat always requires that there be a temperature difference between the heat source and the heat sink. The second law was first formulated by Clausius (1850). Thus

A. *Heat cannot itself flow from a reservoir at lower temperature to one at a higher temperature without there being changes in the environment (Clausius).*

A later statement due to Thomson (1851) is

B. *No machine is possible which removes heat from a heat reservoir and changes it completely into work without changes taking place in the environment.*

The last statement is based on the following definition, due to Ostwald, of a perpetual-motion machine of the *second type:* a machine that undertakes to transform heat drawn from a single reservoir into work without changing anything else in its environment.

A satisfactory statement of the second law based on Ostwald's definition of a perpetual-motion machine of the second type is as follows:

C. *Perpetual motion of the* second type is impossible *even with an ideal, frictionless, perfectly insulated heat engine.*[12]

The above statements point out that in a reversible heat transfer process a part of the heat energy is always *unavailable* for conversion into work. Thus, if 1 lb of a substance acts as a heat reservoir at the temperature T at any instant, and supplies heat Q, by a reversible process, to a reversible engine, the engine always rejects a portion of this heat to the lowest available temperature T_0. The maximum conversion of the heat into work $(1/J)L$, is obtained in a Carnot engine and is given by

$$\frac{\Delta L}{J} = -\int_{T_1}^{T_0} \left(\frac{T - T_0}{T} \right) dQ \qquad (15a)$$

or

$$\frac{\Delta L}{J} = -\int_{T_1}^{T_0} dQ + T_0 \int_{T_1}^{T_0} \frac{dQ}{T} \qquad (15b)$$

Integrating between the temperatures T_1 and T_0

$$\frac{1}{J} \Delta L = - \left[Q - T_0 s \right]_{T_1}^{T_0} \qquad (15c)$$

Equation 15c states that, in a reversible process where the total heat transfer is Q, a quantity of heat equal to $\left[T_0 s \right]_{T_1}^{T_0}$ is unavailable for conversion into work, and the balance can be completely converted into work only in an ideal machine.[10]

Because of the assumption of reversibility all the heat rejected must take place at the temperature T_0. Consequently, in accordance with the second law,

$$dQ = T_0\, ds \qquad (15d)$$

The addition or removal of the heat dQ changes the internal energy of the substance in accordance with the first law. Thus

$$du = dQ - \frac{1}{J} dL \qquad (16)$$

The work obtained, $(1/J)\,dL$, is composed of the maximum useful work $(1/J)\,dL_{max}$ and the work $(1/J)\,p_0\,dv$ required to overcome the pressure of the environment.[48] Hence

$$du = T_0\,ds - \frac{1}{J}\,dL_{max.} - \frac{1}{J}\,p_0\,dv \qquad (17)$$

Integrating between T_1 and T_0, and transposing, gives an expression for the maximum work obtainable from a reversible process. Thus

$$-\frac{1}{J}L_{max.} = u_1 - u_0 - T_0(s_1 - s_0) + \frac{1}{J}p_0(v_1 - v_0) \qquad (18)$$

This last expression is usually presented in the following form· it is called the *availability function* and is denoted by B. Thus

$$B = (u_1 + p_0 v_1 - T_0 s_1) - (u_0 + p_0 v_0 - T_0 s_0) \qquad (19)$$

Since p_0 and T_0 are fixed for a given process, it is seen that the availability is a function of the initial state, i.e., state 1. The change in availability for a reversibile process proceeding from state 1 to state 2 is accordingly

$$\Delta B = (u_2 + p_0 v_2 - T_0 s_2) - (u_1 + p_0 v_1 - T_0 s_1) \qquad (20)$$

In a reversible flow process, where gravitational work and potential energy changes are neglected,[10] the availability change reduces to

$$\Delta B = \Delta h - T_0\,\Delta s = -\frac{1}{J}L_{max} \qquad (21)$$

For a more detailed discussion of availability consult references 2, 3, 8, 9, and 10.

5. Dynamic Equations for Frictionless Flow of Gases

Refer to the general dynamic equation, equation 7, and assume that a gas encounters no friction as it flows along its path, nor does its elevation change. Then $d\mathcal{R} = dz = 0$, and equation 7 reduces to

$$v\,dp + d\left(\frac{w^2}{2g}\right) = 0 \quad \text{or} \quad -\int_1^2 v\,dp = \frac{w_2{}^2}{2g} - \frac{w_1{}^2}{2g} \qquad (22)$$

and equation 7a, in terms of the fluid density ρ, becomes

$$\frac{dp}{\rho} + w\,dw = 0 \quad \text{or} \quad dp = -\rho w\,dw \qquad (22a)$$

Rewriting equation 22a in the following form

$$\frac{dp}{d\rho} \cdot \frac{d\rho}{\rho} = -w\,dw \tag{22b}$$

But, from Chapter 1, equation 79,

$$\frac{dp}{d\rho} = a^2 = (\text{acoustic velocity})^2$$

Hence in the case of the frictionless flow of gases the energy equation becomes

$$\frac{d\rho}{\rho} = -\frac{w}{a^2}\,dw \tag{23a}$$

or

$$\frac{d\rho}{dw} = -\frac{\rho w}{a^2} \tag{23b}$$

Referring to equation 22 it is apparent that the kinetic energy, $E_k = w^2/2g$, derived from expanding a gas in frictionless flow is exactly equal to the work, $-\int v\,dp$, obtainable by expanding the gas in a piston engine.

If the pressure change in flowing from station 1 to station 2 is very small, no sensible error is introduced by using the average of the end pressures, $\frac{1}{2}(p_1 + p_2)$, instead of the actual pressures. A mean value of the specific volume $v_m = 1/\gamma_m$ can then be applied. Hence, for very small pressure changes, the kinetic energy E_k in foot-pounds per pound, is given by

$$E_k = -\int_1^2 v\,dp = v_m(p_1 - p_2) = \frac{p_1 - p_2}{\gamma_m} \tag{24}$$

Substituting equation 24 into 22

$$p_1 + \frac{\gamma_m}{2g}\,w_1{}^2 = p_2 + \frac{\gamma_m}{2g}\,w_2{}^2 = \text{Constant} \tag{25}$$

Equation 25 is recognized as the *Bernoulli equation* for incompressible fluids. It could have been obtained directly from equation 22 by assuming that $\rho = \gamma/g = $ constant. Hence, for the flow of a *non-viscous incompressible fluid* in a horizontal passage,

$$\frac{1}{2g}(w_2{}^2 - w_1{}^2) = \frac{1}{\gamma}(p_1 - p_2) \tag{26}$$

If changes in elevation are encountered by the incompressible fluid, then $dE_p = \rho g\, dz$ and the Bernoulli equation takes the following form

$$dp + \rho g\, dz + \frac{\rho}{2}\, d(w^2) = 0 \tag{27}$$

6. Isentropic Flow Equation for Gases

For an isentropic process $ds = dQ = 0$, and the changes in the internal energy of the gas are due entirely to the work of flow *compression* or *expansion;* this work is represented by the term $(1/J)p\, dv$ in equation 8. If the flow process is an expansion, the temperature of the gas is lowered, which signifies that the internal energy of the gas is decreased; the reverse obtains for a compression. Hence

$$du + \frac{1}{J} p\, dv = 0 \tag{28a}$$

or

$$c_v\, dT + \frac{1}{J} p\, dv = \frac{R}{J}\left(\frac{1}{k-1}\right) dT + \frac{1}{J} p\, dv \tag{28b}$$

The energy equation for isentropic flow and no work done on or removed from the gas is obtained by substituting $dQ = dL = 0$ and equation 28a into equation 8. The result is

$$v\, dp + \frac{w}{g}\, dw = 0 \tag{29}$$

For an isentropic process it follows from 12a

$$0 = dQ = T\, ds = du + \frac{1}{J} p\, dv = dh - \frac{v}{J} dp \tag{30}$$

Hence for a reversible process

$$J\, dh - v\, dp = 0 \tag{31}$$

Substituting for $v\, dp$ from equation 29 into equation 31 gives the following energy equation for the isentropic flow of a fluid. Thus

$$J\, dh + d\left(\frac{w^2}{2g}\right) = 0 \tag{32}$$

and the dynamic equation, equation 22, is

$$v\, dp + d\left(\frac{w^2}{2g}\right) = 0$$

It is seen from equations 22 and 32 that in non-turbulent, friction-less adiabatic flow the energy and dynamic equations are identical. If the pressure in the direction of flow is decreasing (accelerated flow) the flow passage is called a *nozzle;* if it is increasing (decelerated flow) it is a *diffuser.*

For a perfect gas $dh = c_p \, dT$. Substituting this into equation 32 and for c_p in terms of k and R yields

$$\left(\frac{k}{k-1}\right) R \, dT + \frac{1}{g} w \, dw = 0$$

Hence the energy equation for the isentropic flow of a gas can be written in the form

$$kgR \, dT + (k-1) \, w \, dw = 0 \tag{33}$$

Dividing through by $kgRT = a^2$

$$\frac{dT}{T} + (k-1) \frac{w}{a^2} dw = 0$$

Dividing and multiplying the last term by w, the energy equation for the isentropic flow of a gas becomes

$$\frac{dT}{T} + (k-1)M^2 \frac{dw}{w} = 0 \tag{33a}$$

Integrating equation 32 and using the prime to denote that the end point is attained by an isentropic process

$$\frac{1}{2gJ} (w_2'^2 - w_1^2) = h_1 - h_2' = H = \Delta h_t' \quad \text{Btu/lb} \tag{34}$$

In mechanical units

$$w_2'^2 - w_1^2 = 50{,}000 \, \Delta h_t' \quad \text{(fps)}^2 \tag{35}$$

Equation 34 gives the maximum change in kinetic energy obtainable from expanding a fluid from state 1 to state 2. The term $H = (h_1 - h_2')$ is termed the *available energy* for the reasons explained in Section 4; it is also referred to as the *isentropic enthalpy change.*

Assume that the initial velocity w_1 is small enough so that the assumption $w_1 = 0$ is justified. Then the final velocity of the gas is

$$w_2' = 223.7\sqrt{h_1 - h_2'} = 223.7\sqrt{H} = 223.7\sqrt{\Delta h_t'} \tag{36}$$

The velocity w_2' is termed the *isentropic* velocity.

If the initial kinetic energy is not zero, then the isentropic velocity is given by

$$w_2' = \sqrt{2gJH + w_1^2} \quad \text{fps} \tag{37}$$

7. Total Temperature and Ideal Pressure Rise Ratio

In the preceding section it was shown that the energy equation for isentropic flow is given by equation 32. For a perfect gas this equation can be written in the form

$$Jc_p \, dT + d\left(\frac{w^2}{2g}\right) = 0$$

That the process is isentropic is indicated by writing T_2' for the final temperature instead of T_2. Hence the energy equation is

$$c_p T_2' + \frac{w_2'^2}{2gJ} = c_p T_1 + \frac{w_1^2}{2gJ} \tag{38}$$

Solving for the ideal temperature ratio $T_2'/T_1 = \theta$

$$\theta = \frac{T_2'}{T_1} = 1 + \frac{w_1^2}{2gJc_pT_1}\left(1 - \frac{w_2'^2}{w_1^2}\right) \tag{39}$$

Assuming that the flow is a compression process, so that w_2'/w_1 is less than unity, substitute for c_p from equation 1·43 and note that $M_1^2 = w_1^2/a_1^2 = w_1^2/gkRT$; then

$$\theta = 1 + \frac{k-1}{2}M_1^2\left(1 - \frac{w_2'^2}{w_1^2}\right) \tag{40}$$

If the final velocity is zero, the temperature T_2' is called the stagnation or *total temperature* and is denoted by T_t, and the ratio $T_t/T_1 = \Phi$. Thus

$$\Phi = \frac{T_t}{T_1} = 1 + \frac{k-1}{2}M_1^2 = \frac{k-1}{2}\left[M_1^2 + \frac{2}{k-1}\right] \tag{41}$$

The relationship between the temperature change and the corresponding pressure change is obtained from equation 31 and the characteristic equation for perfect gases. Thus

$$J \, dh = v \, dp = Jc_p \, dT = \left(\frac{k}{k-1}\right) R \, dT = RT\frac{dp}{p} \tag{42}$$

From which it follows from equations 42 and 33a

$$\frac{dT}{T} = \left(\frac{k-1}{k}\right)\frac{dp}{p} = -(k-1)M^2\frac{dw}{w} \tag{43}$$

Integrating equation 43 between the limits $T = T_1$, $T = T_t$ $p = p_1$, and $p = p_t$ gives

$$\log_e\frac{T_t}{T_1} = \left(\frac{k-1}{k}\right)\log_e\frac{p_t}{p_1}$$
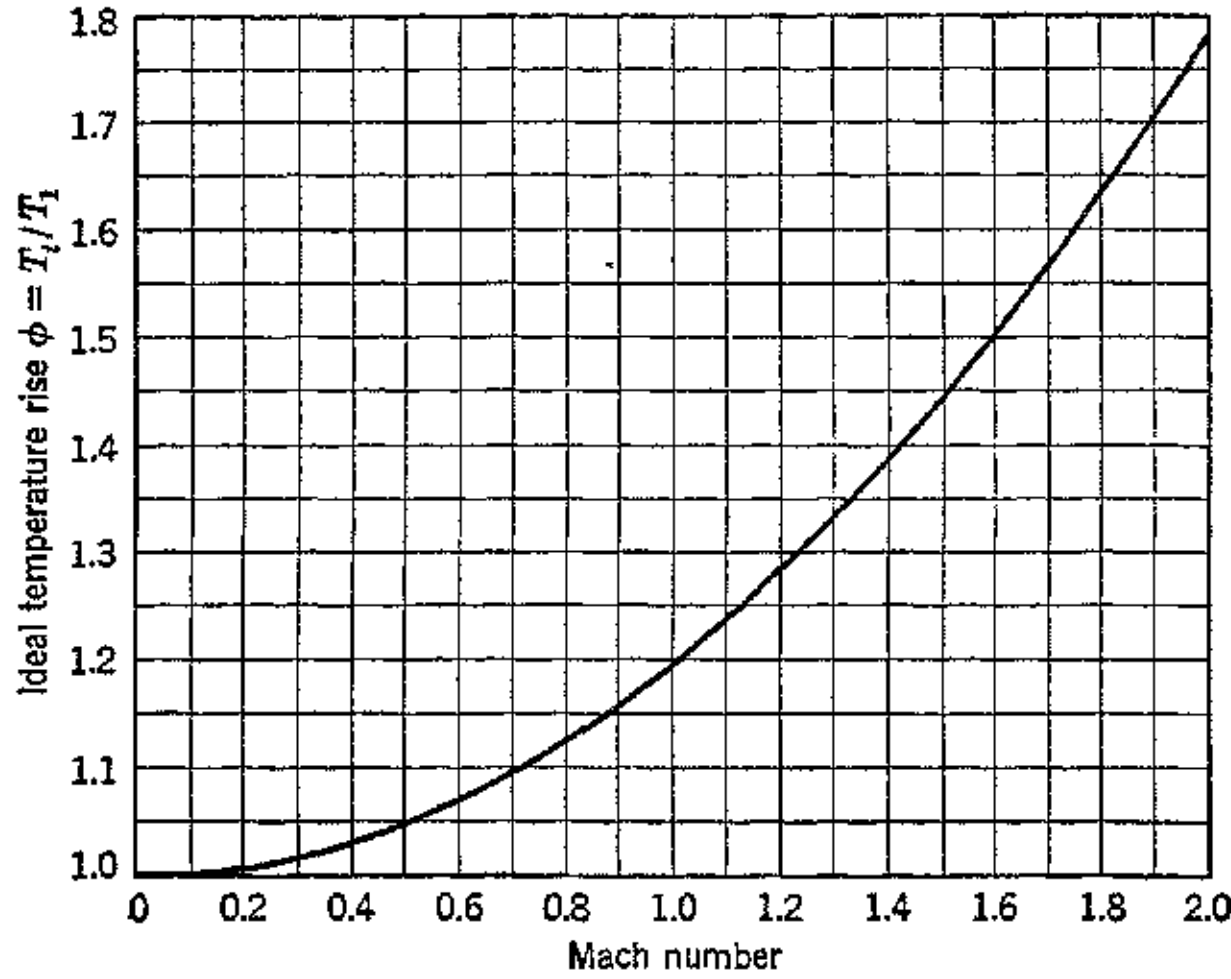
FIG. 3.   Ideal temperature rise ratio for normal air.

The relationship between the *ideal pressure rise ratio* p_t/p_1 and the Mach number is

$$\Phi = \frac{T_t}{T_1} = \left(\frac{p_t}{p_1}\right)^{\frac{k-1}{k}} = \frac{k-1}{2}\left[M_1^2 + \frac{2}{k-1}\right] \tag{44}$$

The total pressure p_t, also called the stagnation pressure, is that corresponding to the pressure in an infinite reservoir from which the fluid is accelerated isentropically to its actual velocity.   It is seen from equation 1·70 that in general $Z_c = \theta - 1$.   For the stagnation condition $\theta = \Phi$.   Hence, using equations 41 and 44,

$$Z_c = \theta - 1 = \Phi - 1 = \frac{k-1}{2}M_1^2 \tag{45}$$

The entering Mach number as a function of the ideal pressure rise ratio is accordingly

$$M_1 = \sqrt{\frac{2}{k-1}(\Phi-1)} = \sqrt{\frac{2}{k-1}Z_c} \qquad (46)$$

The ideal pressure rise ratio resulting from the isentropic deceleration of a gas from an initial Mach number M_1 to a final Mach number M_2 is obtained from the ratio $(p_t/p_1)_{M_1}/(p_t/p_1)_{M_2}$.
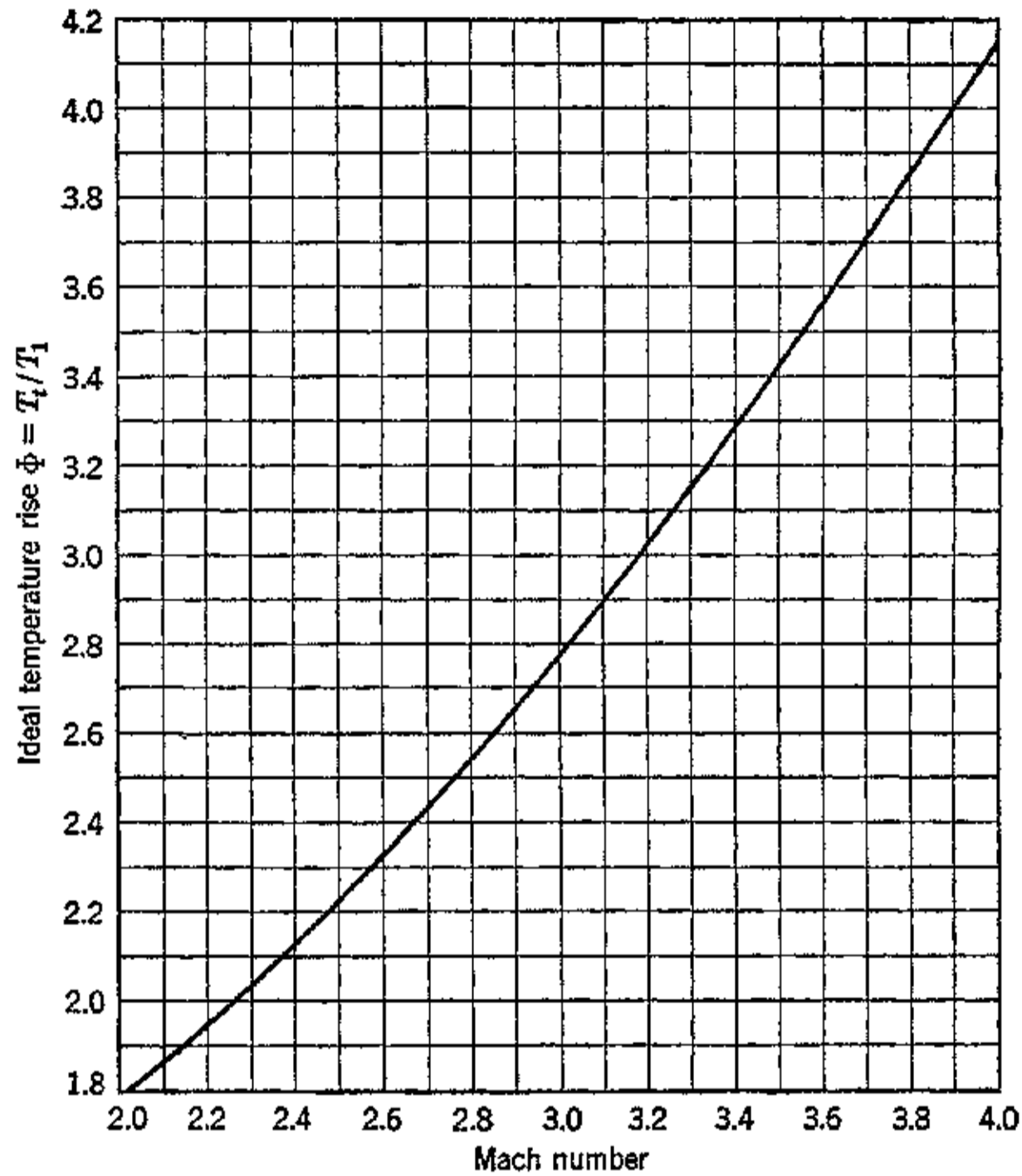
FIG. 4.   Ideal temperature rise ratio for normal air.

For normal air $k = 1.395$ and $R = 53.35$ according to reference 44. Values of the parameter Z_c for normal air are presented in Table 4·5.

Figures 3 and 4 present $\Phi = T_t/T_1$ as a function of M. Figure 5 presents p_t/p_1 as a function of M.
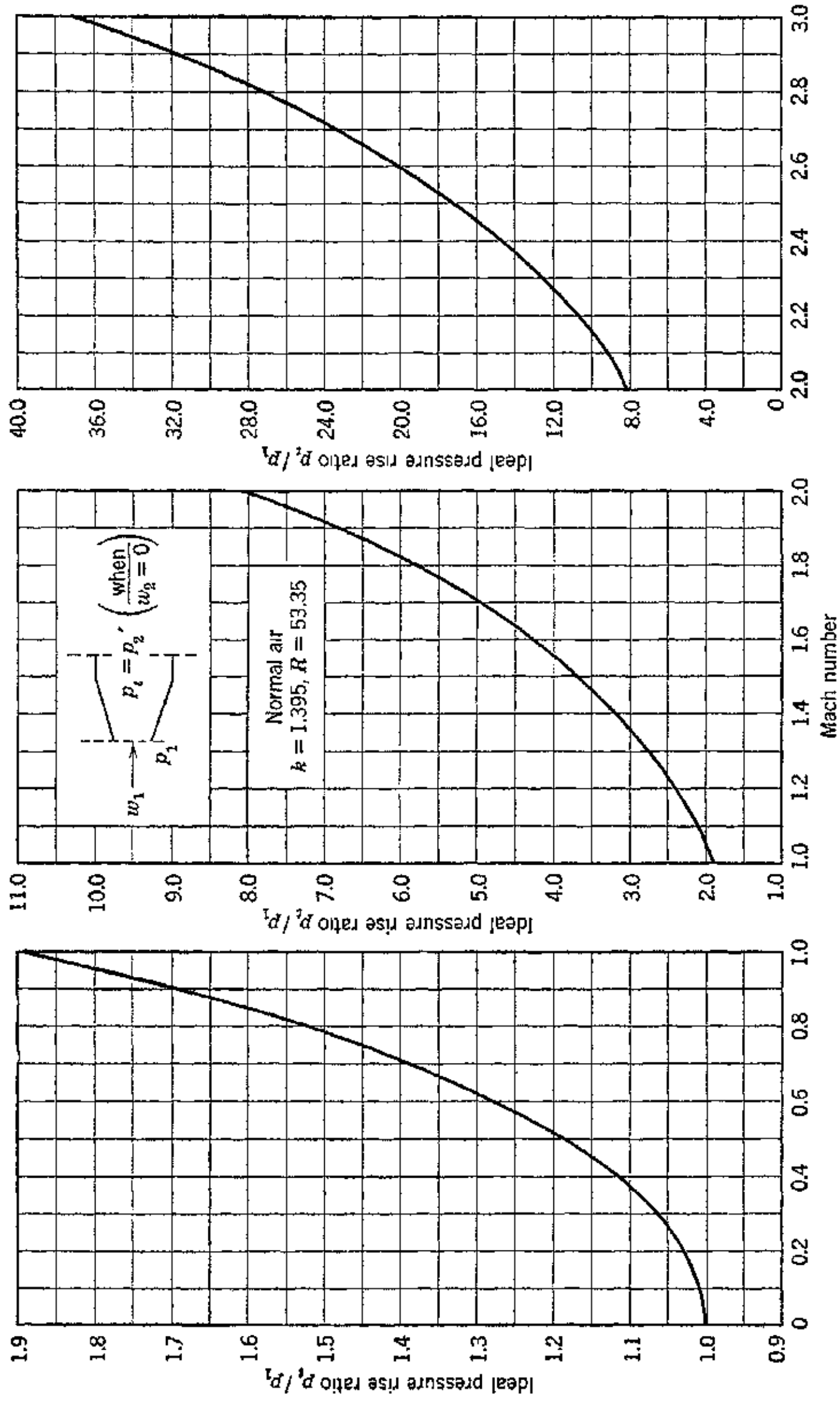
FIG. 5. Ideal pressure rise ratio for normal air.

EXAMPLE. Air at atmosphere pressure and 59 F flows into an ideal diffuser. The entrance velocity is 600 fps. Calculate the ideal final (ram) pressure and the total temperature.

Solution.

$$a_1 = \sqrt{gkRT_1} = \sqrt{32.174 \times 1.395 \times 53.35 \times 519} = 1115 \text{ fps}$$

$$M_1 = \frac{600}{1115} = 0.540$$

From equation 45

$$Z_c = 0.1975 \times (0.54)^2 = 0.0576$$

From Table 4·5

$$\frac{p_t}{p_1} = r_c = 1.219$$

$$p_t = 17.9 \text{ psia} \quad \text{(final pressure)}$$

From equation 41

$$\Phi = \frac{T_t}{T_1} = 1 + \frac{1.395 - 1}{2}(0.540)^2$$

$$= 1 + (0.1975 \times 0.293) = 1.0575$$

$$T_t = 1.0575 \times 519 = 548 \text{ R} \quad \text{(total temperature)}$$

It follows from equation 38 and the foregoing that, for perfect gases in isentropic flow, since c_p is constant,

$$T_1 + \frac{w_1^2}{2gJc_p} = T_{t1}$$

and

$$T_2' + \frac{w_2^2}{2gJc_p} = T_{t2}$$

Hence for perfect gases in isentropic flow the total temperature is a constant.

8. Adiabatic Flow with Friction

Refer to the general form of the energy equation, Section 3, and assume that the external work $dL = 0$. Then

$$dQ = dh + \frac{1}{J}\frac{d(w^2)}{2g} + \frac{1}{J}dE_F + \frac{1}{J}dE_P \qquad (47)$$

The work expended on the gas in overcoming friction is transformed into heat. If the fluid loses no heat to the outside, all the foregoing heat remains with it. This signifies that the entire quantity of heat added to the fluid consists of two parts. The heat supplied from external sources $dQ_{ext.}$ and the heat equivalent of the

work expended in overcoming friction $1/J(dE_F)$. Consequently the heat added dQ is given by

$$dQ = dQ_{ext} + \frac{1}{J} dE_F \qquad (48)$$

Substituting equation 48 into equation 9, noting that $dL = 0$, gives the following equation for the flow of a fluid when no work is done by or taken from the fluid.

$$dQ_{ext.} + \frac{1}{J} dE_F = dh + \frac{1}{J} d\left(\frac{w^2}{2g}\right) + \frac{1}{J} dE_F + \frac{1}{J} dE_P \qquad (49)$$

From equation 49 it follows that the energy equation for 1 lb of fluid when there is friction, no external work, and heat losses is

$$dQ_{ext} = dh + \frac{1}{J} \frac{d(w^2)}{2g} + \frac{1}{J} dE_P \qquad (50)$$

If the change in potential energy is negligible, which is true for gases, and if the flow is adiabatic

$$dh + \frac{1}{J} \frac{d(w^2)}{2g} = 0 \qquad (51)$$

Equation 51, which is the energy equation for the adiabatic flow of a fluid with friction when there is no external work and no change in potential energy, is seen to have the same form as the energy equation for the isentropic flow of a gas; see equation 32. This means that in adiabatic flow, with or without friction, the total energy remains constant.

The difference between the total energy equations for adiabatic flow is not stated explicitly. It does appear, however, in the integration of the energy equation. If the flow is isentropic the enthalpy in the final state, denoted by the subscript 2, is h_2', and when the flow is accompanied by friction the final enthalpy is h_2. The values of h_2' and h_2 for identical values of the expansion ratio p_2/p_1 are different, h_2' being smaller than h_2. Furthermore, the process involving friction is accompanied by an increase in entropy, whereas for isentropic flow $ds = 0$. The two adiabatic processes are compared on the pv and hs planes in Fig. 6.

The energy equation for adiabatic flow with friction integrates to

$$w_2{}^2 - w_1{}^2 = 2gJ(h_1 - h_2) = 2gJ \, \Delta h_t \qquad (52)$$

In the isentropic case w_2 is replaced by w_2' and h_2 by h_2'. The

difference between the enthalpy changes for the two processes is the heat equivalent of the work expended in overcoming friction. Hence

$$h_1 - h_2 = h_1 - h_2' - \frac{1}{J}{}_1(E_F)_2 = H - \frac{1}{J}{}_1(E_F)_2 \qquad (53)$$

For gases

$$h_1 - h_2 = c_p(T_1 - T_2)$$

and

$$h_1 - h_2' = c_p(T_1 - T_2')$$

Assuming c_p constant, or assuming that its average values for the temperature ranges involved are not significantly different, it follows that when adiabatic flow is accompanied by friction $T_2 > T_2'$.
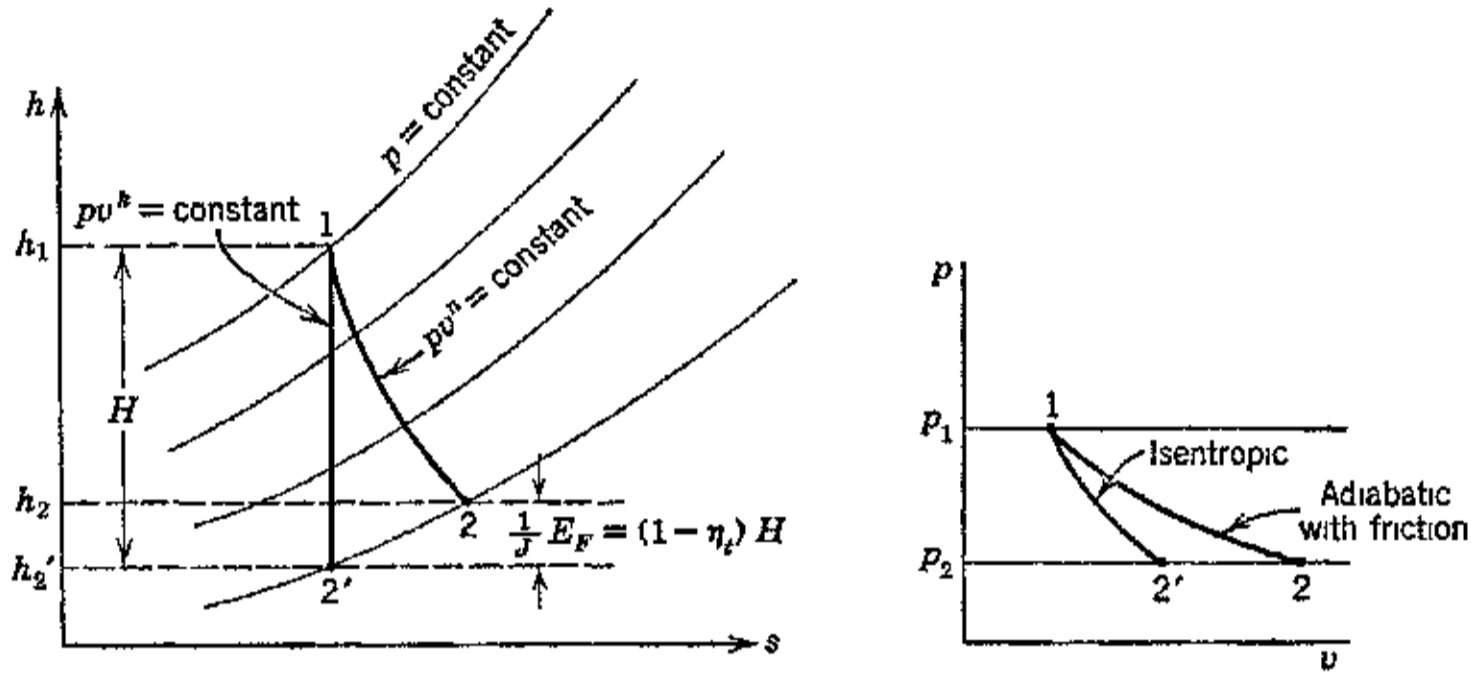
FIG. 6.   Isentropic and polytropic expansions compared on the p-v and h-s planes.

In the case of flow with friction the heat added dQ is given by equation 48. Consequently, the equations of Section 11d, Chapter 1, can be used for calculating entropy changes by using equation 48 above for defining dQ.

9. Efficiency of an Adiabatic Flow Expansion

The ultimate goal of an adiabatic flow expansion is to convert as large a fraction as possible of the available energy H into kinetic energy. This conversion is a maximum when there are no losses and all the kinetic energy associated with the approach velocity w_1 is fully utilized. When the flow is accompanied by friction, shock, and turbulence the enthalpy change $(h_1 - h_2) < H$ and the kinetic energy $w_1^2/2gJ$ may not be utilized completely.

The effectiveness of the passage (nozzle) wherein the flow expansion occurs, in converting the total energy supplied it into kinetic energy,

is termed the nozzle efficiency η_n. The total energy supplied the nozzle is

$$E_T = H + \frac{w_1{}^2}{2gJ} = \frac{(w_2')^2}{2gJ} \qquad (54)$$

The energy converted into kinetic energy is denoted by E_k, where

$$E_k = \Delta h_t + \frac{w_1{}^2}{2gJ} = h_1 - h_2 + \frac{w_1{}^2}{2gJ} = \frac{w_2{}^2}{2gJ} \qquad (55)$$

Consequently the nozzle efficiency is

$$\eta_n = \frac{E_k}{E_T} = \left(\frac{w_2}{w_2'}\right)^2 \qquad (56)$$

In an actual flow process all the approach kinetic energy may not be fully utilized. Instead only the fraction $\varphi_1{}^2 w_1{}^2/2gJ$, where φ_1 is a coefficient less than unity, may be available to the nozzle. In that event the kinetic energy of the final stream is given by

$$\frac{w_2{}^2}{2gJ} = h_1 - h_2 + \varphi_1{}^2 \frac{w_1{}^2}{2gJ} \qquad (57)$$

The actual final velocity can be expressed in terms of the ideal velocity w_2' by introducing the velocity coefficient $\varphi_2 < 1$, where $\varphi_2 = w_2/w_2'$. Hence the general equation for the final velocity of the fluid stream is

$$w_2 = \varphi_2 \sqrt{2gJH + \varphi_1{}^2 w_1{}^2} \qquad (58)$$

As before, $\eta_n = (w_2/w_2')^2$, which will have different values, depending upon the completeness with which the entrance kinetic energy $w_1{}^2/2gJ$ is utilized.

10. Efficiency of Conversion of Enthalpy into Kinetic Energy

Where the approach velocity is zero or negligible, the final velocity of the fluid is due entirely to the transformation of enthalpy into kinetic energy. As before the efficiency of the expansion is $(w_2/w_2')^2$, and, to distinguish this efficiency from the case where the approach velocity is involved, it is denoted by η_t. Hence when $w_1 = 0$

$$\eta_t = \left(\frac{w_2}{w_2'}\right)^2 = \frac{h_1 - h_2}{h_1 - h_2'} = \frac{\Delta h_t}{H} \qquad (59)$$

Introducing the velocity coefficient φ_2, where

$$w_2{}^2 = \varphi_2{}^2 (w_2')^2$$

then

$$\eta_t = \varphi_2{}^2 \quad \text{or} \quad \varphi_2 = \sqrt{\eta_t} \tag{60}$$

If $1/J(E_F)$ is the enthalpy increase due to friction, then

$$\Delta h_t = H - \frac{1}{J} E_F$$

and

$$\eta_t = \frac{H - (1/J)E_F}{H} = 1 - \frac{(1/J)E_F}{H} \tag{61}$$

The expansion process with friction cannot be represented by the equation $pv^k = $ constant, where $k = c_p/c_v$. It can, however, be represented by the polytropic equation $pv^n = $ constant, where $n \neq k$. The relationship between n, k, and η_t will now be derived, assuming that c_p is a constant and small pressure ratios are involved.

11. Efficiency of a Polytropic Expansion

In adiabatic flow with friction $dh \neq 1/J\,(v\,dp)$ but

$$\frac{1}{J} E_F = dh - \frac{1}{J} v\,dp \tag{62}$$

If the change of state is an expansion, as illustrated in Fig. 6, the process is accompanied by a decrease in enthalpy. Hence, the change in available energy for an isentropic expansion is

$$dH = -dh \tag{63}$$

For an adiabatic expansion involving friction it follows from equation 59 that if η_t is constant, which is substantially true for small pressure ratios,

$$dH = -\frac{dh}{\eta_t} = -c_p \frac{dT}{\eta_t} \tag{64}$$

But from equation 62

$$\frac{1}{J} E_F = (1 - \eta_t)\,dH = -\frac{1 - \eta_t}{\eta_t} dh = -\frac{1 - \eta_t}{\eta_t} c_p\,dT \tag{65}$$

Equating equations 62 and 65 and substituting $c_p\,dT = dh$

$$-\frac{1 - \eta_t}{\eta_t} c_p\,dT = c_p\,dT - \frac{1}{J} v\,dp$$

from which it follows that

$$(\eta_t - 1)c_p \, dT = \eta_t c_p \, dT - \eta_t \frac{1}{J} v \, dp$$

or

$$c_p \, dT = \eta_t \frac{1}{J} v \, dp \tag{66}$$

Substituting for $v = \dfrac{RT}{p}$ and $c_p = \dfrac{R}{J}\left(\dfrac{k}{k-1}\right)$ in equation 66

$$R\left(\frac{k}{k-1}\right) dT = \eta_t RT \frac{dp}{p}$$

so that

$$\frac{dT}{T} = \eta_t \left(\frac{k-1}{k}\right)\frac{dp}{p} \tag{67}$$

Integrating equation 67

$$\log_e \frac{T_2}{T_1} = \eta_t \left(\frac{k-1}{k}\right) \log_e \left(\frac{p_2}{p_1}\right) \tag{68}$$

so that

$$\frac{T_2}{T_1} = \left(\frac{p_2}{p_1}\right)^{\eta_t \left(\frac{k-1}{k}\right)}$$

Substituting for T_2/T_1 from the characteristic equation for perfect gases

$$\frac{v_2}{v_1} = \left(\frac{p_1}{p_2}\right)^{1-\eta_t \left(\frac{k-1}{k}\right)} \tag{69}$$

It was pointed out in Section 9 that the change of state equation is $pv^n = $ constant. Hence

$$\frac{v_2}{v_1} = \left(\frac{p_1}{p_2}\right)^{\frac{1}{n}} = \left(\frac{p_1}{p_2}\right)^{1-\eta_t \left(\frac{k-1}{k}\right)} \tag{70}$$

From equation 70 it follows that

$$\frac{1}{n} = \frac{k - \eta_t(k-1)}{k}$$

or

$$n = \frac{k}{k - \eta_t(k-1)} = \frac{k}{\eta_t + k(1 - \eta_t)} \tag{71}$$

Hence

$$\frac{n-1}{n} = \eta_t \left(\frac{k-1}{k}\right)$$

The efficiency of the expansion is given by

$$\eta_t = \frac{(n-1)/n}{(k-1)/k} \tag{72}$$

A similar expression can be derived, by applying the same argument, to an adiabatic compression process with friction. In that case

$$n = \frac{\eta_c k}{1 - k(1 - \eta_c)} \tag{73}$$

and

$$\eta_c = \frac{(k-1)/k}{(n-1)/n} \tag{74}$$

Since the efficiency of an expansion process is denoted by η_t, then for an expansion

$$\frac{p_1}{p_2} = \left(\frac{v_2}{v_1}\right)^{\frac{k}{k - \eta_t(k-1)}} \tag{75}$$

and the corresponding temperature ratio is

$$\frac{T_1}{T_2} = \left(\frac{p_1}{p_2}\right)^{\eta_t\left(\frac{k-1}{k}\right)} \tag{76}$$

For a compression process the efficiency is denoted by η_c; then

$$\frac{p_2}{p_1} = \left(\frac{v_1}{v_2}\right)^{n} = \left(\frac{v_1}{v_2}\right)^{\frac{\eta_c k}{1 - k(1 - \eta_c)}} \tag{77}$$

and

$$\frac{T_1}{T_2} = \left(\frac{p_1}{p_2}\right)^{\frac{n-1}{n}} = \left(\frac{p_1}{p_2}\right)^{\frac{k-1}{\eta_c k}} \tag{78}$$

12. The Continuity Equation for Gases

If the weight rate of flow of a fluid is G lb/sec, then for each cross section of the flow passage

$$G = Aw\gamma = \frac{Aw}{v} = \text{Constant} \tag{79}$$

Equation 79, known as the *continuity equation*, is based on the principle of the conservation of matter. It states that the same

weight of fluid must pass through all cross sections of a flow conduit of any shape. This means that for any two stations in the flow passage

$$G = A_1 w_1 \gamma_1 = A_2 w_2 \gamma_2 = \text{Constant}$$
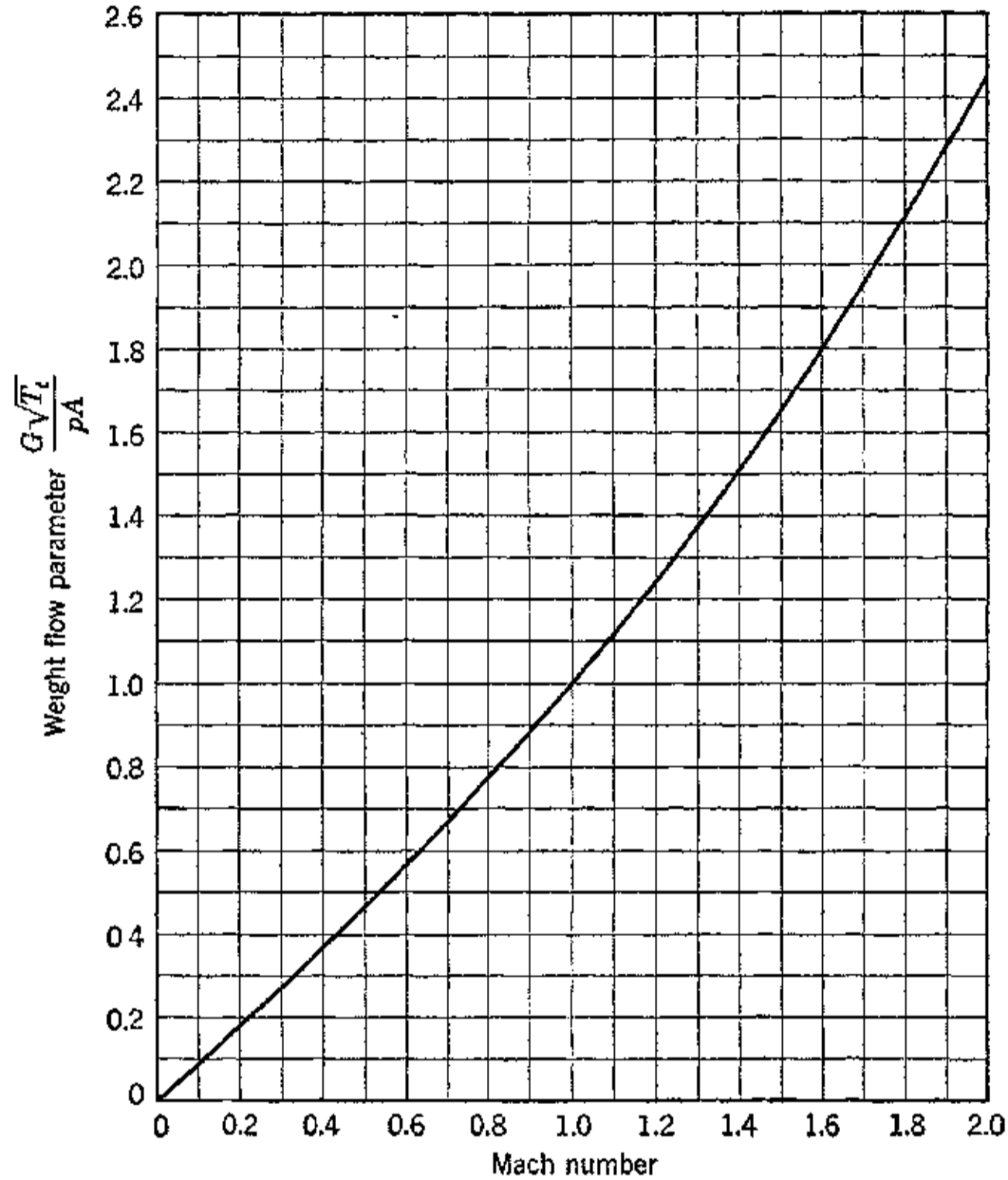
FIG. 7.   Weight flow parameter vs. Mach number for normal air.

For a perfect gas the weight rate of flow can be expressed in terms of the Mach number by applying the characteristic equations for perfect gases. Since $M = w/\sqrt{gkRT}$, equation 79 can be written in the form

$$G = pAM \sqrt{\frac{gk}{RT}} \qquad (80)$$

Substituting for T_t from equation 41 into equation 80

$$G = \frac{pA}{\sqrt{T_t}} M \sqrt{\frac{kg}{R} \left[1 + \frac{k-1}{2} M^2 \right]} \tag{81}$$
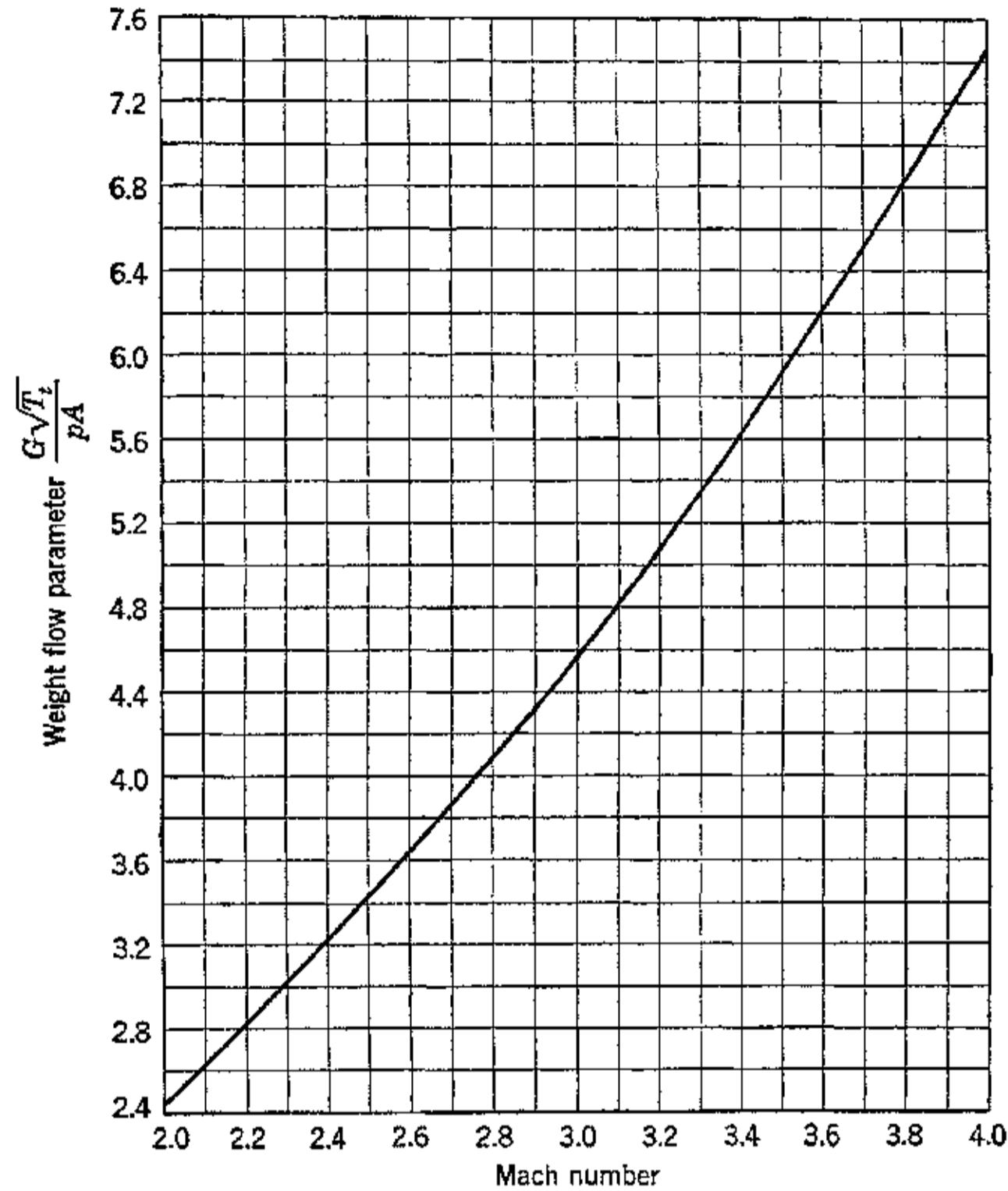
FIG. 8.   Weight flow parameter vs. Mach number for normal air.

For normal air ($k = 1.395$ and $R = 53.35$) equation 81 can be written in the form

$$\frac{G\sqrt{T_t}}{pA} = M\sqrt{0.84[1 + 0.1975M^2]} \quad \text{(for normal air)} \tag{82}$$

Figures 7 and 8 present the parameter $G\sqrt{T_t}/pA$ as a function of Mach number for normal air.

For perfect gases equation 79 can be combined with the characteristic equation 1·29 which gives the following expression for perfect gases.

$$G = w \frac{Ap}{RT} = \text{Constant} \tag{83}$$
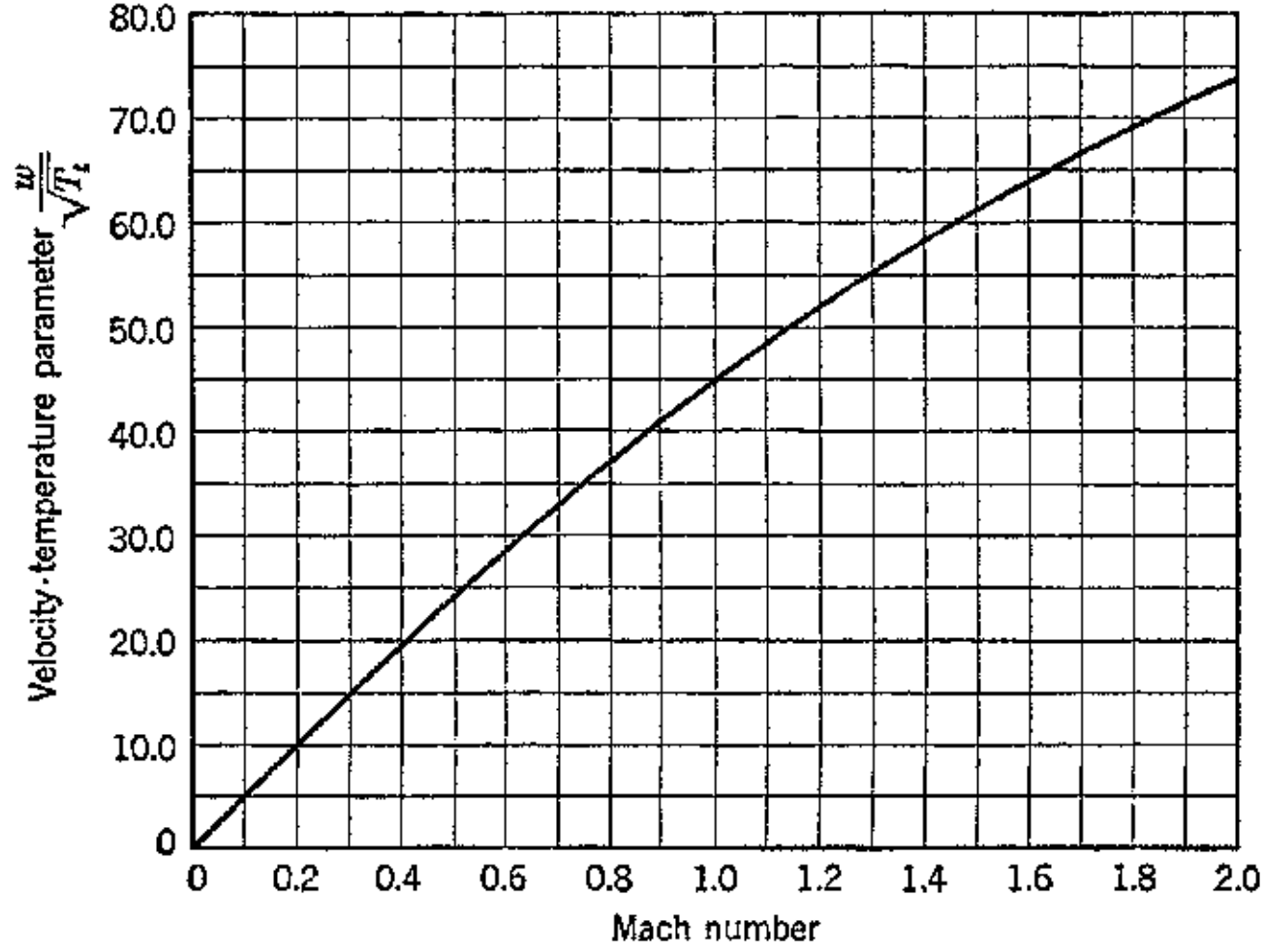
FIG. 9.   Velocity-temperature parameter vs. Mach number for normal air.

Substituting for G from equation 83 into equation 81, and solving for w gives

$$w = \frac{T}{T_t} \sqrt{kgRT_t} \left[1 + \frac{k-1}{2} M^2 \right]^{\frac{1}{2}} M$$

Substituting for T/T_t from equation 41 gives the following results

$$\frac{w}{\sqrt{gkRT_t}} = \frac{M}{\sqrt{1 + \frac{k-1}{2} M^2}} \tag{84}$$

For normal air equation 84 becomes

$$\frac{w}{\sqrt{T_t}} = \frac{49M}{\sqrt{1 + 0.1975M^2}} \tag{85}$$

Figures 9 and 10 present values of $w/\sqrt{T_t}$ as a function of M; the values of T_t are defined by equation 44.
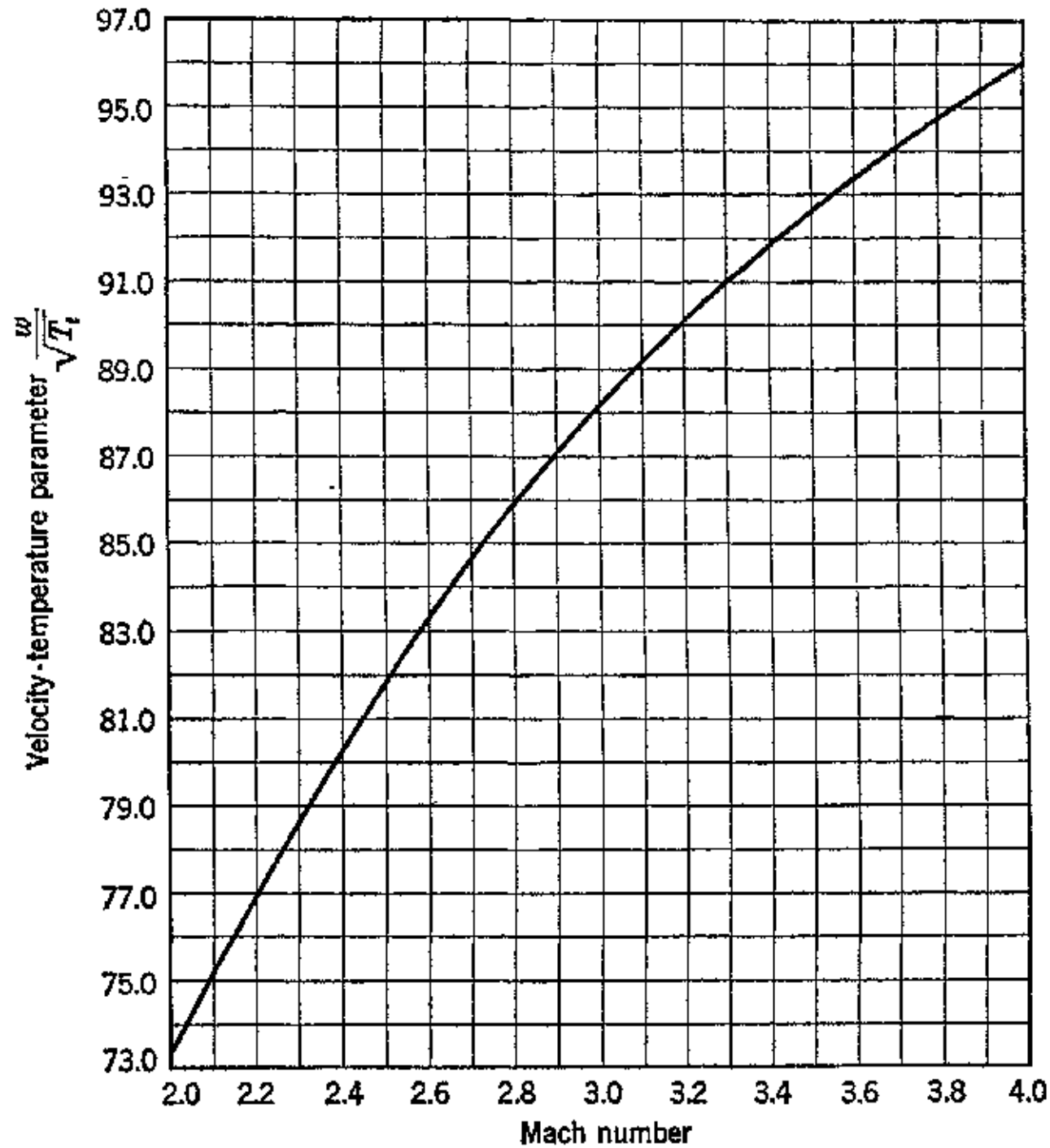
FIG. 10.   Velocity-temperature parameter vs. Mach number for normal air.

EXAMPLE. Air flows through a duct with a velocity of 600 fps. The weight flow is 20 lb/sec. If the area of the duct is 80 sq in. and the Mach number is 0.5, calculate the static pressure.

Solution.

$$\frac{w_1}{\sqrt{T_t}} = \frac{49\,M}{\sqrt{1 + 0.1975\,M^2}}$$

$$\frac{600}{\sqrt{T_t}} = \frac{49 \times 0.5}{\sqrt{1 + 0.1975 \times 0.25}} = \frac{24.5}{\sqrt{1.049}} = 24.0$$

$$T_t = 628 \text{ R}$$

$$\frac{G\sqrt{T_t}}{p_1 A} = M\sqrt{0.845[1 + 0.1975\,M^2]}$$

$$\frac{20 \times 25}{p_1 \times 80} = 0.5\sqrt{0.845 \times 1.0494}$$

$$p_1 = 13.3 \text{ psia}$$

EXAMPLE   Air approaches an ideal diffuser with a Mach number of 0 6   It is desired to attain a stagnation temperature of 600 R.   What must be the initial velocity?

Solution $M = 0 6$ so that $w_1/\sqrt{T_i} = 28 4$ Hence

$$w_1 = 28 4\sqrt{600} = 695 \text{ fps}$$

Refer to equation 83, and differentiate logarithmically, noting that $G = $ constant   The result gives a relationship between relative changes in the variables   Thus

$$\frac{dA}{A} + \frac{dw}{w} + \frac{dp}{p} - \frac{dT}{T} = 0 \tag{86}$$

For a constant weight rate of flow G, the change in velocity is obtained by solving equation 79 for w and differentiating.   Thus

$$dw = G\left[\left(\frac{dv}{A}\right) - v\left(\frac{dA}{A^2}\right)\right] \tag{87}$$

The last equation indicates the dependence of the fluid velocity on the specific volume and cross-sectional area changes.   An expression relating the rate of change of area with velocity (dA/dw) is obtained by differentiating the first form of equation 79 and dividing the result by dw Thus, substituting $\rho = \gamma/g$

$$\frac{1}{A}\frac{dA}{dw} + \frac{1}{w} + \frac{1}{\rho}\frac{dp}{dw} = 0 \tag{88}$$

But, from equation 23b, $dp/dw = -\rho w/a^2$.   Substituting this last expression into equation 88 and solving for dA/dw gives

$$\frac{dA}{dw} = -\frac{A}{w}\left(1 - \frac{w^2}{a^2}\right) = -\frac{A}{w}(1 - M^2) \tag{89}$$

From which it follows that

$$\frac{dw}{w} = -\frac{dA}{A}\left(\frac{1}{1 - M^2}\right) \tag{89a}$$

But from equations 1·78 and 3·33a

$$\frac{dw}{w} = \frac{dM}{M} + \frac{1}{2}\frac{dT}{T} = \frac{dM}{M} - \left(\frac{k-1}{2}\right)M^2\frac{dw}{w}$$

Hence the velocity and Mach number changes are related by the equation

$$\frac{dw}{w} = \frac{dM}{M\left[\dfrac{k-1}{2}M^2 + 1\right]} \tag{90}$$

The relative change in flow area dA/A for the isentropic flow of a perfect gas can be related to the Mach number in the following manner.[34] Thus, from equation 89a

$$\frac{dA}{A} = -\frac{dw}{w}(1 - M^2) \tag{91}$$

Substituting for dw/w from equation 90 yields

$$\frac{dA}{A} = -\frac{(1 - M^2)}{\left[\dfrac{k-1}{2}M^2 + 1\right]}\frac{dM}{M} \tag{92}$$

Integrating the last expression

$$\log_e A = \log_e\left\{\frac{\left[1 + \dfrac{k-1}{2}M^2\right]^{\frac{k+1}{2(k-1)}}}{M}\right\} + C_1 \tag{93}$$

where C_1 is a constant of integration. Equation 93 can be written in the form

$$A = \frac{C_1}{M}\left\{1 + \frac{k-1}{2}M^2\right\}^{\frac{k+1}{2(k-1)}} \tag{94}$$

The integration constant C_1 is evaluated by letting $A = A_0$ when $M = M_0$; then

$$C_1 = \frac{A_0 M_0}{\left\{1 + \dfrac{k-1}{2}M_0{}^2\right\}^{\frac{k+1}{2(k-1)}}} \tag{95}$$

Substituting for C_1 in equation 94 gives the following expression for the area ratio

$$\frac{A}{A_0} = \frac{M_0}{M}\left[\frac{1 + \dfrac{k-1}{2}M^2}{1 + \dfrac{k-1}{2}M_0{}^2}\right]^{\frac{k+1}{2(k-1)}} \tag{96}$$

As shown in reference 34 it is of advantage to let A_0 be unity when $M_0 = 1$, when plotting the relationship between A/A_0 and M. Figures 11 and 12 present A/A_0 as a function of Mach number on the aforementioned basis, for normal air.
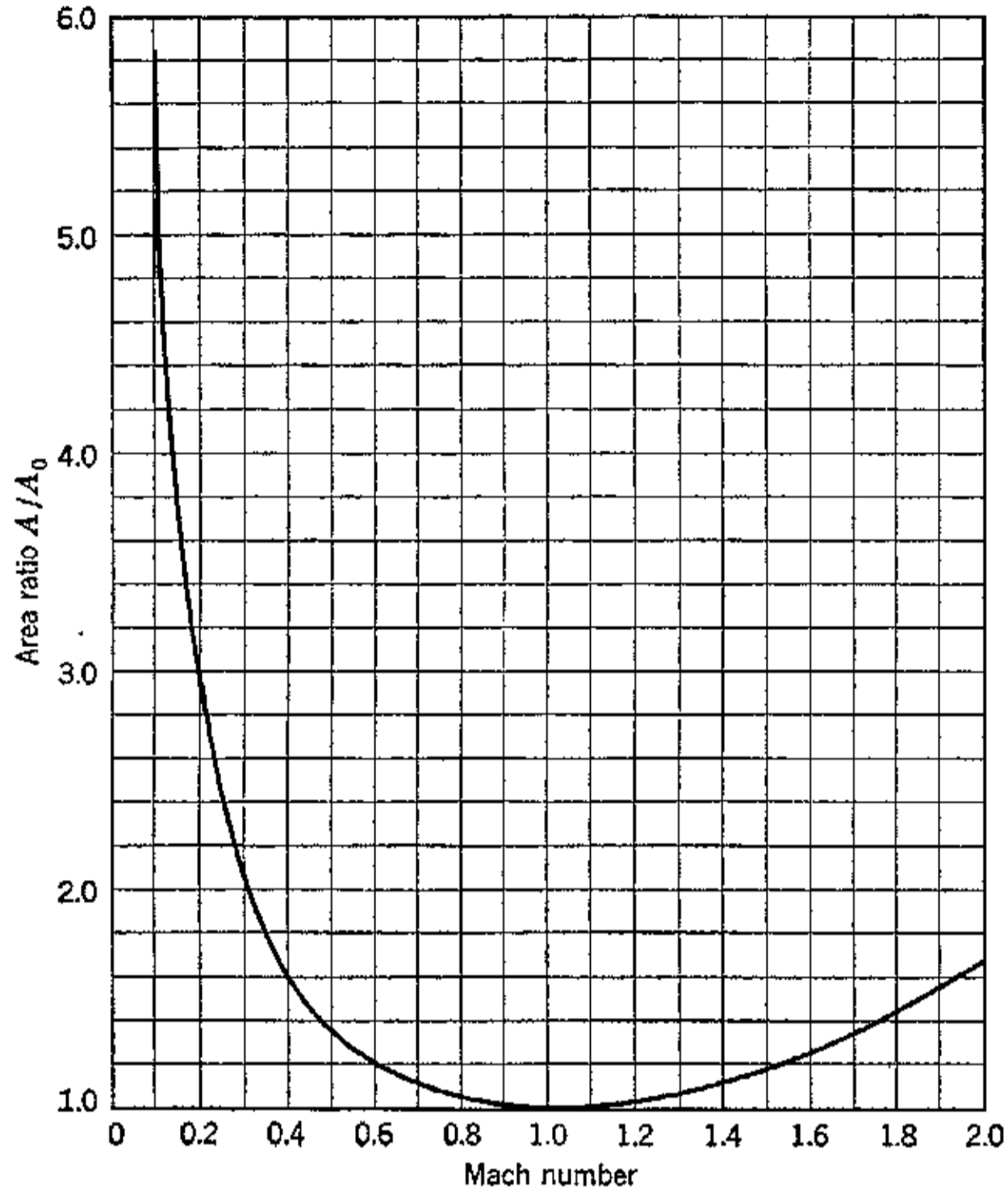
Fig. 11.   Area ratio vs. Mach number for normal air.

For normal air equation 96 becomes

$$\frac{A}{A_0} = \frac{M_0}{M} \left\{ \frac{1 + 0.1975M^2}{1 + 0.1975M_0{}^2} \right\}^{3.032} \tag{97}$$

If $M_0 = 1$ when $A_0 = 1$, then

$$A = \frac{1}{M} \left\{ \frac{1 + 0.1975M^2}{1.1975} \right\}^{3.032} \tag{98}$$
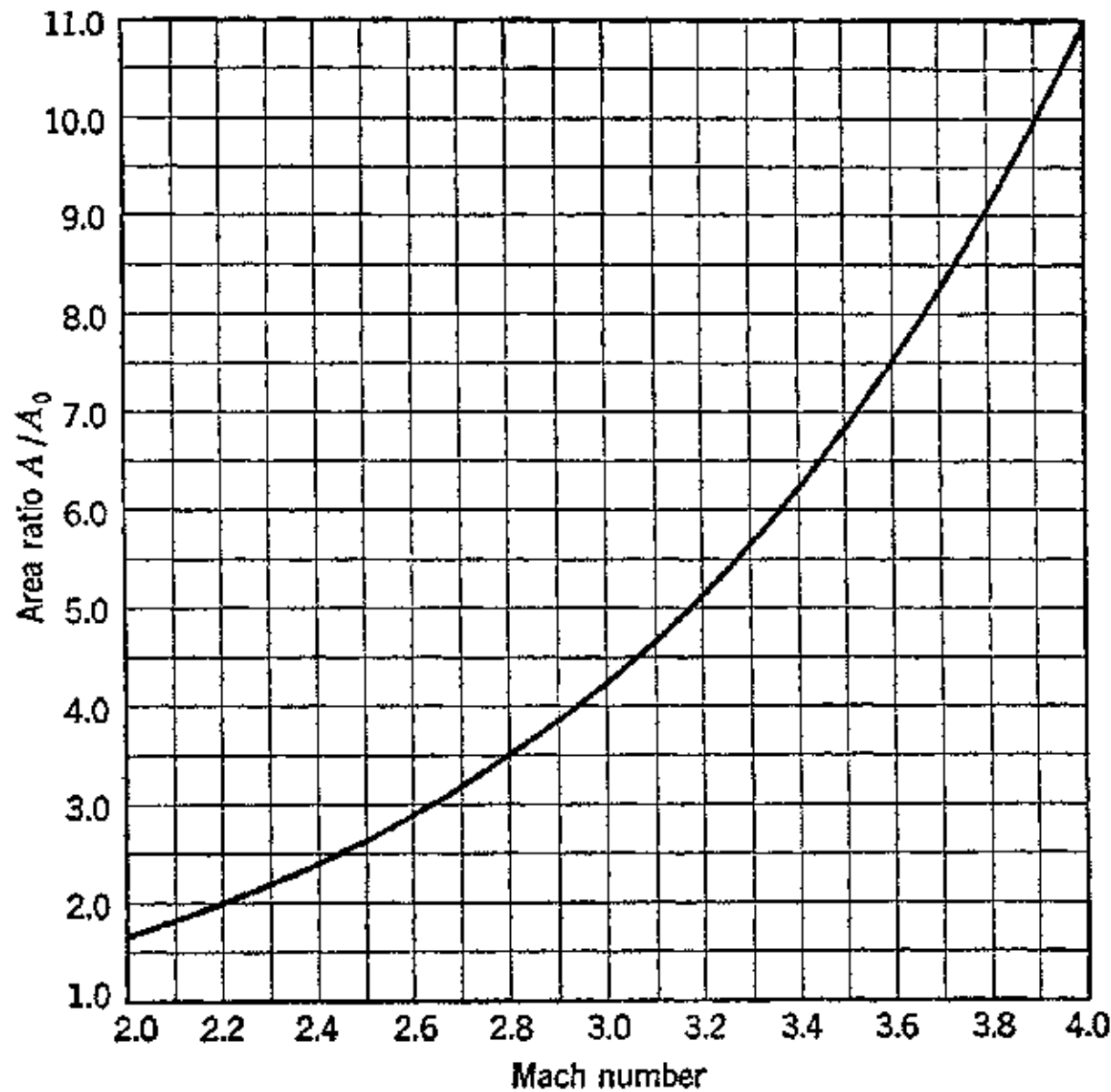
FIG. 12. Area ratio vs. Mach number for normal air.

EXAMPLE. An ideal air diffuser is to reduce the Mach number of the entering air from $M_1 = 0.8$ to $M_2 = 0.2$. Determine its area ratio.
Solution.
From Fig. 11

$$\text{For } M = 0.8 \quad \frac{A}{A_0} = 1.04$$

$$\text{For } M = 0.2 \quad \frac{A}{A_0} = 2.98$$

Hence

$$\text{Area ratio} = \frac{2.98}{1.04} = 2.86$$

13. Discharge Velocity for a Perfect Gas Flowing through a Converging Nozzle

Refer to Fig. 13. Assume that a perfect gas flows out of a large container through a converging nozzle. Let p_1, T_1, and v_1 in the container remain constant with time. Similarly p_2, T_2, and v_2 at the exit section of the convergent nozzle are constants. Since p_1 is greater than p_2 the flow process is an expansion. Further, let it be

assumed that no external work is removed from or done upon the gas and that there is no friction and no heat transfer. The flow process is, therefore, isentropic; and the change in the kinetic energy of the gas in flowing from station 1 to station 2 is given by equation 34, and the isentropic discharge velocity is given by equation 37.
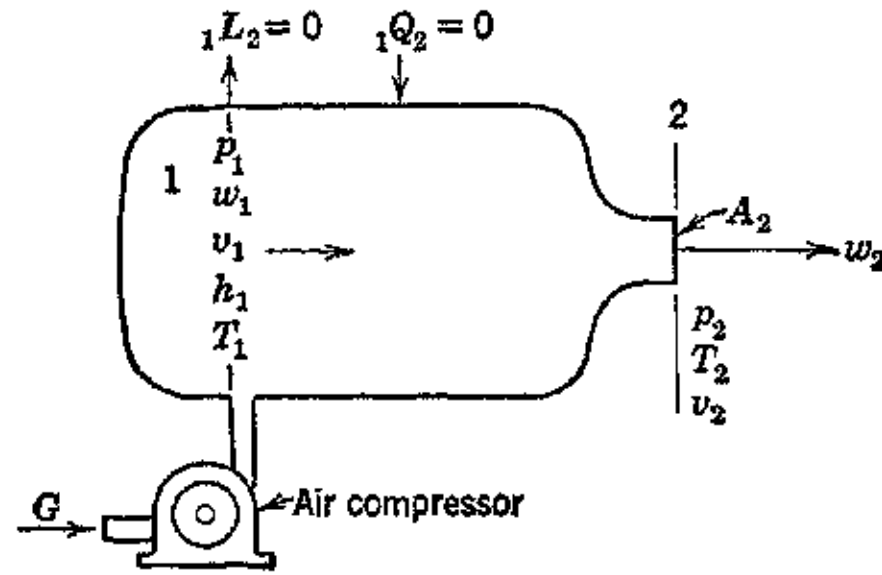
FIG. 13. Flow of gas through a converging nozzle under steady-state condition with no heat added or mechanical work removed.

Substituting for $\Delta h_t' = H$, from equation 1·68 and $RT_1 = p_1 v_1$, the result is

$$w_2' = \sqrt{2g \frac{k}{k-1} RT_1 \left[1 - \left(\frac{p_2}{p_1} \right)^{\frac{k-1}{k}} \right] + w_1{}^2} \qquad (99)$$

or in terms of Z_t (see Chapter 1, Section 11f)

$$w_2' = \sqrt{2gJc_p T_1 \left(\frac{Z_t}{1+Z_t} \right) + w_1{}^2} \quad \text{fps} \qquad (100)$$

If the approach velocity w_1 can be neglected, then, dropping the subscript, the isentropic exhaust velocity

$$w' = \sqrt{2gJc_p T_1 \left(\frac{Z_t}{1+Z_t} \right)} \qquad (101)$$

or

$$w' = 223.7 \sqrt{\frac{k}{k-1} \frac{RT_1}{J} \left(\frac{Z_t}{1+Z_t} \right)} \quad \text{fps} \qquad (102)$$

Equations 101 and 102 demonstrate that the magnitude of the isentropic velocity for a gas is a function of its gas constant, initial temperature, specific heat ratio, and the expansion ratio p_2/p_1. It is evident from the preceding equations that w_2' attains its maximum

value for a given gas and initial temperature when the expression $Z_t/(1 + Z_t)$ reduces to unity, i.e., when $p_2 = 0$. This signifies that the gas attains its maximum isentropic discharge velocity when it
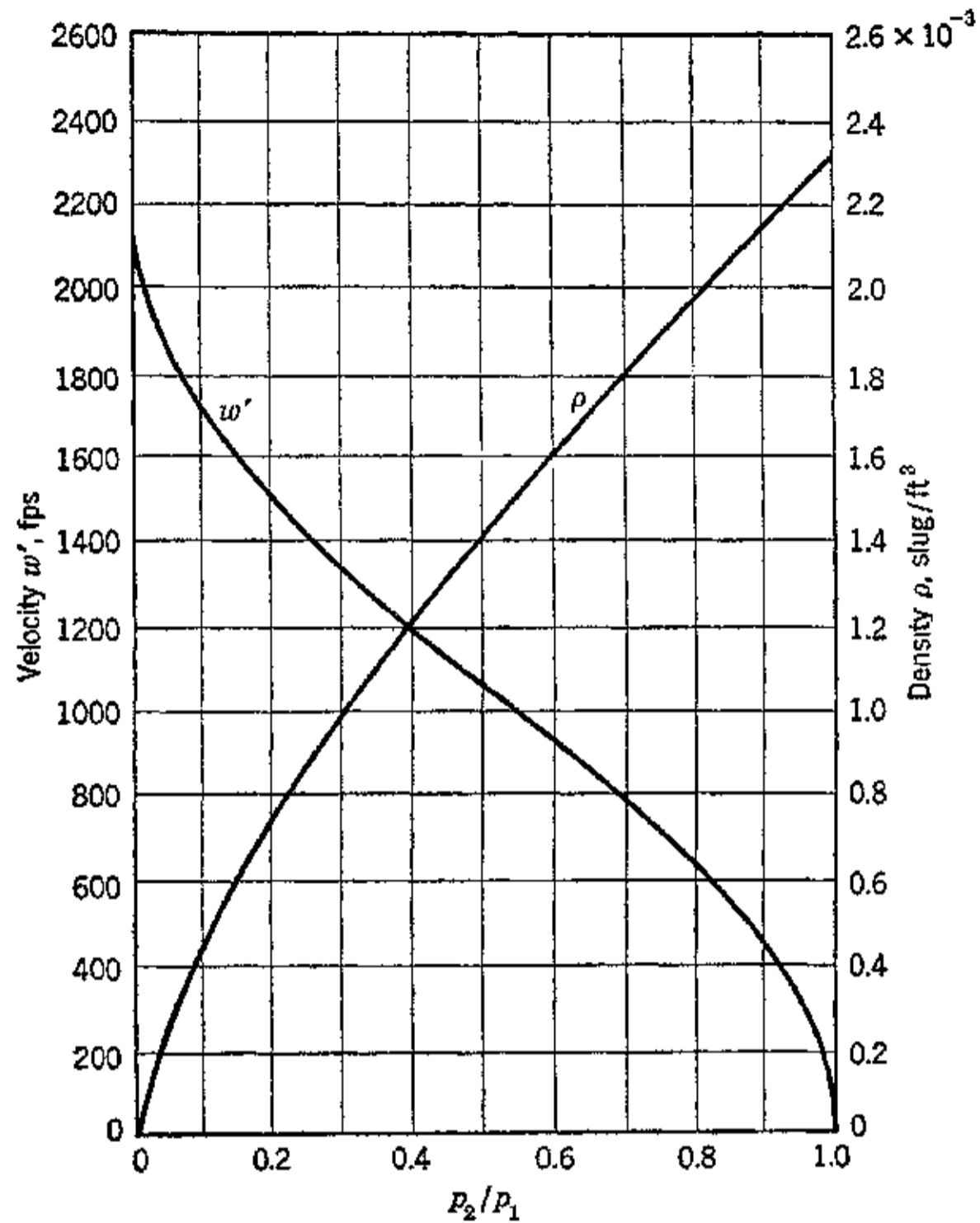
FIG. 14.   Velocity and density of a gas as a function of expansion ratio.   (Reproduced from O. G. Tietjens, A.S.M.E. semi-annual meeting, June 9–11, 1930.)

expands into a vacuum. The maximum isentropic discharge velocity, which is denoted by $w_{max.}'$, is given by

$$w_{max.}' = \sqrt{\frac{2gkRT_1}{k - 1}} \tag{103}$$

Figure 14, taken from reference 16, illustrates the relationship between w' and p_2/p_1 for a gas having the thermodynamic constants $T_1 = 523$ R and $k = 1.405$.

If the flow through the nozzle is accompanied by friction, the

actual exhaust velocity w will be reduced by the energy losses. The actual velocity is related to the isentropic discharge velocity by the velocity coefficient φ, where

$$w = \varphi w' \tag{104}$$

Since the energy losses can be expressed in terms of the kinetic energy of the gas, they are proportional to $(\text{velocity})^2$. The efficiency of the enthalpy conversion into kinetic energy is given by equation 60.

The actual expansion process can be represented by the polytropic equation $pv^n = \text{constant}$. The actual discharge velocity is obtained by replacing $(p_2/p_1)^{\frac{k-1}{k}}$ in equation 99 by $(p_2/p_1)^{\frac{n-1}{n}}$ and noting that $gkRT_1 = a^2$. Thus for small pressure ratios

$$w_2 = \sqrt{\frac{2gk}{k-1} p_1 v_1 \left\{ \left[1 - \left(\frac{p_2}{p_1} \right)^{n\left(\frac{k-1}{k}\right)} \right] + \frac{k-1}{2} M_1^2 \right\}}$$

or

$$w_2 = \sqrt{\frac{2}{k-1} a_1^2 \left\{ \left[1 - \left(\frac{p_2}{p_1} \right)^{\frac{n-1}{n}} \right] + \frac{k-1}{2} M_1^2 \right\}} \tag{105}$$

where n is defined by equation 71.

The last equation expresses the discharge velocity in terms of the inlet acoustic velocity a_1, the inlet Mach number M_1, the expansion ratio p_2/p_1, and k.

The foregoing analysis assumes that the approach kinetic energy is fully utilized. If this is not the case then M_1 is replaced by $\varphi_1^2 M_1^2$.

Values of the parameter $Z_n = (p_2/p_1)^{\frac{n-1}{n}} - 1$ for several values of n are presented in Table 3·1.

The efficiency of the flow expansion process is called the nozzle efficiency η_n and, in general, is defined by the equation

$$\eta_n = \left(\frac{w_2}{w_2'} \right)^2 \tag{105a}$$

The velocity w_2' is given by equation 99, and w_2, the actual discharge velocity, is given by equation 105. When the approach velocity $w_1 \approx 0$, then $\eta_n = \eta_t$, where η_t is defined by equation 72. For the flow expansions occurring in stationary nozzles, such as those for impulse turbines (see Chapter 10), the assumption that $w_1 = 0$ is usually justified, and no serious error is introduced by assuming that $\eta_n = \eta_t = \varphi^2$, where φ is the velocity coefficient defined by equation 104.

TABLE 3·1

Values of $Z_n = \left(\dfrac{p_1}{p_2}\right)^{\frac{n-1}{n}} - 1$

$(p_1 > p_2)$

Values of n

p_1/p_2	1.2	1.25	1.30	1.35	1.40
1.1	0.016	0.019	0.022	0.026	0.028
1.2	.031	.037	.043	.048	.053
1.3	.045	.054	.062	.070	.078
1.4	.058	.070	.081	.091	.101
1.5	.070	.085	.098	.110	.123
1.6	.081	.099	.115	.130	.144
1.7	.092	.112	.130	.147	.164
1.8	.103	.125	.145	.164	.183
1.9	.113	.137	.160	.181	.201
2.0	.123	.149	.174	.197	.219
2.5	.165	.201	.235	.268	.299
3.0	.201	.246	.289	.329	.369
3.5	.232	.284	.336	.383	.431
4.0	.260	.320	.378	.432	.487
4.5	.285	.351	.415	.476	.526
5.0	.307	.380	.449	.517	.584
5.5	.328	.406	.482	.555	.627
6.0	.348	.431	.512	.590	.668
6.5	.366	.454	.540	.624	.707
7.0	.383	.476	.566	.655	.743
7.5	.399	.496	.591	.685	.778
8.0	.414	.516	.616	.714	.811
9.0	.442	.552	.660	.766	.873
10.0	.468	.585	.701	.816	.931
11.0	.491	.616	.739	.862	.984
12.0	.513	.644	.774	.902	1.034
13.0	.533	.670	.807	.942	1.081
14.0	.549	.696	.839	.982	1.126
15.0	.570	.719	.868	1.017	1.168
16.0	.587	.741	.896	1.052	1.208
17.0	.604	.762	.923	1.083	1.247
18.0	.619	.783	.948	1.114	1.284
19.0	.633	.802	.973	1.143	1.319
20.0	.648	.822	.996	1.173	1.354
22.0	.674	.855	1.041	1.227	1.418
23.0	.686	.872	1.063	1.252	1.453
24.0	.698	.887	1.082	1.277	1.479
25.0	.710	.903	1.103	1.302	1.505
26.0	.721	.918	1.121	1.324	1.537
28.0	.743	.947	1.158	1.370	1.591
30.0	.763	.974	1.192	1.413	1.643
32.0	.782	1.000	1.225	1.454	1.692
34.0	.800	1.024	1.256	1.492	1.739
36.0	.817	1.048	1.287	1.515	1.784
38.0	.834	1.071	1.315	1.532	1.827
40.0	.850	1.092	1.343	1.603	1.869
42.0	.863	1.112	1.372	1.632	1.915
44.0	.879	1.133	1.396	1.665	1.953
46.0	.893	1.152	1.423	1.695	1.992
48.0	.906	1.168	1.447	1.728	2.028
50.0	.918	1.187	1.468	1.755	2.065

Table 4·5 may be used for estimates of the enthalpy changes due to compression and expansion of air. For compressions the results will be sufficiently accurate for most purposes, if the initial temperature T_1 is below 600 R. For expansions the error increases as the initial temperature is raised. The error is due to the assumption that k is a constant at all air temperatures, which is not strictly true. For a more detailed discussion of the effect of temperature on the thermodynamic properties of air, see Chapter 4.

EXAMPLE. Air at 25 psia discharges through a converging nozzle. The initial air temperature is 600 R, and the back pressure is 14.7 psia. What is the exhaust velocity, if the efficiency of the expansion is 0.89? Assume $c_p = 0.24$ Btu/lb F.

Solution.

$$r_t = \frac{25.0}{14.7} = 1.70$$

From Table 4·5

$$Z_t = 0.16203 \quad \text{and} \quad \frac{Z_t}{1 + Z_t} = 0.140$$

$$H = c_p T_1 \frac{Z_t}{1 + Z_t} = 0.24 \times 600 \times 0.140 = 20.15 \quad \text{Btu/lb}$$

$$h_1 - h_2 = \eta_t H = 0.89 \times 20.15 = 17.95 \quad \text{Btu/lb}$$

$$w = 223.7\sqrt{17.95} = 945 \quad \text{fps}$$

Check.

$$\varphi = \sqrt{\eta_t} = 0.943$$

$$w = 0.943 \times 223.7\sqrt{20.15} = 945 \quad \text{fps}$$

14. Weight Flow Equation for Nozzle Flow

The weight rate of gas flow through the nozzle, assuming $w_1 = 0$, is obtained by substituting from equations 104 and 101 into the continuity equation 79 and substituting $(k/k - 1)RT_1 = Jc_p T_1$. Thus, if C_c is the contraction coefficient, then

$$G = C_c \varphi A_2 w_2' \gamma_2 = C_c \varphi A_2 \gamma_2 \sqrt{2g \frac{k}{k - 1}\left(\frac{Z_t}{1 + Z_t}\right)RT_1} \quad \text{lb/sec} \quad (106)$$

From $pv^k = $ constant

$$\gamma_2{}^2 = \left(\frac{1}{v_2}\right)^2 = \left(\frac{1}{v_1}\right)^2\left(\frac{p_2}{p_1}\right)^{\frac{2}{k}} \quad (107)$$

Substituting for γ_2 into equation 106 and expressing Z_t in terms of the pressure ratio, see equation 1·70a, the weight flow equation becomes

$$G = C_c \varphi A_2 \sqrt{\frac{2gk}{k - 1}\frac{p_1{}^2}{RT_1}\left[\left(\frac{p_2}{p_1}\right)^{\frac{2}{k}} - \left(\frac{p_2}{p_1}\right)^{\frac{k+1}{k}}\right]} \quad (108)$$

Let

$$C_D = C_c \varphi = \text{discharge coefficient} \qquad (109)$$

$$G = C_D A_2 \sqrt{2g\frac{p_1}{v_1}} \sqrt{\frac{k}{k-1}} \left(\frac{p_2}{p_1}\right)^{\frac{1}{k}} \sqrt{\frac{Z_t}{1+Z_t}} \qquad (110)$$

Let

$$\psi = \sqrt{\frac{k}{k-1}} \sqrt{\frac{Z_t}{1+Z_t}} \left(\frac{p_2}{p_1}\right)^{\frac{1}{k}} \qquad (111)$$

Figure 15 presents curves of ψ vs. p_2/p_1 for different values of k.
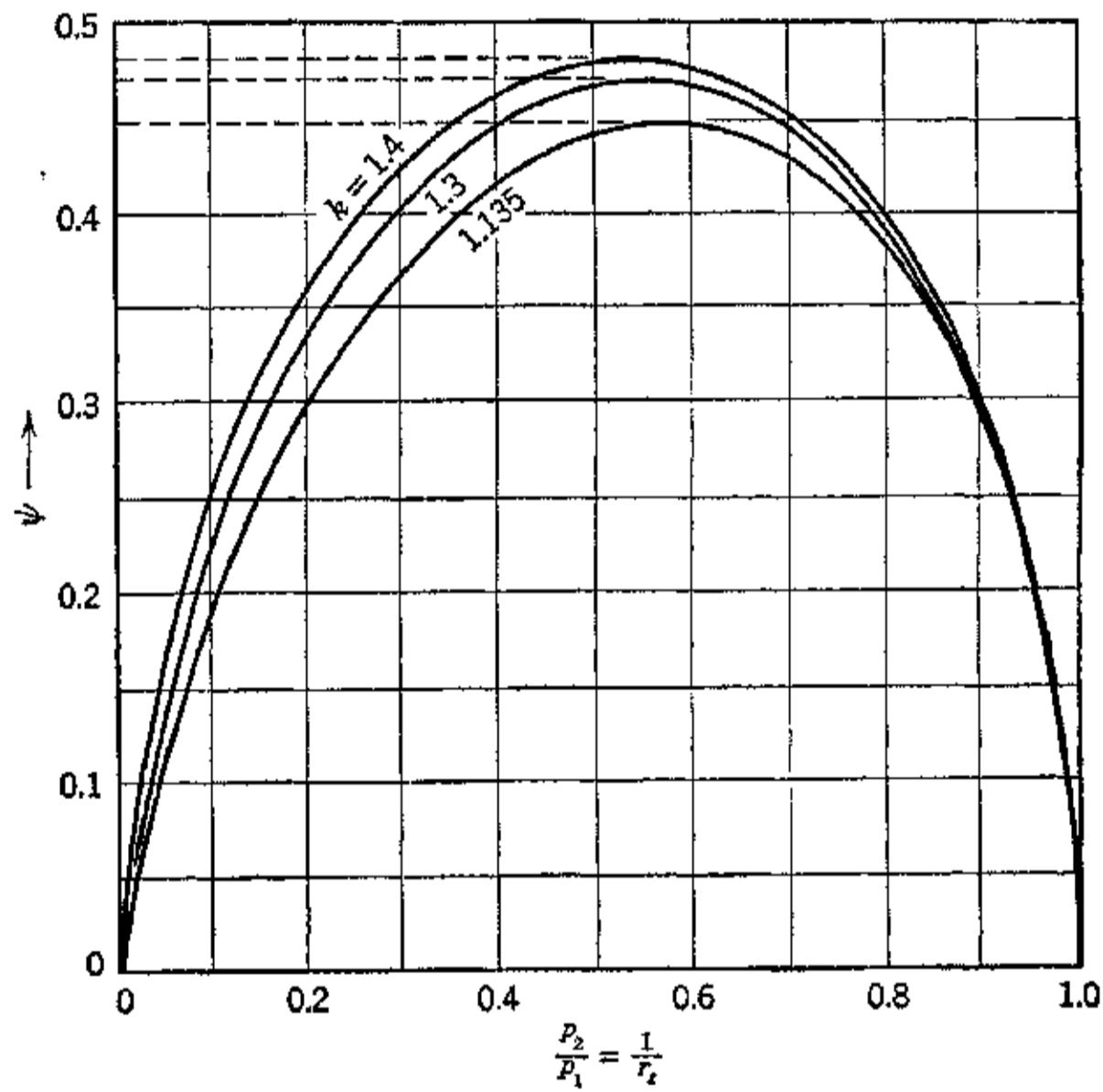
FIG. 15.   Parameter ψ vs. expansion ratio.

The weight rate of flow expressed in terms of ψ is given by

$$G = C_D A_2 \psi \sqrt{2g\frac{p_1}{v_1}} = C_D A_2 \psi \sqrt{2g p_1 \gamma_1} = C_D A_2 \psi \sqrt{\frac{2g}{RT_1}} p_1 \qquad (112)$$

or

$$\frac{G}{A_2} = 8.025 C_D \psi \sqrt{\frac{p_1}{v_1}} \qquad (113)$$

Equation 110 shows that the weight rate of flow for a fixed expansion ratio (ψ = constant) depends only upon the initial temperature of the gas. Under these conditions the weight rate of flow is proportional to $1/\sqrt{T_1}$, which signifies that raising the initial temperature decreases the weight flow.

For well-rounded nozzles the contraction coefficient $C_c \approx 1$

In the discussion following this section it will be assumed that the discharge coefficient $C_D = 1$, and the prime denoting isentropic conditions will be omitted.

15. Effect of Compressibility on the Continuity Relationships

The effect of the compressibility of the gas upon the weight rate of flow can be determined by studying the manner in which the pressure changes affect the specific weight of the gas.[2] Rewriting the continuity equation,

$$f\gamma w = \frac{A}{G} \gamma w = 1 \tag{114}$$

where f is the area through which passes a flow of 1 lb/sec

The area f can be expressed as a function of γ and w, thus

$$\frac{1}{f} = \gamma w \quad \text{lb/ft}^2 \text{ sec} \tag{115}$$

Assume now that the gas is at rest, denoting the rest condition by the subscript 0; then $w = w_0 = 0$, and the corresponding static pressure and specific weight are p_0 and γ_0. Since $w_0 = 0$, it follows that

$$\gamma w = \gamma_0 w_0 = 0 \tag{a}$$

Now assume that the gas is permitted to expand completely into a perfect vacuum so that the final pressure is $p_2 = 0$. Under these conditions the specific volume of the gas becomes infinite and its corresponding specific weight zero; hence $\gamma = 0$. Furthermore, the gas attains the maximum possible velocity corresponding to the expansion ratio, or the value of $w = w_{max}$. For this condition the product γw is again zero, since

$$\gamma w = \gamma w_{max} = 0 \quad \text{(since } \gamma = 0\text{)} \tag{b}$$

Equations (a) and (b) show that there are two limiting conditions where the weight rate of flow is zero. One corresponds to zero pressure drop to cause flow ($w_2 = 0$ and $p_1 = p_2$); the other, to an infinite expansion of the gas where the velocity attains its maximum value but the specific weight is zero ($\gamma_2 = 0$ and $p_2 = 0$). It follows, there-

fore, that there are two limiting values for the back pressure: $p_2 = p_1$ and $p_2 = 0$. Between these limits the curve of weight flow as a function of expansion ratio (or the back pressure p_2) must have at least one maximum point. Investigations have shown [5] that there is only one maximum point between the limits $p_2 = p_1$ and $p_2 = 0$.

The manner in which the discharge velocity and density, $\rho = \gamma/g$, of a gas vary with the expansion ratio is illustrated in Fig. 14.

If the weight flow G for a given nozzle is plotted as a function of the expansion ratio $1/r_t$, as is done in Fig. 16, it is seen that the
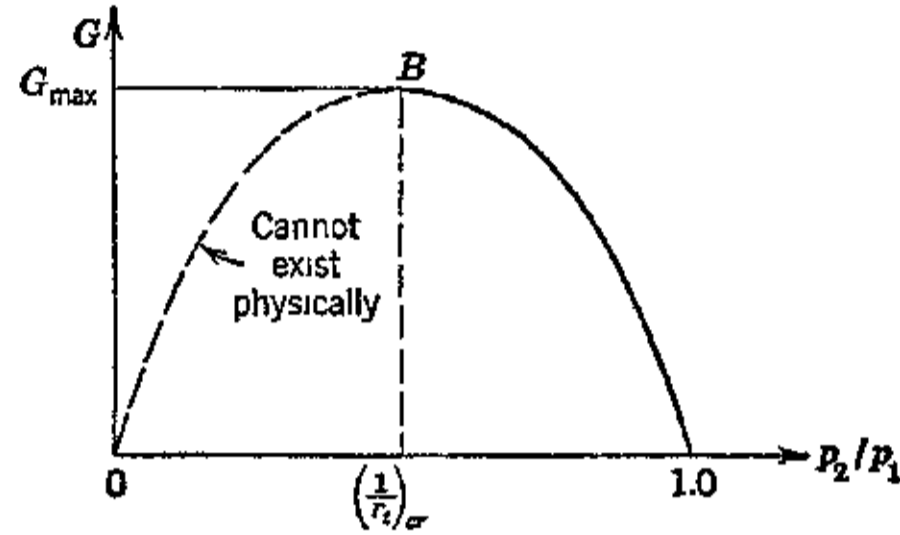
FIG. 16.   Weight flow through a nozzle vs expansion ratio

maximum flow G_{max} will be reached at a particular value of the expansion ratio. This particular value of $1/r_t$ which is denoted by $(1/r_t)_{cr}$, is called the *critical expansion ratio*.

Hence, there is one value of the expansion ratio between $1/r_t = 1$ and $1/r_t = 0$ where the weight flow G attains its maximum value Further decrease in the back pressure does not change the flow; it merely remains fixed at the value G_{max}.

It is evident from equation 112 that the expansion ratio at which the maximum weight flow will occur corresponds to that which makes the parameter ψ a maximum, that is, when

$$\left(\frac{1}{r_t}\right)^{\frac{2}{k}} - \left(\frac{1}{r_t}\right)^{\frac{k+1}{k}} = \text{Maximum} \qquad (116)$$

The value of $1/r_t$ for the maximum weight flow can be obtained by differentiating equation 116

$$d\frac{\left[\left(\frac{p_2}{p_1}\right)^{\frac{2}{k}} - \left(\frac{p_2}{p_1}\right)^{\frac{k+1}{k}}\right]}{d(p_2/p_1)} = 0$$

The result of the differentiation is

$$\left(\frac{p_2}{p_1}\right)_{cr} = \left(\frac{1}{r_t}\right)_{cr} = \left(\frac{2}{k+1}\right)^{\frac{k}{k-1}} \tag{117}$$

Equation 117 gives the expansion ratio corresponding to the maximum weight flow per unit area of the nozzle $(G/A_2)_{max}$. The velocity corresponding to this expansion ratio is called the *critical velocity* and is denoted by w_{cr}.
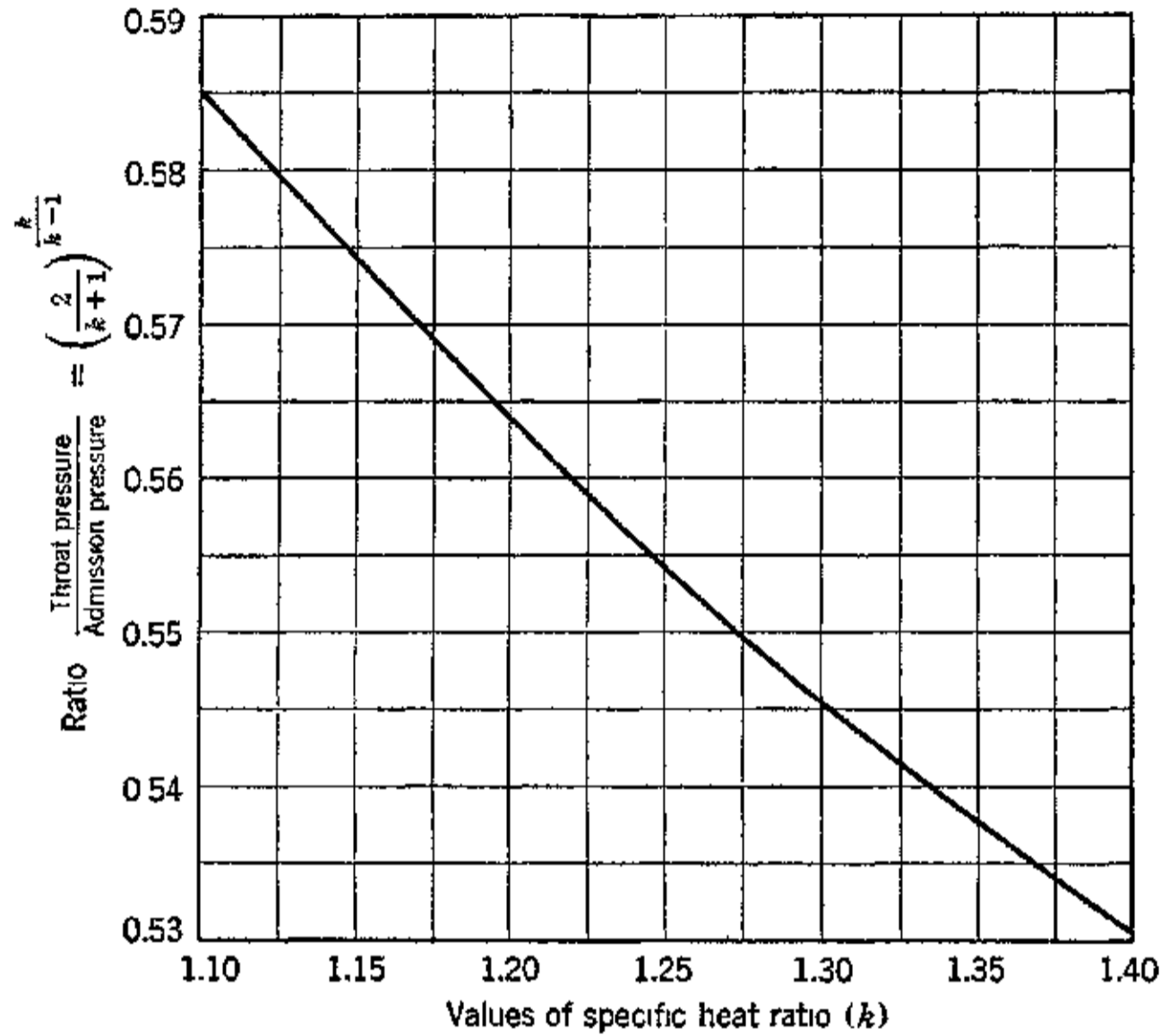
FIG. 17.   Values of critical pressure ratio as a function of the specific heat ratio.

Equation 117 shows that the critical expansion ratio depends only upon the specific heat ratio for the gas.   Figure 17 presents the values of the critical expansion ratio as a function of the specific heat ratio k.

16. Critical Velocity

The equation for the critical velocity is obtained by substituting the critical expansion ratio from equation 117 into equation 102 and expressing it in terms of p_1 and v_1.   Thus

$$\frac{w_{cr}^2}{2g} = \frac{k}{k-1} p_1 v_1 \left[1 - \left\{ \left(\frac{2}{k+1}\right)^{\frac{k}{k-1}} \right\}^{\frac{k-1}{k}} \right]$$

which reduces to

$$\frac{w_{cr}{}^2}{2g} = \frac{k}{k+1} p_1 v_1 \qquad (118)$$

Hence the critical velocity is

$$w_{cr} = \sqrt{\frac{2gk}{k+1} p_1 v_1} = \sqrt{\frac{2gk}{k+1} RT_1} \qquad (119)$$

Equation 119 can be rewritten in the form

$$w_{cr} = \sqrt{2g \frac{k}{k+1} \frac{p_1 v_1}{p_{cr} v_{cr}} p_{cr} v_{cr}} \qquad (a)$$

Since the process has been assumed to be isentropic

$$\frac{p_{cr}}{p_1} = \left(\frac{v_1}{v_{cr}}\right)^k \qquad (b)$$

Hence

$$\frac{p_1 v_1}{p_{cr} v_{cr}} = \left[\left(\frac{2}{k+1}\right)^{\frac{k}{k-1}}\right]^{\frac{1-k}{k}} = \left(\frac{2}{k+1}\right)^{-1} = \frac{k+1}{2} \qquad (c)$$

Substituting from (c) into (a) gives the following expression for the critical velocity

$$w_{cr} = \sqrt{gk p_{cr} v_{cr}} = a_2 \qquad (120)$$

From Chapter 1, Section 12, it is seen that, when the critical velocity prevails at the nozzle exit section (area A_2), it is identical with the local acoustic velocity a_2.

17. Maximum Weight Flow

The foregoing has established that the maximum weight rate of flow of gas $G_{\max}$ occurs when the parameter $\psi = \psi_{\max}$. This value is obtained when the converging nozzle operates with the critical expansion ratio. When this occurs the velocity in the exit section is the local sonic value. The value of $\psi_{\max}$ is obtained by substituting for the critical expansion ratio in the equation for ψ. Hence

$$\psi_{\max} = \left(\frac{2}{k+1}\right)^{\frac{1}{k-1}} \sqrt{\frac{k}{k+1}} \qquad (121)$$

Substituting for $\psi = \psi_{max}$ into equation 112 gives the expression for the maximum weight flow of gas through the nozzle. Thus

$$G_{max} = A_2 \left(\frac{2}{k+1}\right)^{\frac{1}{k-1}} \sqrt{\frac{k}{k+1}} \sqrt{\frac{2g}{RT_1}} p_1 \qquad (122)$$

For gases with $k = 1.4$

$$G_{max} = 3.89 A_2 \sqrt{\frac{p_1}{v_1}} = 3.89 \frac{A_2 p_1}{\sqrt{RT_1}} \qquad (123)$$

The maximum values of ψ are indicated by the broken lines in Fig. 15.

It should be borne in mind that the flows calculated by the above equation will be too high in any actual example. To obtain the correct flow, the result must be multiplied by an experimentally determined discharge coefficient.

The foregoing demonstrates that the calculated plot of G vs. p_2/p_1, for the range $p_2/p_1 = 0$ to unity, is correct until the value of p_2/p_1 is reduced from unity to the critical ratio, for which the acoustic velocity is attained in the exit section or throat. Since disturbances beyond the throat can no longer be propagated upstream, the flow behaves as if there had been no further reduction in the back pressure; it has no way of recognizing the reduction in pressure. Consequently, when the back pressure is equal to or less than the critical value the nozzle discharges the same flow, the *critical flow*, $G_{cr} = G_{max}$. The broken-line portion of the curve in Fig. 16 does not exist physically.
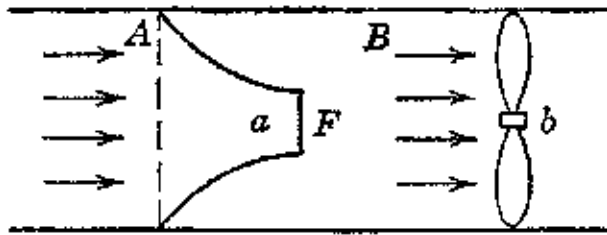
FIG. 18.   Induced flow through a nozzle and duct.

The aforementioned conditions can be explained by considering the arrangement illustrated in Fig. 18 taken from reference 2. Assume that a gas held at constant pressure flows from the region A through the nozzle of area A into the confined space B where the critical back pressure is maintained at the nozzle outlet by the exhaust fan b. The gas flows out of the nozzle exit section into space B with the acoustic velocity. Let the fan exhaust the gas from the space B at a more rapid rate than that at which it is being discharged by the nozzle. The pressure in the space B will fall below the critical value, and the reduction in the pressure will cause a pressure wave to travel from the fan blades toward the nozzle exit section with the speed of sound. The gas is being discharged, however, with the same velocity. The pressure wave stands at the exit section of the nozzle;

that is, it is impossible for the reduction in pressure to propagate itself upstream into the nozzle. The exit velocity of the gas remains unchanged and does not rise above the acoustic velocity or change the state of the gas in region A even if the region B is completely evacuated. This fact was known to St. Venant and Wantzel (1839) and was explained both theoretically and experimentally by Grashof (1875) and by Zeuner (1900).

Experiments show that the shape of the jet discharging from a nozzle is different depending on whether the back pressure is above or below the critical value. When the back pressure is above the critical pressure, the jet issues as a cylindrical parallel stream, its surface being gradually retarded by the surrounding gas, so that a mixing zone is produced in which the velocity of the jet finally drops to that of the surroundings. This is illustrated in Fig. 19.
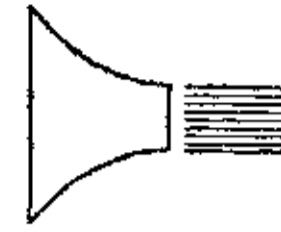
FIG. 19. Shape of jet discharged from a converging nozzle with supercritical back pressure.

When the back pressure is less than the critical pressure, the jet expands as it discharges from the nozzle, as indicated in Fig. 20; here the pressure of the gas in the jet leaving the nozzle is the critical pressure which is higher than the back pressure. The sudden reduction in pressure causes the gas to expand in an explosive fashion. The gas particles are accelerated radially and owing to their inertia move beyond their equilibrium positions, thereby creating a pressure reduction in the core of the jet that causes the particles to reverse themselves. This phenomenon is periodic. The jet becomes thinner in some sections and thicker in others, so that standing waves are observed. These are associated with loud noise and decrease the available energy of the gas.

FIG. 20. Shape of jet discharged from a converging nozzle with subcritical back pressure.

Consider now that the back pressure p_2 is held constant and the upstream pressure p_1 is continuously increased from the initial value $p_1 = p_2$. As p_1 is increased the weight rate of flow is increased in accordance with equations 112 and 113 until the critical pressure ratio is reached. Thus, for gases with $k = 1.4$, the critical pressure ratio occurs when $p_2/p_1 = 0.5283$ or when $p_1/p_2 = 1/0.5283 = 1.89/1$. When $p_1/p_2 = 1.89$ the velocity in the nozzle exit section is the local acoustic velocity a_2.

For gases with $k = 1.4$, it was shown that
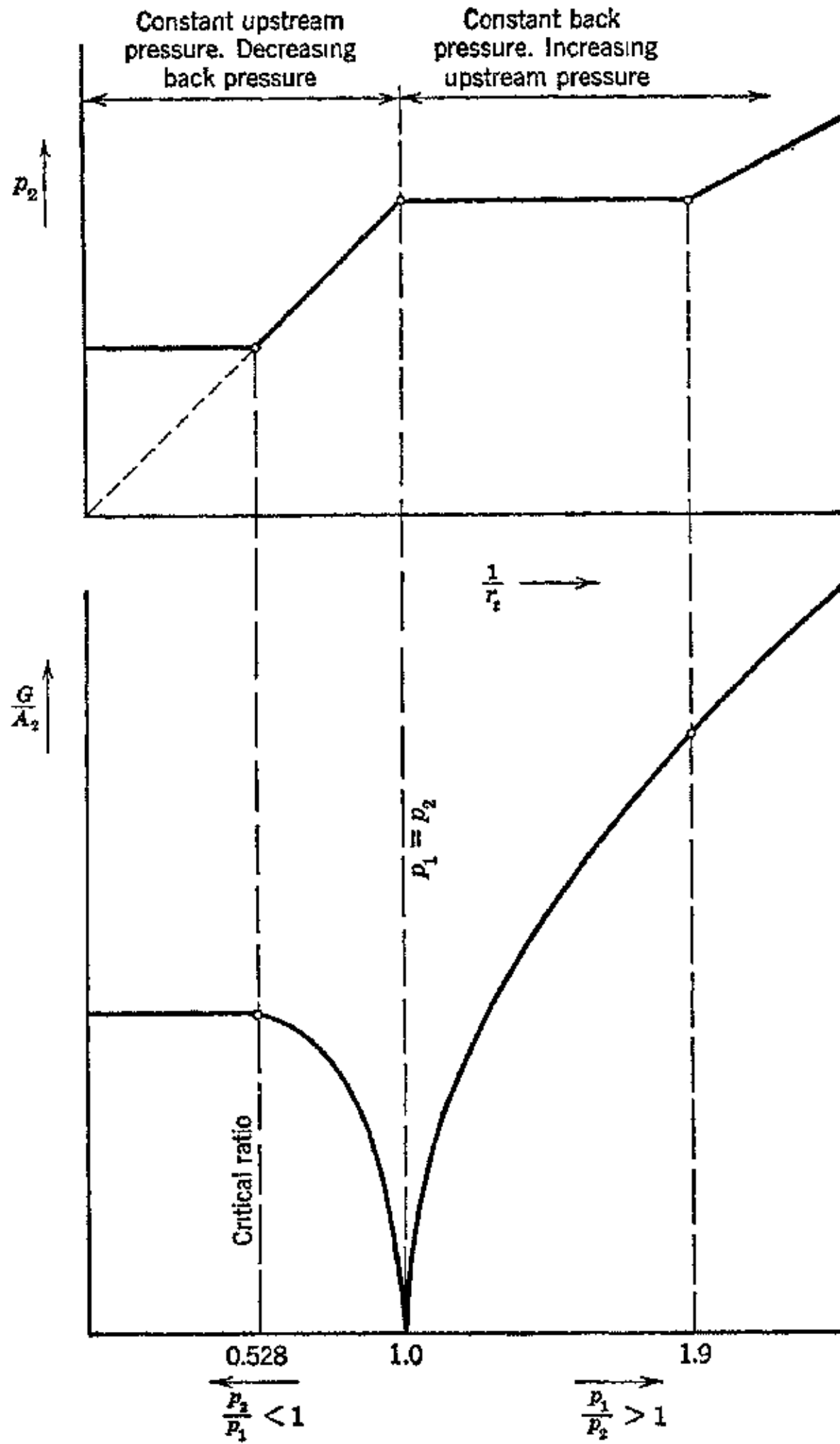
$$\left(\frac{G}{A_2}\right)_{max} = \frac{3.89 p_1}{\sqrt{RT_1}}$$

FIG. 21. Nozzle characteristics with constant upstream pressure and variable back pressure, and with constant back pressure and variable upstream pressure. (Reproduced from O. G. Tietjens, A.S.M.E., semi-annual meeting, June 9–11, 1930)

Hence, if T_1 is held constant and p_1 is further increased above that corresponding to $p_1/p_2 = 1.89$, the weight flow increases linearly with p_1. This increase is due to the increased specific weight of the gas crossing the exit area A_2. The volumetric rate of discharge is unaffected by increasing p_1, as is seen from the following. Let Q_{max} denote the volumetric rate of flow per unit area corresponding to $p_2/p_1 = 0.5283$. Then

$$Q_{max} = \left(\frac{G}{A_1}\right) v_1 = 3.89 \sqrt{RT_1}$$

which is seen to be independent of p_1

The exit velocity is given by equation 119 and for $k = 1.4$ becomes

$$w_2 = a_2 = \sqrt{2g \frac{k}{k+1} RT_1} = 6.13 \sqrt{RT_1}$$

which is also independent of the pressure p_1.

The two types of back-pressure conditions are illustrated in Fig. 21, which is based on reference 16.

18. The Converging-Diverging or De Laval Nozzle

Figure 22 represents an isentropic expansion on the pv plane.
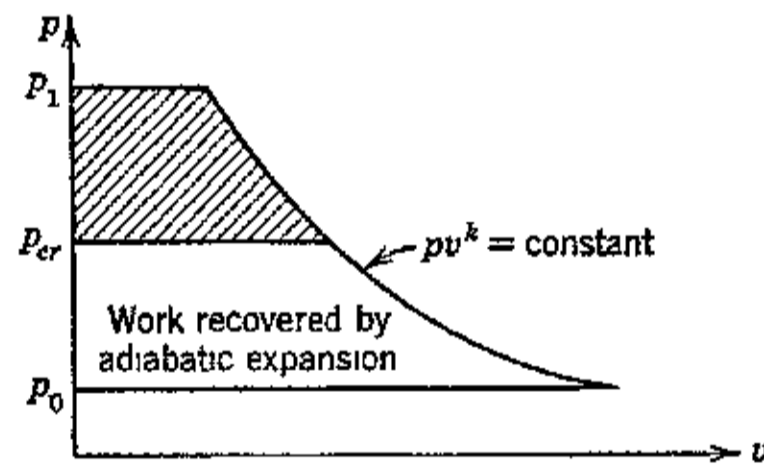
FIG. 22. Work recovered by expansion from critical pressure to correct back pressure

From the preceding sections it follows that, when a gas expands in a converging nozzle, the enthalpy transformable into kinetic energy is limited to that represented by the upper cross-hatched portion of the diagram, that is, the area of the diagram located above the critical pressure p_{cr}. The area of the diagram below p_{cr} is not transformed into kinetic energy but is used up in frictional heat and noise after the gas jet emerges from the converging nozzle.[4]

De Laval showed that the total enthalpy drop corresponding to the pressure drop $(p_1 - p_2)$ could be transformed into kinetic energy if a divergent downstream cone is added to the converging nozzle. This form of nozzle is called the De Laval nozzle and is illustrated in Fig. 23.

The phenomenon which takes place in a De Laval nozzle can be explained by means of the equations derived for the converging
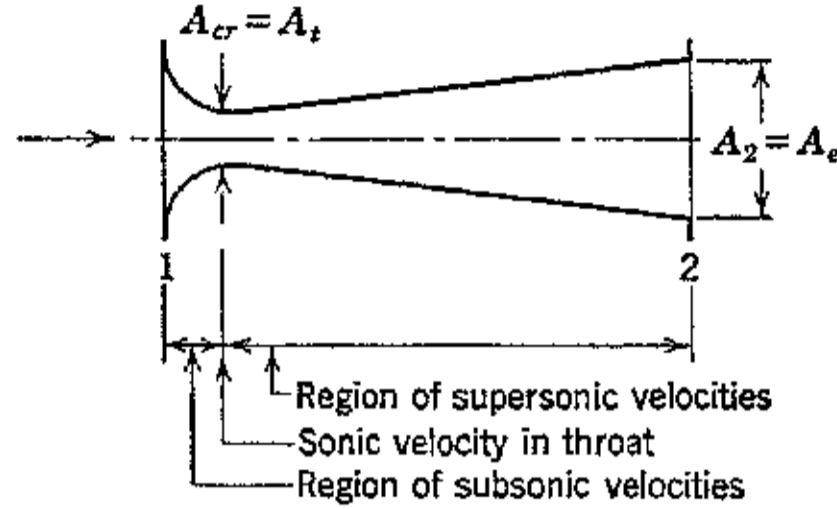
FIG. 23. The De Laval nozzle.

nozzle. Thus it was shown that, for isentropic flow and zero velocity of approach, the kinetic energy E_k derived from the expansion of 1 lb of gas is given by

$$E_k = \frac{w_2{}^2}{2g} \quad \text{ft-lb/lb} \tag{a}$$

where

$$\frac{w_2{}^2}{2g} = -\int_1^2 v \, dp = \frac{k}{k-1} p_1 v_1 \left[1 - \left(\frac{p_2}{p_1}\right)^{\frac{k-1}{k}} \right] \tag{b}$$

from which, assuming $\varphi = 1$, and dropping the subscript, the velocity equation becomes

$$w = \sqrt{2gE_k} = \sqrt{-2g \int_1^2 v \, dp} = \sqrt{\frac{2gk}{k-1} p_1 v_1 \left(\frac{Z_t}{1+Z_t}\right)} \quad \text{fps} \tag{c}$$

The interpretation of these equations can be illustrated graphically as shown in Fig. 24 by the following procedure.[2]

(a) Curve E_k shows how the kinetic energy changes with the back pressure. Thus, when $p_2 = p_1$, $E_k = 0$, and when $p_2 = 0$, $E_k = [k/(k-1)]p_1 v_1$. The intermediate values are obtained by means of equations (a) and (b). The total mechanical work transformed into kinetic energy is the area to the left of the kinetic-energy curve E_k, between the pressure limits p_1 and p_2.

(b) The curve denoted by w is the velocity curve for different back pressures. It is obtained by integrating the kinetic-energy curve between the pressures p_1 and p_2 for different values of the back pressure p_2. This procedure gives a series of values of total kinetic energy for different back pressures. The corresponding velocities are
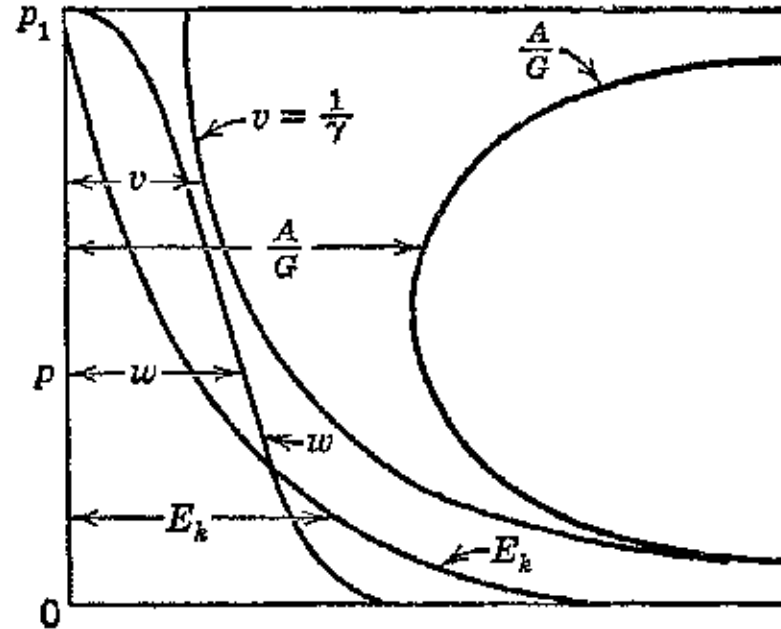
FIG. 24. Flow conditions in a De Laval nozzle. (Reproduced from E. Schmidt, *Einführung in die technische Thermodynamik*, Julius Springer, Berlin, 1936.)

obtained by taking the square root of these kinetic energies and multiplying them by $\sqrt{2g}$. In this manner a curve of the velocity w as a function of back pressure is obtained.

(c) Curve v shows the specific volume as a function of the back pressure. It is obtained from the kinetic energy relationship

$$\frac{w^2}{2g} = E_k = -\int_1^2 v \, dp$$

The value of the specific volume is computed for several values of p_2, and the result is plotted as a function of p_2.

(d) The curve marked A/G is the nozzle area per unit weight flow as a function of the back pressure. It is obtained by applying the continuity equation, $A = Gv/w$. From the curves for v and w the ratio A/G is calculated. It is seen that as the back pressure is decreased the area per unit weight flow A/G first decreases, then attains a minimum value, and then increases again as already explained.

EXAMPLE. High-pressure air at 100 psig and 500 R discharges through a well-rounded nozzle. The back pressure is 14.7 psia. Find the isentropic exhaust velocity. Assume $c_p = 0.243$.

$$p_1 = 100 + 14.7 = 114.7 \quad \text{psia}$$

$$p_2 = 14.7$$

$$r_t = \frac{p_1}{p_2} = \frac{114.7}{14.7} = 7.81$$

From Table 4·5

$$Z_t = 0.7890$$

$$w' = 223.7\sqrt{0.243 \times 500 \times \frac{0.7890}{1.7890}} = 1640 \quad \text{fps}$$

If the velocity coefficient $\varphi = 0.96$, then the actual velocity is

$$w_2 = w'\varphi = 0.96 \times 1640 = 1570 \quad \text{fps}$$

19. Area Ratio for Complete Expansion

It has been shown that for a converging nozzle the parameter ψ cannot exceed the value $\psi = \psi_{max.}$.

Refer to Fig. 25, where ψ is plotted as a function of $1/r_t$. For continuity, the product $A\psi$ must remain constant at all sections of the nozzle.
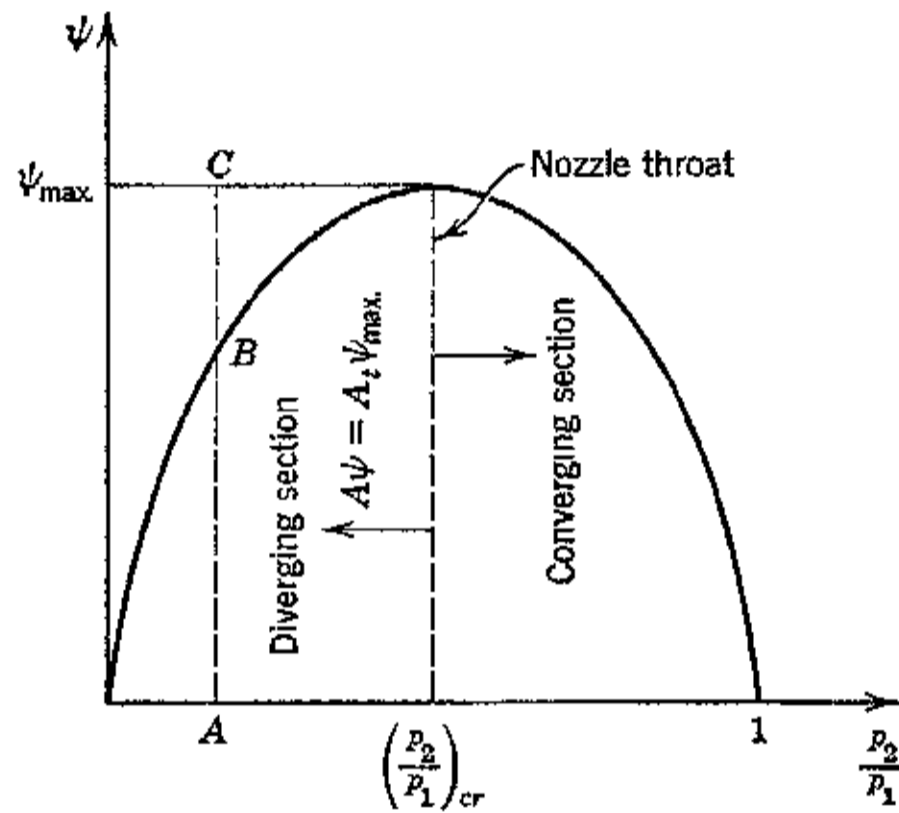
FIG. 25.   Relationships for converging-diverging flow passage.

In a nozzle constructed with a divergent discharge section following the narrowest section (the throat), the parameter ψ must decrease in the divergent outlet section in order to maintain continuity. This signifies that for such a nozzle, or flow passage, the pressure beyond the throat section can continue to decrease. The conditions in the divergent section are illustrated in Fig. 25. They correspond to that part of the ψ vs. $1/r_t$ curve lying to the left of $1/r_t = (p_2/p_1)_{cr}$.

At any arbitrary cross-sectional area A of the divergent portion

$$A\psi = A_t\psi_{max.} = \text{Constant} \tag{124}$$

where $A_t = A_2 = A_{cr} =$ cross-sectional area of the nozzle throat in square feet.

Refer to Fig. 25. From equation 124 the area ratio, based on the throat area, at any section is

$$\frac{A}{A_t} = \frac{\psi_{\text{max.}}}{\psi} = \frac{AC}{AB} \qquad (125)$$

From the curve of Fig. 25 the area ratio A/A_t required to transform the enthalpy into kinetic energy for expansion to the critical ratio can be determined.

By substituting the values of ψ and $\psi_{\text{max.}}$ from equations 111 and 121 into equation 125, the ratio of the throat area A_t to the exit area $A_2 = A_e$ is obtained. Thus

$$\frac{A_t}{A_e} = \frac{\psi_e}{\psi_{\text{max.}}} = \left(\frac{k+1}{2}\right)^{\frac{1}{k-1}} \sqrt{\frac{k+1}{k-1}\left[\left(\frac{p_e}{p_1}\right)^{\frac{2}{k}} - \left(\frac{p_e}{p_1}\right)^{\frac{k+1}{k}}\right]}$$

or

$$\frac{A_t}{A_e} = \left(\frac{k+1}{2}\right)^{\frac{1}{k-1}}\left(\frac{p_e}{p_1}\right)^{\frac{1}{k}}\sqrt{\frac{k+1}{k-1}\left[1 - \left(\frac{p_e}{p_1}\right)^{\frac{k-1}{k}}\right]} \qquad (126)$$

Equation 126 gives the area ratio required to expand a gas adiabatically from an initial pressure p_1 to a pressure $p_2 = p_e$ at the exit section, p_e being lower than the throat pressure p_t. It is seen that the area ratio depends only on the specific heat ratio k and the expansion ratio $p_2/p_1 = p_e/p_1$.

An expression for the ratio of the velocities at the exit section and the throat is obtained by combining equations 102 and 120. Let $w_t = w_{cr}$ denote the throat velocity, and w_e the velocity in the exit section; then

$$\frac{w_e}{w_t} = \sqrt{\frac{k+1}{k-1}\left[1 - \left(\frac{p_e}{p_1}\right)^{\frac{k-1}{k}}\right]} \qquad (127)$$

Figure 26 presents the curves of A_e/A_t as functions of p_e/p_1 for several values of k, and Fig. 27 presents w_e/w_t as a function of p_e/p_1.

The conditions when the back pressure p_2 is reduced to zero, so that $p_1/p_2 =$ infinity, are of special interest. Assuming that $k = 1.4$, and that the area ratio is infinitely large, the ratio of the exit velocity to the throat velocity is

$$\frac{w_e}{w_t} = \sqrt{\frac{k+1}{k-1}\left[1 - \left(\frac{p_e}{p_1}\right)^{\frac{k-1}{k}}\right]} = \sqrt{\frac{k+1}{k-1}} = 2.45$$

Hence for the limiting case (when $p_e = 0$) the ideal exit velocity is 2.45 times the acoustic velocity corresponding to the conditions in the throat section.
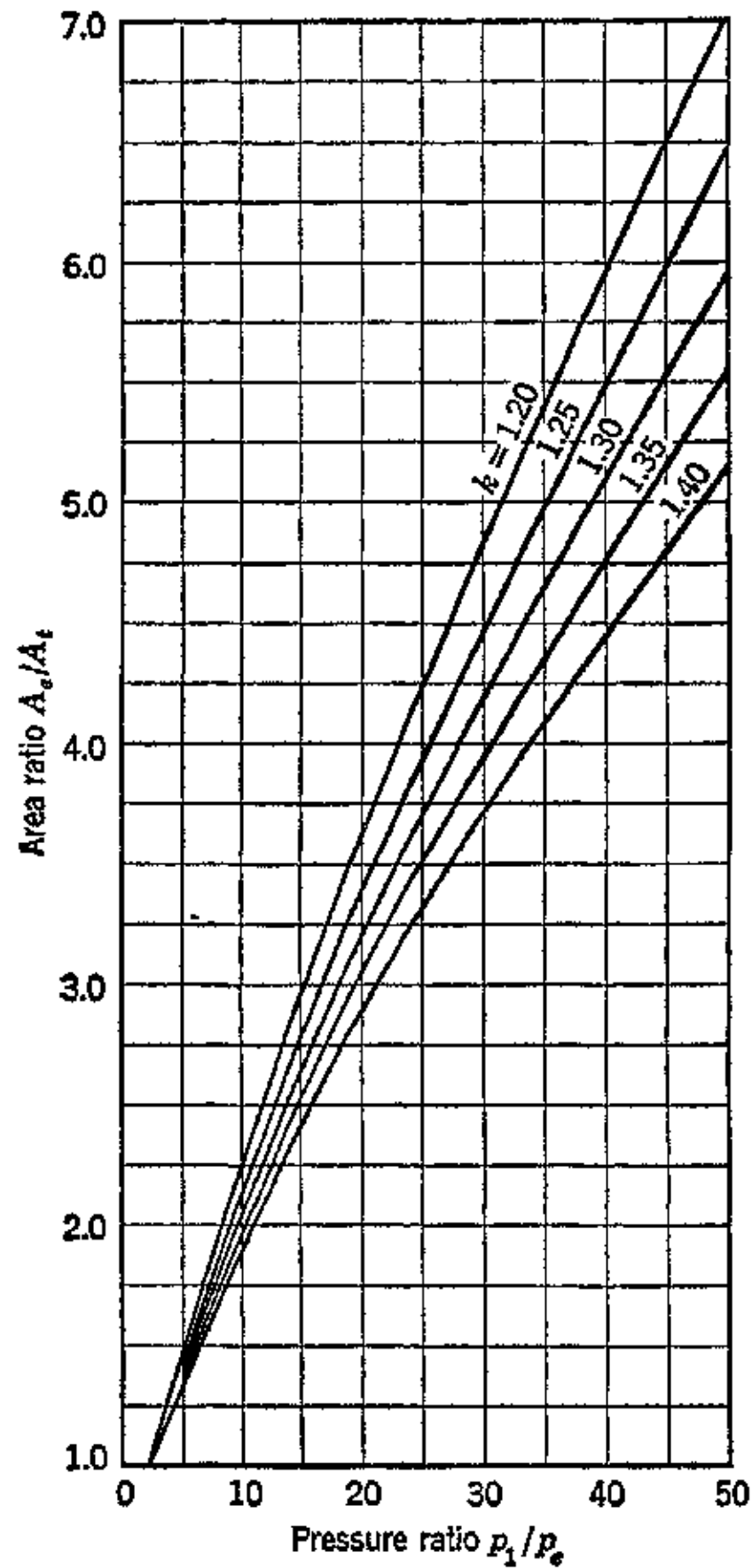
Fig. 26.   Nozzle area ratio for complete expansion for various values of the specific heat ratio.

According to the equation for an adiabatic expansion, when $p_2 = 0$, the temperature ratio T_2/T_1 is given by

$$\frac{T_2}{T_1} = \left(\frac{p_2}{p_1}\right)^{\frac{k-1}{k}} = 0$$

The last equation indicates that if the expansion could be carried to $p_2 = 0$ the corresponding temperature of the gas at the exit from
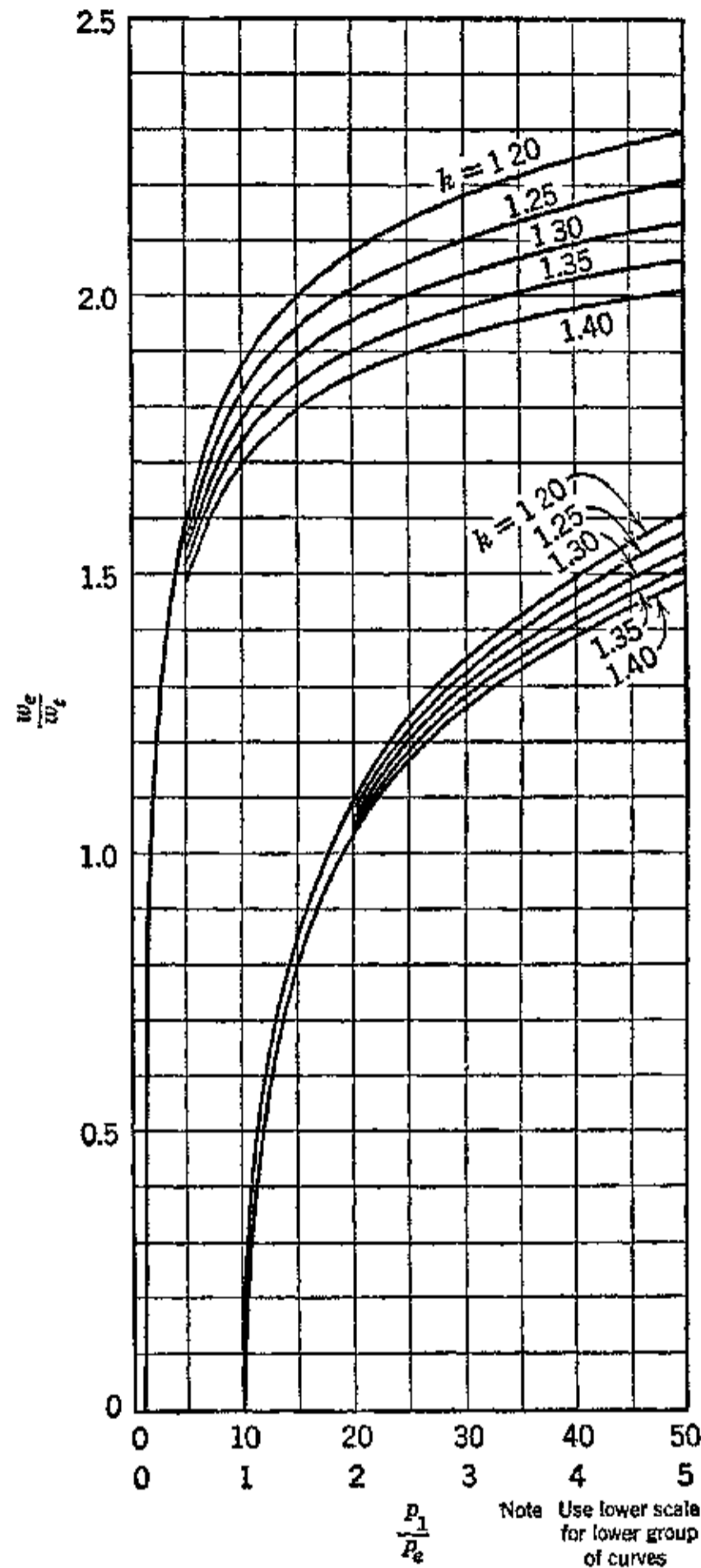
FIG. 27.   Ratio of exit velocity to throat velocity for different values of the specific heat ratio.

the nozzle must fall to absolute zero, assuming that the gas does not liquefy.   The entire enthalpy of the gas is then converted into kinetic energy, and the gas molecules no longer possess any random motion but move similarly in parallel paths.

20. General Discussion of Flow through a Converging-Diverging Passage

The equations for the ideal weight rate of flow G, derived above, show that if G is constant, as required by continuity, then for each cross-sectional area of the divergent part of the nozzle there is a corresponding expansion ratio p_t/p_x, where p_x is the pressure at the section in question. Hence if A_x denotes the area corresponding to p_x, and A_t is the throat area, then for the maximum weight flow (acoustic velocity in the throat) the ratio p_x/p_1 can be plotted as a function of A_x/A_t for the critical flow $G_{max.}$ or different percentages of $G_{max.}$. Such a plot is illustrated in Fig. 28.
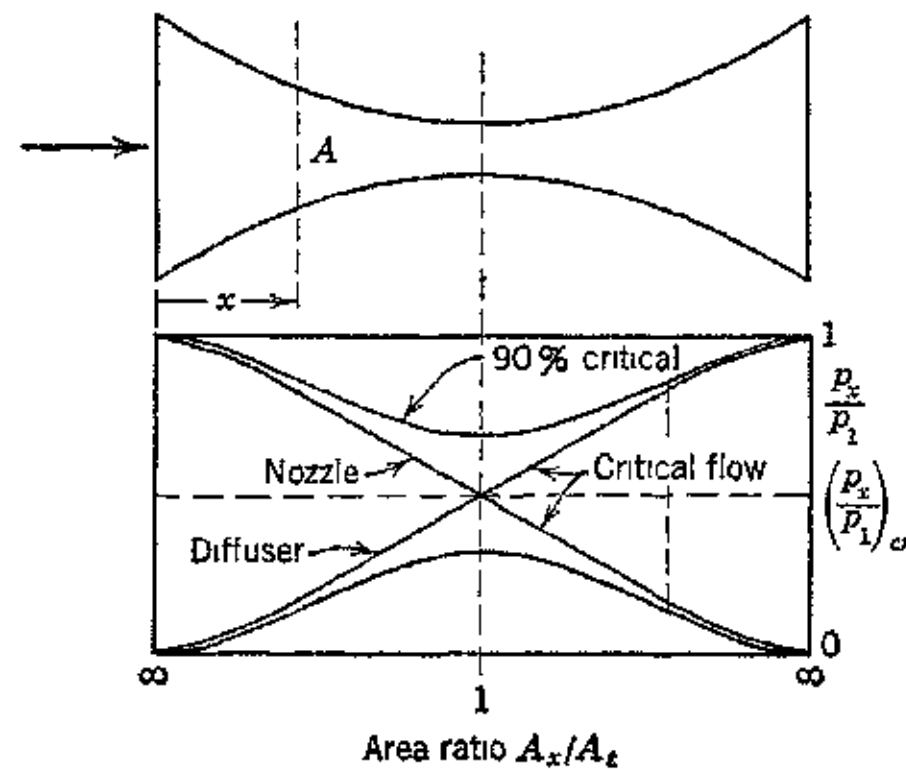
FIG. 28.   Variation in pressure ratio along a converging-diverging passage.

Figure 28 shows that for a given cross-sectional area there are two values of p_x/p_1 which satisfy the equation for the maximum weight flow. One value corresponds to an expansion of the fluid, or nozzle action; the other to a compression, or diffuser action. The two curves, one marked nozzle and the other labeled diffuser, intersect at the throat section. As far as energy and continuity considerations are concerned two different processes are possible. There can be an expansion from the nozzle entrance to the throat and either a further expansion with supersonic velocity in the divergent section or a recompression of the gas, depending upon the magnitude of the back pressure. If the weight flow is less than the critical value, there is only one ideal exit pressure which satisfies the flow equation. From the continuity equation $G = Aw/v = $ constant

$$\frac{dA}{A} + \frac{dw}{w} - \frac{dv}{v} = 0 \qquad (128)$$

From the energy equation for isentropic flow

$$-v\,dp = \frac{w}{g}\,dw$$

Hence

$$-\frac{dw}{w} = \frac{gv\,dp}{w^2}$$

For an isentropic process $pv^k = $ constant, and

$$\frac{dp}{p} + k\frac{dv}{v} = 0$$

Substituting for dw/w and dv/v into equation 128

$$\frac{dA}{A} = \frac{gkpv - w^2}{w^2kp}dp$$

and finally

$$\frac{dA}{A} = \frac{1}{k}\left(\frac{1}{M^2} - 1\right)\frac{dp}{p} \tag{129}$$

Equation 129 relates the pressure and area changes and the Mach number. The relationship between the velocity and area changes and the Mach number is given by equation 91, which is repeated here for convenience:

$$\frac{dA}{A} = -(1 - M^2)\frac{dw}{w} \tag{130}$$

Equations 129 and 130 are extremely helpful in studying the effect of changing the area of the flow passage for different flow velocities, i.e., Mach numbers.

Consider now the conditions to be satisfied when the flow passage is to be employed for accelerating the flow of a compressible fluid. Because the fluid velocity is increasing, its pressure must be falling as it passes through the passage. Hence dp in equation 129 is negative while dw in equation 130 is positive.

If a fluid enters a flow passage with a subsonic velocity ($M < 1$), then for dw to be positive requires dA/A to be negative; that is, the passage must converge. Conversely, if the entrance velocity is supersonic ($M > 1$), then to produce a velocity increase (dw positive and dp negative) requires that dA/A be positive; that is, the passage must diverge.

The foregoing shows that a continuous flow passage which is to accelerate the velocity of the gas from an initial subsonic value to a

supersonic value must comprise a convergent section followed by a divergent section. In other words the flow passage must have the general features of the De Laval nozzle.

Consider now the case for decelerating a fluid to obtain a flow compression. Here the pressure is to increase (dp positive) and the velocity decrease (dw negative). If the gas velocity is subsonic ($M < 1$), it follows, from equations 129 and 130, that dA/A must be positive. Flow compression of a subsonic flow requires a divergent passage. Conversely, if the flow is supersonic ($M > 1$), to obtain a flow compression dA/A must be negative; the passage must converge. Hence, if a flow deceleration begins with a supersonic velocity and is to end with a subsonic velocity the flow passage must first converge and then diverge. If a flow compression begins and ends with supersonic velocities, the flow passage must converge continuously.

Summarizing, a converging-diverging passage, such as a De Laval nozzle, can produce the following flow phenomena. If the entering velocity is subsonic, the velocity continues to increase and the pressure to decrease up to the throat section. If the velocity in the throat is still subsonic, a flow compression occurs in the divergent section. If the velocity in the throat is the local sonic value, either a flow expansion with supersonic velocities or a flow compression with subsonic velocities can occur in the divergent section. Which of these flow phenomena will occur depends upon the pressure at the exit of the converging-diverging passage.
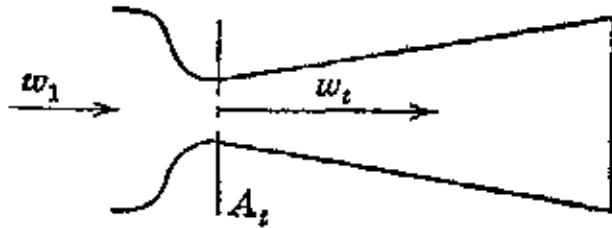
FIG. 29. A converging-diverging flow passage.

To illustrate these important facts further, consider the flow conditions in a passage constructed from a converging passage connected to one which diverges as illustrated in Fig. 29.

Let w_1 = entrance velocity, w_t = throat velocity. Four different cases can be distinguished.

Case I ($w_1 < a$, $w_t < a$). The velocity of the gas increases in the converging section until the throat section is reached. In the diverging section the velocity decreases. Correspondingly, the pressure decreases in the converging section until the throat section is reached and then increases again. Owing to friction and to separation of the jet from the wall, especially if the divergence is too large, the pressure does not reach its initial value. The variation in the velocity and pressure along the passage is illustrated in Fig. 30.

Case II ($w_1 < a$, $w_t = a$). The gas velocity increases in the converging section with a corresponding decrease in pressure. Acoustic

velocity is attained at the throat. Beyond the throat the velocity increases in the diverging section with a corresponding diminution in pressure. This corresponds to a pure expansion flow where, apart
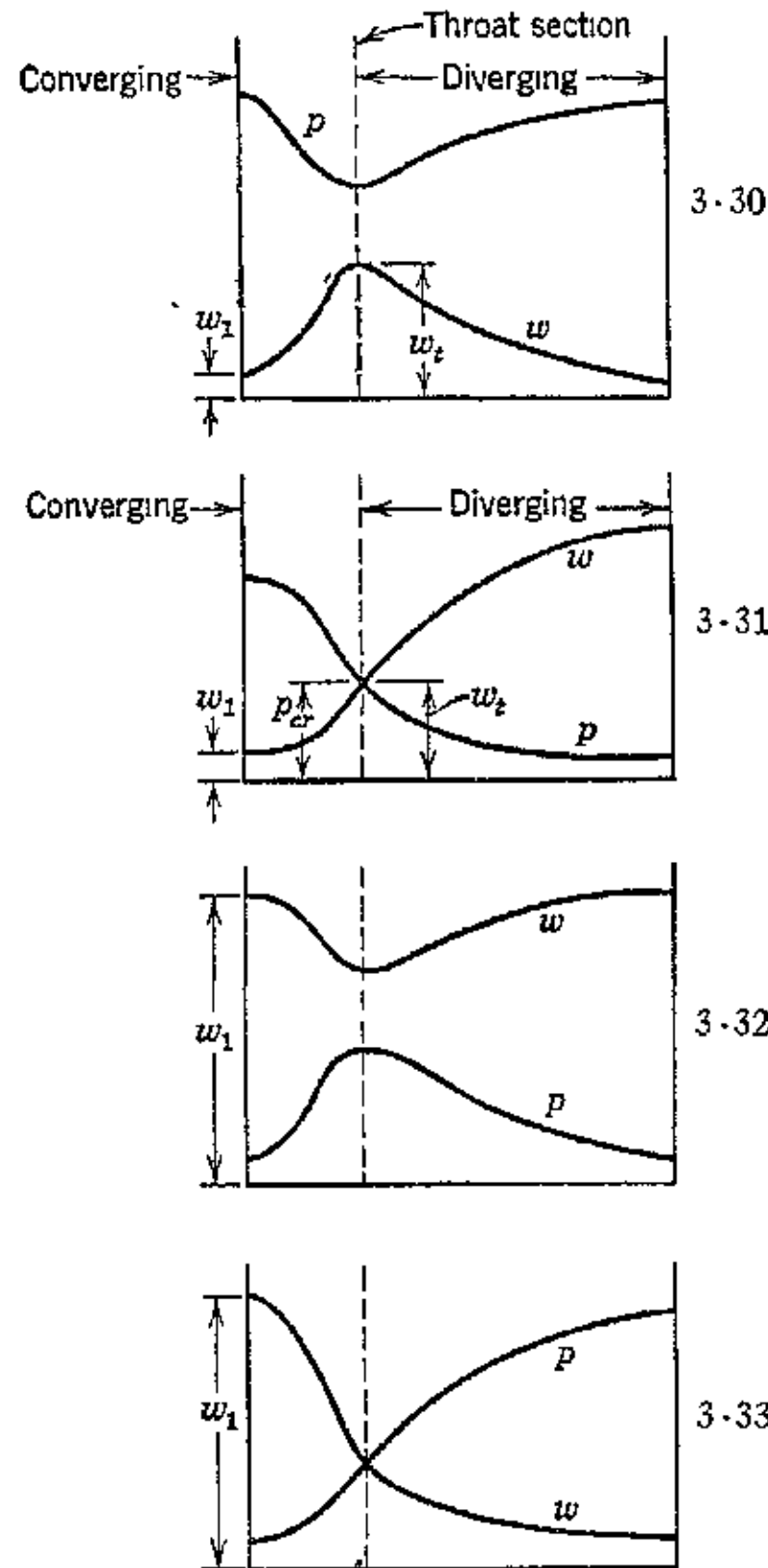
FIGS. 30–33.   Effect of entrance and throat velocities on pressure distribution in a converging-diverging passage.

from losses due to wall friction, all the pressure drop is transformed into kinetic energy. This case is illustrated in Fig. 31.

Case III $(w_1 > a, w_t > a)$. The gas enters the converging section with supersonic velocity and decreases in this section while the pressure increases. Since $w_t > a$ the flow accelerates again in the diverging section with a consequent decrease in the pressure. See Fig. 32.

Case IV ($w_1 > a$, $w_t = a$). The flow conditions in the converging section are similar to those for Case III. The velocity decreases until the acoustic velocity is reached in the throat, and in the diverging section it continues to decrease while the pressure increases. This case corresponds to a pure flow compression, in which, as in Case I, there are large separation losses in the diverging section. The losses due to jet separation exceed those resulting from wall friction. The conditions are illustrated in Fig. 33.

The converging-divergent nozzles used with rocket motors are designed to bring the velocity of the combustion gases from subsonic to supersonic flow. This is desirable because the higher the exhaust velocity of the gases the greater is the thrust developed for a given weight rate of flow.

21. Effect of Back Pressure on a Converging-Diverging Nozzle

It was shown that for a given back pressure the area ratio of the nozzle must have a definite value to obtain complete expansion of the gas. The question naturally arises, what is the effect of changing the back pressure in operating a given nozzle?

For a given area ratio there is one correct value for the back pressure p_2. If the back pressure falls below the correct value the conditions inside the nozzle are unaffected. The disturbance created by lowering p_2 propagates itself only with the acoustic velocity while the jet discharges with supersonic velocity. The discharging jet expands, however, as it reaches the exit in much the same manner as that for a jet from a converging nozzle discharging into a region with subcritical back pressure.

Raising the back pressure above the correct value causes a pressure wave to propagate with sonic speed into the boundary of the jet which is emerging with supersonic speed. The superposition of both velocities produces a pressure wave with an inclined front. This forms at the corner of the exit section from the nozzle and forces its way into the jet.
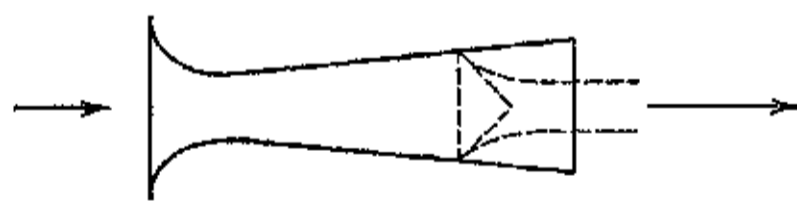
FIG. 34. Jet separation and shock due to incorrect back pressure.

A pressure wave starts at the exit edge forming a Mach angle wave front similar to that formed at the nose of a projectile moving with supersonic speed. In this pressure wave the pressure suddenly increases from that in the exit section to that of the surroundings, causing a *compression shock*, and is called a *shock wave*. Behind the shock wave, the jet contracts

to a smaller cross section corresponding to the effect of the external pressure on the local specific volume. If the exit pressure is increased further, the jet separates from the wall of the nozzle as illustrated in Fig. 34.
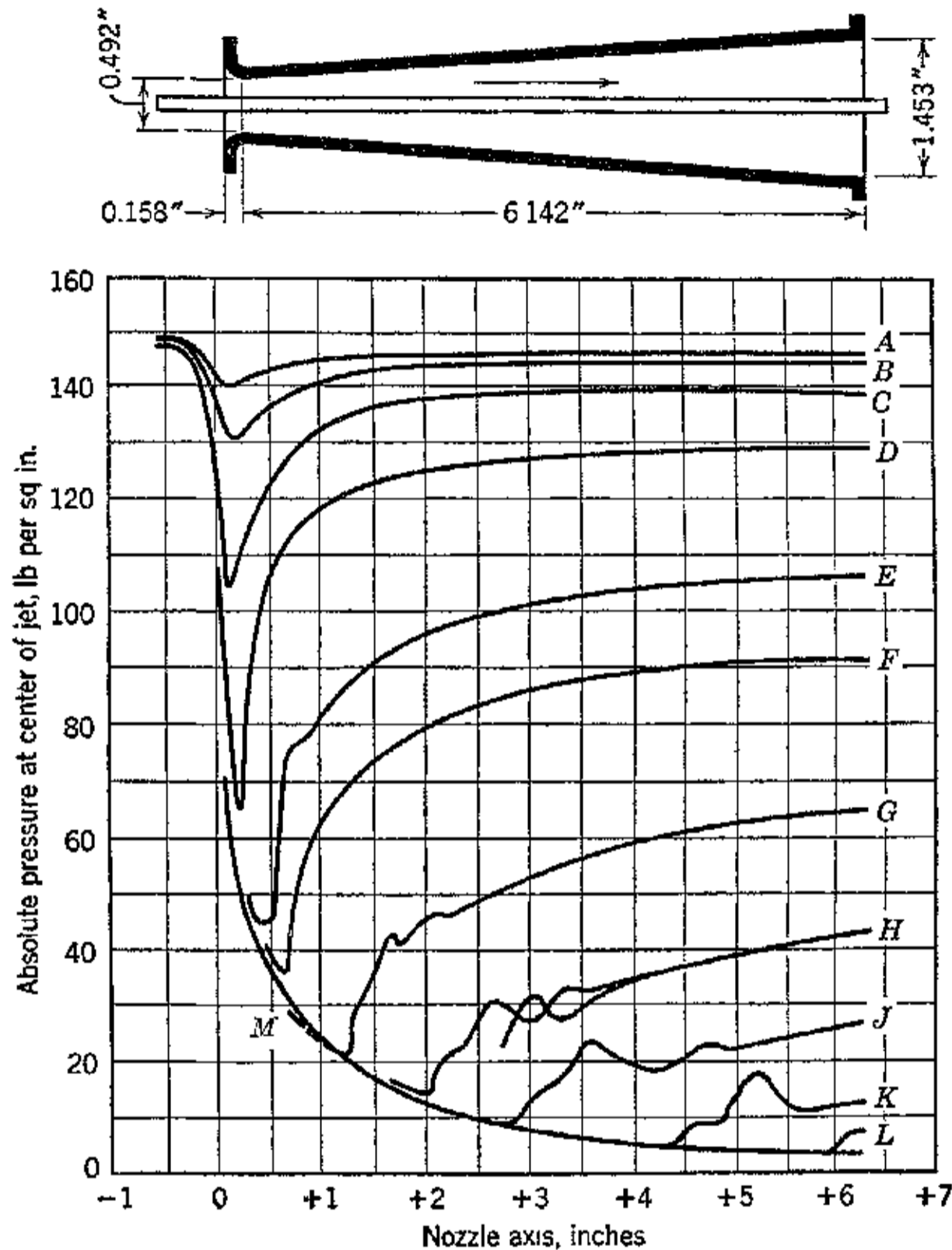
Fig. 35.   Effect of back pressure on the pressure along the axis of a De Laval nozzle. (Reproduced from A. Stodola, *Steam and Gas Turbines*, Vol. 1, McGraw-Hill Book Co., 1927.)

At the wall, because of friction, the jet velocity falls to zero so that the boundary layer is moving with subsonic speed. The excessive external pressure propagates through the boundary layer and tears the jet away from the wall.

The foregoing conclusions regarding the effect of incorrect back pressure are based on the experiments of A. Stodola, who measured

the variation in pressure along the axis of a converging-diverging nozzle operating with different back pressures. The results obtained are illustrated in Fig. 35.

Reference to Fig. 35 shows that, when the back pressure was correct, curve M, the pressure along the axis of the nozzle was the lowest for the tests and is the limiting condition for all of them. As the back pressure was slightly increased, the pressure along the axis showed a sharp increase or shock close to the nozzle exit. Further increase in the back pressure intensified the shock and it moved further inside the nozzle; see curves K, J, H, G. The waves illustrated on these curves are standing pressure waves that propagated themselves back into the jet.

In curve D, the acoustic velocity was not quite attained, but the shock wave traveled upstream and occurred close to the throat section.

Curves such as C, B, and A are typical for flows in the range of subsonic velocities; the expanded part of the nozzle transforms the velocity back into pressure again. This type of flow is normal for incompressible fluids, and these curves are similar to those for water flowing through a venturi meter.

22. Some Aspects of Nozzle Design

Tests have demonstrated that the transformation of pressure energy into kinetic energy in a nozzle can be accomplished with a high degree of efficiency. Measurements by M. S. Kisenko [31] show that even with nozzles having rough interior surfaces the velocity coefficient $\varphi = w/w' = 0.92$. For a correctly designed nozzle with a smooth, well-polished interior surface, values of $\varphi = 0.96$ to 0.98 are attainable. The exact geometry of the converging approach section is not critical. All that is required is that it make a smooth transition with the throat section. Consequently the throat section can be made quite short. Though a well-rounded entrance is not essential, it is of advantage in that it permits of a shorter approach section. The geometry of nozzles for measuring the flow of fluids should be patterned after the standards recommended by the A.S.M.E. Special Research Committee on Fluid Meters and should be installed in accordance with the recommendations of that committee. These nozzles are designed with a well-rounded entrance, usually of elliptical shape. In nozzles which are to be used for reaction propulsion devices, such as rocket motors, the approach section need not be well rounded. It can be a conical convergence, and no measurable loss in thrust will be experienced for a range of included angles varying from 50° to 70°.

The total included angle (2α) of the conical divergence of the nozzle must be held between certain limits if separation of the jet from the nozzle walls is to be avoided. From the point of view of light weight and minimum heat losses the divergence angle α should be as large as permissible in jet-propulsion nozzles. According to reference 31 the most favorable value for the cone angle (2α) for thrust motor nozzles is approximately 25°. This conclusion is based on tests where the pressure in the outlet section of the nozzle was kept equal to the pressure of the surrounding atmosphere. Most rocket motor nozzles operate with the pressure in the outlet section slightly above that of the surrounding atmosphere (see Chapter 12), and the divergence angle for such a nozzle can be as high as $\alpha = 17°$ without any serious loss in thrust. In general, it is recommended that the divergence angle α be less than 15°.

On the basis of his tests Kisenko concluded in addition to the results discussed above that (1) a nozzle with a conical divergence and ending with a cylindrical portion gives a better velocity distribution than a conventional De Laval nozzle; (2) a nozzle designed in accordance with the Frankl method [38] gives uniformly distributed velocity and static pressure distribution and increases the jet reaction 2 to 3 per cent.

23. Compression Shock

The experiments of Stodola described in the preceding section present a phenomenon associated with supersonic flow. It was seen that if the back pressure was higher than that required to give maximum discharge with subsonic exit velocity, but less than that to produce complete expansion of the gas at the exit section, then smooth flow consistent with the pressure ratio and given area ratio is not possible.[6] A more or less discontinuous rise in pressure occurs at some location in the divergent portion of the nozzle, the location being influenced by the magnitude of the back pressure. Because of the shock wave the fluid experiences a large loss in kinetic energy and leaves the nozzle with subsonic velocity. The loss in kinetic energy is larger than the increase in pressure energy; since the process is a non-reversible adiabatic the loss in kinetic energy is converted into heat which remains in the fluid.[16]

The type of flow described above can exist only if the fluid moves with supersonic speed upstream to the shock. The normal velocity of the fluid leaving the shock is always subsonic.[6]

Figure 36 illustrates the manner in which the pressure may change in the direction of flow along the nozzle. The lowest curve illustrates

the pressure variation along the nozzle with the correct back pressure
(isentropic expansion). The dotted curves are lines of constant total
energy for three different back pressures. The vertical lines represent
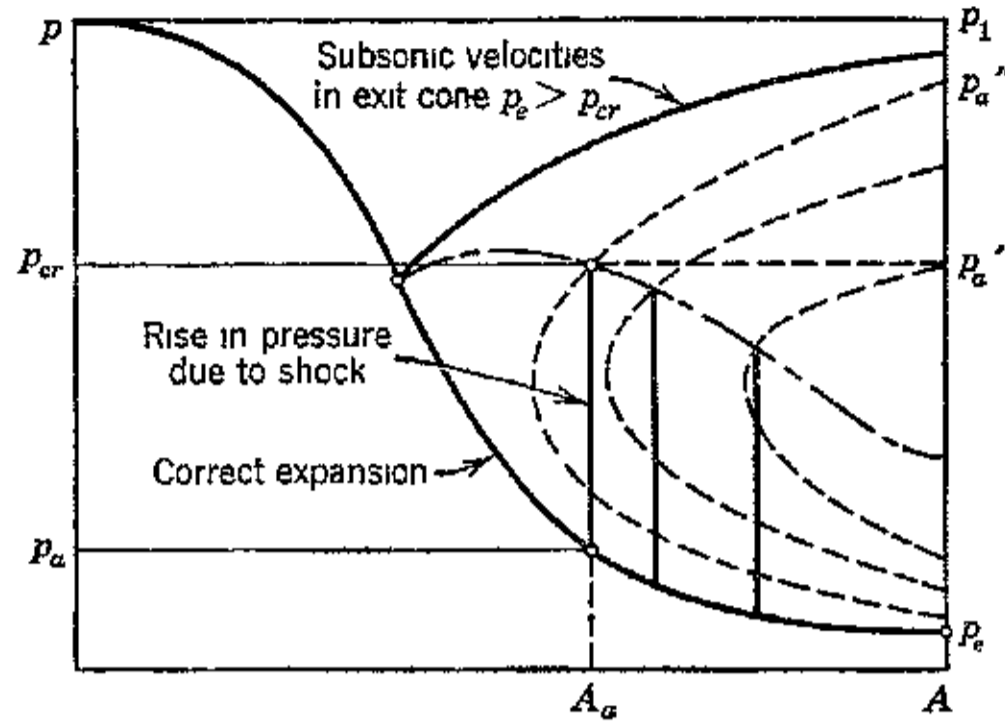
FIG 36.   Effect of back pressure upon the static pressure along a converging-
diverging passage.

the increased pressure due to shock. Thus if the pressure decreases
adiabatically to the area A_a, and the back pressure is p_a'', the pres-
sure increases rapidly from the value p_a to the value p_a' due to shock
and then more gradually to the final back pressure p_a''. A method for
calculating the constant energy lines is presented in reference 16

Refer to Fig. 37. Let it be assumed that the fluid flows in a direc-
tion perpendicular to a shock wave which is assumed fixed in space
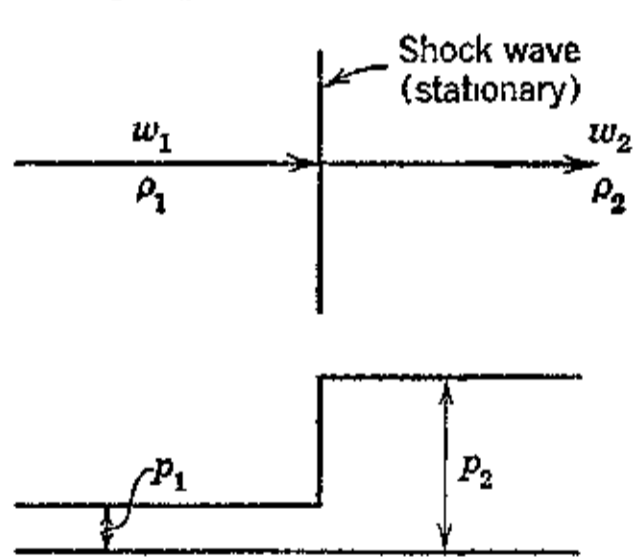
FIG 37.   Isentropic flow through
a discontinuity

Then by continuity the rate of mass
flow m is

$$m = \rho_1 w_1 = \rho_2 w_2 \qquad (131)$$

The momentum equation for the
fluid flowing through the shock, since
the flow area is constant, is given by

$$p_2 - p_1 = m(w_1 - w_2) \qquad (132)$$

The work done per second by the
pressures p_1 and p_2, respectively, is
$p_1 w_1$ and $p_2 w_2$. The increase in kinetic
energy is $(m/2)(w_2^2 - w_1^2)$. The
change in the internal energy of the gas in flowing through the shock
wave, foot-pounds per slug, is from equation 1·50.

$$J(u_1 - u_2) = J c_v(T_2 - T_1) = \frac{1}{k - 1}\left(\frac{p_2}{\rho_2} - \frac{p_1}{\rho_1}\right) \qquad (133)$$

Hence the energy equation for the flow through the shock wave is

$$p_1 w_1 - p_2 w_2 + \frac{m}{2}(w_2{}^2 - w_1{}^2) = \frac{m}{k-1}\left(\frac{p_2}{\rho_2} - \frac{p_1}{\rho_1}\right) \quad (134)$$

or

$$p_1 w_1 - p_2 w_2 + \frac{m}{2}(w_2 - w_1)(w_2 + w_1) = \frac{m}{k-1}\left(\frac{p_2}{\rho_2} - \frac{p_1}{\rho_1}\right) \quad (135)$$

Substituting from equation 132 into equation 135 gives

$$p_1 w_1 - p_2 w_2 - \left(\frac{p_1 - p_2}{2}\right)(w_2 + w_1) = \frac{m}{k-1}\left(\frac{p_2}{\rho_2} - \frac{p_1}{\rho_1}\right) \quad (136)$$

Rearranging and dividing by m

$$\frac{1}{2}(p_1 + p_2)\left(\frac{w_1 - w_2}{m}\right) = \frac{1}{k-1}\left(\frac{p_2}{\rho_2} - \frac{p_1}{\rho_1}\right) \quad (137)$$

But, from equation 131, $w_1/m = 1/\rho_1$ and $w_2/m = 1/\rho_2$; hence equation 137 becomes

$$\frac{1}{2}(p_1 + p_2)\left(\frac{1}{\rho_1} - \frac{1}{\rho_2}\right) = \frac{1}{k-1}\left(\frac{p_2}{\rho_2} - \frac{p_1}{\rho_1}\right) \quad (138)$$

Equation 138 relates the pressures and densities on the two sides of the shock wave. Since the process is irreversible it is accompanied by an increase in entropy. It can be shown [28] that because of the requirement that the entropy of the gas must increase after the gas flows through the shock wave, the latter is always a compression wave. The density ratio is from equation 138

$$\frac{\rho_2}{\rho_1} = \frac{(k-1)p_1 + (k+1)p_2}{(k-1)p_2 + (k+1)p_1} \quad (139)$$

or

$$\frac{\rho_2}{\rho_1} = \frac{\dfrac{p_2}{p_1}\left(\dfrac{k+1}{k-1}\right) + 1}{\dfrac{p_2}{p_1} + \left(\dfrac{k+1}{k-1}\right)} \quad (140)$$

The preceding equations assume that there is a discontinuity in the flow process. In a real fluid no discontinuity can exist and the propagation of a shock wave of the permanent type is explained from the bases of the viscosity of the fluid or its thermal conductivity, which make this type of wave possible.[28]

Shock-wave phenomena are of importance in connection with flight at supersonic speed because of their effect on the aerodynamic resistance to flight. They are of importance also in diffusers for supersonic ramjets.
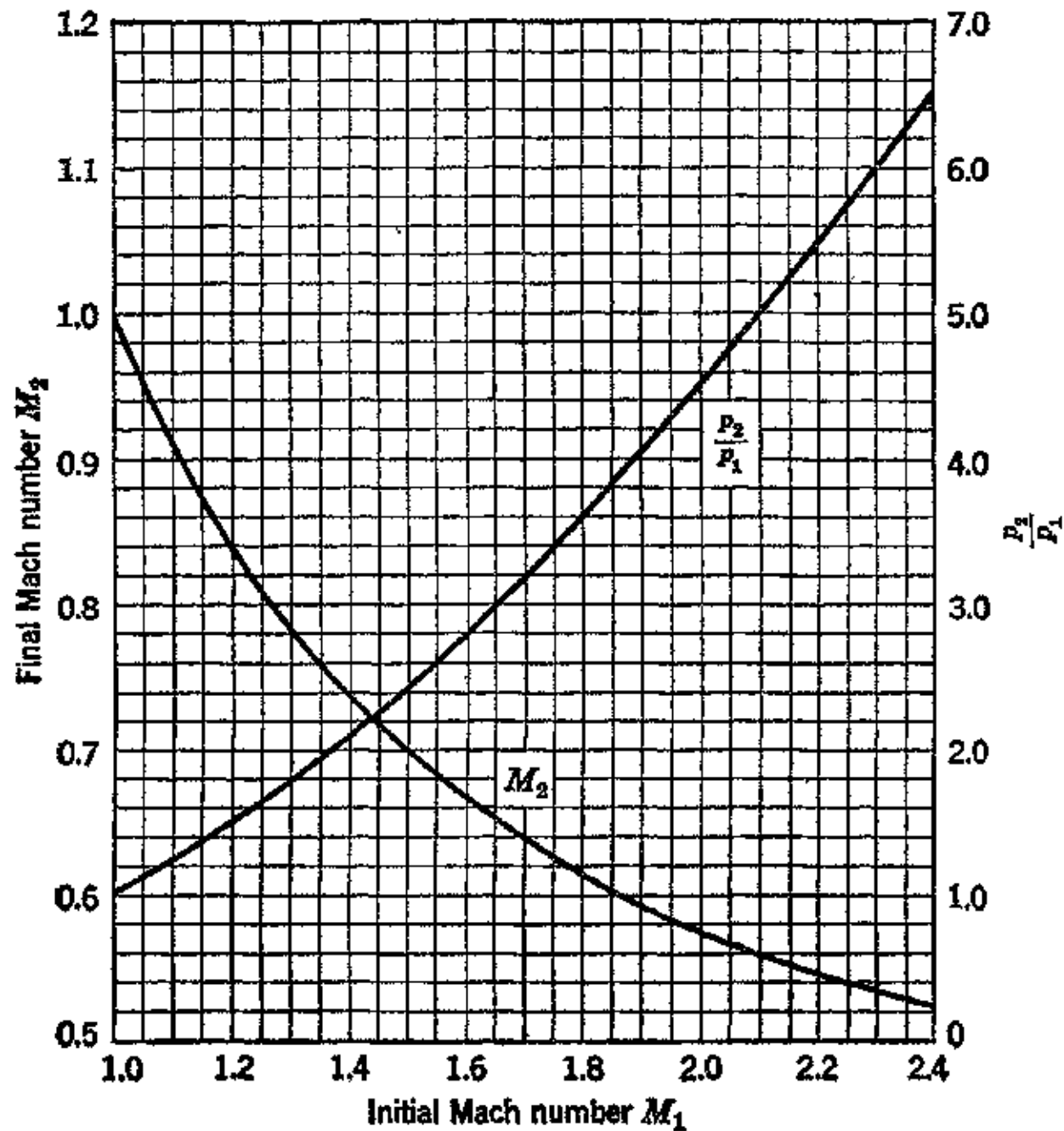
FIG. 38. Final Mach number and pressure ratio as a function of initial Mach number for a normal shock (normal air).

The relationship between the Mach number M_1 of the gas upstream to a plane compression shock and M_2 after the shock [34] is given by

$$\frac{1 + kM_1{}^2}{M_1\sqrt{M_1{}^2 + \dfrac{2}{k-1}}} = \frac{1 + kM_2{}^2}{M_2\sqrt{M_2{}^2 + \dfrac{2}{k-1}}} \tag{141}$$

The corresponding equation for the pressures p_1 and p_2 is

$$\frac{p_1}{p_2} = \frac{1 + kM_2{}^2}{1 + kM_1{}^2} \tag{142}$$

This last relationship is plotted in Fig. 38.

In addition to plane or normal compression shocks of the aforementioned type, shocks of the following characteristics are associated with the supersonic flow of gas entering a device such as a diffuser.

1. Normal shock upstream to the entrance, with no pressure recovery downstream.

2. Normal shock upstream with subsonic velocities accompanied by pressure recovery downstream.

3. Oblique shock fronts followed by subsonic speed, or a succession of oblique shocks.

The above does not include all the shock phenomena associated with supersonic air flow approaching ducts, but it does include the principal types. Further, discussion of supersonic air flow is beyond the scope of this book. Nevertheless, because of the importance of this subject of shock waves to high-speed aircraft and diffusers, some of the principal equations, taken from reference 29, are presented below for convenience. The specific heat ratio for air used in these equations is $k = 1 4$

$$\frac{p_2}{p_1} = \frac{1}{6}(7M_1^2 - 1) \tag{143}$$

$$\frac{p_1}{p_2} = \frac{1}{6}(7M_2^2 - 1) \tag{144}$$

$$\frac{w_2}{w_1} = \frac{\rho_1}{\rho_2} = \frac{M_1^2 + 5}{6M_1^2} \tag{145}$$

$$\frac{p_2 - p_1}{p_2 + p_1} = \frac{7}{5}\left(\frac{\rho_2 - \rho_1}{\rho_2 + \rho_1}\right) \tag{146}$$

$$M_2^2 = \frac{M_1^2 + 5}{7M_1^2 - 1} \tag{147}$$

$$w_1 w_2 = a^2 \tag{148}$$

$$\frac{T_2}{T_1} = \frac{a_2^2}{a_1^2} = \left(\frac{7M_1^2 - 1}{6}\right)\left(\frac{5 + M_1^2}{6M_1^2}\right) \tag{149}$$

24. General Equation for Flow of Gases in Pipes.

The general dynamic equation for the flow of a gas, including friction and neglecting elevation changes ($dz = 0$), is given by equation 6. In that equation the friction force $d\Re$ depends upon the area of the passage wall in contact with the gas and the friction per unit

area τ of the wall surface. Let y be the *wetted perimeter* and dx the length of passage under consideration; then the wall area in contact with the fluid is $y\,dx$. The total friction force acting on the fluid element $d\mathcal{R}$ is given by

$$d\mathcal{R} = \tau y\,dx \tag{150}$$

The friction force per unit area is usually stated in terms of a friction coefficient f, where f is defined, as in reference 13, by the equation

$$f = \frac{\tau}{\frac{1}{2}\rho w^2} = \frac{2g\tau}{\gamma w^2} \tag{151}$$

Hence the friction force per unit area is

$$\tau = \frac{\gamma w^2}{2g} f \tag{152}$$

Substituting for τ gives the following expression for the friction force

$$d\mathcal{R} = \frac{\gamma}{2g} w^2 fy\,dx \tag{153}$$

Let $m = A/y =$ the hydraulic radius; then the dynamic flow equation becomes

$$v\,dp + \frac{w}{g}\,dw + f\frac{w^2}{2g}\frac{dx}{m} = 0 \tag{154}$$

For perfect gases this equation can also be written in the form presented earlier in Section 2, as equation 7a. Thus

$$dp = -\frac{p}{gRT}f\frac{w^2}{2m}\,dx - \frac{p}{gRT}w\,dw \tag{155}$$

Sometimes it is more convenient to state the flow equation in terms of the weight rate of gas flow G lb/sec. Substituting for w and dw from equations 79 and 87 into equation 155 gives

$$v\,dp + \frac{1}{g}\left(\frac{G}{A}\right)^2\left(v\,dv - \frac{v^2}{A}\,dA\right) + \frac{1}{2g}\left(\frac{G}{A}\right)^2 f\frac{v^2}{m}\,dx = 0 \tag{156}$$

For a straight passage of constant cross-sectional area, such as a pipe or duct, $dA = 0$, so that

$$v\,dp + \frac{1}{g}\left(\frac{G}{A}\right)^2 v\,dv + \frac{1}{2g}\left(\frac{G}{A}\right)^2 f\frac{v^2}{m}\,dx = 0 \tag{157}$$

It can be shown by dimensional analysis [27] that the friction coefficient f is a function of the Reynolds number R_e, and the Mach number M. Experiments by J. H. Keenan with steam [13] and by W. Frössel with air [14] indicate that in the regime of turbulent flow the friction coefficient is practically independent of the Mach number. Their experiments also indicated that f is the same function of R_e for both compressible and incompressible fluids.

For smooth pipes Nikuradze [28] has proposed the following relation between f and R_e

$$\frac{1}{\sqrt{f}} = 0.3959 + 4 \log_{10} (R_e \sqrt{f}) \qquad (158)$$

The following equation by Koo correlates the data for long smooth pipes [30] for Reynolds numbers ranging from 3×10^3 to 3×10^6.

$$f = 0.00140 + 0.125 R_e^{-0.32} \qquad (159)$$

For a range of R_e values from 5×10^3 to 200×10^3 the following equation correlates the data for smooth pipes

$$f = 0.046 R_e^{-0.2} \qquad (160)$$

R. P. Genereaux [15] suggests, on the basis of his analysis of pipe friction data, the following simpler equation as being sufficiently accurate for most engineering purposes.

$$f = 0.04 R_e^{-0.16} \qquad (161)$$

This equation is applicable for Reynolds numbers ranging from 4×10^3 to 20×10^6. In the usual range of Reynolds numbers, 250,000 to 500,000, the friction coefficient may be assumed to be a constant at the value 0.005 (N.A.C.A.T.M. 844).

If a constant value of f is applicable, or if a mean value for the length of passage is used, then since $m = D/4$ for a pipe, where D is the diameter in feet, equation 157 becomes

$$\int_1^2 \frac{dp}{v} + \frac{1}{g}\left(\frac{G}{A}\right)^2 \log_e \frac{v_2}{v_1} + \frac{2}{g}\left(\frac{G}{A}\right)^2 f \frac{dx}{D} = 0 \qquad (162)$$

Before proceeding to a discussion of the integration of equation 162 it should be noted that the friction coefficient f is that used in the *Fanning equation* for pipe friction loss. According to the Fanning equation, the pressure loss in a pipe due to friction dp_F is given by

$$dp_F = \frac{f \gamma w^2}{2gm} dx = \frac{4f\gamma w^2}{2gD} dx = 2f\left(\frac{G}{A}\right)^2 \frac{v}{gD} dx \qquad (163)$$

Many books use the D'Arcy formula for evaluating pipe friction loss. In that equation, if dz_F is the head loss due to friction, then

$$dp_F = \gamma \, dz_F = f' \frac{w^2\gamma}{2gD} dx = f' \left(\frac{G}{A}\right)^2 \frac{v}{2gD} dx \qquad (164)$$

From the foregoing equation it is seen that the *friction factor f'* in the D'Arcy equation is four times the friction coefficient f in the Fanning equation. The friction coefficient used in this book is that based on the Fanning equation.

Reference to equation 156 will show that, if the equation is divided by v, the specific volume, so that its dimensions are force per unit area, then the third term is identical with the pressure loss due to friction as defined by the Fanning equation.

For more detailed discussions of the friction coefficient for pipe flow the reader is referred to references 13, 14, 20, 21, 22, and 47.

It is apparent that for a conduit of constant area equation 86 reduces to

$$\frac{dp}{p} = \frac{dT}{T} - \frac{dw}{w} \qquad (165)$$

But from equation 155

$$\frac{dp}{p} = -\frac{1}{gRT} fw^2 \frac{dx}{2m} - \frac{1}{gRT} w \, dw \qquad (166)$$

which can be written in the form

$$\frac{dp}{p} = -kM^2 f \frac{dx}{2m} - kM^2 \frac{dw}{w} \qquad (167)$$

Equating 165 and 167

$$-f \frac{kM^2}{2m} dx - kM^2 \frac{dw}{w} = \frac{dT}{T} - \frac{dw}{w} \qquad (168)$$

If there is no change in total energy, the friction heat remains in the gas Substituting from equations 43 and 90 for dT/T and dw/w in equation 168 gives the following expression for $(fk/2m)dx$

$$\frac{fk}{2m} dx = \frac{(1 - M^2) \, dM}{M^3 \{[(k-1)/2]M^2 + 1\}} \qquad (169)$$

Equation 169 can be integrated by expanding it into a series. It is simpler, however, as pointed out in reference 34 to perform the integration by either the trapezoid or Simpson's rules [46] for the distance x which changes the initial Mach number to the value $M = 1$. Thus

$$\frac{fkx}{2m} = \int_{M=M}^{M=1} \frac{(1 - M^2)\, dM}{M^3\{1 + [(k - 1)/2]M^2\}} \qquad (170)$$

For normal air the last equation becomes

$$\frac{fkx}{2m} = \int_{M=M}^{M=1} \frac{(1 - M^2)\, dM}{M^3\{0.1975M^2 + 1\}} \qquad (171)$$
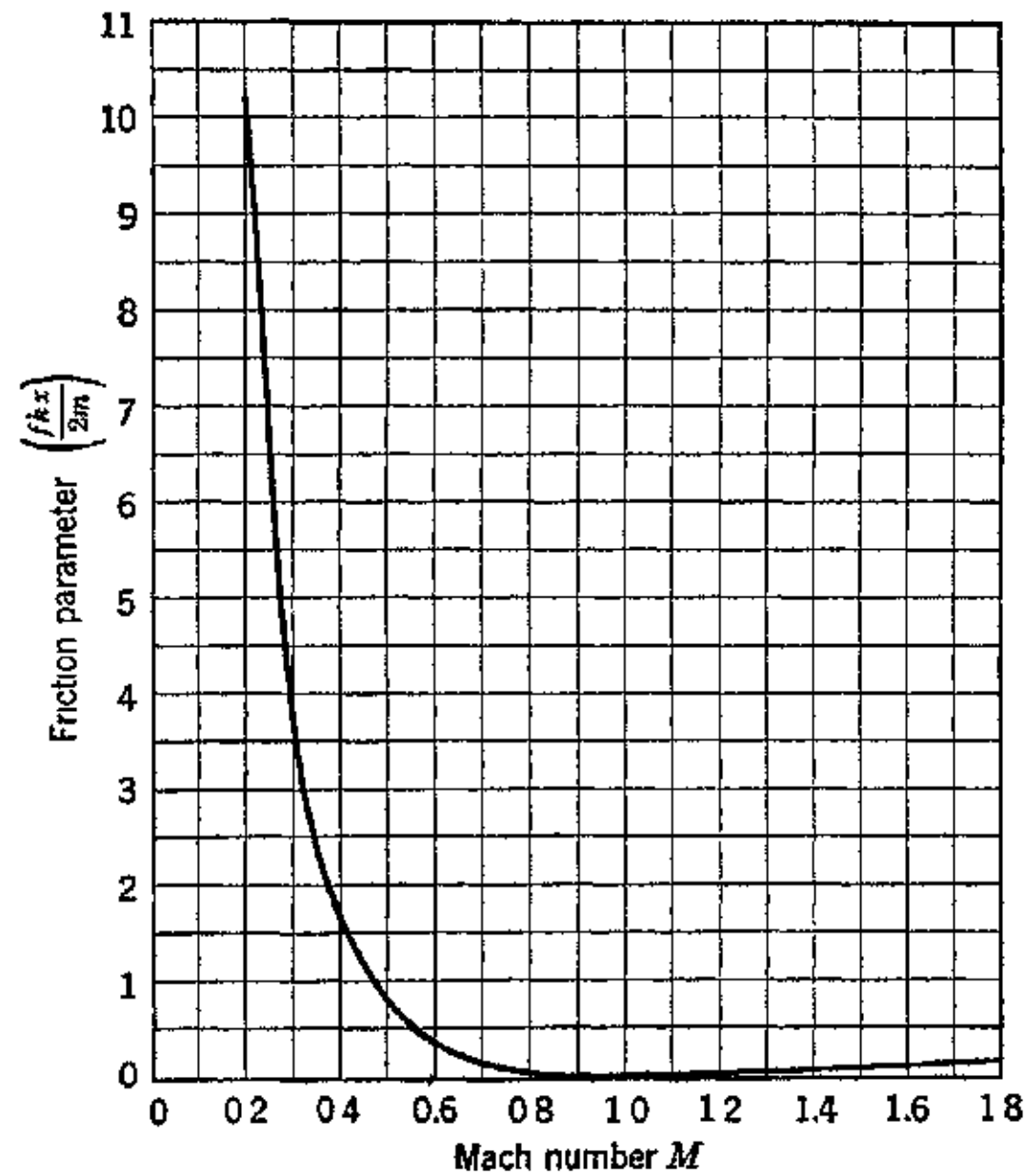
FIG. 39. Friction parameter as a function of Mach number for flow in a straight constant-area duct.

Figures 39 and 40 present the friction parameter $(fkx/2m)$ as a function of M. The curves were obtained by using Simpson's rule From this curve the length of straight pipe required to change the Mach number from one value to another when the flow involves friction is readily determined.
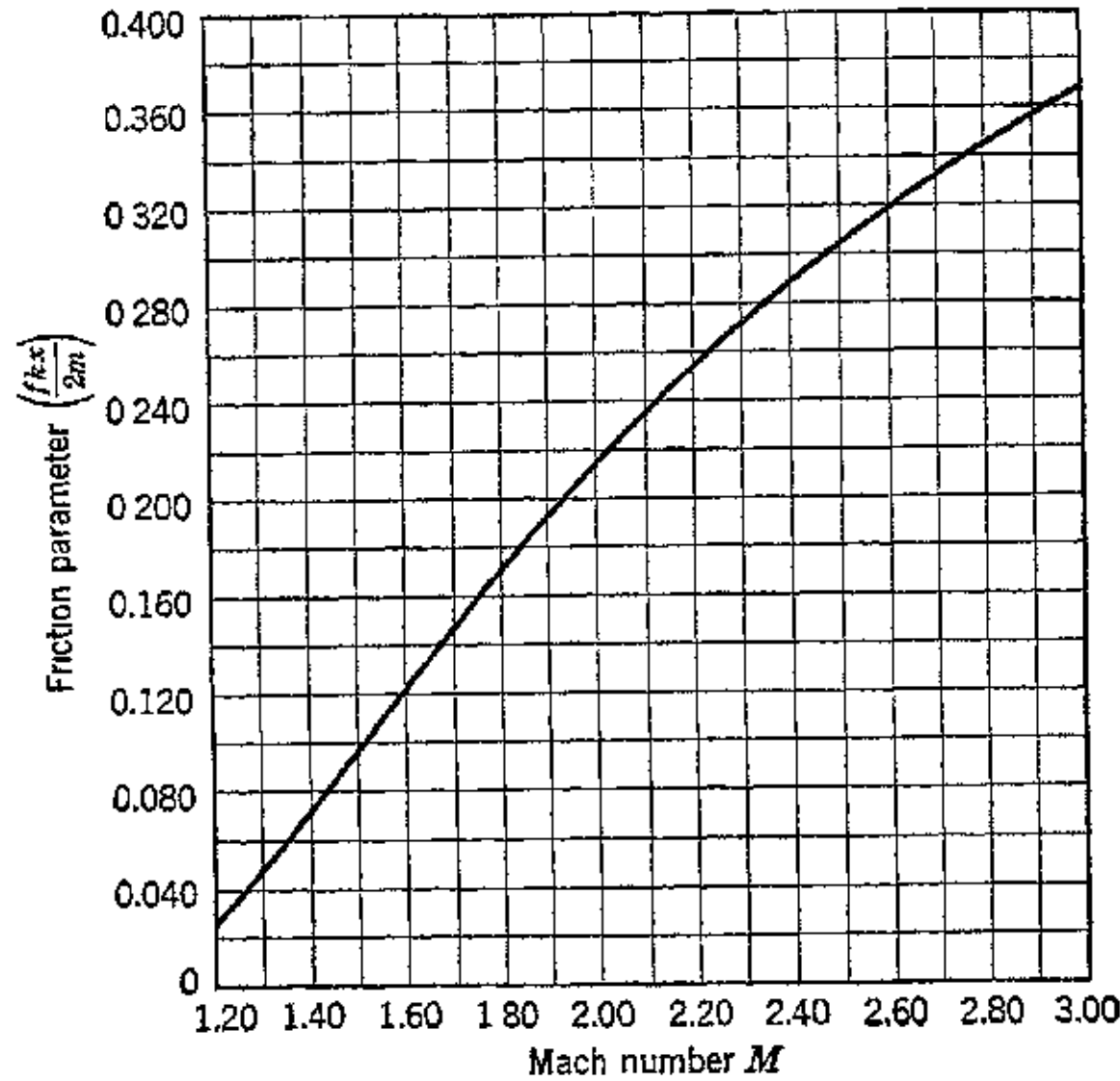
FIG. 40. Friction parameter as a function of Mach number for flow in a straight constant-area duct.

25. Flow in Pipes with Friction and No Heat Transfer (dQ = O)

This type of flow is comparable to that for a perfectly insulated pipe or to flow so rapid that no appreciable heat transfer can take place. The friction energy heats up the gas and changes its specific volume and enthalpy. As pointed out in Section 8, the relationship between the pressure and specific volume is given by pv^n = constant, where $n \neq k$. The equation for the condition of the gas as it flows along the pipe can be determined by the methods of references 12 and 13 presented below.

It has been pointed out by A. Stodola [12] that the energy and continuity equations give no implicit information regarding the influence of pipe friction. Thus, if h_i is the initial enthalpy of the fluid and h is its enthalpy at any point in the pipe, the aforementioned equations become

$$h_i - h = \frac{w^2}{2Jg} - \frac{w_i^2}{2Jg} \tag{172}$$

and

$$Gv = Aw \tag{173}$$

Further, since the weight rate of flow G lb/sec is constant for all cross-sectional areas A, then

$$w^2 = \left(\frac{G}{A}\right)^2 v^2 \tag{174}$$

Substituting equation 174 into equation 172 gives the following equation for any section of the pipe

$$h + \left(\frac{G}{A}\right)^2 \frac{v^2}{2gJ} = h_t \tag{175}$$

Equation 175 is the equation for a Fanno line (see references 12 and 3), and is applicable irrespective of the law of friction that prevails. By applying this equation a family of curves can be drawn for $G/A =$ constant for the same value of the initial enthalpy $h = h_t$. A plot of the Fanno lines [3] will show that, since the flow process is such that the change in the condition of the gas must involve an increase in entropy, the velocity of a gas expanding in a cylindrical pipe can never exceed its acoustic velocity.

For perfect gases, the enthalpy is, in general, given by

$$h = \frac{k}{J(k-1)} pv = \frac{B}{J}(pv) \tag{176}$$

where the constant $B = k/(k-1)$.

Consider any two sections in the flow path and write their Fanno-line equations, denoting the sections by the subscripts 1 and 2, and substitute for the corresponding values of h_1 and h_2 from equation 176. Then

$$h_t = \frac{B}{J}(p_1 v_1) + \left(\frac{G}{A}\right)^2 \frac{v_1^2}{2gJ} - \frac{w_t^2}{2gJ} = \frac{B}{J}(p_2 v_2) + \left(\frac{G}{A}\right)^2 \frac{v_2^2}{2gJ} - \frac{w_t^2}{2gJ}$$

or in general

$$\left(\frac{G}{A}\right)^2 \frac{v_1^2}{2gJ} + \frac{B}{J} p_1 v_1 = \left(\frac{G}{A}\right)^2 \frac{v_2^2}{2gJ} + \frac{B}{J} p_2 v_2 \tag{177}$$

But $(G/A)^2 = (w_1/v_1)^2 = (w_2/v_2)^2$. Substituting for $(G/A)^2$ into equation 177 gives

$$\frac{w_1^2}{2gJB} + \frac{p_1 v_1}{J} = \frac{w_2^2}{2gJB} + \frac{p_2 v_2}{J} \tag{178}$$

Rearranging and substituting for $B = k/(k-1)$

$$p_1 v_1 \left[1 + \frac{(k-1)w_1^2}{2gkp_1 v_1} \right] = p_2 v_2 \left[1 + \frac{(k-1)w_2^2}{2gkp_2 v_2} \right] \tag{179}$$

Noting that $a^2 = gkpv$ and $M = w/a$, equation 179 can be written in the following form.

$$pv \left[1 + \frac{k-1}{2} M^2 \right] = \text{Constant} \tag{180}$$

Equation 180 is the Fanno-line equation in a different form.

To obtain a relationship between the pressure p and the specific volume v for the gas at any point it is simpler to substitute for the enthalpy h from equation 176 into equation 175, solve for p, and differentiate; note that B, h, and G/A are constants. The result is

$$dp = - \frac{1}{2gB} \left(\frac{G}{A} \right)^2 dv - \frac{Jh_i}{B} \frac{dv}{v^2} \tag{181}$$

Dividing equation 181 by v gives the following expression for the first term of equation 162

$$\frac{dp}{v} = - \frac{1}{2gB} \left(\frac{G}{A} \right)^2 \frac{dv}{v} - \frac{Jh_i}{B} \frac{dv}{v^3} \tag{182}$$

Substituting from equation 181 into equation 162 and integrating between the limits 1 and 2, assuming that f is constant (that is, a mean value is to be used for the pipe length in question) and letting $x_2 - x_1 = l =$ the length of the pipe, the following result is obtained.

$$\frac{Jh_i}{2B} \left(\frac{1}{v_2{}^2} - \frac{1}{v_1{}^2} \right) + \frac{1}{g} \left(\frac{G}{A} \right)^2 \left(1 - \frac{1}{2B} \right) \log_e \frac{v_2}{v_1} + \frac{2}{g} \left(\frac{G}{A} \right)^2 f \frac{l}{D} = 0 \tag{183}$$

Substituting for $B = k/(k-1)$ and solving for fl/D gives

$$\frac{fl}{D} = \frac{g}{2} \left(\frac{A}{G} \right)^2 \left[\frac{Jh_i}{2} \left(\frac{k-1}{k} \right) \left(\frac{1}{v_1{}^2} - \frac{1}{v_2{}^2} \right) - \frac{1}{g} \left(\frac{G}{A} \right)^2 \left(\frac{k+1}{2k} \right) \log_e \frac{v_2}{v_1} \right] \tag{184}$$

But from equation 175

$$h_i = \left(\frac{G}{A} \right)^2 \frac{v_1{}^2}{2gJ} + \frac{B}{J} p_1 v_1 = \left(\frac{G}{A} \right)^2 \frac{v_2{}^2}{2gJ} + \frac{B}{J} p_2 v_2$$

Substituting for h_i into equation 184, noting that $(G/A)^2 = w^2/v^2$, that $w_1/w_2 = v_1/v_2$, and $gkpv = a^2$, the result is

$$\frac{4fl}{D} = - \left(\frac{k+1}{2k} \right) \log_e \left(\frac{w_2}{w_1} \right)^2 + \frac{1}{k} \left(\frac{1}{M_1{}^2} + \frac{k-1}{2} \right) \left[1 - \left(\frac{w_1}{w_2} \right)^2 \right] \tag{185}$$

From equation 185 the values of $4fl/D$ for a given value of the initial Mach number M_1 can be calculated for a series of values of
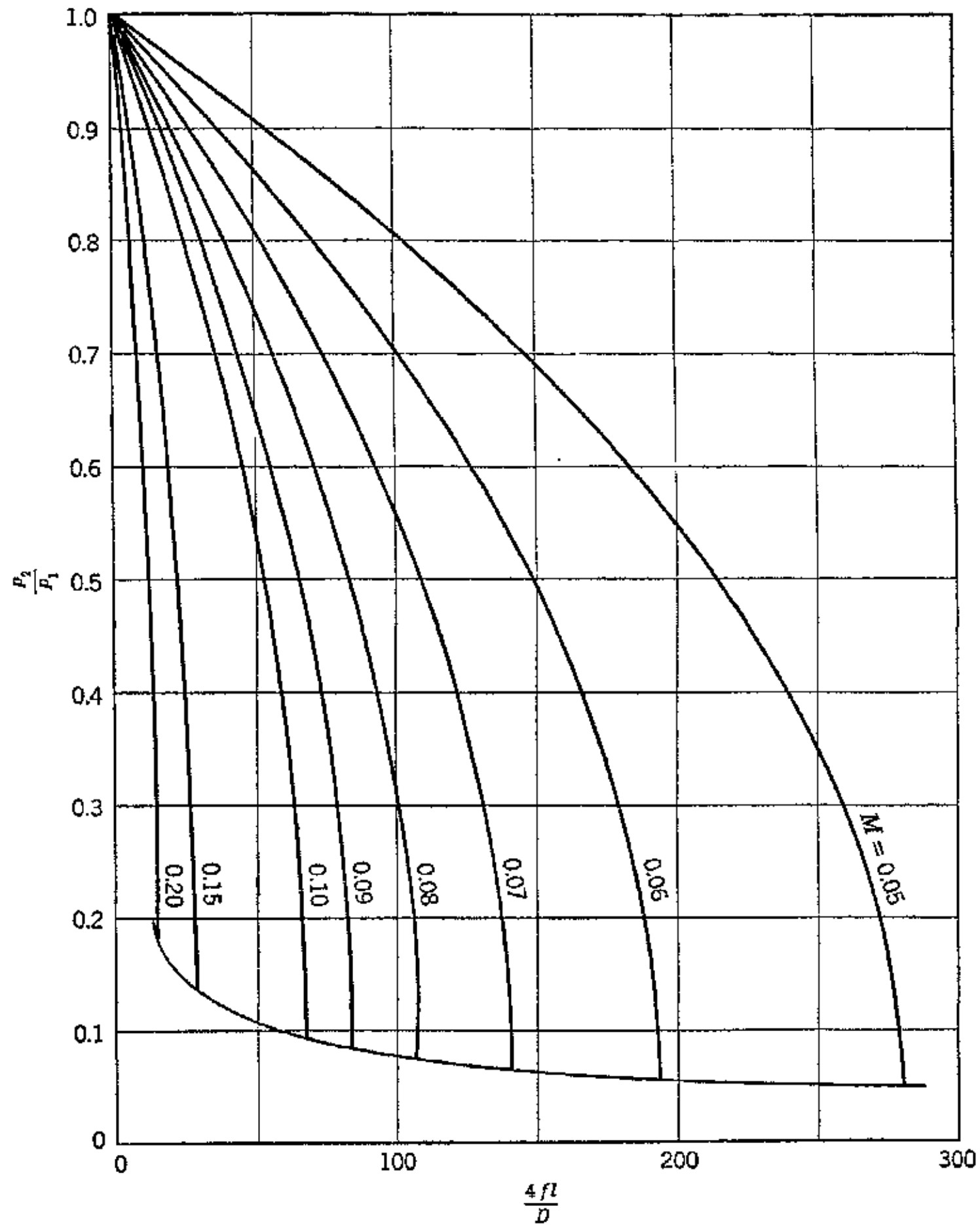
FIG. 41.   Pressure ratio vs. friction parameter for different Mach numbers for adiabatic flow in a straight pipe.

$w_2/w_1 = v_2/v_1$.   If the value of the friction factor is given or known, it is then a simple matter to determine the velocity corresponding to a given pipe length.   It should be noted that the maximum attainable velocity is limited to the local acoustic value.

Figures 41 and 42 are plots of the ratio p_2/p_1 as a function of $4fl/D$ for different initial Mach numbers as the parameter. Similarly, Figs. 43 and 44 present $4fl/D$ vs. $w_2/w_1 = v_2/v_1$ for different constant values of the Mach number.
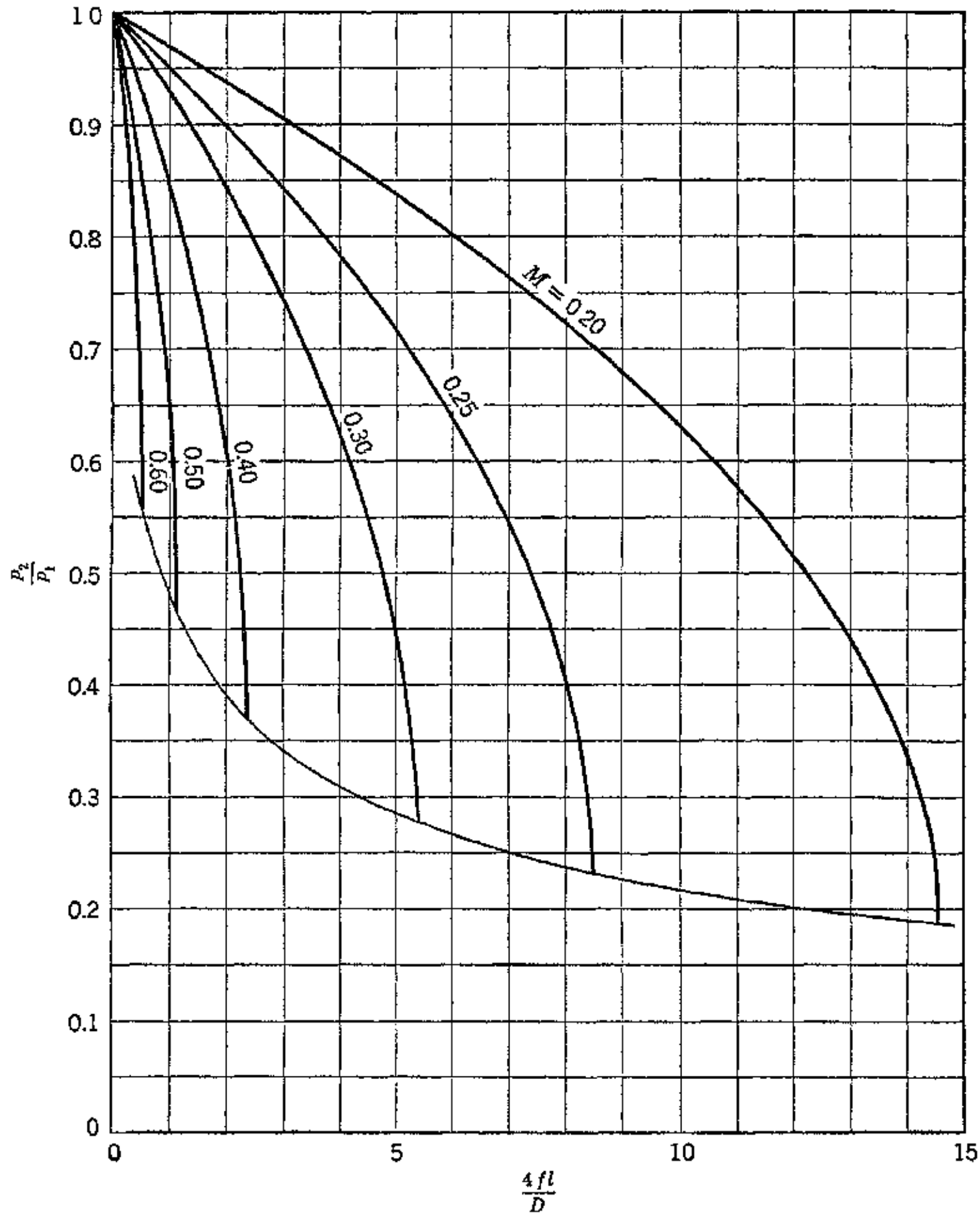
FIG. 42.   Pressure ratio vs. friction parameter for different Mach numbers for adiabatic flow in a straight pipe.
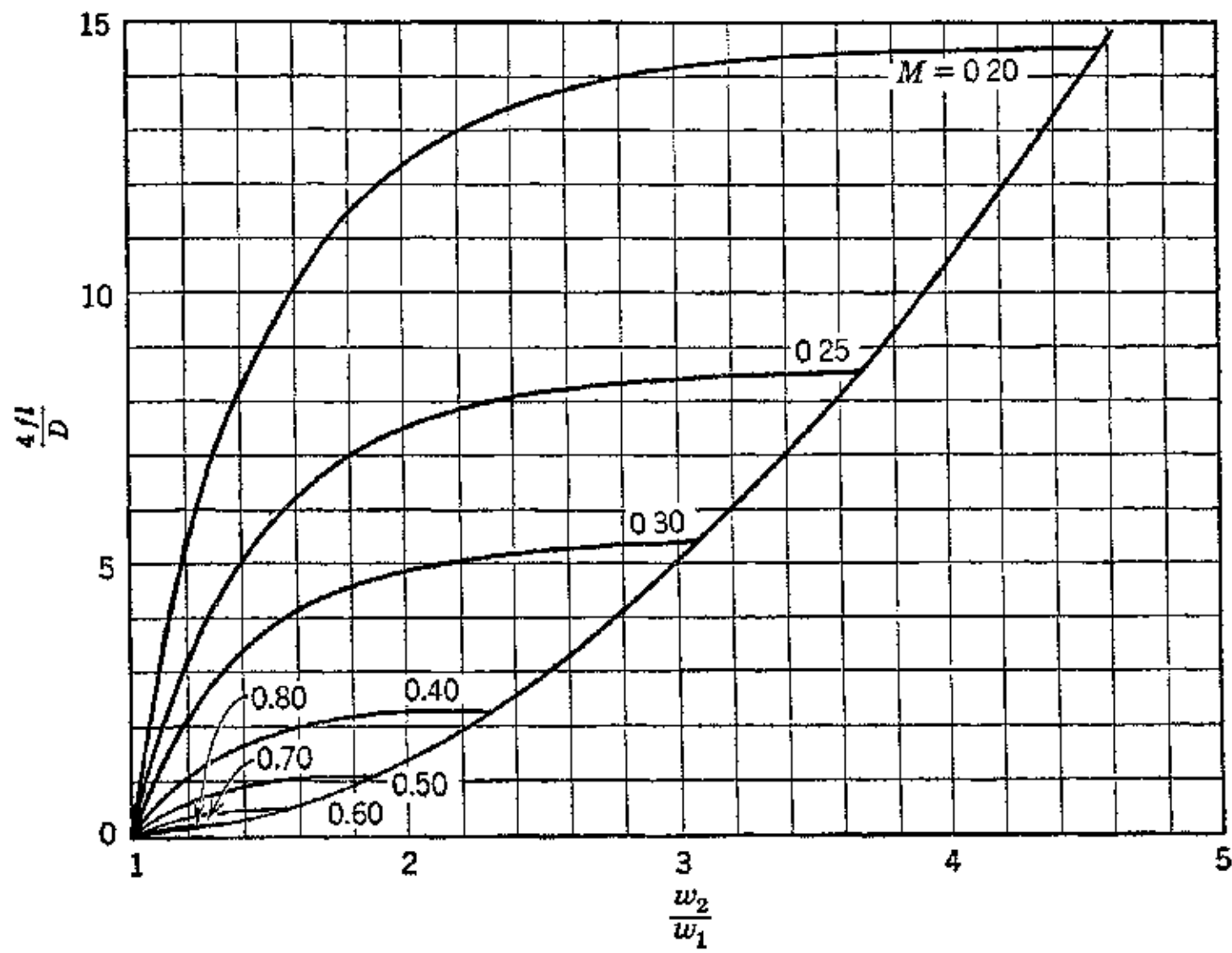
FIG. 43. Friction parameter vs. velocity ratio for different Mach numbers for adiabatic flow in a straight pipe.
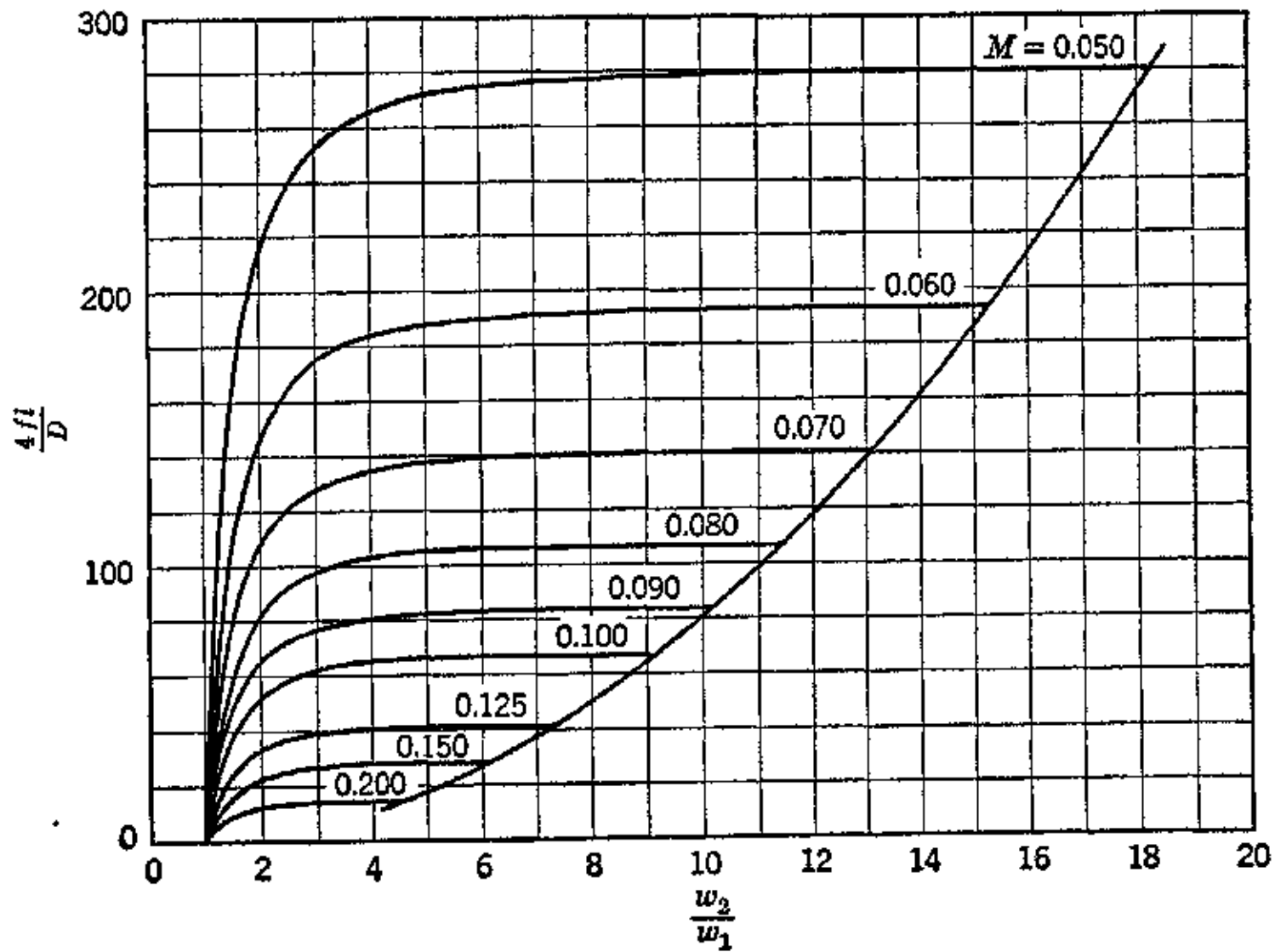
FIG. 44. Friction parameter vs. velocity ratio for different Mach numbers for adiabatic flow in a straight pipe.

141

26. Limiting Conditions for Adiabatic Flow with Friction

The equation for the condition of the fluid as it flows along the pipe, equation 172, does not hold in the neighborhood of $p = 0$; in fact, it is true down to a definite limiting pressure p_L.[7] This arises from the fact that the friction loss in the pipe cannot decrease to zero except at the exit end of the pipe. Beyond this location, owing to the absence of wall friction, it is possible for the gas to expand isentropically to lower pressures than the limiting pressure p_L. The value of p_L, and the corresponding value of v_L, can be determined by equating the slopes of the isentropic condition curve $pv^k =$ constant and that of the actual condition curve equation 161 at the state point corresponding to the coordinates p_L and v_L. Following the method of references 7 and 49, let $b = \dfrac{k-1}{2gk}\left(\dfrac{G}{A}\right)^2$, then equation 178 becomes, on solving for p,

$$p = \frac{p_1 v_1 + b v_1^2}{v} - bv \qquad (186)$$

and the slope of the curve is given by

$$\frac{dp}{dv} = -\frac{(p_1 v_1 + b v_1^2)}{v^2} - b \qquad (187)$$

For the isentropic expansion beyond p_L, differentiating $pv^k =$ constant gives

$$\frac{dp}{dv} = -\frac{kp}{v} \qquad (188)$$

Hence, substituting the limiting conditions p_L and v_L

$$\frac{kp_L}{v_L} = \frac{p_1 v_1 + b v_1^2}{v_L^2} + b \qquad (189)$$

from which

$$p_L v_L = \frac{p_1 v_1 + b v_1^2}{k} + \frac{b v_L^2}{k} \qquad (190)$$

This value of $p_L v_L$ must be equal to that obtainable from equation 186. Combining equation 186 with equation 190 and solving for the ratio of specific volumes, the result is

$$\left(\frac{v_L}{v_1}\right)^2 = \left(\frac{k-1}{k+1}\right)\left(1 + \frac{p_1}{b v_1}\right) \qquad (191)$$

Substituting for $b = \dfrac{k-1}{2gk}\left(\dfrac{G}{A}\right)^2 = \dfrac{k-1}{2gk}\left(\dfrac{w_1}{v_1}\right)^2$, and $a_1{}^2 = gkp_1v_1$,

into equation 191 gives the following equation for the specific volume ratio

$$\frac{v_L}{v_1} = \frac{w_L}{w_1} = \left\{\frac{k-1}{k+1}\left[1 + \frac{2}{(k-1)M_1{}^2}\right]\right\}^{1/2} \tag{192}$$

The pressure ratio p_L/p_1 is obtained in a similar manner [49] by solving equation 190 and substituting for $b = \dfrac{k-1}{2gk}\left(\dfrac{w_1}{v_1}\right)^2$ and $a_1{}^2 = gkp_1v_1$. Thus

$$\frac{p_L}{p_1} = M_1{}^2\left\{\frac{k-1}{k+1}\left[1 + \frac{2}{(k-1)M_1{}^2}\right]\right\}^{1/2} \tag{193}$$

Since the ratio $G/A = w/v$ is constant throughout the length of the pipe, it follows that

$$\frac{w_L}{w_1} = \frac{v_L}{v_1} \tag{194}$$

Hence, equation 192 gives the ratio of the limiting velocity w_L to the initial velocity w_1, as well as the specific volume ratio.

The acoustic velocity at the exit from the pipe is given by

$$a_L = \sqrt{kgp_Lv_L} = \sqrt{kgp_1v_1\frac{p_Lv_L}{p_1v_1}} = a_1\sqrt{\frac{p_Lv_L}{p_1v_1}} \tag{195}$$

Substituting for v_L/v_1 and p_L/p_1 from equations 192 and 193, respectively, into equation 195, the following equation is obtained for the acoustic velocity at the exit section

$$a_L = w_1\left\{\frac{k-1}{k+1}\left[1 + \frac{2}{(k-1)M_1{}^2}\right]\right\}^{1/2} \tag{196}$$

Equation 196 is the same as equation 192 for the limiting velocity w_L for irreversible adiabatic flow. This signifies that as the gas flows through the pipe its pressure decreases until the gas attains a velocity corresponding to the acoustic velocity for the local pressure and specific-volume conditions. Any further reduction of the back pressure into which the pipe discharges has no effect on the gas velocity.

The limiting values of the ratios $w_L/w_1 = v_L/v_1$, and p_L/p_1 for air, plotted as functions of the entering Mach number for adiabatic flow with friction, are presented in Fig. 45.

It is apparent from these curves and the discussions of the preceding sections that where gases are transported at high velocities in ducts great care must be exercised in their design. As discussed in connection with the flow through nozzles, the maximum weight rate of flow through a duct is attained when the local acoustic velocity is attained in any section perpendicular to the main direction of flow. This has an important bearing on the design of the flow passages for gas turbines and thermal jet engines,[45] and an analysis of the
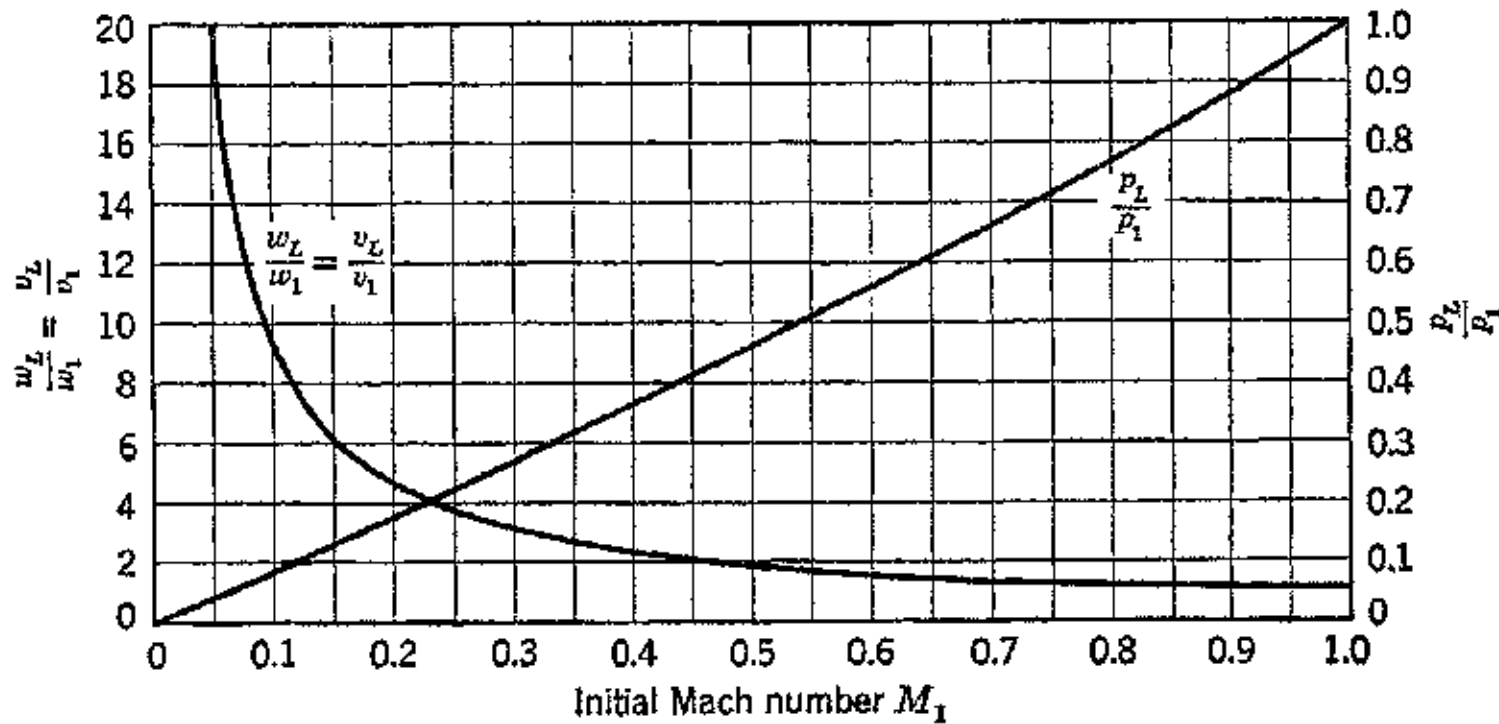
FIG. 45. Limiting velocity and pressure ratios for adiabatic flow in a straight pipe as functions of initial Mach number.

flow path to determine the Mach numbers under the different flow conditions is essential if "choking" of the flow at some point is to be avoided.

27. Isothermal Flow in Pipes with Friction

The dynamic equation for the flow of a compressible fluid in a pipe is given by equation 157, which is repeated here for convenience. Thus, with $m = D/4$

$$v\,dp + \frac{1}{g}\left(\frac{G}{A}\right)^2 v\,dv + \frac{2f}{g}\left(\frac{G}{A}\right)^2 \frac{v^2}{D}\,dx = 0 \qquad (197)$$

For isothermal flow the Reynolds number remains constant since the dynamic viscosity is a function mainly of the temperature. Hence, the friction coefficient f is also constant. The equation of state is

$$pv = \text{Constant}$$

or

$$\frac{dp}{p} = -\frac{dv}{v} \quad \text{(isothermal flow)} \qquad (198)$$

The continuity equation gives the relationship

$$\frac{dw}{w} = \frac{dv}{v} \tag{199}$$

Substituting $(G/A)^2 = (w/v)^2$ into equation 197

$$v\,dp + \frac{1}{g}w^2\frac{dv}{v} + \frac{2f}{g}\frac{w^2}{D}dx = 0 \tag{200}$$

or

$$p\,dp + \frac{w^2p^2}{gpv}\left(\frac{dv}{v} + 2f\frac{dx}{D}\right) = 0 \tag{201}$$

Substituting for $dv/v = dw/w$ from equation 199 gives

$$\frac{gv\,dp}{w^2} + \frac{dw}{w} + 2f\frac{dx}{D} = 0 \tag{202}$$

Combining equations 198 and 199 with equation 202 as is done in reference 19,

$$\frac{gpv}{w^2}\left(\frac{dp}{p}\right) - \frac{dp}{p} + 2f\frac{dx}{D} = 0 \tag{203}$$

The limiting values of $p = p_L$ and $w = w_L$ occur when $f\,dx/D = 0$. Substituting, $f\,dx/D = 0$ into equation 203 shows that at the limiting condition

$$\frac{gpv}{w_L{}^2} = 1$$

or the limiting velocity is given by

$$w_L = \sqrt{gp_L v_L} = a_L/\sqrt{k} \tag{204}$$

This equation indicates that the maximum attainable velocity with isothermal flow w_L is less than the acoustic velocity.

The pressure ratio corresponding to the limiting velocity is obtained by combining equation 204 with the continuity equation and the equation of state. Thus

$$\frac{p_L}{p_1} = \frac{v_1}{v_L} = \frac{w_1}{w_L} = \frac{w_1}{a_1}\sqrt{k} = M_1\sqrt{k} \tag{205}$$

By combining the continuity equation, the equation of state, and equation 201, letting $l = x_2 - x_1$, integrating, and rearranging as is done in reference 19, the result is

$$\frac{4fl}{D} = \frac{1}{kM_1{}^2}\left[1 - \left(\frac{p_2}{p_1}\right)^2\right] - 2\log_e\left(\frac{p_1}{p_2}\right) \tag{206}$$

28. *Effect of Friction in Gas Flow*

It has been pointed out in preceding sections that the heat generated in overcoming frictional resistance to flow goes into heating up the gas. This heat increases the random motion of the gas molecules and increases the entropy of the gas. The energy converted into friction decreases the available energy as illustrated in Fig. 6. The available energy decrease is given by

$$T \, ds = \frac{1}{J} E_F = \frac{v}{J} dp_F \qquad (207)$$

where dp_F is the pressure drop due to friction.

The entropy increase can be expressed in terms of the Mach number by applying the method of reference 34. Thus, from equation 207

$$ds = \frac{v}{JT} dp_F \qquad (208)$$

The pressure drop dp_F, due to friction, in the distance dx is from equation 7a, given by

$$dp_F = \frac{pk}{gkRT} \cdot fw^2 \frac{dx}{2m} \qquad (209)$$

Combining 208 and 209 and substituting $M^2 = w^2/gkRT$

$$ds = \frac{R}{J} M^2 \frac{fk \, dx}{2m} \qquad (210)$$

Substituting for $\dfrac{fk \, dx}{2m}$ from equation (169)

$$ds = \frac{R}{J} M^2 \frac{(1 - M^2) \, dM}{M^3 \left[\left(\dfrac{k - 1}{2} \right) M^2 + 1 \right]} \qquad (211)$$

The rate of change in the entropy of the gas with Mach number, ds/dM, is accordingly

$$\frac{ds}{dM} = \frac{R}{J} \frac{(1 - M^2)}{M \left[\left(\dfrac{k - 1}{2} \right) M^2 + 1 \right]} \qquad (212)$$

Equation 212 illustrates an important effect produced by frictional resistance to flow. Thus, when $M = 1$ the derivative $ds/dM = 0$,

which means that this is the condition for the maximum value of the entropy. Since all natural processes tend to approach the condition for maximum entropy, as pointed out in Section 4, the foregoing signifies that, in flow with friction only, the velocity of the gas tends to reach the local acoustic value.

29. Diffuser Action or Compression Flow

Diffusers are of importance to all types of propulsion equipment which induct air from the atmosphere. For bodies moving through the air at either subsonic or sonic speeds the function of the air intake system is to decelerate the air with the minimum of friction so that a large portion of the ideal pressure rise will be recovered. In air intakes moving at supersonic speeds the phenomenon is complicated by the formation of shock waves at the entrance. The discussions here are limited to diffusers for subsonic air flow.

The problems of diffusion arise in the intake air systems of aircraft engines, in the discharge passages from high-speed rotary compressors, and many other applications. Diffusion as a flow process is not as efficient as the reverse process, the expansion of a gas to secure high velocities.

(a) **Ram Efficiency.** The final pressure attained in the diffuser outlet is termed the *ram pressure*, and the ratio of the actual pressure rise effected by the diffuser to the ideal value is called the *ram efficiency* η_r. If p_1 is the static pressure of the entering air, the ideal pressure rise, $\Delta p'$, is given by

$$\Delta p' = p_t - p_1 \tag{213}$$

where p_t is defined by equation 44.

The actual final pressure is $p_2 < p_t$, so that the actual pressure rise $\Delta p = p_2 - p_1$. The ram efficiency is accordingly

$$\eta_r = \frac{\Delta p}{\Delta p'} = \frac{p_2 - p_1}{p_t - p_1} \tag{214}$$

The temperature rise in the diffuser is determined likewise from equation 44. It should be noted, as pointed out in reference 29, that the expression for the ideal temperature rise

$$\Phi = \frac{T_t}{T_1} = 1 + \left(\frac{k-1}{2}\right) M_1{}^2$$

is applicable to the processes of bringing a free stream of gas to stagnation either isentropically or after traversing a shock wave. This means that Φ depends only on the initial Mach number.

(b) **Effect of Friction on Diffusion Process.** It can be shown that the velocity gradient for a flow passage is given by

$$\frac{dw}{dx} = \frac{w}{1 - M^2}\left(\frac{fkM^2}{2m} - \frac{1}{A}\frac{dA}{dx}\right)$$ (215)

If the cross-sectional area of the passage is constant throughout its length, $dA/dx = 0$, and the velocity gradient dw/dx is positive if the flow is subsonic ($M < 1$). Conversely, if the flow is supersonic ($M > 1$) the velocity gradient is negative.

For a divergent passage, dA/dx is positive. Consequently, if the gas enters the diffuser with subsonic velocity, the condition for the accomplishment of a flow compression is that

$$\frac{1}{A}\frac{dA}{dx} > \frac{fkM^2}{2m}$$ (a)

Since the friction factor f has, in general, a value of approximately 0.005, so that the friction term tends to be smaller than the area term, the divergent passage with subsonic flow tends to produce a flow compression (negative velocity gradient). The effect of friction is to oppose this action and will prevent diffusion when

$$\frac{1}{A}\frac{dA}{dx} = \frac{fkM^2}{2m}$$ (b)

If r is the radius of the cross section of a conical diffuser,[34] then $A = \pi r^2$ and $m = r/2$. Hence

$$\frac{dA}{dx} = \frac{dA}{dr}\frac{dr}{dx} = 2\pi r\frac{dr}{dx}$$ (c)

and

$$\frac{1}{A}\frac{dA}{dx} = \frac{2}{r}\frac{dr}{dx}$$ (d)

where dr/dx is the tangent of the angle made by the diffuser wall and the longitudinal axis of the passage.

For a subsonic conical diffuser, therefore, there will be no diffusion when

$$\frac{dr}{dx} = \frac{fkM^2}{2}$$ (e)

It is seen from the above that the effect of friction, in a subsonic diffuser, is to accelerate the gas velocity and oppose the normal diffusion action. In the interests of securing the greatest possible rise in pressure, the friction should be kept as small as possible.

(c) **Energy Efficiency of Diffuser.** The efficiency of the diffuser on an energy basis is that fraction of the kinetic energy which is converted into pressure rise. It can be determined by comparing the kinetic energy which would be obtained by expanding the diffused gas back to the entrance pressure with that obtainable from an expansion from the 100 per cent ram pressure p_t. Since no work is removed from the gas, the stagnation temperature T_t is the same for both expansions. Hence

$$\eta_D = \frac{1 - (p_1/p_2)^{\frac{k-1}{k}}}{1 - (p_1/p_t)^{\frac{k-1}{k}}} \tag{216}$$

Multiplying the numerator and denominator by $(p_t/p_1)^{\frac{k-1}{k}}$ gives the following equation

$$\eta_D = \frac{(p_t/p_1)^{\frac{k-1}{k}} - (p_t/p_2)^{\frac{k-1}{k}}}{(p_t/p_1)^{\frac{k-1}{k}} - 1} \tag{217}$$

Substituting from equation 44 into equation 217

$$\eta_D = 1 - \frac{2}{(k-1)M^2}\left[\left(\frac{p_t}{p_2}\right)^{\frac{k-1}{k}} - 1\right] \tag{218}$$

For normal air with $k = 1.395$ this becomes

$$\eta_D = 1 - \frac{5.06}{M^2}\left[\left(\frac{p_t}{p_2}\right)^{\frac{k-1}{k}} - 1\right] \tag{219}$$

In this last equation M is the Mach number of the air at the entrance to the diffuser.

Let $Z_D = (p_t/p_2)^{\frac{k-1}{k}} - 1$; then the efficiency equation becomes

$$\eta_D = 1 - \frac{2}{(k-1)M^2}Z_D = 1 - \frac{5.06}{M^2}(Z_D) \tag{220}$$

EXAMPLE. Air enters a diffuser at 520 R and 14.7 psia. Its entrance velocity relative to the diffuser walls is 600 fps. The design of the diffuser is such that its energy efficiency is 0.8. Calculate the air pressure at the discharge section.

Solution.

$$M_1 = \frac{w_1}{\sqrt{gkRT_1}} = 0.535 \quad \text{and} \quad M_1^2 = 0.281$$

From equation 45

$$Z_C = 0.1975M^2 = 0.0555$$

From Table 4·5

$$p_t = 1.219p_1$$

From equation 220

$$0.8 = 1 - \frac{5.06Z_D}{0.281} = 1 - 18.0Z_D$$

$$18.0Z_D = 0.2 \quad \text{so that} \quad Z_D = 0.0111$$

Hence from Table 4·5

$$\frac{p_t}{p_2} = 1.040$$

$$p_2 = 1.161p_1$$

REFERENCES

1. L. Prandtl and O. G. Tietjens, *Applied Hydro- and Aeromechanics*, McGraw-Hill Book Co., 1934.
2. E. Schmidt, *Einführung in die technische Thermodynamik* Julius Springer, Berlin, 1936.
3. J. H. Keenan, *Thermodynamics*, McGraw-Hill Book Co., 1941.
4. N. P. Bailey, *Principles of Heat Engineering*, John Wiley & Sons, 1942.
5. L. Prandtl and O. Tietjens, *Fundamentals of Hydro- and Aeromechanics*, McGraw-Hill Book Co., 1934.
6. Th. von Kármán, *Problems of Flow in Compressible Fluids*, Univ. of Penna., Bicentennial Conference.
7. R. A. Dodge and M. J. Thompson, *Fluid Mechanics*, McGraw-Hill Book Co., 1937.
8. R. C. Wenner, *Thermochemical Calculations*, McGraw-Hill Book Co., 1941.
9. H. C. Weber, *Thermodynamics for Chemical Engineers*, John Wiley & Sons, 1939.
10. B. F. Dodge, *Chemical Engineering Thermodynamics*, McGraw-Hill Book Co., 1944.
11. L. E. Steiner, *Introduction to Chemical Thermodynamics*, McGraw-Hill Book Co., 1941.
12. A. Stodola, *Steam and Gas Turbines*, McGraw-Hill Book Co., 1927.
13. J. H. Keenan, "Friction Coefficients for the Compressible Flow of Steam," *J. Applied Mechanics*, March, 1939, pp. A11–A20.
14. W. Frössel, "Strömung in glatten, geraden Rohren mit Über- und Untergeschallgeschwindigkeit," *Forschung auf dem Gebiete Ingenieurwesens*, Vol. 7, 1936, pp. 75–84 (Translation *N.A.C.A.T.M.* 844, 1938).
15. R. P. Genereaux, "Fluid Flow Design Methods," *Ind. Eng. Chem.*, Vol. 29, No. 4, pp. 385–388.

16. O. G. TIETJENS, "Flow of Gases at a Rate Exceeding the Acoustic Velocity," A.S.M.E., Semi-annual meeting, June 9–11, 1930, Applied Mechanics Division.

17. W. E. LOBO, L. FRIEND, and G. T. SKAPERDAS, "Pressure Drop in the Flow of Compressible Fluids," *Ind. Eng. Chem.*, July, 1942, pp. 822–823.

18. R. C. BINDER, "Incompressible vs. Compressible Flow in Pipes," *Chem. and Met. Eng.*, June, 1944, p. 99.

19. R. C. BINDER, "Limiting Isothermal Flow in Pipes," *Trans. A.S.M.E.*, April, 1944, pp. 221–223.

20. B. A. BAHKMETEFF, *The Mechanics of Turbulent Flow*, Princeton University Press, 1936.

21. R. J. S. PIGOTT, "The Flow of Fluids in Closed Conduits," *Mech. Eng.*, August, 1933, pp. 497–501.

22. L. M. VAN DER PYL, "The Flow of Fluids in Pipes," *Instruments*, January, 1935, pp. 1–4.

23. B. A. BAHKMETEFF, "The Reynolds Number," *Mech. Eng.*, October 1936, pp. 625–630.

24. A. EGLI, "The Leakage of Gases through Narrow Channels," *J. Applied Mechanics*, 1936, pp. A63–A67.

25. E. S. DENNISON, "Graphical Solution of Fluid-Friction Problems," *Trans. A.S.M.E.*, 1945.

26. F. W. LAVERTY and F. M. McNALL, "High-Pressure Pipe Line Research," *Trans. A.S.M.E.*, April, 1944, pp. 215–218.

27. H. ROUSE, *Fluid Mechanics for Hydraulic Engineers*, McGraw-Hill Book Co., 1938.

28. G. I. TAYLOR and J. W. MACCOLL, "The Mechanics of Compressible Fluids," *Aerodynamic Theory* by F. W. Durand, Vol. III, Division H.

29. C. E. PAPPAS and M. G. HARRISON, "Analyzing the Aspects of Future Flight," *Aviation*, November, 1945, pp. 131–134.

30. W. H. McADAMS, *Heat Transmission*, McGraw-Hill Book Co., 1942.

31. M. S. KISENKO, "Comparative Results of Tests on Several Different Types of Nozzles," *N.A.C.A.T.M.* 1066, June, 1944.

32. E. OWER, *The Measurement of Air Flow*, Chapman & Hall, London, England, 1927.

33. F. I. FRANKL, "Supersonic Flows with Axial Symmetry," *Akedemie RKKA*, Vol. 1, 1934.

34. N. P. BAILEY, "Thermodynamics of Air at High Velocities," *J. Inst. Aero Sci.*, July, 1944.

35. G. BIRTWISTLE, *The Principles of Thermodynamics*, Cambridge University Press, 1925.

36. J. R. PARTINGTON, *Chemical Thermodynamics*, Constable and Co., 1924.

37. C. S. ROBINSON, *The Thermodynamics of Firearms*, McGraw-Hill Book Co., 1943.

38. A.S.M.E., *Report of Special Research Committee on Fluid Meters*, Part 1.

39. G. FLÜGEL, *Die Dampfturbinen*, Julius Springer, Berlin.

40. A. BUSEMAN, "Gas Dynamik," *Handb. Experimental-Physik*, Bd. Iv, 1. Teil, Akad. Verlagsgesellschaft, Leipzig.

41. G. B. SCHILBAUER, "Jet Propulsion with Special Reference to Thrust Augmenters," *N.A.C.A.T.N.* 442, 1933.

42. A. H. Shapiro, "Nozzles for Supersonic Flow without Shock Fronts," *Trans. A.S.M.E.*, Vol. 66, 1944, pp. A93-A100.

43. L. Crocco, "Gallerie aerodinamische per alta velocita," *L'Aeronautica*, Vol. XV, fase. 3, March, 1935, pp. 237-275; XV, fase. 7 and 8, July and August, 1935, pp. 735-778.

44. Moss and Smith, "Engineering Computations for Air and Gases," *Trans. A.S.M.E.*, Vol. 52, 1930, paper A.P.M. 52-8.

45. W. R. Hawthorne, "Factors Affecting the Design of Jet Turbines," S.A.E. Annual Meeting, Detroit, Mich., Jan. 7-11, 1946.

46. Th. von Kármán and M. Biot, *Mathematical Methods in Engineering*, McGraw-Hill Book Co., 1940, Chapter 1.

47. L. F. Moody, "Friction Factors for Pipe Flow," *Trans. A.S.M.E.*, November, 1944.

48. J. H. Keenan, *Mech. Eng.*, Vol. 54, 1932, pp. 195-204.

49. W. Schule, *Technical Thermodynamics* (translated by E. W. Geyer), Chapter IV, Sir Isaac Pitman & Sons, 1933.

THERMODYNAMIC PROPERTIES OF AIR

1. Introduction

The working fluid employed in gas turbine power plants and thermal jet engines, regardless of the cycle adopted, consists mainly of heated air containing a small admixture of combustion products derived from the combustion of the fuel utilized to raise the temperature of the air. In analyzing the various cycles which hold promise, either for gas turbine propeller-drive propulsion plants or for straight thermal jet propulsion, the thermodynamic properties of the working
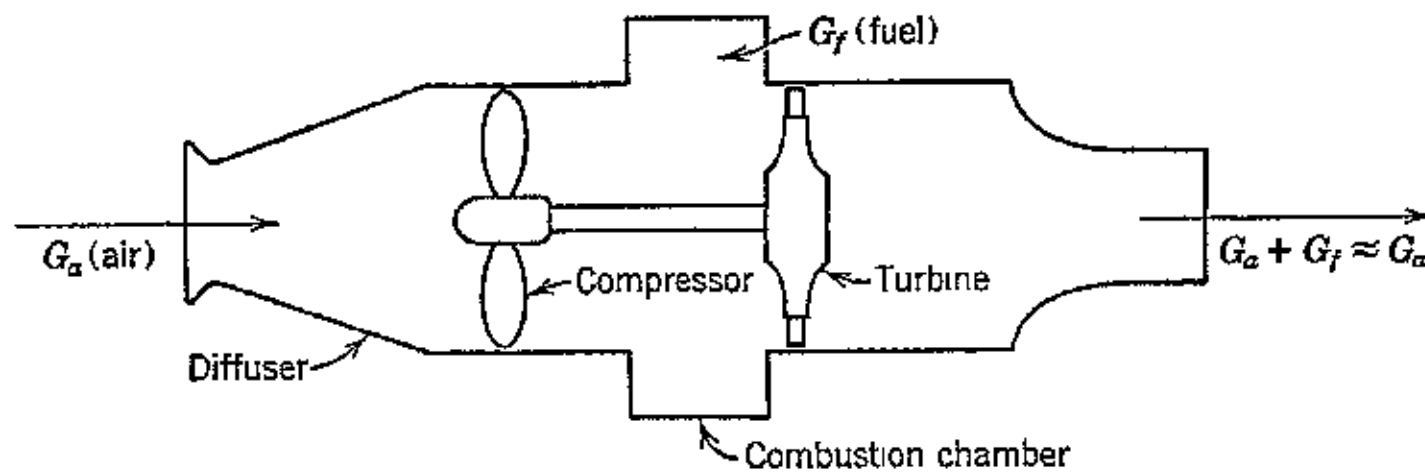
FIG. 1. Principal components of a thermal jet engine.

fluid enter. Consequently, thermodynamic data pertaining to the working fluid must be available so that the thermodynamic relationships can be calculated with reasonable engineering accuracy.

Figure 1 illustrates an elementary form of thermal jet engine. The quantity of air G_a lb/sec enters the diffuser wherein its pressure is raised before it flows into the compressor. The compressor raises the pressure of the air still more and then discharges it into the combustion chamber. Here, a fuel is introduced at substantially ambient temperature and burned under practically isobaric conditions, thereby raising the temperature of the working fluid to the desired value.

The hot working fluid leaving the combustion chamber consists of a mixture of heated air and the products of combustion of the fuel with a portion of the air. The mixture contains a large excess

of air, usually between three and seven times the quantity required to burn the fuel completely. No serious error is introduced, therefore, if it is assumed that the fluid entering the turbine is entirely heated air. In the turbine the working fluid expands, converting thermal energy into mechanical work. The turbine is so designed that it furnishes exactly the amount of work needed to drive the air compressor. The turbine exhaust gases are then discharged through the exhaust nozzle.

Several variations of the above arrangement are possible. For the present, however, it should be noted that the main thermodynamic processes involved are compressions and expansions. If each component of the thermal jet engine were an ideal piece of apparatus, the compression and expansion processes would be isentropic. Owing to various heat and friction losses, the actual processes are not isentropic.

The exact analysis of any cycle should take into consideration the effect of the fuel-air ratio as well as the variation in the specific heat, but since the former is small, it can be neglected without introducing any sensible error; this is equivalent to assuming that the working fluid is dry air. The effect of temperature on the value of the specific heat of air, however, should, in general, be taken into account.

The purpose of this chapter is to discuss some of the thermodynamic properties of air, to present data concerning its specific heat, and to describe methods for taking into account the variation of the specific heat when analyzing thermodynamic processes.

2. Deviation of Air from Perfect Gas

If air were a perfect gas, it would behave in accordance with the characteristic equation for perfect gases discussed in Chapter 1. Thus

$$pv = RT \quad \text{or} \quad \frac{pv}{RT} = 1 \tag{1}$$

Equation 1 assumes that the specific heat of the perfect gas is a constant. For air, this law does not hold exactly, although for most gases it is followed with sufficient closeness for engineering computations. The major discrepancies arise from the fact that the value of the specific heat of air is not a constant but is affected by both pressure and temperature. Table 4·1 presents data taken by Holborn and Otto showing the degree to which air deviates from the perfect-gas law.[1] More exact equations of state are those of Beattie

and Bridgeman; [17] see also references 18, 24, 25, and 26. For data on the deviation of other gases from the perfect-gas law see reference 2.

TABLE 4·1

VALUES OF pv/RT FOR AIR

(Holborn and Otto, *Zeit. Physik*, Bd. 33, 1935)

Abs Pressure		Temperature, °C				
kg/cm²	psi	0	50	100	150	200
0	0	1	1	1	1	1
10	142	0.9945	0.9990	1.0012	1.0025	1.0031
20	284	.9895	0 9984	1.0027	1.0051	1.0064
30	426	.9851	0 9981	1.0045	1.0078	1.0097
40	568	.9812	0.9982	1 0065	1.0108	1.0132
50	710	.9779	0.9986	1.0087	1.0139	1.0168
60	852	.9751	0.9993	1.0112	1.0172	1.0205
70	994	.9730	1.0004	1.0139	1.0206	1.0243
80	1136	.9714	1.0018	1.0169	1.0242	1.0282
90	1278	.9704	1.0036	1.0201	1.0279	1 0322
100	1420	.9699	1.0057	1.0235	1.0319	1.0364

Examination of Table 4·1 shows that the deviation in the behavior of air from the perfect-gas law is influenced by the predominating pressure and temperature. It should be noted that, since the specific heat at constant pressure c_p is not constant, the specific heat ratio $k = c_p/c_v$ is also a function of the pressure and temperature.

The range of operating pressures for thermal jet-propulsion engines and gas-turbine power plants, as judged by the pressure ratios obtainable with light-weight compressors at this time, is between 50 and 100 psia. In this pressure range the effect of pressure on the specific heat c_p and on the specific heat ratio k is so small that it can be ignored. This is readily apparent from the data in Fig. 2, which presents the instantaneous values of c_p in Btu/lb F and the specific heat ratio $k = c_p/c_v$ as functions of the air temperature in degrees Fahrenheit for different constant pressures.[3]

It is seen from Fig. 2 that for pressures below 150 psia the specific heat c_p and the specific heat ratio k can be assumed to be defined by the curves for zero pressure. At a temperature of 0 F and zero pressure the value of c_p is 0.240 Btu/lb and the corresponding value of $k = c_p/c_v = 1.40$. It is seen that for the temperature range 0 F to 4000 F the effect of moderate pressures can be ignored, but the effect of temperature is appreciable.

Assuming that the curve for $p = 0$ is applicable, it is seen that c_p changes from 0.24 at 0 F to 0.275 at 1500 F, an increase of 15 per cent. As the temperature is increased, the value of c_p increases almost linearly at the rate of 0.015 Btu/lb/1000 F. Since the work of either a compression or an expansion process varies directly with c_p, the actual mean value of c_p for the temperature range involved should be used.
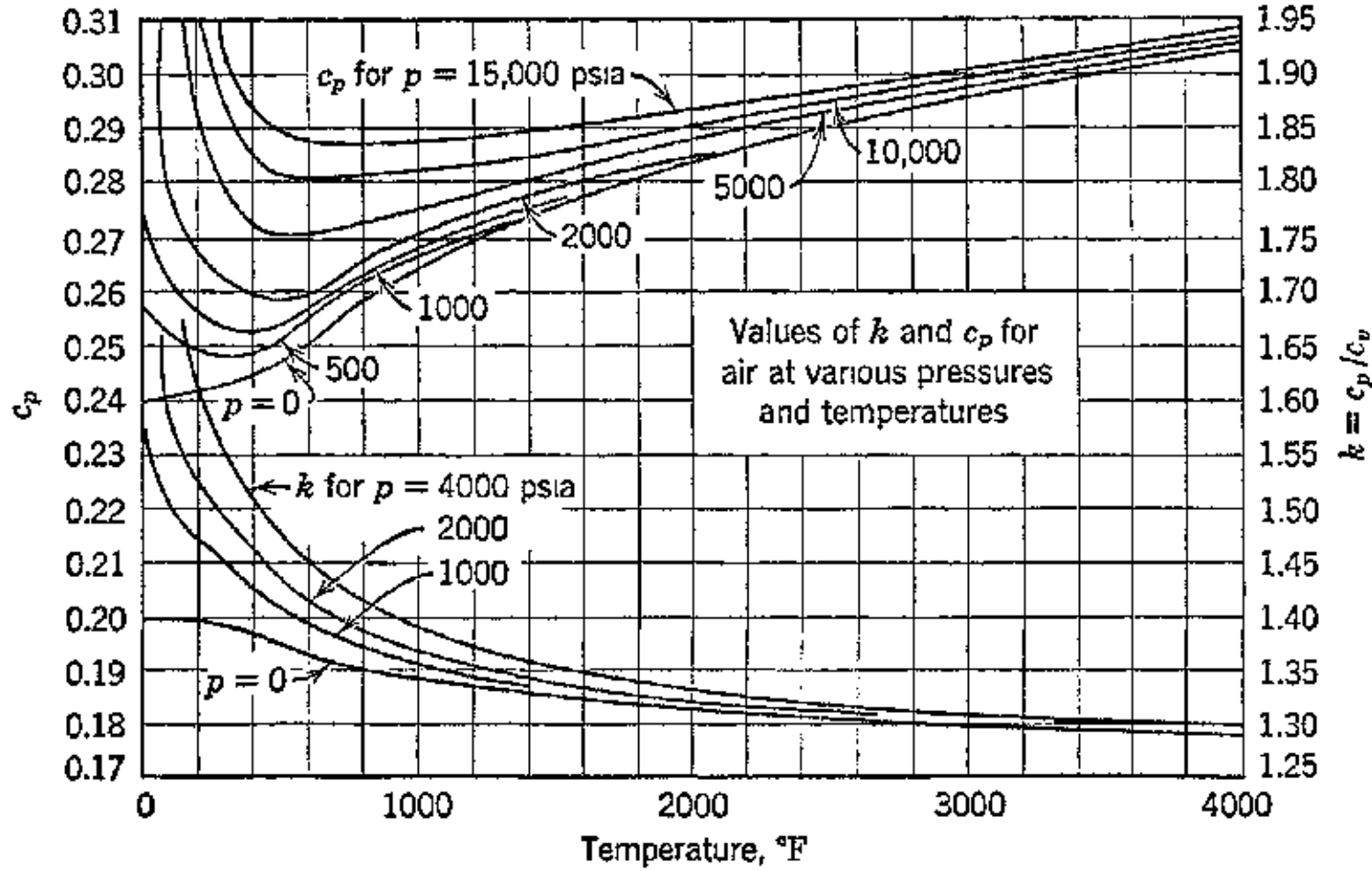
Fig. 2. Specific heat and specific heat ratio for air at different pressures as a function of temperature. (Reproduced from F. O. Ellenwood, N. Kulik, and N. R. Gay, *Cornell Univ. Eng. Expt. Sta.*, *Bul.* 30, October 1942.)

3. Data on Specific Heat of Air

The most recent measurements of the instantaneous values of specific heats of gases, and also those considered most accurate, are due to Professor R. C. H. Heck,[4] and to H. L. Johnston and A. T. Chapman.[5] For a critical discussion and analysis of specific-heat data the reader is referred to reference 3, from which Fig. 2 is taken.

The data obtained by Professor Heck apply for the range of temperatures above 600 R. Below 600 R the data of Johnston for oxygen and nitrogen indicate that no serious error is introduced by assuming the specific heat to be constant. These data, however, are based on zero pressure. At low temperature, errors are introduced by this assumption if the pressure is high.

Figure 3 presents the instantaneous values of the specific heat c_p, and $k = c_p/c_v$, for air as a function of temperature. At temperatures below 500 R, c_p is assumed to be constant at the value $c_p = 0.24$. The specific-heat values for air plotted in the figure were computed from the experimentally determined values for nitrogen, oxygen,
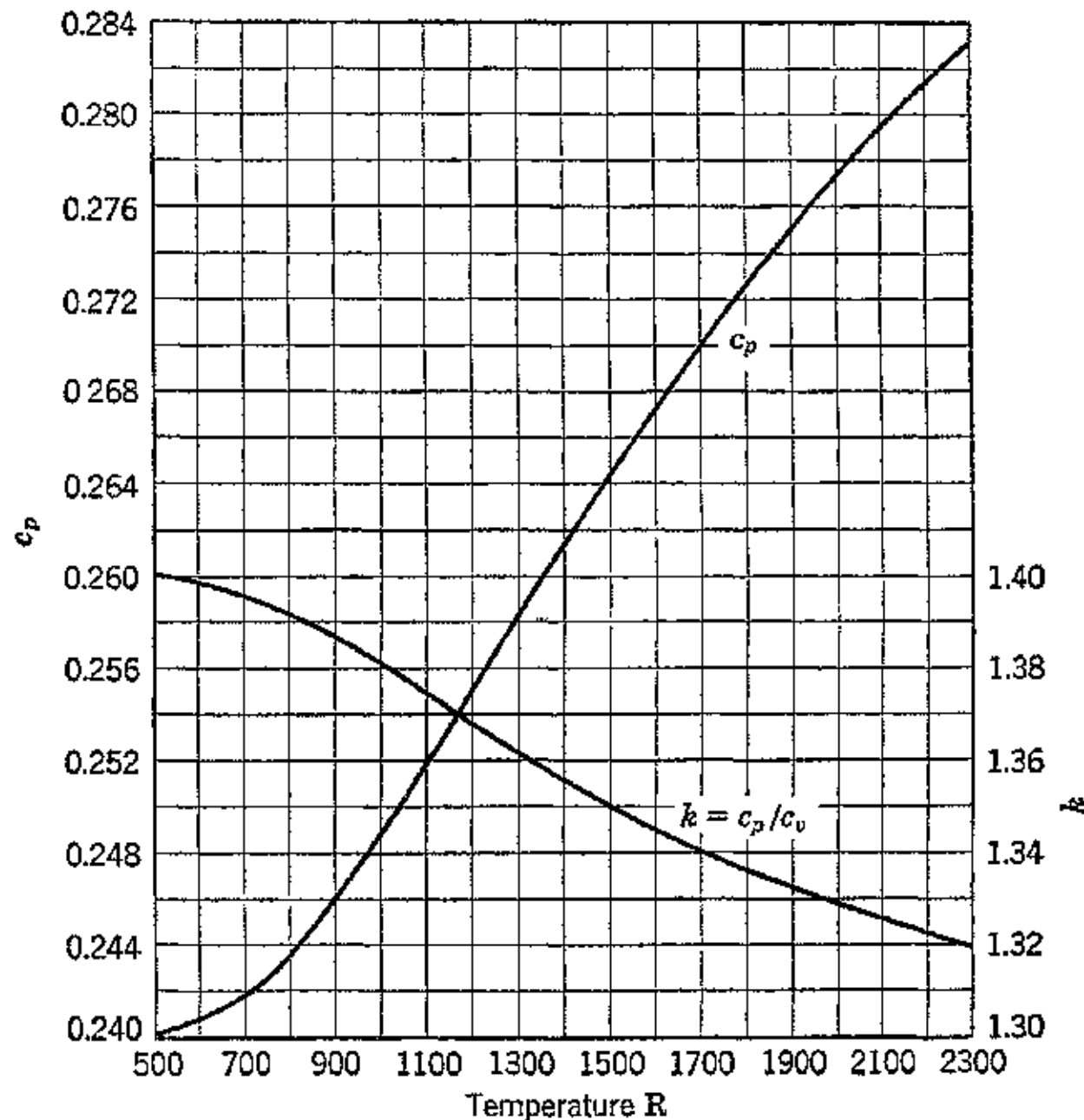
FIG. 3. Instantaneous values of the specific heat and specific heat ratio for air as a function of temperature. (Based on data of Prof. R. C. H. Heck, *Mech. Eng.*, Vol. 63, 1941, pp. 126–135.)

and argon obtained by Heck. The following gas composition, on a weight basis, was assumed for dry air: nitrogen 75.6 per cent, oxygen 23.0 per cent, and argon 1.4 per cent. The specific heat of argon was assumed to be constant and equal to 4.964 Btu/lb mole F.

The functional relationships between the specific heats of the more common gases have been expressed in mathematical form by Sweigert and Beardsley.[6] The Sweigert and Beardsley equations are assembled in Table 4·2. They are based on the experimental data of Heck previously referred to.

TABLE 4·2

INSTANTANEOUS VALUES OF SPECIFIC HEATS OF GASES

(Bulletin 2, Ga. School of Technology, by R. L. Sweigert and M. W. Beardsley)

Gas or Vapor	Specific Heat Equation mc_p in Btu/lb mole R	Range	Maximum Error
O_2	$mc_p = 11.515 - \dfrac{172}{\sqrt{T}} + \dfrac{1530}{T}$	540–5000	1.1 %
	$mc_p = 11.51 - \dfrac{172}{\sqrt{T}} + \dfrac{1530}{T} + \dfrac{0.05}{1000}(T - 4000)$	5000–9000	0.3
N_2	$mc_p = 9.47 - \dfrac{3.47 \times 10^3}{T} + \dfrac{1.16 \times 10^6}{T^2}$	540–9000	1.7
CO	$mc_p = 9.46 - \dfrac{3.29 \times 10^3}{T} + \dfrac{1.07 \times 10^6}{T^2}$	540–9000	1.1
H_2	$mc_p = 5.76 + \dfrac{0.578}{1000} T + \dfrac{20}{\sqrt{T}}$	540–4000	0.8
	$mc_p = 5.76 + \dfrac{0.578}{1000} T + \dfrac{20}{\sqrt{T}} - \dfrac{0.33}{1000}(T - 4000)$	4000–9000	1.4
H_2O	$mc_p = 19.86 - \dfrac{597}{\sqrt{T}} + \dfrac{7500}{T}$	540–5400	1.8
CO_2	$mc_p = 16.2 - \dfrac{6.53 \times 10^3}{T} + \dfrac{1.41 \times 10^6}{T^2}$	540–6300	0.8
CH_4	$mc_p = 4.52 + 0.00737T$	540–1500	1.2
C_2H_4	$mc_p = 4.23 + 0.01177T$	350–1100	1.5
C_2H_6	$mc_p = 4.01 + 0.01636T$	400–1100	1.5
C_8H_{18}	$mc_p = 7.92 + 0.0601T$	400–1100	Est. 4
$C_{12}H_{26}$	$mc_p = 8.68 + 0.0889T$	400–1100	Est. 4

Figure 4 compares the empirical values of c_p with those calculated by using the Sweigert and Beardsley equations. No equation was presented by Sweigert and Beardsley for the specific heat of air. Further, it should be noted that all their data are on a molar basis.

The Sweigert and Beardsley equations are of two forms

$$c_p = a - \frac{b}{T} + \frac{c}{T^2} \qquad (a)$$

and

$$c_p = a - \frac{b}{\sqrt{T}} + \frac{c}{T} \qquad (b)$$

where a, b, and c are constants.
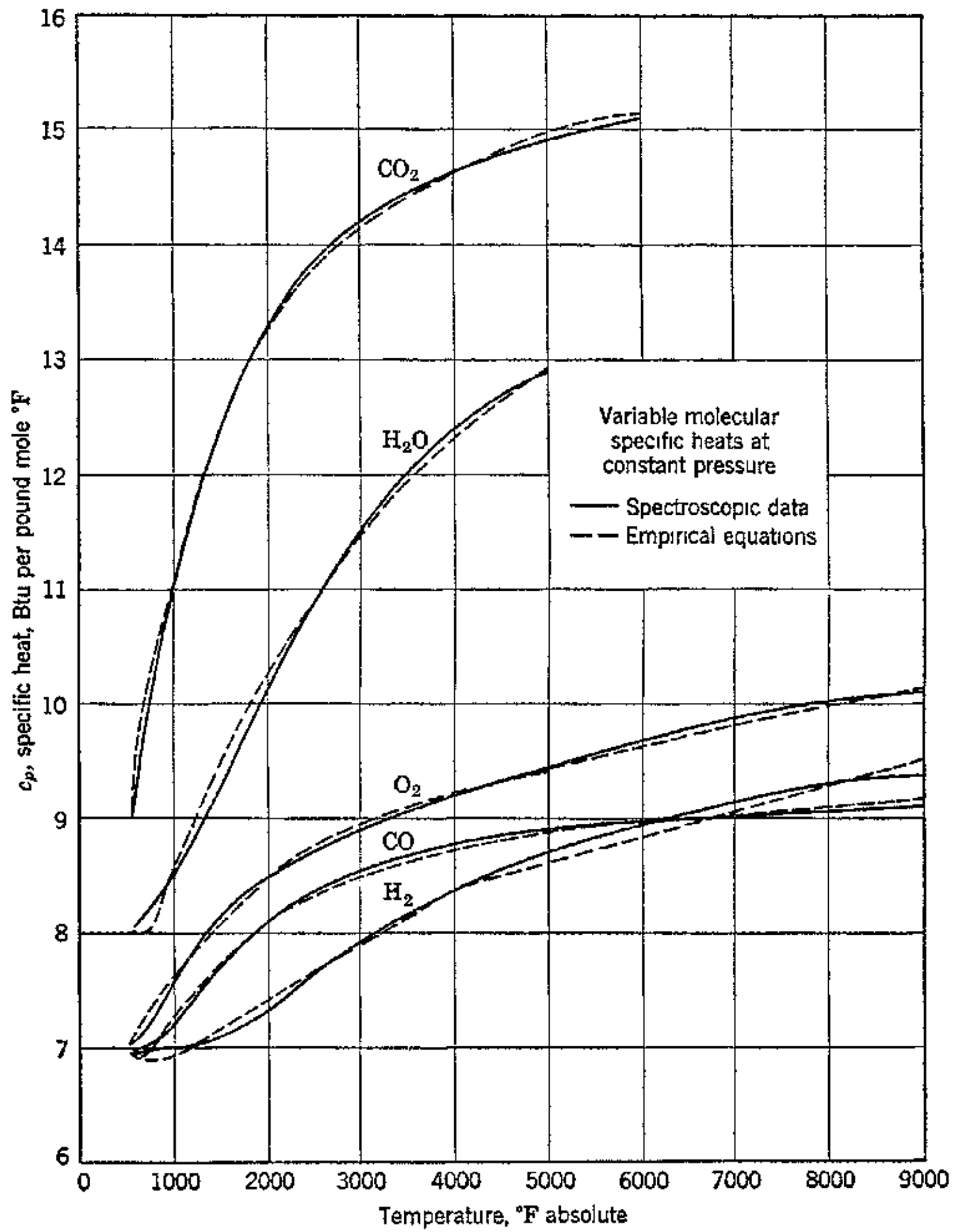
Fig. 4. Comparison of measured and calculated values of the specific heat for various gases. (Reproduced from R. L. Sweigert and M. W. Beardsley, *Georgia School of Technology, State Eng. Expt. Sta., Bul.,* Vol. 1, No. 3, June 1936.)

The equation for the instantaneous specific heat of dry air can be derived by applying the Sweigert and Beardsley equations to the composition of air. The volume composition of dry air at sea level is [7]

	PER CENT BY VOLUME
Nitrogen	78.03
Oxygen	20.99
Argon	0.94
Carbon dioxide	0.03
Hydrogen	0.01
Neon	0.00123
Krypton	0.00005
Xenon	0.000006

From the above it is apparent that for practical purposes it can be assumed that dry air is composed of only the first three elements in the list. This gives the weight composition 75.5 per cent nitrogen, 23.2 per cent oxygen, and 1.35 per cent argon. Consequently, air can be assumed to consist of 1 mole oxygen plus 3.71 moles nitrogen plus 0.045 mole argon. The molecular weight of air is accordingly

$$m_{air} = \frac{3.717 \times 28.016 + 1 \times 32 + 0.047 \times 39.94}{4.764} = 28.97$$

The gas constant for air is

$$R = \frac{1545}{28.97} = 53.35 \text{ ft-lb/lb F}$$

and

$$\frac{R}{J} = \frac{53.35}{778} = 0.06854 \text{ Btu/lb F}$$

The specific heat equation for air is obtained from those for nitrogen and oxygen, and by adding $0.047 \times 4.964 = 0.232$ Btu/lb mole F for the argon. Thus

CONSTITUENT	MOLES $\times$ MOLAR SPECIFIC HEAT		
Nitrogen	35.20	$- 1.29 \times 10^4/T + 4.30 \times 10^6/T^2$	
Oxygen	$11.515 - 172/\sqrt{T} + 1.53 \times 10^3/T$		
Argon	0.232		
4.764 moles of air	$46.947 - 172/\sqrt{T} -$	$11,370/T + 4.31 \times 10^6/T^2$	
$(mc_p)_{air}$	$9.85 - 36.1/\sqrt{T} -$	$2,387/T +$	$905,000/T^2$

Using 1 mole of oxygen mixed with 3.78 moles of nitrogen, for the composition of air, Professor J. Smallwood [10] obtained the following molar specific heat equation for air

$$(mc_p)_{air} = 9.90 - \frac{36}{\sqrt{T}} - \frac{2420}{T} + \frac{917,000}{T^2}$$

Dividing through by $m = 28.97$ the instantaneous specific heat equation for air in Btu/lb F is obtained, thus

$$c_p = 0.342 - 1.25T^{-\frac{1}{2}} - 82.4T^{-1} + 31,200T^{-2} \qquad (2)$$

4. Mean Specific Heat

The data and equations presented in the preceding sections were concerned with the instantaneous values of the specific heat at different temperatures. In many problems a knowledge of the values of the mean specific heat between the temperature limits of the problem is of great value.

The value of the mean specific heat $\bar{c}_p$ is determined from the relationship

$$\bar{c}_p = \frac{1}{T_2 - T_1} \int_{T_1}^{T_2} c_p \, dT \qquad (3)$$

To solve this equation the instantaneous specific heat as a function of temperature must be substituted in the equation. Table 4·3 presents values of the mean specific heat for air as a function of temperature.[8,9]

TABLE 4·3

MEAN VALUES OF THE MOLAR SPECIFIC HEAT OF AIR

Temperature F	$m\bar{c}_p$ Btu/lb mole F	Temperature F	$m\bar{c}_p$ Btu/lb mole F
32	6.940	1500	7.431
100	6.944	1600	7.469
200	6.958	1700	7.505
300	6.985	1800	7.548
400	7.012	1900	7.583
500	7.038	2000	7.615
600	7.071	2100	7.649
700	7.110	2200	7.680
800	7.149	2300	7.714
900	7.188	2400	7.736
1000	7.224	2500	7.768
1100	7.264	2600	7.795
1200	7.300	2700	7.829
1300	7.344	2800	7.853
1400	7.387	2900	7.876

EXAMPLE. How much heat must be supplied to raise the temperature of 10 lb of air per second from 100 F to 1200 F?

$$Q = G[\bar{c}_p(1200 - 32) - \bar{c}_p(100 - 32)]$$

From Table 4 3

$$\bar{c}_p \text{ at } 1200 \text{ F} = \frac{7.30}{28.97} = 0.252 \quad \text{Btu/lb}$$

$$\bar{c}_p \text{ at } \;\;100 \text{ F} = \frac{6\,944}{28.97} = 0.240$$

$$Q = 10[0.252 \times 1168 - 0.240 \times 68]$$

$$= 10[294 - 16.3] = 2777 \text{ Btu/sec}$$

From equation 2 the heat required can be calculated as follows:

$$Q = G \int_{560}^{1660} (0.342 - 1.25T^{-\frac{1}{2}} - 82.4T^{-1} + 31{,}200T^{-2})\, dT$$

$$= 10 \left\{ 0.342 \left[T \right]_{560}^{1660} - 2.50 \left[\sqrt{T} \right]_{560}^{1660} - 82.4 \left[\log_e T \right]_{560}^{1660} - 31{,}200 \left[\frac{1}{T} \right]_{560}^{1660} \right.$$

5. Temperature Entropy Diagram for Air

The entropy change of a perfect gas is given by

$$\int_0^1 ds = \int_{T_0}^T c_p \frac{dT}{T} - \frac{R}{J} \int_{p_0}^p \frac{dp}{p} \tag{4}$$

The entropy at any state calculated above some arbitrary zero value, corresponding to T_0, and unit pressure is

$$s - s_0 = \int_{T_0}^T c_p \frac{dT}{T} - \frac{R}{J} \log_e \frac{p}{p_0} \tag{5}$$

Let

$$\phi = \int_{T_0}^T c_p \frac{dT}{T} \tag{6}$$

A change in entropy between any two states is given by

$$s - s_0 = \phi - \phi_0 - \frac{R}{J} \log_e \frac{p}{p_0} \tag{7}$$

For air $R = 53.35$ and $R/J = 0.06854$ Btu/lb F. Substituting for R/J in equation 7 the equation for entropy change becomes

$$s - s_0 = \phi - 0.06854 \log_e \frac{p}{p_0} \tag{8}$$

Values of $(R/J) \log_e p$ for air, based on $p_0 = 1$ psia, can be obtained from Figs. 5 and 6. From equation 8 it is seen that the entropy change is a function of ϕ and of the pressure ratio $p/p_0 = r_c$.
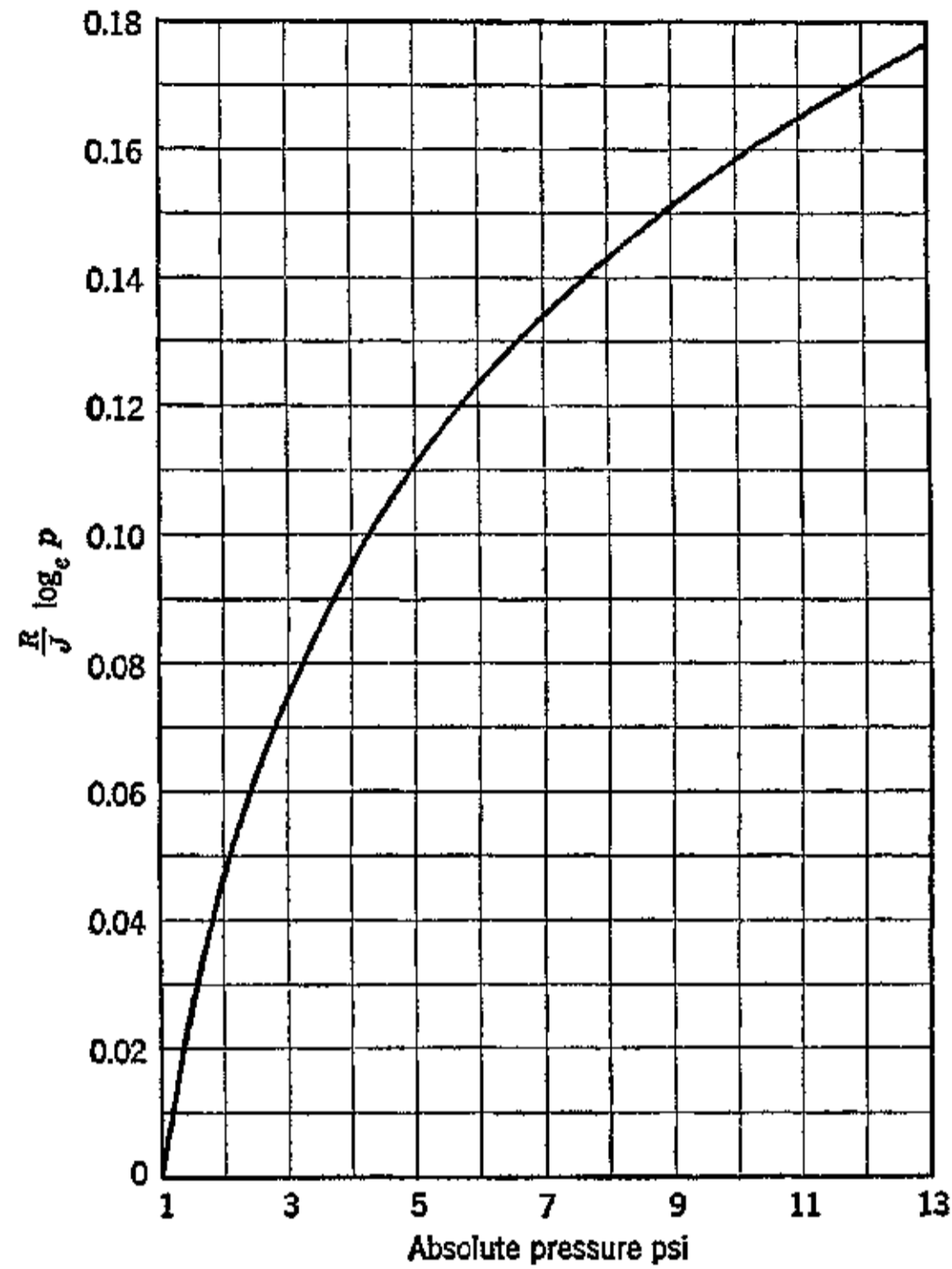
FIG. 5. Values of $R/J \log_e p$ for air, based on $p_0 = 1$.

Referring to equations 4 and 2, let the datum points be $T_0 = 400$ and $p_0 = 1$ psia. Then the increment in entropy at a constant pressure gives the following expression

$$(\Delta s)_p = 0.340 \log_e \frac{T}{T_0} - 2.50 \left[\frac{T^{\frac{1}{2}} - T_0^{\frac{1}{2}}}{(TT_0)^{\frac{1}{2}}} \right] - 82.5 \left[\frac{T - T_0}{TT_0} \right]$$

$$+ 15,600 \left[\frac{T^2 - T_0^2}{(TT_0)^2} \right] \quad (9)$$

Equation 9 gives the entropy change for a condition where the pressure remains constant. From this equation the temperature-entropy curve for one constant pressure can be calculated. For other constant pressures, the relation

$$(\Delta s)_T = 0.06854 \log_e \frac{p}{p_0} = 0.06854 \log_e r_c \tag{10}$$

is used, the subscript T denoting an entropy change where the temperature is held constant.
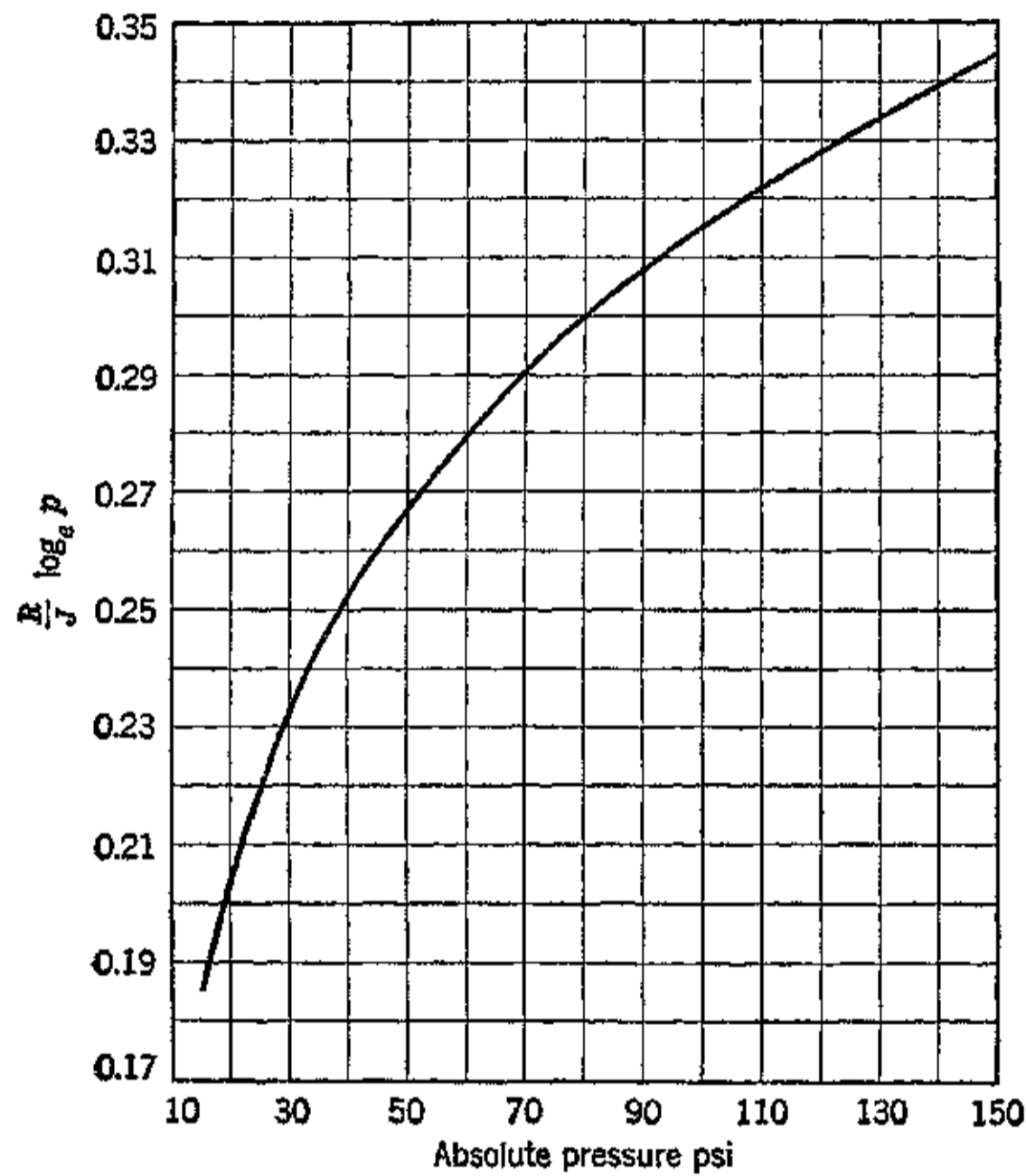
Fig. 6. Values of $R/J \log_e p$ for air, based on $p_0 = 1$.

It is apparent from the foregoing that the temperature-entropy chart will be a family of parallel curves displaced from each other by distances proportional to the logarithm of the pressure ratio. Figure 7 illustrates the temperature-entropy diagram.[16]
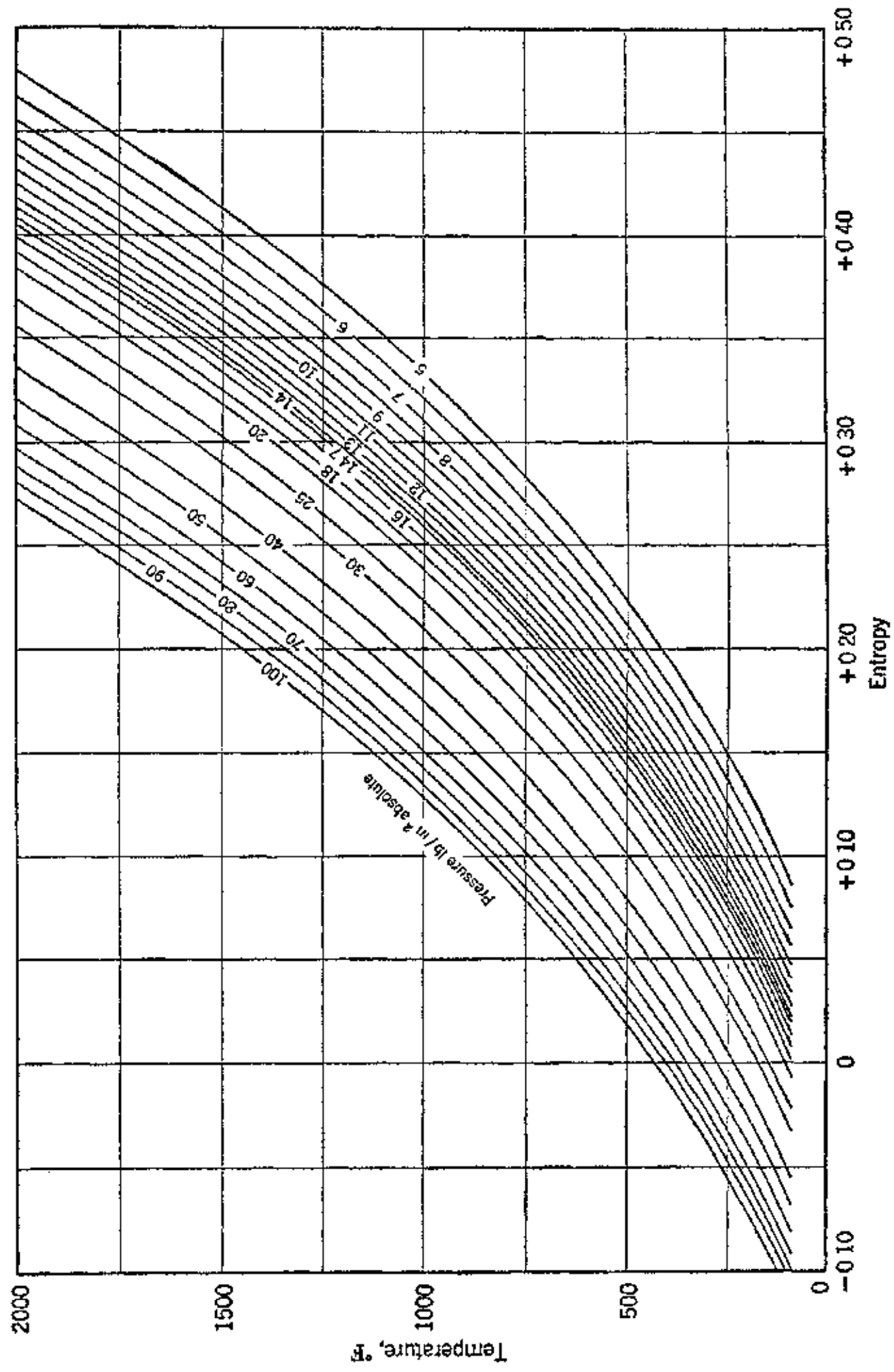
Fig. 7.   Temperature-entropy diagram for air.
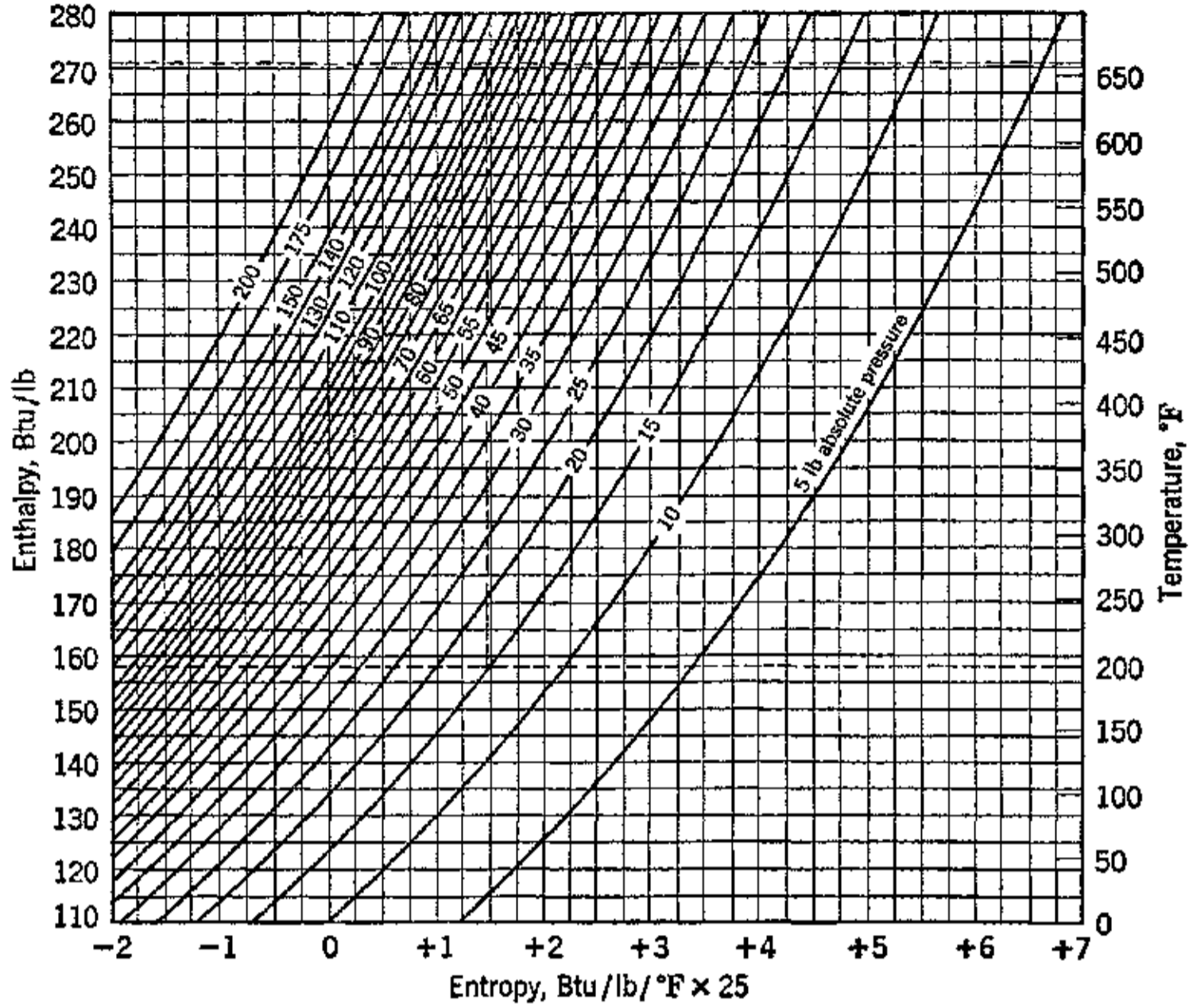
FIG. 8.   Enthalpy-entropy chart for air.   (Reproduced from *Power*, March 1941.)

6. The Entropy-Enthalpy Chart

In the analysis of gas-turbine cycles, diffusers, and nozzles, the processes involved are dependent on enthalpy changes. An enthalpy change is given by

$$\Delta h = \int c_p \, dT \tag{11}$$

where for air

$$c_p = 0.342 - 1.25T^{-\frac{1}{2}} - 82.4T^{-1} + 31,200T^{-2} \quad \text{Btu/lb F}$$

Substituting for c_p in equation 11

$$\Delta h = \int_{T_0}^{T} 0.342 \, dT - 1.25 \int_{T_0}^{T} \frac{dT}{T^{\frac{1}{2}}} - 82.4 \int_{T_0}^{T} \frac{dT}{T} + 31,200 \int_{T_0}^{T} \frac{dT}{T^2} \tag{12}$$

If $T_0 = 400$ R, so that $h = 0$ at that temperature, then equation 12

can be integrated to give the enthalpy change above and below that datum. Thus

$$\Delta h = 0.342 \left[T \right]_{400}^{T} - 2.50 \left[T^{1/2} \right]_{400}^{T} - 82\ 4 \left[\log_e T \right]_{400}^{T}$$

$$- 31,200 \left[\frac{1}{T} \right]_{400}^{T} \quad (13)$$

From equations 9 and 13 the enthalpy-entropy chart can be constructed by using the pressure p as a parameter. In this chart the lines of constant temperature can be drawn. Such charts unless drawn to a very large scale are not sufficiently accurate for gas design purposes for turbines and thermal jet engines. For rough calculations Fig. 8 is useful.[11]

7. Gas Tables

In making thermodynamic analyses, the specific heat equations are cumbersome and time-consuming. A great deal of labor can be avoided by using tables of the thermodynamic properties of the gas in question. Such a table for air has been compiled by Keenan and Kaye.[12,13] A portion of this table has been reproduced here in Table 4·4. Tables of a similar nature for other gases are to be found in reference 14.

In evaluating the thermodynamic properties presented in Table 4·4 the specific heat of air c_p was taken from Professor Heck's data for temperatures above 600 R, and c_p was assumed to have the constant value 0.240 for temperatures below 600 R, in accordance with the work of Johnston and Walker.[15]

It was pointed out in Chapter 1 that the internal energy of a gas is a function of temperature; thus

$$u = f(T) = c_v T = h - \frac{RT}{J} \quad \text{Btu/lb} \quad (14)$$

Similarly for the enthalpy of a gas

$$h = f(T) = c_p T \quad \text{Btu/lb} \quad (15)$$

This means that the values of u and h for air can be tabulated as functions of the temperature by using known values of the specific heat.

TABLE 4·4

Thermodynamic Properties of Dry Air

(Keenan and Kaye, *Trans. A.S.M.E.*, 1943, p. A123.)

Temperature R T	Enthalpy Btu/lb h	Diff.	Internal Energy Btu/lb u	Relative Pressure p_r	Diff.	Relative Volume $v_r \times 10^4$	Diff.	$\int c_p\, dt$ ϕ	Diff.
300	−24.00	1.20	−44.56	0.3554		20,537		.06904	
305	−22.80	1.20	−43.70	0.3870	0.0316	19,705	832	.06507	.00397
310	−21.60	1.20	−42.85	0.4096	0.0226	18,920	785	.06117	.00390
315	−20.40	1.20	−41.99	0.4332	0.0236	18,178	742	.05733	.00384
320	−19.20	1.20	−41.13	0.4578	0.0246	17,476	702	.05355	.00378
325	−18.00	1.20	−40.28	0.4833	0.0255	16,810	666	.04983	.00372
330	−16.80	1.20	−39.42	0.5098	0.0265	16,180	630	.04617	.00366
335	−15.60	1.20	−38.56	0.5374	0.0284	15,583	597	.04256	.00361
340	−14.40	1.20	−37 70	0.5661	0.0287	15,016	567	.03900	.00356
345	−13.20	1.20	−36.85	0.5958	0.0297	14,478	538	.03550	.00350
350	−12.00	1.20	−35.99	0.6266	0.0308	13,966	512	.03205	.00345
355	−10.80	1.20	−35.13	0.6585	0.0319	13,479	487	.02865	.00340
360	− 9.60	1.20	−34.28	0.6916	0.0321	13,016	463	.02529	.00336
365	− 8.40	1.20	−33.42	0.7258	0.0342	12,574	442	.02198	.00331
370	− 7.20	1.20	−32.56	0.7612	0.0354	12,153	421	.01871	.00327
375	− 6.00	1.20	−31.71	0.7978	0.0366	11,752	401	.01549	.00322
380	− 4.80	1.20	−30.85	0.8356	0.0378	11,369	383	.01231	.00318
385	− 3.60	1.20	−29.99	0.8747	0.0391	11,003	366	.00918	.00313
390	− 2.40	1.20	−29.13	0.9152	0.0405	10,654	349	.00608	.00310
395	− 1.20	1.20	−28.28	0.9569	0.0417	10,320	334	.00302	.00296
400	0	1.20	−27.42	1.0000	0.0431	10,000	320	0	.00302
405	1.20	1.20	−26.56	1.0445	0.0445	9,694	306	.00293	.00293
410	2.40	1.20	−25.70	1.0903	0.0448	9,401	293	.00593	.00300
415	3.60	1.20	−24.85	1.1376	0.0473	9,120	281	.00884	.00291
420	4.80	1.20	−23.99	1.1863	0.0487	8,851	269	.01171	.00287
425	6.00	1.20	−23.13	1.2365	0.0502	8,593	258	.01455	.00284
430	7.20	1.20	−22.27	1.2882	0.0517	8,345	248	.01736	.00281
435	8.40	1.20	−21.41	1.3415	0.0533	8,107	238	.02014	.00278
440	9.60	1.20	−20.56	1.3962	0.0547	7,879	228	.02288	.00274
445	10.80	1.20	−19.70	1.4525	0.0563	7,659	220	.02559	.00271
450	12.00	1.20	−18.84	1.5104	0.0579	7,448	211	.02827	.00268
455	13.20	1.20	−17.98	1.5700	0.0696	7,245	203	.03092	.00265
460	14.40	1.20	−17.13	1.6312	0.0612	7,050	195	.03354	.00262
465	15.60	1.20	−16.27	1.6942	0.0630	6,861	189	.03613	.00259
470	16.80	1.20	−15.41	1.7589	0.0647	6,680	181	.03870	.00257
475	18.00	1.20	−14.56	1.8253	0.0664	6,505	175	.04124	.00254
480	19.20	1.20	−13.70	1.8935	0.0682	6,337	168	.04376	.00252
485	20.40	1.20	−12.84	1.9634	0.0699	6,175	162	.04625	.00249
490	21.60	1.20	−11.98	2.0352	0.0718	6,019	156	.04871	.00243
495	22.80	1.20	−11.13	2.1089	0.0737	5,868	151	.05114	.00246

TABLE 4-4 (*Continued*)

THERMODYNAMIC PROPERTIES OF DRY AIR

(Keenan and Kaye, *Trans. A.S.M.E.*, 1943, p. A123.)

Temperature R T	Enthalpy Btu/lb h	Diff.	Internal Energy Btu/lb u	Relative Pressure p_r	Diff.	Relative Volume $v_r \times 10^4$	Diff.	$\int c_p\,dt$ ϕ	Diff.
500	24.00	1.20	−10.27	2.1845	0.0756	5,722	146	.05355	.00241
505	25.20	1.20	− 9.41	2 262	0 0775	5,582	140	.05594	.00239
510	26.40	1.20	− 8.55	2.342	0 080	5,446	136	.05831	.00237
515	27.60	1.20	− 7.70	2.423	0.081	5,315	131	.06065	.00234
520	28.80	1.20	− 6.84	2.506	0.083	5,188	127	.06297	.00232
525	30.00	1.20	− 5.98	2.592	0.084	5,065	123	.06527	.00230
530	31.20	1.20	− 5.12	2.679	0.087	4,946	119	.06754	.00227
535	32.41	1.21	− 4.27	2.768	0.089	4,831	115	.06979	.00225
540	33.61	1.20	− 3.41	2.860	0.092	4,720	111	.07202	.00223
545	34.81	1.20	− 2.55	2.954	0.094	4,612	108	.07424	.00222
550	36.01	1.20	− 1.69	3.050	0.096	4,508	104	.07644	.00220
555	37.21	1.20	− 0.83	3.148	0.098	4,407	101	.07862	.00218
560	38.41	1.20	0.03	3.249	0.101	4,309	98	.08077	.00215
565	39.61	1.20	0.89	3.352	0.103	4,214	95	.08290	.00213
570	40.82	1.21	1.74	3.457	0.105	4,122	92	.08502	.00212
575	42.02	1.20	2.60	3.564	0.107	4,033	89	.08712	.00210
580	43.22	1.20	3.46	3.674	0.110	3,946	87	.08920	.00208
585	44.42	1.20	4.32	3.787	0.113	3,862	84	.09126	.00206
590	45.62	1.20	5.18	3.902	0.115	3,780	82	.09331	.00205
595	46.83	1.21	6.04	4.019	0.117	3,701	79	.09534	.00203
600	48.03	1.20	6.90	4.139	0.120	3,624	77	.09735	.00201
605	49.23	1.20	7.76	4 261	0.122	3,550	74	.09935	.00200
610	50.44	1.21	8.62	4.386	0.125	3,477	73	.10133	.00198
615	51.64	1.20	9.48	4.514	0.128	3,406	71	.10329	.00196
620	52.84	1.20	10.34	4.644	0.130	3,338	68	.10524	.00195
625	54.05	1.21	11.20	4.777	0.133	3,271	67	.10718	.00194
630	55.26	1.21	12.06	4.913	0.136	3,206	65	.10910	.00192
635	56.46	1.20	12.92	5.051	0.138	3,143	63	.11101	.00191
640	57.66	1.20	13.79	5.192	0.141	3,082	61	.11290	.00189
645	58.86	1.20	14.65	5.336	0.144	3,022	60	.11478	.00188
650	60.07	1.21	15.51	5.483	0.147	2,964	58	.11664	.00186
655	61.28	1.21	16.37	5.633	0.150	2,907	57	.11849	.00185
660	62.48	1.20	17.23	5.786	0.153	2,852	55	.12032	.00183
665	63.69	1.21	18.10	5.941	0.155	2,798	54	.12214	.00182
670	64.89	1.20	18.97	6.100	0.159	2,746	52	.12395	.00181
675	66.10	1.21	19.83	6.262	0.162	2,695	51	.12574	.00179
680	67.31	1.21	20.70	6.427	0.165	2,645	50	.12752	.00178
685	68.52	1.21	21.57	6.595	0.168	2,596	49	.12929	.00177
690	69.72	1.20	22.43	6.766	0.171	2,549	47	.13105	.00176
695	70.93	1.21	23.29	6.941	0.175	2,503	46	.13280	.00175

TABLE 4·4 (*Continued*)

THERMODYNAMIC PROPERTIES OF DRY AIR

(Keenan and Kaye, *Trans. A.S.M.E.*, 1943, p. A123.)

Temperature R T	Enthalpy Btu/lb h	Diff.	Internal Energy Btu/lb u	Relative Pressure p_r	Diff.	Relative Volume $v_r \times 10^4$	Diff.	$\int c_p \, dt$ ϕ	Diff.
700	72.14	1.21	24.16	7.119	0.178	2,458	45	.13453	.00173
705	73.35	1.21	25.02	7.301	0.182	2,415	43	.13625	.00172
710	74.56	1.21	25.89	7.485	0.184	2,372	43	.13796	.00171
715	75.77	1.21	26.76	7.672	0.187	2,330	42	.13966	.00170
720	76.98	1.21	27.63	7.863	0.191	2,289	41	.14134	.00168
725	78.19	1.21	28.50	8.057	0.194	2,250	39	.14301	.00167
730	79.40	1.21	29.36	8.255	0.198	2,211	39	.14468	.00167
735	80.61	1.21	30.23	8.457	0.202	2,173	38	.14634	.00166
740	81.82	1.21	31.10	8.662	0.205	2,136	37	.14799	.00165
745	83.04	1.22	31.97	8.871	0.209	2,099	37	.14962	.00163
750	84.25	1.21	32.84	9.084	0.213	2,064	35	.15124	.00162
755	85.46	1.21	33.71	9.300	0.216	2,030	34	.15285	.00161
760	86.68	1.22	34.58	9.520	0.220	1,995.8	34.2	.15445	.00160
765	87.89	1.21	35.45	9.744	0.224	1,962.7	33.1	.15604	.00159
770	89.10	1.21	36.33	9.972	0.228	1,930.4	32.3	.15762	.00158
775	90.31	1.21	37.20	10.204	0.232	1,898.9	31.5	.15920	.00158
780	91.53	1.22	38.07	10.439	0.235	1,868.1	30.8	.16077	.00157
785	92.75	1.22	38.95	10.678	0.239	1,837.9	30.2	.16232	.00155
790	93.97	1.22	39.82	10.921	0.243	1,808.4	29.5	.16386	.00154
795	95.18	1.21	40.69	11.169	0.248	1,779.6	28.8	.16540	.00154
800	96.40	1.22	41.57	11.421	0.252	1,751.4	28.2	.16693	.00153
805	97.62	1.22	42.45	11.676	0.255	1,723.7	27.7	.16844	.00151
810	98.84	1.22	43.32	11.936	0.260	1,696.6	27.1	.16995	.00151
815	100 06	1.22	44.20	12.200	0.264	1,670.1	26.5	.17145	.00150
820	101.28	1.22	45.08	12.469	0.269	1,644.2	25.9	.17295	.00150
825	102.50	1.22	45.95	12.742	0.273	1,618.8	25.4	.17444	.00149
830	103.72	1.22	46.83	13.019	0.277	1,593.9	24.9	.17591	.00147
835	104.94	1.22	47.71	13.301	0.282	1,569.5	24.4	.17737	.00146
840	106.16	1.22	48.59	13.587	0.286	1,545.6	23.9	.17883	.00146
845	107.39	1.23	49.47	13.878	0.291	1,522.2	23.4	.18028	.00145
850	108.61	1.22	50.35	14.173	0.295	1,499.3	22.9	.18172	.00144
855	109.83	1.22	51.23	14.473	0.300	1,476.9	22.4	.18316	.00144
860	111.05	1.22	52.11	14.778	0.305	1,454.9	22.0	.18459	.00143
865	112.28	1.23	53.00	15.088	0.310	1,433.3	21.6	.18601	.00142
870	113.51	1.23	53.88	15.402	0.314	1,412.2	21.1	.18742	.00141
875	114.74	1.23	54.76	15.721	0.319	1,391.5	20.7	.18883	.00141
880	115.96	1.22	55.65	16.045	0.324	1,371.2	20.3	.19023	.00140
885	117.19	1.23	56.54	16.374	0.329	1,351.2	20.0	.19162	.00139
890	118.42	1.23	57.42	16.708	0.334	1,331.6	19.6	.19300	.00138
895	119.65	1.23	58.30	17.047	0.339	1,312.5	19.1	.19438	.00138

TABLE 4·4 (*Continued*)

THERMODYNAMIC PROPERTIES OF DRY AIR

(Keenan and Kaye, *Trans. A.S.M.E.*, 1943, p. A123.)

Temperature R T	Enthalpy Btu/lb h	Diff.	Internal Energy Btu/lb u	Relative Pressure p_r	Diff.	Relative Volume $v_r \times 10^4$	Diff.	$\int c_p \, dt$ ϕ	Diff.
900	120.88	1.23	59.19	17.391	0.344	1,293.7	18.3	.19575	.00137
905	122.11	1.23	60.08	17.740	0.349	1,275.3	18.4	.19711	.00136
910	123.34	1.23	60.97	18.095	0.355	1,257.2	18.1	.19847	.00136
915	124.57	1.23	61.86	18.455	0.360	1,239.5	17.7	.19982	.00135
920	125.80	1.23	62.75	18.820	0.365	1,222.1	17.4	.20116	.00134
925	127.04	1.24	63.64	19.191	0.371	1,205.0	17.1	.20250	.00134
930	128.27	1.23	64.53	19.567	0.376	1,188.2	16.8	.20383	.00133
935	129.50	1.23	65.42	19.949	0.382	1,171.8	16.4	.20515	.00132
940	130.73	1.23	66.31	20.336	0.387	1,155.6	16.2	.20647	.00132
945	131.97	1.24	67.21	20.728	0.392	1,139.7	15.9	.20778	.00131
950	133.21	1.24	68.10	21.126	0.398	1,124.2	15.5	.20909	.00131
955	134.45	1.24	68.99	21.530	0.404	1,108.9	15.3	.21039	.00130
960	135.69	1.24	69.89	21.940	0.410	1,093.8	15.1	.21168	.00129
965	136.93	1.24	70.79	22.356	0.416	1,079.0	14.8	.21297	.00129
970	138.17	1.24	71.68	22.778	0.422	1,064.6	14.4	.21425	.00128
975	139.41	1.24	72.58	23.205	0.427	1,050.4	14.2	.21552	.00127
980	140.65	1.24	73.48	23.639	0.434	1,036.4	14.0	.21679	.00127
985	141.89	1.24	74.38	24.079	0.440	1,022.6	13.8	.21805	.00126
990	143.14	1.24	75.28	24.525	0.445	1,009.1	13.5	.21931	.00126
995	144.38	1.25	76.18	24.977	0.452	995.9	13.2	.22056	.00125
1,000	145.62	1.24	77.08	25.44	0.463	982.9	13.0	.22181	.00125
1,010	148.11	2.49	78.88	26.37	0.93	957.4	22.5	.22429	.00248
1,020	150.60	2.49	80.69	27.33	0.96	932.9	24.5	.22675	.00246
1,030	153.10	2.50	82.50	28.32	0.99	909.2	23.7	.22919	.00244
1,040	155.60	2.50	84.31	29.34	1.02	886.2	23.0	.23160	.00241
1,050	158.10	2.50	86.13	30.38	1.04	864.0	22.2	.23399	.00239
1,060	160.60	2.50	87.95	31.45	1.07	842.6	21.4	.23636	.00237
1,070	163.11	2.51	89.77	32.55	1.10	821.8	20.8	.23871	.00235
1,080	165.62	2.51	91.59	33.68	1.13	801.7	20.1	.24105	.00234
1,090	168.13	2.51	93.42	34.84	1.16	782.2	19.5	.24337	.00232
1,100	170.65	2.52	95.25	36.02	1.18	763.4	18.8	.24567	.00230
1,110	173.17	2.52	97.08	37.24	1.22	745.1	18.3	.24795	.00228
1,120	175.69	2.52	98.92	38.49	1.25	727.4	17.7	.25021	.00226
1,130	178.22	2.53	100.76	39.77	1.28	710.2	17.2	.25245	.00224
1,140	180.75	2.53	102.60	41.09	1.32	693.6	16.6	.25468	.00223
1,150	183.28	2.53	104.45	42.44	1.35	677.5	16.1	.25689	.00221
1,160	185.81	2.53	106.30	43.82	1.38	661.9	15.6	.25909	.00220
1,170	188.35	2.54	108.15	45.23	1.41	646.7	15.2	.26127	.00218
1,180	190.89	2.54	110.01	46.68	1.45	631.9	14.8	.26343	.00216
1,190	193.43	2.54	111 87	48.17	1.49	617.6	14 3	.26558	.00215

TABLE 4·4 (*Continued*)

THERMODYNAMIC PROPERTIES OF DRY AIR

(Keenan and Kaye, *Trans. A.S.M.E.*, 1943, p. A123.)

Temperature R T	Enthalpy Btu/lb h	Diff.	Internal Energy Btu/lb u	Relative Pressure p_r	Diff.	Relative Volume $v_r \times 10^4$	Diff.	$\int c_p\, dt$ ϕ	Diff.
1,200	195.98	2.55	113.73	49.69	1.52	603.8	13.8	.26771	.00213
1,210	198.53	2.55	115.60	51.25	1.56	590.3	13.5	.26983	.00212
1,220	201.08	2.55	117.47	52.85	1.60	577.2	13.1	.27193	.00210
1,230	203.64	2.56	119.34	54.48	1.63	564.5	12.7	.27402	.00209
1,240	206.20	2.56	121.21	56.15	1.67	552.1	12.4	.27609	.00207
1,250	208.76	2.56	123.09	57.86	1.71	540.1	12.0	.27815	.00206
1,260	211.33	2.57	124.97	59.61	1.75	528.4	11.7	.28019	.00204
1,270	213.90	2.57	126.86	61.40	1.79	517.0	11.4	.28222	.00203
1,280	216.47	2.57	128.75	63.24	1.84	506.0	11.0	.28424	.00202
1,290	219.05	2.58	130.64	65.12	1.88	495.3	10.7	.28625	.00201
1,300	221.63	2.58	132.53	67.04	1.92	484.8	10.5	.28824	.00199
1,310	224.21	2.58	134.43	69.00	1.96	474.6	10.2	.29022	.00198
1,320	226.80	2.59	136.33	71.01	2.01	464.7	9.9	.29219	.00197
1,330	229.39	2.59	138.23	73.06	2.05	455.1	9.6	.29414	.00195
1,340	231.98	2.59	140.13	75.16	2.10	445.7	9.4	.29608	.00194
1,350	234.58	2.60	142.04	77.31	2.15	436.5	9.2	.29801	.00193
1,360	237.18	2.60	143.95	79.51	2.20	427.6	8.9	.29993	.00192
1,370	239.78	2.60	145.87	81.75	2.24	418.9	8.7	.30184	.00191
1,380	242.39	2.61	147.79	84.04	2.29	410.5	8.4	.30373	.00189
1,390	245.00	2.61	149.71	86.38	2.34	402.3	8.2	.30561	.00188
1,400	247.61	2.61	151.64	88.77	2.39	394.3	8.0	.30748	.00187
1,410	250.22	2.61	153.57	91.21	2.44	386.5	7.8	.30934	.00186
1,420	252.84	2.62	155.50	93.71	2.50	378.9	7.6	.31119	.00185
1,430	255.46	2.62	157.44	96.26	2.55	371.5	7.4	.31303	.00184
1,440	258.08	2.62	159.38	98.86	2.60	364.2	7.3	.31486	.00183
1,450	260.71	2.63	161.32	101.52	2.66	357.1	7.1	.31668	.00182
1,460	263.34	2.63	163.26	104.23	2.71	350.2	6.9	.31849	.00181
1,470	265.97	2.63	165.21	107.00	2.77	343.5	6.7	.32029	.00180
1,480	268.61	2.64	167.16	109.83	2.83	336.9	6.6	.32207	.00178
1,490	271.25	2.64	169.11	112.71	2.88	330.5	6.4	.32385	.00178
1,500	273.89	2.64	171.07	115.66	2.95	324.2	6.3	.32562	.00177
1,510	276.54	2.65	173 03	118.66	3.00	318.1	6.1	.32738	.00176
1,520	279.19	2.65	174.99	121.72	3.06	312.2	5.9	.32913	.00175
1,530	281.84	2.65	176.96	124.85	3.13	306.4	5.8	.33087	.00174
1,540	284.49	2.65	178.93	128.04	3.19	300.7	5.7	.33260	.00173
1,550	287.15	2.66	180.90	131.29	3.25	295.1	5.6	.33432	.00172
1,560	289.81	2.66	182.88	134.61	3.32	289.7	5.4	.33603	.00171
1,570	292.47	2.66	184.86	137.99	3.38	284.4	5.3	.33773	.00170
1,580	295.14	2.67	186.84	141.44	3.45	279.2	5.2	.33942	.00169
1,590	297.81	2.67	188.82	144.96	3.52	274.2	5.0	.34110	.00168

TABLE 4·4 (*Continued*)

THERMODYNAMIC PROPERTIES OF DRY AIR

(Keenan and Kaye, *Trans. A.S.M.E.*, 1943, p. A123.)

Temperature R T	Enthalpy Btu/lb h	Diff.	Internal Energy Btu/lb u	Relative Pressure p_r	Diff.	Relative Volume $v_r \times 10^4$	Diff.	$\int c_p\, dt$ ϕ	Diff.
1,600	300.48	2.67	190.81	148.55	3.59	269.3	4.9	.34278	.00168
1,610	303.15	2.67	192.80	152.21	3.66	264.4	4.9	.34445	.00167
1,620	305.83	2.68	194.79	155.93	3.72	259.7	4.7	.34611	.00166
1,630	308.51	2.68	196.78	159.72	3.79	255.1	4.6	.34776	.00165
1,640	311.19	2.68	198.78	163.59	3.87	250.6	4.5	.34940	.00164
1,650	313.88	2.68	200.78	167.54	3.95	246.2	4.4	.35103	.00163
1,660	316.57	2.69	202.78	171.56	4.02	241.9	4.3	.35265	.00162
1,670	319.26	2.69	204.79	175.66	4.10	237.7	4.2	.35427	.00162
1,680	321.95	2.69	206.80	179.83	4.17	233.6	4.1	.35588	.00161
1,690	324.65	2.70	208.81	184.08	4.25	229.5	4.1	.35748	.00160
1,700	327.35	2.70	210.82	188.4	4.32	225.57	3.93	.35907	.00159
1,720	332.75	5.40	214.86	197.3	8.9	217.94	7.63	.36223	.00316
1,740	338.16	5.41	218.90	206.5	9.2	210.63	7.31	.36536	.00313
1,760	343.59	5.43	222.96	216.1	9.6	203.62	7.01	.36846	.00310
1,780	349.03	5.44	227.03	226.0	9.9	196.90	6.72	.37153	.00307
1,800	354.48	5.45	231.11	236.3	10.3	190.46	6.44	.37458	.00305
1,820	359.94	5.46	235.20	246.9	10.6	184.29	6.17	.37760	.00302
1,840	365.41	5.47	239.30	257.9	11.0	178.37	5.92	.38059	.00299
1,860	370.89	5.48	243.41	269.3	11.4	172.68	5.69	.38355	.00296
1,880	376.38	5.49	247.52	281.1	11.8	167.22	5.46	.38648	.00293
1,900	381.88	5.50	251.65	293.3	12.2	161.97	5.25	.38939	.00291
1,920	387.39	5.51	255.79	305.9	12.6	156.93	5.04	.39228	.00289
1,940	392.91	5.52	259.93	318.9	13.0	152.09	4.84	.39514	.00286
1,960	398.44	5.53	264.09	332.3	13.4	147.44	4.65	.39797	.00283
1,980	403.97	5.53	268.26	346.2	13.8	142.96	4.48	.40078	.00281
2,000	409.51	5.54	272.43	360.6	14.4	138.65	4.31	.40357	.00279
2,020	415.07	5.56	276.61	375.5	14.9	134.50	4.15	.40633	.00276
2,040	420.64	5.57	280.80	390.8	15.3	130.51	3.99	.40907	.00274
2,060	426.21	5.57	285.00	406.6	15.8	126.67	3.84	.41179	.00272
2,080	431.79	5.58	289.21	422.9	16.3	122.97	3.70	.41449	.00270
2,100	437.38	5.59	293.43	439.7	16.8	119.40	3.57	.41716	.00267
2,120	442.98	5.60	297.66	457.1	17.4	115.96	3.44	.41981	.00265
2,140	448.58	5.60	301.89	475.0	17.9	112.65	3.31	.42244	.00263
2,160	454.19	5.61	306.13	493.4	18.4	109.46	3.19	.42505	.00261
2,180	459.81	5.62	310.38	512.4	19.0	106.38	3.08	.42764	.00259
2,200	465.43	5.62	314.64	532.0	19.6	103.40	2.98	.43021	.00257
2,220	471.06	5.63	318.90	552.1	20.1	100.53	2.87	.43276	.00255
2,240	476.70	5.64	323.17	572.8	20.7	97.76	2.77	.43529	.00253
2,260	482.35	5.65	327.45	594.2	21.4	95.08	2.68	.43780	.00251
2,280	488.01	5.66	331.73	616.2	22.0	92.49	2.59	.44029	.00249

TABLE 4·4 (*Continued*)

THERMODYNAMIC PROPERTIES OF DRY AIR

(Keenan and Kaye, *Trans. A.S.M.E.*, 1943, p. A123.)

Temperature R T	Enthalpy Btu/lb h	Diff.	Internal Energy Btu/lb u	Relative Pressure p_r	Diff.	Relative Volume $v_r \times 10^4$	Diff.	$\int c_p \, dt$ ϕ	Diff.
2,300	493.67	5.66	336.02	638.9	22.7	90.00	2.49	.44276	.00247
2,320	499.34	5.67	340.32	662.2	23.3	87.59	2.41	.44521	.00245
2,340	505.02	5.68	344.62	686.1	23.9	85.26	2.33	.44765	.00244
2,360	510.70	5.68	348.93	710.7	24.6	83.01	2.25	.45007	.00242
2,380	516.39	5.69	353.25	736.1	25.4	80.83	2.18	.45247	.00240
2,400	522.09	5.70	357.58	762.2	26.1	78.72	2.11	.45485	.00238
2,420	527.79	5.70	361.92	788.9	26.7	76.69	2.03	.45722	.00237
2,440	533.50	5.71	366.26	816.4	27.5	74.72	1.97	.45957	.00235
2,460	539.22	5.72	370.60	844.7	28.3	72.81	1.91	.46190	.00233
2,480	544.94	5.72	374.95	873.8	29.1	70.96	1.85	.46422	.00232
2,500	550.67	5.73	379.31	903.6	29.8	69.17	1.79	.46652	.00230
2,520	556.41	5.74	383.67	934.2	30.6	67.44	1.73	.46880	.00228
2,540	562.15	5.74	388.04	965.6	31.4	65.76	1.68	.47107	.00227
2,560	567.90	5.75	392.42	997.9	32.3	64.13	1.63	.47333	.00226
2,580	573.65	5.75	396.80	1,031.0	33.1	62.55	1.58	.47557	.00224
2,600	579.41	5.76	401.19	1,065.0	34.0	61.03	1.52	.47779	.00222
2,620	585.17	5.76	405.58	1,099.8	34.8	59.55	1.48	.48000	.00221
2,640	590.94	5.77	409.98	1,135.6	35.6	58.11	1.44	.48219	.00219
2,660	596.72	5.78	414.38	1,172.3	36.7	56.72	1.39	.48437	.00218
2,680	602.50	5.78	418.79	1,210.0	37.7	55.37	1.35	.48654	.00217
2,700	608.28	5.78	423.21	1,248.6	38.6	54.06	1.31	.48869	.00215
2,720	614.07	5.79	427.63	1,288.1	39.5	52.79	1.27	.49083	.00214
2,740	619.87	5.80	432.06	1,328.6	40.5	51.56	1.23	.49295	.00212
2,760	625.67	5.80	436.49	1,370.1	41.5	50.36	1.20	.49506	.00211
2,780	631.48	5.81	440.92	1,412.7	42.6	49.19	1.17	.49716	.00210
2,800	637.29	5.81	445.36	1,456.3	43.6	48.06	1.13	.49924	.00208
2,820	643.11	5.82	449.81	1,500.9	44.6	46.97	1.09	.50131	.00207
2,840	648.93	5.82	454.26	1,546.6	45.7	45.90	1.07	.50337	.00206
2,860	654.75	5.82	458.72	1,593.5	46.9	44.86	1.04	.50541	.00204
2,880	660.58	5.83	463.18	1,641.5	48.0	43.86	1.00	.50744	.00203
2,900	666.42	5.84	467.65	1,690.6	49.1	42.88	0.98	.50946	.00202
2,920	672.26	5.84	472.12	1,740.8	50.2	41.93	0.95	.51147	.00201
2,940	678.11	5.85	476.60	1,792.2	51.4	41.01	0.92	.51347	.00200
2,960	683.96	5.85	481.08	1,844.8	52.6	40.11	0.90	.51545	.00198
2,980	689.82	5.86	485.56	1,898.7	53.9	39.24	0.87	.51742	.00197
3,000	695.68	5.86	490.05	1,954.	55.3	38.39	0.85	.51938	.00196
3,020	701.54	5.86	494.54	2,010.	56.	37.56	0.83	.52133	.00195
3,040	707.41	5.87	499.04	2,068.	58.	36.75	0.81	.52327	.00194
3,060	713.28	5.87	503.54	2,127.	59.	35.97	0.78	.52520	.00193
3,080	719.16	5.88	508.05	2,187.	60.	35.21	0.76	.52711	.00191

The equation for an entropy change ds is given by

$$ds = c_p \frac{dT}{T} - \frac{v}{JT} dp = c_p \frac{dT}{T} - \frac{RT}{pTJ} dp = c_p \frac{dT}{T} - \frac{R}{J} \frac{dp}{p} \qquad (16)$$

From equation 16 it is seen that the entropy of a gas is a function of both its pressure and temperature. Consequently, to compile a general table of entropy values requires calculating them at different temperatures for each constant pressure. In general, from equation 16 the entropy above the base temperature T_0 and base pressure p_0 is given by

$$s = \int_{T_0}^{T} c_p \frac{dT}{T} - \frac{R}{J} \log_e \frac{p}{p_0} = \phi - \frac{R}{J} \log_e \frac{p}{p_0} \qquad (17)$$

In an isentropic process, however, $ds = 0$ so that

$$\frac{v}{J} dp = c_p \, dT$$

or

$$\frac{dp}{p} = \frac{Jc_p}{R} \frac{dT}{T} \quad \text{(isentropic process)} \qquad (17a)$$

If the subscript zero is used to designate the base condition for the gas table, then an isentropic process is given by

$$\log_e \frac{p}{p_0} = \frac{J}{R} \int_{T_0}^{T} c_p \frac{dT}{T} \qquad (18)$$

From equation 18 it is seen that the pressure ratio p/p_0, termed the *relative pressure*, is a single-valued function of the temperature once the base temperature T_0 has been designated. The same remarks are applicable to the volume ratio v/v_0, since for gases

$$\frac{v}{v_0} = \frac{p_0}{p} \frac{T}{T_0} \qquad (19)$$

The base conditions for Table 4·4 are $T_0 = 400$ R, $p_0 = 1$ psia, and $h_0 = 0$; then the pressure ratio equation for an isentropic process reduces to

$$\log_e p = \frac{J}{R} \int_{400}^{T} c_p \frac{dT}{T} \qquad (20)$$

For an isentropic process between the temperature limits T_1 and T_2, . the ratio of p_1 and p_2 is equal to the ratio of the relative pressures

$p_1/p_0 = p_{r1}$ and $p_2/p_0 = p_{r2}$. Similarly for the corresponding volume ratios. The table lists the values of $10,000v/v_0$, where v/v_0 is calculated from equation 19.

A change in entropy between conditions 1 and 2 is determined from the table as follows. Using equation 7

$$s_2 - s_1 = \phi_2 - \phi_1 - \frac{R}{J} \log_e \frac{p_2}{p_1}$$

$$= \phi_2 - \phi_1 - 0.6854 \log_e \frac{p_2}{p_1} \tag{21}$$

The value of the internal energy at any temperature T can be calculated from the enthalpy by means of the expression

$$u = h - \frac{RT}{J} \quad \text{Btu/lb}$$

At the base temperature of the table (400 R) the enthalpy has been set arbitrarily at the value zero. Hence at 400 R

$$u = 0 - \frac{53.35}{778} \times 400 = -27.42 \quad \text{Btu/lb}$$

Hence, at the base temperature of the table, the values of the properties of air are as follows:

$$T_0 = 400 \text{ R}, \quad u_0 = -27.42 \text{ Btu/lb}, \quad h_0 = 0 \text{ Btu/lb}$$

$$p_r = 1.0, \quad v_r = 10,000, \quad \text{and} \quad \phi_0 = \int c_p \frac{dT}{T} = 0$$

EXAMPLE. Air is compressed from 1 atm pressure and 520 R temperature to 3 atm pressure. What work must be supplied to the compressor under the following conditions: (a) compressor efficiency $\eta_c = 1.0$; (b) compressor efficiency $\eta_c = 0.6$? Also find (c) entropy change corresponding to (b).

Solution.

(a) $T_1 = 520$ R, from Table 4·4, $p_{r1} = 2.506$, $h_1 = 28.80$ Btu/lb, and $p_{r2} = 3 \times p_{r1} = 3 \times 2.506 = 7.518$.

Entering Table 4·4 at $p_{r2} = 7.518$ gives the temperature corresponding to an isentropic compression $T_{2s} = 711$ R and $h_{2s} = 78.16$ Btu/lb.

$\Delta h_c' =$ isentropic compression work $= 78.16 - 28.80 = 49.36$ Btu/lb

(b) $\eta_c = 0.60$

$$\Delta h_c = \text{Work of compression} = \frac{\Delta h_c'}{\eta_c} = \frac{49.36}{0.6} = 82.27 \quad \text{Btu/lb}$$

$$h_2 = h_1 + \Delta h_c = 28.80 + 82.27 = 111.07 \quad \text{Btu/lb}$$

T_2 from Table 4·4 is 860 R.

(c) The entropy change is given by

$$\Delta s = \phi_2 - \phi_1 - 0.06854 \log_e \frac{p_2}{p_1}$$

$$\frac{p_2}{p_1} = 3.0 \qquad \log_e \frac{p_2}{p_1} = 1.09861 \qquad T_1 = 520 \text{ R} \qquad \phi_1 = 0.06297$$

$$T_2 = 860 \text{ R} \qquad \phi_2 = 0.18459$$

Hence

$$\Delta s = 0.18459 - 0.06297 - 0.06854 \times 1.09861$$

$$= 0.04635 \quad \text{Btu/lb F}$$

The entropy change can also be calculated from values of ϕ_2 and ϕ_{2s}. Thus

From (a) at $T_{2s} = 711$ R the value of $\phi_{2s} = 0.13824$

From (b) at $T_2 = 860$ R the value of $\phi_2 = 0.18459$

$$\Delta s = \phi_2 - \phi_{2s} = 0.04635 \quad \text{Btu/lb F}$$

EXAMPLE. A stream of air under steady state conditions enters a nozzle with a velocity of 100 fps, a pressure of 10 atm, and a temperature of 1500 R. The back pressure into which the nozzle discharges is 1 atm. Find: (a) the exit velocity of the jet, assuming unity velocity coefficient; (b) ratio of entrance area to discharge area.

Solution.

(a) $T_1 = 1500$ R, $p_{r1} = 115.66$, $h_1 = 273.89$ Btu/lb, $c_1 = 100$ fps, $p_2/p_1 = 1/10$; hence $p_{r2} = 115.66/10 = 11.566$. From Table 4·4 the following values are obtained for thermodynamic properties corresponding to $p_{r2} = 11.566$

$$T_{2s} = 804.84 \text{ R} \quad \text{and} \quad h_{2s} = 97.09 \quad \text{Btu/lb}$$

The work of isentropic expansion $\Delta h_t'$ is given by

$$\Delta h_t' = (h_1 - h_{2s}) = \frac{c_2{}^2 - c_1{}^2}{2gJ} = 273.89 - 97.09 = 176.8 \quad \text{Btu/lb}$$

Hence

$$c_2 = \sqrt{2gJ(176.8) + c_1{}^2} = 2978 \text{ fps}$$

The exit velocity $c_2 = 2980 + 100 = 3080$ fps.

(b) *Area Ratio.* From continuity, see Chapter 3, it follows that

$$G = \frac{A_1 c_1}{v_1} = \frac{A_2 c_2}{v_2}$$

Hence

$$\frac{A_1}{A_2} = \frac{c_2}{c_1} \cdot \frac{v_1}{v_2} = \frac{v_{r1}}{v_{r2}} \cdot \frac{c_2}{c_1}$$

From Table 4·4, $v_{r1} = 324.2$ and $v_{r2} = 1735.7$

$$\frac{A_1}{A_2} = \frac{324.2}{1735.7} \cdot \frac{3080}{100} = 5.76$$

EXAMPLE. A 5000-cu-ft tank contains air at $p_1 = 60$ psia and $T_1 = 1000$ R. The air is discharged from the tank into the atmosphere through a nozzle, until the mass of air contained in the tank has been reduced to one-half its original value. Assuming that there are no heat or friction losses, so that the process is isentropic, find the pressure and temperature of the air remaining in the tank.

Solution. From Table 4·4, $T_1 = 1000$ R, $v_{r1} = 982$ 9, $p_{r1} = 25.44$, and $p_1 = 60$ psia. Since one-half the mass of gas still occupies 5000 cu ft, the final specific volume is twice the original. Thus

$$v_2 = 2v_1 \quad \text{so that} \quad v_{r2} = 2v_{r1} = 1965.8$$

The corresponding value for $p_{r2} = 9.722$ and for $T_2 = 764.5$ R.

$$p_2 = p_1 \times \frac{p_{r2}}{p_{r1}} = 60 \times \frac{9.722}{25.44} = 22.87 \quad \text{psia}$$

8. Normal Air Table—Correction-Factor Method for Calculating Compression and Expansion Work

In determining the work for a flow compression or expansion it is at times more convenient to use Table 4·5 than Table 4·4. Table 4·5 can be used in conjunction with Fig. 9 for compressors and Fig. 10 for expansion processes. These figures present correction factors by which the perfect-gas values obtained by using Table 4·5 are corrected to take into account the variation of the specific heat of air with temperature. For normal air, assumed to be a perfect gas, the isentropic work corresponding to a flow compression $\Delta h_c'$ is as given in Chapter 1

$$\Delta h_c' = c_p T_1 Z_c \quad \text{(for normal air)} \tag{22}$$

For air at moderate pressures and temperature the A.S.M.E. Power Test Code for compressors uses $c_p = 0.243$ Btu/lb F.

$$\Delta h_c' = 0.243 T_1 Z_c \quad \text{Btu/lb} \tag{23}$$

The corresponding isentropic work when the variation in specific heat with the air temperature is taken into amount is given by

$$\Delta h_c' = 0.243 K_c T_1 Z_c \quad \text{Btu/lb} \tag{24}$$

where K_c = correction factor from Fig. 9.

$Z_c = \left(\dfrac{p_2}{p_1}\right)^{0.283} - 1$ from Table 4·5.

T_1 = inlet temperature, R.

The actual work of compression, where η_c is the efficiency of the compression, is given by the equation

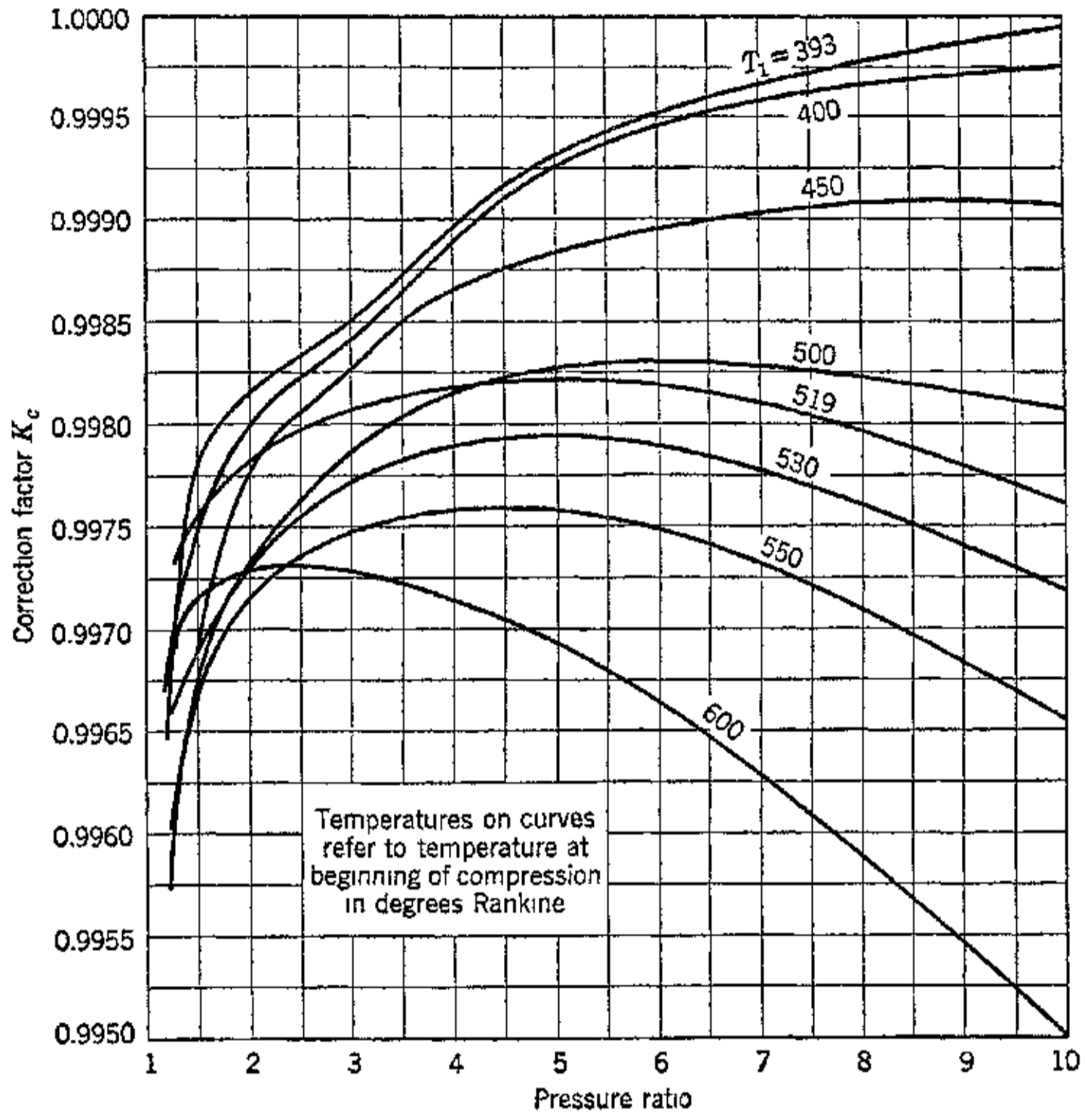$$\Delta h_c = \frac{0.243 K_c T_1 Z_c}{\eta_c} \quad \text{Btu/lb} \tag{25}$$

FIG. 9.   Correction factor K_c vs. pressure ratio (compression processes).

TABLE 4.5

Values of Z for Standard Air and Perfect Diatomic Gases

$$Z = \left(\frac{p_1}{p_0}\right)^{0.283} - 1 \quad \text{or} \quad Z = r^{0.283} - 1$$

r		0	1	2	3	4	5	6	7	8	9
1.00	0.00	000	028	057	085	113	141	169	198	226	254
1.01		282	310	338	366	394	422	450	478	506	534
1.02		552	590	618	646	673	701	729	757	785	812
1.03	0.01	840	868	895	923	951	978	006	034	061	089
1.04		116	144	171	199	226	253	281	308	336	363
1.05		390	418	445	472	500	527	554	581	608	636
1.06		663	690	717	744	771	798	825	852	879	906
1.07	0.02	933	960	987	014	041	068	095	122	148	175
1.08		202	229	255	282	309	336	362	389	416	442
1.09		469	495	522	549	575	602	628	655	681	708
1.10		734	760	787	813	840	866	892	919	945	971
1.11	0.03	997	024	050	076	102	129	155	181	207	233
1.12		259	285	311	337	363	389	415	441	467	493
1.13		519	545	571	597	623	649	675	700	726	752
1.14		778	804	829	855	881	906	932	958	983	009
1.15	0.04	035	060	086	111	137	162	188	213	239	264
1.16		290	315	341	366	391	417	442	467	493	518
1.17		543	569	594	619	644	670	695	720	745	770
1.18		796	821	846	871	896	921	946	971	996	021
1.19	0.05	046	071	096	121	146	171	196	221	245	270
1.20		295	320	345	370	394	419	444	469	493	518
1.21		543	567	592	617	641	666	691	715	740	764
1.22		789	813	838	862	887	911	936	960	985	009
1.23	0.06	034	058	082	107	131	155	180	204	228	253
1.24		277	301	325	350	374	398	422	446	470	495
1.25		519	543	567	591	615	639	663	687	711	735
1.26		759	783	807	831	855	879	903	927	951	974
1.27		998	022	046	070	094	117	141	165	189	212
1.28	0.07	236	260	283	307	331	354	378	402	425	449
1.29		472	496	520	543	567	590	614	637	661	684
1.30		708	731	754	778	801	825	848	871	895	918
1.31		941	965	988	011	035	058	081	104	128	151
1.32	0.08	174	197	220	243	267	290	313	336	359	382
1.33		405	428	451	474	497	520	543	566	589	612
1.34		635	658	681	704	727	750	773	795	818	841
1.35	0.09	864	887	910	932	955	978	001	023	046	069
1.36		092	114	137	160	182	205	228	250	273	295
1.37		318	341	363	386	408	431	453	476	498	521
1.38		543	566	588	611	633	655	678	700	723	745
1.39		767	790	812	834	857	879	901	923	946	968
1.40	0.10	990	012	035	057	079	101	123	145	168	190
1.41		212	234	256	278	300	322	344	366	389	411
1.42		433	455	477	499	521	542	564	586	608	630
1.43		652	674	696	718	740	761	783	805	827	849
1.44	0.11	871	892	914	936	958	979	001	023	045	066
1.45		088	110	131	153	175	196	218	239	261	283
1.46		304	326	347	369	390	412	433	455	476	498
1.47		520	541	562	584	605	627	648	669	691	712
1.48		734	755	776	798	819	840	862	883	904	925
1.49		947	968	989	010	032	053	074	095	116	138
1.50	0.12	159	180	201	222	243	264	286	307	328	349
1.51		370	391	412	433	454	475	496	517	538	559
1.52		580	601	622	643	664	685	706	726	747	768
1.53		789	810	831	852	872	893	914	935	956	977
1.54	0.13	997	018	039	060	080	101	122	142	163	184
1.55		205	225	246	266	287	308	328	349	370	390
1.56		411	431	452	472	493	513	534	554	575	595
1.57		616	636	657	677	698	718	739	759	780	800
1.58		820	841	861	881	902	922	942	963	983	003
1.59	0.14	024	044	064	085	105	125	145	165	186	206
1.60		226	246	267	287	307	327	347	367	387	408
1.61		428	448	468	488	508	528	548	568	588	608
1.62		628	648	668	688	708	728	748	768	788	808
1.63		828	848	868	888	908	928	948	968	988	007

Proportional Parts

	29	28	27	26	25	24
1	2.9	2.8	2.7	2.6	2.5	2.4
2	5.8	5.6	5.4	5.2	5.0	4.8
3	8.7	8.4	8.1	7.8	7.5	7.2
4	11.6	11.2	10.8	10.4	10.0	9.6
5	14.5	14.0	13.5	13.0	12.5	12.0
6	17.4	16.8	16.2	15.6	15.0	14.4
7	20.3	19.6	18.9	18.2	17.5	16.8
8	23.2	22.4	21.6	20.8	20.0	19.2
9	26.1	25.2	24.3	23.4	22.5	21.6

r		0	1	2	3	4	5	6	7	8	9
2.00		672	689	707	724	741	758	775	792	810	827
2.01		844	861	878	895	913	930	947	964	981	998
2.02	0.22	015	032	049	066	084	101	118	135	152	169
2.03		186	203	220	237	254	271	288	305	322	339
2.04		356	373	390	407	424	441	458	474	491	508
2.05		525	542	559	576	593	610	627	644	660	677
2.06		694	711	728	745	762	778	795	812	829	846
2.07		863	879	896	913	930	946	963	980	997	013
2.08	0.23	030	047	064	080	097	114	130	147	164	181
2.09		197	214	231	247	264	281	297	314	331	347
2.10		364	380	397	414	430	447	463	480	497	513
2.11		530	546	563	579	596	613	629	646	662	679
2.12		695	712	728	745	761	778	794	811	827	844
2.13		860	877	893	909	926	942	959	975	992	008
2.14	0.24	024	041	057	074	090	106	123	139	155	172
2.15		188	204	221	237	253	270	286	302	319	335
2.16		351	368	384	400	416	433	449	465	481	498
2.17		514	530	546	563	579	595	611	627	644	660
2.18		676	692	708	724	741	757	773	789	805	821
2.19		838	854	870	886	902	918	934	950	966	983
2.20		999	015	031	047	063	079	095	111	127	143
2.21	0.25	159	175	191	207	223	239	255	271	287	303
2.22		319	335	351	367	383	399	415	431	447	463
2.23		479	495	511	526	542	558	574	590	606	622
2.24		638	654	669	685	701	717	733	749	765	780
2.25		796	812	828	844	859	875	891	907	923	938
2.26	0.26	954	970	986	001	017	033	049	064	080	096
2.27		112	127	143	159	175	190	206	222	237	253
2.28		269	284	300	316	331	347	363	378	394	409
2.29		425	441	456	472	488	503	519	534	550	566
2.30		581	597	612	628	643	659	675	690	706	721
2.31		737	752	768	783	799	814	830	845	861	876
2.32	0.27	892	907	923	938	954	969	984	000	015	031
2.33		046	062	077	092	108	123	139	154	169	185
2.34		200	216	231	246	262	277	292	308	323	338

Proportional parts

22	23	20	21	18	19	16	17
1 2.2	1 2.3	1 2.0	1 2.1	1 1.8	1 1.9	1 1.6	1 1.7
2 4.4	2 4.6	2 4.0	2 4.2	2 3.6	2 3.8	2 3.2	2 3.4
3 6.6	3 6.9	3 6.0	3 6.3	3 5.4	3 5.7	3 4.8	3 5.1
4 8.8	4 9.2	4 8.0	4 8.4	4 7.2	4 7.6	4 6.4	4 6.8
5 11.0	5 11.5	5 10.0	5 10.5	5 9.0	5 9.5	5 8.0	5 8.5
6 13.2	6 13.8	6 12.0	6 12.6	6 10.8	6 11.4	6 9.6	6 10.2
7 15.4	7 16.1	7 14.0	7 14.7	7 12.6	7 13.3	7 11.2	7 11.9
8 17.6	8 18.4	8 16.0	8 16.8	8 14.4	8 15.2	8 12.8	8 13.6
9 19.8	9 20.7	9 18.0	9 18.9	9 16.2	9 17.1	9 14.4	9 15.3

r		0	1	2	3	4	5	6	7	8	9
1.64	0.15	027	047	067	087	107	126	146	166	186	206
1.65		225	245	265	284	304	324	344	363	383	403
1.66		423	442	462	481	501	521	540	560	580	599
1.67		619	638	658	678	697	717	736	756	775	795
1.68		814	834	853	873	892	912	931	951	970	990
1.69	0.16	009	028	048	067	087	106	125	145	164	184
1.70		203	222	242	261	280	299	319	338	357	377
1.71		396	415	434	454	473	492	511	531	550	569
1.72		588	607	626	646	665	684	703	722	741	760
1.73		780	799	818	837	856	875	894	913	932	951
1.74		970	989	008	027	046	065	084	103	122	141
1.75	0.17	160	179	198	217	236	255	274	292	311	330
1.76		349	368	387	406	425	443	462	481	500	519
1.77		538	556	575	594	613	631	650	669	688	706
1.78		725	744	762	781	800	818	837	856	874	893
1.79		912	930	949	968	986	005	023	042	061	079
1.80	0.18	098	116	135	153	172	191	209	228	246	265
1.81		283	302	320	339	357	376	394	412	431	449
1.82		468	486	505	523	541	560	578	596	615	633
1.83		652	670	688	707	725	743	762	780	798	816
1.84		835	853	871	890	908	926	944	962	981	999
1.85	0.19	017	035	054	072	090	108	126	144	163	181
1.86		199	217	235	253	271	289	308	326	344	362
1.87		380	398	416	434	452	470	488	506	524	542
1.88		560	578	596	614	632	650	668	686	704	722
1.89		740	758	776	794	811	829	847	865	883	901
1.90		919	937	954	972	990	008	026	044	061	079
1.91	0.20	097	115	133	150	168	186	204	221	239	257
1.92		275	292	310	328	345	363	381	399	416	434
1.93		452	469	487	504	522	540	557	575	593	610
1.94		628	645	663	681	698	716	733	751	768	786
1.95		804	821	839	856	874	891	909	926	944	961
1.96		979	996	013	031	048	066	083	101	118	135
1.97	0.21	153	170	188	205	222	240	257	275	292	309
1.98		327	344	361	379	396	413	431	448	465	482
1.99	0.21	500	517	534	552	569	586	603	620	638	655

TABLE 4·5 (*Continued*)

VALUES OF Z FOR STANDARD AIR AND PERFECT DIATOMIC GASES

r		0	1	2	3	4	5	6	7	8	9
2.35		354	369	384	400	415	430	446	461	476	492
2.36		507	522	538	553	568	583	599	614	629	644
2.37		660	675	690	705	721	736	751	766	781	797
2.38		812	827	842	857	873	888	903	918	933	948
2.39		964	979	994	009	024	039	054	070	085	100
2.40	0.28	115	130	145	160	175	190	205	220	236	251
2.41		266	281	296	311	326	341	356	371	386	401
2.42		416	431	446	461	476	491	506	521	536	551
2.43		566	581	596	611	626	641	656	671	686	701
2.44		716	730	745	760	775	790	805	820	835	850
2.45		865	879	894	909	924	939	954	969	984	993
2.46	0.29	013	028	043	058	073	087	102	117	132	147
2.47		162	176	191	206	221	235	250	265	280	295
2.48		309	324	339	353	368	383	398	412	427	442
2.49		457	471	486	501	515	530	545	559	574	589
2.50		604	618	633	647	662	677	691	706	721	735
2.51		750	765	779	794	808	823	838	852	867	881
2.52		896	911	925	940	954	969	984	998	013	027
2.53	0.30	042	056	071	085	100	114	129	144	158	173
2.54		187	202	216	231	245	260	274	289	303	318
2.55		332	346	361	375	390	404	419	433	448	462
2.56		476	491	505	520	534	548	563	577	592	606
2.57		620	635	649	663	678	692	707	721	735	750
2.58		764	778	793	807	821	836	850	864	879	893
2.59		907	921	936	950	964	979	993	007	021	036
2.60	0.31	050	064	079	093	107	121	136	150	164	178
2.61		193	207	221	235	249	264	278	292	306	320
2.62		335	349	363	377	391	405	420	434	448	462
2.63		476	490	505	519	533	547	561	575	589	603
2.64		618	632	646	660	674	688	702	716	730	744
2.65		759	773	787	801	815	829	843	857	871	885
2.66		899	913	927	941	955	969	983	997	011	025
2.67	0.32	039	053	067	081	095	109	123	137	151	165
2.68		179	193	207	221	235	249	262	276	290	304
2.69		318	332	346	360	374	388	402	416	429	443
2.70		457	471	485	499	513	527	540	554	568	582
2.71		596	610	624	637	651	665	679	693	707	720
2.72		734	748	762	776	789	803	817	831	845	858
2.73		872	886	900	913	927	941	955	968	982	996
2.74	0.33	010	023	037	051	065	078	092	106	119	133
2.75		147	161	174	188	202	215	229	243	256	270
2.76		284	297	311	325	338	352	366	379	393	407
2.77		420	434	448	461	475	488	502	516	529	543
2.78		556	570	584	597	611	624	638	651	665	679
2.79		692	706	719	733	746	760	773	787	801	814
2.80		828	841	855	868	882	895	909	922	936	949
2.81		963	976	990	003	017	030	044	057	070	084
2.82	0.34	097	111	124	138	151	165	178	191	205	218
2.83		232	245	259	272	285	299	312	326	339	352
2.84		366	379	393	406	419	433	446	459	473	486
2.85		500	513	526	540	553	566	580	593	606	620
2.86		633	646	660	673	686	700	713	726	739	753
2.87		765	779	793	806	819	832	846	859	872	885
2.88		899	912	925	939	952	965	978	991	005	018
2.89	0.35	031	044	058	071	084	097	110	124	137	150
2.90		163	176	190	203	216	229	242	255	269	282
2.91		295	308	321	334	347	361	374	387	400	413
2.92		426	439	452	466	479	492	505	518	531	544
2.93		557	570	584	597	610	623	636	649	662	675
2.94		688	701	714	727	740	753	767	780	793	806
2.95		819	832	845	858	871	884	897	910	923	936
2.96		949	962	975	988	001	014	027	040	053	066
2.97	0.36	079	092	105	118	131	144	157	169	182	195
2.98		208	221	234	247	260	273	286	299	312	324
2.99		337	350	363	376	389	402	415	428	440	453

Proportional parts:

	14	15
1	1.4	1.5
2	2.8	3.0
3	4.2	4.5
4	5.6	6.0
5	7.0	7.5
6	8.4	9.0
7	9.8	10.5
8	11.2	12.0
9	12.6	13.5

	12	13
1	1.2	1.3
2	2.4	2.6
3	3.6	3.9
4	4.8	5.2
5	6.0	6.5
6	7.2	7.8
7	8.4	9.1
8	9.6	10.4
9	10.8	11.7

r	0	1	2	3	4	5	6	7	8	9
7.6	0.7753	0.7760	0.7766	0.7773	0.7779	0.7786	0.7792	0.7799	0.7806	0.7812
7.7	0.7819	0.7825	0.7832	0.7838	0.7845	0.7851	0.7858	0.7864	0.7871	0.7877
7.8	0.7884	0.7890	0.7897	0.7903	0.7910	0.7916	0.7923	0.7929	0.7936	0.7942
7.9	0.7949	0.7955	0.7961	0.7968	0.7974	0.7981	0.7987	0.7993	0.8000	0.8006
8.0	0.8013	0.8019	0.8025	0.8032	0.8038	0.8044	0.8051	0.8057	0.8063	0.8070
8.1	0.8076	0.8082	0.8089	0.8095	0.8101	0.8108	0.8114	0.8120	0.8126	0.8133
8.2	0.8139	0.8145	0.8151	0.8158	0.8164	0.8170	0.8176	0.8183	0.8189	0.8195
8.3	0.8201	0.8207	0.8214	0.8220	0.8226	0.8232	0.8238	0.8245	0.8251	0.8257
8.4	0.8263	0.8269	0.8275	0.8281	0.8288	0.8294	0.8300	0.8306	0.8312	0.8318
8.5	0.8324	0.8330	0.8336	0.8343	0.8349	0.8355	0.8361	0.8367	0.8373	0.8379
8.6	0.8385	0.8391	0.8397	0.8403	0.8409	0.8415	0.8421	0.8427	0.8433	0.8439
8.7	0.8445	0.8451	0.8457	0.8463	0.8469	0.8475	0.8481	0.8487	0.8493	0.8499
8.8	0.8505	0.8511	0.8517	0.8523	0.8529	0.8535	0.8541	0.8547	0.8552	0.8558
8.9	0.8564	0.8570	0.8576	0.8582	0.8588	0.8594	0.8600	0.8605	0.8611	0.8617
9.0	0.8623	0.8629	0.8635	0.8641	0.8646	0.8652	0.8658	0.8664	0.8670	0.8676
9.1	0.8681	0.8687	0.8693	0.8699	0.8705	0.8710	0.8716	0.8722	0.8728	0.8734
9.2	0.8739	0.8745	0.8751	0.8757	0.8762	0.8768	0.8774	0.8779	0.8785	0.8791
9.3	0.8797	0.8803	0.8808	0.8814	0.8819	0.8825	0.8831	0.8837	0.8842	0.8848
9.4	0.8854	0.8859	0.8865	0.8871	0.8876	0.8882	0.8888	0.8893	0.8899	0.8905
9.5	0.8910	0.8916	0.8921	0.8927	0.8933	0.8938	0.8944	0.8949	0.8955	0.8961
9.6	0.8966	0.8972	0.8977	0.8983	0.8989	0.8994	0.9000	0.9005	0.9011	0.9016
9.7	0.9022	0.9028	0.9033	0.9039	0.9044	0.9050	0.9055	0.9061	0.9066	0.9072
9.8	0.9077	0.9083	0.9088	0.9094	0.9099	0.9105	0.9110	0.9116	0.9121	0.9127
9.9	0.9132	0.9138	0.9143	0.9149	0.9154	0.9159	0.9165	0.9170	0.9176	0.9181
10.0	0.9187	0.9192	0.9198	0.9203	0.9208	0.9214	0.9219	0.9225	0.9230	0.9235
10.1	0.9241	0.9246	0.9252	0.9257	0.9262	0.9268	0.9273	0.9278	0.9284	0.9289
10.2	0.9295	0.9300	0.9305	0.9311	0.9316	0.9321	0.9327	0.9332	0.9337	0.9343
10.3	0.9348	0.9353	0.9358	0.9364	0.9369	0.9374	0.9380	0.9385	0.9390	0.9396
10.4	0.9401	0.9406	0.9411	0.9417	0.9422	0.9427	0.9432	0.9438	0.9443	0.9448
10.5	0.9453	0.9459	0.9464	0.9469	0.9474	0.9480	0.9485	0.9490	0.9495	0.9500
10.6	0.9506	0.9511	0.9516	0.9521	0.9526	0.9532	0.9537	0.9542	0.9547	0.9552
10.7	0.9558	0.9563	0.9568	0.9573	0.9578	0.9583	0.9589	0.9594	0.9599	0.9604
10.8	0.9609	0.9614	0.9619	0.9625	0.9630	0.9635	0.9640	0.9645	0.9650	0.9655
10.9	0.9660	0.9665	0.9671	0.9676	0.9681	0.9686	0.9691	0.9696	0.9701	0.9706
11.0	0.9711	0.9716	0.9721	0.9726	0.9732	0.9737	0.9742	0.9747	0.9752	0.9757
11.1	0.9762	0.9767	0.9772	0.9777	0.9782	0.9787	0.9792	0.9797	0.9802	0.9807
11.2	0.9812	0.9817	0.9822	0.9827	0.9832	0.9837	0.9842	0.9847	0.9852	0.9857
11.3	0.9862	0.9867	0.9872	0.9877	0.9882	0.9887	0.9892	0.9897	0.9902	0.9907
11.4	0.9912	0.9916	0.9921	0.9926	0.9931	0.9936	0.9941	0.9946	0.9951	0.9956
11.5	0.9961	0.9966	0.9971	0.9975	0.9980	0.9985	0.9990	0.9995	1.0000	1.0005
11.6	1.0010	1.0015	1.0019	1.0024	1.0029	1.0034	1.0039	1.0044	1.0049	1.0054
11.7	1.0058	1.0063	1.0068	1.0073	1.0078	1.0083	1.0087	1.0092	1.0097	1.0102
11.8	1.0107	1.0112	1.0116	1.0121	1.0126	1.0131	1.0136	1.0140	1.0145	1.0150
11.9	1.0155	1.0160	1.0164	1.0169	1.0174	1.0179	1.0184	1.0188	1.0193	1.0198
12.0	1.0203	1.0207	1.0212	1.0217	1.0222	1.0226	1.0231	1.0236	1.0241	1.0245

r	0	1	2	3	4	5	6	7	8	9
3.0	0.3647	0.3659	0.3672	0.3685	0.3698	0.3711	0.3723	0.3736	0.3749	0.3761
3.1	0.3774	0.3786	0.3799	0.3811	0.3824	0.3836	0.3849	0.3861	0.3874	0.3886
3.2	0.3898	0.3911	0.3923	0.3935	0.3947	0.3959	0.3971	0.3984	0.3996	0.4008
3.3	0.4020	0.4032	0.4044	0.4056	0.4068	0.4080	0.4091	0.4103	0.4115	0.4127
3.4	0.4139	0.4150	0.4162	0.4174	0.4186	0.4197	0.4209	0.4220	0.4232	0.4244
3.5	0.4255	0.4267	0.4278	0.4290	0.4301	0.4313	0.4324	0.4335	0.4347	0.4358
3.6	0.4369	0.4380	0.4392	0.4403	0.4414	0.4425	0.4437	0.4448	0.4459	0.4470
3.7	0.4481	0.4492	0.4503	0.4514	0.4525	0.4536	0.4547	0.4558	0.4569	0.4580
3.8	0.4591	0.4602	0.4612	0.4623	0.4634	0.4645	0.4656	0.4666	0.4677	0.4688
3.9	0.4698	0.4709	0.4720	0.4730	0.4741	0.4752	0.4762	0.4773	0.4783	0.4794
4.0	0.4804	0.4815	0.4825	0.4835	0.4846	0.4856	0.4867	0.4877	0.4887	0.4898
4.1	0.4908	0.4918	0.4928	0.4939	0.4949	0.4959	0.4970	0.4980	0.4990	0.5000
4.2	0.5010	0.5020	0.5030	0.5040	0.5050	0.5060	0.5070	0.5080	0.5090	0.5100
4.3	0.5110	0.5120	0.5130	0.5140	0.5150	0.5160	0.5170	0.5179	0.5189	0.5199
4.4	0.5209	0.5219	0.5228	0.5238	0.5248	0.5258	0.5267	0.5277	0.5287	0.5296
4.5	0.5306	0.5316	0.5325	0.5335	0.5344	0.5354	0.5363	0.5373	0.5382	0.5392
4.6	0.5401	0.5411	0.5420	0.5430	0.5439	0.5449	0.5458	0.5467	0.5477	0.5486
4.7	0.5495	0.5505	0.5514	0.5523	0.5533	0.5542	0.5551	0.5560	0.5570	0.5579
4.8	0.5588	0.5597	0.5606	0.5616	0.5625	0.5634	0.5643	0.5652	0.5661	0.5670
4.9	0.5679	0.5688	0.5697	0.5706	0.5715	0.5724	0.5733	0.5742	0.5751	0.5760
5.0	0.5769	0.5778	0.5787	0.5796	0.5805	0.5814	0.5822	0.5831	0.5840	0.5849
5.1	0.5858	0.5867	0.5875	0.5884	0.5893	0.5902	0.5910	0.5919	0.5928	0.5936
5.2	0.5945	0.5954	0.5962	0.5971	0.5980	0.5988	0.5997	0.6006	0.6014	0.6023
5.3	0.6031	0.6040	0.6048	0.6057	0.6065	0.6074	0.6082	0.6091	0.6099	0.6108
5.4	0.6116	0.6125	0.6133	0.6142	0.6150	0.6159	0.6167	0.6175	0.6184	0.6192
5.5	0.6200	0.6209	0.6217	0.6225	0.6234	0.6242	0.6250	0.6258	0.6267	0.6275
5.6	0.6283	0.6291	0.6300	0.6308	0.6316	0.6324	0.6332	0.6340	0.6349	0.6357
5.7	0.6365	0.6373	0.6381	0.6389	0.6397	0.6405	0.6413	0.6421	0.6430	0.6438
5.8	0.6446	0.6454	0.6462	0.6470	0.6478	0.6486	0.6494	0.6502	0.6509	0.6517
5.9	0.6525	0.6533	0.6541	0.6549	0.6557	0.6565	0.6573	0.6581	0.6588	0.6596
6.0	0.6604	0.6612	0.6620	0.6628	0.6635	0.6643	0.6651	0.6659	0.6666	0.6674
6.1	0.6682	0.6690	0.6697	0.6705	0.6713	0.6721	0.6729	0.6736	0.6744	0.6752
6.2	0.6759	0.6767	0.6774	0.6782	0.6789	0.6797	0.6805	0.6812	0.6820	0.6827
6.3	0.6835	0.6843	0.6850	0.6858	0.6865	0.6873	0.6880	0.6888	0.6895	0.6903
6.4	0.6910	0.6918	0.6925	0.6933	0.6940	0.6948	0.6955	0.6963	0.6970	0.6978
6.5	0.6985	0.6992	0.7000	0.7007	0.7014	0.7021	0.7028	0.7036	0.7043	0.7050
6.6	0.7058	0.7065	0.7073	0.7080	0.7087	0.7095	0.7102	0.7110	0.7117	0.7124
6.7	0.7131	0.7138	0.7145	0.7153	0.7160	0.7167	0.7174	0.7181	0.7189	0.7196
6.8	0.7203	0.7210	0.7217	0.7224	0.7232	0.7239	0.7246	0.7253	0.7260	0.7267
6.9	0.7274	0.7281	0.7288	0.7295	0.7302	0.7309	0.7316	0.7323	0.7330	0.7338
7.0	0.7345	0.7352	0.7359	0.7366	0.7373	0.7380	0.7386	0.7393	0.7400	0.7407
7.1	0.7414	0.7421	0.7428	0.7435	0.7442	0.7449	0.7456	0.7463	0.7470	0.7477
7.2	0.7483	0.7490	0.7497	0.7504	0.7511	0.7518	0.7524	0.7531	0.7538	0.7545
7.3	0.7552	0.7559	0.7565	0.7572	0.7579	0.7586	0.7592	0.7599	0.7606	0.7613
7.4	0.7620	0.7626	0.7633	0.7640	0.7646	0.7653	0.7660	0.7666	0.7673	0.7680
7.5	0.7687	0.7693	0.7700	0.7706	0.7713	0.7720	0.7726	0.7733	0.7740	0.7746

NOTE: Taken from "Engineering Computations for Air and Gases," by Moss and Smith, Trans. A.S.M.E., Vol. 52, 1930, paper APM-52-8. For nozzles, $r = p_1/p_3$. For compressors and exhausters, $r = p_2/p_1$.

Example. What will be the temperature rise in a single-stage compressor, assuming $\eta_c = 0.85$ and $T_1 = 528$ R, for pressure ratios r_c varying from 1.5 to 12.0?

Solution.
$$\Delta h_c' = 0.243 \times 528 \times K_c \times Z_c$$

The average value of K_c from Fig. 9 is 0.996. Hence the equation for isentropic compression work is
$$\Delta h_c' = 128.3 Z_c \quad \text{Btu/lb}$$

The results of the calculations are presented below.

r_c	Z_c	$\Delta h_c' =$ 128.3Z_c	$\Delta h_c =$ $\dfrac{\Delta h_c'}{\eta_c}$	$\Delta t'$	Average c_p	Δt	T_2
1.5	0.12159	15.58	18.35	75.5	0.2395	76.6	604.6 R
2.0	.21672	27.80	32.7	134.4	.2405	136.0	664
2.5	.29604	37.95	44.7	184	.2408	186	714
3.0	.3647	46.70	55.0	226	.2411	228	756
3.5	.4255	54.55	65.3	269	.2417	243	771
4.0	.4804	61.60	72.6	298	.2418	288	816
5.0	.5769	74.0	87.1	358	.2423	359	880
6.0	.6604	84.7	99.8	412	.2428	411	939
8.0	.8013	102.6	120.5	497	.2438	496	1014
10.0	.9187	117.8	138.7	572	.2448	569	1097
12.0	1.0203	131.0	154.0	632	.2456	627	1155

$\Delta t'$ = temperature rise based on constant $c_p = 0.243$.
Δt = temperature rise based on average c_p using Fig. 3.
Z_c = from Table 4-5.
$T_2 = t + T_1$, R.

For an expansion process analogous equations can be derived. Thus the work of an isentropic expansion is given by

$$\Delta h_t' = 0.243 T_1 K_t \frac{Z_t}{1 + Z_t} \tag{26}$$

where T_1 = initial temperature of air, R.
$Z_t = r_t^{0.283} - 1$; for values see Table 4-5.
$r_t = p_1/p_2$.
p_1 = initial pressure.
p_2 = final pressure.
K_t = correction factor for variation in specific heat of air; see Fig. 10.

Similarly the work of an actual expansion, through a turbine of efficiency η_t, for example, is given by

$$\Delta h_t = 0.243 T_1 K_t \eta_t \frac{Z_t}{1 + Z_t} \tag{27}$$
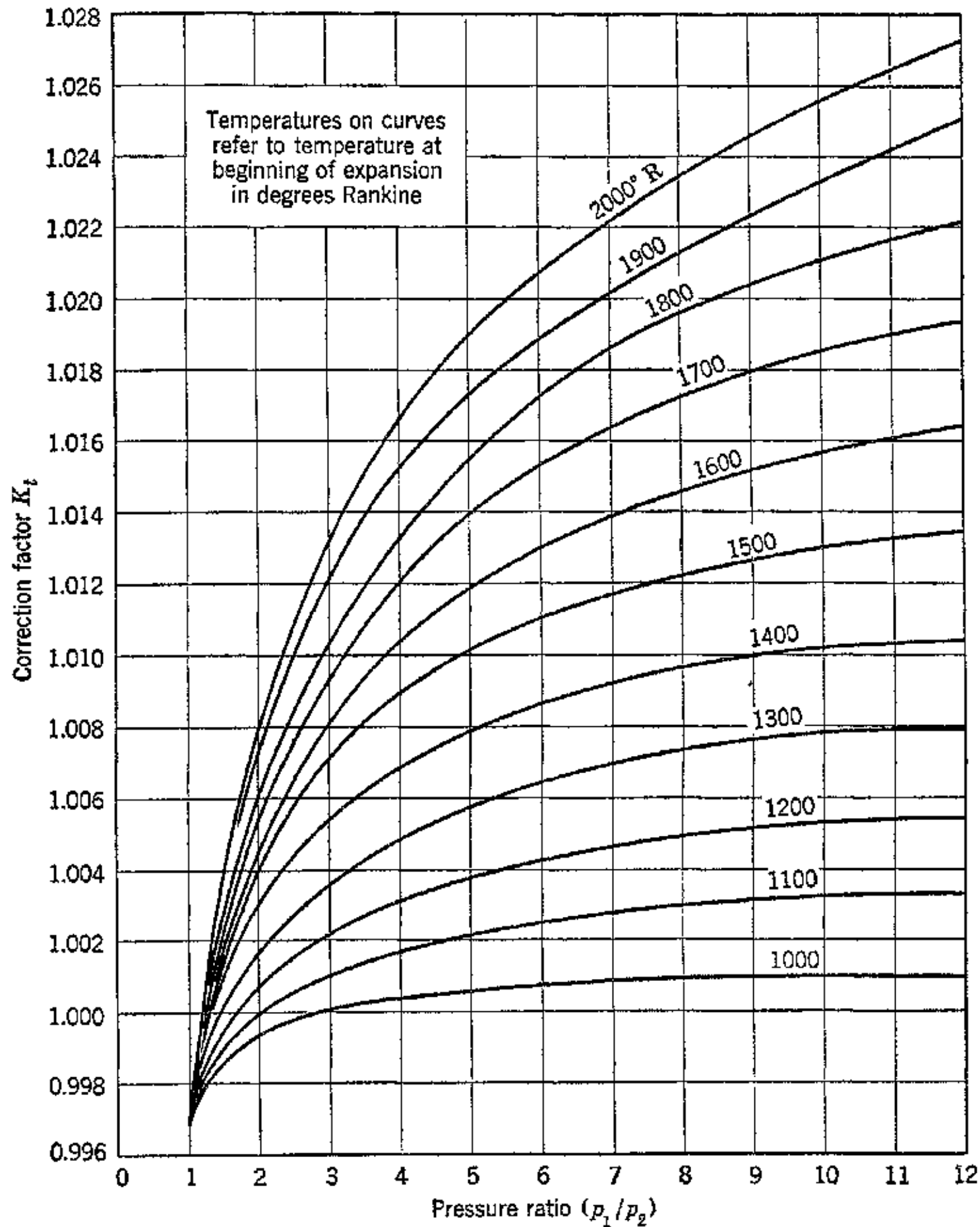
Fig. 10. Correction factor K_t vs. pressure ratio for air (expansion processes).

Example. A turbine operates on heated air. The inlet temperature is 1660 R, $p_1 = 5$ atm, and $p_2 = 1$ atm. The efficiency of the turbine is $\eta_t = 0.875$, and its mechanical efficiency is $\eta_m = 0.98$. Find the horsepower developed per pound of air flow per second and the final temperature.

Solution.

$$r_t = \frac{p_1}{p_2} = 5$$

From Table 4·5, $Z_t = 0.5769$. From Fig. 10, $K_t = 1.013$.

$$\Delta h_t = 0.243 \times 1660 \times 1.013 \times 0.875 \cdot \frac{0.5769}{1.5769} = 131.2 \quad \text{Btu/lb}$$

The actual output $= \Delta h_t \times \eta_m = 131.2 \times 0.98 = 128.5$ Btu/lb.

$$\text{Hp/lb sec} = \frac{128.5}{0.707} = 181.7$$

Check using Table 4·4: $T_1 = 1660$, $h_1 = 316.57$, $p_{r1} = 171.56$, $p_{r2} = 171.56/5 = 34.31$, $h_{2s} = 166.44$, $T_{2s} = 1083$, $\Delta h_t' = 316.57 - 166.44 = 150.13$ Btu/lb, $\Delta h_t = \Delta h_t' \times \eta_t = 150.13 \times 0.875 = 131.2$ Btu/lb (check), $h_2 = h_1 - \Delta h_t = 316.57 - 131.20 = 185.37$ Btu/lb.

The final temperature from Table 4·4 is

$$T_2 = 1158.6 \text{ R}$$

Using the correction-factor method, the final temperature is determined as follows:

$$\Delta t' = \frac{\Delta h_t}{0.243} = \frac{131.2}{0.243} = 540 \text{ R drop in temperature}$$
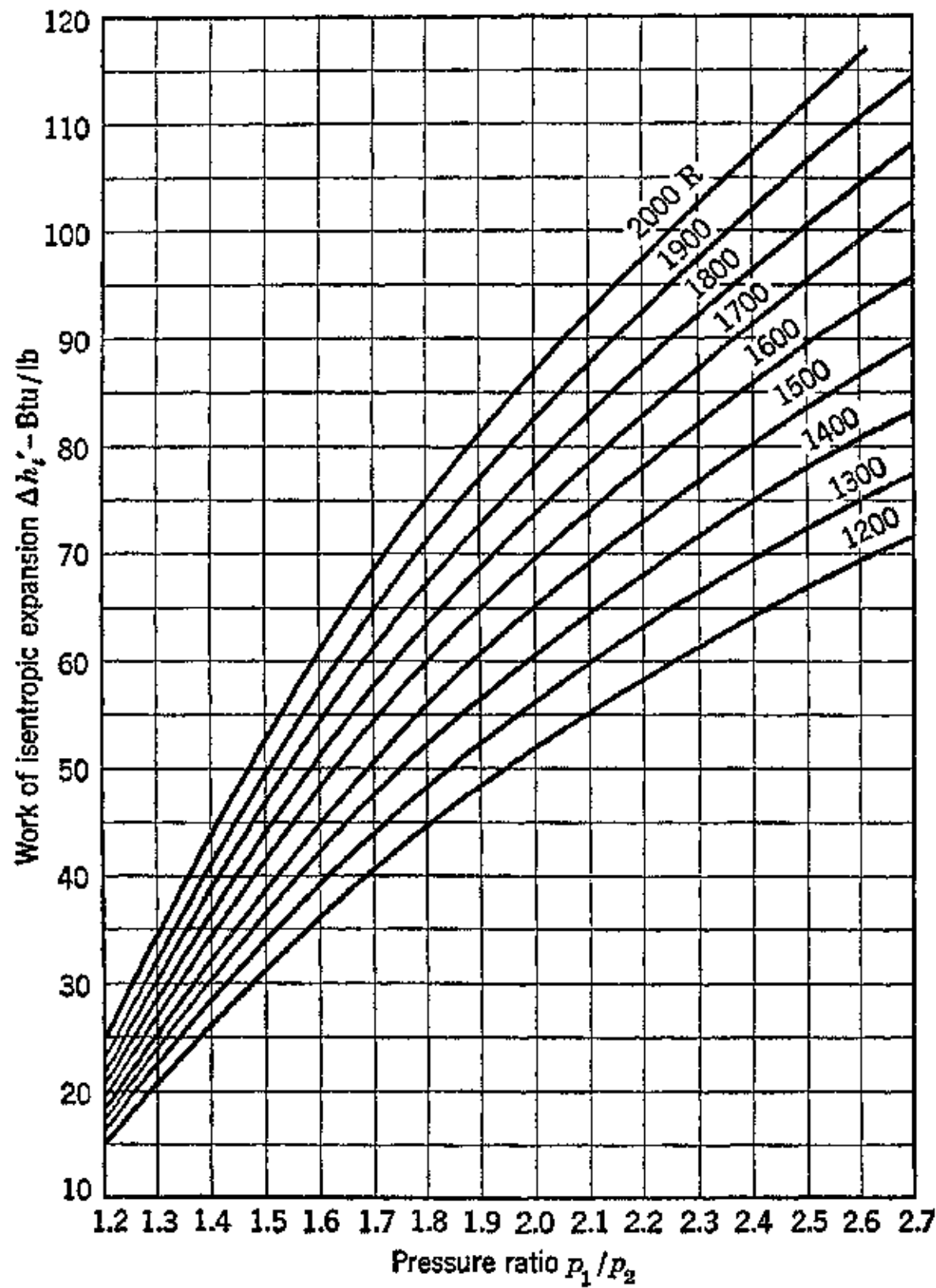
FIG. 11.   Isentropic work of expansion vs. pressure ratio.

This assumes that $c_p = 0.243$ and is constant. This temperature drop is, therefore, approximate. The first approximation to the actual value of c_p is obtained by using the value of c_p from Fig. 3 for the average temperature based on $\Delta t' = 540$ F. Thus $(T_2)_{av.} = 1380$ and $(c_p)_{av.} = 0.2608$; this gives $\Delta t = 505$. The next trial $(c_p)_{av.} = 0.2602$, and finally $\Delta t = 502$ degrees. The final temperature is $T_2 = 1660 - 502 = 1158$ R.

For rough calculations the works of isentropic expansion and compression may be taken directly from Figs. 11 and 12 respectively.
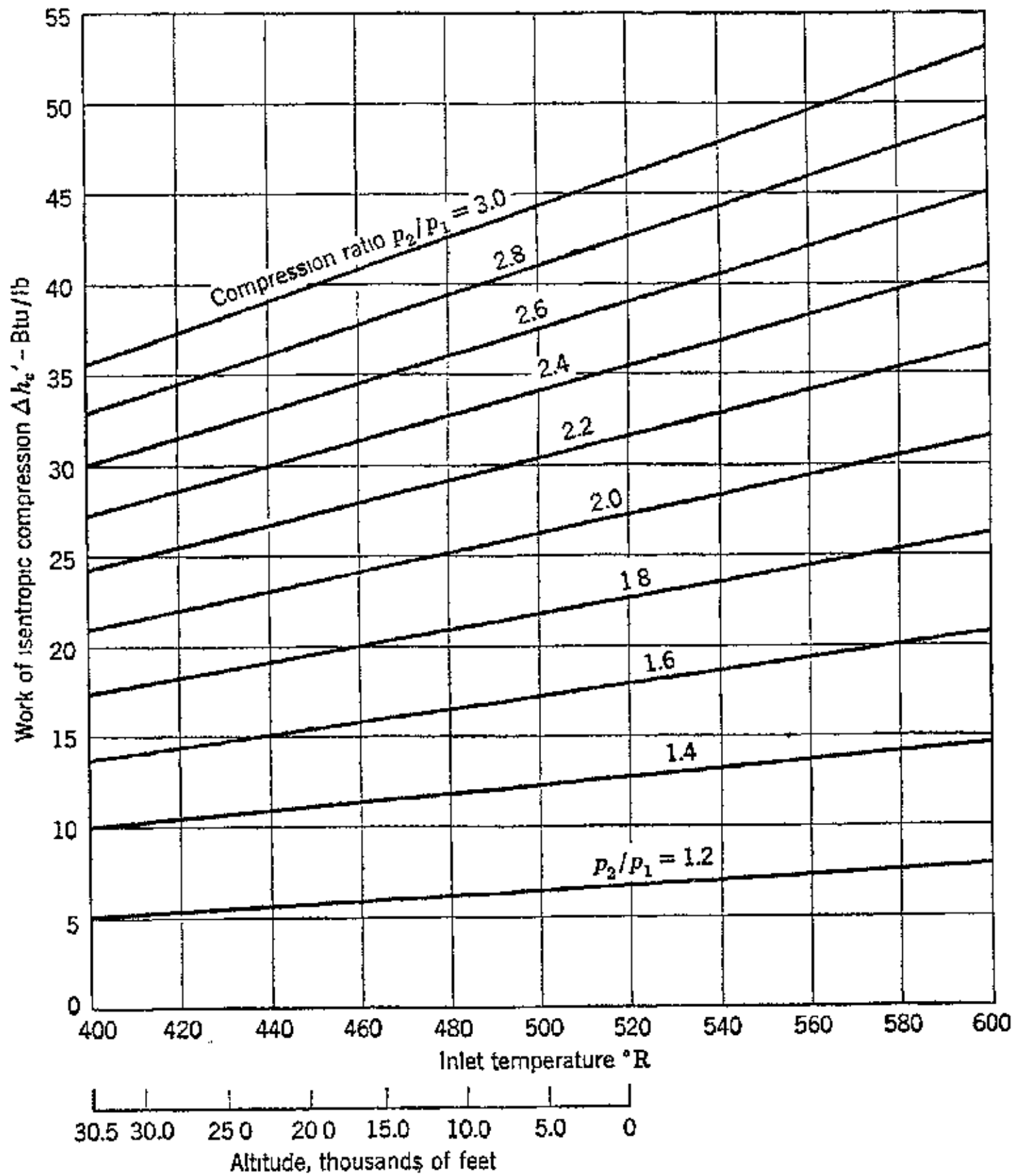
FIG. 12. Isentropic work of compression as a function of initial temperature (or altitude) for different pressure ratios.

REFERENCES

1. HOLBORN and OTTO, *Zeit. Physik*, Bd. 33, 1935.
2. J. GOLDSBURY and J. R. HENDERSON, "Turbines for Power from Industrial Power Gases," *Trans. A.S.M.E.*, May, 1942, p. 287.
3. F. O. ELLENWOOD, N. KULIK, and N. R. GAY, "The Specific Heats of Certain Gases over Wide Ranges of Pressures and Temperatures," *Cornell University Eng. Expt. Sta., Bul.* 30, October, 1942.
4. R. C. H. HECK, "The New Specific Heats," *Mech. Eng.*, Vol. 63, 1941, pp. 126–135.
5. H. L. JOHNSTON and A. T. CHAPMAN, "Heat Capacity Curves of the Simpler Gases, IV," *J. Am. Chem. Soc.*, Vol. 56, 1934, p. 1045.
6. R. L. SWEIGERT and M. W. BEARDSLEY, "Empirical Specific Heat Equations Based upon Spectrographic Data," *Georgia School of Technology, State Engineering Experiment Station, Bul.*, Vol. 1, No. 3, June, 1936.
7. L. S. MARKS, *Mechanical Engineers' Handbook*, McGraw-Hill Book Co., Fourth Ed., 1941, p. 550.
8. JUSTI and LÜDER, *Arch. f. Wärmewirtschaft*, Bd. 16, 1935, p. 323.
9. E. SCHMIDT, *Einführung in die technische Thermodynamik*, J. Springer, 1936, p. 44.
10. J. C. SMALLWOOD, "Equations for the Specific Heats of Gases," *Ind. Eng. Chem.*, July, 1942, p. 863.
11. "Heat Temperature—Entropy Chart for Air," Data Sheet No. 104, *Power*, March, 1941.
12. J. H. KEENAN and J. KAYE, "A Table of Thermodynamic Properties of Air," *Trans. A.S.M.E.*, 1943, p. A123.
13. J. H. KEENAN and J. KAYE, *Thermodynamic Properties of Air*, John Wiley & Sons, 1945.
14. N. P. BAILEY, *Heat Power Engineering*, John Wiley & Sons, pp. 47–54.
15. H. L. JOHNSTON and M. K. WALKER, "Heat Capacity Curves of the Simpler Gases, III," *J. Am. Chem. Soc.*, Vol. 55, 1933, p. 172.
16. F. C. MARGGRAFF and A. H. SENNER, A Temperature-Entropy Diagram for Air Based on Spectroscopic Specific Heats.
17. J. A. BEATTIE and O. C. BRIDGEMAN, "A New Equation of State for Fluids, I, Application to Gaseous Ethyl Ether and Carbon Dioxide," *J. Am. Chem. Soc.*, Vol. 49, 1927, p. 1665; "II, Application to Helium, Neon, Argon, Hydrogen, Nitrogen, Oxygen, Air, and Methane," *J. Am. Chem. Soc.*, Vol. 50, 1928, p. 3133.
18. C. S. ROBINSON, *The Thermodynamics of Fire Arms*, McGraw-Hill Book Co., 1943, pp. 17–21.
19. R. V. GERHART, F. C. BRUNNER, H. S. SAGE, and W. N. LACEY, "Thermodynamic Properties of Air," *Mech. Eng.*, April, 1942, p. 270.
20. E. D. EASTMAN, "Specific Heats of Gases at High Temperatures," *J. Am. Chem. Soc.*, Vol. 55, July, 1933.
21. E. JUSTI, "The Specific Heat of Gas Mixtures," *Feuerungstechnik*, Vol. 26, 1938, p. 313.
22. W. M. D. BRYANT, "Empirical Molar Heat Equations from Spectographic Data," *Ind. Eng. Chem.*, Vol. 25, 1933, p. 820.
23. B. F. DODGE, *Chemical Engineering Thermodynamics*, McGraw-Hill Book Co., p. 371.

24. J. R. PARTINGTON, *Chemical Thermodynamics*, Constable and Co., London, 1924, Chapter 1.

25. G. BIRTWISTLE, *The Principles of Thermodynamics*, Cambridge University Press, London, Chapter 4.

26. R. R. WENNER, *Thermochemical Calculations*, McGraw-Hill Book Co., 1941, Chapters V and XVI.

27. J. R. PARTINGTON and W. G. SCHILLING, *The Specific Heat of Gases*, Ernest Benn, London, 1924.

28. J. CHIPMAN and M. G. FONTANA, "A New Approximate Equation for Heat Capacities at High Temperatures," *J. Am. Chem. Soc.*, Vol. 57, 1935, p. 48.

29. O. LUTZ and F. WOLF, *I.S. Tafel für Luft und Verbrennungsgase*, Julius Springer, 1938.

AIRPLANE PERFORMANCE CALCULATIONS

1. Introduction

This chapter discusses the factors governing the basic performance characteristics of the airplane and presents procedures for estimating its performance characteristics. Sufficient aerodynamic theory is introduced to give a physical understanding of the equations and the principles involved. In developing the subject matter the references given at the end of the chapter have been used freely.

Principal Notation

a = acoustic velocity, fps.

$AR = (kb)^2/S$ = geometrical effective aspect ratio.

$AR_e = eAR = eb^2/S$ = virtual aspect ratio ($k = 1$).

$b_e = eb^2$.

b = wing span, ft.

C = chord length, ft, or climb speed, in fpm, as indicated in text.

C_D = drag coefficient = $391D/\sigma V^2 S$ (V in mph).

C_{Di} = induced drag coefficient = $C_L^2/\pi AR$.

$C_{D\pi}$ = proper drag coefficient.

C_{DP} = parasite drag coefficient.

C_{DP_e} = effective parasite drag coefficient.

C_L = lift coefficient = $391W/\sigma V^2 S$ (V in mph).

D = drag in level flight, lb.

D_i = induced drag, lb.

D_{ld} = minimum drag for level flight, lb.

e = airplane efficiency factor (Oswald).

$eb^2 = AR_e S$ = (effective span)^2, ft^2.

f = equivalent parasite area = $C_{DP_e}S$, ft^2.

F_T = thrust factor = $1/\sqrt{KK'}$ = $1.772\, b/W(e/f)^{\frac{1}{2}}$.

F_V = speed factor = $(K/K')^{\frac{1}{4}}$ = $1/14.85\,(\sigma b/W)^{\frac{1}{2}}(fe)^{\frac{1}{4}}$.

$K = \sigma f/391$ lb hr^2/mi^2.

$K' = 124.5/\sigma e(W/b)^2$ lb mi^2/hr^2.

$K_\nu = \nu_0/\nu =$ kinematic viscosity ratio for air.

$L =$ lift of wings, lb.

$l_p = W/f =$ parasite loading, psf.

$l_s = W/eb^2 =$ effective span loading, psf.

$(L/D)_{max} =$ maximum value of lift-drag ratio for airplane.

$M =$ Mach number.

$M_{cr} =$ critical Mach number $=$ the free stream Mach number at which sonic velocity is attained on the wing.

$P =$ power, ft-lb/min or hp as specified in text.

$P_a =$ power available.

$P_r =$ power required.

$P_e = P_a - P_r =$ excess power.

$p =$ pressure, psf.

$p_{ud} =$ pressure of undisturbed stream, psf.

$p_t = p_{ud} + \frac{1}{2}\rho V^2 =$ stagnation or total pressure, psf.

$q = \frac{1}{2}\rho V^2 =$ dynamic pressure, psf   (V in fps).

$R =$ range, mi.

$R_e =$ Reynolds number.

$S =$ wing area, sq. ft.

$\mathfrak{I} =$ thrust, lb.

$\mathfrak{I}_n =$ net thrust, lb.

$\mathfrak{I}_{ld} =$ minimum thrust for level flight, lb.

$V =$ true air speed, fps or mph, as indicated in text.

$V_{min} =$ minimum speed.

$V_s =$ stalling speed.

$V_{ld} =$ speed for minimum drag.

$V_C =$ speed for maximum rate of climb.

$V_{max} =$ maximum airplane speed, neglecting compressibility.

$W =$ gross weight, lb.

$w = W/S =$ wing loading, psf.

Greek Symbols

$\rho =$ air density, slug/ft^3.

$\rho_0 =$ air density at sea level $= 0.002378$ slug/ft^3.

$\sigma = \rho/\rho_0 =$ density ratio.

$\eta =$ efficiency.

$\eta_P =$ propulsion efficiency.

$\nu =$ kinematic viscosity of air, ft^2/sec.

ν_0 = kinematic viscosity of air at sea level.

α = angle of attack.

μ = absolute viscosity = $\rho\nu$.

β = Mach angle.

φ = $3/\sigma 3_0$ = thrust factor.

2. Forces Acting on the Airplane

The operating principle of all aircraft stems from the property of a thin inclined flat plate to provide a lifting force when moved horizontally through the air.[1] Experiments show that the forces exerted by a fluid upon a body immersed in it depend only upon the physical characteristics of the fluid and its velocity relative to the body (see Chapter 1, Section 2). Consequently, the experimental measurements of aerodynamic forces are made in a wind tunnel wherein the body is held stationary and the air is blown past it.
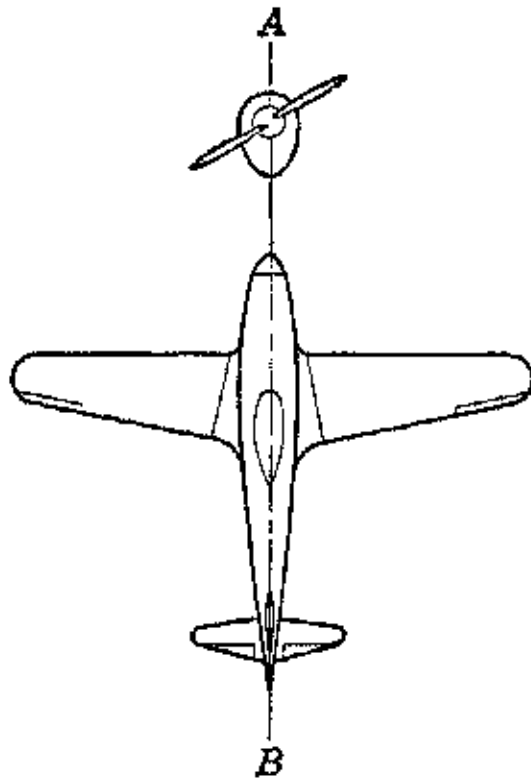
FIG. 1.   Plane of symmetry of an airplane.

An airplane in flight is acted upon by the forces due to gravitational attraction and those due to aerodynamic effects.[2] The resultant of the gravitational forces can be represented by a single force, equal to the weight of the airplane, acting vertically downward through the center of gravity (cg). The air reactions may be represented by three mutually perpendicular forces acting through the cg and three moments acting around the axes formed by the lines of action of the aforementioned forces.

For the purposes at hand, it is assumed that the controls are adjusted to maintain the airplane in steady rectilinear flight, which means that there is no acceleration. Consequently the resultant of all the external forces and the resultant moment or couple are equal to zero. It is also assumed that the airplane is symmetrical about the plane AB; see Fig. 1. It is further assumed that the resultant air reaction and the force due to gravity lie in the plane of symmetry.

When the flight speed is constant, the flight path, with reference to the horizontal, may be inclined upward, inclined downward, or horizontal.[2] If the propulsion force is zero, then the only steady flight possible in still air is the steady descent; i.e., the flight path is inclined downward. When the airplane is being propelled in steady

flight the flight path is, in general, either a steady climb or horizontal.

Figure 2 is a free-body diagram for the forces acting upon an airplane in steady climb. The angle made by the flight path is denoted by θ, and the speed of the airplane along the flight path is V. For simplicity the thrust $\mathfrak{I}$ developed by the propulsion system is assumed to act along the flight path. For a conventional airplane $\mathfrak{I}$ is the

Propeller Propulsion
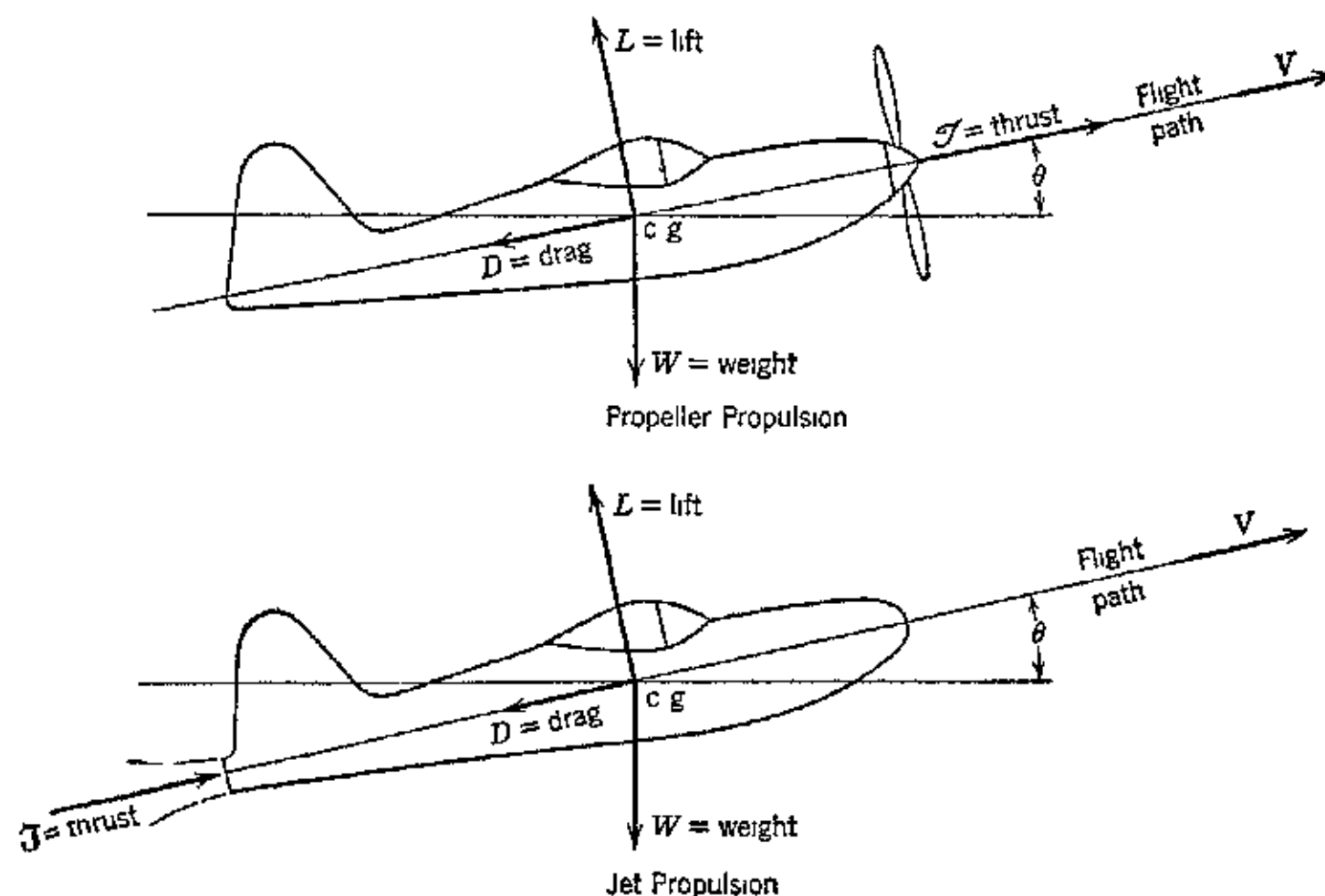
Jet Propulsion

FIG. 2.   Forces acting on an airplane in steady rectilinear flight.

propeller thrust, and for a jet-propelled airplane it is the reaction force of the gaseous jet.

Four forces, therefore, act upon the airplane: the drag D, lift L, weight W, and propulsion thrust $\mathfrak{I}$. The vector sum of these four forces, or of their components in any direction, must be equal to zero.

3. Equilibrium Equations

Because of the assumption of equilibrium, the sums of the forces acting perpendicular and parallel to the flight path must each be zero. Acting perpendicular to the flight path are the lift L and the weight component $W \cos \theta$. Acting parallel to the flight path are the drag D, the weight component $W \sin \theta$, and the thrust $\mathfrak{I}$. Hence

$$L - W \cos \theta = 0 \quad \text{or} \quad L = W \cos \theta \tag{1}$$

and

$$\mathfrak{I} - D - W \sin \theta = 0 \quad \text{or} \quad \mathfrak{I} = D + W \sin \theta \tag{2}$$

The climb angle θ is ordinarily less than 20°, and for that value $\cos \theta = 0.93969$. Consequently, it is sufficiently accurate to assume that $\cos \theta = 1$ and $\sin \theta = 0$. Substituting these values for $\cos \theta$ and $\sin \theta$ in equations 1 and 2, respectively, reduces them to $L = W$ and $3 = D$. The weight and speed of the airplane are related by equations 3 and 4.

$$L = W = C_L q S = \tfrac{1}{2}\rho V^2 C_L S \quad (V \text{ in fps}) \tag{3}$$

From equation 3

$$C_L = \frac{W}{qS} = \frac{2w}{\rho V^2} \tag{4a}$$

or

$$C_L = \frac{391w}{\sigma V^2} \quad (V \text{ in mph}) \tag{4b}$$

where $w = W/S$ is the *wing loading* of the airplane in pounds per square foot, and $\sigma = \rho/\rho_0$.

From equation 3 the following expression for the speed of an airplane in terms of the lift coefficient C_L, the wing loading w, and the density of the air ρ is obtained.

$$V = \sqrt{\frac{2w}{\rho C_L}} \quad \text{fps} \tag{5a}$$

The airplane speed V can be expressed in terms of the density ratio σ by introducing the sea-level value for the density of air ($\rho_0 = 0.002378$ slug/ft^3). Then, the true air speed V is given by

$$V = 29.0 \sqrt{\frac{w}{C_L}} \cdot \sqrt{\frac{1}{\sigma}} \quad \text{fps} \tag{5b}$$

or

$$V = 19.77 \sqrt{\frac{w}{\sigma C_L}} \quad \text{mph} \tag{5c}$$

Values of $\sqrt{1/\sigma}$ are given in Table 1·6.

From equation 3 it is apparent that the lift is directly proportional to the density of the air. Consequently, to maintain the same lift and attitude at higher altitudes, the airplane must travel at higher speeds.

The *minimum speed*, $V_{\min}$, at which an airplane can fly in steady rectilinear flight depends upon the maximum value of its lift co-

efficient $C_{L_{max}}$. Thus

$$C_{L_{max}} = 391 \sqrt{\frac{w}{V_{min}{}^2 \sigma}} \quad (V \text{ in mph}) \qquad (6a)$$

or

$$V_{min} = V_s = 19.77 \sqrt{\frac{w}{C_{L_{max}}}} \cdot \sqrt{\frac{1}{\sigma}} \quad (V \text{ in mph}) \qquad (6b)$$

The minimum speed, V_{min}, is called the *stalling speed* and is denoted by V_s. The stalling speed corresponds to the landing speed without power.

The wing loading w used in equation 6 is the total weight of the airplane divided by the net wing area. It does not include that portion of the wing intercepted by the fuselage. At small angles of attack the lift is comparable to that obtainable from a wing extending through the fuselage. At large angles of attack, however, the lift obtained is substantially that due to the net wing area. For a fuller discussion of the effect of wing arrangement and fairing, the reader is referred to *N.A.C.A. Tech. Report* 540.

4. Power Relationships

Refer to equation 2, and multiply each side by the speed of the airplane V. Thus

$$3V = DV + WV \sin \theta \quad \text{ft-lb/sec} \qquad (6c)$$

The product $3V$ is termed the *thrust power* and is the useful work furnished by the propulsion plant. In the conventional airplane the thrust power is supplied by the engine-driven propeller. The engine delivers the *propulsion power*, P, which is equal to its brake horsepower, but because of inherent losses in the operation of the propeller a portion of the propulsion horsepower is lost. The propulsion power minus the losses entailed in converting it into propulsion thrust is the power available P_a or thrust horsepower (see Chapter 2). Thus, if η_P is the propulsion efficiency of the propeller, then the *power available* P_a for propelling the airplane is given by

$$P_a = \eta_P P = \frac{3V}{550} \quad \text{hp} \quad (V \text{ in fps}) \qquad (7a)$$

or

$$P_a = \eta_P P = \frac{3V}{375} \quad \text{hp} \quad (V \text{ in mph}) \qquad (7b)$$

The first term on the right-hand side of equation 6c, that is DV, represents the *power required* P_r to keep the airplane in level flight, D being the total drag of the airplane. Hence

$$P_r = \frac{DV}{550} \quad \text{hp} \quad (V \text{ in fps}) \tag{8a}$$

or

$$P_r = \frac{DV}{375} \quad \text{hp} \quad (V \text{ in mph}) \tag{8b}$$

The drag of the airplane can be represented by an equation analogous to the lift equation 3. Thus

$$D = \mathfrak{Z} = C_D q S = \tfrac{1}{2}\rho V^2 C_D S \tag{9}$$

where C_D is the drag coefficient for the complete airplane; the reader is referred to Chapter 1, where this equation was derived by dimensional analysis. Combining equations 8 and 9, the following equations for the power required are obtained.

$$P_r = \frac{DV}{550} = \frac{\tfrac{1}{2}\rho V^3 C_D S}{550} \quad \text{hp} \quad (V \text{ in fps}) \tag{10a}$$

or

$$P_r = \frac{\rho V^3 C_D S}{350} = \frac{\sigma \rho_0 V^3 C_D S}{350} \quad \text{hp} \quad (V \text{ in mph}) \tag{10b}$$

It is seen from the above equations that the power required to overcome the drag of the airplane increases with the cube of its speed and directly as the density of the air. Substituting the value of the sea-level density ρ_0 into the above equations, the power-required equation becomes

$$P_r = \frac{\sigma V^3 C_D S}{146{,}600} \quad (V \text{ in mph}) \tag{11}$$

For a fixed attitude, increasing the power available above that required for level flight does not cause the airplane to fly faster in horizontal flight, but to climb, the rate of climb depending upon the magnitude of the difference $P_a - P_r$. Conversely, if the power available is reduced below that of the power required the airplane glides down until the work done by the falling airplane equals the difference $P_r - P_a$ or its equivalent $(DV - P_a)$.

If P_a exceeds DV at any fixed attitude, horizontal flight can be reestablished by reducing the thrust developed by the propulsion system. With a fixed attitude there is only one speed at each altitude that gives level flight.

5. Rate of Climb

Let h be the altitude of the airplane at any instant; then, since the term $V \sin \theta$ in equation 6c is equal to dh/dt, this term gives the rate at which the airplane is climbing.   Hence equation 6c becomes

$$\frac{W \, dh}{dt} = 3V - DV \quad \text{ft-lb/sec} \tag{12}$$

and the rate of climb for the airplane is given by

$$\frac{dh}{dt} = \frac{3V - DV}{W} \quad \text{fps} \tag{13}$$

If P_a and P_r are in horsepower, the last equation becomes

$$\frac{dh}{dt} = \frac{550(P_a - P_r)}{W} = 550 \frac{P_e}{W} \quad \text{fps} \tag{14}$$

where $P_e = (P_a - P_r)$ is termed the *excess horsepower*.   It is obvious that the maximum climbing rate for the airplane coincides with the maximum value for the excess horsepower.

6. Drag of Airplane

In equation 8, which gives the power required for horizontal flight, the drag D is the resistance of the complete airplane and includes the drags of all the components — the wings, nacelles, fuselage, radiators, etc.   The total drag of the airplane is usually divided into the *parasite drag* and the *induced drag of the wings*.

In the older literature, the parasite drag is defined as that portion of the total drag of the airplane not associated with the lifting elements, that is, all drags except wing drag.

(a) **Drag of the Wings.** The wing drag is denoted by D_1.   This drag is divided into two components, the *profile drag* D_0 and the *induced drag* D_i.   The profile drag consists of the resistance due to skin friction, shearing stresses in the boundary layer, and a part of the pressure drag due to eddies in the wake of the slipstream passing over the wing.   The magnitude of the profile drag is a function of the angle of attack of the wing and is expressible as a function of the lift coefficient C_L.   As stated above, the profile drag D_0 is classified in the modern literature as a part of the total parasite drag of the airplane.[4]

The drag of the wings D_1 is, therefore, given by

$$D_1 = D_0 + D_i \tag{15}$$

The induced drag D_i is an aerodynamic resistance resulting from the wings' having a finite length (or aspect ratio), which causes circulatory flow around the wing (see Chapter 2) to produce downwardly directed trailing vortices at its tips as illustrated in Fig. 3. The kinetic energy to maintain these vortices must be supplied by the propulsion system and consequently subtracts from the power available for rectilinear flight. These trailing vortices produce the same effect as an increase in frictional resistance or drag.[6]
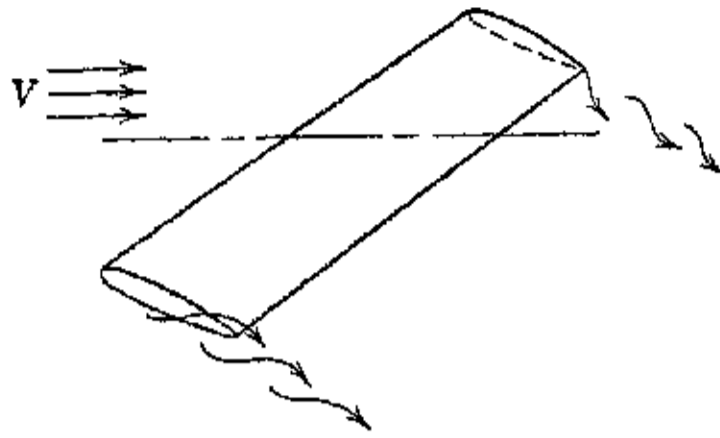
FIG. 3.   Vortex formation at wing tips.

The physics of the situation can be explained in elementary terms as follows.[4,6] The pressure acting on the under side of the wing, being higher than that on the top surface, causes the air to flow from under the wing over the wing tips. The net result is that the entire slipstream is given a virtual downward component, as illustrated in Fig. 4. This causes the relative air velocity to become directed downward with the so-called *induced angle of attack* α_i, which has the effect of a reduction in the angle of attack relative to the resultant air-velocity vector and gives the lift force a virtual rotation in the direction of motion. The phenomenon of induced drag arises purely from hydrodynamic considerations and would be present even if the air were an inviscid fluid.[4]
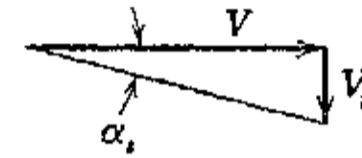
FIG. 4. Effect of induced drag on angle of attack.

The magnitude of the induced drag coefficient C_{Di} depends upon the lift coefficient and the effective aspect ratio of the wings AR. Thus, for monoplanes,

$$C_{Di} = \frac{C_L{}^2 S}{\pi b^2} = \frac{C_L{}^2}{\pi AR} \qquad (16)$$

where b is the wing span and S the projected area of the wings.

The induced drag can be expressed in terms of the weight and speed of the airplane by substituting for the lift coefficient from equation 4. Thus

$$D_i = \frac{2W^2}{\rho V^2 S \pi AR} = \frac{2W^2}{\rho V^2 \pi b^2} \quad (V \text{ in fps}) \qquad (17)$$

If the airplane speed is given in miles per hour, then equation 17 becomes

$$D_i = \frac{124.5}{\sigma V^2} \left(\frac{W}{b}\right)^2 \quad (V \text{ in mph}) \tag{18}$$

It is apparent from equation 18 that for a given airplane at a specified altitude the induced drag varies inversely as the square of the flight speed. The higher the speed, the smaller the induced drag.

The power required to overcome the induced drag will be denoted by P_{ri} and is given by

$$P_{ri} = \frac{D_i V}{375} = \frac{0.332}{V\sigma} \left(\frac{W}{b}\right)^2 \quad (V \text{ in mph}) \tag{19}$$

Equation 19 shows that the power consumed in overcoming induced drag decreases with the flight speed but increases with the altitude.

(b) Parasite Drag. The parasite drags other than the profile drag of the wings D_0 are usually subdivided into (a) those having magnitudes which vary with the angle of attack and (b) those which are independent of the angle of attack.

The parasite drags belonging to category (a) above are the drags of those components having square or rectangular cross sections: nacelles, hulls, floats, tail surfaces, fuselages, etc. The drag coefficient applicable to this form of parasite drag is called the *proper drag coefficient* $C_{D\pi}$ and is defined by

$$C_{D\pi} = \frac{\Delta D}{qS_\pi} = \text{Proper drag coefficient} \tag{20}$$

where ΔD = the drag contributed by the part in question to the total parasite drag.

S_π = the proper area of components. For nacelles, fuselage, etc., it is the total projected frontal area of the part including any wing area covered by it.

The drags of those components that are independent of the attack angle are defined in terms of a drag coefficient f, which has the dimensions of an area,[4] thus

$$f = \frac{D_2}{q} = \text{Equivalent parasite area} \tag{21}$$

where D_2 = parasite drag of component, lb.

$q = \frac{1}{2}\rho V^2$ = dynamic pressure, lb/ft².

EXAMPLE. An airplane has wing area of 1000 ft². The wing profile drag coefficient $C_{D0} = 0.010$. The projected frontal area of fuselage is 100 ft², and its proper drag coefficient $C_{D_{\pi}} = 0.08$. The tail surface is 150 ft², and its proper drag coefficient is 0.0075. The nacelles add an equivalent parasite area $f = 5.0$ ft². Find the parasite drag coefficient of the complete airplane.

Solution.

Wing profile drag	$1000 \times 0.010 \times q$	$= 10q$
Fuselage proper drag	$100 \times 0.08 \times q$	$= 8q$
Tail surface proper drag	$150 \times 0.0075 \times q$	$= 1.125q$
Nacelle drag	$5.0 \times q$	$= 5q$
	Total drag	$= 24.125q$

$$C_{DP} = \frac{\text{Total drag}}{Sq} = \frac{24.125}{1000} = 0.024$$

7. Effect of Altitude on the Power Required and Flight Speed

The horsepower required to maintain the airplane in level flight at any speed was shown to be

$$P_r = \frac{DV}{375} \quad (V \text{ in mph})$$

where the drag D is defined by

$$D = D_p + \frac{C_L^2 qS}{\pi AR}$$

where D_p is the total parasite drag, including the profile drag of the wings. For a fixed attitude of the airplane, the required power P_r is a function of both the flight speed and the altitude. The manner in which P_r varies with speed and altitude is determined from the following considerations.[7]

Since the lifting force L is equal to the airplane weight W, it is a constant for level flight at all altitudes. These two numerically equal forces are given by equation 3. For a fixed attitude the factors S and C_L in that equation have the same values regardless of the altitude. Since the force $W = L$ is also independent of altitude, to maintain level flight the dynamic pressure q must have the same magnitude at all altitudes. The speed of the airplane at any altitude is given by equation 5a, and, if the subscript zero is used to denote sea-level conditions, the sea-level speed is

$$V_0 = \sqrt{\frac{2W}{\rho_0 C_L S}}$$

and the ratio of the speed V at any altitude to the sea-level speed V_0

is determined from the ratio V/V_0. Thus, letting $\sigma = \rho/\rho_0$, the speed at any altitude is given by

$$V = V_0 \sqrt{\frac{1}{\sigma}} \tag{22}$$

It is seen from equation 22 that with a fixed attitude the speed at any altitude is equal to the speed for level flight at sea level multiplied by $\sqrt{1/\sigma}$.

The characteristics of the power required for level flight are determined in a similar manner.[7] For a fixed attitude the *glide ratio* for the airplane (L/D) is independent of the altitude. Hence the drag D has the same magnitude at altitude that it has at sea level. If $D_0 V_0$ is the power required for level flight at sea level, the power required at altitude is $D_0 V$. Hence, from equation 9 and the considerations discussed above it follows that the power required at altitude is given by

$$D_0 V = D_0 V_0 \sqrt{\frac{1}{\sigma}} \tag{23}$$

Equation 23 shows that the required power at altitude for the condition where C_L = constant is the product of the sea-level power and $\sqrt{1/\sigma}$.

8. Effect of Speed on the Drag of an Airplane

It is shown in reference 10 that the drag of a moving body submerged to a great depth in a fluid is given by

$$D = \rho V^2 S \varphi[\alpha, R_e, M, r_1, r_2 \cdots] \tag{24}$$

where α = angle of attack.

$R_e = Vl\rho/\mu$ = Reynolds number.

$M = V/a$ = Mach number.

l = a characteristic length for the body.

a = acoustic velocity, fps.

V = relative velocity of fluid to body.

S = a characteristic area of the body.

$r_1, r_2 \cdots$ denotes certain scale ratios of length and velocity.

$\varphi \cdots$ denotes that a functional relationship exists between the parameters enclosed by the brackets.

The above equation is applicable to the motion of an airfoil through the air of the atmosphere or to a moving airplane, since the latter can be replaced by an equivalent airfoil.

For an airfoil moving with a constant speed the drag coefficient C_D and the lift coefficient C_L are functions of the angle of attack α. These coefficients are also functions of the Reynolds number R_e. In evaluating the Reynolds number the chord length of the airfoil C ft is taken as the characteristic length.[10] Thus, at standard sea-level conditions

$$R_e = \frac{VC\rho}{\mu} = 6{,}378\,VC \quad (V \text{ in fps}) \tag{25a}$$

or

$$R_e = 9{,}354\,VC \quad (V \text{ in mph}) \tag{25b}$$

At altitudes other than sea level the Reynolds numbers are obtained by multiplying the sea-level values by K_ν, the ratio of the kinematic viscosity of air at sea level to its value at the altitude in question. Thus

$$R_e = 6{,}378\,VCK_\nu \quad (V \text{ in fps}) \tag{26a}$$

where $K_\nu = \nu_0/\nu$.

If V is in miles per hour the Reynolds number at any altitude is given by

$$R_e = 9{,}354\,VCK_\nu \quad (V \text{ in mph}) \tag{26b}$$

Values of the kinematic viscosity ratio for air K_ν as a function of altitude are presented in Fig. 5.
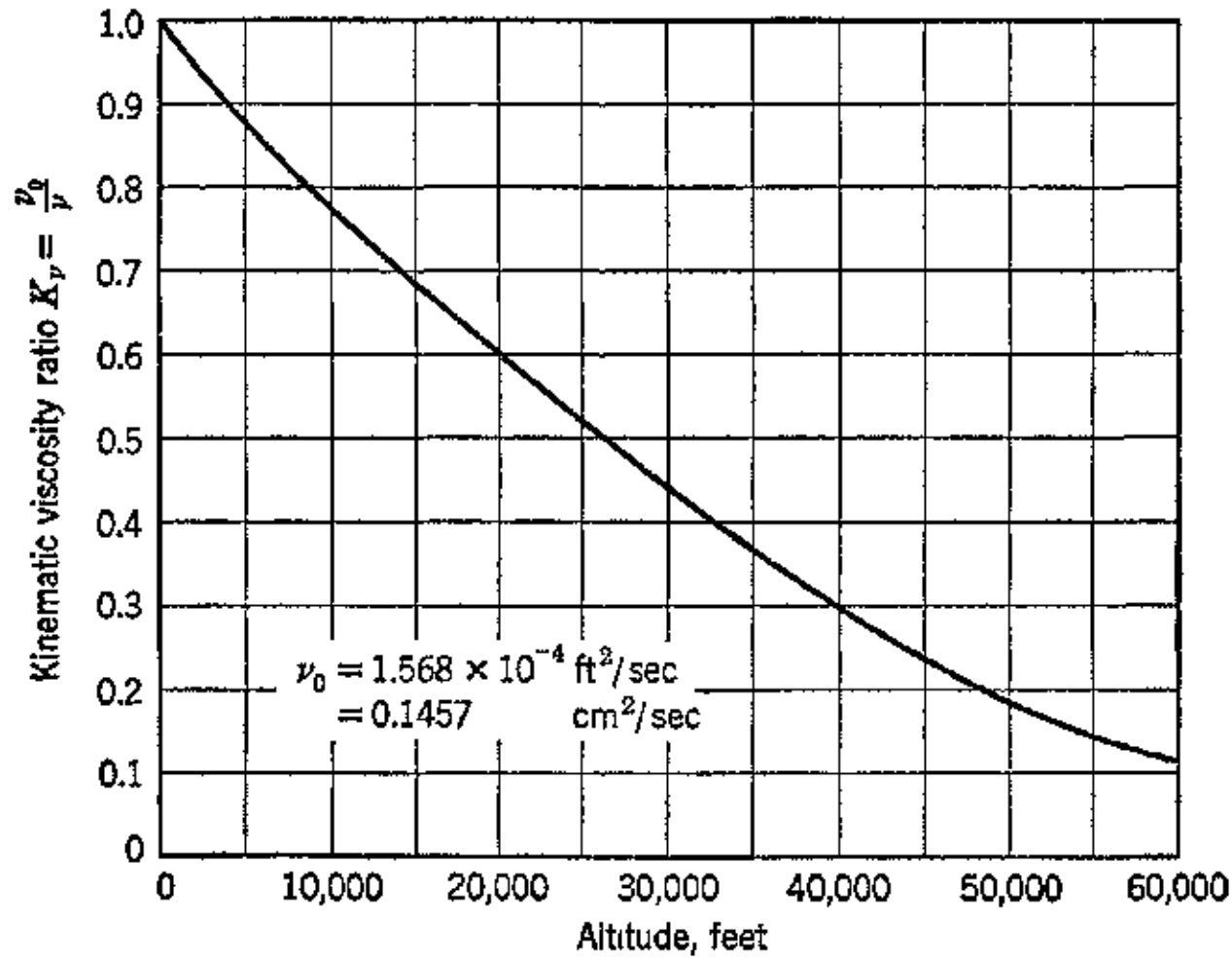
FIG. 5. Kinematic viscosity ratio for air as a function of altitude.

The effect of the Reynolds number on the lift and drag coefficients is termed the *scale effect;* it is used in adapting the data obtained from testing models in the wind tunnel to the full-size object. From Fig. 5 it is apparent that as the altitude is increased the Reynolds number at the same flight speed decreases.

The effect of increasing the Mach number is discussed in subsequent sections.

9. Effect of Speed on Dynamic Pressure

When a body moves through air at the low speeds, the air can be assumed to behave as an incompressible fluid. This assumption is valid, however, as long as the speed of the propelled body is small compared to the acoustic-velocity of the surrounding medium.

The effect of speed upon the dynamic pressure, by virtue of the change in air density, can be deduced by the methods used in references 4 and 5. Thus, if the Bernoulli theorem is applied first to a point remote from a stationary body with air flowing past it with the relative velocity V, and then to a point on the body where the air is brought to rest, the total pressure p_t is given by

$$p_t = p_{ud} + \tfrac{1}{2}\rho V^2 \tag{27}$$

When the air is assumed to be an incompressible fluid the equation for the dynamic or stagnation pressure is

$$q = \tfrac{1}{2}\rho V^2 \tag{28}$$

When the compressibility of the air is taken into account it can be shown (reference 5, p. 226) that with isentropic compression the dynamic pressure equation is

$$q' = p_{ud} \left\{ \left[1 + \frac{\rho_{ud} V_{ud}^2}{2 p_{ud}} \cdot \frac{k-1}{k} \right]^{\frac{k}{k-1}} - 1 \right\} \tag{29}$$

where V_{ud} = velocity of air in undisturbed region.

p_{ud} = pressure in undisturbed air stream.

q' = dynamic pressure based on isentropic compression of the air.

To compare equation 29 with the incompressible case, equation 28, expand equation 29 by the binomial theorem. Thus

$$q' = p_{ud} \left\{ 1 + \frac{\rho_{ud} V_{ud}^2}{2 p_{ud}} + \frac{1}{2k} \left(\frac{\rho_{ud} V_{ud}^2}{2 p_{ud}} \right) + \cdots - 1 \right\}$$

or

$$q' = \frac{\rho_{ud} V_{ud}^2}{2} \left(1 + \frac{\rho_{ud} V_{ud}^2}{4k p_{ud}} + \cdots \right) \tag{30}$$

Introducing the acoustic velocity a_{ud} and Mach number M_{ud}, for the undisturbed stream, then from Chapter 3

$$a_{ud}{}^2 = \frac{k p_{ud}}{\rho_{ud}} \quad \text{and} \quad M_{ud}{}^2 = \frac{V_{ud}{}^2}{a_{ud}{}^2}$$

Then equation 30 becomes

$$q' = \frac{\rho_{ud} V_{ud}{}^2}{2} \left(1 + \frac{M_{ud}{}^2}{4} + \cdots \right) \tag{31}$$

From equation 31 the error introduced in the dynamic pressure equation by neglecting the term $M_{ud}{}^2/4$ is readily calculated. It is seen that, at the Mach number $M_{ud} = 0.5$, the error due to neglecting compressibility is 6.25 per cent.
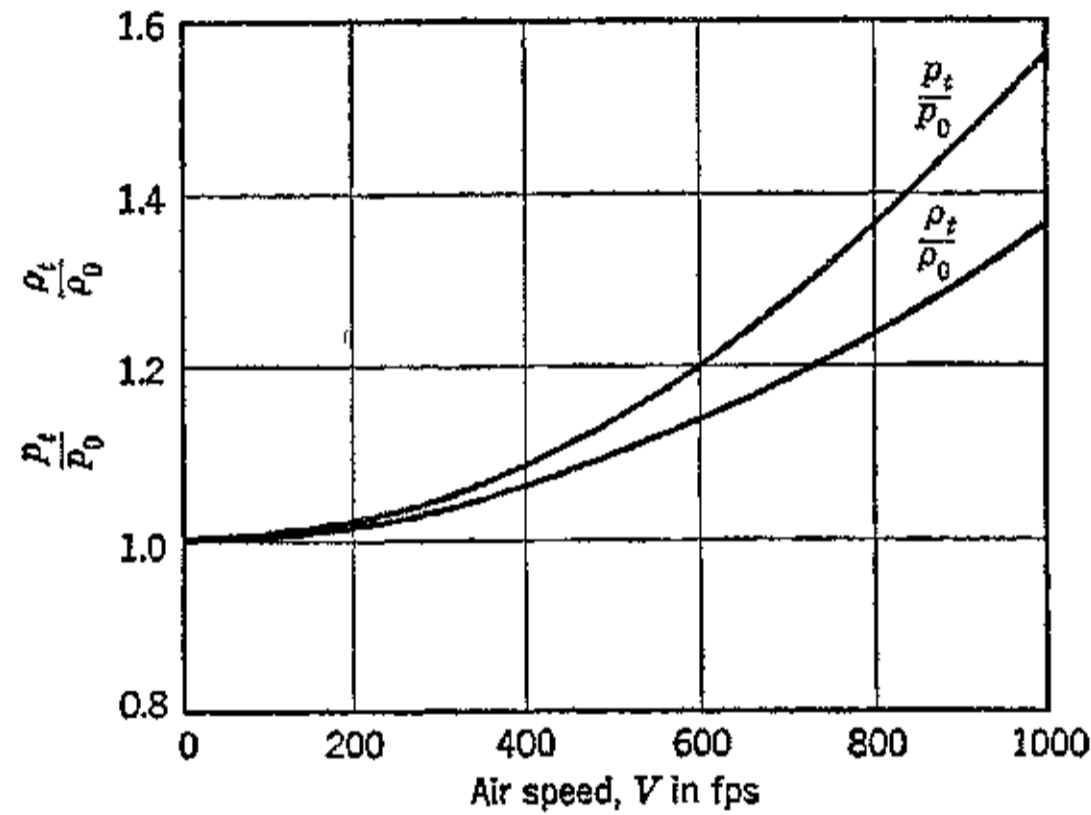
FIG. 6. Effect of speed on the stagnation pressure and density of air at sea level.

Table 5·1 presents values of the stagnation pressure for air coming to rest from different speeds, assuming incompressibility in one case and adiabatic compression in the other. From the table it is seen that the assumption of incompressibility introduces an error of approximately 1 per cent for a speed of 280 fps. Figure 6 illustrates the effect of speed on the density of the air brought to rest with adiabatic compression.

10. Effect of Compressibility on Lift and Drag Coefficients

It is customary to express the lift and drag for an airfoil in terms of the quadratic formulas used for incompressible fluids even where the effect of the compressibility of the fluid medium cannot be

TABLE 5·1

Pressure of Air Coming to Rest from Various Speeds

N.A.C.A. Tech. Report 316

Air Speed fps	Barometric Pressure plus Impact Pressure in Standard Atmospheres		Impact Pressure lb/ft^2	
	Incompressible	Adiabatic	Incompressible	Adiabatic
0	1.00000	1.00000	0.000	0.000
10	1.00005	1.00005	0.119	0.119
20	1.00022	1.00022	0.476	0.476
30	1.00050	1.00050	1.070	1.070
40	1.00089	1.00089	1.903	1 903
50	1.00140	1.00140	2.973	2 975
60	1.00202	1.00202	4.281	4.285
70	1.00275	1.00275	5.827	5.833
80	1.00359	1.00360	7.611	7.621
90	1.00455	1.00455	9.633	9.649
100	1.00561	1.00562	11.892	11.916
110	1.00679	1.00681	14.390	14.424
120	1.00808	1.00811	17.125	17.174
130	1.00949	1.00952	20.098	20.166
140	1.01101	1.01105	23.308	23.401
150	1.01264	1 01269	26 758	26.877
160	1.01438	1.01445	30.444	30.600
170	1.01623	1.01633	34.368	34.567
180	1.01820	1.01832	38.530	38.784
190	1.02028	1.02042	42.931	43.242
200	1.02247	1.02265	47.569	47.952
210	1.02477	1.02499	52.444	52.909
220	1.02719	1.02745	57.558	58.119
230	1.02971	1.03003	62.909	63.580
240	1.03236	1.03273	68.500	69.293
250	1.03511	1.03555	74.327	75.263
260	1.03797	1.03849	80.392	81.488
270	1.04095	1.04155	86.694	87.966
280	1.04404	1.04474	93.234	94.708
290	1.04724	1.04804	100.01	101.71
300	1.05056	1.05148	107.03	108.97
310	1.05398	1.05503	114.28	116.50
320	1.05752	1.05872	121.78	124.30
330	1.06118	1.06252	129.51	132.36
340	1.06494	1.06646	137.47	140.69
350	1.06882	1.07052	145.68	149.30
360	1.07280	1.07472	154.12	158.17
370	1.07691	1.07904	162.80	167.32
380	1.08112	1.08350	171.72	176.75
390	1.08545	1.08808	180.88	186.47
400	1.08988	1.09281	190.27	196.46
410	1 09443	1.09766	199.91	206.74
420	1.09910	1.10266	209.78	217.31
430	1.10388	1.10779	219.89	228.17
440	1.10876	1.11305	230.22	239.30
450	1.11376	1.11846	240.81	250.76
460	1.11888	1.12401	251.65	262.50
470	1.12410	1.12970	262.69	274.55
480	1.12944	1.13553	274.00	286.89
490	1.13489	1.14151	285.54	299.55
500	1.14045	1.14763	297.30	312.50
550	1.16994	1.18051	359.73	382.10
600	1.20225	1.21728	428.12	459.94
700	1.27528	1.30342	582.71	642.28
800	1.35955	1.40813	761.10	863.93
900	1.45506	1.53392	963.27	1130.2
1000	1.56180	1.68372	1189.2	1447.3
1100	1.67978	1.86121	1439.0	1823.0
1200	1.80899	2.07050	1712.5	2266.0
1300	1.94944	2.31650	2009.8	2786.8
1400	2.10113	2.60489	2330.9	3397.2
1500	2.26405	2.94219	2675.7	4111.2

ignored. The lift and drag coefficients for an airfoil calculated on the aforementioned basis are plotted as a function of the Mach number in Fig. 7. In that figure it is seen that as the Mach number is raised from 0.3 to 0.5 the lift and drag coefficients increase rather slowly. Increasing M above 0.5 produces larger rates of increase in the values of C_L and C_{D0} until the value M approximately 0.7 is reached. Further increase in M results in a rapid decrease in C_L and a large increase in C_{D0}. The rapid increase in drag coefficient above $M = 0.6$ is attributed to the fact that the air passing over the top surfaces of the airfoil attains local sonic and supersonic velocities.

Fig. 7. Effect of compressibility on lift and drag coefficients. (Reproduced from J. Stack, *N.A.C.A.T.R.* 492, 1934.)

11. Pressure Disturbances in Compressible Fluids

The essential difference in the flow phenomena accompanying subsonic and supersonic velocities can be explained in a simple manner.[9] Thus, consider the motion of a spherical sound wave emanating from the source designated as O in Fig. 8, and assume that the fluid surrounding the source of disturbance is at rest prior to the creation of the disturbance.

The center O becomes the source from which sound waves are propagated in all directions with the acoustic velocity, and each sound wave, moving with a constant speed, traverses an equal radial distance in the same time interval t. The result is a spherical wave of radius at, where a is the acoustic velocity.

Now consider a body traveling with subsonic speed in a fluid. As each point of the body contacts previously undisturbed fluid it becomes a source of pressure disturbances. Its effect is similar to that described for the sound source illustrated in Fig. 8. The pressure disturbances created by each point of the body are
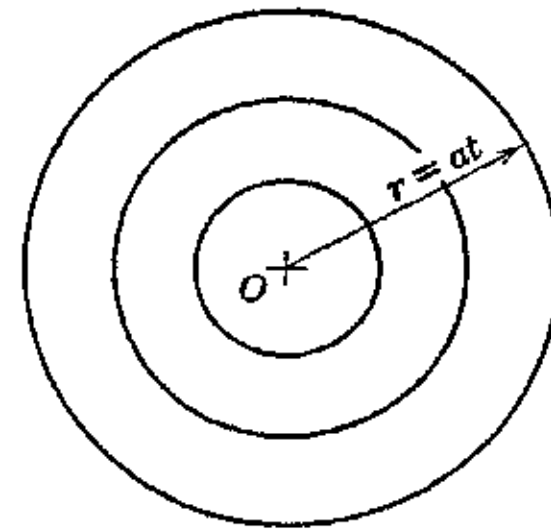
Fig. 8. Propagation of sound waves from a point source.

propagated through the fluid with the local sonic velocity, which is a constant if the fluid medium is assumed to be homogeneous and at a constant temperature.

Refer to Fig. 9. Assume that a body moves in a previously undisturbed homogeneous fluid at constant temperature, with the speed c. Let the instant when the body is at A be the starting point for the discussion. The disturbance created by the body will traverse the distance at from point A in the time interval t. In this same time interval the body originally at A will move to the point A'; the distance $AA' = ct$. In a second time interval t the body will be at A'' and the disturbance at a''. The distance $A'A'' = ct$ and $a'a'' = at$. Since a is greater than c, the disturbance, or wave front produced by it, moves faster than the body and always precedes it. This means that the disturbance is always moving away from the body, and the body, which assumes the successive positions A, A', A'', etc., always remains inside the spherical
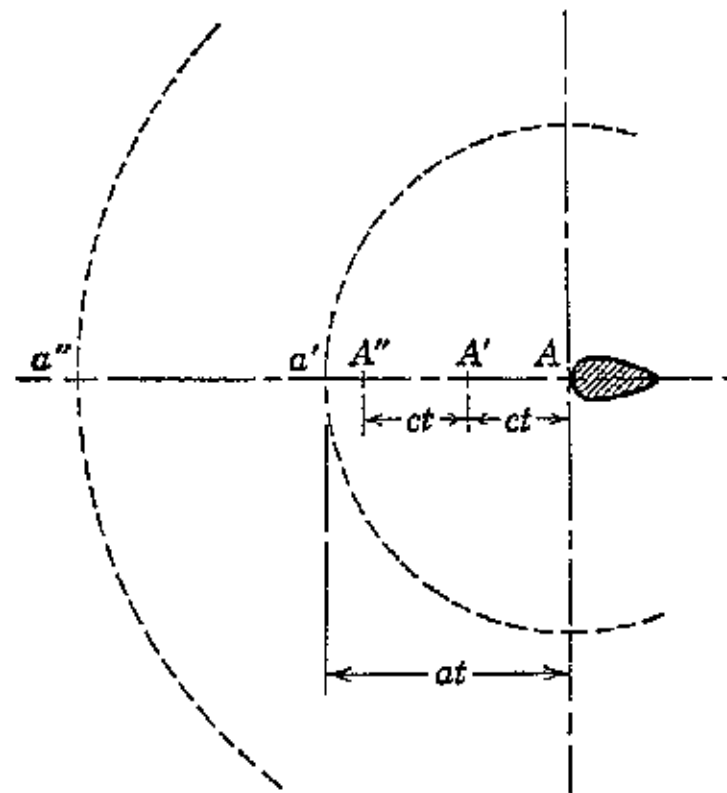
FIG. 9.   Disturbance produced by a body moving with subsonic speed.

wave front. Hence when a body travels with subsonic speed the disturbances it creates are said to "clear away" from it.

Consider now the case illustrated in Fig. 10, where the body travels with a speed u greater than a; that is, its speed is supersonic. In the time interval t the front of the disturbance is the spherical surface having the radius at. The body in this same interval moves to the position A', and the distance traversed is $AA' = ut$. In this case the wave front of the disturbance lags behind the point on the body that creates the disturbance. The source of the disturbance, point A, moves so that it precedes the propagation of the disturbance which it creates. Consequently in all its positions A', A'', etc., the moving body is located outside of the disturbance wave fronts it has produced. In fact, the body must pass through every wave front emanating from the successive positions it occupied in moving along its path of motion. These wave fronts are enveloped by a conical sur-

face of half-angle β corresponding to the angle $AA'C$ in the figure. From geometry it is seen that

$$\sin \beta = \frac{AC}{AA'} = \frac{at}{ut} = \frac{a}{u} = \frac{1}{M}$$

The angle β is called the *Mach angle*, and its magnitude is determined by the ratio of the flight velocity to the local acoustic velocity.[8]
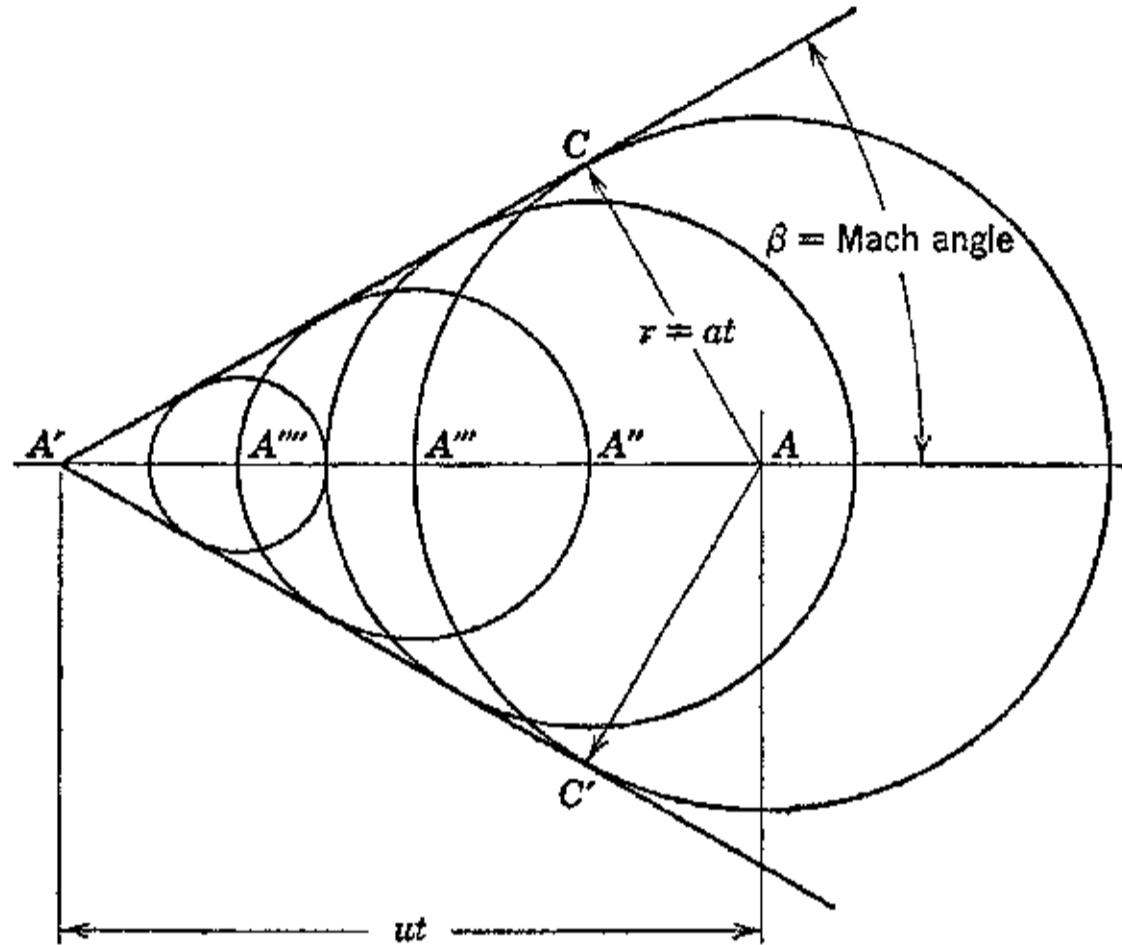
FIG. 10. Disturbance produced by a body moving with supersonic speed.

The foregoing discussion shows that all the disturbances in the case of supersonic speed remain inside the conical enveloping surface CAC'. In the regions beyond the conical surface the conditions are unaffected by the moving body. The conical surface, therefore, forms a *wave front* termed a *Mach wave*, a weak shock. The shock-wave phenomenon is accompanied by an increase in drag above the subsonic value; this drag increase has been termed *wave drag*. The wave drag is of the same order as the skin friction discussed earlier.

If the speed of an airplane (or airfoil) through the air is gradually increased, the drag begins to increase rapidly as unity Mach number is approached. At unity Mach number, or very close to it, the drag coefficient increases to two or more times its subsonic value.[17] If the speed of the airplane could be increased so that it exceeded the speed of sound, the drag coefficient would decrease again, although its value would be larger than the subsonic values.* In the Mach

* See Fig. 22, p. 522.

number range $M = 0.85$ to 1.2, called the *transonic range*, the flow conditions around an airfoil are unsteady, and, as pointed out in reference 14, wind-tunnel tests indicate that in this speed range there is great probability that the airplane will experience severe buffeting and stable flight will be difficult to achieve.

The Mach number of the free stream for which some point on the surface of a body first experiences the local sonic velocity is called the critical Mach number M_{cr}. When this condition is first reached the effects of the shock wave are quite small. As the Mach number is increased the intensity of the shock wave increases markedly with an accompanying large increase in the value of the drag coefficient. The shock wave disturbs the normal flow pattern for the airfoil, and there is a decrease in the lift coefficient. The breakdown in the normal flow pattern is termed the *shock stall*.

The aforementioned phenomena introduce problems which must be overcome before supersonic speeds can be attained. As pointed out in reference 14, level flight speeds at $M = 0.75$ have been attained by modern aircraft, and in some cases the speed has been limited not by the power plant but by the shock-stall phenomenon of the air frame. This same phenomenon limits the operating-speed range of propellers because the tips operate at speeds approaching the speed of sound.[13]

12. Basic Aerodynamic Performance Equations

The calculation of the performance characteristics of an airplane is simplified by replacing the complete airplane by a wing with elliptical lift distribution. Let C_{DP_e} be the effective profile drag of the equivalent wing, assumed constant, and AR_e the effective geometrical aspect ratio for the airplane. Then

$$AR_e = eAR = eb^2/S \qquad (32)$$

where e is known as the Oswald efficiency factor.[10]

It can be assumed that the drag coefficient of the equivalent wing is a parabolic function of the lift coefficient.[8] Let C_D be the drag coefficient for the airplane or its equivalent wing and C_L the lift coefficient; then

$$C_D = C_{DP_e} + \frac{C_L^2}{\pi AR_e} \qquad (33)$$

The geometrical aspect ratio $AR = b^2/S$ can be calculated from the dimensions of the airplane. Consequently, the only items in equation 33 which require empirical determination, or must be estimated, are C_{DP_e} and e, both of which are constants.

The total drag of the airplane is obtained by substituting equation 33 into equation 9. If V is in miles per hour, then the thrust required for level flight $\mathfrak{I}$ is given by

$$\mathfrak{I} = D = \left(C_{DP_e} + \frac{C_L{}^2}{\pi AR_e}\right)\frac{\sigma V^2 S}{391} \quad (V \text{ in mph}) \tag{34}$$

Introducing the parasite area $f = C_{DP_e}S$, $eb^2/S = AR_e$, and $W = C_L V^2 S\sigma/391$ into equation 34 gives

$$\mathfrak{I} = D = \frac{\sigma f V^2}{391} + \frac{124.5}{\sigma e}\left(\frac{W}{b}\right)^2 \frac{1}{V^2} \tag{35}$$

Or in terms of the parasite and span loadings l_p and l_s

$$\mathfrak{I} = D = 0.00255\sigma \frac{W}{l_p} V^2 + 124.5 \frac{l_s W}{\sigma V^2} \tag{36}$$

For a given airplane at a fixed altitude the coefficients of V^2 in equation 36 are constants. Let

$$K = 0.00255\sigma \frac{W}{l_p} = 0.00255\sigma f \tag{37}$$

and

$$K' = 124.5 \frac{W}{\sigma} l_s = \frac{124.5}{\sigma e}\left(\frac{W}{b}\right)^2 \tag{38}$$

Hence the thrust required for level flight is given by the equation [11]

$$\mathfrak{I} = D = KV^2 + \frac{K'}{V^2} \tag{39}$$

It follows from equations 37 and 38 that

$$\sqrt{KK'} = \sqrt{0.3175 W^2 \frac{l_s}{l_p}} = 0.5634 W \sqrt{\frac{l_s}{l_p}} \tag{40}$$

Following the procedure of reference 11, let

$$F_T = \text{thrust factor} = \frac{1}{\sqrt{KK'}} = \frac{1.775}{W}\sqrt{\frac{l_p}{l_s}} \tag{41}$$

and

$$F_V = \text{speed factor} = \left(\frac{K}{K'}\right)^{\frac{1}{4}} = (KF_T)^{\frac{1}{2}} = 0.06727 \frac{\sqrt{\sigma}}{(l_p l_s)^{\frac{1}{4}}} \tag{42}$$

Multiplying both sides of equation 39 by $F_T = 1/\sqrt{KK'}$ gives

$$\Im F_T = \frac{KV^2}{\sqrt{KK'}} - \frac{K'}{V^2\sqrt{KK'}} \tag{43}$$

But, from equation 42, $K/\sqrt{KK'} = \sqrt{K/K'} = F_V^2$. Hence equation 43 becomes

$$\Im F_T = F_V^2 V^2 + \frac{1}{F_V^2 V^2} \tag{44}$$

The values of $\Im F_T$ in equation 44 are those required to maintain the airplane in level flight.

Figure 11 presents the values of $\Im F_T$ required for level flight as a function of $F_V V$. The curve is applicable without correction only in the range of flight speeds where the effects of compressibility may be neglected. At higher flight speeds a compressibility correction must be applied to the results obtained by using Fig. 11. Approximate corrections for the effect of compressibility are presented in Fig. 12. For the derivation of the compressibility correction consult reference 11.

When the airplane is in level unaccelerated flight $\Im = D$ and $L = W$. Hence, the required thrust for level flight is given by

$$\Im = \frac{W}{L/D} \tag{45}$$

It has been pointed out that the ratio L/D determines the glide angle for the airplane. The maximum value of this ratio, denoted by $(L/D)_{\text{max.}}$, corresponds to the smallest value of the glide angle. For the minimum glide angle the effective parasite drag coefficient and the effective induced drag coefficient are equal to each other.[4]

Let the subscript ld denote at the condition $(L/D)_{\text{max}}$. It follows from equation 45 that the condition $(L/D)_{\text{max.}}$ corresponds to that for which the required thrust for unaccelerated level flight has its minimum value. The flight speed corresponding to $(L/D)_{\text{max}}$ is denoted by V_{ld}, and its value is obtained from equation 44. Differentiating equation 44 with respect to V and setting the result equal to zero gives the following equation for V_{ld}

$$V_{ld} = \frac{1}{F_V} = 14.86 \frac{(l_p l_s)^{\frac14}}{\sqrt{\sigma}} \tag{46}$$
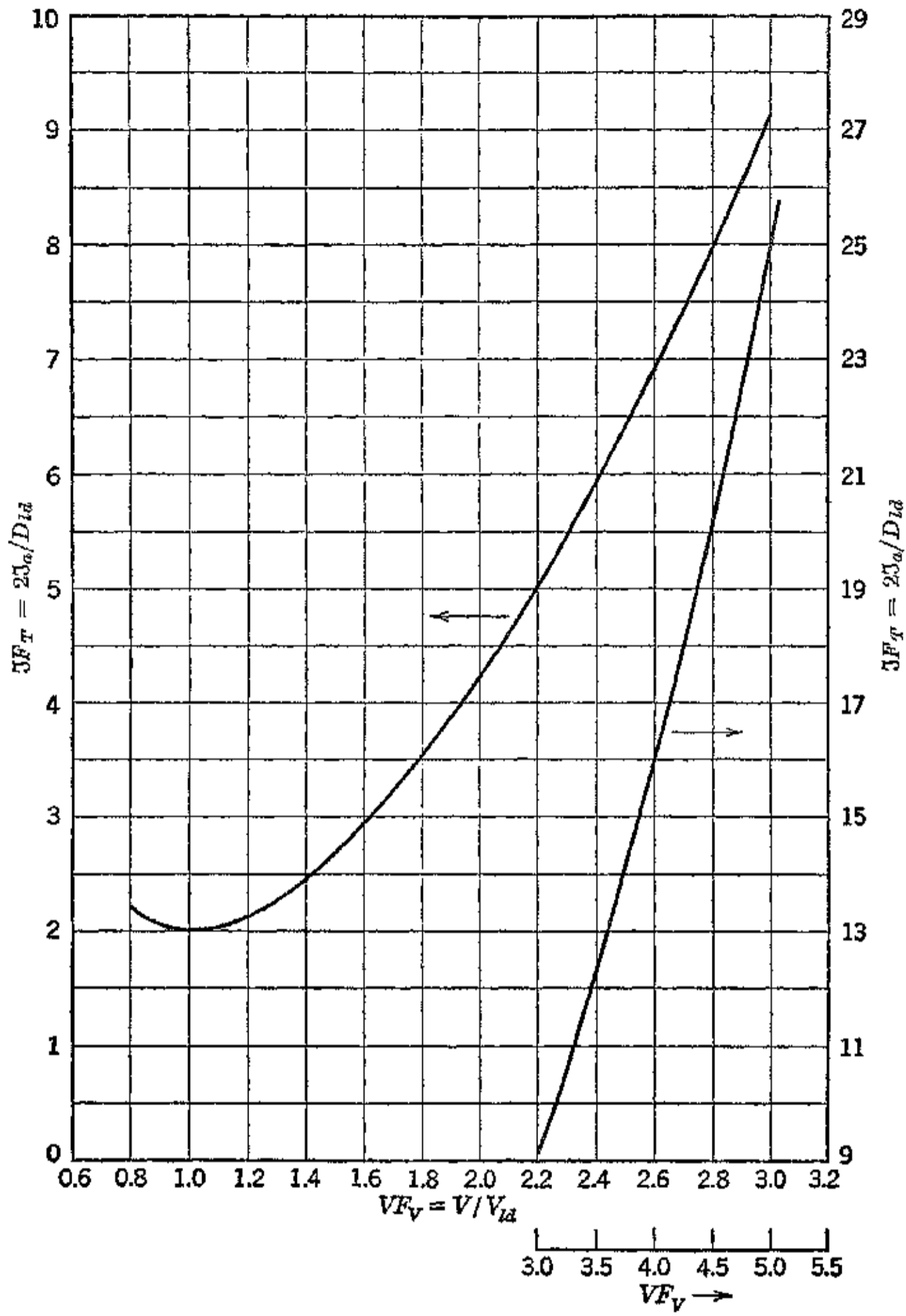
Fig. 11. Values of $3F_T$ for level flight as a function of VF_V (incompressible flow)
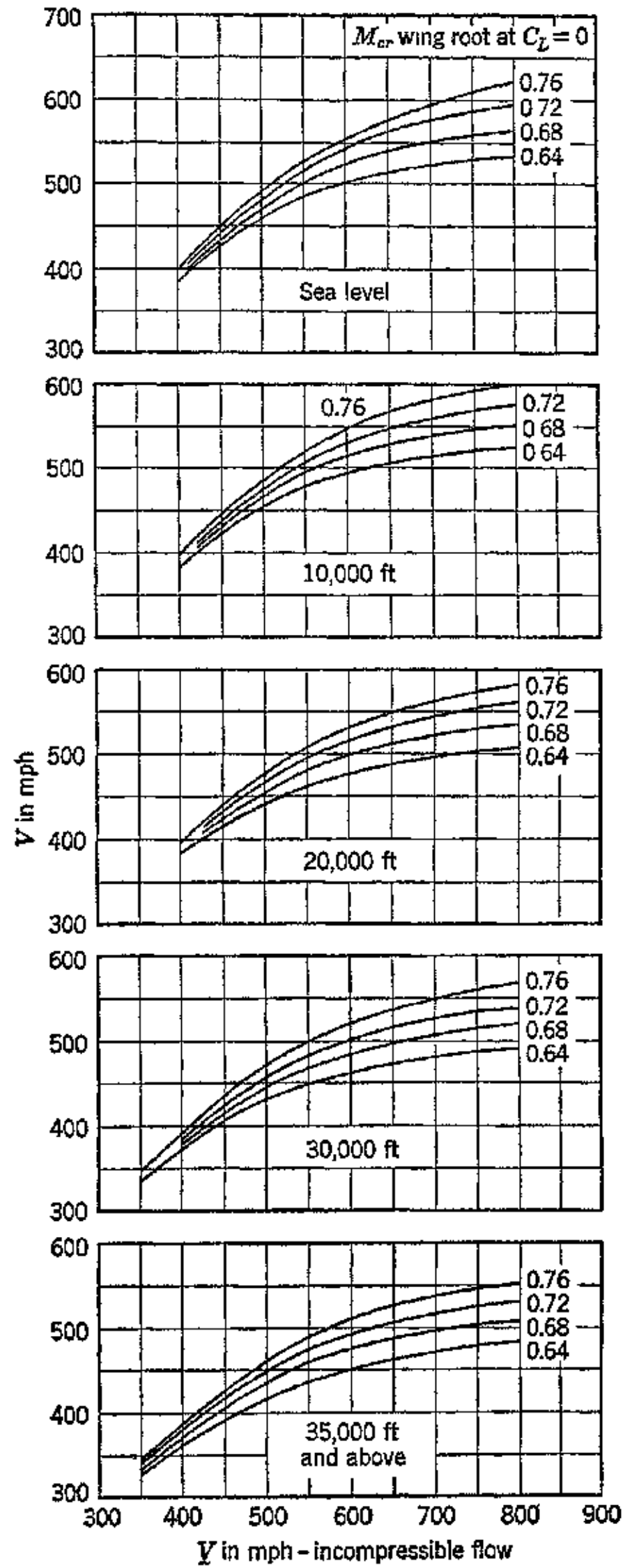
FIG. 12.   Approximate corrections for the effect of compressibility.   (Reproduced from R. E. Hage, *A.A.F. Tech. Rept.* 5193, A.S.T.C.)

Substituting for $V = V_{ld}$ into equation 44, and solving for $\mathfrak{I} = \mathfrak{I}_{ld} = D_{ld}$ gives

$$\mathfrak{I}_{ld} = D_{ld} = \frac{2}{F_T} = 1.128 W \sqrt{\frac{l_s}{l_p}} = 1.128 \frac{W}{b} \sqrt{\frac{f}{e}} \qquad (47)$$

It follows from equations 46 and 47 that at the condition $(L/D)_{max}$

$$F_V V_{ld} = 1 \quad \text{and} \quad F_T D_{ld} = 2 \qquad (48)$$

Once the values of F_V and F_T for the airplane have been determined the speed for minimum drag V_{ld} is readily calculated, and also the corresponding drag D_{ld}.

Following the method of reference 12, introduce the following two ratios.

$$\frac{\mathfrak{I}_a}{D_{ld}} = \text{Thrust ratio} = \frac{\text{Net available thrust}}{\text{Required thrust}} \qquad (49)$$

and

$$\frac{V}{V_{ld}} = \text{Speed ratio} = \frac{\text{Airplane flight speed}}{\text{Speed for minimum drag}} \qquad (50)$$

The above ratios can be related to each other by combining equations 44, 46, and 47. The result is

$$\frac{\mathfrak{I}_a}{D_{ld}} = \frac{\mathfrak{I}_a F_T}{2} = \frac{1}{2}\left[F_V{}^2 V^2 + \frac{1}{F_V{}^2 V^2} \right] \qquad (51)$$

But, from equation 46, $F_V{}^2 = 1/V_{ld}{}^2$. Hence equation 51 becomes

$$\frac{\mathfrak{I}_a}{D_{ld}} = \frac{1}{2}\left[\left(\frac{V}{V_{ld}}\right)^2 + \left(\frac{V_{ld}}{V}\right)^2 \right] \qquad (52)$$

Equation 52 shows that the curve $F_T\mathfrak{I}$ vs. $F_V V$ presented in Fig. 11 is, therefore, a plot of $2\mathfrak{I}_a/D_{ld}$ as a function of V/V_{ld}.

The condition for minimum required thrust power is determined from equation 44. Multiply both sides of equation 44 by $F_V V$. The resulting equation is a power relationship.

$$\mathfrak{I}F_T \cdot F_V V = F_V{}^3 V^3 + \frac{1}{F_V V}$$

Differentiate the above equation with respect to $F_V V$ and equate the result to zero. Solving for $F_V V$ gives $F_V V = (\frac{1}{3})^{\frac{1}{4}} = 0.76$. Substituting the foregoing result into equation 44 yields $\mathfrak{I}F_T = 2.31$. Hence, at the condition for minimum required power $F_V V = 0.76$

and $F_T 3 = 2.31$. Comparing the foregoing values with those corresponding to the speed for minimum required thrust V_{ld} shows that the speed for minimum power is $0.76 V_{ld}$, i.e., 0.76 times the speed for minimum drag.

For certain purposes it is convenient to express the thrust horsepower required to maintain level flight as a function of l_p, l_s, V, and σ. Let P_r denote thrust horsepower to maintain level flight; then with V in miles per hour

$$P_r = \frac{DV}{375} = \frac{6.8W}{l_p}\sigma\left(\frac{V}{100}\right)^3 + \frac{0.332W}{\sigma V}l_s \quad \text{hp} \qquad (53)$$

The preceding equations are the basic ones for determining the principal performance characteristics of the airplane assuming incompressible flow conditions. In general, the following performance criteria are of interest:

(a) Maximum level flight velocity.

(b) True air speed for maximum climbing speed.

(c) Maximum rate of climb.

(d) Time to climb from one altitude to another.

(e) Maximum range.

The determination of these characteristics is discussed in the subsequent sections. The methods used are based on references 4, 11, 12, and 13.

13. Maximum Level-Flight Speed

The maximum level-flight speed at any altitude is that corresponding to the value of $F_V V$ at the intersection of the curves for $3_a F_T$ and $3 F_T$, where the subscript a denotes *available*. To construct the curve $3_a F_T$ vs. $F_V V$ the thrust characteristics of the propulsion plant as a function of the flight speed and the altitude must be available or estimated. The maximum level-flight speed is obtained by dividing the value of $F_V V$, at the intersection of the $3_a F_T$ and $3 F_T$ curves, by F_V.

It should be realized that the value of the maximum level-flight speed, denoted by V_{max}, obtained in the manner described above will be correct only in the speed range where compressibility effects may be neglected ($M < 0.6$ approximately). Consequently, at Mach numbers greater than $M = 0.6$ a compressibility correction must be applied to obtain the correct value of V_{max}.

The application of the above-described procedure is illustrated by the following example based on reference 11.

EXAMPLE. An airplane is equipped with a turbojet engine having the following thrust characteristics at 35,000 ft.

V mph (incompressible)	300	400	500	600
$\Im_a$ lb	1220	1215	1240	1220

The principal dimensions of the airplane are as follows:

$$W = 12,000 \text{ lb} \quad S = 300 \text{ ft}^2 \quad b = 40 \text{ ft} \quad f = 4 \text{ ft}^2$$

$$e = 0.82 \quad \text{and} \quad M_{cr} \text{ at } C_L = 0 \text{ is } 0.72$$

Find the maximum level-flight speed at 35,000 ft.

Solution. From Table 1·6, $\sigma = 0.3098$.

$$l_p = \frac{12,000}{4} = 3000 \qquad l_a = \frac{12,000}{0.82 \times 1600} = 9.15$$

$$F_T = \frac{1.772}{12,000} \sqrt{\frac{3000}{9.15}} = 0.00267$$

$$F_V = 0.06734 \frac{\sqrt{0.3098}}{(3000 \times 9.15)^{1/4}} = 0.00291$$

V (incompressible)	300	400	500	600
VF_V	0.873	1.163	1.455	1.745
$\Im_a F_T$	3.27	3.24	3.32	3.27

The $\Im_a F_T$ curve is plotted as a broken line in Fig. 11. The intersection of the $\Im_a F_T$ and $\Im F_T$ curves gives $V_{max} F_V = 1.68$. Hence $V_{max} = 1.68/0.00291 = 578$ mph. From Table 1·6 at 35,000 ft, $a = 976.1$ fps $= 666$ mph. Hence $M = \frac{578}{666} = 0.867$.

Compressibility correction from Fig. 12 indicates that the actual value of $V_{max} = 480$ mph.

14. Speed for Maximum Rate of Climb

It was shown in section 4 that if V is in feet per second the rate of climb of an airplane in feet per second is given by equation 12. Let V be in miles per hour; then the rate of climb C in feet per minute is given by

$$C = 88 V \frac{(\Im_a - D)}{W} = 88 V \frac{\Im_e}{W} \tag{54}$$

where $\Im_a - D = \Im_e$ = the excess thrust. Multiplying the numerator and denominator of equation 54 by $F_T F_V$ gives

$$C = \frac{88(VF_V)(\Im_e F_T)}{W F_T F_V} \tag{55}$$

Since the product $WF_T F_V$ is constant for a given airplane at a given altitude, the climbing rate at a given altitude is practically proportional to the product $VF_V \cdot \Im_e F_T$.

If $\Im_a F_T$ and $\Im F_T$ are plotted as functions of VF_V, the speed for the maximum rate of climb will correspond to that value of VF_V at

which the difference between the ordinates of the $\mathfrak{I}_a F_T$ and $\mathfrak{I} F_T$ curves multiplied by the corresponding value of VF_V has the largest value. Consequently to obtain an analytic expression for the speed for best climb, $\mathfrak{I}_a$ must be expressible as a function of V.
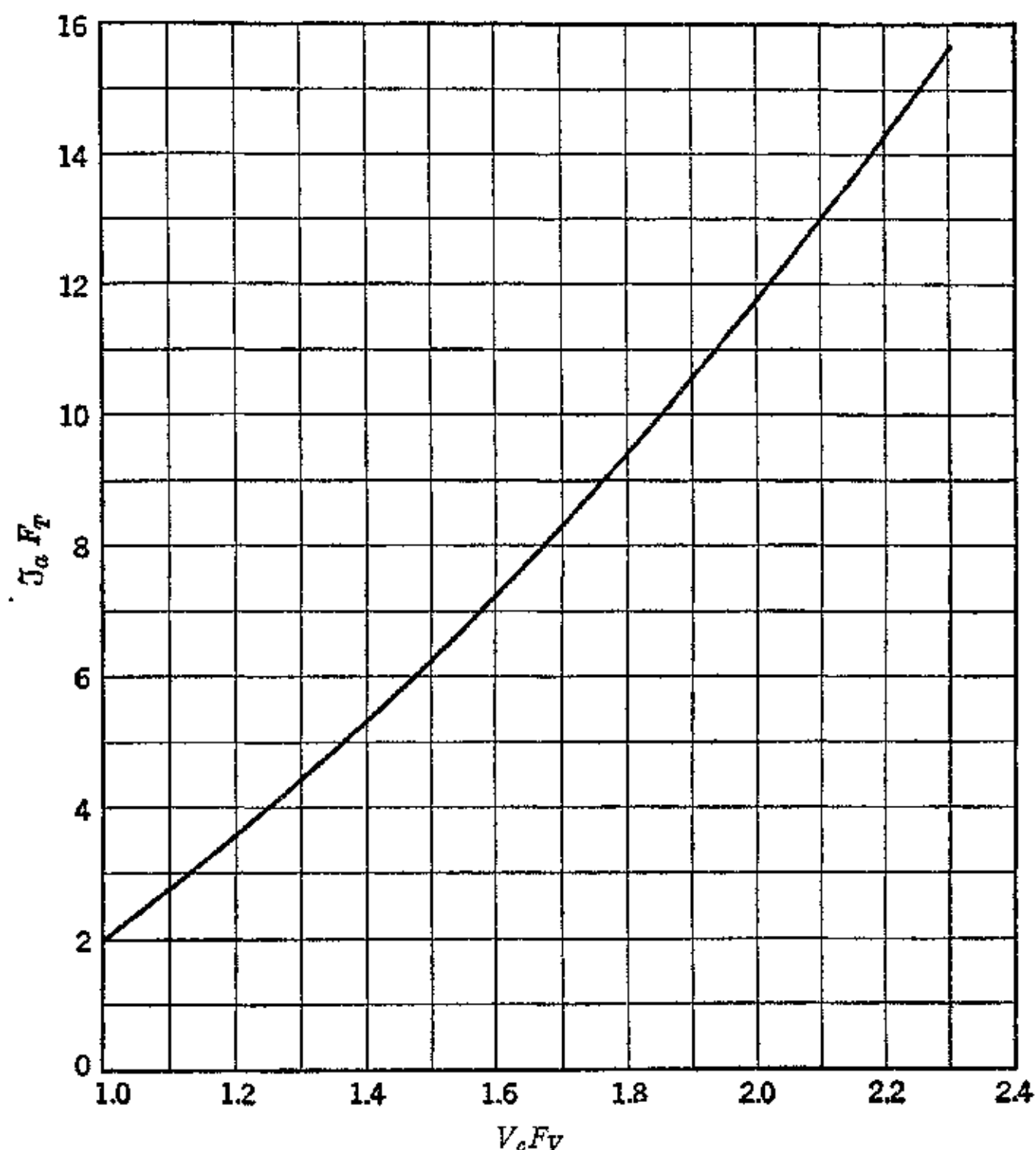
FIG. 13.   Parameter $\mathfrak{I}_a F_T$ vs. parameter $V_e F_V$ (incompressible flow).

For turbojet-propelled aircraft at a given altitude $\mathfrak{I}_a F_T$ is practically constant. For rocket-jet-propelled aircraft $\mathfrak{I}_a F_T$ is substantially constant and varies only slightly with the altitude. Assuming that $\mathfrak{I}_a F_T$ is a constant for jet-propelled aircraft at a given altitude, then the maximum value of $(\mathfrak{I}_e F_T)(F_V V)$ can be found analytically.

$$(VF_V)(\mathfrak{I}_e F_T) = VF_V \left(\mathfrak{I}_a F_T - F_V{}^2 V^2 - \frac{1}{F_V{}^2 V^2} \right) \qquad (56)$$

Differentiating equation 56 with respect to VF_V and setting the result equal to zero, the value of VF_V which makes the product (VF_V)

$(\mathfrak{J}_e F_T)$ a maximum can be determined. Let $V_C F_V$ denote the value of $V F_V$ for best climb; then the result of the differentiation is

$$V_C F_V = \left[\frac{\mathfrak{J}_a F_T - \sqrt{\mathfrak{J}_a{}^2 F_T{}^2 - 12}}{6} \right]^{\frac{1}{2}} \tag{57}$$

Equation 57 gives the value of $V F_V$ for best climb assuming incompressible flow.

The relationship expressed by equation 57 is plotted in Fig. 13 It is applicable to incompressible flow conditions, and to propulsion plants which are characterized by delivering a constant value for $\mathfrak{J}_a F_T$ at each altitude. If $\mathfrak{J}_a F_T$ does not remain constant at a fixed altitude then an average value should be used. According to reference 11 the appropriate average value is that between $V F_V = 1$ and where the $\mathfrak{J}_a F_T$ curve intersects the $\mathfrak{J} F_T$ curve. The flight speed which gives the maximum rate of climb is denoted by V_C.

EXAMPLE. Determine the speed for best climb at 35,000 ft altitude for the airplane of the problem discussed on page 216.
Solution.

Average value	$\mathfrak{J}_a F_T$	$= 3.05$
From Fig. 12	$V_C F_V$	$= 1.13$
From Fig. 11	$\mathfrak{J} F_T$	$= 2.08$

Hence

$$\mathfrak{J}_e F_T = 3.05 - 2.08 = 0.97$$

$$\mathfrak{J}_e = \frac{0.97}{0.00267} = 363$$

$$V_C = \frac{1.13}{0.00291} = 388 \quad \text{mph}$$

The above value of V_C is for incompressible flow. From Fig. 12, the value of V_C corrected for compressibility is 370 mph.

A useful relationship between V_C, V_{ld}, $\mathfrak{J}_a$, and D_{ld} is obtained by expressing the rate of climb in terms of the available horsepower P_a and the required horsepower P_r. If V is in miles per hour, and C in feet per minute, equation 14 becomes

$$C = \frac{33,000}{W} (P_a - P_r) \tag{58}$$

Substituting for P_r from equation 53,

$$C = 33,000 \left[\frac{\mathfrak{J}_a V}{375 W} - \frac{6.8}{l_v} \sigma \left(\frac{V}{100} \right)^3 - \frac{0.332 l_s}{\sigma V} \right] \quad \text{fpm} \tag{59}$$

Differentiating equation 59 with respect to time t, equating the result to zero, and introducing the ratios $\Im_a/D_{ld}$ and V/V_{ld}, as is done in reference 12, gives

$$\frac{\Im_a}{D_{ld}} = \frac{1}{2}\left[3\left(\frac{V_C}{V_{ld}}\right)^2 - \left(\frac{V_{ld}}{V_C}\right)^2\right]$$

(60)

Figure 14 presents $\Im_a/D_{ld}$ as a function of V_C/V_{ld}.
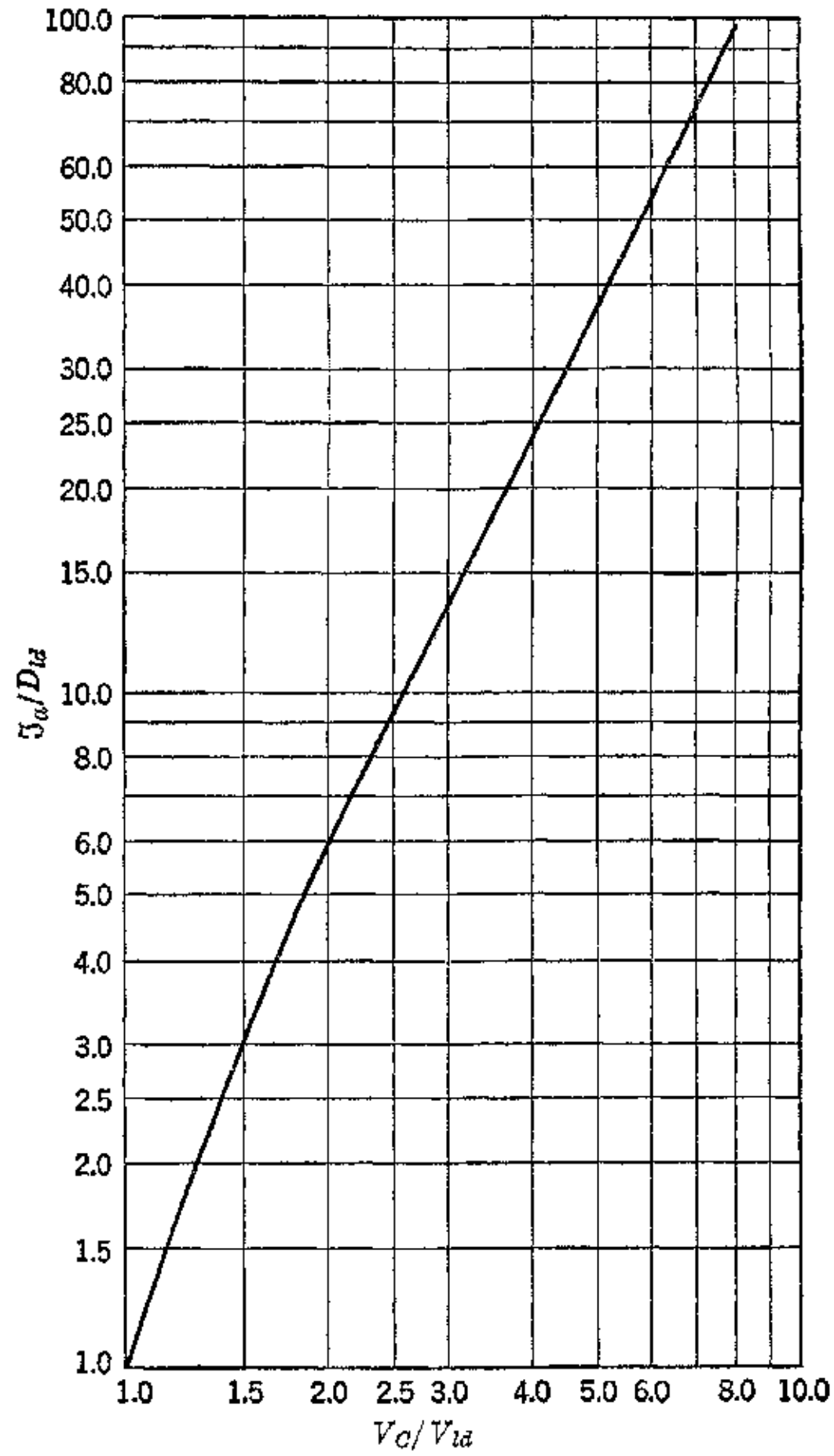
FIG. 14.   Ratio $\Im_a/D_{ld}$ vs. ratio V_C/V_{ld} (incompressible flow).

15. Maximum Rate of Climb

The maximum rate of climb, denoted by $C_{max.}$, is obtained by substituting the value $V = V_C$ in equation 54. If equation 60 is substituted into equation 59, the maximum rate of climb can be expressed by the following equation.[12]

$$C_{max.} = \frac{V_C f_2}{(L/D)_{max}} \tag{61}$$

where

$$f_2 = 176 \left[\frac{3_a}{D_{ld}} - \left(\frac{V_C}{V_{ld}} \right)^2 \right] \tag{62}$$
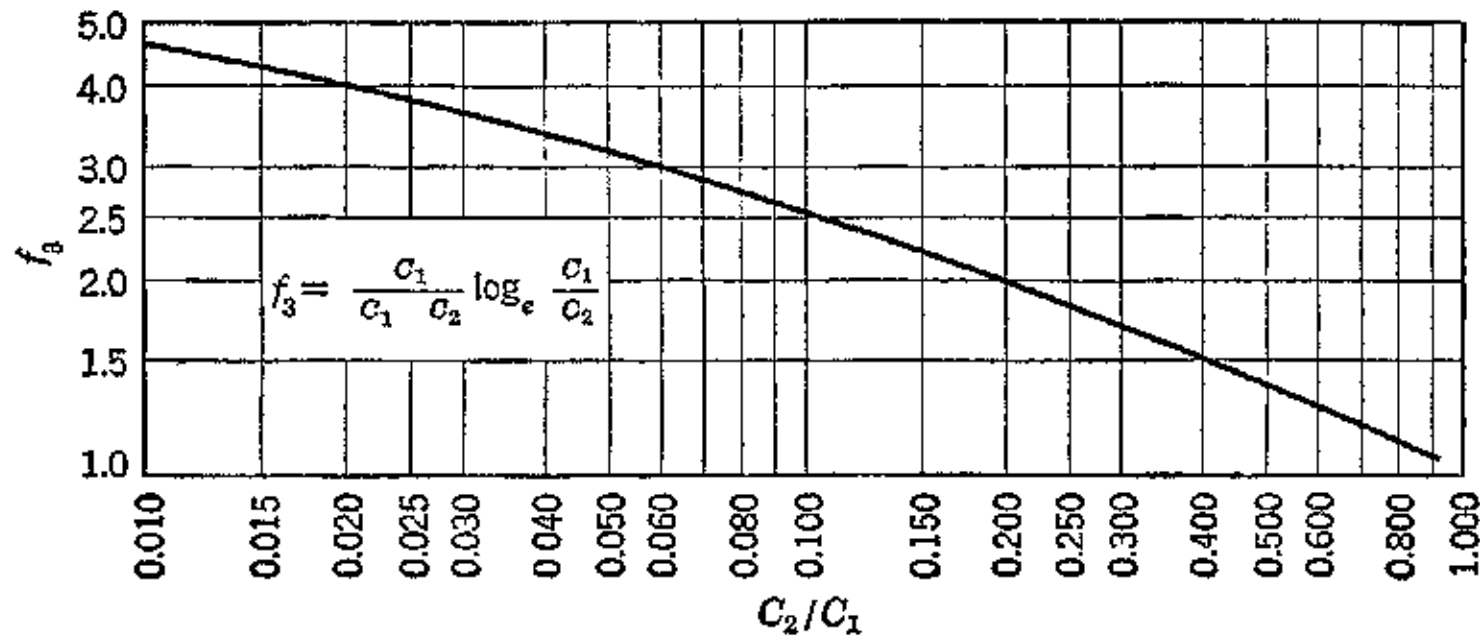
Fig. 15. Values of maximum rate of climb parameter f_3 as a function C_2/C_1 (incompressible flow). (Based on S. R. Puffer and J. S. Alford, paper 45-A-49, A.S.M.E. annual meeting, New York, Nov. 26–29, 1945.)

16. Time to Climb

For an airplane propelled by a turbojet engine it may be assumed that between any two altitudes the rate of climb is a linear function of the altitude.[11] Hence if C is the rate of climb at any altitude h, and C_1 and C_2 are the climb rates at altitudes h_1 and h_2 respectively, then

$$C - C_1 = \frac{C_2 - C_1}{h_2 - h_1} (h - h_1) \tag{63}$$

Since, in general, the time to climb is given by

$$t = \int_0^h \frac{1}{C} dh \tag{64}$$

then

$$t_C = \int_{t_1}^{t_2} dt = \int_{h_1}^{h_2} \frac{1}{C} dh \tag{65}$$

But from equation 63

$$C = \frac{C_1 h_2 - C_2 h_1 - h(C_1 - C_2)}{h_2 - h_1} \tag{66}$$

Substituting equation 66 into equation 65 and integrating

$$t_C = \frac{h_2 - h_1}{C_1 - C_2} \log_e \frac{C_1}{C_2} \tag{67}$$

To simplify equation 67, let

$$t_C = \frac{h_2 - h_1}{C_1} f_3 \tag{68}$$

then the parameter f_3 is given by

$$f_3 = \frac{C_1}{C_1 - C_2} \log_e \frac{C_1}{C_2} = \frac{1}{1 - (C_2/C_1)} \log_e \frac{C_1}{C_2} \tag{69}$$

Figure 15 presents values of the parameter f_3 as a function of C_2/C_1.

17. Fuel to Climb from One Altitude to Another

It is shown in reference 12 that, if it is assumed that there is a linear relationship between the rate of fuel consumption and altitude, which is reasonably correct for turbojet engines, then since

$$G_f - G_{f1} = \frac{G_{f2} - G_{f1}}{h_2 - h_1} (h - h_1) \tag{70}$$

where G_{f1} = fuel consumption rate in lb/min at h_1,
$\quad\;\; G_{f2}$ = fuel consumption rate in lb/min at h_2,

the weight of fuel consumed in climbing is given by

$$W_{fC} = \int_{C_1}^{C_2} \frac{G_f}{C} dh \tag{71}$$

Substituting equations 63 and 70 into equation 71 and integrating gives the result presented below.

$$W_{fC} = \frac{G_{f1}}{C_1} (h_2 - h_1) f_4 \tag{72}$$

where

$$f_4 = \frac{C_1}{C_1 - C_2} \left\{ 1 - \frac{G_{f2}}{G_{f1}} + \left[1 - \frac{(G_{f1} - G_{f2})/G_{f1}}{(C_1 - C_2)/C_1} \right] \log_e \frac{C_1}{C_2} \right\} \tag{73}$$

Figure 16 presents values of the fuel factor f_4 as a function of the rate-of-climb ratio C_2/C_1, with the fuel-consumption ratio G_{f2}/G_{f1} as a parameter. The aforementioned figure is reproduced with the permission of the authors from reference 12.
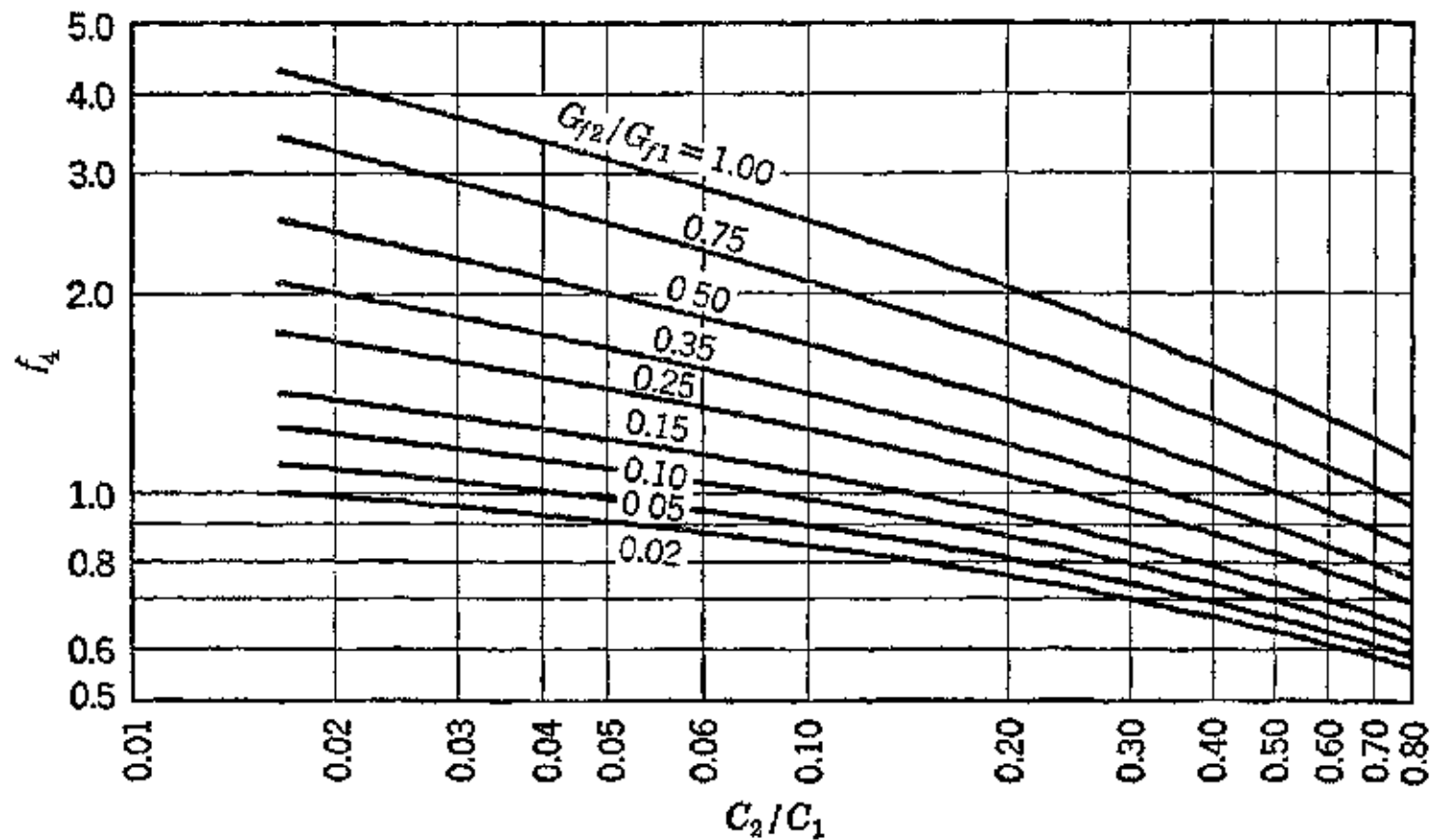
FIG. 16. Values of fuel factor f_4 vs. rate-of-climb ratio C_2/C_1 (incompressible flow). (Based on S. R. Puffer and J. S. Alford, *loc. cit.*)

18. Range of Aircraft

The accurate determination of the flight conditions yielding maximum range involves tedious tabular and graphical procedures beyond the scope of this book. Useful formulas giving approximate results have been developed by Breguet and by Diehl. Thus for aircraft propelled by a reciprocating engine and propeller the two most commonly used formulas are as follows [3]

(a) Breguet's logarithmic formula for range is

$$R = 863.5 \frac{\eta}{w_f} \frac{L}{D} \log_{10} \frac{W_0}{W_E} \quad \text{miles} \tag{74}$$

and

(b) Diehl's exponential formula

$$R = \frac{375}{n} \frac{\eta_0}{w_{f0}} \frac{L}{D} \left[1 - \left(\frac{W_E}{W_0} \right)^n \right] \quad \text{miles} \tag{75}$$

A more convenient equation for range which is also used quite generally is

$$R = 1250 \frac{\eta_0}{w_{f0}} \frac{L}{D} \left[1 - \left(\frac{W_E}{W_0} \right)^{0.3} \right] \quad \text{miles} \tag{76}$$

In the above equations the symbols have the following significance:

η = average efficiency of propeller.

η_0 = efficiency of the propeller at the beginning.

w_f = average specific fuel consumption of engines, lb/bhp-hr.

w_{f0} = specific fuel consumption of the engines at the beginning of flight, lb/bhp-hr.

L = lift of airplane, lb.

D = drag of airplane, lb.

W_0 = weight of airplane at take-off, lb.

W_E = weight of airplane at end of the flight when the fuel is exhausted, lb.

$W_f = W_0 - W_E$ = weight of fuel consumed, lb.

n = exponent depending for its value on the characteristics of the airplane.

Equation 76 gives accurate results for the following operating conditions

(a) $W_E/W_0 > 0.70$.
(b) Final engine speed > 1200 rpm.
(c) Flight is conducted at constant L/D; not necessarily $(L/D)_{max}$.
(d) Automatic rich carburetor setting is not used.
(e) Flight is made with a fixed blade angle setting for the propellers.

For *jet-propelled airplanes* equipped with a turbojet power plant, an approximate range formula can be derived by the same approach as Breguet's. Thus let w_f' be the specific fuel consumption of the thermal jet engine in pounds per hour per pound thrust. If D is the drag (the required thrust) to be overcome to maintain level flight, the decrease in the weight of the airplane dW is given by

$$\frac{dW}{dt} = -D \times w_f'$$

If it is assumed that the specific fuel consumption of the turbojet engine is constant, the maximum range of the jet-propelled airplane results when the flight is conducted at constant flight speed.[12] Consequently, as the airplane weight is reduced by virtue of the consumption of fuel, the flight altitude is increased just enough to keep the flight speed constant at the reduced thrust output. On these

assumptions, the range corresponding to the flight duration t is given by

$$R = \int_0^t V\,dt = \int_{W_0}^{W_E} -\frac{V\,dW}{Dw_f'} = \int_{W_E}^{W_0} \frac{1}{w_f'} \frac{dW}{(D/V)} \qquad (77)$$

As a result of the assumption of constant specific fuel consumption, the maximum range will occur at the flight speed V_{MR} for which D/V is a minimum. This speed is given by

$$V_{MR} = \frac{19.55}{\sqrt{\sigma}} (l_p l_s)^{1/4} \quad \text{mph} \qquad (78)$$

The corresponding L/D ratio is given by

$$\left(\frac{L}{D}\right)_{MR} = 0.767 \frac{b_e}{\sqrt{f}} = 0.865 \left(\frac{L}{D}\right)_{\text{max.}} \qquad (79)$$

The required thrust $\mathfrak{I}_{MR}$ (or the drag D_{MR}) for maximum range is

$$\mathfrak{I}_{MR} = D_{MR} = 1.305 \frac{W}{b_e} \sqrt{f} \qquad (80)$$

For aircraft propelled by reciprocating engines and propellers the speed for maximum range is close to that for $(L/D)_{\text{max}}$, where

$$\left(\frac{L}{D}\right)_{\text{max.}} = 0.886 \frac{b_e}{\sqrt{f}} \qquad (81)$$

The speed corresponding to $(L/D)_{\text{max.}}$ is V_{ld}, which is given by equation 46. It follows, therefore, that, to obtain the maximum range from a jet-propelled airplane, it must fly at slightly more than 30 per cent higher speed than would be required if it were propelled by a propeller. Further, the drag must be approximately 15 per cent greater at its maximum range speed than it is at the maximum range speed for propeller propulsion.

The value of $(D/V)_{\text{min}}$ for jet-propelled airplanes is given by [12]

$$\left(\frac{D}{V}\right)_{\text{min.}} = 0.0667 \sqrt{\frac{\sigma W}{b_e}} \cdot f^{3/4} \quad \text{(lb/mi/hr)} \qquad (82)$$

Introducing the *thrust factor* ϕ, where

$$\phi = \frac{\mathfrak{I}}{\sigma \mathfrak{I}_0} = \frac{\text{Actual thrust available at altitude}}{\sigma \times \text{Gross thrust at sea level and zero speed}}$$

and $\sigma = \rho/\rho_0 = $ density ratio, and substituting $(D/V)_{\text{min}}$ into equa-

tion 77 and integrating gives the following approximate equation for the maximum range of the jet-propelled airplane

$$R_{\text{max.}} = \frac{14.80}{w_f'} \left[\frac{\phi_{av} \mathfrak{z}_0}{f} \right]^{1/2} \left(\frac{L}{D} \right)_{\text{max}} \log_e \frac{W_0}{W_E} \tag{83}$$

or

$$R_{\text{max}} = \frac{13.1}{w_f'} (\phi_{av} \mathfrak{z}_0)^{1/2} \frac{b_e}{f} \log_e \frac{W_0}{W_E} \tag{84}$$

The maximum range can also be expressed in terms of the constant flight speed for maximum range V_{MR}. At that speed $\mathfrak{z}_{MR} = D_{MR}$, so that

$$\sqrt{\sigma} = (1.305)^{1/2} \frac{W^{1/2} f^{1/4}}{(\phi \mathfrak{z}_0)^{1/2} b_e^{1/2}}$$

Substituting for $\sqrt{\sigma}$ in equation 78 and substituting for l_p and l_s, the following equation is obtained for V_{MR}

$$V_{MR} = 17.15 \sqrt{\frac{\phi \mathfrak{z}_0}{f}} \tag{85}$$

As pointed out in reference 12, equation 85 shows that the flight velocity for maximum range is constant if the thrust factor ϕ is constant. Substituting this result into equation 77 gives the following

$$R_{\text{max}} = \int_{W_E}^{W_0} \frac{V \, dW}{w_f' D} = \frac{V_{MR}}{w_f'} \left(\frac{L}{D} \right)_{MR} \int_{W_E}^{W_0} \frac{dW}{W} \tag{86}$$

Hence, the maximum range for the jet-propelled airplane can be estimated from the equation

$$R_{\text{max.}} = \frac{V_{MR}}{w_f'} \left(\frac{L}{D} \right)_{MR} \log_e \frac{W_0}{W_E} = 0.865 \frac{V_{MR}}{w_f'} \left(\frac{L}{D} \right)_{\text{max}} \log_e \frac{W_0}{W_E} \tag{87}$$

REFERENCES

1. TH. VON KÁRMÁN and J. M. BURGERS, "General Aerodynamic Theory Perfect Fluids," *Aerodynamic Theory* by F. W. Durand, Vol. II, Division E, pp. 1–15.
2. B. MELVILLE JONES, "Dynamics of the Airplane," *Aerodynamic Theory* by F. W. Durand, Vol. V, Division N, pp. 5–19.
3. W. S. DIEHL, *Engineering Aerodynamics*, Ronald Press Co., 1936, pp. 362–434.
4 C. B. MILLIKAN, *Aerodynamics of the Airplane*, John Wiley & Sons, 1941.
5. L. PRANDTL and C. G. TIETJENS, *Fundamentals of Hydro- and Aeromechanics*, McGraw-Hill Book Co , 1934, pp 224–229.

6 L. PRANDTL and C. G. TIETJENS, *Applied Hydro- and Aeromechanics*, McGraw-Hill Book Co., 1934, pp. 144–226.

7. L. V. KERBER, "Airplane Performance," *Aerodynamic Theory* by F. W. Durand, Vol. V, Division O, pp. 224–270.

8 W. L. COWLEY, *Aerodynamics of the Airplane*, Ronald Press Co., pp. 142–156.

9 B. A. BAKHMETEFF, *Mechanics of Fluids*, Compendium of Course C. E. 261, Columbia University, Morningside Heights, New York.

10 W. B. OSWALD, "General Formulas and Charts for the Calculation of Airplane Performance," *N.A.C.A. Tech. Report* 408, 1932.

11. R. E. HAGE, *A A.F. Tech. Report* 5193, A A.F. Air Service Technical Command (unclassified).

12. S. R. PUFFER and J. S. ALFORD, "The Gas Turbine in Aviation," Paper No. 45-A-49, A S.M E. Annual Meeting, New York, N. Y., Nov. 26–29, 1945.

13. W. S. DIEHL, *Mechanical Engineers' Handbook* by L. S. Marks, Fourth Ed., 1941, p. 1536.

14. C. E. PAPPAS and M. G. HARRISON, "Analyzing the Aspects of Future Flight," *Aviation*, November, 1945, pp. 131–134.

15. E. J. BULBAN, "Nazi Jet-Bats Which Never Took Wing," *Aviation*, October, 1945, p. 172.

16. "Nazis Brinked the Fantastic in Drive to Re-Command Air," *Aviation*, November, 1945, p 178.

17. TH. VON KÁRMÁN and N. B. MOORE, "Resistance of Slender Bodies Moving with Supersonic Velocities, with Special Reference to Projectiles," *Trans. A.S.M.E.*, APM-54-27, 1932, pp. 303–310.

THE AIRPLANE PROPELLER

1. Introduction

The function of the propeller is to convert the torque delivered to it by the power plant into a thrust for propelling the airplane. If the airplane is in steady horizontal flight, the thrust developed by the propeller is equal to the drag of the airplane. If the airplane is climbing, the propeller thrust must overcome not only the drag but also the weight component of the airplane, $W \sin \theta$ (see Fig. 5·2).

The conventional propeller consists of two or more equally spaced radial blades which are rotated at a substantially uniform angular velocity. A blade section taken at any arbitrary radius from the center of rotation is shaped like an airfoil. Consequently, each blade section experiences the aerodynamic reactions that would be experienced by an airfoil of like section moving through the air in a similar manner. At any given radius the section of one blade forms with the corresponding sections on the other blades of the propeller a series of similar airfoils which follow each other as the propeller rotates.

As the hub of the propeller is approached, the blade sections become more nearly circular. The shape of the blade near the hub is dictated by the strength requirements rather than aerodynamic considerations, and that portion of each blade close to the hub contributes little if any propeller action. Figure 1 taken from *N.A.C.A. Tech. Report* 237 presents a sectional analysis of a typical propeller blade.

The forward motion or advance of the propeller as it moves through the air surrounding it resembles that of a screw advancing into a solid nut. For this reason, the term "airscrew" is frequently applied to the airplane propeller.

When the propeller rotates, its action produces a slipstream composed of the entire body of air which flows through the circle, or disk area, swept by the propeller blades. This is illustrated in Fig. 2.

The torque of the propeller imparts a rotational motion to the air passing through it. The pressure of the air immediately behind the propeller is raised, and in front of it the pressure is decreased. The

227

Blade thickness or ordinate
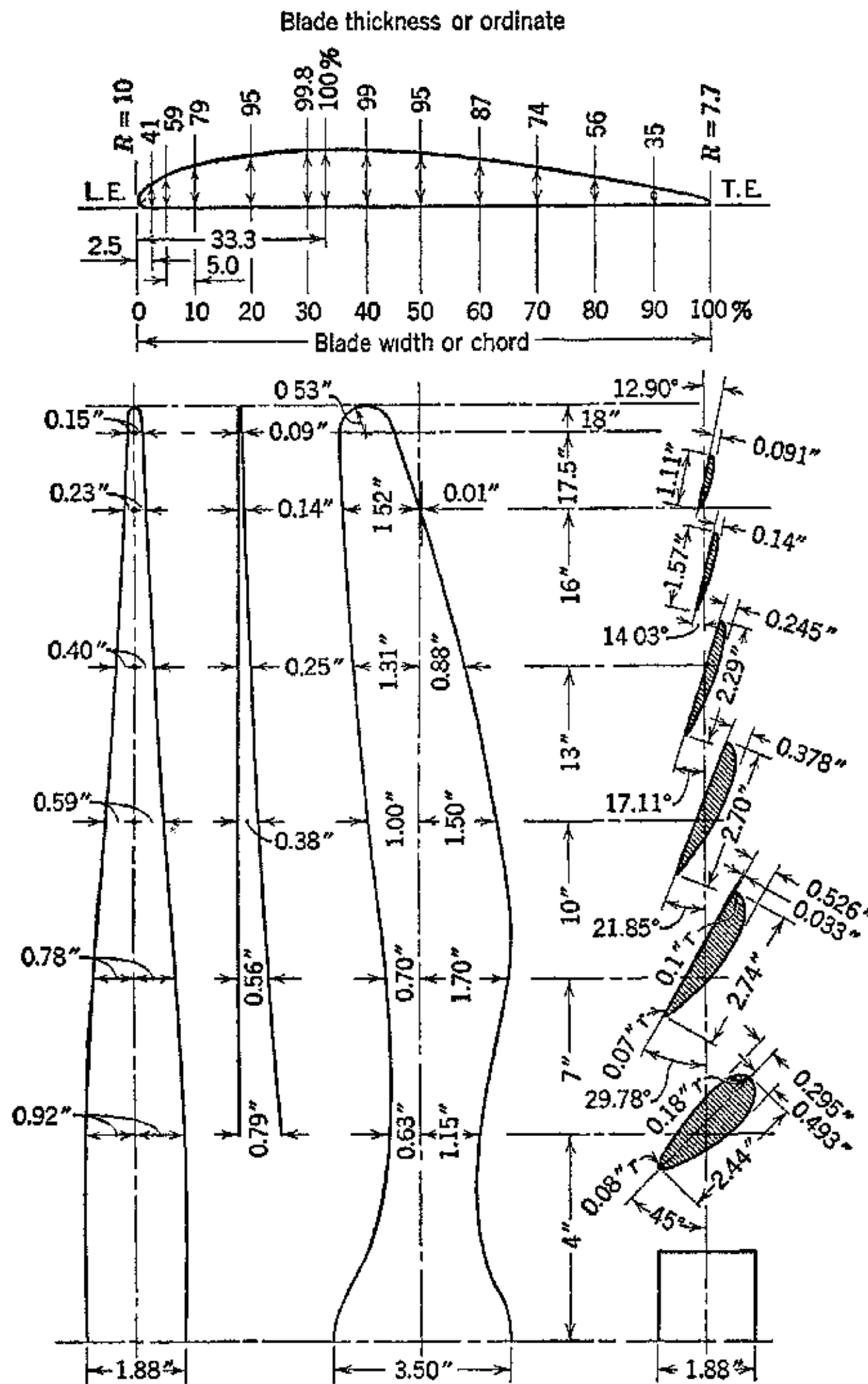
FIG. 1. Sectional analysis of a typical propeller blade. (Reproduced from *N.A.C.A. Tech. Rept.* 237.)

air is sucked toward the front of the propeller and pushed away behind it. The air attains its maximum axial velocity at some dis-
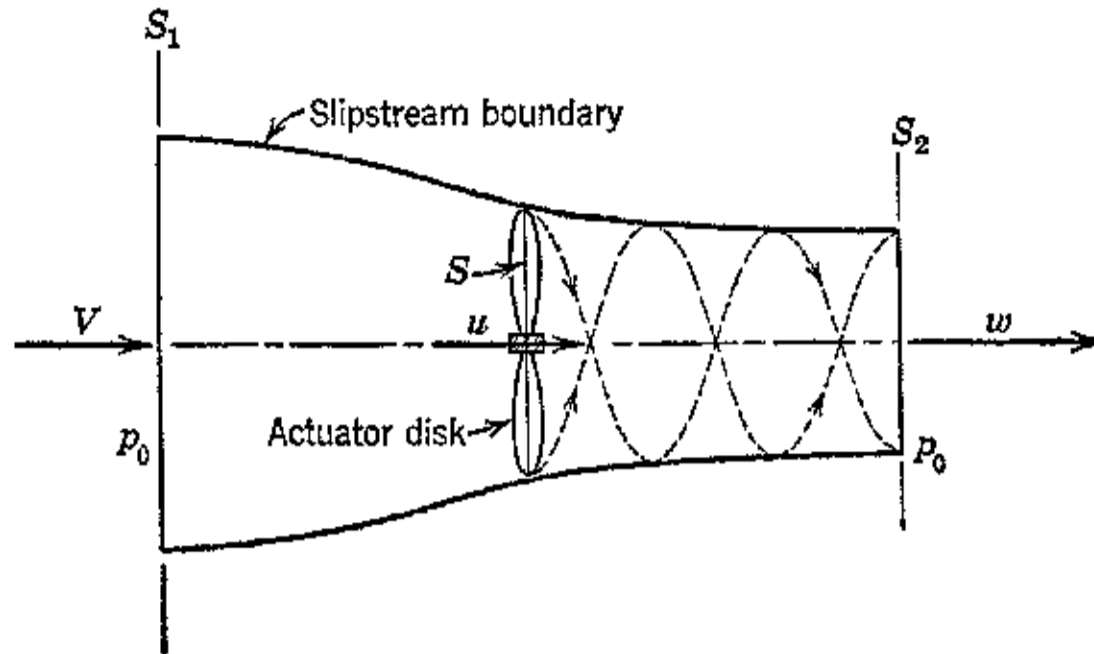
FIG. 2.   Effect of propeller torque on air passing through the propeller.

tance behind the propeller, but there is an increase in the air velocity in front of the propeller.

One of the principal reasons for the interest in jet propulsion for high-speed flight arises from the limitations which the compressibility of the air places on the permissible tip speeds for propellers. Jet propulsion becomes attractive for high-speed aircraft because the compressibility of the air does not affect its thrust output.

2. Pitch and Slip

Figure 3 represents an element of a propeller blade located at a distance r from the axis of rotation. The length $Oc = 2\pi r$ is the linear
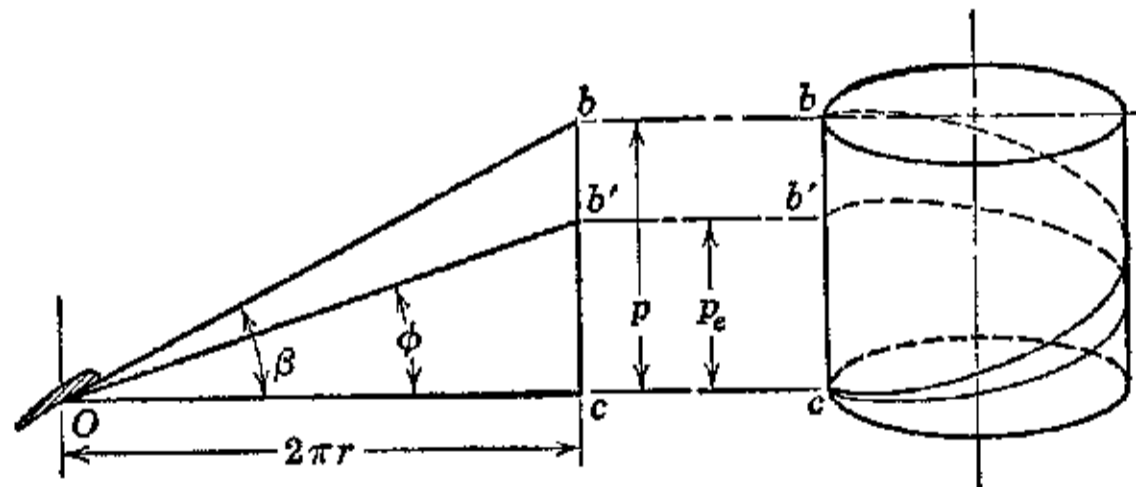
FIG. 3.   Pitch and helix angle for a propeller element.

equivalent of the circumferential distance described in one revolution by a point on a blade element of the propeller. The perpendicular distance cb corresponds to the axial distance the point would travel

if it advanced along the geometric helix angle β. This advance is the *geometric pitch* p. Hence

$$p = bc = 2\pi r \tan \beta = \pi D \tan \beta \tag{1}$$

EXAMPLE. A propeller is 12 ft in diameter. At the ¾ radius the blade angle is 30°. What is the geometric pitch at the ¾ radius?
Solution.

$$p = 3.1416 \times \tfrac{3}{4} \times 12 \times \tan 30$$

$$= 3.1416 \times 9 \times 0.57735 = 16.3 \quad \text{ft}$$

The actual advance of the point in question is governed by the forward speed of the airplane V. Thus, if the propeller makes n rps, the time required for one revolution is $t_1 = 1/n$ sec. Consequently, the actual advance, which is the distance cb', is given by

$$cb' = \frac{V \,(\text{fps})}{n \,(\text{rps})} \quad \text{ft/rev} \tag{2}$$

The ratio $cb'/\pi D$, where D is the propeller diameter in feet, determines the effective helix angle for the blade element and is denoted by ϕ. The effective pitch is

$$p_e = \pi D \tan \phi \tag{3}$$

EXAMPLE. The forward velocity of an airplane is 300 fps. The propeller diameter is 10 ft. What is the effective pitch of the propeller if it makes 30 rps?
Solution.

$$cb' = \frac{V}{n} = \frac{300}{30} = 10 \quad \text{ft/rev}$$

$$\tan \phi = \frac{cb'}{\pi D} = \frac{10}{31.416}$$

$$p_e = 3.1416 \times 10 \times \frac{10}{31.416} = 10 \quad \text{ft}$$

The distance bb', Fig. 3, is a measure of the distance the propeller lags behind the distance it would advance if the air were an incompressible fluid. This lag is called the *slip*.

From Fig. 4 it is seen that the geometric pitch p can be conceived as the corresponding advance of the blade element for a fictitious forward velocity V_0 for which $\phi = \beta$. For this condition the propeller thrust is zero, for there can be no positive thrust when there is no slip. The ratio of the slip to the geometric pitch is given by

$$\frac{bb'}{bc} = \frac{(p - p_e)}{p} = \frac{(V_0 - V)}{V_0} \tag{4}$$

The above ratio influences the magnitude of the propeller thrust and is usually written in the form

$$\text{Slip} = 1 - \frac{p_e}{p} = 1 - \frac{V}{V_0} = 1 - \frac{V}{np} \tag{5}$$

where n = rps.

Equation 5 defines what is termed the *slip function*, and its magnitude is usually 0.15 to 0.25. The slip function is often expressed as the actual reduction in the linear advance.
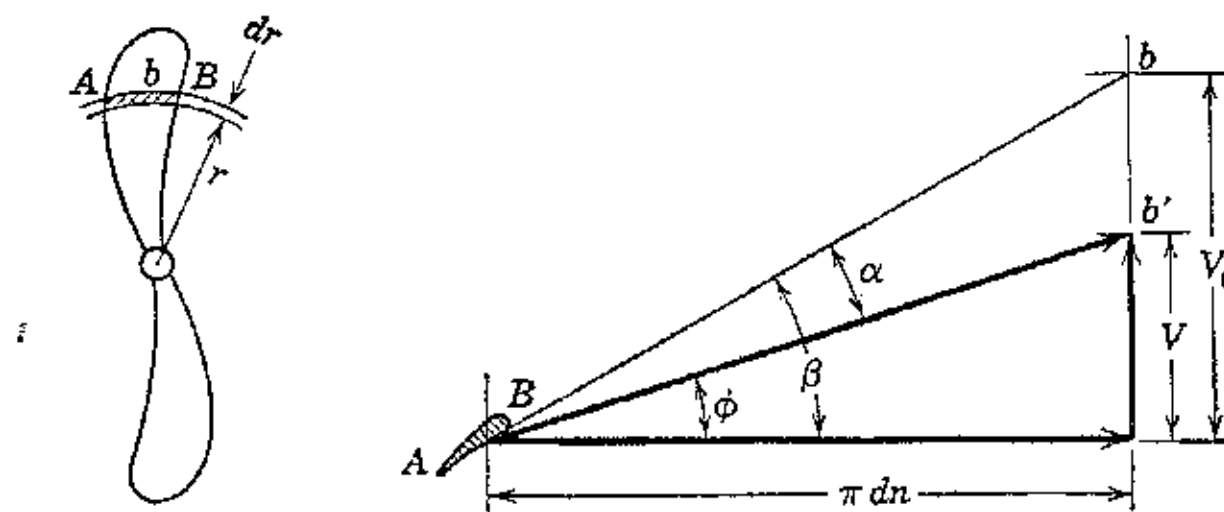
FIG. 4. Velocity relationships for a blade element.

EXAMPLE. An airplane has a forward velocity of 400 fps. It is equipped with a 12-ft propeller rotating at 1800 rpm. What is the slip? (Assume that the average blade angle is 30°.)

Solution.

$$p = \pi \times 12 \times \tan 30 = 16.3 \quad \text{ft}$$

$$\text{Slip} = 1 - \frac{400 \times 60}{1800 \times 16.3} = 1 - 0.822 = 0.178$$

3. Axial Momentum Theory

This theory, due originally to Rankine and to Froude, may be considered to be that of an ideal propeller operating in a perfect fluid. It assumes that the propeller is an actuator disk which produces a change in the axial momentum of a slipstream consisting of the entire body of air moved by the propeller. This body of air flows through the actuator disk and is bounded by a stream tube as illustrated in Fig. 5.

Applying the relative coordinate system (see Chapter 2, section 6) to the air flow relative to the propeller, it is seen that there are two distinct bodies of air: (1) the slipstream which flows through the propeller, and (2) the undisturbed air outside the slipstream boundary. The air in the slipstream is accelerated as it approaches the

propeller disk. This produces a contraction of the slipstream by virtue of its increasing velocity with a corresponding decrease in pressure until the disk area is reached. As the air passes through the propeller disk its pressure is raised by an amount designated
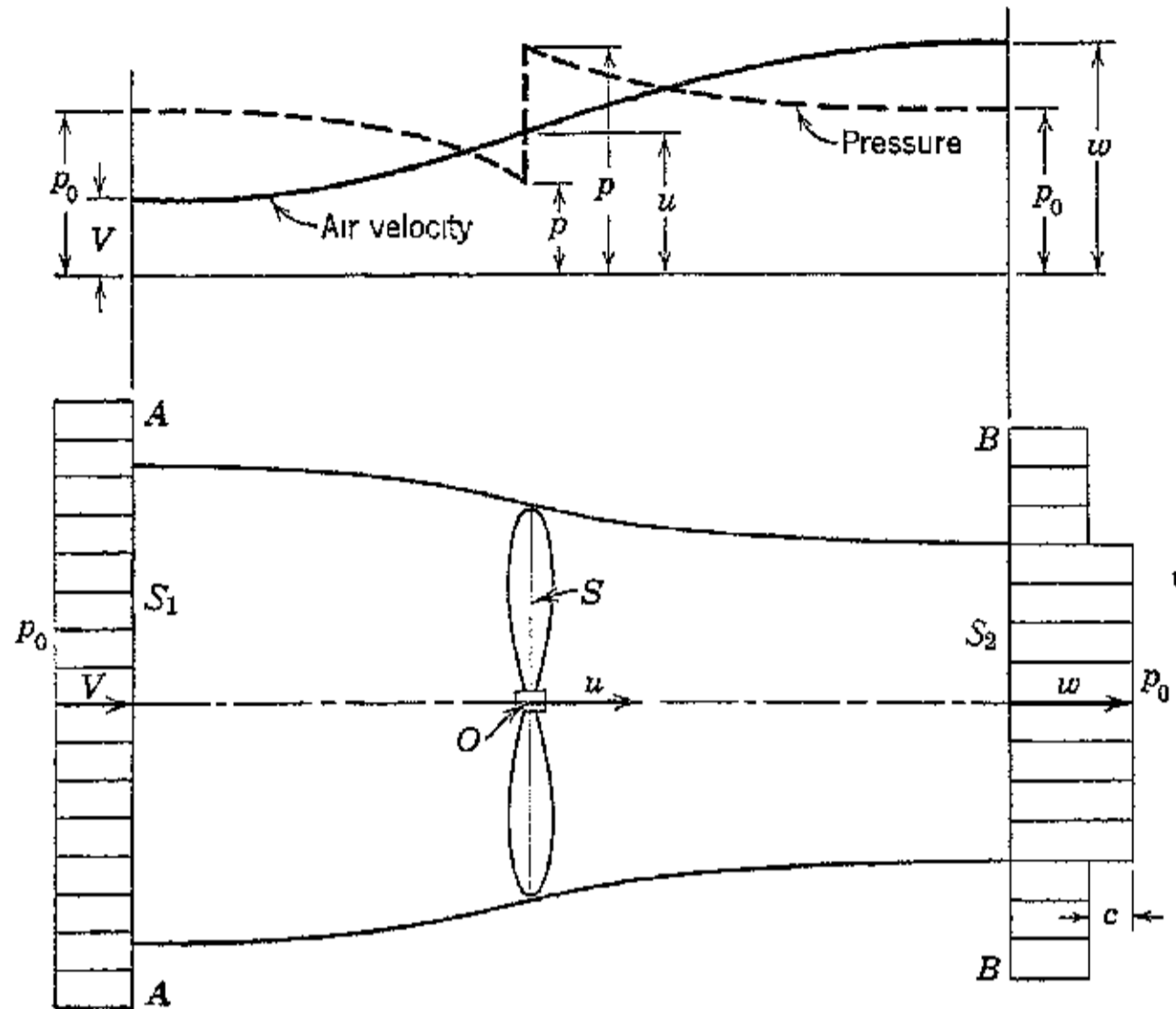
FIG. 5. Momentum theory applied to the ideal propeller.

by Δp. The slipstream continues to the outer boundary or ultimate wake where the pressure decreases to that of the surroundings p_0.

Let $\mathfrak{I}$ = propeller thrust, lb.

D = propeller diameter, ft.

S = propeller disk area, sq ft.

G = air flow rate through the slipstream, lb/sec.

m = air-mass flow rate through the slipstream, slug/sec.

V = forward speed of propeller, fps.

u = slipstream velocity in disk section, fps.

w = slipstream velocity in the ultimate wake, fps.

$\nu = V/w$ = velocity ratio.

ρ = density of air, slug/ft^3.

p = pressure, lb/sq ft.

$\mathbf{M}$ = momentum, slug-ft/sec.

$P_T = \mathfrak{I}V$ = thrust power, ft-lb/sec.

P = propulsion power, ft-lb/sec.
P_L = leaving loss, ft-lb/sec.
η_i = internal efficiency.
η_P = propulsion efficiency.
$\eta = \eta_i \eta_P$ = overall efficiency.
η_b = blade efficiency.

Assume that the control surfaces S_1 and S_2 are located where the pressures acting upon them are the undisturbed pressures, so that $p_1 = p_2 = p_0$. The momentum change for the air is confined to the slipstream boundary, and S_1 and S_2 need be extended only to form the perpendicular boundaries of the slipstream.

Assume now that the velocities of the fluid crossing S_1 and S_2 are uniform over these surfaces, and are V and w respectively. Since $p_1 = p_2$, equation 2·13 reduces to

$$\mathfrak{J} = w \int_{S_2} m_2 \, dS_2 - V \int_{S_1} m_1 \, dS_1 \qquad (6)$$

where m_1 and m_2 are the mass flow rates per unit area

The expressions under the integral signs represent the mass of air flowing through the propeller disk and, by continuity, since no air flows across the slipstream boundary, are equal to each other. Hence

$$m = \int_{S_1} m_1 \, dS_1 = \int_{S_2} m_2 \, dS_2 \qquad (7)$$

If it is assumed that the air density ρ is constant, which is reasonably correct for a propeller, then if G is the weight rate of air flow

$$\mathfrak{J} = m(w - V) = \frac{G}{g}(w - V) \qquad (8)$$

Let $\nu = V/w$ = velocity ratio; then

$$\mathfrak{J} = \frac{G}{g} w(1 - \nu) \qquad (9)$$

or the thrust per pound of air flow per second is

$$\frac{\mathfrak{J}}{G} = \frac{w}{g}(1 - \nu) \qquad (10)$$

Equation 10 indicates how the thrust developed, per pound of fluid flowing through the propulsion system per second, varies with the exit velocity w and the velocity ratio ν Figure 6 illustrates this relationship for several different values of the relative exit velocity w.

It is seen that, as the velocity ratio approaches unity, the thrust per pound of air flow per second approaches zero. Consequently, to develop thrust under conditions close to unity velocity ratio, the quantity of working fluid required becomes very large. Consequently, a large exit area would be needed for passing the fluid. For a fixed velocity ratio the size of the required exit area increases as the speed of the airplane decreases. Hence, the propeller with its
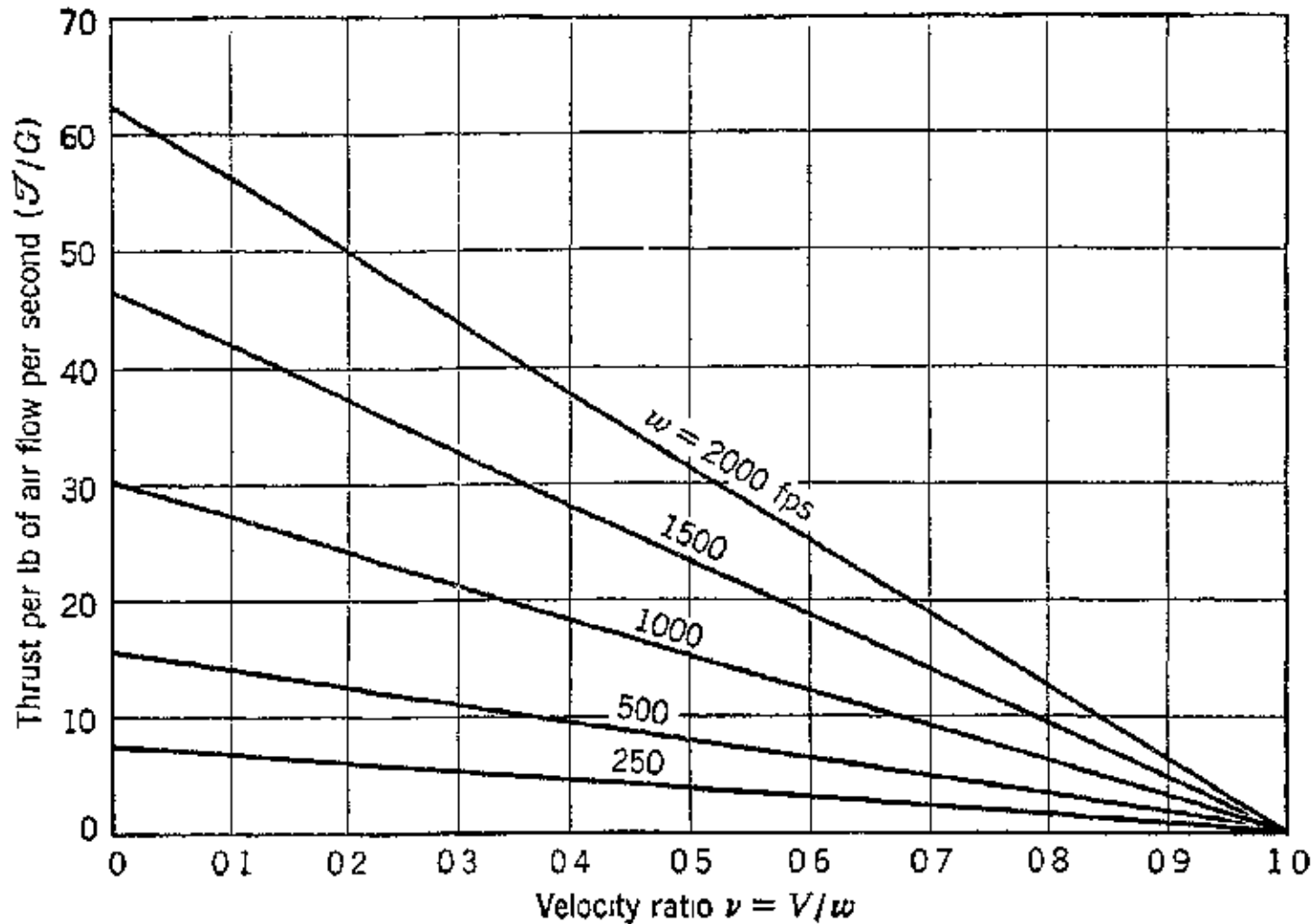
FIG. 6.　Thrust per pound of air per second vs. velocity ratio for the ideal propeller.

ability to handle extremely large quantities of air at velocity ratios close to unity is well adapted to the propulsion of bodies at moderate and low speeds. This is particularly true since, as will be seen later, operation close to unity velocity ratio gives high propulsion efficiency.

4. Propulsion Power and Ideal Propulsion Efficiency

The term *propulsion power* P was introduced in Chapter 2 in the discussion of hydraulic jet propulsion. When applied to a propeller, P is the power furnished by the prime mover, and a portion of this power is converted into the *thrust power* $P_T = \mathcal{T}V$ required to keep the propelled body in motion. It is obvious that the magnitude of the difference $P - P_T$ measures the energy losses associated with the propulsion system. As explained in Chapter 2, the ratio of the

thrust power to the propulsion power is termed the propulsion efficiency η_P. Thus

$$\eta_P = \frac{P_T}{P} = \frac{5V}{P}.$$ (11)

In the ideal case considered here the total energy loss is that associated with the kinetic energy of the air ejected from the slipstream. This loss, which has been called the leaving loss (see Chapter 2), is accordingly

$$P_L = \frac{m}{2}(w - V)^2$$ (12)

In general the ideal propulsion efficiency is given by the equation

$$\eta_P = \frac{5V}{P} = \frac{5V}{5V + P_L}$$ (13)

Substituting for the thrust from equation 9 and for the exit loss from equation 12 gives

$$\eta_P = \frac{2V}{V + w} = \frac{2\nu}{1 + \nu}$$ (14)

where $\nu = V/w$ is the *velocity ratio*. Equation 14 is identical to that for the propulsion efficiency of the hydraulic jet propulsion system discussed in Chapter 2. Figure 7 is a plot of η_P as a function of ν for several constant flight speeds. On the same diagram is a plot of the thrust per pound of air flow per second as a function of the velocity ratio. It will be seen in Chapter 8 that these curves are also applicable to thermal jet propulsion.

Equation 14 shows that to obtain high propulsion efficiency the velocity ratio for the propeller must be close to unity. This means that, for a given flight speed V, the smaller the velocity of the air leaving the ultimate wake the higher the propulsion efficiency. This is quite understandable, for the exit loss depends upon the square of the absolute velocity of the air leaving the slipstream. Consequently, since this absolute velocity c is equal to $(w - V)$, the smaller the exit velocity w, the smaller is the kinetic-energy loss. To decrease w while developing the same thrust necessitates increasing the mass rate of flow through the propeller disk. This would require using a propeller of larger diameter with a smaller loading per unit area of blade surface, which in an actual case increases the frictional losses.

The *thrust power*, in terms of the velocity ratio, is given by

$$P_T = \Im V = mw^2(1 - v)v \tag{15}$$

This equation shows that, for a constant rate of air flow through the propulsion system, the thrust power is a quadratic function of the
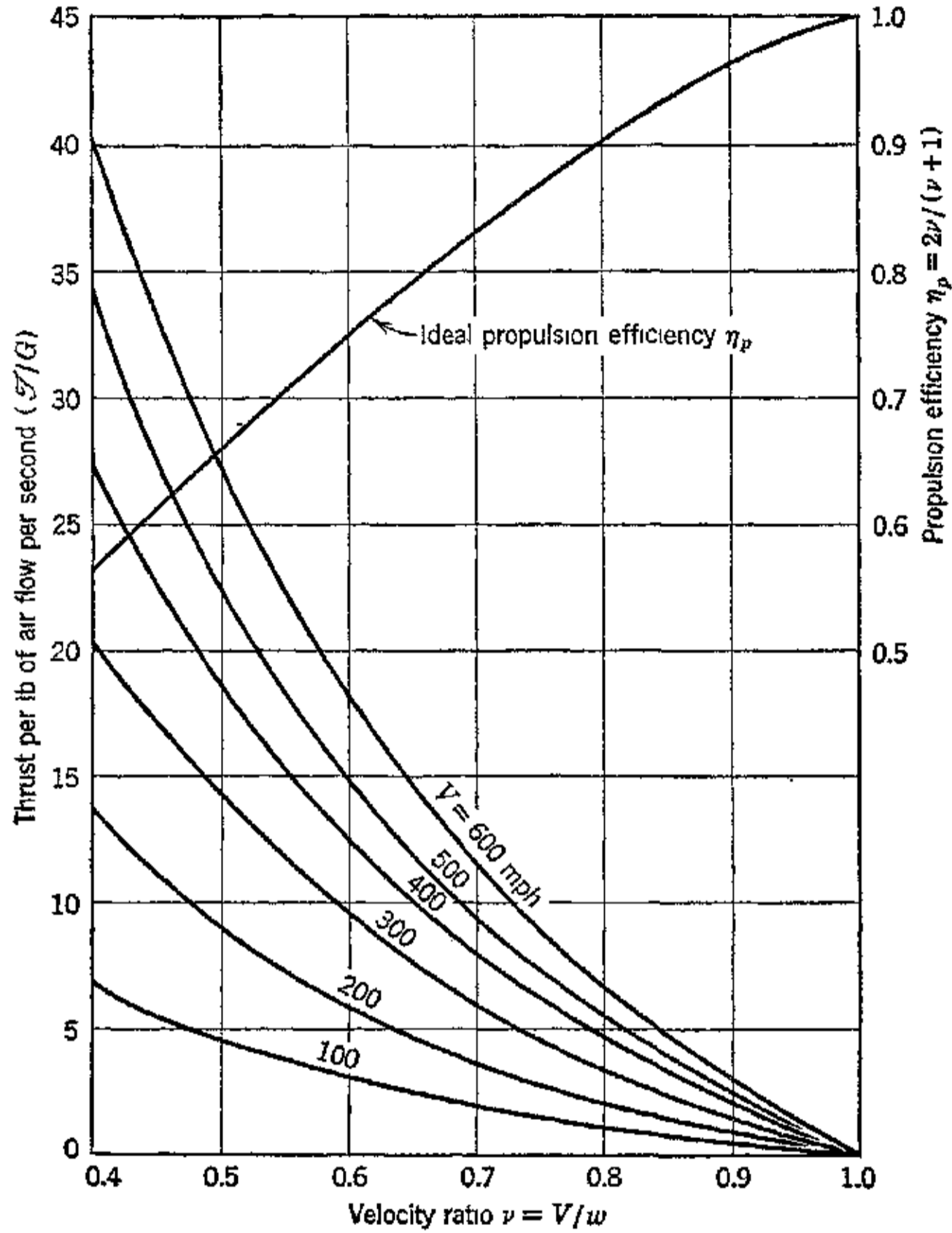
Fɪɢ. 7. Thrust per pound of air flow and ideal propulsion efficiency as functions of velocity ratio, for the ideal propeller.

velocity ratio. Referring to Chapter 2, the maximum value for the thrust power under these conditions occurs when the velocity ratio $v = V/w = 0.5$, and the corresponding value of the propulsion efficiency is $\eta_P = 0.667$. It is seen, therefore, that the velocity ratios

for maximum thrust power and maximum propulsion efficiency are not identical.

5. Propulsion Power and Discharge Area

A relationship can be derived relating the propulsion power P, the flight speed V, the propeller diameter D, the air density ρ, and the ideal propulsion efficiency η_P. Thus for the ideal propeller

$$P = 5V + P_L = \frac{m}{2} w^2 (1 - \nu^2) \quad \text{ft-lb/sec} \tag{16}$$

The mass rate of flow of air through the actuator disk circle is given by equation 7, which in terms of the propeller diameter D becomes

$$m = \frac{\pi D^2}{4} \rho u \quad \text{slug/sec} \tag{17}$$

Substituting for m in equation 16, and noting that $u = (V + w)/2 = V/\eta_P$, gives the following equation for the propulsion power

$$P = \frac{\pi D^2 \rho}{8} \frac{V^3}{\eta_P} \cdot \frac{w^2}{V^2} \left(1 - \frac{V^2}{w^2} \right)$$

or

$$P = \frac{\pi D^2 \rho}{8} \cdot \frac{V^3}{\eta_P} \cdot \left(\frac{w^2}{V^2} - 1 \right)$$

But

$$\frac{w^2}{V^2} = \left(\frac{2 - \eta_P}{\eta_P} \right)^2 \tag{a}$$

so that

$$\left(\frac{w^2}{V^2} - 1 \right) = \frac{1}{\eta_P^2} (4 - 4\eta_P) = \left(\frac{2}{\eta_P} \right)^2 (1 - \eta_P) \tag{b}$$

Substituting from (a) and (b) into the last equation for P gives

$$P = D^2 \rho V^3 \frac{\pi}{2} \left(\frac{1 - \eta_P}{\eta_P^3} \right) \tag{18}$$

so that

$$\frac{P}{D^2 \rho V^3} = \frac{\pi}{2} \left(\frac{1 - \eta_P}{\eta_P^3} \right) \tag{19}$$

or

$$\frac{V^3 D^2 \rho}{P} = \frac{2}{\pi} \frac{\eta_P^3}{1 - \eta_P} \tag{20}$$

Rearranging and taking the cube root of both sides of the equation gives

$$V\sqrt[3]{\frac{D^2\rho}{P}} = \frac{0.86\eta_P}{\sqrt[3]{1 - \eta_P}} \qquad (21)$$

In this equation the density ρ refers to the average density of the air in the plane of the propeller. Owing to the increase in pressure
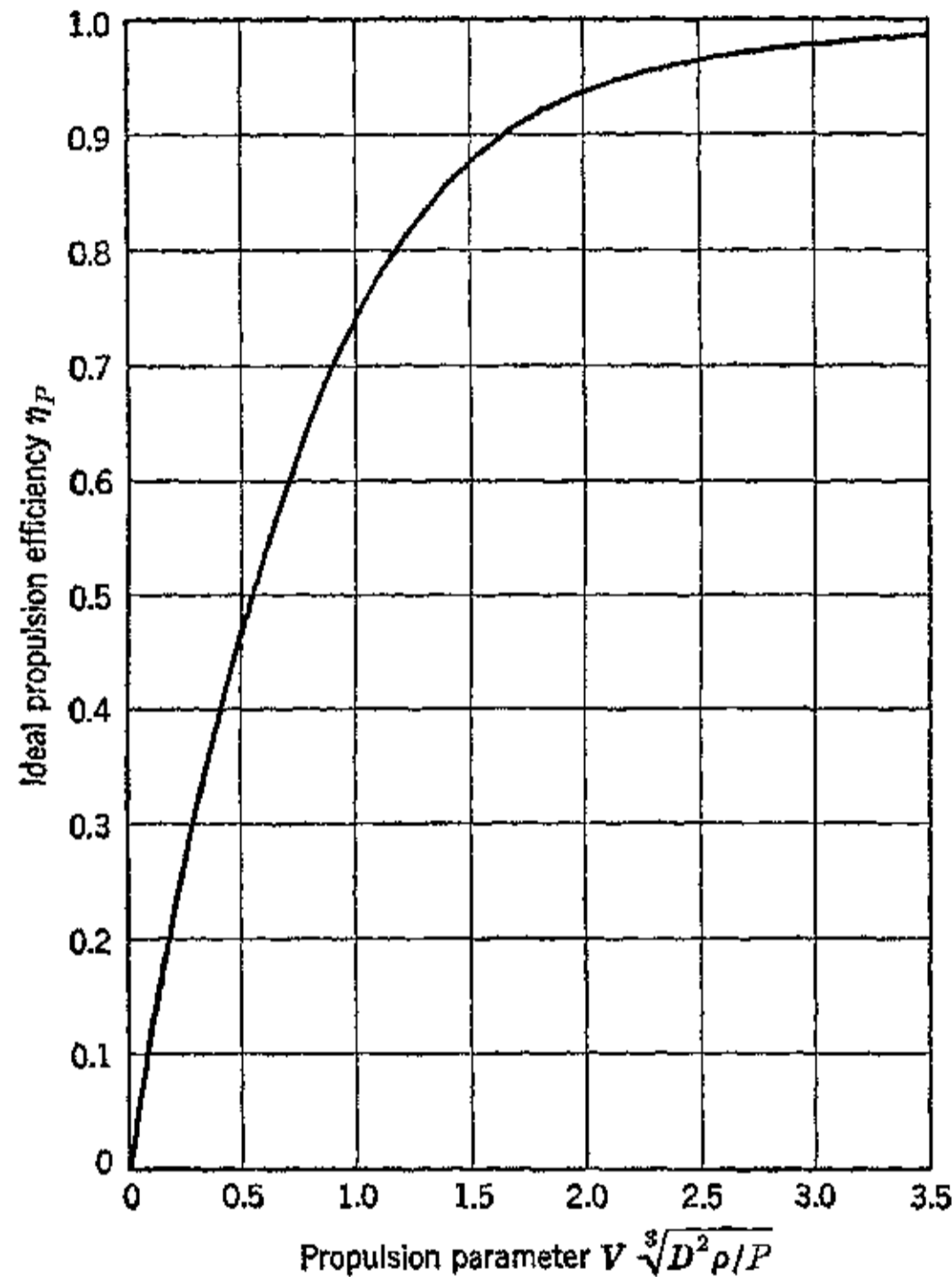
FIG. 8.   Ideal propulsion efficiency vs. propulsion parameter for the ideal propeller.

in the plane of the actuator disk the air density is somewhat higher than the atmospheric pressure. This difference enters to the one-third power and is sufficiently small to be neglected for estimating purposes.

Figure 8 is a plot of the propulsion parameter $V\sqrt[3]{D^2\rho/P}$ as a function of the ideal propulsion efficiency. This curve gives the maximum attainable propulsion efficiency for the propeller system.

It is seen that, to obtain high values of propulsion efficiency with low airplane speeds, the diameter of the propeller must be large, assuming the other factors to be constant.

The propulsion efficiency of an actual propeller will be approximately 0.85 per cent of the value of the ideal propulsion efficiency. This is due to the various losses neglected in the consideration of the ideal case.

The plant or *overall efficiency* η of the propeller type of propulsion system is the product of the thermal or internal efficiency η_i for the power plant and the actual propulsion efficiency. Thus

$$\eta = \eta_P\, \eta_i = \frac{\text{Useful work } (\Im V)}{\text{Energy supplied}} \tag{22}$$

6. Relationship between Thrust and Ideal Propulsion Efficiency

It can be shown [18] that for the ideal propeller the relationship between thrust and propulsion efficiency can be expressed in the form

$$\frac{\Im}{\rho S V^2} = \frac{2(1 - \eta_P)}{\eta_P^{2}} \tag{23}$$

This relationship is illustrated in Fig. 9. It is seen that, if the thrust is maintained at a constant value, then decreasing either V or S reduces the propulsion efficiency. Conversely, for a given flight
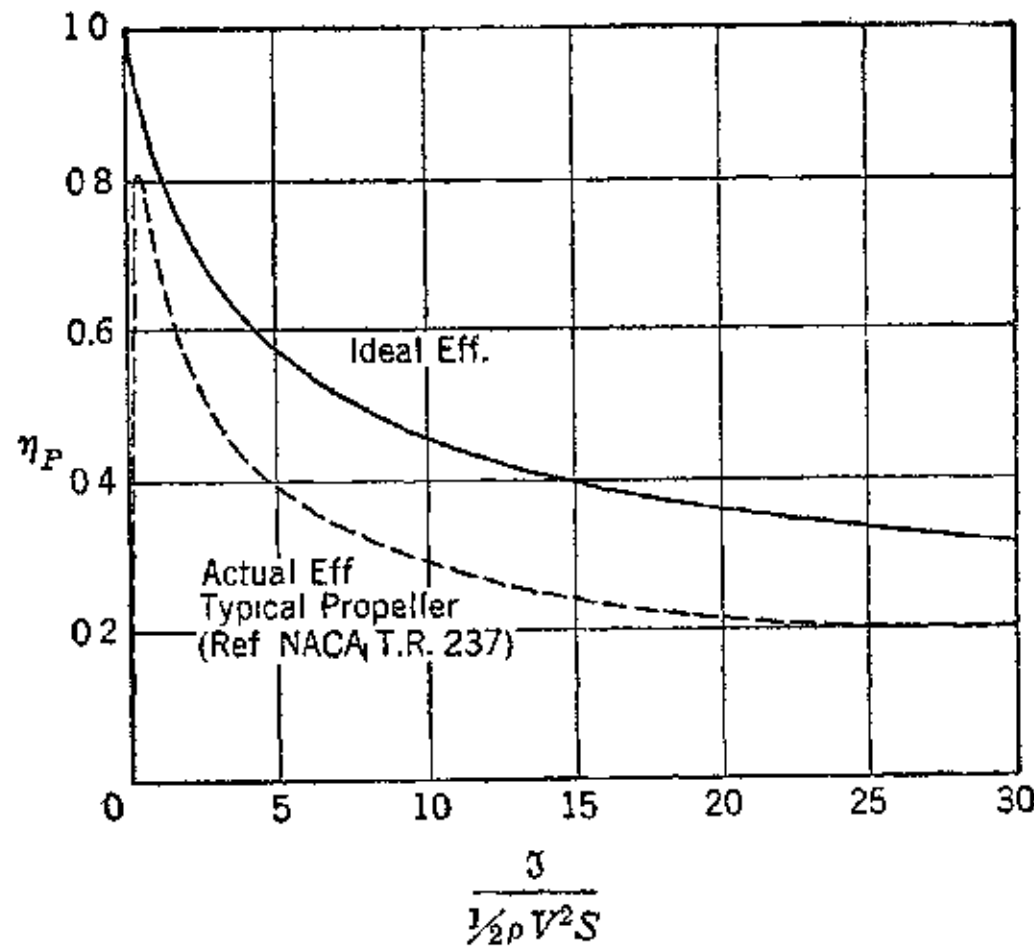
FIG. 9. Actual and ideal efficiency curves for a propeller. (Reproduced from W. C. Nelson, *Airplane Propeller Principles*, John Wiley & Sons.)

speed V, and propeller disk area S, increasing the thrust decreases the propulsion efficiency. This lowered efficiency is to be expected, since a thrust increase requires increasing the exit velocity w, with a corresponding increase in the exit loss P_L.

The momentum theory is only a first approximation to the action of the propeller and cannot be used for design purposes. Though it gives a good insight into operating behavior, it neglects such factors as the drag of the blades, energy losses due to slipstream rotation, blade interference effects, and compressibility effects. Because of these losses an actual propeller requires power to rotate it at zero thrust, which is somewhat analogous to the power required for idling an internal-combustion engine. Consequently, the efficiency curve of an actual propeller drops to zero when the thrust is zero, while for an ideal propeller the propulsion efficiency is unity.

7. Simple Blade Element Theory

The propeller may be assumed to be a rotating airfoil. If the radial flow of the air due to slipstream contraction is neglected, and the flow assumed two-dimensional, then Fig. 10 illustrates the velocity vectors for a blade element located at an arbitrary radius r from the axis of rotation O. The projection of the axis of rotation is OO', the plane of rotation is Oc, and the blade angle is β.
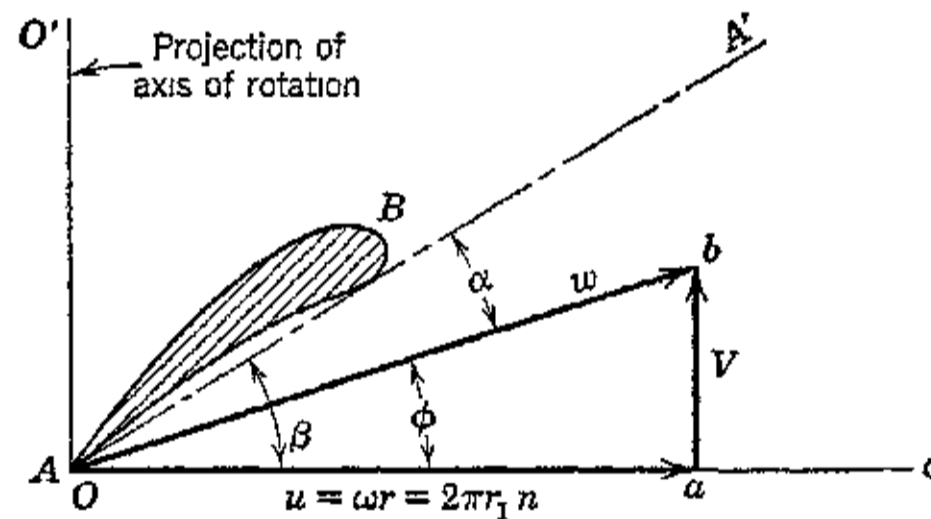
FIG. 10.   Vector diagram for a blade element of a propeller.

Vector Oa represents the circumferential velocity of the blade element, and the vector ab, the forward speed of the airplane V. The relative velocity of the blade element with respect to the immobile air is the vector sum $Ob = Oa + ab$. The relative velocity, denoted by w, is

$$w = \sqrt{u^2 + V^2} = \sqrt{(\pi n d)^2 + V^2} \tag{24}$$

where $d = 2r$.

The angle between the chord line AA' for the blade element and the tangential velocity u is denoted by β. If the blade element is assumed fixed in space and the air flows toward it with a velocity equal in magnitude to w, then the aerodynamic forces acting on the element can be determined by applying conventional airfoil theory. To illustrate, the blade element AB can be considered to be an airfoil placed at an angle of attack α with respect to the direction of the air which approaches it with the velocity w. Obviously,

$$\alpha = \beta - \phi \tag{25}$$

The magnitude of angle ϕ is a function of the velocity ratio V/u and is determined from

$$\tan \phi = \frac{V}{u} = \frac{V}{2\pi rn} = \frac{V}{\pi nd} \tag{26}$$

or

$$\phi = \tan^{-1} \left(\frac{V}{\pi nd} \right) \tag{27}$$

Figure 11 illustrates the forces acting on blade element, which are the elementary lift force dL and the drag dD. The resultant of the
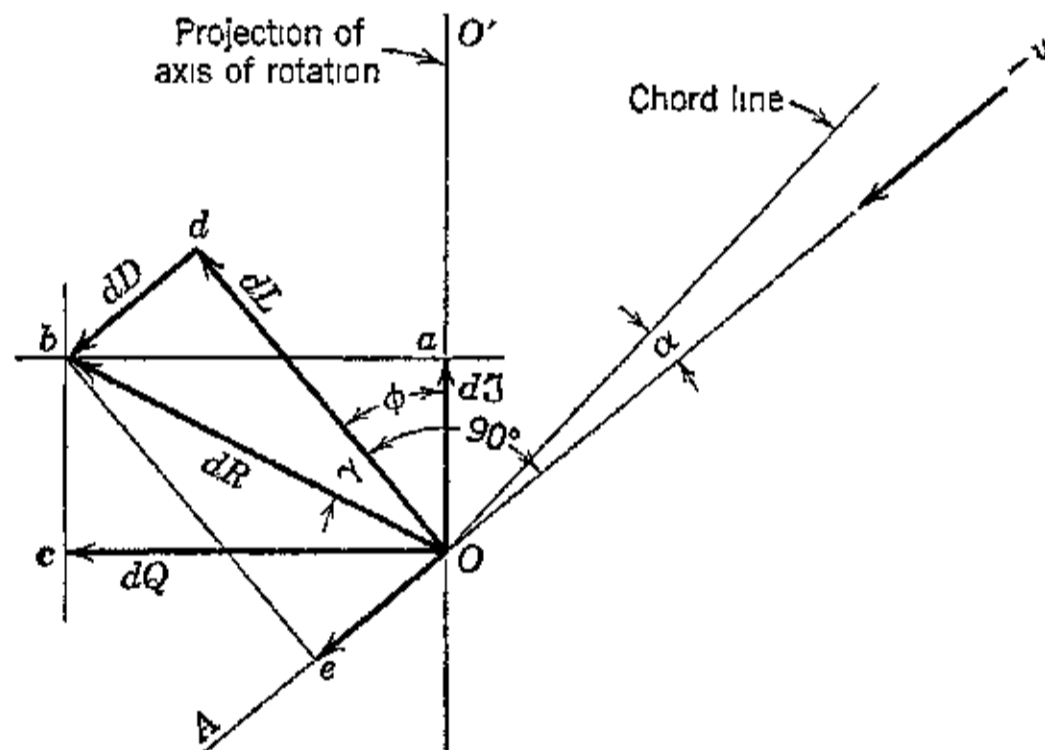
Fig. 11. Aerodynamic forces acting on a blade element.

lift and drag forces is denoted by dR, and dR has been resolved into the thrust component $d\mathfrak{I}$, and the torque component dQ.

The power required to rotate the element is denoted by P' and is given by

$$P' = 2\pi nr\, dQ \tag{28}$$

The thrust power developed by the blade element is denoted by P_T', where

$$P_T' = V\,d\Im \tag{29}$$

Hence the propulsion efficiency of the blade element, denoted by η_b, is

$$\eta_b = \frac{P_T'}{P'} = \frac{V\,d\Im}{2\pi n r\,dQ} \tag{30}$$

Since the forces $d\Im$ and dQ are functions of the angles β, ϕ, and α, the effect of these angles on η_b is of interest. Let b be the width of the blade element at radius r, and C_L its lift coefficient. Then

$$dL = C_L \tfrac{1}{2}\rho w^2 b\,dr \tag{31}$$

Similarly, if C_D is the drag coefficient, then

$$dD = C_D \tfrac{1}{2}\rho w^2 b\,dr \tag{32}$$

From Fig. 11 it is seen that the resultant dR is given by

$$\frac{dL}{dR} = \cos\gamma \tag{33}$$

Hence

$$dR = \frac{dL}{\cos\gamma} = \frac{1}{2}\rho w^2 b\,dr\left(\frac{C_L}{\cos\gamma}\right) \tag{34}$$

A diagram such as Fig. 11 can be drawn for every element of the propeller blade. The value of $V/\pi n d$ will be different for each element, and the blade-angle distribution or twist built into the propeller blade affects the magnitude of the forces acting on the different elements. Consequently, to obtain a single overall characteristic for the propeller, the blade angle of a specific blade element is used to define the operating conditions for the complete propeller regardless of whether it is of the fixed-pitch or variable-pitch type. It is customary to specify the blade angle for a propeller as the value of β at the three-quarter radius.

From Fig. 11, it is seen that

$$d\Im = dR\cos(\phi + \gamma) \tag{35}$$

Substituting for dR from equation 34, and for dL from equation 31, and noting that $w = V/\sin\phi$, equation 35 becomes

$$d\Im = \frac{1}{2}\rho V^2 b\,dr C_L\,\frac{\cos(\phi + \gamma)}{\cos\gamma\sin^2\phi} \tag{36}$$

Equation 36 can be applied to several elements of a complete blade, and the thrust loading can be determined by integrating the curve of $d\mathfrak{I}$ as a function of blade radius.

The torque force dQ is given by

$$dQ = dR \sin (\phi + \gamma) \tag{37}$$

Substituting for dR, noting that $w = V/\sin \phi$, gives

$$dQ = \frac{1}{2} \rho V^2 b \, dr C_L \frac{\sin (\phi + \gamma)}{\cos \gamma \sin^2 \phi} \tag{38}$$

Substituting for $d\mathfrak{I}$ and dQ from equations 36 and 38 respectively into equation 30 gives the following equation for the blade element efficiency η_b.

$$\eta_b = \frac{\tan \phi}{\tan (\phi + \gamma)} \tag{39}$$

Thus it is seen that according to the blade element theory the efficiency of the propeller depends only on the angles ϕ and γ. The angle ϕ is a function of the velocity ratio V/u, while the angle γ depends only on the L/D ratio. It can be shown that the condition for maximum efficiency is given by

$$\phi = \frac{\pi}{4} - \frac{\gamma}{2} = 45° - \frac{\gamma}{2} \tag{40}$$

The above indicates that the propeller attains its maximum efficiency when the angle ϕ is slightly less than 45°. Since $\tan \phi = V/u$ this signifies that η_P decreases with an increase in the radius of the propeller blade, a conclusion in direct opposition to that derived from the momentum theory. The simple blade element theory does not explain propeller action accurately, but it gives better design criteria than the momentum theory.

8. The Blade Angle β

As pointed out in the preceding, for a given blade angle β, the angle of attack $\alpha = (\beta - \phi)$ is a function of the velocity ratio V/u.

For $V = 0$, with $\phi = 0$, angle α has its maximum value. Hence the maximum thrust is obtained when the airplane is stationary, i.e., at take-off. As the forward speed V increases the angle α decreases and with it the thrust. A speed is finally reached where the thrust is zero.

For a blade of airfoil cross section, the lift is zero at a negative value of α. Consequently the thrust becomes zero at a speed some-

what higher than V_0. Figure 12 illustrates the manner in which C_L and C_D vary with angle of attack. Figure 13 illustrates the effect of thickness ratio of the airfoil section on these coefficients. The manner in which thrust, torque, and efficiency vary with V/u for a given blade setting is illustrated in Fig. 14.
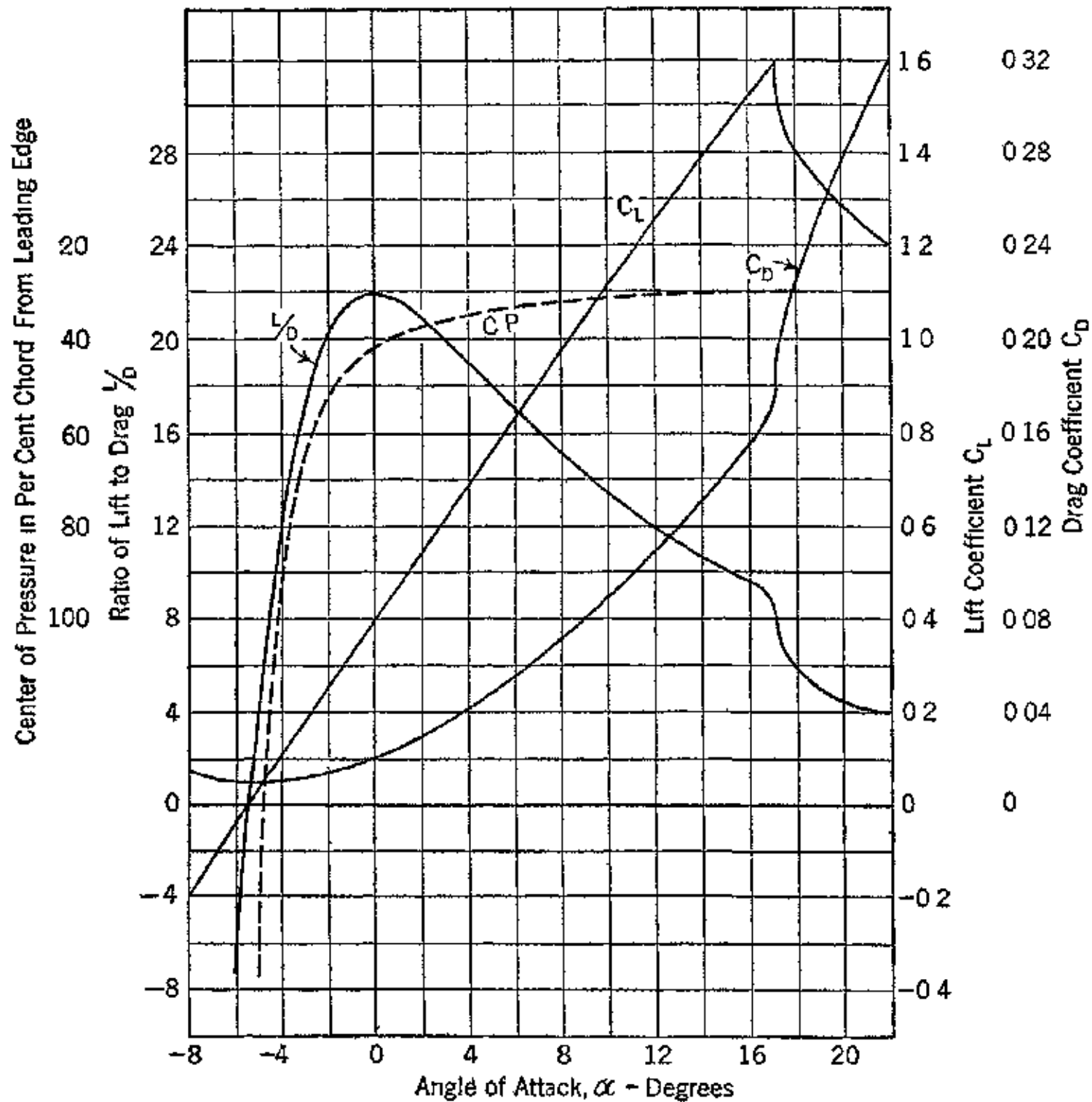
FIG. 12. Test of Clark airfoil at $R_e = 6 \times 10^6$ (aspect ratio $= 6$) (Reproduced from W. C. Nelson, *Airplane Propeller Principles*, John Wiley & Sons)

9. The Angle of Attack $\alpha = (\beta - \phi)$

It has been pointed out that the angle of attack α is dependent upon the velocity V. Consequently, the mode of operation of the propeller will depend on the value of V, because both C_L and C_D vary with α. Referring to Fig. 12 it is seen that C_L is a linear function of α up to the stall angle, and C_D is a quadratic function. Since
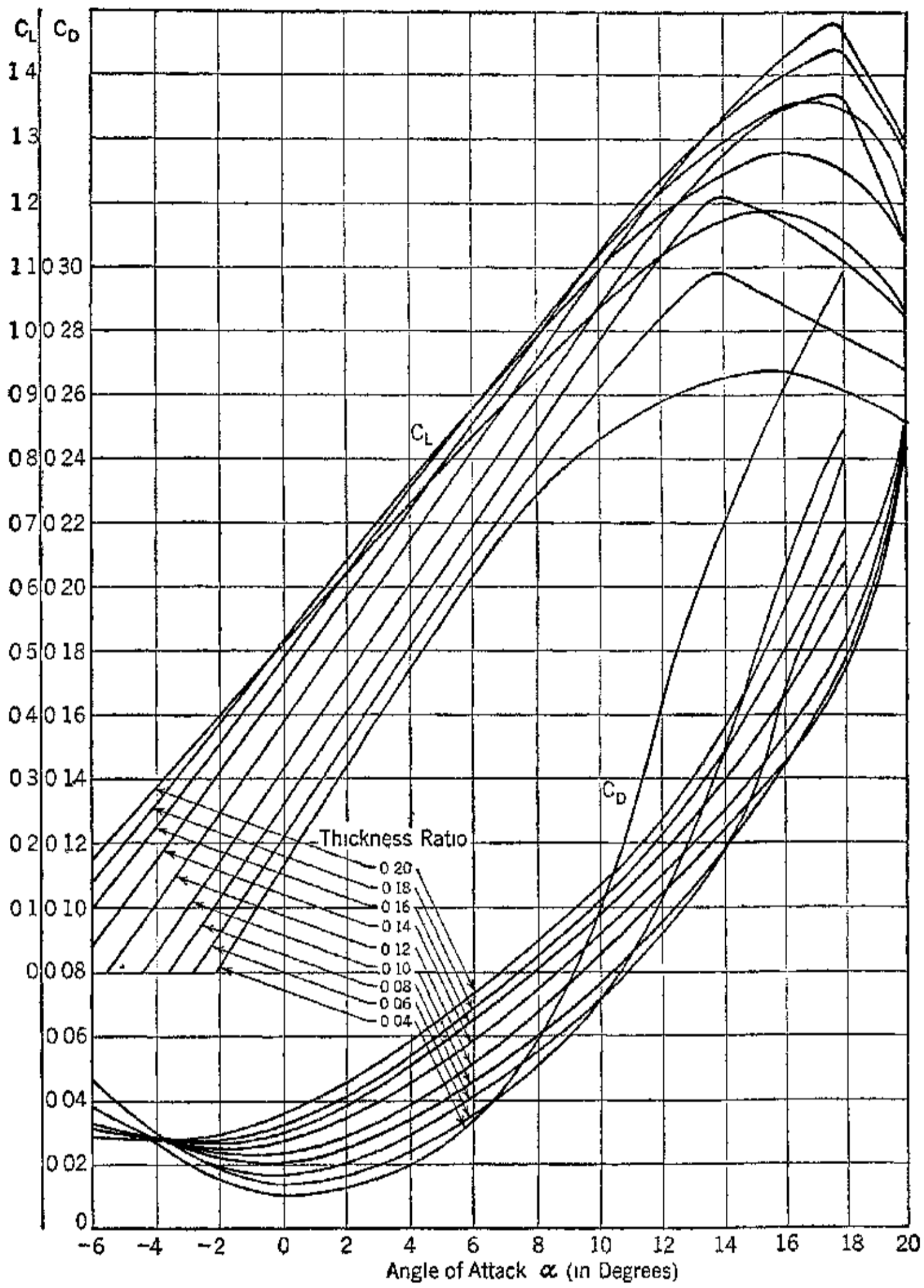
Fig 13. Test of R A F propeller section for aspect ratio 6   (Reproduced from
W C Nelson, *Airplane Propeller Principles*, John Wiley & Sons)

these two coefficients determine the thrust and torque of the propeller they also affect its behavior.

Assuming a constant blade angle let the speed ratio V/u be varied. As this ratio is increased, the propeller operates successively as a fan, propeller, brake, and windmill.[14] Most of the operation is conducted in the true propeller state. The static thrust which is obtained at take-off occurs with the propeller in the fan state. In the braking
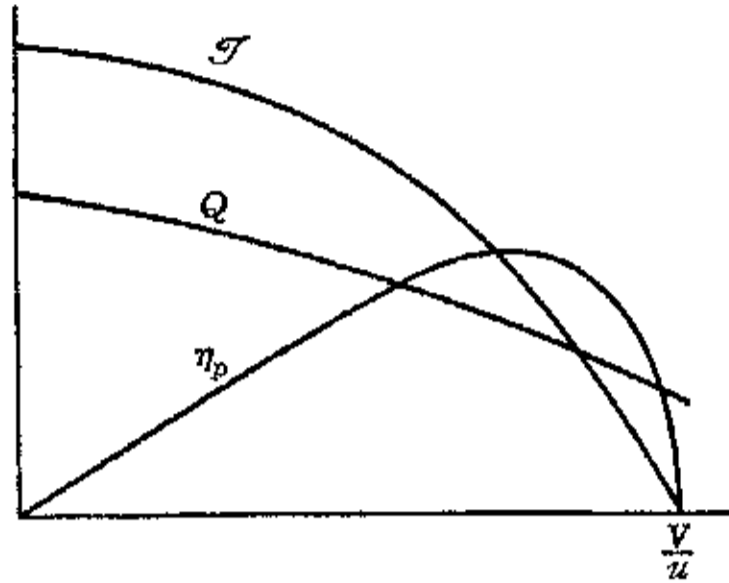
FIG. 14.   Propeller performance characteristics as a function of speed ratio.

state, the propeller actually adds drag to the airplane. The windmill state must be avoided because it can cause damage to the engine by overspeeding it.

10. Geometric Pitch Distribution

Figure 15 illustrates a blade of a propeller. The respective radii to different blade elements are denoted by r_1, r_2, r_3 $\cdots$, and their respective diameters by d_1, d_2, d_3 $\cdots$. The propeller diameter is denoted by D.

At any section of the propeller the geometric pitch is given by

$$p = \pi d \tan \beta \tag{41}$$

Consequently, if the geometric pitch is to be the same at all sections of the blade, the angle β must increase as the propeller hub is approached.

It has been shown that the torque and the thrust developed by the propeller depend on the speed ratio V/u. Since $u = 2\pi r n = \pi d n$, an equivalent expression more convenient to use is

$$J = \frac{V}{Dn} \tag{42}$$

where n = propeller revolutions per second.

The dimensionless ratio $J = V/Dn$ is called the *advance ratio* and is the parameter against which all test data on propellers are plotted. If V is in miles per hour, D in feet, N the propeller rpm (engine rpm $\times$ gear ratio), then equation 42 becomes

$$J = \frac{88V}{ND} \quad (V \text{ in mph, } D \text{ in ft}) \tag{43}$$
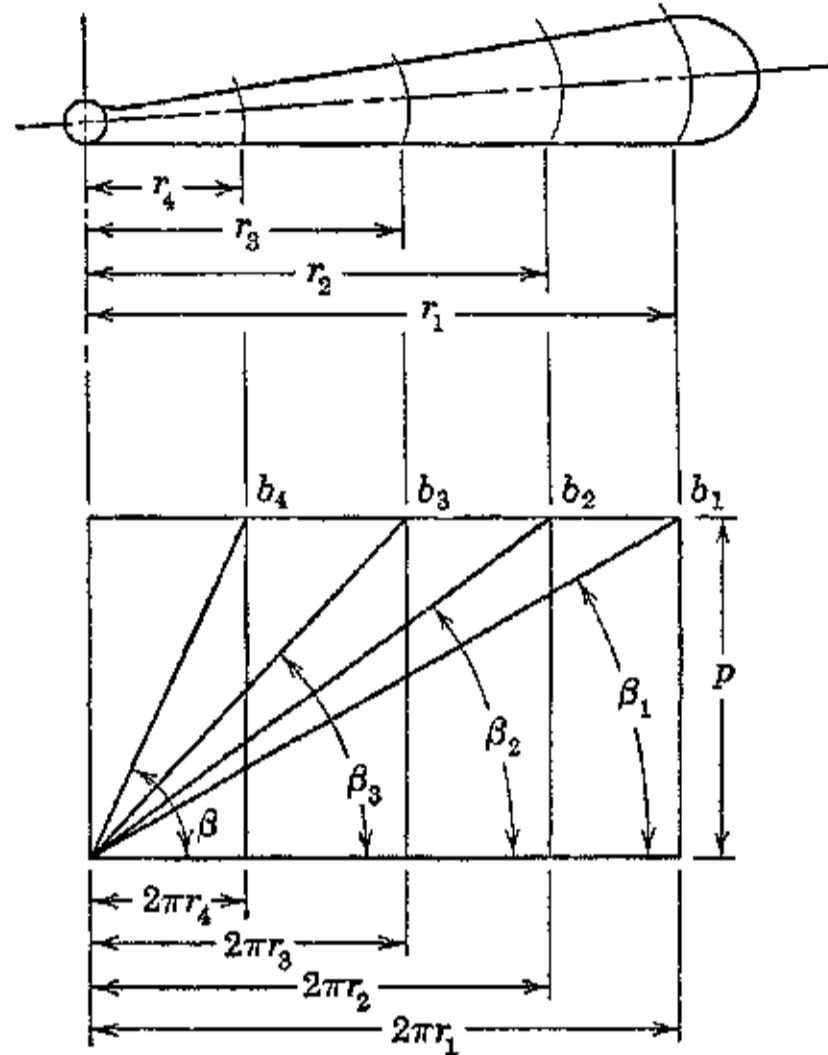
Fig. 15.   Geometric pitch distribution for a propeller blade.

11. Thrust, Torque, and Power Coefficients

From the physics of the situation and neglecting any effects that compressibility introduces, the following variables can affect the thrust developed by the propeller: its velocity V, its revolutions per second n, its diameter D, and the air density ρ. Hence the following functional relationship can be written.

$$F(V, n, D, \rho, \mathfrak{I}) = 0 \tag{44}$$

Since there are five variables and three principal dimensions, there should be two dimensionless ratios. (See Chapter 1 ,Section 2.) Thus

$$\pi_1 = Vn^a D^b \rho^c \tag{a}$$

and

$$\pi_2 = n^x D^y \rho^z \mathfrak{I} \tag{b}$$

Solving these equations by the method described in Chapter 1 gives the following

$$\pi_1 = \frac{V}{nD} = J \tag{45}$$

and

$$\pi_2 = \frac{\Im}{n^2 D^4 \rho} \tag{46}$$

Hence

$$\frac{\Im}{n^2 D^4 \rho} = \varphi \left(\frac{V}{nD} \right) \tag{47}$$

For a constant value of V/nD, let $\varphi(V/nd) = $ constant $= C_T$, then

$$C_T = \frac{\Im}{n^2 D^4 \rho} \tag{48}$$

where the value of C_T depends upon V/nD as well as n, D, and ρ.

The relationships for the power and torque of the propeller can be derived in an analogous manner. Thus

$$\Im = C_T D^4 n^2 \rho \tag{49}$$

$$Q = C_Q D^5 n^2 \rho \tag{50}$$

$$P = C_P D^5 n^3 \rho \tag{51}$$

The efficiency of the propeller can be expressed in terms of the torque and power coefficients and the advance ratio. Thus

$$C_T = \frac{\Im}{\rho n^2 D^4} \tag{48}$$

$$C_Q = \frac{Q}{\rho n^2 D^5} \tag{52}$$

$$C_P = \frac{P}{\rho n^3 D^5} \tag{53}$$

Since the efficiency is

$$\eta_P = \frac{\Im V}{P}$$

where $\Im$ is the *effective thrust;* the propulsion efficiency is given by

$$\eta_P = \frac{C_T}{C_P} \frac{V}{Dn} = J \frac{C_T}{C_P} \tag{54}$$

The efficiency of the propeller, therefore, depends directly upon the ratio of the thrust coefficient to the power coefficient and upon the advance ratio.

In testing a propeller a set of C_T and C_P curves is determined for each blade angle. By exploring a range of blade angles sufficient to cover all possible operating conditions, the propeller performance can be established over the entire operating range.

Figure 16 illustrates the manner in which C_T and C_P vary with the advance ratio J for a fixed blade angle. (For detailed data on this subject see *N.A.C.A. Tech. Report* 642.)

FIG. 16. Thrust and torque coefficients for a constant blade angle as functions of the advance ratio.

Figure 17 illustrates the effect of the blade angle on C_T for different values of V/nD. It is seen that as V/nD approaches zero the thrust coefficient increases for all blade angles.
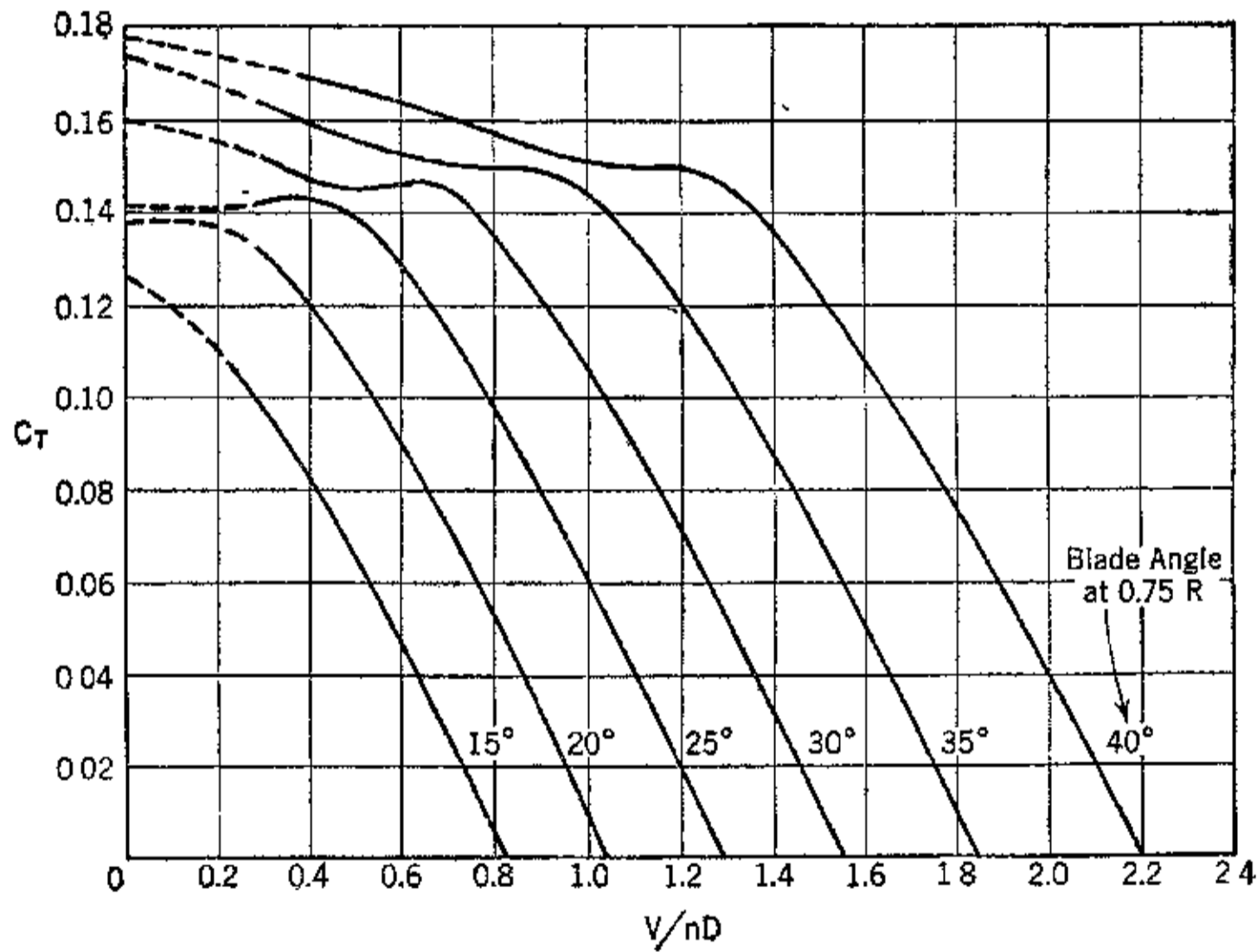
FIG. 17. Thrust coefficient curves for three-bladed propeller. (Reproduced from W. C. Nelson, *Airplane Propeller Principles*, John Wiley & Sons.)

12. Speed Power Coefficient (C_S)

A coefficient which is helpful in studying propeller action is the speed-power coefficient C_S, developed by F. E. Weick.[12] Its derivation is presented below.
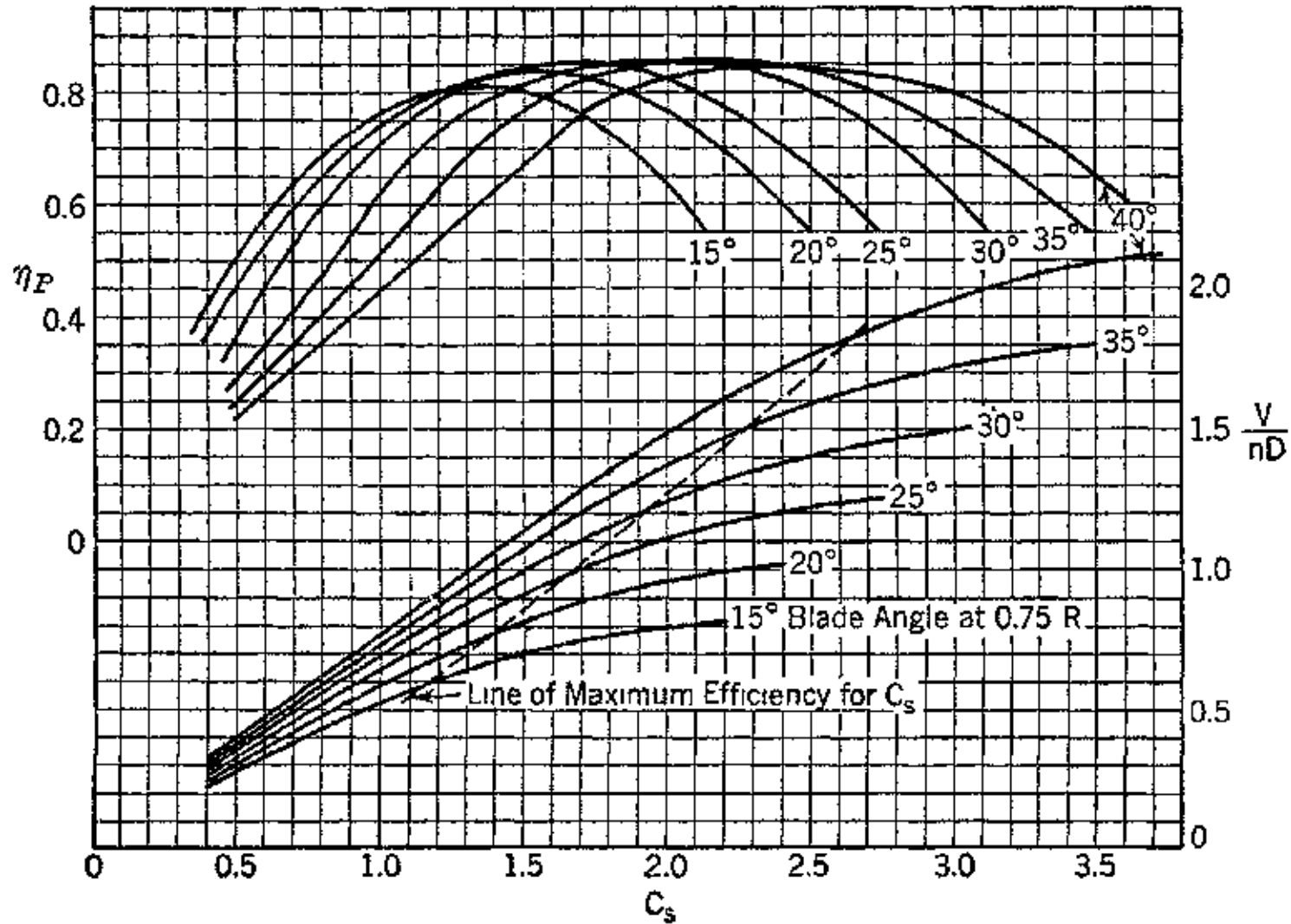
FIG. 18. Propeller chart for a three-bladed propeller. (Reproduced from W. C. Nelson, *Airplane Propeller Principles*, John Wiley & Sons.)

C_S is obtained by modifying the power coefficient C_P to obtain a coefficient depending primarily on speed and power. Thus

$$C_P = \frac{P}{\rho n^3 D^5}$$

Let $K = (V/nD)^5/C_P$. Then

$$K = \frac{V^5}{n^5 D^5} \cdot \frac{\rho n^3 D^5}{P} = \frac{\rho V^5}{P n^2} \tag{55}$$

Let the speed-power coefficient C_S be defined by

$$C_S = \sqrt[5]{K}$$

Then

$$C_S = V \cdot \sqrt[5]{\frac{\rho}{P n^2}} \tag{56}$$

For a constant ρ and n, the coefficient C_S depends on the forward speed V and the power P.

Figure 18 is a plot of propeller efficiency η_P and advance ratio J as a function of C_S for different blade angles. For use at all altitudes the density ρ is replaced by $\sigma = \rho/\rho_0$, where $\rho_0 = 0.002378$ slug/ft^3. Then

$$C_S = \frac{0.638\,V\ (\text{mph}) \times \sigma^{\frac{1}{5}}}{N^{\frac{2}{5}}\ (\text{rpm}) \cdot P^{\frac{1}{5}}\ (\text{bhp})} \tag{57}$$

13. The Torque-Speed Coefficient (C_{QS})

In high-speed aircraft it is important to be able to determine the thrust in the take-off range. It is primarily for this purpose that the torque-speed coefficient was derived.[11] This is based on plotting propeller characteristics using a coefficient in which the rotative speed of the propeller has been eliminated.

Starting with equation 52, multiply both sides by the dimensionless product $(V/nD)^{-2}$, thereby eliminating the speed n. Let

$$K = C_Q \left(\frac{nD}{V}\right)^2 = \frac{Q}{\rho n^2 D^5} \cdot \left(\frac{nD}{V}\right)^2$$

Let

$$C_{QS} = \sqrt{\frac{1}{K}} = V\sqrt{\frac{\rho D^3}{Q}} \tag{58}$$

In a supercharged engine operating at full throttle the bmep, and hence the torque, are substantially constant throughout the usual flight range. Hence C_{QS} can be assumed independent of engine speed. Consequently, C_{QS} is directly proportional to the forward velocity of the airplane for a given engine, propeller, and altitude.

The torque Q is calculated from the rated horsepower and speed of the engine, thus

$$Q = 5250 \quad \text{bhp/rpm} \quad \text{lb-ft}$$

Since ρ, D, and Q are constants for a given engine, altitude, and propeller diameter, the general expression for C_{QS} is

$$C_{QS} = V \times \text{Constant}$$

From equation 48 it follows that the ratio $C_T/C_Q = 5D/Q$ is also independent of the propeller rotation speed n. The ratio C_T/C_Q is, therefore, directly proportional to the effective thrust. By plotting C_T/C_Q as a function of C_{QS} a curve relating thrust and air speed is obtained. This is done for various blade angles, and then lines of

constant V/nD are superimposed to give the performance chart, Fig. 19. These curves for each blade angle are in reality plots of
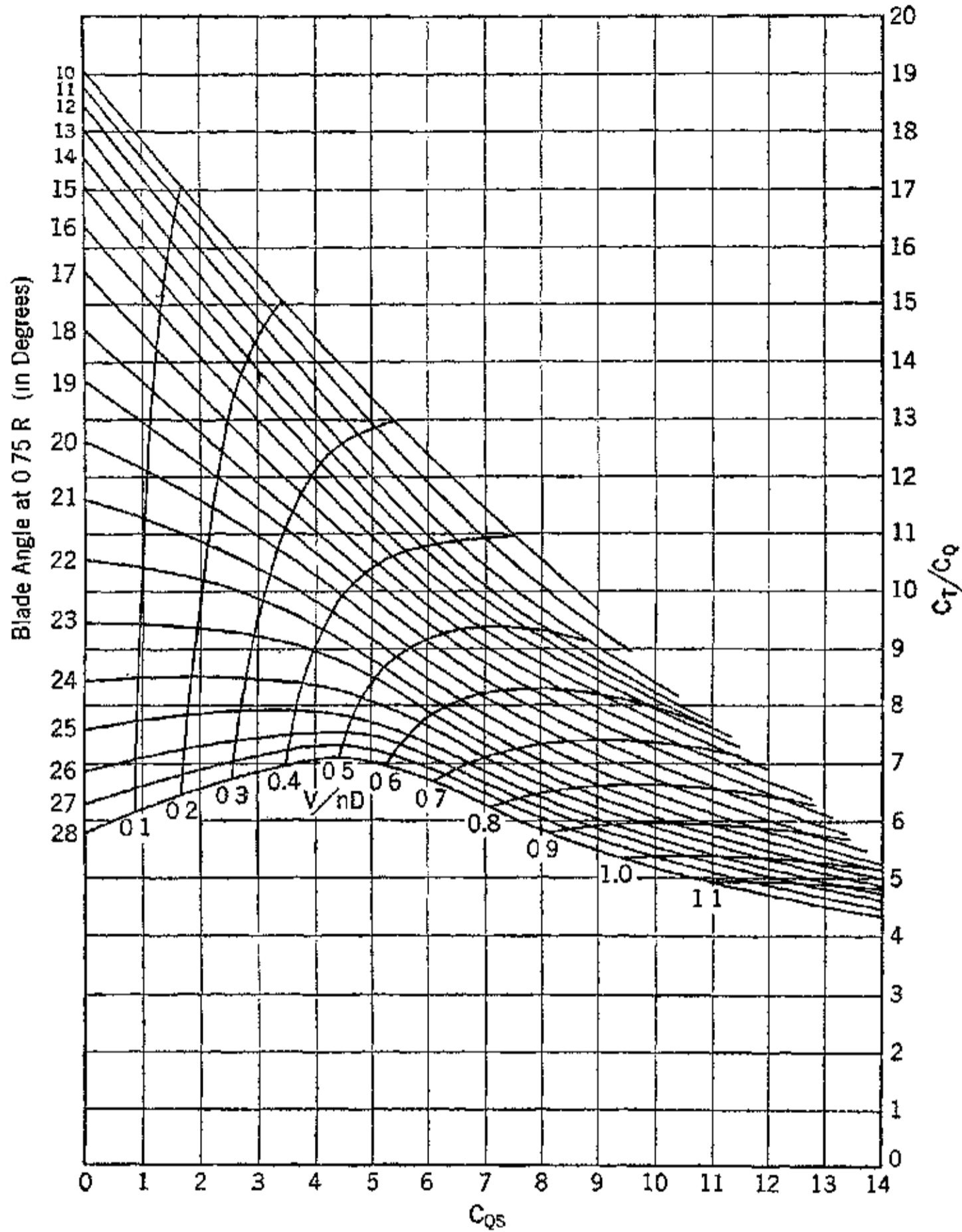
FIG 19. Propeller performance chart for a 9-ft-diameter adjustable-pitch propeller. (Reproduced from W. C Nelson, *Airplane Propeller Principles*, John Wiley & Sons.)

thrust vs. velocity for a given propeller and engine throttle setting. It is apparent that the thrust decreases rapidly as the blade angle, for a fixed V/nD, is increased, particularly at the lower values of

V/nD. At high forward velocities the minimum usable blade angle is dependent on the maximum allowable engine rpm, which tends to increase as the blade angle is made smaller.

At take-off (small value of V/nD) it is desirable to develop the largest possible thrust. This requires a small blade angle. Consequently, a fixed-pitch propeller must compromise the requirements for safe operation with those for take-off. The angle must be large
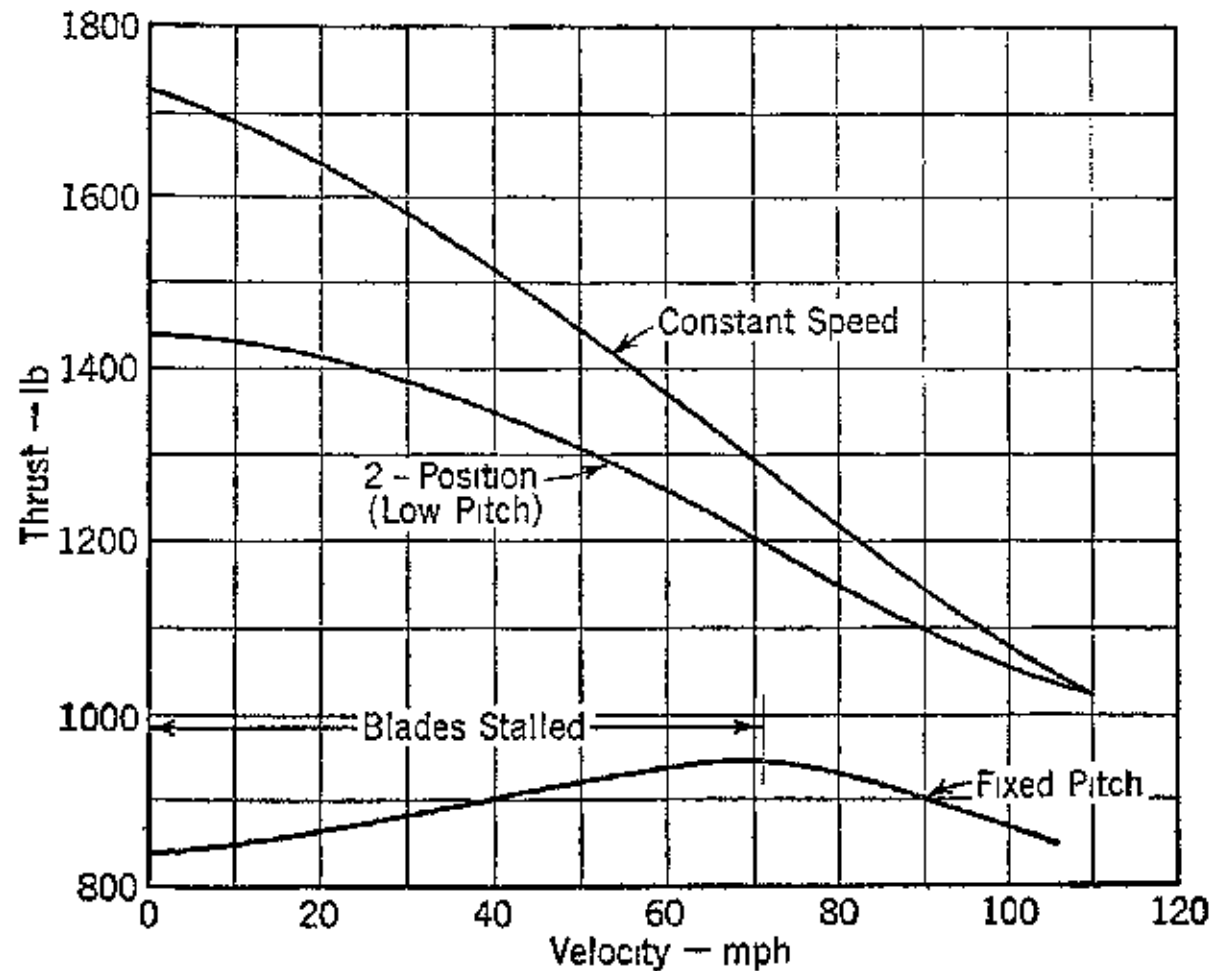
FIG. 20. Propeller thrust during take-off. (Reproduced from W C. Nelson, *Airplane Propeller*, John Wiley & Sons)

enough to prevent overspeeding the engine in flight with a consequent diminution in the static thrust for take-off. This difficulty is overcome by using a variable-pitch propeller which permits adjusting the blade angle according to the requirements. For high-speed aircraft the variable-pitch propeller operates at constant speed; it acts as the governor to prevent the engine from overspeeding. Most modern aircraft are equipped with constant-speed propellers.[20]

Figure 20 illustrates the manner in which the thrust of a variable-pitch propeller and that of a fixed-pitch propeller vary during the take-off run.

In general, the thrust of the propeller increases, inversely proportional to the forward speed of the airplane, illustrating that the conventional propeller, as mentioned previously, is inherently a low-speed device.

14. Compressibility Effects and Propeller Limitations

It was pointed out in Chapter 5 that as the relative velocity between an airfoil and the surrounding air approached the sonic velocity all the characteristics of the aerodynamic phenomena changed. The
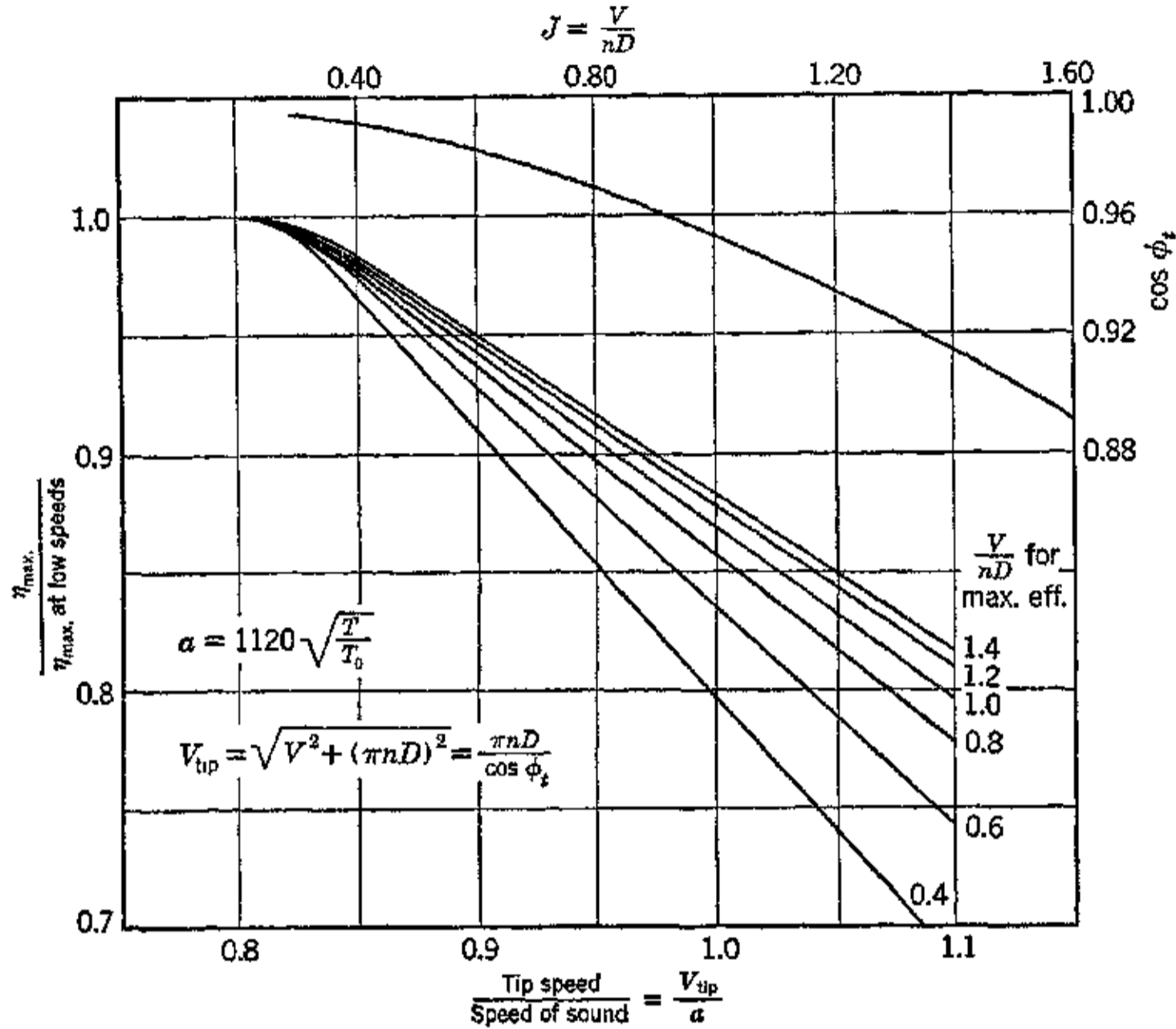
Fig. 21. Effect of tip speed on propeller efficiency. (Reproduced from W. C. Nelson, *Airplane Propeller Principles,* John Wiley & Sons.)

lift coefficient C_L decreases rapidly, and there is a large increase in the value of the drag coefficient C_D. The propeller is subject to these effects.

Since the pressure waves travel through the air with the velocity of sound, a shock wave is formed at the leading edge of the propeller blade when its pitch line velocity approaches the sonic velocity a. This phenomenon appears at lower tip speeds when the airplane is at high altitude, owing to decrease in the value of the sonic velocity with altitude. The effect is more pronounced if the airfoil section is thick, for then the phenomenon is encountered at reduced tip speeds.

Because of the shock waves the coefficient C_T is reduced and C_P is increased, thereby adversely affecting the efficiency of the propeller. As the tip speed approaches the sonic speed there is a large increase in the noise of the propeller. Figure 21 presents wind-tunnel and flight-test data illustrating the effect of the ratio V_{tip}/a on the reduction in propeller efficiency.[21] The tests were conducted using different thin metal blades.

For aircraft capable of flight speeds of 400 mph or more, the value of nD must be limited so that large compressibility losses will be avoided. This is usually accomplished by using a small-diameter propeller or by driving the propeller through a gear reduction.

Although compressibility effects are mainly high-speed phenomena, they may be encountered at the low speeds corresponding to take-off conditions, where the angle of attack of the blades is large. The compressibility effects may then occur at Mach numbers as low as 0.55.

In general, losses in propulsive efficiency due to compressibility effects become evident at Mach numbers M ranging from 0.5 to 0.7 and greater.[6] Tests indicated that at $M = 0.8$ the loss in thrust power was of the order of 20 per cent.

It is because of the aforementioned limitation of the propeller at high flight speeds that other methods of propulsion which do not encounter these difficulties are of interest. Such a method is offered by jet propulsion. Like all new developments, however, jet propulsion must demonstrate its possibilities by extensive field use. It is to be expected, therefore, that most aircraft built in the immediate future, at least, will employ propeller propulsion with either a reciprocating engine or gas turbine for the power plant, and jet propulsion will be applied mainly to high-performance aircraft.

Published data regarding jet-propelled planes are meager, but they indicate that propeller propulsion, employing either a gas turbine or a reciprocating internal-combustion engine, develops more thrust per pound of fuel consumed than does a thermal jet engine until the flight speed of the airplane approaches 500 mph. The exact flight speed for equal rates of fuel consumptions will be governed by the speed at which compressibility seriously affects the performance of the propeller and the success of engineering developments in reducing the fuel consumption of the turbojet engine.

REFERENCES

1. E. P. HARTMAN and D. BIERMAN, "Static Thrust and Power Characteristics of Six Full-Scale Propellers," *N.A.C.A. Tech. Report* 684.
2. JOHN STARK, W. F. LINDSEY, and R. E. LITTELL, "The Compressibility Burble and the Effect of Compressibility on Pressures and Forces Acting on an Airfoil," *N.A.C.A. Tech. Report* 646.
3. D. BIERMAN and E. HARTMAN, "The Aerodynamic Characteristics of Six Full-Scale Propellers Having Different Airfoil Sections," *N.A.C.A. Tech. Report* 650.
4. D. BIERMAN and E. HARTMAN, "Tests of Two Full-Scale Propellers with Different Pitch Distributions, at Blade Angles up to 60°," *N.A.C.A. Tech. Report* 658.
5. R. M. PINKERTON, "The Variation with Reynolds Number of Pressure Distribution over an Airfoil Section," *N.A.C.A. Tech. Report* 613.
6. D. BIERMAN and E. HARTMAN, "The Effect of Compressibility in the Take-off and Climbing Range," *N.A.C.A. Tech. Report* 639.
7. E. P. HARTMAN and D. BIERMAN, "The Negative Thrust and Torque of Several Full-Scale Propellers and Their Application to Various Flight Problems," *N.A.C.A. Tech. Report* 641.
8. L. J. BRIGGS, G. F. HULL, and H. L. DRYDEN, "Aerodynamic Characteristics of Airfoils at High Speeds," *N.A.C.A. Tech. Report* 207.
9. JOHN STACK, "The Compressibility Burble," *N.A.C.A. Tech. Report* 543.
10. JOHN STACK and A. E. VON DOENHOFF, "Tests of 16 Related Airfoils at High Speeds," *N.A.C.A. Tech. Report* 492.
11. E. P. HARTMAN, "Working Charts for the Determination of Propeller Thrust at Various Speeds," *N.A.C.A. Tech. Report* 481.
12. F. E. WEICK, "Working Charts for the Selection of Aluminum Alloy Propellers of Standard Form to Operate with Various Aircraft Engines and Bodies," *N.A.C.A. Tech. Report* 350.
13. OBER, SHATSWELL, "Estimation of the Variation of Thrust Horsepower with Air Speed," *N.A.C.A. Tech. Note* 446.
14. W. C. NELSON, *Airplane Propeller Principles*, John Wiley & Sons, New York, 1944.
15. W. S. DIEHL, *Engineering Aerodynamics*, Ronald Press Co., New York.
16. W. F. DURAND, *Aerodynamic Theory*, Vol. IV.
17. C. B. MILLIKAN, *Aerodynamics of the Airplane*, John Wiley & Sons, New York, 1941.
18. A. GLAUERT, *The Elements of Aerofoil and Airscrew Theory*, The Macmillan Co., New York.
19. M. J. ZUCROW, "Jet Propulsion and Rockets for Assisted Take-off," A.S.M.E., Los Angeles, Calif., June 11, 1945.
20. F. W. CALDWELL, E. MARTIN, and T. B. RHINES, "The Constant Speed Propeller," *Trans. S.A.E.*, 1937, p. 23.
21. H. M. McCOY, "A Discussion of Propeller Efficiency," *J. Aero. Sci.*, Vol. 1, No. 6, April, 1939, p. 220.

THE GAS-TURBINE POWER PLANT

1. Introduction

The basic concepts underlying gas-turbine power-plant cycles have stimulated inventors and engineers for many years. It is only recently, however, that real progress toward producing a practical
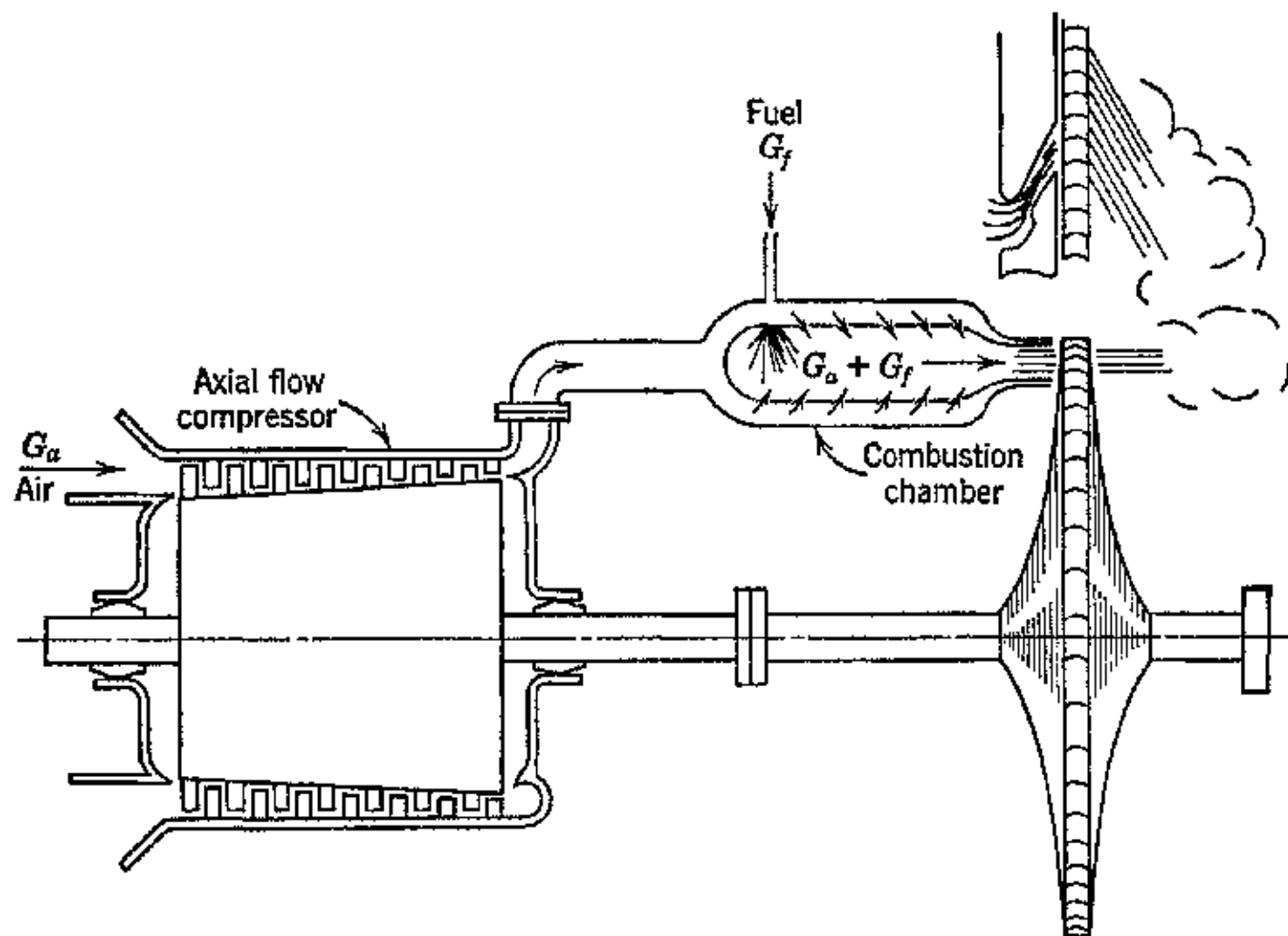
FIG. 1. Elements of a gas-turbine power plant. (Reproduced from S. A. Tucker, *Mechanical Engineering*, June 1944.)

gas-turbine plant has been possible, and its development has now reached that stage where judgments of its potentialities can be made.

The arrangement of the elements of a modern continuous-combustion gas-turbine power plant is illustrated in Fig. 1. Three major elements are required to execute its power cycle: a compressor, a combustion chamber, and a turbine. The compressed air leaving

257

the compressor flows to the internally fired combustion chamber wherein it is heated to a high temperature. The air then expands in the turbine. The useful power developed by the plant is the difference between the work produced by the turbine and that required to drive the compressor, less any parasitic losses due to radiation, pressure drops, leakage, power to drive accessories, etc.

The power plant illustrated in Fig. 1 is frequently called a constant-pressure gas turbine. This is really a misnomer; the term arose from the necessity of distinguishing this type of power cycle from the explosion or constant-volume cycle utilized in the Holzwarth gas turbine. As pointed out by Dr. Adolph Meyer, neither the combustion-chamber pressure nor the pressure at the turbine inlet remains absolutely constant but both vary with the load on the plant. The more appropriate designation suggested by Dr. A. Meyer is the *continuous-combustion gas turbine.*[1]

According to Dr. J. T. Retalliata the history of the gas turbine can be traced back to Hero of Alexandria.[2] The first important design, however, was that disclosed in a patent issued to John Barber, an Englishman, in 1791. The plant disclosed by John Barber was intended to operate on distilled coal, wood, or oil. It incorporated a compressor driven through chains and gears by a turbine operated by the combustion gases. Since that time there has been a steady increase in the number of gas-turbine patents, but the efforts of the early inventors to produce a practical plant were, on the whole, entirely unsuccessful.

In their efforts to produce a simple power plant to replace the more complex steam power plant with its reciprocating steam engine, steam boiler, and manifold auxiliaries, the early inventors paid no heed to the question of thermal efficiency. Furthermore, it appears that they did not appreciate the relationship between the turbine output, the compressor power requirements, and the useful output of the gas-turbine plant. Their work and progress should not be disparaged, however, but should be appraised in accordance with the background of the thermodynamic and aerodynamic knowledge available to them. Furthermore, the seriousness of the metallurgical problems with which they had to cope should not be overlooked.

The first approach to the modern conception of the gas-turbine plant was that described in a patent issued to Dr. F Stolze in 1872 [3] The Stolze plant consisted of a multistage axial-flow compressor coupled directly to a multistage reaction turbine. The air leaving the compressor was heated in an externally fired combustion chamber before its admission into the turbine. Tests of this plant were made

in 1900 and 1904. The unit was unsuccessful. The lack of success was primarily due to the inefficiency of the axial-flow compressor. This is quite understandable since the basis for modern axial-flow-compressor design is aerodynamics, a science which was little developed at that time. Figure 2 illustrates the arrangement of the Stolze gas-turbine plant.
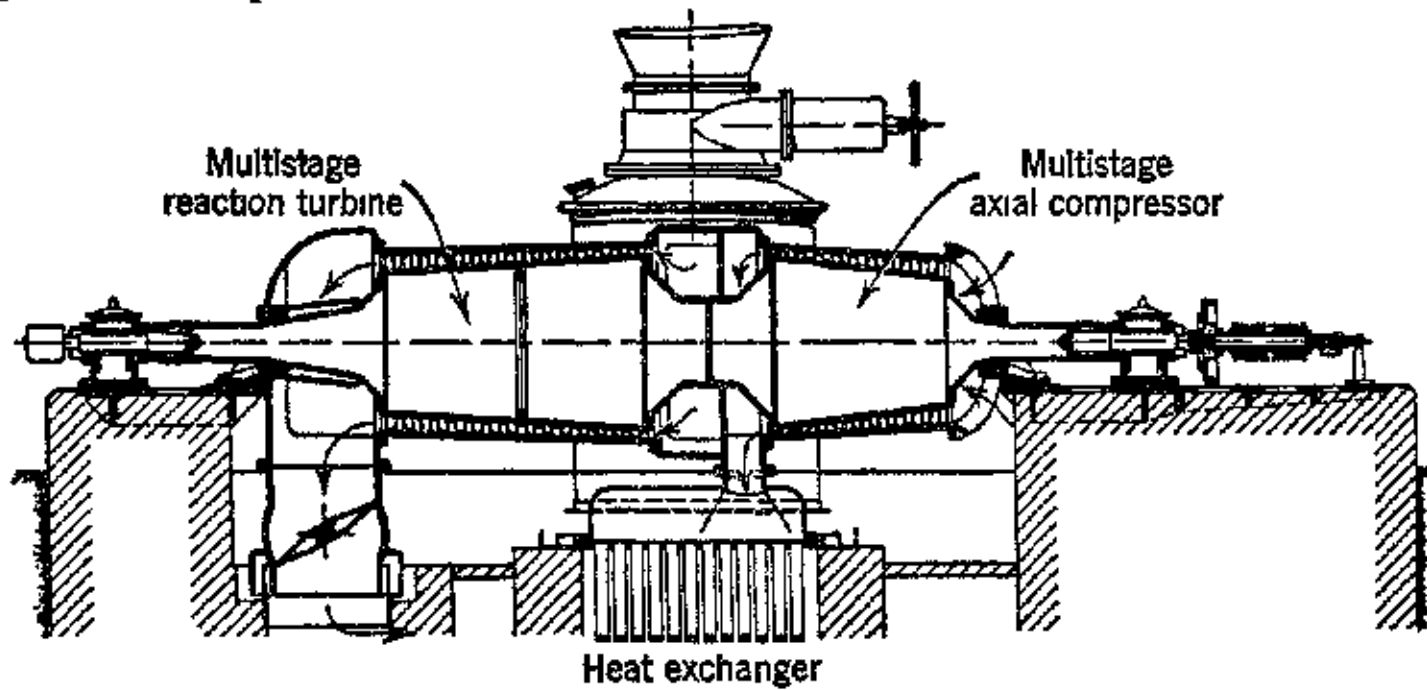
FIG. 2.   Stolze gas-turbine power plant.   (Reproduced from A Meyer, *Inst. Mech Eng Proc*, 1939, Vol. 141, p. 197)

It is worth noting that this lack of aerodynamic information led Sir Charles Parsons, the inventor of the reaction turbine, to abandon the development of the axial-flow compressor in 1908 after building 30 compressors of that type. His efforts to improve the efficiency of the axial-flow compressor met with little success, and at that time the more highly efficient centrifugal compressor was introduced by Rateau.[4]

Several experimental gas turbines were built by the Société des turbomoteurs in Paris during 1903 to 1906. These gas turbines operated on a cycle similar to that of modern gas turbines   The most significant unit had a multistage centrifugal compressor, 25 impellers working in series, a two-row impulse wheel turbine with water injection to cool the turbine blades and disk, and an internally fired liquid-fuel combustion chamber. The operating temperature for the turbine was 1030 F, and the thermal efficiency of the unit was slightly less than 3 per cent. This unit was probably the first gas turbine to produce net useful work. The low thermal efficiency was due to the poor efficiency of the compressors and too low an operating temperature.

An important step in the advance of the gas-turbine art must be credited to the development of the Velox steam generator.[5]   This

steam generator is a boiler fired under pressure, the pressure being produced by a compressor driven by a gas turbine actuated by the flue gases of the boiler. A part of the pressure developed by the compressor is employed to produce high gas velocities in the heat-transmitting parts of the boiler, thereby ensuring high rates of heat transfer. For this development to be successful, a compressor of high efficiency was essential; otherwise, the exhaust gas turbine would be unable to develop the power required to drive the compressor and the deficiency would have to be supplied by another source; this would have reduced the efficiency of the steam generator.

The problem was solved by the Brown-Boveri Company by the development of a multistage reaction turbine and a multistage axial-flow compressor, the design taking into account the results of the latest research in the field of aerodynamics.

A similar application for the gas turbine was found in oil refineries making gasoline by the Houdry process.[6] Air is compressed by an axial-flow compressor and delivered to the catalyst chamber where it is heated to high temperature. It is then returned to the turbine, wherein it expands to produce the energy required for operating the compressor. The excess power is furnished to an electric generator.

A parallel development which has also contributed to the development of the gas turbine is the exhaust-gas-driven supercharger. In this application the gas turbine is an accessory. But its application to aircraft engines has served to accelerate the development of the high-speed centrifugal compressor and the high-temperature high-speed turbine. The large number of installations of this type of equipment on aircraft engines [7] and diesel engines (Buchi system) [8] has provided a real incentive to metallurgists to develop high-temperature materials and has quickly produced a wealth of operating experience upon which future gas-turbine developments can be safely based.

To return for a few moments to the difficulties encountered by the early inventors, their troubles were of two kinds. First was the low efficiencies of the compressors and turbines available in those days, and second there was a lack of materials suitable for high-temperature service. Consequently, the permissible operating temperatures were inadequate for the available component machines. This is readily understandable from Fig. 3, which illustrates the minimum turbine-inlet temperature to obtain useful output from the gas-turbine plant as a function of machine efficiency, the latter being the product of the efficiency of the compressor and the efficiency of the turbine.

Today the obstacles mentioned above have been largely overcome.

Compressors and turbines are available or can be designed with efficiencies ranging from 0.80 to 0.90. Further, materials are available with good strength properties at operating temperatures ranging from 1200 to 1600 F. Though 1600 F appears to be the present practical limit, there is every indication that operating temperatures
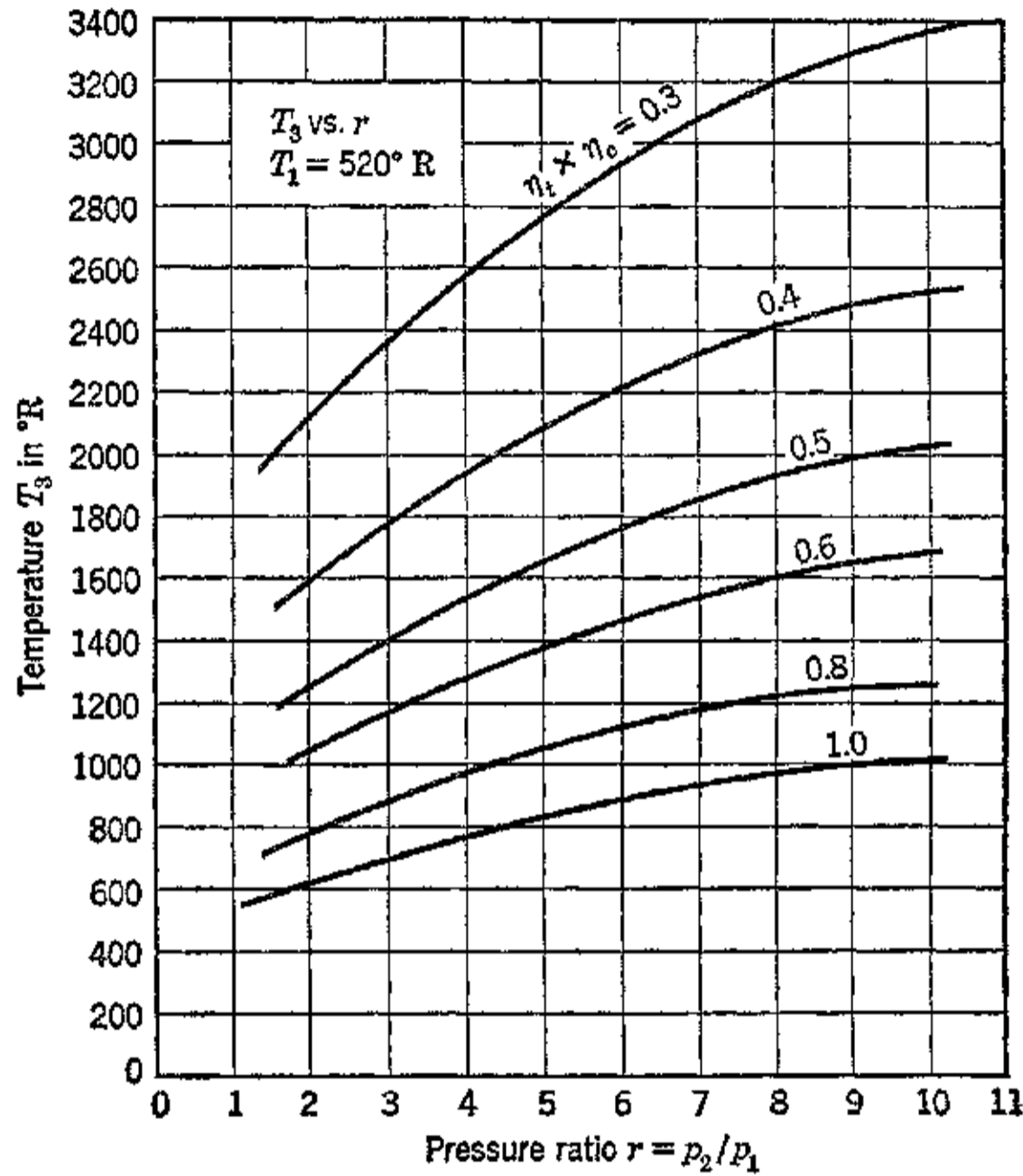
Fig. 3.   Minimum turbine inlet temperature to produce useful work.

as high as 1900 F are a distinct possibility.[19] A section through a modern continuous-combustion gas-turbine plant is presented in Fig. 4.

The gas turbine is of interest to aeronautical engineers for several reasons. The problems associated with increasing the size of light-weight internal-combustion-engine plants seem to be leading to a practicable limit to this size of plant.[9] No such limitation is basic to the gas-turbine plant, and in the larger sizes a favorable power-weight ratio should be feasible with careful design. Furthermore, the gas-turbine power plant can utilize grades of fuel not suitable for high-performance spark-ignition engines.
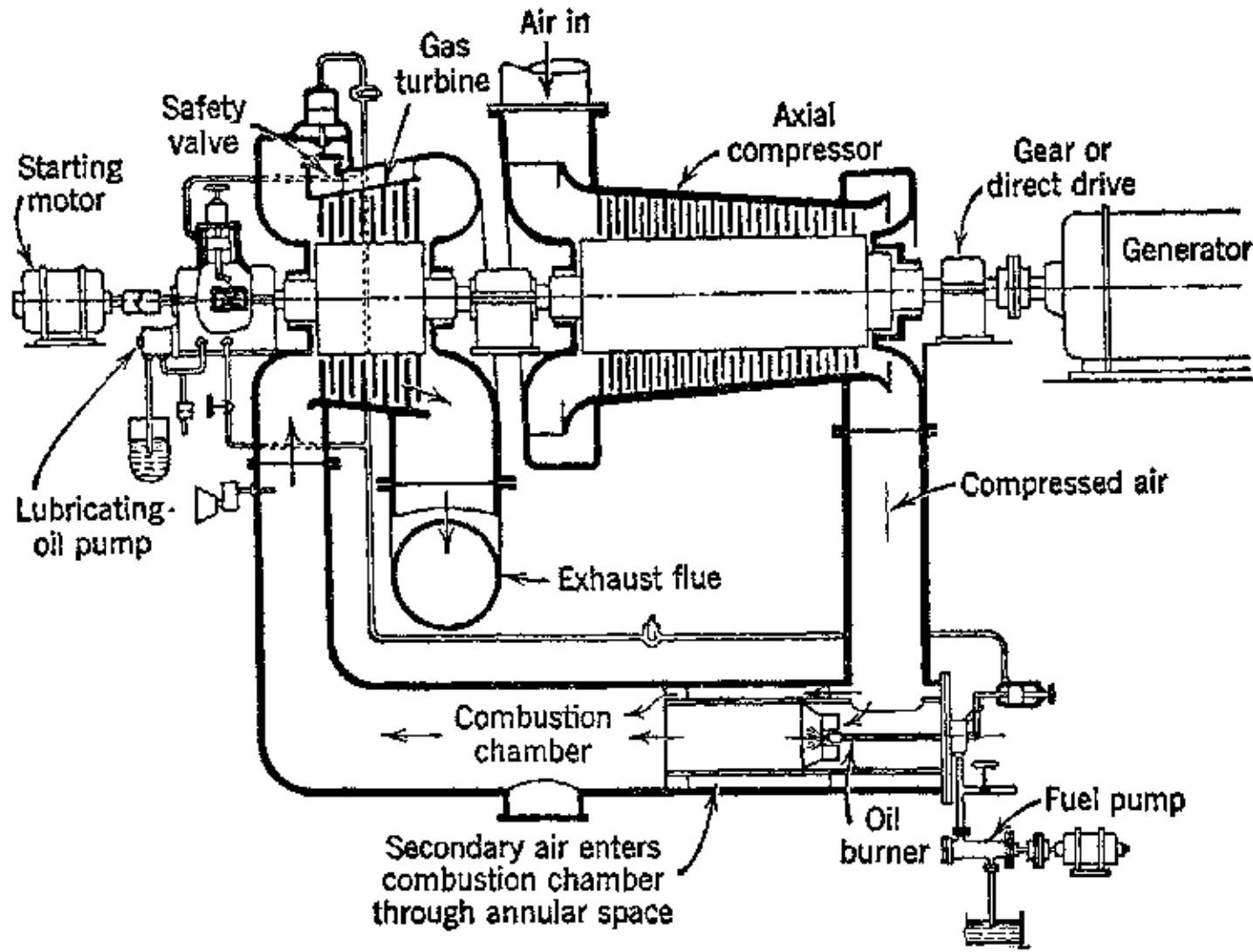
FIG. 4. Section through a modern continuous-combustion gas-turbine power plant. (Reproduced from S. A. Tucker, *loc. cit.*)

This chapter is concerned with the analysis of the continuous-combustion gas turbine as a basic power plant which can be adapted to the propeller propulsion of aircraft.

2. Ideal Open-Cycle Gas Turbine

Figure 5 is a diagrammatic illustration of an open-cycle gas-turbine plant. Atmospheric air enters the compressor C, wherein it is compressed. It then flows to the combustion chamber B, wherein fuel

c = compressor
t = turbine
B = combustion chamber
G_f = fuel flow, lb/sec
G_a = air flow, lb/sec
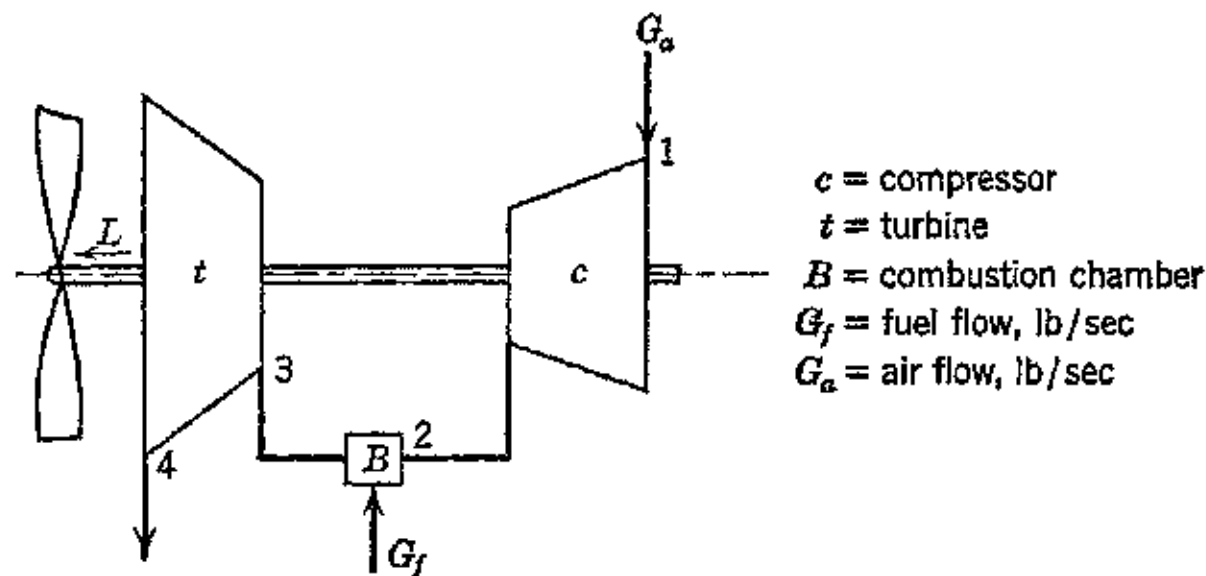
FIG. 5. Diagrammatic sketch of the elements of an open-cycle gas-turbine power plant for airplane propulsion.

is burned to raise its temperature to the permissible turbine inlet temperature. The gases entering the turbine t, assuming a temperature of approximately 1200 F, will contain approximately 600 per cent excess air. This highly heated mixture of a small amount of combustion products and air expands in the turbine to the atmospheric pressure. The excess work developed by the turbine, above that required to operate the compressor, is absorbed by the propeller or other means according to the application for which the plant is intended.

The ideal cycle for this plant is illustrated on the pv-plane in Fig. 6 and on the Ts-plane in Fig. 7.
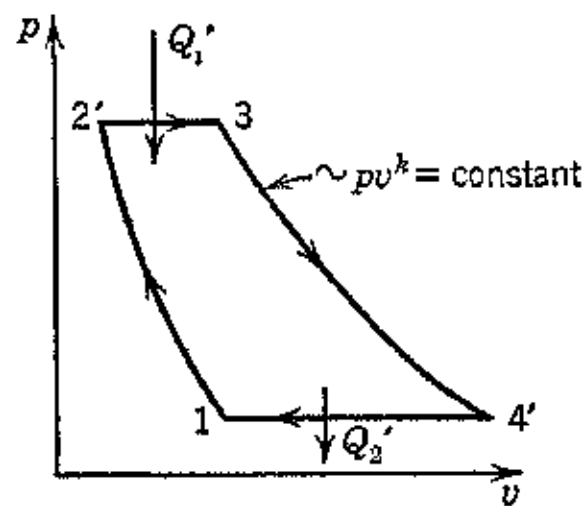
FIG. 6.   Ideal gas-turbine cycle
on the p-v plane.
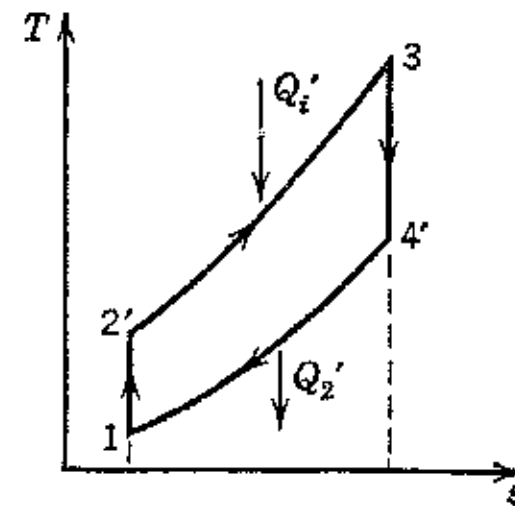
FIG. 7.   Ideal gas-turbine
cycle on the T-s plane.

As a first approximation, the characteristics of the plant will be determined, assuming that the working fluid is a perfect gas, that the component parts of the plant are 100 per cent efficient, and that there are no losses due to friction, radiation, pressure drop, etc.

Notation

L = net work delivered by the gas turbine power plant, ft-lb/lb.

L_t = work developed by an ideal turbine, ft-lb/lb.

L_c = work required by an ideal compressor, ft-lb/lb.

A = area, sq ft.

η_a = efficiency of an ideal non-regenerative air cycle.

η_{aR} = efficiency of an ideal regenerative air cycle.

r = pressure ratio of compressor (cycle pressure ratio for ideal plant).

k = c_p/c_v.

T_1 = temperature at inlet to compressor, R.

T_2' = temperature at outlet of an ideal compressor for which $\eta_c = 1.0$, R.

T_3 = temperature at inlet to turbine, R.

T_4' = temperature at outlet of ideal turbine for which $\eta_t = 1.0$, R.

$$\theta = \frac{T_2'}{T_1} = r^{\frac{k-1}{k}}.$$

$Z = \theta - 1.$

Q_i' = heat supplied to ideal combustion chamber to raise temperature of gases from T_2' to T_3.

Δh_c = compression work including all internal losses except mechanical efficiency = $L_c/J\eta_c$, Btu/lb.

η_c = internal efficiency of compressor.

Δh_t = turbine output = $L_t\eta_t/J$, Btu/lb.

η_t = internal efficiency of turbine.

η_R = effectiveness of regenerator.

η_B = efficiency of combustion chamber.

η_M = mechanical efficiency of turbine and compressor drives.

Q_i = heat actually supplied to the working fluid = Q_i'/η_B.

T_2 = actual temperature at end of compression, R.

T_3 = temperature at inlet to turbine, R.

T_4 = actual temperature at end of turbine expansion, R.

λ_R = losses in regenerator = $(1 - \eta_R)$.

λ_P = losses due to pressure drop.

$y = 1 - \eta_B(1 - \eta_t\eta_a).$

$$z = \lambda_R\left(\frac{1}{\theta} + \frac{\eta_a}{\eta_c}\right).$$

η_{cp} = compressor efficiency adjusted to take care of pressure drop in the plant layout.

Assuming that the working fluid is a perfect gas and that all the machine components are 100 per cent efficient, the useful work of an ideal gas turbine plant is, in general, given by

$$L = L_t - L_c \quad \text{ft-lb/lb.} \tag{1}$$

The heat supplied to the ideal plant is $Q_i' = c_p(T_3 - T_2')$ Btu per pound. The ideal cycle efficiency is

$$\eta_a = \frac{L}{JQ_i'} = \frac{L_t - L_c}{JQ_i'} \tag{2}$$

Assuming that the compression process 1–2′ and the expansion process 3–4′ are isentropic, the changes in enthalpy will be

$$L_c = Jc_p(T_2' - T_1) \quad \text{and} \quad L_t = Jc_p(T_3 - T_4')$$

Hence substituting for L_t and L_c in equation 2 gives the following

$$\eta_a = \frac{c_p[(T_3 - T_4') - (T_2' - T_1)]}{c_p(T_3 - T_2')} \tag{3}$$

For a perfect gas c_p = constant. Hence the ideal cycle efficiency

$$\eta_a = 1 - \frac{T_4' - T_1}{T_3 - T_2'} \tag{4}$$

For this ideal cycle the pressure ratio for the compression process is the same as it is for the expansion process. For a cycle made up of two pairs of similar curves

$$T_2'T_4' = T_1 T_3$$

Hence

$$\frac{T_2'}{T_1} = \frac{T_3}{T_4'} = \left(\frac{p_2}{p_1}\right)^{\frac{k-1}{k}} = r^{\frac{k-1}{k}} = \theta \tag{5}$$

where r = pressure ratio = p_2/p_1.
Hence

$$\eta_a = 1 - \frac{\left(\frac{1}{r}\right)^{\frac{k-1}{k}} T_3 - \left(\frac{1}{r}\right)^{\frac{k-1}{k}} T_2'}{T_3 - T_2'}$$

or, finally, the efficiency of the ideal non-regenerative cycle is

$$\eta_a = 1 - \left(\frac{1}{r}\right)^{\frac{k-1}{k}} = 1 - \frac{1}{\theta} \tag{6}$$

From equation 6 it is seen that the efficiency of the ideal cycle for the gas-turbine power plant depends only upon its pressure ratio r and the specific heat ratio k. The efficiency of the ideal cycle is independent of the temperatures of the cycle.
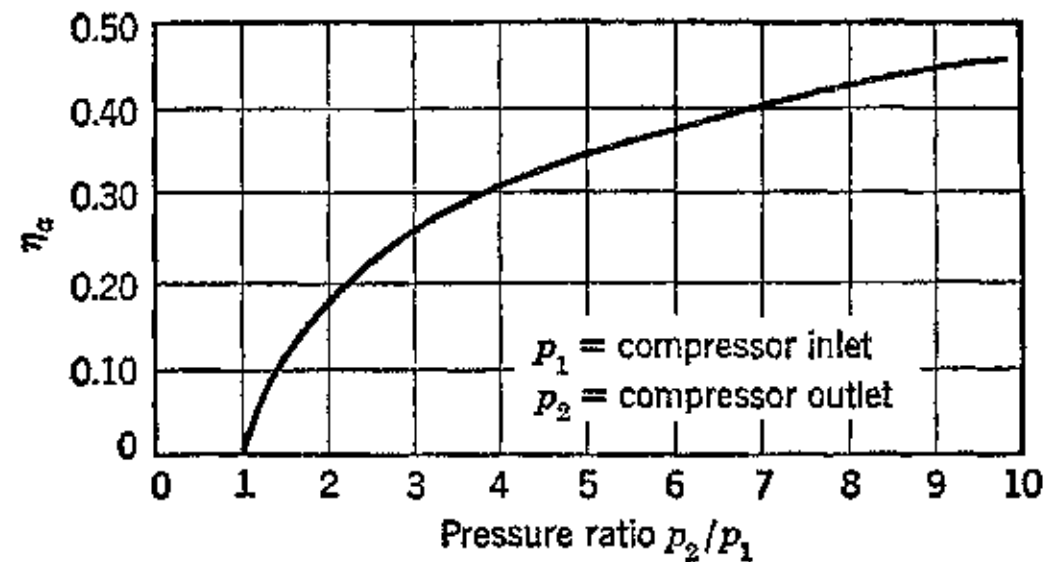
FIG. 8.   Air cycle efficiency vs. pressure ratio for the ideal open-cycle gas-turbine power plant.

From Fig. 8 it is seen that the ideal gas-turbine plant has the potentiality of giving high efficiency if the pressure ratio for the cycle is large enough.

Table 7·1 presents values of $r^{\frac{k-1}{k}}$ for different values of $k = c_p/c_v$.

TABLE 7·1

TABLE OF POLYTROPIC COMPRESSIONS

$$\theta = \frac{T_2'}{T_1} = \left(\frac{p_2}{p_1}\right)^{\frac{k-1}{k}} = r^{\frac{k-1}{k}}$$

r	$k = 1.4$	$k = 1.3$	$k = 1.2$	$k = 1.1$
1.1	1.028	1.022	1.016	1.009
1.2	1.053	1.043	1.031	1.017
1.3	1.078	1.062	1.045	1.024
1.4	1.101	1.081	1.085	1.031
1.5	1.123	1.098	1.070	1.038
1 6	1.144	1.115	1.081	1.044
1.7	1.164	1.130	1.092	1.050
1.8	1.183	1.145	1.103	1.055
1.9	1.201	1.160	1.113	1.060
2.0	1.219	1.174	1.123	1.065
2.5	1.299	1.235	1.165	1.087
3.0	1.369	1.289	1.201	1.105
3.5	1.431	1.336	1.232	1.121
4.0	1.487	1.378	1.260	1.134
4.5	1.537	1.415	1.285	1.147
5.0	1.583	1.449	1.307	1.157
5.5	1.627	1.482	1.328	1.167
6.0	1.668	1.512	1.348	1.177
6.5	1.707	1.540	1.366	1.186
7.0	1.742	1.566	1 383	1.194
7.5	1.778	1.591	1.399	1.201
8.0	1.811	1.616	1.414	1.208
8.5	1.843	1.639	1.429	1.215
9.0	1.873	1.660	1.442	1.221
9.5	1.903	1.681	1.455	1.227
10.0	1.931	1.701	1.468	1.233

EXAMPLE. An ideal gas-turbine plant operating with the cycle illustrated in Fig. 6 has a pressure ratio $p_2/p_1 = 6.0$. What is its efficiency?

$$\eta_a = 1 - \left(\frac{1}{r}\right)^{\frac{k-1}{k}}$$

From Table 7·1, $r^{\frac{k-1}{k}} = 1.668$; $\left(\frac{1}{r}\right)^{\frac{k-1}{k}} = 0.60.$

$$\eta_a = 1 - 0.6 = 0.40$$

3. Ideal Regenerative Cycle

Referring to Fig. 7 it is seen that the gases in the turbine exhaust are discharged at the temperature T_4'. If this temperature is higher than T_2', the temperature at which the compressed air enters the combustion chamber, it is possible to recover a portion of the thermal energy in the exhaust gases from the turbine by the expedient of inserting a heat exchanger, called a *regenerator*, in the paths of these two gas streams in the manner illustrated in Fig. 9. The heat transferred from the turbine exhaust to the air leaving the compressor, by the regenerator, effects a reduction in the quantity of heat which must be added in the combustion chamber to obtain the gas temperature T_3 at the inlet to the turbine. This reduction in the supply of heat is possible provided T_4' is higher than T_2', which it usually is.
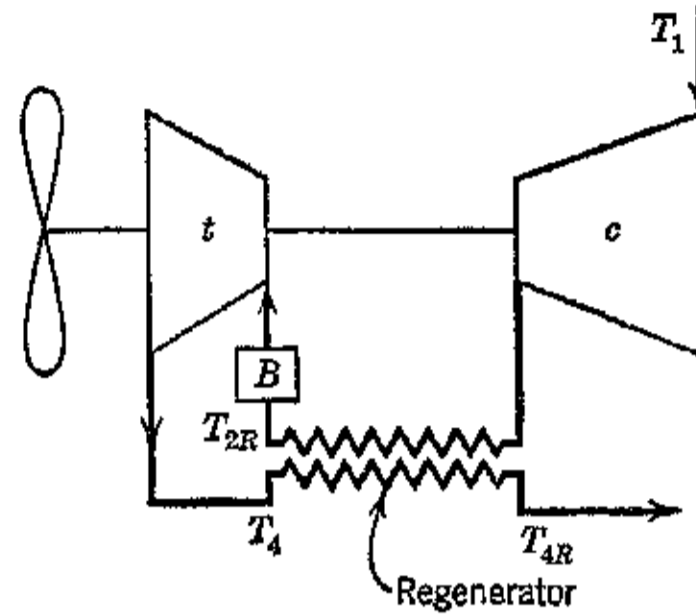
FIG. 9. Elements of the open-cycle regenerative gas-turbine power plant.

The reduction in the quantity of heat added in the combustion chamber, assuming an ideal regenerator and constant specific heats for the gases, is Q_R, where

$$Q_R = c_p(T_4' - T_2') \quad \text{Btu/lb} \tag{7}$$

Hence the heat which is supplied to the combustion chamber of a gas turbine utilizing the ideal regenerative cycle is given by

$$Q_{iR}' = Q_i' - Q_R = c_p(T_3 - T_2') - c_p(T_4' - T_2') \tag{8}$$

The efficiency of this ideal regenerative cycle is given by

$$\eta_{aR} = \frac{(T_3 - T_4') - (T_2' - T_1)}{(T_3 - T_2') - (T_4' - T_2')}$$

which in accordance with equation 3 can be written

$$\eta_{aR} = 1 - \frac{T_2' - T_1}{T_3 - T_4'} \tag{9}$$

From equation 5

$$T_1 = \frac{T_2'}{\theta} \quad \text{and} \quad T_4' = \frac{T_3}{\theta}$$

and, substituting these expressions for T_1 and T_3 in equation 9, the result is

$$\eta_{aR} = 1 - \frac{T_2'}{T_3} = 1 - \frac{T_1}{T_3} r^{\frac{k-1}{k}} = 1 - \frac{T_1}{T_3} \theta \qquad (10)$$

From equation 10 it is seen that for the ideal regenerative gas turbine the cycle efficiency is dependent upon the inlet temperature
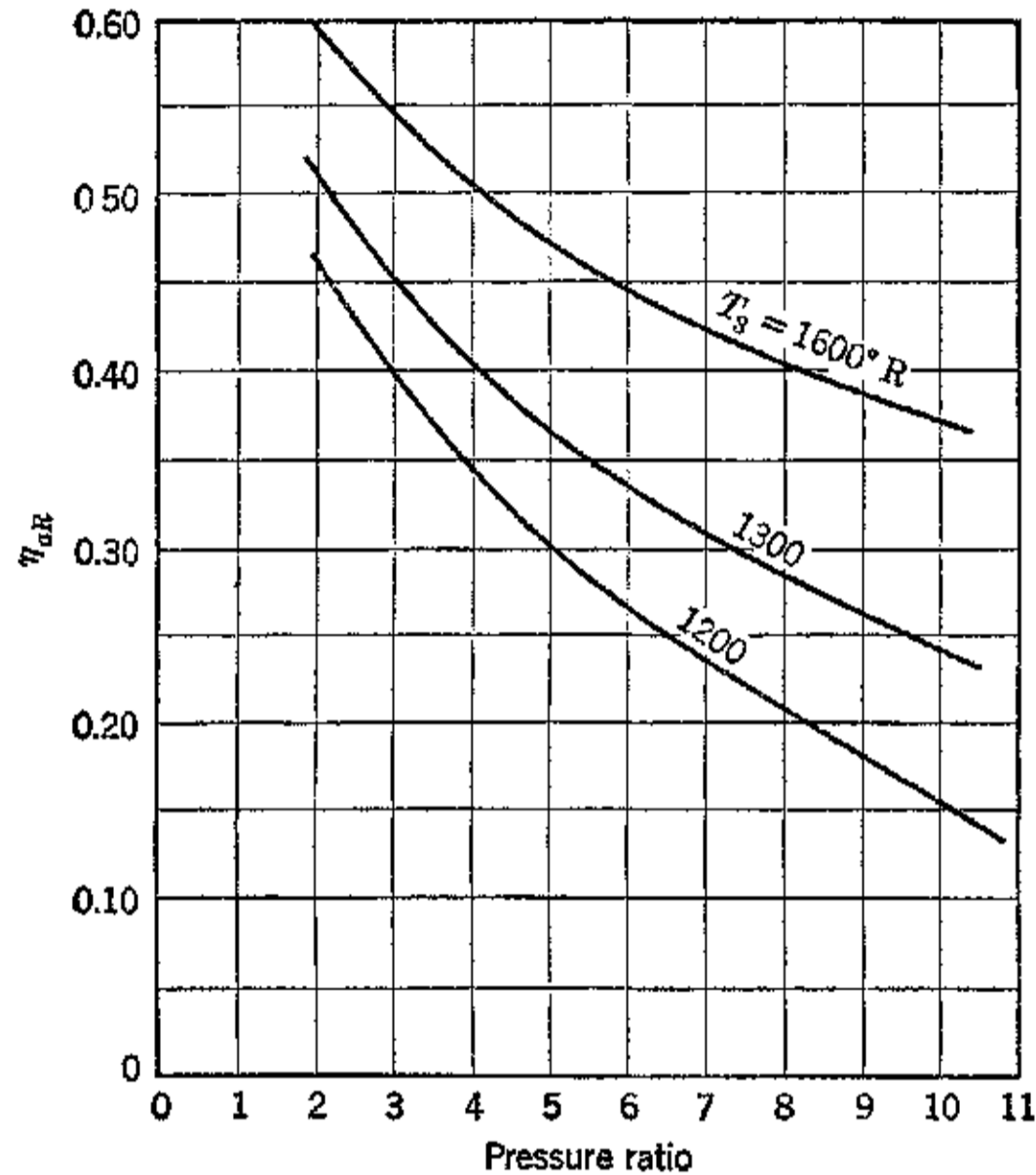
FIG. 10.   Characteristics of the ideal open-cycle regenerative gas-turbine power plant.

to the compressor T_1, the inlet temperature to the turbine T_3, the cycle pressure ratio r, and the specific heat ratio k.

From the relationship $\theta = T_2'/T_1 = r^{\frac{k-1}{k}}$ it is apparent that increasing the pressure ratio r raises the temperature at the end of compression T_2'. Consequently, if the turbine inlet temperature T_3 is fixed the cycle efficiency η_{aR} will be lowered if the pressure ratio is increased. This is readily seen from Fig. 10. Since the lower pressure ratios correspond to part-load operation, the regenerative cycle has the advantage of maintaining plant efficiency at part-load operation.

EXAMPLE. An ideal gas turbine is operated on the regenerative cycle. The inlet temperature to the turbine is 1200 R, the air entering the compressor is at a temperature of 520 R, and the pressure ratio is 6. Assuming that $k = c_p/c_v = 1.4$, find the ideal cycle efficiency (a) for the conditions listed above; (b) for an inlet temperature to the turbine of 1600 R; (c) for an inlet temperature to the turbine of 1200 R and a pressure ratio of 10.

Solution.

(a) $\eta_{aR} = 1 - \dfrac{T_1}{T_3}\theta = 1 - \dfrac{520}{1200} \times 1.668 = 0.277$

(b) $\eta_{aR} = 1 - \dfrac{520}{1600} \times 1.668 = 0.458$

(c) $\eta_{aR} = 1 - \dfrac{520}{1200} \times 1.931 = 0.155$

The ideal cycles discussed in the preceding cannot be executed in practice, but by careful design the discrepancies can be kept small enough to give actual efficiencies that are attractive. It should be realized, however, that thermal efficiency is not the only criterion in deciding upon the application of prime movers. Such factors as cheap fuel, low maintenance costs, compactness of plant, simplicity, and low weight are frequently of greater importance. This new form of power plant will undoubtedly be subjected to intensive development for aircraft use in the future, since it potentially offers the possibility of low weight-to-power ratio.

4. Causes of Departure of Actual Cycle from Ideal Cycle

The actual cycle for a continuous-combustion gas turbine deviates in several respects from the ideal cycles discussed in Sections 2 and 3. The differences arise from the causes discussed below:

(a) **Compression Process.** In the actual compressor there are losses due to friction, heat transfer, shock, and the like. Consequently, the flow compression of the air is not conducted under the isentropic conditions assumed in the ideal cycle. Thus, if

> r_c = pressure ratio of compressor,
>
> $\bar{c}_{pc}$ = average specific heat at constant pressure for compression process,
>
> Δh_c = actual compression work, Btu/lb,
>
> L_c = isentropic compression work, ft-lb/lb,

then

$$J\Delta h_c = \frac{L_c}{\eta_c} = J\bar{c}_{pc}(T_2 - T_1) = J\bar{c}_{pc}\frac{(T_2' - T_1)}{\eta_c} \qquad (11)$$

or

$$\Delta h_c = \bar{c}_{pc}T_1 \frac{r_c^{\frac{k-1}{k}} - 1}{\eta_c} = \bar{c}_{pc}T_1 \frac{(\theta - 1)}{\eta_c} \qquad (11a)$$

The value of η_c depends upon the type of air compressor, its pressure ratio, and the weight of air passing through it. For modern high-speed centrifugal compressors a value $\eta_c = 0.75$ appears to be reasonable for estimating purposes; for axial-flow compressors $\eta_c = 0.85$ to 0.90. According to C. R. Soderberg and R. B. Smith a value of $\eta_c = 0.847$ is attainable with the constant-displacement helical lobe rotary compressor invented by Alf Lysholm, Ljungstom Company, Sweden.[11] The marine gas turbine developed by the Elliott Company employs Lysholm compressors.[12,13,14]

PROBLEM. Calculate the efficiency of a compressor operating with a pressure ratio of 3.0 if the entering air is at 500 R and the exit air is at 700 R.

Solution. From Chapter 4, Section 4, the heat added per mole of air is

$$Q = m\bar{c}_{pc}(240 - 32) - m\bar{c}_{pc}(40 - 32) \quad \text{Btu/mole}$$

From Table 4·3

$$\bar{c}_{pc} \text{ at } 240 = \frac{6.969}{28.97} = 0.2406$$

$$\bar{c}_{pc} \text{ at } 40 = \frac{6.941}{28.97} = 0.2396$$

$$\Delta h_c = Q = .2406 \times 208 - .2396 \times 8 = 48.12 \quad \text{Btu/lb}$$

From Table 4·4

$$h_1 = 24.00 \qquad p_{r1} = 2.1845 \qquad p_{r2} = 2.1845 \times 3 = 6.5535$$

$$h_2' = 68.17 \qquad \frac{L_c}{J} = h_2' - h_1 = 44.17 \quad \text{Btu/lb}$$

$$\eta_c = \frac{L_c/J}{\Delta h_c} = \frac{44.17}{48.12} = .917$$

(*b*) **Expansion Process in the Turbine.** The expansion of the heated gas in the turbine is accompanied by various losses. Consequently, the actual work performed by the turbine is less than that obtainable from an ideal machine. Because of the injection of fuel in the combustion chamber, the mass flow of gases is greater in the turbine than the air flow through the compressor; this is discussed in detail in Section 4(*d*).

It should be further noted that owing to the pressure loss in the combustion chamber the expansion ratio for the turbine is smaller than the pressure ratio for the compressor.

In general

$$J\Delta h_t = \eta_t L_t \tag{12}$$

where L_t = isentropic expansion work in turbine ft-lb/lb.

η_t = internal efficiency of turbine.

r_t = expansion ratio of turbine.

$\bar{c}_{pt}$ = mean specific heat for operating temperature range of turbine.

Hence

$$\Delta h_t = \eta_t \bar{c}_{pt} T_3 (1 - r_t^{-\frac{k-1}{k}}) = \eta_t \bar{c}_{pt} T_3 \left(1 - \frac{1}{\theta}\right) \qquad (13)$$

where T_3 is the temperature at the inlet to the turbine.

The internal efficiency of the turbine is affected by its size and the number of stages. For single-stage impulse machines, values ranging from 0.80 to 0.85 can be expected, depending upon the care taken to reduce the blading losses, nozzle friction, leakage, etc.; for multistage machines of either the impulse or reaction types higher internal efficiencies can be expected. For analytic studies, a value of $\eta_t = 0.85$ appears to be reasonable.

(c) The Regenerator. This apparatus does not transfer 100 per cent of the heat in the turbine exhaust gases to the compressed air leaving the compressor as assumed in the ideal regenerative cycle. As a matter of fact, 100 per cent effectiveness cannot be obtained unless the heat-transfer surface has infinite area. The effectiveness of the regenerator will be denoted by η_R.

Figure 11 illustrates the heat-balance conditions for the regenerator.
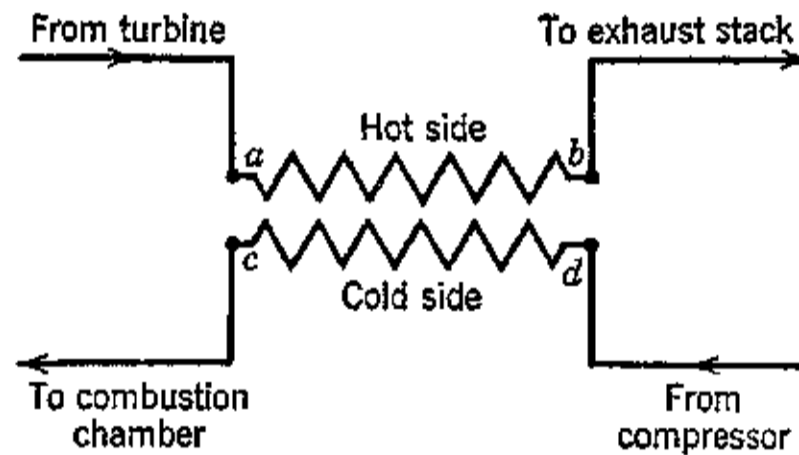
FIG. 11. Heat balance for the regenerator.

Let h denote the enthalpy of the fluid in Btu/lb above a given datum. If the locations in Fig. 11 are used as subscripts, then

h_c = enthalpy leaving regenerator (cold side).
h_d = enthalpy entering regenerator (cold side).
h_a = enthalpy entering regenerator (hot side).
h_b = enthalpy leaving regenerator (hot side).

The regenerator is a counterflow heat exchanger. The cold gases flow through a tube bundle, and the hot gases flow around them. In practice, it is important to keep the pressure drops through the

regenerator as low as possible. A large pressure drop on the cold side increases the required pressure ratio of the compressor and consequently the compression work. Similarly, a large pressure drop on the hot gas side of the regenerator raises the turbine back pressure, thereby reducing the pressure ratio of the turbine and consequently its output.

From the foregoing, it is seen that the gain due to exhaust-gas heat recovery is partly offset by the pressure drop involved in carrying the fluids through the regenerator. For a given heat-transfer-surface area the pressure drop will increase with the efficiency of the regenerator since, to obtain higher rates of heat transfer, the velocity of the gases past the heating surfaces must be greater. For estimating purposes, the enthalpy loss corresponding to different regenerator efficiencies can be assumed to be those listed below. These values assume well-designed heat-transfer equipment, and unless care is exercised in the design of the regenerator either its size will become unreasonable or the losses will be greater than those listed.[11]

REGENERATOR EFFECTIVENESS η_R	ENTHALPY LOSS IN BTU/LB
0.50	0.55
0.75	1.10
0.90	2.75

Since the regenerator is a device for reclaiming some of the heat energy in the turbine exhaust, effectiveness is defined in terms of the rise in the enthalpy on the cold side referred to the enthalpy of the exhaust gases above that of the compressed air leaving the compressor

$$\eta_R = \frac{h_c - h_d}{h_a - h_d} \tag{14}$$

In terms of the temperatures

$$\eta_R = \frac{\bar{c}_p(T_c - T_d)}{\bar{c}_p(T_a - T_d)} \tag{15}$$

where $\bar{c}_p$ is the mean value of the specific heat at constant pressure for the temperature ranges involved.

(d) **Combustion Chamber.** Not all the thermal energy of the fuel injected into the combustion chamber is recovered as increased temperature of the working fluid; there are losses due to radiation and

imperfect combustion. Figure 12 illustrates the thermal conditions at the combustion chamber. Let

G_f = rate of fuel addition, lb/sec.

G_a = rate of air flow, lb/sec.

$G_g = G_f + G_a$ = rate of gas flow, lb/sec.

H_c = lower heat value of fuel.

h_f = enthalpy of fuel above some fixed temperature, Btu/lb.

r_{fa} = fuel-air ratio, G_f/G_a.

H_f = enthalpy of fuel above 400 R, datum of Table 4·4, Btu/lb.

h_a = enthalpy of air at entrance to combustion chamber, above 400 R, datum of Table 4·4, Btu/lb.

Q_i = the thermal energy supplied to the combustion chamber in the form of fuel, Btu/lb of air.

Q_i' = the heat actually imparted to the working fluid, Btu/lb of air.

η_B = efficiency of combustion chamber.

$\bar{c}_p$ = mean specific heat at constant pressure for the temperature range T_c to T_e, Btu/lb F.

T_c = temperature at entrance to combustion chamber, R.

T_e = temperature at exit from the combustion chamber, R.

The air and fuel entering the combustion chamber are mixed under adiabatic conditions, so that the final enthalpy of the mixture is equal to the sum of the enthalpies of the air and the fuel entering the combustion chamber. The fuel-air ratio, the pounds of fuel per pound of air, is calculated from the combustion efficiency η_B, the lower heating value of the fuel H_c, and the temperature rise which occurs. Thus

$$r_{fa} = \frac{G_f}{G_a} = \frac{\bar{c}_p(T_e - T_c)}{H_c \times \eta_B} \frac{G_g}{G_a} \tag{16}$$

The rate of gas flow through the combustion chamber is

$$G_g = G_a + G_f = \left(1 + \frac{G_f}{G_a}\right) G_a \tag{17}$$

If the ratio G_f/G_a is sufficiently small it can be assumed that the mixture of air and completely vaporized fuel obeys the perfect-gas laws for air. This assumption is well justified for gas turbines because of the large excess air employed.
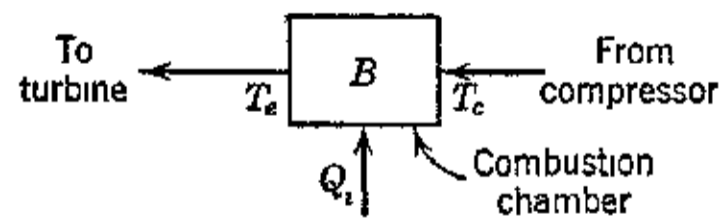
Fig 12. Heat balance for the combustion chamber.

The heat actually supplied to the working fluid is expressed by the equation

$$Q_i = \frac{Q_i'}{\eta_B} = \frac{\bar{c}_p}{\eta_B}(T_e - T_c) \tag{18}$$

The enthalpy per pound of fuel-air mixture entering the combustion chamber is composed of two parts: the enthalpy of the entering fuel plus the enthalpy of the air.

The enthalpy per pound of mixture, assuming the fuel and air to have the same chemical aggregation, is determined as follows. Each pound of fuel-air mixture contains $G_f/(G_f + G_a)$ pounds of fuel and $G_a/(G_f + G_a)$ pounds of air. If the enthalpies of the fuel vapor and of the air are assumed to be zero at 400 R, the base of Table 4·4, then the enthalpy of the liquid fuel at the temperature T_L R can be represented by an equation of the form

$$H_f = aT_L + C \quad \text{Btu/lb of fuel} \tag{19}$$

where a and C are constants, and T_L is the liquid temperature in degrees R.

According to Keenan and Kaye, *Trans. A.S.M.E.*, 1943, p. A123, for liquid octane $a = 0.5$ and $C = -375$.

The enthalpy of 1 lb of mixture entering the combustion chamber after mixing is given by

$$h_c = \frac{G_f}{G_a + G_f} \cdot H_f + \frac{G_a}{G_a + G_f} h_a \tag{20}$$

The enthalpy per pound of mixture leaving the combustion chamber, h_e, is h_c plus the enthalpy of combustion. Thus

$$h_e = h_c + \frac{G_f}{G_f + G_a} H_c \eta_B \tag{21}$$

EXAMPLE. Consider the gas turbine of Fig. 5. Assume the temperature of the air leaving the compressor to be 820 R. The temperature of the air leaving the combustion chamber is 1700 R, $\eta_B = 0.98$, $H_c = 19{,}240$ Btu/lb. Find: (a) fuel air ratio; (b) enthalpy of liquid fuel (octane) entering combustion chamber at 520 R; (c) total enthalpy per pound of mixture after mixing fuel and air; (d) total enthalpy per pound of mixture leaving combustion chamber.

Solution. Assuming that the fuel addition does not affect the specific heat of the mixture, so that it may be assumed to be air, then, from Fig. 4·3, $\bar{c}_p = 0.26$

(a) *Using equation* 16

$$r_{fa} = \frac{0.260(1700 - 820)}{19{,}240 \times 0.98}\frac{G_g}{G_a} = 0.0121\frac{G_g}{G_a}$$

or

$$G_f = 0.01228 G_a \quad \text{lb/sec}$$

(b) *Using equation* 19

$$H_f = 0.5 \times 520 - 375 = -115 \quad \text{Btu/lb of fuel}$$

(c) *Using equation* 20: From Table 4·4, the enthalpy of the air entering at the temperature 820 R is h_{a2} = 101.26 Btu/lb of air

$$h_2 = \frac{0.01228 G_a}{1.01228 G_a} H_f + \frac{G_a}{1.0121 G_a} h_{a2}$$

$$= 0.0120(-115) + 0.99(101.26)$$

$$= 98.61 \quad \text{Btu/lb of mixture}$$

(d) *Using equation* 21

$$h_3 = 98.61 + 0.01213 \times 19{,}240 \times 0.99 = 327.3 \quad \text{Btu/lb of mixture}$$

Check from Table 4·4: T_3 = 1695 R.

(e) Mechanical Losses. In addition to the thermal losses and thermodynamic deviations discussed above, there are mechanical losses due to friction in the bearings and in any gearing between the turbine and the propeller. These losses may be taken into account collectively by introducing the factor η_M, the *mechanical efficiency*.

Since the compressor and turbine are similar types of machines, their bearing losses are of the same relative magnitude for the enthalpy changes per pound of fluid passing through them. Consequently, for analytical purposes, it can be assumed that η_M is the same for both the compressor and the turbine. In the design of a plant this point has to be investigated, and the actual values of η_M for each component of the plant is used in the design calculations. For well-designed equipment the mechanical efficiency will be of the order of 0.96 to 0.98.

(f) Parasite Losses. In the operating cycle of an actual gas turbine there are parasite losses arising from pressure drops in the piping, regenerator, etc. These losses necessitate increasing the pressure ratio of the compressor and reduce the net useful work of the gas turbine.

The parasite losses will be denoted by Δh_L. The net output of the plant which is denoted by L is, therefore, given by

$$L = \eta_M \left(\eta_t L_t - \frac{1}{\eta_c} L_c \right) - J \Delta h_L \quad \text{ft-lb/lb} \tag{22}$$

(g) Variation of Specific Heat of Working Substance. As pointed out in Chapter 4, the specific heat of the working substance is not constant but varies with the temperature. Consequently, the specific-heat ratio k also is a function of temperature. Data on the specific heat of air have been presented in Chapter 4, and methods for taking its variation into account are also presented in that chapter.

It should be noted that there is a small gain in the mass of fluid flowing through the system after it has passed through the combustion chamber. Furthermore, there is a slight change in its chemical composition. These effects will be neglected here.

In designing a gas-turbine plant, all the factors enumerated above must be given consideration, since the selection of the operating conditions and the sizes of the units should be based on the most accurate knowledge that can be obtained. Errors in estimating piping losses will affect both the efficiency and power output of the actual plant. Neglect of the variation in the specific heat will lead to incorrect blade path for the turbine, especially if it is of the multi-stage reaction type.

From the foregoing it is seen that the efficiency of an actual plant of the type illustrated in Fig. 5 can be determined as follows

$$\text{Net work} = L = \eta_M \eta_t L_t - \eta_M \frac{1}{\eta_c} L_c - J \Delta h_L$$

$$\text{Heat supplied} = \frac{1}{\eta_B} Q_i'$$

so that

$$\eta = \frac{\eta_M \left(\eta_t L_t - \frac{1}{\eta_c} L_c \right) - J \Delta h_L}{\frac{1}{\eta_B} J Q_i'} \tag{23}$$

In judging the usefulness of a prime mover, other criteria in addition to the cycle efficiency must be given consideration. Two important criteria are the air rate and the work ratio discussed below.

5. Air Rate, W_a

This is the amount of fluid which must be handled per unit of power output. This is a criterion of the size of the plant. The air rate is usually expressed in terms of pounds of air inducted by the compressor per horsepower-hour. Thus

$$W_a = \frac{2545}{\text{Net output in Btu/lb of air}} \tag{24}$$

Obviously, the lower the value of W_a, the smaller the plant

6. Work Ratio, U

This is the ratio of the net work available for driving the load to the total internal power developed by the turbine.   Thus

$$U = \frac{\text{Net output of plant}}{\text{Output of turbine}} \tag{25}$$

This criterion gives an indication of the size of the machinery which must be installed to produce a given power output for useful purposes. The higher the work ratio, the smaller is the power plant that must be installed for a given net output.

7. Simplified Analysis of Plant Efficiency

A general equation for the efficiency of the simple gas-turbine plant cannot be derived owing to the large number of variables involved.   By making certain simplifying assumptions it is possible, however, to obtain an expression which can readily be applied to analysis of the plant.   These simplifying assumptions do not introduce any significant errors when the methods of this section are used to obtain general characteristics.   Thus let it be assumed that (a) the working fluid is a perfect gas; (b) there is no increase in the quantity of working fluid due to the addition of fuel in the combustion chamber; and (c) there are no pressure drops.

Assumption (a) introduces an error since it neglects the variation in the specific heat and specific heat ratio k of the working fluid with temperature.   The error it introduces in the compression portion of the cycle is less than 1 per cent for a pressure ratio as high as 6. The error is of the order of 2 per cent for the expansion portion of the cycle.   Where an exact analysis is necessary, as in plant design, the variation of the specific heat and k must be taken into consideration.

Assumption (b) introduces a small error in the direction of conservatism.   Further, this error is partly offset by assumption (a).   The combination of these two assumptions tends to nullify the error introduced by each.

The flow of gases through the turbine is $(1 + r_{fa})G_a$ lb/sec, where G_a is the air flow through the compressor.

Assumption (c) can be readily taken into account by either deducting the pressure losses from the cycle pressure at the locations where the pressure losses occur or by reducing the actual efficiency of the compressor by an amount sufficient to compensate for the pressure losses.   In an exact analysis of an actual plant, however, the pressure

drops should be taken into consideration at the appropriate places in the cycle.

The general expression for the efficiency of the simple gas-turbine plant, based on the foregoing assumptions, is equation 23. In this equation the quantity Q_i'/η_B is the actual heat supplied per pound of air by the combustion of fuel in the combustion chamber. It is equal to the heat required to raise the temperature of the compressed air discharged by the compressor to the temperature at the turbine inlet times $1/\eta_B$. Because the compression of the air is not isentropic the air leaving the compressor is at a higher temperature than
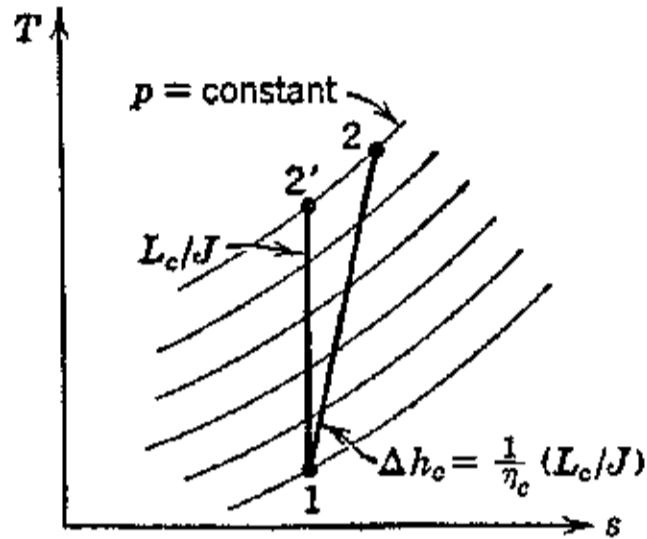
FIG. 13. Compression process on T-s plane.
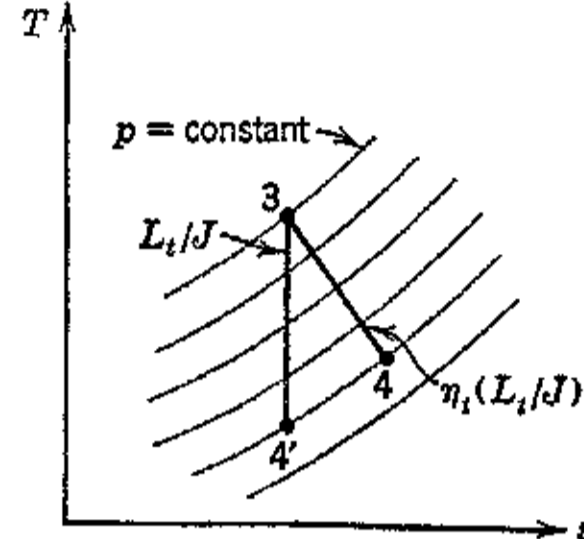
FIG. 14. Expansion process on T-s plane.

the isentropic compression temperature for the same pressure ratio. This is illustrated in Fig. 13, where the actual and isentropic compression processes are illustrated on the Ts plane. The curve 12' represents the isentropic case, and 12 represents the actual compression. The corresponding compression works are L_c and $J \, \Delta h_c = L_c/\eta_c$.

(a) **Temperature at End of Compression.** The temperature rise in the compressor and its internal efficiency η_c are related by the expressions

$$\eta_c = \frac{L_c}{J \, \Delta h_c} = \frac{\text{Isentropic compression work}}{\text{Actual compression work}} \tag{26}$$

Using assumption (a), this becomes

$$\eta_c = \frac{c_p(T_2' - T_1)}{c_p(T_2 - T_1)} = \frac{T_2' - T_1}{T_2 - T_1} \tag{27}$$

It has been shown that for an isentropic compression from p_1 to p_2, so that $r = p_2/p_1$, the initial and final temperatures are related by the expression

$$\frac{T_2'}{T_1} = \left(\frac{p_2}{p_1}\right)^{\frac{k-1}{k}} = r^{\frac{k-1}{k}} = \theta$$

Hence

$$T_2' = T_1\theta \quad \text{or} \quad T_1 = \frac{T_2'}{\theta} \tag{28}$$

Substituting for T_1 into equation 27, an expression for the discharge temperature from the compressor in terms of T_2' and η_c is obtained. Thus

$$T_2 = T_1 + \frac{T_2' - T_1}{\eta_c}$$

which can be transformed to give

$$T_2 = \frac{T_2'}{\theta} + \left(T_2' - \frac{T_2'}{\theta}\right)\frac{1}{\eta_c} = \frac{T_2'}{\theta} + \frac{T_2'}{\eta_c}\left(1 - \frac{1}{\theta}\right) \tag{29}$$

The factor $1 - (1/\theta)$ is identical with the expression for the efficiency of an ideal simple plant η_a; see equation 6. Hence equation 29 can be transformed to give

$$T_2 = \frac{T_2'}{\theta} + \frac{T_2'}{\eta_c}\eta_a = T_2'\left(\frac{1}{\theta} + \frac{\eta_a}{\eta_c}\right) \tag{30}$$

Values of $T_2' = T_1\theta$ for different pressure ratios, and values of k, can be determined from Table 7·2. Values of η_a can be taken from Fig. 8.

EXAMPLE. An air compressor has an inlet temperature of 520 R. Assuming that $k = 1.4$, and perfect gas laws, what is the discharge temperature of the air for a pressure ratio of 2: (a) $\eta_c = 1.0$; (b) $\eta_c = 0.9$; (c) $\eta_c = 0.85$?

Solution. From equation 30

$$T_2 = T_2'\left(\frac{1}{\theta} + \frac{\eta_a}{\eta_c}\right)$$

For $r = 2$, from Table 7·1, $\theta = 1.219$.
From equation 28, $T_2' = 520 \times 1.219 = 633$ R.
From Eq. 6, $\eta_a = 1 - (1/\theta) = 1 - 0.821 = 0.179$.

$$T_2 = 633\left(0.821 + \frac{0.179}{\eta_c}\right)$$

(a) $T_2 = T_2' = 633 (0.821 + 0.179) = 633$ R.
(b) $T_2 = 633(0.821 + 0.199) = 645$ R.
(c) $T_2 = 633(0.821 + 0.211) = 653$ R.

EXAMPLE. Find the discharge temperature of the air leaving compressor for which the pressure ratio is 6, the inlet temperature 520 R, and the internal efficiency 0.80. Compare result with value if variation in specific heat is taken into account.

From Table 7·1, for $k = 1.4$ and $r = 6$, $T_2 = 1.668 T_1$.

$$\frac{1}{\theta} = \frac{1}{1.668}$$

From equation 6

$$\eta_a = 1 - \frac{1}{1.668} = 1 - 0.6 = 0.40$$

From equation 30

$$T_2 = 1.668T_1\left(0.6 + \frac{0.4}{0.8}\right)$$

$$= 1.668T_1 \times 1.10 = 1.835 \times 520 = 954 \text{ R (constant } c_p \text{ assumed)}$$

Check, using Table 4·4:

For $T_1 = 520$ $h_1 = 28\ 80$ $p_{r1} = 2.506$

$p_{r2} = 2.506 \times 6 = 15.036$ $h_2' = 112.07$ Btu/lb

$L_c/J = 112.07 - 28.80 = 83.27$ Btu/lb

$$\Delta h_c = \frac{1}{\eta_c} L_c/J = \frac{83.27}{0.8} = 104.1 \text{ Btu/lb}$$

$h_2 = 104.1 + 28.8 = 132.9$ Btu/lb

From Table 4·4, $T_2 = 948$ R (variable c_p). It is seen from the above comparison that the error in T_2 due to neglecting the variation in c_p with temperature is 0.6 per cent.

(b) **Temperature of Turbine Exhaust.** This temperature is determined in a manner similar to that used for determining T_2. The actual expansion is compared with the isentropic expansion in Fig. 14. Hence the efficiency of the turbine is given by

$$\eta_t = \frac{T_3 - T_4}{T_3 - T_4'} \tag{31}$$

From equation 31

$$T_4 = T_3 - \eta_t(T_3 - T_4') \tag{32}$$

But, from equation 5, $T_4' = T_3/\theta$. Substituting this expression into equation 32 gives the following equation for the turbine exhaust temperature T_4

$$T_4 = T_3\left[1 - \eta_t\left(1 - \frac{1}{\theta}\right)\right] = T_3(1 - \eta_t\eta_a) \tag{33}$$

From equation 33 it is seen that the enthalpy change taking place in the turbine depends only upon the ideal cycle efficiency η_a and the internal efficiency of the turbine η_t.

EXAMPLE. A turbine is supplied with air heated to 1660 R, its internal efficiency is 0.80, the expansion ratio is 6.0. Find the exhaust temperature for the gases (a) $c_p = $ constant; (b) $c_p = f(T)$.

Solution.

(a) From Table 7·1 for $k = 1.4$ and $r = 6$, $\theta = 1.668$ and $\eta_a = \left(1 - \dfrac{1}{\theta}\right) = 0.40$.

From equation 33

$$T_4 = 1660[1 - 0.80 \times 0.40] = 0.68 \times 1660 = 1130 \ R(c_p \text{ constant})$$

(b) From Table 4·4

$$T_3 = 1660 \ R \qquad h_3 = 316.57 \ \text{Btu/lb} \qquad p_{r3} = 171.56$$

$$p_{r4} = \frac{171.56}{6} = 28.59 \qquad h_4' = 153.9 \ \text{Btu/lb}$$

$$L_t/J = h_3 - h_4' = 316.57 - 153.9 = 162.67 \ \text{Btu/lb}$$

$$\Delta h_t = \eta_t L_t/J = 0.8 \times 162.67 = 130.14 \ \text{Btu/lb}$$

$$h_4 = h_3 - \Delta h_t = 186.43 \ \text{Btu/lb}$$

$$T_4 = 1163 \ R \quad (c_p \text{ variable})$$

Because the compression and expansion processes are not isentropic, as discussed in the foregoing, the actual cycle for the simple gas turbine plant differs from the ideal cycle. Figure 15 illustrates the actual cycle on the *h-s* plane.[10]

8. Heat Supplied and Cycle Efficiency

The actual quantity of heat furnished the cycle Q_i is that required to raise the temperature of the air from the compressor discharge temperature T_2 to the turbine throttle temperature T_3. This is equal to the enthalpy change corresponding to the temperature increase $(T_3 - T_2)$ less the heat recovered in the regenerator plus the thermal losses in the combustion chamber.

Assuming that the specific heat is constant and the efficiency of the combustion chamber is η_B, the heat supplied to the working fluid is $Q_i' = \eta_B Q_i$, and the heat furnished to the cycle is

$$Q_i = \frac{Q_i'}{\eta_B} = \frac{c_p}{\eta_B}[(T_3 - T_2) - \eta_R(T_4 - T_2)]$$

Rearranging, this becomes

$$Q_i = \frac{c_p}{\eta_B}[T_3 - T_2(1 - \eta_R) - \eta_R T_4] \tag{34}$$
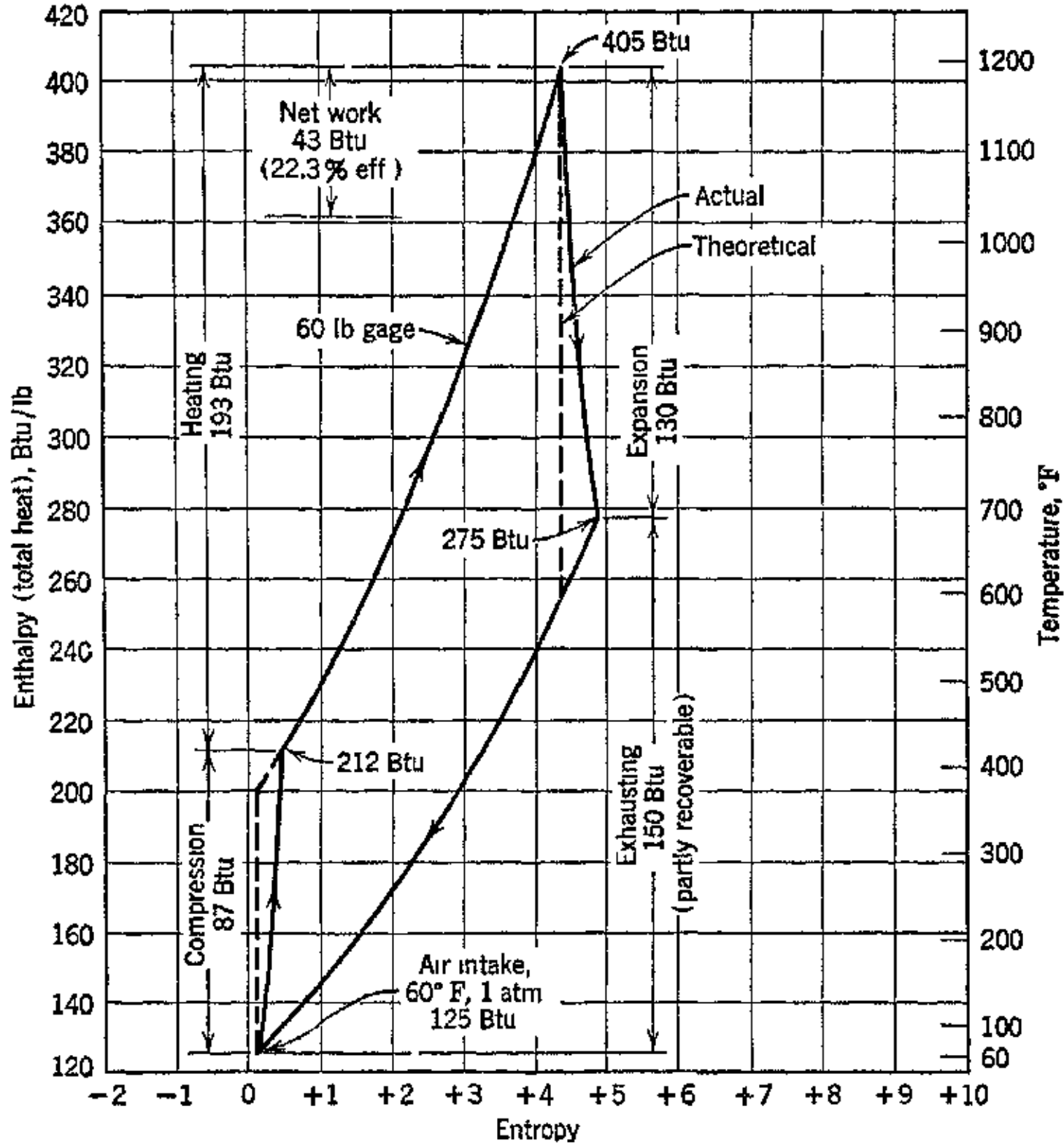
FIG 15   Actual open cycle on the enthalpy-entropy plane   (Reproduced from
S A Tucker, *loc cit*)

The expression $(1 - \eta_R)$ represents the fraction of the thermal
energy in the turbine exhaust gases not recovered in the regenerator.
This loss is denoted by λ_R But from equation 30

$$T_2 = T_2' \left(\frac{1}{\theta} + \frac{\eta_a}{\eta_c} \right) \qquad (a)$$

and from equation 33

$$T_4 = T_3(1 - \eta_t \eta_a) \qquad (b)$$

Substituting from (a) and (b) into equation 34 and letting λ_R
$= (1 - \eta_R)$,

$$Q_t = \frac{c_p}{\eta_B} \left[T_3 \{ 1 - \eta_R(1 - \eta_t \eta_a) \} - T_2' \lambda_R \left(\frac{1}{\theta} + \frac{\eta_a}{\eta_c} \right) \right] \qquad (35)$$

For brevity, let

and

$$y = 1 - \eta_R(1 - \eta_t\eta_a)$$

$$z = \lambda_R \left(\frac{1}{\theta} + \frac{\eta_a}{\eta_c}\right)$$

Then the equation for the heat supplied to the cycle becomes

$$Q_i = \frac{c_p}{\eta_B}[T_3y - T_2'z] \tag{36}$$

The output of the gas-turbine power plant, neglecting mechanical losses, is given by

$$L = \eta_t L_t - \frac{1}{\eta_c}L_c$$

This can be written in the form

$$L = \eta_t L_t - \frac{1}{\eta_c}L_c = Jc_p\left[\eta_t(T_3 - T_4') - \frac{1}{\eta_c}(T_2' - T_1)\right]$$

By eliminating T_1 and T_4' and noting that $\eta_a = 1 - (1/\theta)$, the above expression becomes

$$\frac{L}{J} = c_p\eta_a\left(\eta_t T_3 - \frac{1}{\eta_c}T_2'\right) \tag{37}$$

The net output of the plant in mechanical units, taking mechanical losses into account, is $\eta_M L$.

Substituting for Q_i and L into the plant-efficiency equation 23, assuming that the parasite losses Δh_L are taken into account by proper adjustment of the compressor or turbine efficiency, the final equation for the efficiency of the gas turbine is

$$\eta = \eta_M \eta_B \eta_a \frac{\eta_t T_3 - (1/\eta_c)T_2'}{yT_3 - zT_2'} \tag{38}$$

Equation 38 is the general expression for the efficiency of a simple gas-turbine plant of either the regenerative or non-regenerative type. It is not entirely accurate in view of the simplifying assumptions used in its derivation. For studying the effect of changing the various factors which influence the plant performance it is useful and sufficiently correct.

To reduce the amount of calculation required in applying this equation, Table 7·2 has been prepared. This table presents the values of θ, $1/\theta$, η_a, and $\eta_a\theta$ for different pressures and for $k = 1\,4$

TABLE 7-2

VALUES OF θ, $1/\theta$, η_a, AND $\eta_a\theta$

$$\theta = \frac{T_2'}{T_1} = \left(\frac{p_2}{p_1}\right)^{\frac{k-1}{k}} = r^{\frac{k-1}{k}} \quad (k = 1.40)$$

r	θ	$1/\theta$	η_a	$\eta_a\theta$
1.0	1.000	1.000	0	0
1.1	1.028	0.9728	0.0272	0.0279
1.2	1.053	.9497	.0503	.0529
1.3	1.078	.9276	.0724	.0780
1.4	1.101	.9083	.0917	.1009
1.5	1.123	.8905	.1095	.1229
1.6	1.144	.8741	.1259	.1440
1.7	1.164	.8591	.1409	.1640
1.8	1.183	.8453	.1547	.1830
1.9	1.201	.8326	.1674	.2010
2.0	1.219	.8205	.1797	.2191
2.5	1.299	.7698	.2302	.2990
3.0	1.369	.7305	.2695	.3689
3.5	1.431	.6988	.3012	.4310
4.0	1.487	.6725	.3275	.4870
4.5	1.537	.6506	.3494	.5370
5.0	1.583	.6317	.3683	.5831
5.5	1.627	.6146	.3854	.6270
6.0	1.668	.5995	.4005	.6680
6.5	1.707	.5858	.4142	.7070
7.0	1.742	.5741	.4259	.7419
7.5	1.778	.5624	.4376	.7780
8.0	1.811	.5522	.4478	.8110
8.5	1.843	.5426	.4574	.8429
9.0	1.873	.5339	.4661	.8730
9.5	1.903	.5255	.4745	.9029
10.0	1.931	.5179	.4821	.9309

9. Characteristics of the Non-Regenerative Plant

The general characteristics of the non-regenerative plant can be determined from equation 38. Since the inlet air temperature T_1 is generally known this equation is more useful when written in the form

$$\eta = \eta_M \eta_B \eta_a \frac{\eta_t T_3 - (\theta T_1/\eta_c)}{y T_3 - z\theta T_1} \tag{39}$$

For the non-regenerative plant the regenerator efficiency $\eta_R = 0$ and the factors denoted by y and z have the values indicated below.

$$y = 1 - \eta_R(1 - \eta_t\eta_a) = 1$$

and

$$z = (1 - \eta_R)\left(\frac{1}{\theta} + \frac{\eta_a}{\eta_c}\right) = \left(\frac{1}{\theta} + \frac{\eta_a}{\eta_c}\right)$$

Substituting for y and z in the efficiency equation listed above gives

$$\eta = \eta_a\eta_B\eta_M \frac{\eta_t T_3 - (T_1\theta/\eta_c)}{T_3 - T_1[1 + (\theta\eta_a/\eta_c)]} \tag{40}$$

This equation shows that the efficiency of the plant will depend on

(a) The ideal cycle efficiency η_a.

(b) The combustion chamber efficiency η_B.

(c) The mechanical efficiency η_M.

(d) The internal efficiency of the turbine η_t.

(e) The internal efficiency of the compressor η_c.

(f) The pressure ratio and the specific heat ratio, since θ is a function of r and k.

(g) The inlet temperature to the turbine T_3.

(h) The inlet temperature to the compressor T_1.

In view of the above list of factors which affect the efficiency of the plant it is not possible to represent the plant efficiency by a single curve. To determine the plant characteristics it is necessary to select a basic plant as a starting point and then study the effect of varying each factor separately.

The *basic plant* which will be used for determining the characteristics of the non-regenerative gas turbine assumes the following:

$$\eta_M = 1.00, \quad \eta_B = 1.00, \quad \eta_t = 0.85, \quad \eta_c = 0.84, \quad \eta_R = 0, \quad k = 1.4$$

The plant-efficiency equation, using the above data, becomes

$$\eta = \eta_a \frac{0.85 T_3 - 1.193 T_1\theta}{T_3 - T_1(1 + 1.191\eta_a\theta)}$$

10. Effect of Pressure Ratio on Performance of Non-Regenerative Gas Turbine

The pressure ratio of the turbine has a bearing upon the size of the equipment as well as upon its efficiency. In operating the gas turbine the part-load operation is obtained by changing its speed, which reduces its pressure ratio. This is accomplished by lowering

the temperature at the turbine throttle, by reducing the quantity of fuel supplied to the combustion chamber. With the reduced operating speed the efficiencies of the compressor and turbine units are
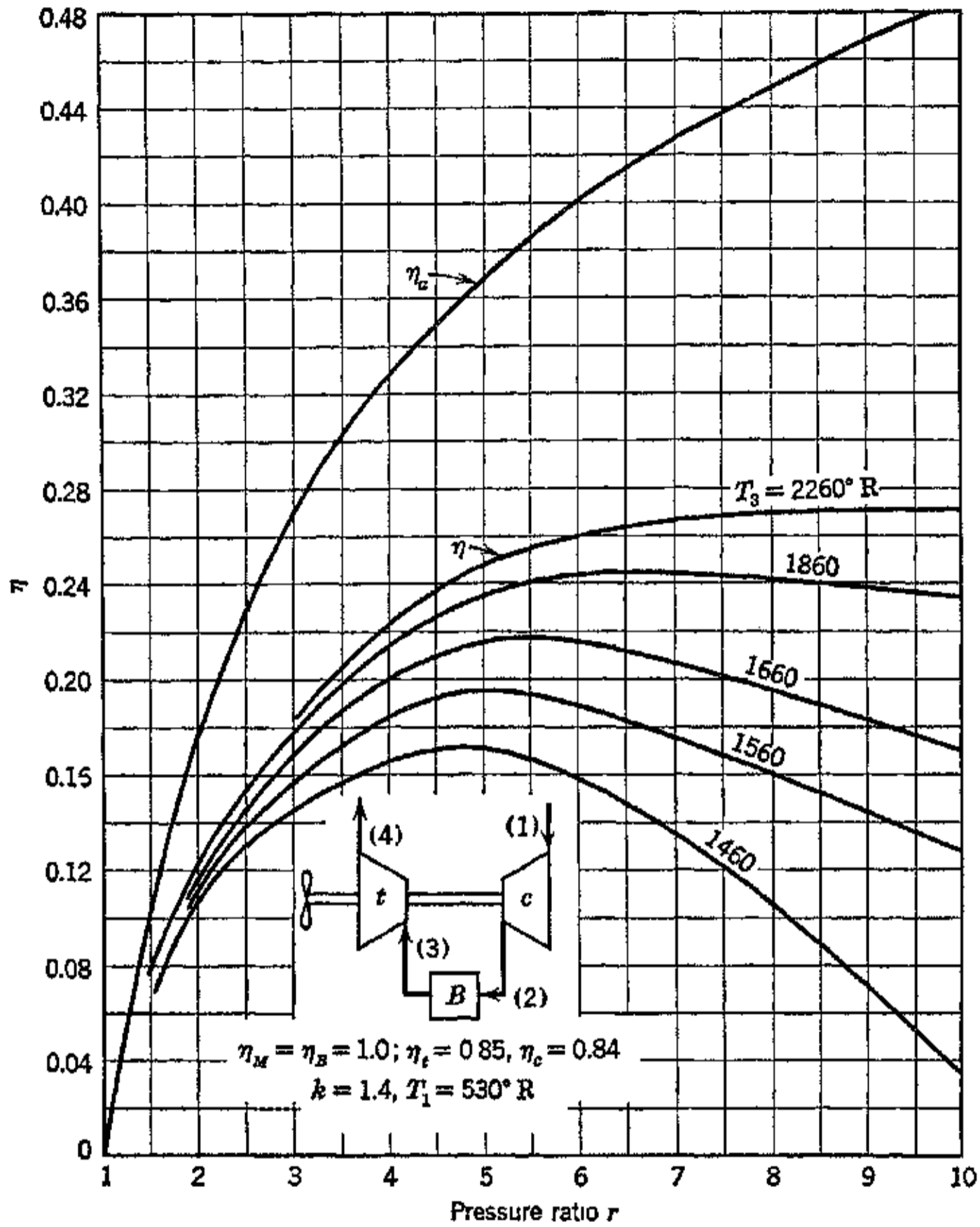
FIG. 16. Air-cycle efficiency vs pressure ratio for an open-cycle gas-turbine power plant.

reduced, and to determine the part-load performance the efficiency curves of these machines as functions of speed must be known or estimated.

This section considers the effect of pressure ratio on the full-load performance only.

It will be assumed that the inlet temperature to the air compressor is $T_1 = 530$ R and that the turbine inlet temperature is $T_3 = 1660$ R. The efficiency equation for the basic plant accordingly becomes

$$\eta = \eta_a \left[\frac{1410 - 632\theta}{1660 - 530(1 + 1.191\eta_a\theta)} \right] = \eta_a \frac{A}{B} = K_1\eta_a$$
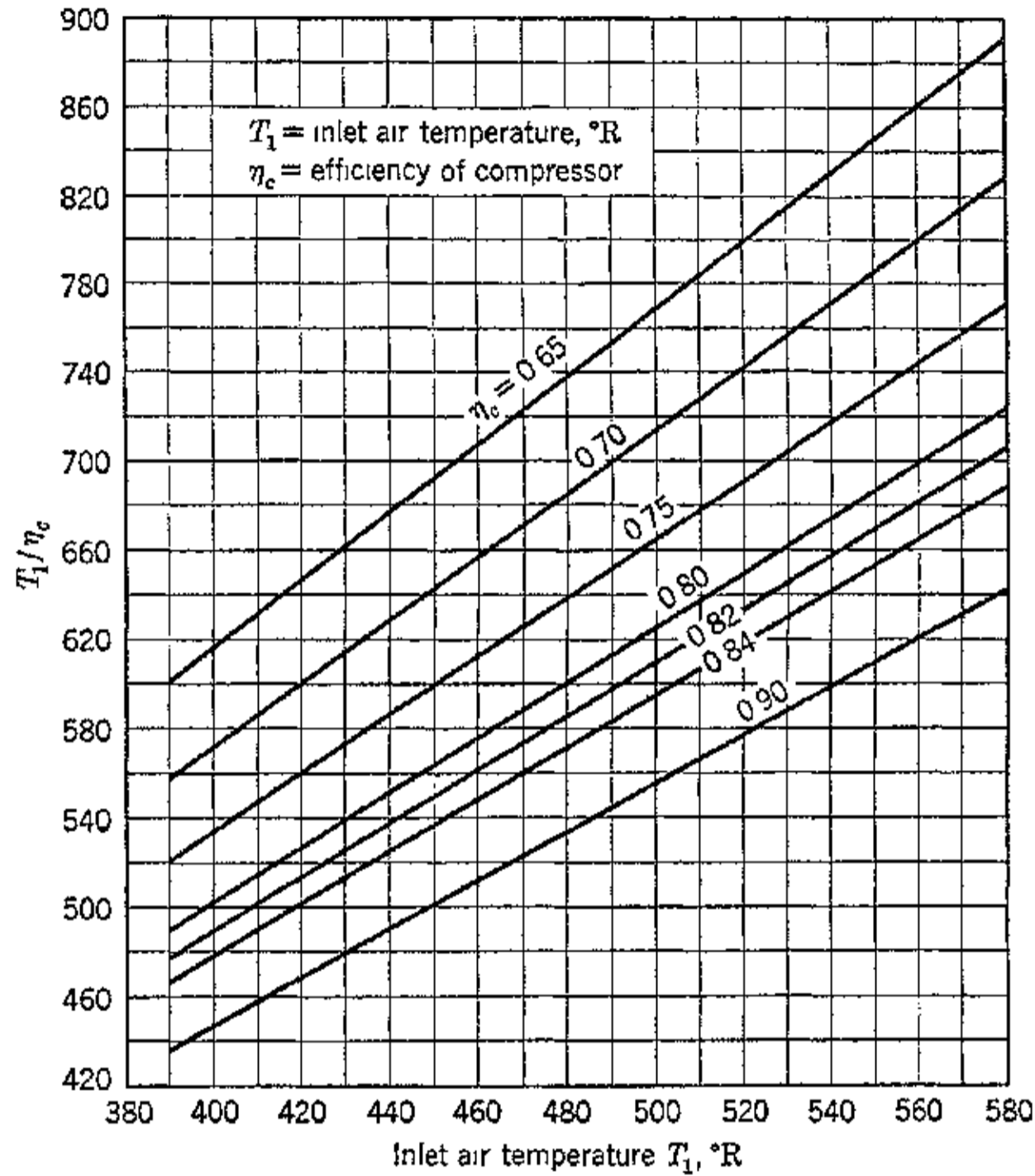
FIG. 17.   Values of T_1/η_c vs inlet air temperature.

The detailed calculations for a pressure range varying from $r = 2$ to $r = 10$ are tabulated in Table 7·3. The results are plotted in Fig. 16.

It is seen from Fig. 16 that as the pressure ratio is increased for a given throttle temperature the cycle efficiency is raised until a maximum value is attained. Further increase in pressure ratio then decreases the cycle efficiency. This indicates that there is a best pressure ratio corresponding to any given throttle temperature (see references 16 and 17 for additional data).

TABLE 7·3

EFFECT OF PRESSURE RATIO ON CYCLE EFFICIENCY

(Non-regenerative, open-cycle gas turbine)

Based on perfect-gas laws, air as working fluid

Data: $\eta_M = \eta_B = 1.0$, $\eta_t = 0.85$, $\eta_c = 0.84$, $k = 1.4$, $T_1 = 530$ R, $T_3 = 1660$ R

Cycle efficiency equation: $\eta = \eta_a \left[\dfrac{1410 - 632\theta}{1660 - 530(1 + 1.191\eta_a\theta)} \right] = K_1\eta_a$

r	$1410 - 632\theta$	$1660 - 530(1 + 1.193\theta)$	K_1	η_a	η
1.5	703	1054	0.668	0.1095	0.073
2.0	642	992	.646	.1797	.116
3.0	548	897	.611	.2695	.165
4.0	473	823	.575	.3275	.188
6.0	359	709	.506	.4005	.203
8.0	269	619	.435	.4478	.195
10.0	193	543	.355	.4821	.171

To help reduce the labor involved in making calculations of cycle efficiency, Figs. 17 and 18 are presented.

11. Effect of Intake Temperature

The intake temperature enters into the general equation for the plant efficiency by virtue of its effect on the isentropic compression temperature T_2'. The compression work for a fixed pressure ratio is proportional to the absolute temperature at the inlet to the compressor, that is, to T_1. Consequently, if the intake temperature is reduced and all other variables remain unchanged, the power output is increased and the efficiency of the cycle raised. To illustrate the effect of changing T_1, consider a gas-turbine plant having the following characteristics

$$\eta_M = 1.00, \qquad \eta_B = 1.00, \qquad \eta_t = 0.85, \qquad \eta_c = 0.84$$

$$T_3 = 1660 \text{ R}, \qquad \eta_R = 0, \qquad r = 6, \qquad k = 1.4$$

(a) Plant Efficiency. The efficiency equation for this type of plant is

$$\eta = \eta_a\eta_B\eta_M \frac{\eta_t T_3 - (T_1\theta/\eta_c)}{T_3 - T_1[1 + (\theta\eta_a/\eta_c)]}$$

From Table 7·2, for $r = 6.0$, $\eta_a = 0.400$.
From Table 7·2, for $r = 6.0$, $\theta = 1.668$.

From plant data, $\eta_a \eta_B \eta_M = 0.400$; $\eta_t T_3 = 1410$; $T_1 \theta / \eta_c = 1.980 T_1$; $\eta_a / \eta_c = 0.477$; $\theta \eta_a / \eta_c = 0.794$.
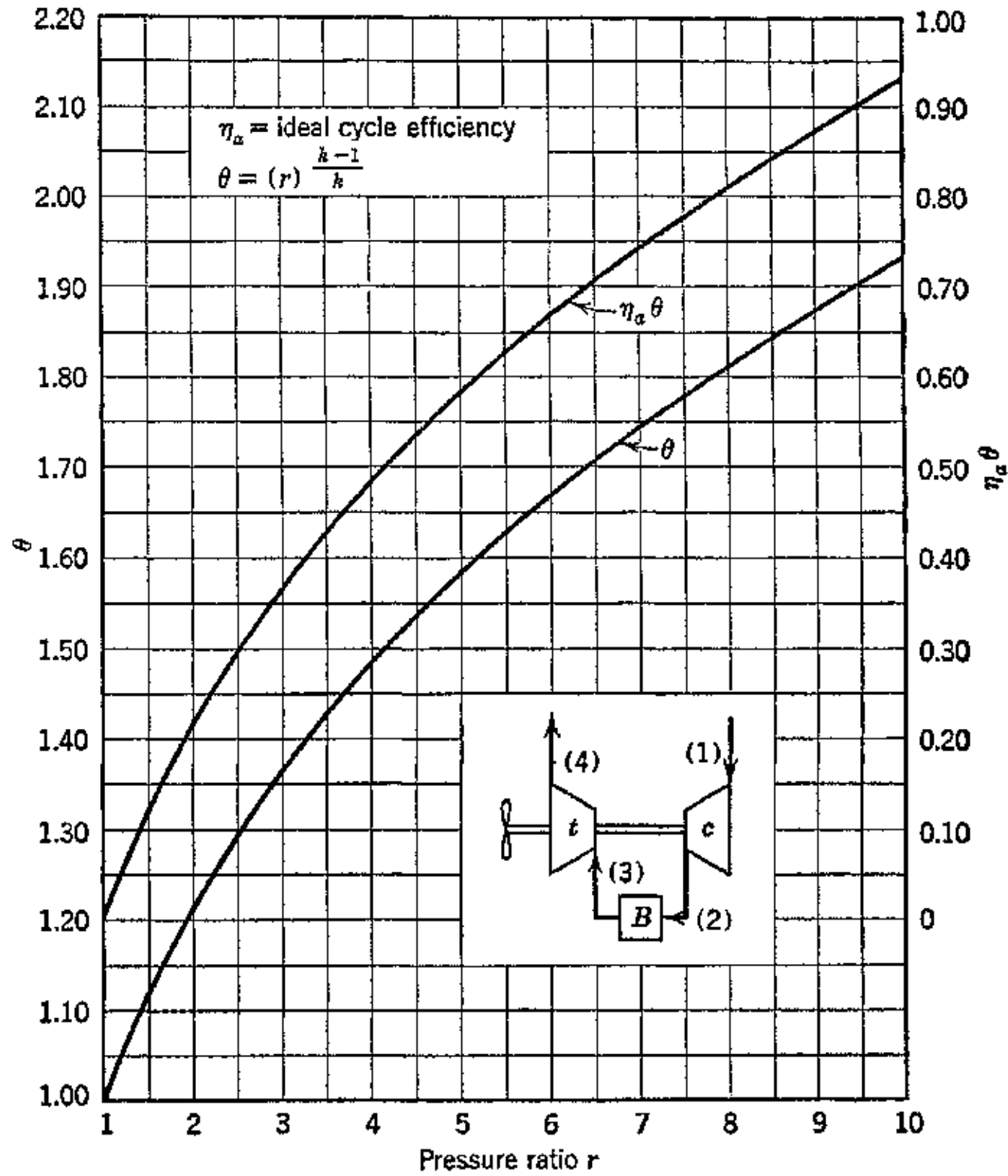
Fig. 18.   Parameters θ and $\eta_a \theta$ vs. pressure ratio.

The equation for the cycle efficiency reduces to

$$\eta = \frac{0.40(1410 - 1.98 T_1)}{1660 - 1.78 T_1}$$

If the plant is designed for an intake temperature $T_1 = 530$ R and a pressure ratio of 6, the cycle efficiency is $\eta = 0.201$. If none of the operating conditions are changed and the inlet temperature is lowered to 500 R, a drop of 30 R, the efficiency of the cycle becomes $\eta = 0.218$. This is equivalent to an improvement in the plant

efficiency of 9 per cent. Reducing the temperature T_1 to 430 R raises the cycle efficiency to $\eta = 0.249$. This demonstrates that the efficiency of an aircraft gas-turbine power plant will increase with the operating altitude.

The effect of inlet air temperature on the *air rate* W_a and the *work ratio* U for this same plant is determined in the following manner.

(b) **Air Rate.** This criterion has been defined in Section 5 and is given by

$$W_a = \frac{2545}{L/J}$$

For the plant in question, operating with the pressure ratio $r = 6$ and $T_3 = 1660$ R, the isentropic turbine output, taking into consideration the variation in specific heat with temperature, is $L_t/J = 162.8$ Btu/lb. Hence, the actual output is $\Delta h_t = 162.8 \times \eta_t = 162.8 \times 0.85 = 138.3$ Btu/lb. The turbine output in Btu per pound of air is independent of the intake air temperature. The latter only affects the work required to operate the compressor and the heat which must be supplied in the combustion chamber. The compression work at 530 R is

$$\Delta h_c = \frac{L_c/J}{\eta_c} = \frac{84.8}{0.84} = 101.0 \quad \text{Btu/lb}$$

The results of calculation of the effect of the temperature of the air at the inlet to the compressor T_1, upon the compression work Δh_c, the plant output L, and the air rate W_a, are tabulated below.

T_1 °R	Δh_c Btu/lb	L/J Btu/lb	W_a lb air/hp-hr
400	76.3	62.0	41.0
460	87.7	50.6	50.3
500	95.5	42.8	59.5
530	101.0	37.3	68.3
575	109.5	28.8	88.3
600	114.3	24.0	106.2

It is seen that reducing the inlet air temperature 30 F from the design value $T_1 = 530$ R reduces the weight of air which must be handled to obtain the same power output to 86 per cent of the design value, or 14 per cent. The decrease in required plant air capacity is consequently approximately 5 per cent per 10 F reduction in air temperature.

(c) **Work Ratio.** The work ratio U is defined as the ratio of the net output of the plant to the output of the turbine. Thus

$$U = \frac{L}{L_t}$$

For the plant conditions assumed here the gross turbine work $L_t/J = 138.3$ Btu/lb. The plant outputs corresponding to different
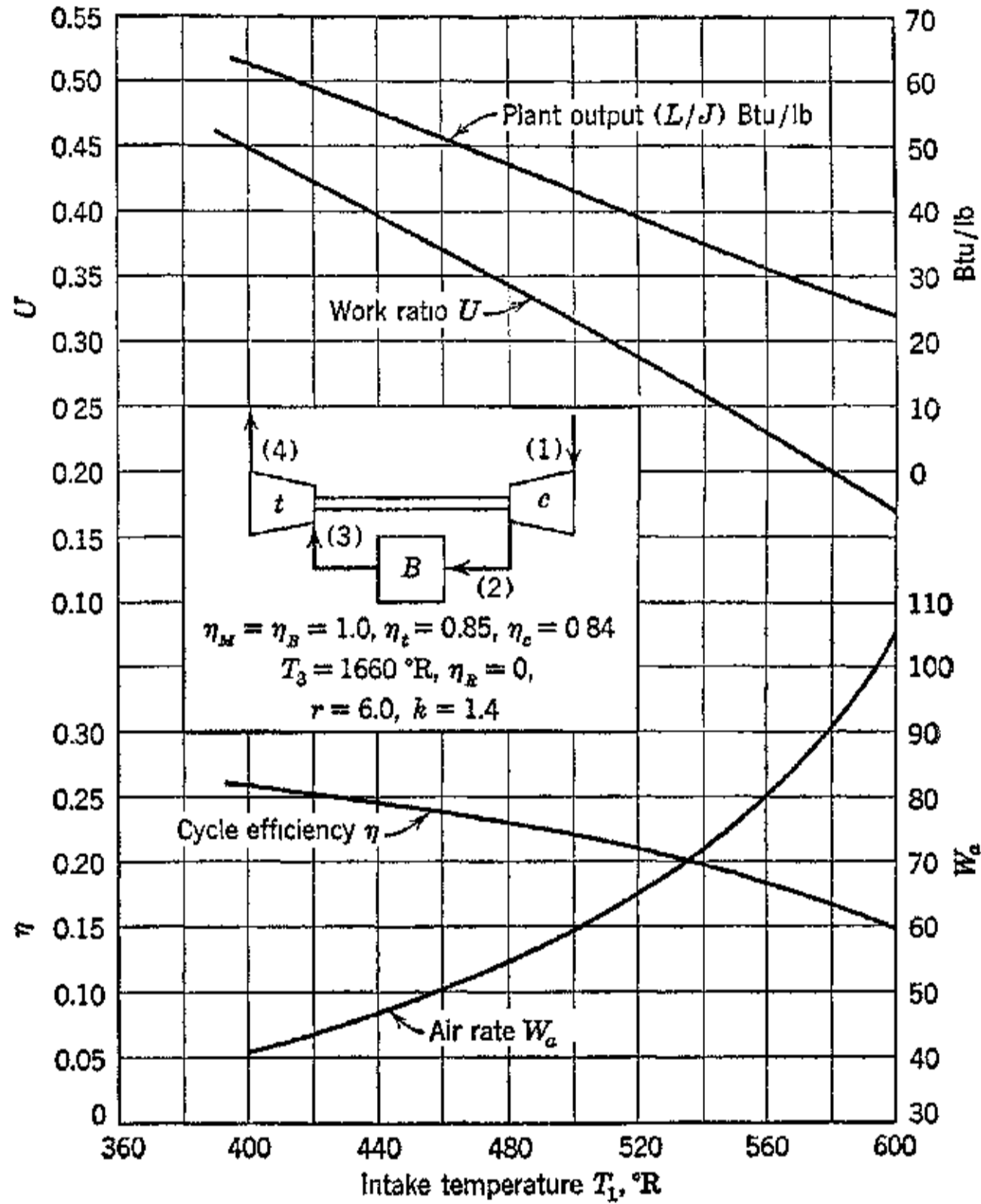
FIG. 19. Effect of inlet air temperature upon the performance characteristics of the open-cycle gas-turbine power plant.

values of T_1 are listed in the preceding table. The work ratio U as a function of T_1 is presented in Fig. 19.

It is seen from Fig. 19 that with $T_1 = 530$ R the plant output is only 26.9 per cent of the total work done by the turbine. Reduc-

ing the inlet air temperature to 500 R increases the plant output, owing to the reduction in compression work, to 30.9 per cent of the turbine gross power. This is equivalent to a 15 per cent increase in power output for a reduction of 30 F in the inlet air temperature.

12. Effect of Machine Efficiency

It has been mentioned in a preceding section that the power output and thermal efficiency of the open-cycle gas turbine are affected by the efficiencies of the air compressor and the turbine. The less efficient the latter machines, the higher must be the temperature T_3 of the working fluid entering the turbine. The minimum value for the required turbine throttle temperature to produce useful work can be determined in the following manner.

For convenience let it be assumed that $\eta_M = \eta_B = 1$, $T_1 = 520$ R, and $\eta_c = \eta_t$. Since the useful work L is the difference between the gross output of the turbine Δh_t and the work required by the compressor Δh_c, the output of the plant is zero when $\Delta h_t = \Delta h_c$. Substituting, for these works from equations 11 and 13, the condition for zero output is

$$\eta_t T_3 \left(\frac{Z}{1 + Z} \right) = \frac{T_1}{\eta_c} Z$$

where $Z = \theta - 1 = (T_2'/T_1) - 1$.

Hence useful work is obtained from the open-cycle gas turbine provided that $\eta_t T_3 > T_2'/\eta_c$. Since the isentropic compression temperature T_2' depends upon the pressure ratio of the gas turbine, there is, of course, a minimum throttle temperature corresponding to each pressure ratio.

The turbine inlet temperature T_3 corresponding to zero output is accordingly given by $T_3 = T_2'/\eta_c\eta_t$.

EXAMPLE. Calculate the minimum turbine throttle temperature for useful work from an open-cycle gas turbine under the following conditions.

$$r = 2, 4, 6, 10$$

$$\eta_t\eta_c = 0.3, 0.4, 0.5, 0.6, 0.7, 0.8, 0.9$$

$$T_1 = 520 \text{ R}, \quad k = 1.4$$

$$T_2' = \theta T_1, \text{ Table 7 1}$$

The results of the calculations are presented in Table 7 4.

TABLE 7·4

Pressure Ratio r	Isentropic Compression Temperature T_2'	Turbine Throttle Temperatures T_3 R						
		Machine Efficiency values $\eta_t\eta_c$						
		0 3	0.4	0.5	0.6	0.7	0.8	0.9
2	633	2120	1580	1270	1060	905	790	705
4	777	2580	1950	1560	1290	1110	990	865
6	880	2930	2200	1760	1470	1260	1100	980
10	1010	3360	2520	2020	1680	1440	1260	1110

These results have already been presented graphically in Fig. 3.

Examination of Fig. 3 or the preceding table makes it apparent why the early inventors were unable to produce any useful output with their gas-turbine plants. As an example, consider Armengaud's gas turbine. This plant was equipped with air compressors for which $\eta_c = 0.65$. If it is assumed that the turbine efficiency was of this same magnitude, then the product $\eta_c\eta_t = 0.42$. An open-cycle gas-turbine plant having this machine efficiency, neglecting all other losses, will produce zero net output for a pressure ratio of 2 when the turbine inlet temperature is as high as 1500 R (1040 F). This is very close to the temperature and pressure ratio actually employed.

Modern compressors and turbines have efficiencies of the order of 0.80 to 0.90. For such machines, assuming that $\eta_t\eta_c = 0.725$, useful work can be produced with turbine throttle temperatures as low as 500 F.

Raising the turbine inlet temperature is very effective in increasing the plant output of a modern plant. Thus consider a plant equipped with machinery for which $\eta_t = \eta_c = 0.80$.

The plant output in Btu per pound is given by

$$\frac{L}{J} = \eta_a\eta_M\left(\eta_t T_3 - \frac{1}{\eta_c}T_2'\right)c_p$$

Thus, if $\eta_M = 0.98$, $r = 6.0$, $T_1 = 520$ R, then $\eta_a = 0.40$; $T_2' = 875$ R; $1/\eta_c T_2' = 1090$ R. Hence

$$L/J = 0.4 \times 0.98(0.8T_3 - 1090)c_p$$

$$L/J = 0.392(0.8T_3 - 1090)c_p \quad \text{Btu/lb}$$

The effect of turbine inlet temperature upon the plant air rate is illustrated in Fig. 20. Raising the turbine inlet temperature from

T_3 = 1400 R to T_3 = 1600 R increases the output of this particular plant from L/J = 11.5 Btu/lb to L/J = 73.0 Btu/lb—an increase of more than 600 per cent. The corresponding reduction in the air rate is from 220 lb of air per hp-hr to 34.8. The great effect that high turbine throttle temperature has upon the performance characteristics of the gas-turbine plant must continually be kept in mind. The results discussed above demonstrate the importance of metal-lurgical developments to this type of power plant.
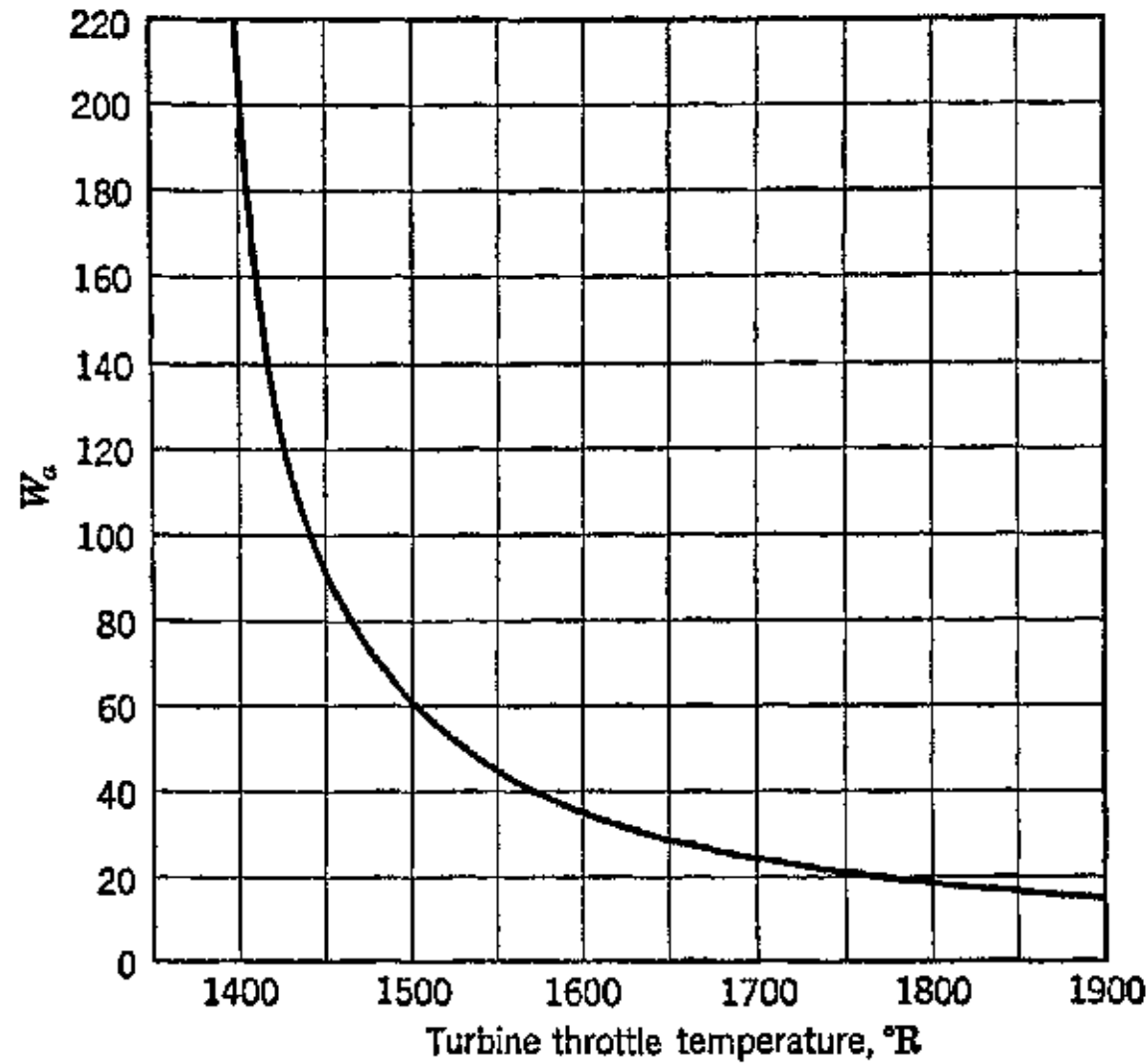
FIG. 20.   Effect of turbine inlet temperature upon the air rate.   (T_1 = 520 R, r = 6.0, η_M = 0.98.)

13. The Effect of Pressure Losses

The importance of designing the continuous-combustion gas turbine so that the pressure losses are kept at a minimum value has been mentioned in the preceding. These losses occur in the piping connecting the air compressor and the combustion chamber, in the combustion chamber itself, in the piping connecting the combustion chamber and the turbine, in the discharge stack, and in the regenerator if one is included.

The pressure drops which affect the compressor make it necessary to increase its pressure ratio in order to overcome them. This obviously increases the compression work required above that for the theoretical plant without pressure drops. The pressure drops

upstream and downstream to the turbine reduce its expansion ratio and, therefore, its output. Consequently, if they are too large the turbine throttle temperature to produce a required net output may have to be too high to give reliable operation.

In analyzing a gas-turbine plant these losses can be taken into account by several methods all of which will give the correct values for plant efficiency, air rate, and work ratio. Thus, the piping losses can be evaluated so that they can be added together and subtracted directly from the turbine output without introducing corrections for the changed compressor and turbine pressure ratios. Another method is to reduce the actual efficiencies of the turbine and compressor by amounts that account for the pressure losses. These methods are entirely satisfactory for making plant studies. Where the actual design of a plant is involved, the pressure drops should be taken into consideration at the exact locations where they occur, since the selection of the final pressure ratios of the turbine and compressor must be made with full cognizance of the actual pressure ratios involved.

The following numerical example illustrates the procedure where all losses are combined and subtracted from the turbine output.

DATA

$\eta_t = 0.90$, $\eta_c = 0.85$, $\eta_R = 0.75$, $\eta_B = 0.98$, $T_1 = 528$ R, $T_3 = 1617$ R

Losses

Combustion chamber	$\lambda_B = 0.54$	Btu/lb
Piping	$\lambda_P = 0.90$	
Regenerator	$\lambda_R = 0.90$	
	$\Delta h_L = 2.34$	Btu/lb

Regenerator equation, $T_{2R} - T_2 = 0.75(T_4 - T_2)$.

TURBINE

Pressure Ratio r	$\dfrac{L_t}{J}$	$\dfrac{\eta_t L_t}{J}$	T_3/T_4'	c_p (av.)	$T_3 - T_4$	T_4	$\dfrac{\eta_t L_t}{J} - \Delta h_L$
2.5	90.5	81.4	1.292	0.2565	317	1300	79.1
4.0	128.5	116.0	1.472	.2595	447	1170	113.7
6.0	158.2	142.0	1.652	.2577	552	1065	139.7

	Compressor		Regenerator			
r	$\dfrac{L_c}{J}$	$\dfrac{L_c}{\eta_c J}$	T_2	$0.75T_4$	$0.25T_2$	T_{2R}
2.5	37.9	44.6	713	975	178	1153
4.0	61.5	72.3	827	879	207	1086
6.0	84.6	99.6	938	800	237	1037

COMBUSTION CHAMBER

r	$T_3 - T_{2R}$	c_p (av.)	Q_i'	$\dfrac{1}{\eta_B} Q_i'$
2.5	464	0 2600	120.5	123 0
4.0	531	2590	137.5	140 2
6.0	580	.2582	149.6	153.0

POWER AND EFFICIENCY

r	$\dfrac{\eta_t L_t}{J} - \dfrac{L_c}{\eta_c J} - \Delta h_L$	hp/lb sec (air)	η	W_a lb/hp-hr	Work Ratio U
2.5	34.5 Btu/lb	48.7	28.0	74.0	0.425
4.0	41.04	58.4	29.5	61.5	.357
6.0	40.1	57.1	26.4	62.9	.283

The method whereby the efficiencies η_c and η_t are altered to compensate for the pressure drops is based on the following thermodynamic considerations.

If the pressure ratio for the cycle without pressure drop is r_c, the compression work assuming no pressure drops is

$$\Delta h_c = \frac{1}{\eta_c} \frac{L_c}{J} \quad \text{Btu/lb} \tag{41}$$

Owing to the pressure drops which must be overcome by the compressor, its actual pressure ratio must be larger than r_c. The corresponding compression work will also be larger than the Δh_c above.
Let

r_{cp} = pressure ratio of compressor to take care of pressure drop
Δh_{cp} = compression work corresponding to r_{cp}

Then,

$$\Delta h_{cp} = \frac{1}{\eta_c} \frac{L_{cp}}{J} = \frac{1}{\eta_{cp}} \frac{L_c}{J} \tag{42}$$

where L_{cp} = isentropic compression work corresponding to r_{cp} in ft-lb/lb.

η_{cp} = adjusted compressor efficiency to take care of pressure loss with compression ratio r_c.

The ratio

$$\frac{\eta_{cp}}{\eta_c} = \frac{\Delta h_c}{\Delta h_{cp}} = \frac{L_c}{L_{cp}} \tag{43}$$

But $r_c = p_2/p_1$ and

$$r_{cp} = \frac{p_2 + \Delta p}{p_1} = \frac{p'}{p_1}$$

where Δp = pressure drop.

$$p' = p_2 + \Delta p = p_2 \left(1 + \frac{\Delta p}{p_2} \right) \tag{44}$$

The actual value of the pressure loss Δp is determined from the velocities in the piping, its friction factor, and its configuration. Where possible the data should be obtained by actual test of a model or mock-up of the proposed layout.

The values of L_{cp} and L_c can be determined by the method discussed in Chapter 4, if the variation of the specific heat of the air with temperature is to be taken into account. For the analytical purposes being discussed here, the air will be assumed to behave in accordance with the laws of perfect gases. Consequently, with the foregoing assumption the compression work required with zero pressure loss is

$$\Delta h_c = \frac{c_p T_1}{\eta_c} Z_c = \frac{c_p T_1}{\eta_c} (\theta - 1) \tag{45}$$

Similarly

$$\Delta h_{cp} = \frac{1}{\eta_c} c_p T_1 Z_{cp} \quad \text{Btu/lb} \tag{46}$$

The work Δh_{cp} is greater than Δh_c by the additional compression required to overcome the pressure drop.

An equivalent expression for Δh_{cp} can be written if the compressor efficiency is decreased and the compression ratio r_c is used instead of r_{cp}. Thus

$$\Delta h_{cp} = \frac{1}{\eta_{cp}} \cdot c_p T_1 Z_c \tag{47}$$

Expressions 46 and 47 must be equal. Hence

$$\frac{1}{\eta_c} c_p T_1 Z_{cp} = \frac{1}{\eta_{cp}} c_p T_1 Z_c$$

or

$$\frac{\eta_{cp}}{\eta_c} = \frac{Z_c}{Z_{cp}} \tag{48}$$

From equation 48 the adjusted efficiency of the compressor can be calculated.

The equations for the output of the turbine with pressure drop are obtained in an analogous manner.

$$\Delta h_t = \eta_t \frac{L_t}{J} = \eta_t c_p T_3 \frac{Z_t}{1 + Z_t} \quad \text{Btu/lb} \tag{49}$$

and

$$\Delta h_{tp} = \eta_t \frac{L_{tp}}{J} = \eta_t c_p T_3 \frac{Z_{tp}}{1 + Z_{tp}} \quad \text{Btu/lb} \tag{50}$$

where $Z_t = (r_t)^{\frac{k-1}{k}} - 1.$

$Z_{tp} = (r_{tp})^{\frac{k-1}{k}} - 1.$

r_t = pressure ratio of turbine with no pressure loss.

r_{tp} = pressure ratio of turbine with pressure loss.

η_t = actual efficiency of turbine.

η_{tp} = efficiency of turbine compensated to take care of pressure loss.

For the case where there is pressure drop, equation 50 becomes

$$\Delta h_{tp} = \eta_{tp} c_p T_3 \frac{Z_t}{1 + Z_t} \tag{51}$$

The adjusted efficiency of the turbine η_{tp} is obtained like the adjusted efficiency of the compressor η_{cp}. Hence,

$$\Delta h_{tp} = \eta_{tp} c_p T_3 \frac{Z_t}{1 + Z_t} = \eta_t c_p T_3 \frac{Z_{tp}}{1 + Z_{tp}} \tag{52}$$

and

$$\eta_{tp} = \eta_t \left(\frac{Z_{tp}}{1 + Z_{tp}} \cdot \frac{1 + Z_t}{Z_t} \right) \tag{53}$$

Since Z_t and Z_c are equal for the conditions of zero pressure loss, $r_t = r_c$ and the subscripts t and c can be dropped. Thus

$$\frac{\eta_{cp}}{\eta_c} = \frac{Z}{Z_{cp}} \tag{54}$$

and

$$\frac{\eta_{tp}}{\eta_t} = \frac{1 + Z}{Z} \cdot \frac{Z_{tp}}{1 + Z_{tp}} \tag{55}$$

If the pressure losses are combined in one machine, no adjustment is needed in the efficiency of the other machine. If the pressure drops are to be segregated into those affecting each machine, both the compressor and turbine efficiencies require adjustment.

In making the calculations it is convenient to express the pressure drops as a percentage of the design pressure ratio.

To illustrate the method for determining the effect of pressure loss consider the following example.

EXAMPLE. A stationary non-regenerative gas-turbine plant has a design pressure ratio of 6.0. Assume that the pressure loss up to the turbine is 5 psi and that the back pressure in the turbine is raised (by resistances) 2 psi. Calculate the reduction in output due to the pressure loss.

For compressor

$$r = 6, \quad r_{cp} = 6 + \frac{5}{14.7} = 6.34$$

For turbine

$$r = 6, \quad r_{tp} = 6 - \frac{2}{14.7} = 5.863$$

For $k = 1.395$ and $r = 6$

$$Z = 0.6604 = Z_t = Z_c$$

$$Z_{cp} = 0.6865, \quad Z_{tp} = 0.6496$$

$$\frac{\eta_{cp}}{\eta_c} = \frac{Z}{Z_{cp}} = \frac{0.6604}{0.6865} = 0.963$$

$$\frac{\eta_{tp}}{\eta_t} = \frac{Z_{tp}}{1 + Z_{tp}} \cdot \frac{1 + Z}{Z} = \frac{0.6496}{1.6496} \times \frac{1.6604}{0.6604} = 0.99$$

If $\eta_c = \eta_t = 0.85$, $c_p = 0.243$, $T_1 = 520$ R, $T_3 = 1600$ R, then $\eta_{cp} = 0.818$ and $\eta_{tp} = 0.842$.

Output with pressure loss

$$\frac{L_p}{J} = \eta_{tp}\frac{L_t}{J} - \frac{1}{\eta_{cp}}\frac{L_c}{J}$$

$$= 0.842 \times 0.243 \times 1600 \times 0.398 - \frac{1}{0.818} \times 0.243 \times 520 \times 0.6604$$

$$= 130.5 - 102.0 = 28.5 \quad \text{Btu/lb}$$

Output without pressure loss

$$\frac{L}{J} = 0.85 \times 0.243 \times 1600 \times 0.398 - \frac{1}{0.85} \times 0.243 \times 520 \times 0.6604$$

$$= 132 - 98.4 = 33.6 \quad \text{Btu/lb}$$

The loss in output is 15.2 per cent even with a highly efficient compressor and turbine.

14. Effect of Stage Intercooling of Compressor

The effect of intercooling between the stages of the compressor is best illustrated by means of a numerical example. Thus consider two simple gas-turbine plants operating between the same tempera-

ture limits and pressure ratio. Assume that each plant has identical equipment, and the basic data are

$$\eta_t = 0.90, \qquad \eta_c = \eta_{c1} = \eta_{c2} = 0.85$$

$$T_1 = 528 \text{ R}, \qquad T_{2b} = 546 \text{ R}, \qquad T_3 = 1617 \text{ R}$$

$$\lambda_B = 0.54 \text{ Btu/lb}, \qquad \lambda_p = 0.90 \text{ Btu/lb}, \qquad \lambda_{ic} = 0.36 \text{ Btu/lb}$$

$$\eta_B = 1.00, \qquad \Sigma\lambda_1 = 1.44 \text{ Btu/lb}, \qquad \Sigma\lambda_2 = 1.80 \text{ Btu/lb}$$

Consider the plant utilizing intercooling, and assume equal stages of compression for compressors c_1 and c_2.

	TURBINE			COMPRESSOR c_1		
r	$\dfrac{L_t}{J}$	$\dfrac{\eta_t L_t}{J}$	$\dfrac{\eta_t L_t}{J} - \Sigma\lambda_2$	$\dfrac{L_{c1}}{J}$	$\dfrac{L_{c1}}{\eta_c J}$	T_{2a}
2.5	90.3	81.3	79.5	17.75	20 9	615.5
4.0	129 4	116.5	114.7	27 78	32 7	664
6.0	158.0	142.2	140.0	37.0	43.5	709
10.0	192.0	172.8	171.0	48.3	57.0	764

	COMPRESSOR c_2		TOTAL COMPRESSOR WORK	NET OUTPUT
r	$\dfrac{L_{c2}}{\eta_c J}$	T_{2b}	$\dfrac{L_{c1} + L_{c2}}{\eta_c J}$	$\dfrac{\eta_t L_t}{J} - \dfrac{1}{\eta_c J}(L_{c1} + L_{c2}) - \Sigma\lambda_2$
2.5	21.5	636	42.4	$79.5 - 42.4 = 37.1$ Btu/lb
4.0	33.8	687	66.5	$114 7 - 66.5 = 48.2$
6.0	45.2	734	88.7	$140.0 - 88.7 = 51.3$
10.0	60.1	795	117.1	$171.0 - 117.1 = 53.9$

	COMBUSTION CHAMBER				PERFORMANCE		
r	$\bar{c}_p$	$T_3 - T_{2B}$	Δh_B	η	hp/lb sec	W_a	Work Ratio (U)
2.5	0.2527	981	248	14.9	52.6	68.5 lb/hp-hr	0.466
4.0	.2534	930	236	20.5	69.6	52.6	.419
6.0	.2540	873	225	22.8	72.5	49.6	.365
10.0	.2549	822	211	25.6	76.3	47.3	.316

The results for plant 1 are compared with those for plant 2 in Table 7·5. From this comparison it is seen that the benefits of intercooling between stages is to reduce the size of plant required. Its effect on efficiency is slight and is beneficial only at high pressure ratios. At the low pressure ratios the heat removed from the first stages is larger than the reduction in power required to operate the

compressor without intercooling. Consequently, since this same quantity of heat must be furnished as an additional quantity in the combustion chamber, the cycle efficiency is slightly lower.

TABLE 7-5

COMPARISON OF SAME PLANT WITH AND WITHOUT INTERCOOLING

Pressure Ratio	η		hp/lb sec		Air Rate, W_a		Work Ratio, U	
	Plant 1	Plant 2	Plant 1	Plant 2	Plant 1	Plant 2	Plant 1	Plant 2
2.5	15.4	14.9	50.0	52.6	72.0	68.5	0.44	0.466
4.0	20.6	20.5	59.0	69.6	61.0	52.6	.368	.419
6.0	23.4	22.8	57.8	72.5	62.5	49.6	.290	.365
10.0	23.5	25.6	44.5	76.3	80.5	47.3	.185	.316

15. Development Possibilities of the Aircraft Gas Turbine

The trend in aviation has been to faster and still faster airplanes. This has necessitated the development of more powerful internal-combustion engines having increased complexity. It appears that the practical limit to engine size is being approached, so that new forms of power plants, such as the gas turbine and certain forms of thermal jet engines must be given thorough consideration. According to reference 9 the trend in the weights of large-output reciprocating engines is as illustrated in Fig. 21.
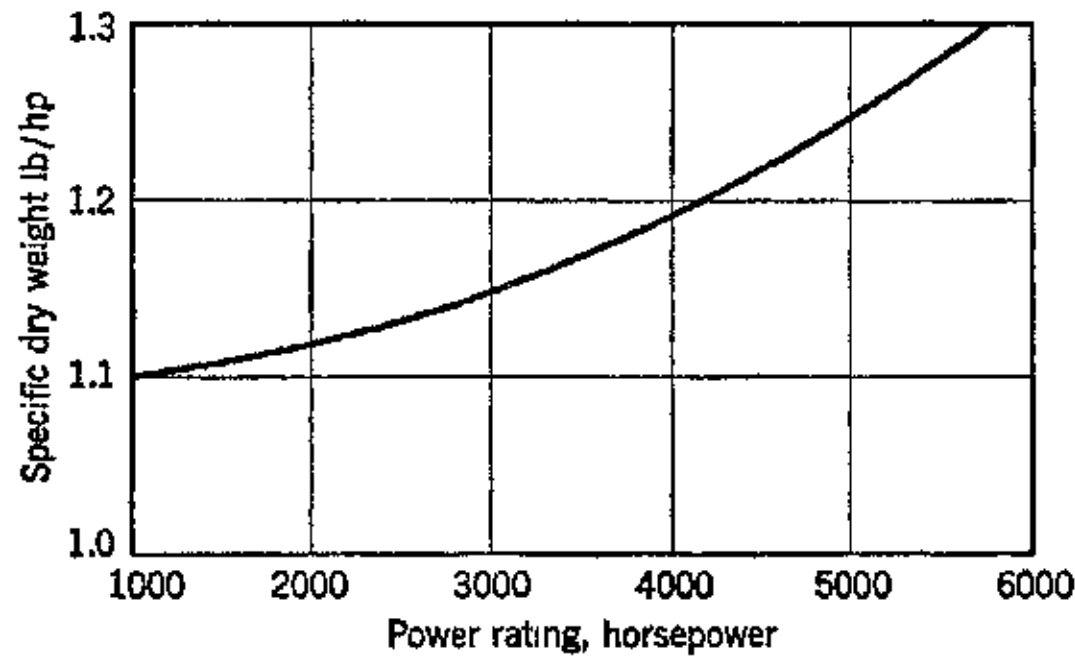
FIG. 21.   Trend in reciprocating engine weights.   (Based on Sir A. H. Roy Fedden, *Proc. Royal Aero. Soc.*, May 25, 1944.)

The development possibilities of the gas turbine for aircraft, called the *turboprop engine*, are such that its potentialities and its problems deserve detailed consideration.

(*a*) **Potentialities.** The analysis presented in this chapter indicates that the open-cycle continuous gas turbine driving a propeller has

great potentialities as an aircraft power plant. It is apparent that its future is closely allied to the engineering development of more efficient air compressors and turbines, particularly air compressors. Another major factor will be the future development of alloys permitting operation at higher temperatures than are currently possible. According to F. W. Godsey and C. D. Flagle,[18] operation with gases entering the turbine at 1500 F is a possibility today. Such a power plant with turbine and compressor efficiencies of 0.85, operating with a pressure ratio of 10, will achieve a cycle efficiency of $\eta = 0.26$ under standard sea-level conditions. At an altitude of 15,000 ft this cycle efficiency will increase to approximately 30 per cent.

The effect that machine efficiency has upon the cycle efficiency has been discussed in this chapter. It can be said generally that, if an improvement of 1 per cent is effected in machine efficiency, the corresponding improvement in the cycle efficiency will be approximately 3 per cent. Since the machines currently in use have not been developed to the state where they achieve the maximum efficiencies that appear to be attainable, there is justification in the belief that the future will bring more efficient compressors and turbines.

The importance of metallurgical developments to the future of the gas turbine cannot be overemphasized, since a permissible increase in turbine inlet temperature markedly increases the net output and the cycle efficiency.

An important consideration that should not be disregarded is that the problems to be solved in order to improve the efficiency and the horsepower per pound weight of the gas-turbine plant are mechanical engineering and metallurgical problems. The developments can follow well-established procedures without any regard to fuel technology.[9] This is a distinct advantage. The development of the reciprocating internal-combustion engine, on the other hand, is considerably dependent upon the progress in the development of better anti-knock fuels.

For aircraft designers to accept the continuous-combustion gas turbine as an airplane power plant in the immediate future, this prime mover must be designed to have a lower weight-to-power ratio than is obtainable with the reciprocating engine. Otherwise a sacrifice in range will be necessary. This requirement should not be difficult to meet. According to the literature (reference 18) it appears to be a distinct possibility, today, for the installed weight of the turboprop engine to be less than three-quarters of the weight of an equivalent piston engine.

One of the many attractive features of the continuous-combustion gas turbine is its ability to employ cheap, low-grade fuels such as kerosene or distillates. This freedom from special fuels should be welcome to the aeronautical engineer. Other advantages are freedom from such problems as detonation, supercharging, vapor lock, and engine cooling. Furthermore, since all the machine elements of the gas turbine involve solely rotating parts there is considerably less vibration than there is with reciprocating engines and there should be
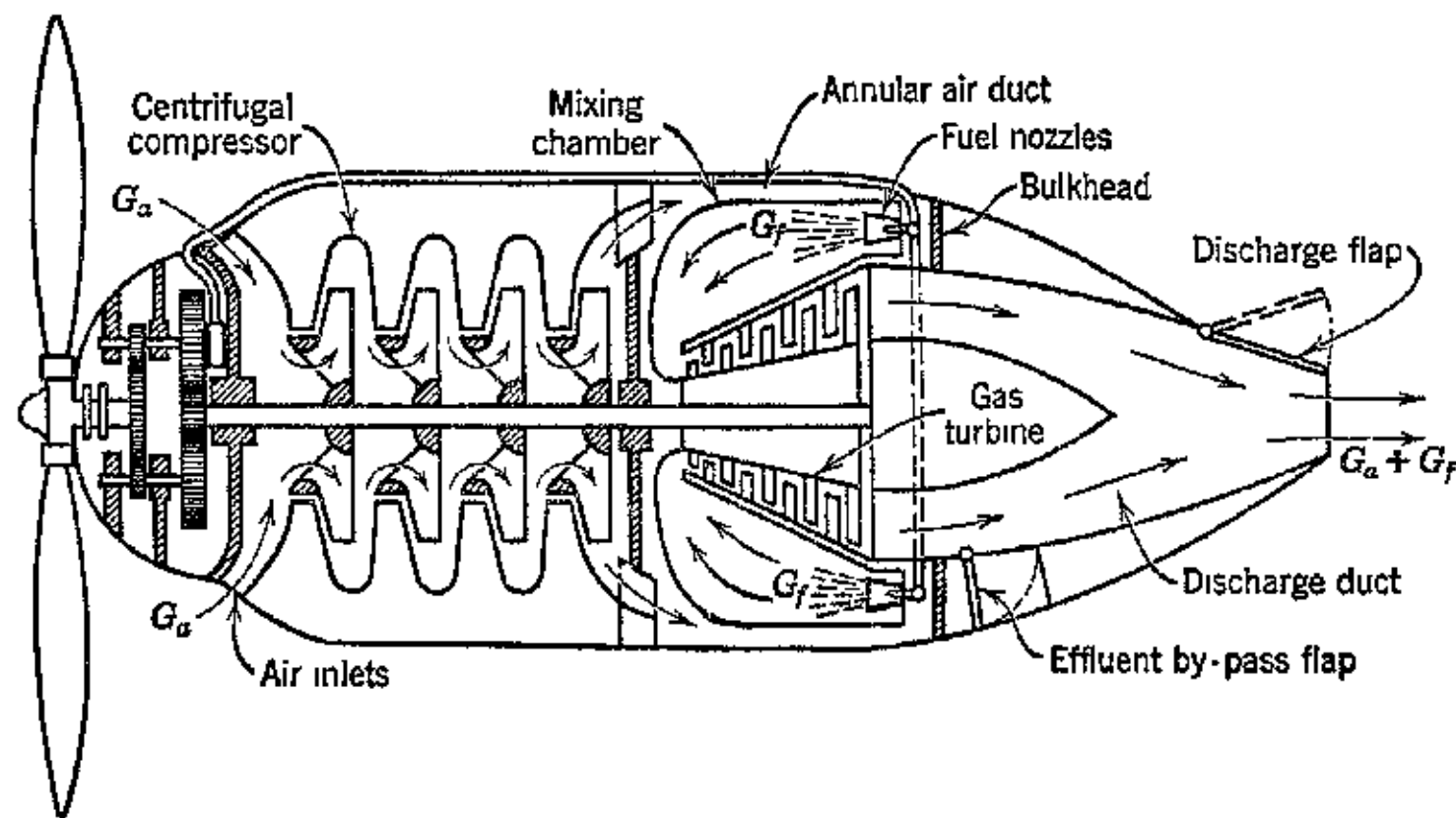
FIG. 22. Turboprop engine with auxiliary jet propulsion design of Ljungström Ångturbin. (From *Gas Turbines and Jet Propulsion for Aircraft*, published by Aircraft Books, Inc., N. Y. C.)

a reduction in maintenance. It seems probable that, except for periodic renewals of parts of the combustion chamber, the periods between major overhauls should be several times that currently the practice for reciprocating internal-combustion engines.

Another factor of great importance to the airplane designer is that the diameter of the gas turbine can be made less than one-half the diameter of an equivalent internal-combustion engine. Consequently, the smaller frontal area of the gas turbine makes it possible to reduce airplane drag to much lower values than are possible with a reciprocating-engine power plant. Furthermore, its smaller diameter offers the possibility of submerging the gas turbine in the wing thereby giving the airplane greater aerodynamic cleanliness than is now possible.

Figure 22 illustrates an application of the aircraft gas turbine. This is a patent disclosure of the Ljungströms Company, Sweden.

The gas turbine comprises a four-stage centrifugal compressor driven by a five-stage reaction turbine. The propeller is driven through gearing. For a fuller description see Chapter 8, reference 1. The arrangement gives propeller propulsion with auxiliary thermal jet propulsion.

Another arrangement for propeller drive with auxiliary thermal jet propulsion is shown in Fig. 23, which is a conception of the
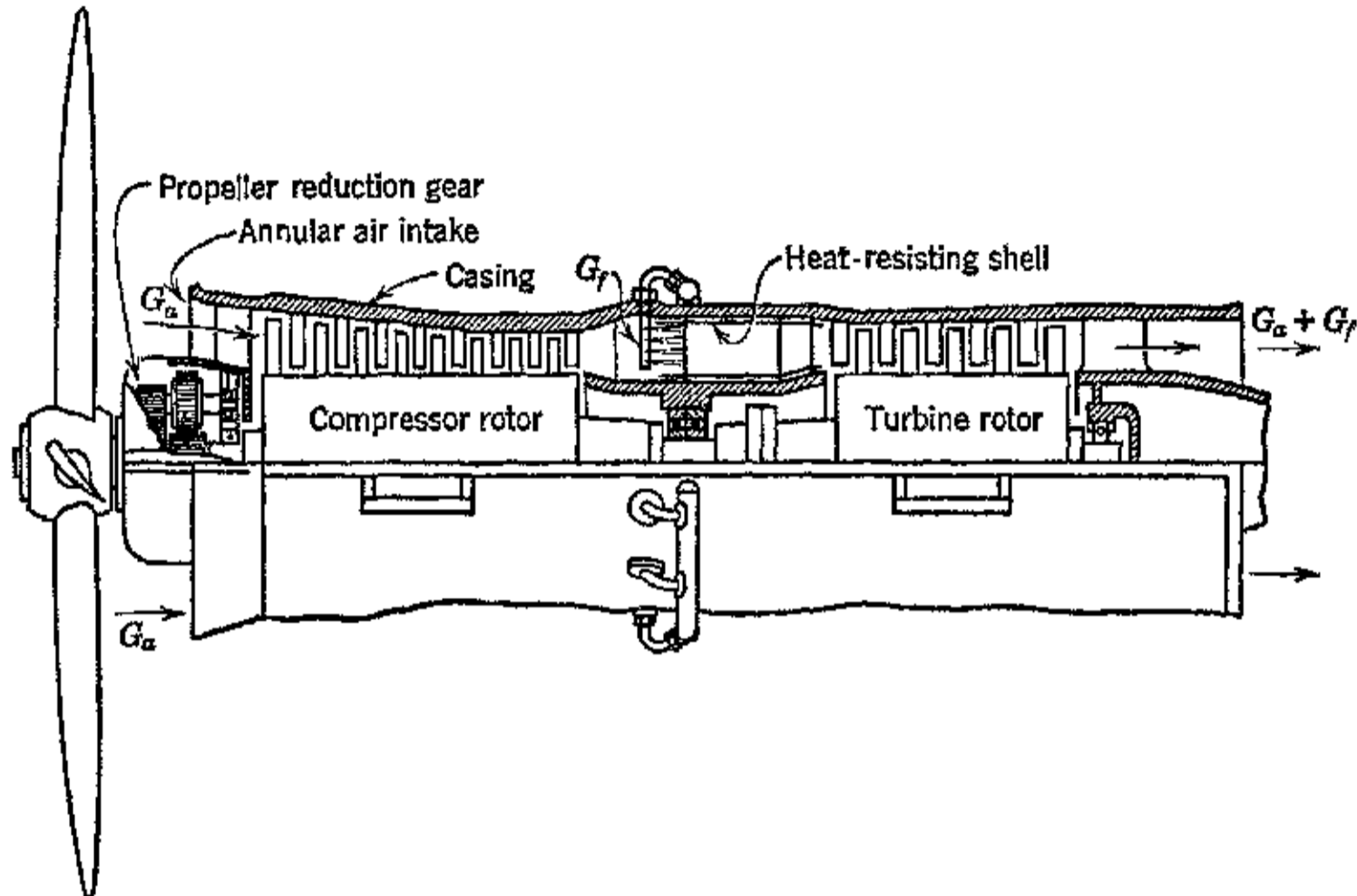
FIG. 23.   Brown-Boveri design of a turboprop engine with auxiliary jet propulsion. (From *Gas Turbines and Jet Propulsion for Aircraft*, published by Aircraft Books, Inc., N. Y. C.)

Brown-Boveri Company. A multistage axial flow compressor and a multistage turbine are used. The particular feature of this unit is that the air flow continues in the longitudinal direction throughout the flow path.

(b) Metallurgy. The benefits that accompany the possible use of higher temperatures at the inlet to the turbine have been pointed out in the preceding. The solution of the problem of permitting higher operating temperatures is entirely one of metallurgical development. Alloys must be developed that are capable of withstanding dynamic loads under highly stressed conditions and have satisfactory creep characteristics at elevated temperatures.

Great progress has been achieved in this field during the past few years, and there is reason to believe that the future will bring alloys that will permit higher turbine inlet temperatures.

(c) **Compressors.** The importance of developing more efficient air compressors is apparent from the preceding sections. Three types of compressors have been employed or considered for gas turbines: the centrifugal compressor, the axial flow compressor, and the positive-displacement compressor.

The centrifugal compressor is the one most widely used for general purposes. Its application to turbo-supercharging has resulted in the development of light-weight designs capable of sustained operation at high rotative speeds. Most of the emphasis in this work has been directed to improving the efficiency and power output of the reciprocating internal-combustion engine rather than the efficiency of the centrifugal air compressor, the primary impetus being the overall reduction in engine weight.

In recent years the developments in connection with the centrifugal compressor have placed greater emphasis on efficiency. According to K. Campbell and J. E. Talbert, "Some Advantages and Limitations of Centrifugal and Axial Aircraft Compressors," *J.S.A.E.*, October, 1945, efficiencies of more than 80 per cent have been obtained experimentally with pressure ratios of 2.4:1 and 77 per cent with 3.0:1 pressure ratio. Despite this improvement in efficiency, these values must be raised still more if this type of air compressor is to play the dominant role in aircraft gas-turbine development, where the efficiency must be as high as possible.

Another limitation of the centrifugal compressor which appears unfavorable is its single-stage pressure ratio. It does not appear likely that this will be increased significantly above 4:1.0. Consequently, to obtain the high pressure ratios which will eventually be realized as the development of the aircraft gas turbine proceeds will necessitate multistaging. This increases the weight and complexity of the compressor installation and decreases the overall efficiency of the air-compressor system.

At present the axial-flow compressor appears to hold out the greatest promise for securing a high-efficiency compressor system of low weight and bulk. Efficiencies from 5 to 10 points higher than the maximum obtainable with centrifugal machines have been reported. The disadvantages suffered by the axial-flow machine is its low pressure ratio per stage, 1.05 to 1.15 atmospheres. Consequently, to obtain high pressure ratio, multistaging is required, which results in a rather lengthy machine necessitating careful design to secure low weight.

The axial-flow compressor is still in the early stages of its development, and few published data are available regarding its performance. It appears, however, that improvements are to be expected as the

aerodynamic knowledge of the flow of air through airfoil lattices becomes available. Furthermore, if it is developed so that higher peripheral speeds can be utilized improvements in pressure ratio per stage, efficiency, and reduced weight will be effected. It appears, therefore, that the axial-flow compressor will play an important role in the future development of the continuous-combustion gas turbine for aircraft and other applications. The eventual compressor plant for high pressure ratio turboprop engines will no doubt be a combination of the axial and centrifugal machines.

Another type of compressor that may exert an influence in the stationary and marine gas-turbine power plant field is the positive displacement helical lobe compressor invented by A. Lysholm of Sweden. This machine can be operated with high-rotative speed so that light-weight designs may be possible. Tests of an experimental Lysholm compressor of 10,000-cfm capacity operating at a pressure ratio of approximately 2.5 gave an adiabatic efficiency of 82 to 84 per cent.

(d) **Turbine.** No serious or unusual problems appear to be connected with the design of an efficient turbine to operate on heated gas, since there is no essential difference between such a turbine and the conventional steam turbine. The only real differences are those inherent in the high inlet temperatures. To obtain reasonable efficiencies the inlet temperature to the turbine must be above 1200 F. Operation at temperatures above this is possible today, since materials having sufficiently high endurance strength, low creep rate, and oxidation resistance have been developed. These developments, which originated in the field of turbo-supercharging, have made available a rich store of experience in the field of high-temperature metals. As mentioned above, further metallurgical advances are to be expected so that higher turbine inlet temperatures appear to be a distinct possibility.

There should be no insurmountable problems in developing a turbine of low weight. Owing to the low operating pressures, the turbine casing can be of light construction. Attention must be given to the solution of problems arising from thermal distortions. These are, however, largely design problems requiring careful analysis of the factors influencing the distortions. The same remarks are applicable to the solution of problems involving the expansion and contraction of parts assembled together. Care must be exercised in the design to preclude the possibility of damaging any of the parts because of these movements.

(e) **Combustion Chamber.** The problems pertinent to the combustion chamber are those connected with the maintenance of reliable

combustion under high loadings and the prevention of "burnouts."
The available refractory steels appear to have satisfactory properties
to withstand the type of service if adequately protected. By judi-
cious employment of the combustion air to cool the hot walls and
the use of protective coatings, it should be possible to obtain reason-
able life. Development in the application of ceramic coatings to
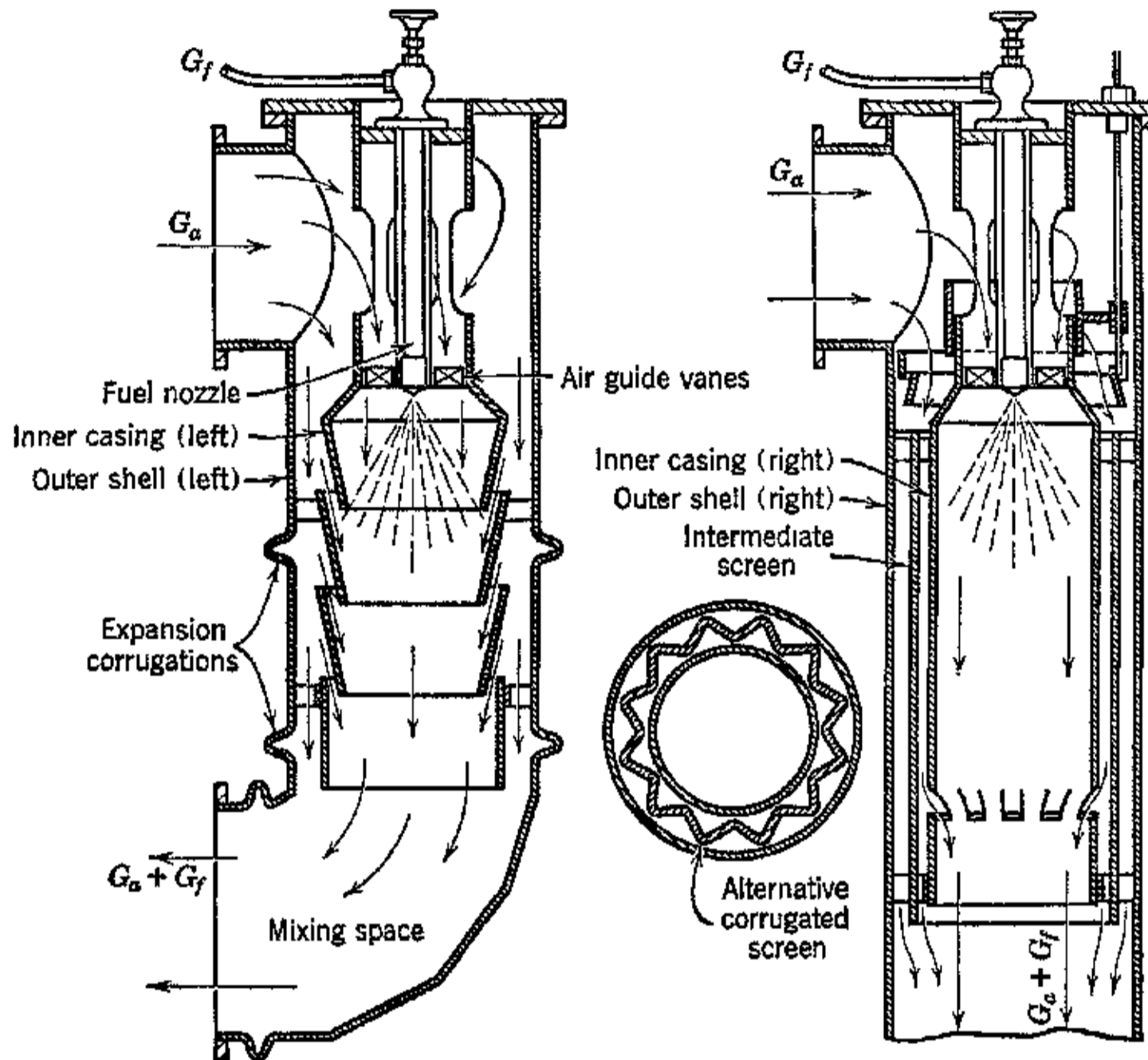
FIG. 24. Two designs of combustion chambers by Brown-Boveri. (From *Gas
Turbines and Jet Propulsion for Aircraft*, published by Aircraft Books, Inc., N. Y. C.)

alloy steels may aid in this connection and also make it possible to
employ higher heat releases. Major requirements confronting the
designer are the securing of flow conditions which will give clean and
stable combustion and high efficiency without introducing a serious
pressure loss. The deleterious effects of pressure losses upon the
efficiency of the cycle have been discussed in Section 13.

Two forms of combustion-chamber design developed by the Brown-
Boveri Company, Switzerland, are illustrated in Fig. 24. Both
designs utilize the excess air for cooling the region wherein combus-

tion takes place. The air then mixes with the combustion products and reduces their temperature to the desired value. It is important to have thorough mixing of the two fluid streams so that no flame will enter the turbine casing.

(f) **Regenerator.** Present knowledge of heat exchangers indicates that the regenerator will be difficult to integrate into the aircraft gas turbine. Despite its beneficial effect on part-load economy its space requirements and weight mitigate against its use in aircraft power plants. A light-weight, compact, highly efficient regenerator that could be adapted to airplane use would be of great value. Whether it is possible to develop such a heat exchanger can be answered only by vigorous prosecution of fundamental research in the heat-transfer field.

For stationary and marine applications, however, where space and weight limitations are not so severe as they are for aircraft, the regenerator has a definite place. The marine gas turbine built by the Elliott Company utilizes a regenerator and the reheat cycle. The thermal efficiency of this machine under test was slightly higher than 29 per cent.[14] This gas turbine also employs Lysholm compressors.

(g) **Piping.** The piping problems that arise can be solved by careful design. As already mentioned, the main problem is to arrange the piping so that dangerous stresses due to thermal distortion are avoided. The flow path for the working fluid should be arranged to keep the pressure losses at the lowest possible value. Because of the low operating pressures, the main stress considerations will be those related to the expansion and contraction of the connected components of the gas turbine. The foregoing difficulties will be greatly reduced if care is exercised to keep the piping for the high-temperature gases as short as possible. It is of advantage in this connection to locate the combustion chamber as close to the turbine as possible.

REFERENCES

1. A. Meyer, "The Gas Turbine, Its History, Development and Prospects," *Inst. Mech. Eng. Proc.*, 1939, Vol. 141, p. 197.
2. J. T. Retalliata, "The Gas Turbine, I, II, III," *Electric Review*, Allis Chalmers, December, 1941, March, 1942.
3. H. H. Supplee, *The Gas Turbine*, Lippincott, Philadelphia, Pa., 1920.
4. G. Stoney, "Scientific Activities of the Late Hon. Sir Charles A. Parsons," *Engineering*, 1937, Vol. 144, p. 695.
5. A. Meyer, "Velox Steam Generator," *Trans. A.S.M.E.*, 1935.
6. A. Meyer, *Oil and Gas Journal*, Vol. 37, p. 40, 1938.

7. O. W. SCHEY, "Comparative Performance of Superchargers," *N.A.C.A. Ann Report, 1931–1932.*

8. A. BUCHI, "Supercharging of Internal Combustion Engines with Blowers Driven by Exhaust Gas Turbines," *Trans. A.S.M.E.*, OGP-59-2, 1937.

9. SIR A. H. ROY FEDDEN, *Proc. Royal Aero. Soc.*, May 25, 1944.

10. S. A. TUCKER, "Gas Turbines," *Mech. Eng.*, June, 1944, p. 363.

11. C. R. SODERBERG and R. B. SMITH, "The Gas Turbine as a Possible Marine Prime Mover," *Trans. Soc. Naval Arch. and Marine Engineers*, Nov. 11, 1943.

12. C. R. SODERBERG and R. B. SMITH, "First Marine Gas Turbine," *Marine Age*, August, 1945, p. 22.

13. C. R. SODERBERG and R. B. SMITH, *Gas Turbine Issue*, Powerfax, Elliott Company, Jeanette, Pa.

14. C. R. SODERBERG and R. B. SMITH, "The Elliott Gas Turbine," *Industry and Power*, September, 1945.

15. *N.A.C.A. Tech. Memo 975.*

16. J. K. SALISBURY, "The Basic Gas Turbine Plant and Some of Its Variants," *Mech. Eng.*, June, 1944, p. 375.

17. F. K. FISHER and C. A. MEYER, "Gas Turbine Developments Portend Power Changes," *Industry and Power*, May, 1944, p. 64.

18. F. W. GODSEY and C. D. FLAGLE, "The Place of the Gas Turbine in Aviation," *Westinghouse Engineer*, June, 1945, p. 121.

19. S. R. PUFFER and J. S. ALFORD, "The Gas Turbine in Aviation—Its Past and Future," paper presented at A.S.M.E., June 14, 1945, Los Angeles, Calif.

20. A. STODOLA, "Leistungsversuche an einer Verbrennungsturbine," *Zeit. V.D.I.*, Vol. 84, 1940, p. 17.

21. J. ACKERET and C. KELLER, "Aerodynamische Warmekraftmaschine mit geschlossenem Kreislauf," *Zeit. V.D I.*, Vol. 85, 1941, p. 491.

22. G. JENDRASSIK, "Versuche an einer neuen Brennkraftturbine," *Zeit. V.D.I.*, Vol. 83, 1939, p. 792.

23. B. WEISSENBERG, "Betrachtungen zur Gasturbinenfrage," *Stahl u. Eisen*, Vol. 61, March, 1941, p. 305.

24. A. STODOLA, *Steam and Gas Turbines*, Vol. 2, McGraw-Hill Book Co., New York.

25. H. C. HAMMAR and E. JOHANSSON, "Thermodynamics of a New Type of Marine Machinery with Pneumatic Power Transmission," *Inst. Marine Engrs. Trans.*, Vol. 51, April, 1939, pp. 139–154.

THE GAS-TURBINE TYPE OF THERMAL JET ENGINE (THE TURBOJET ENGINE)

1. Introduction

In the preceding chapter the principles underlying the operation of the continuous-combustion gas turbine were discussed, and methods were presented for determining its characteristics. It has been pointed out that the gas turbine bears a basic relationship to that form of thermal jet engine called the turbojet engine since it forms an integral part of the latter. This chapter discusses the basic principles of jet propulsion for aircraft by means of the gas-turbine type of thermal jet (turbojet) engine and presents methods for analyzing its characteristics.

In general, the term *thermal jet engine* refers to any jet-propulsion device which utilizes air from its surroundings together with the combustion of a fuel to produce the fluid jet for propulsion purposes. The operating principle is to induct air into the unit, increase its pressure, heat it to a relatively high temperature by the combustion of a fuel, and then eject the heated air containing combustion gases with a velocity substantially higher than that of the entering air. The reaction force or thrust is proportional to the rate of change of the momentum of the fluid leaving and entering the unit.

Thermal jet engines may be classified into the three main groups discussed below.

(*a*) **The Ramjet or Athodyd (Aero-THermO-DYnamic-Duct).** This is the simplest form of the thermal jet engine. It consists of a suitably shaped duct equipped with appropriate fuel burners. The entering air has its velocity energy converted into static pressure or ram as it flows to the burner section of the duct. Fuel is burned continuously in the air, and the heated gases are ejected at high velocity at the rear of the duct in the form of a jet. The device is a continuous-firing duct operating with a continuous flow of atmospheric air.

The manner in which the ramjet may be applied to an airplane is illustrated in Fig. 1, which is a design exhibited by the French engineer René Leduc, at the Paris Salon de l'aviation in 1938.[1] The atmospheric air enters the annular scoop surrounding the cabin, its temperature is raised by the fuel burners located near the midsection of the airplane, and the air is discharged to the rear at high velocity. Since the operation of the ramjet depends upon the ram pressure of the entering air it is inherently a very high-speed device, and to obtain sufficient ram pressure it must be launched by some auxiliary
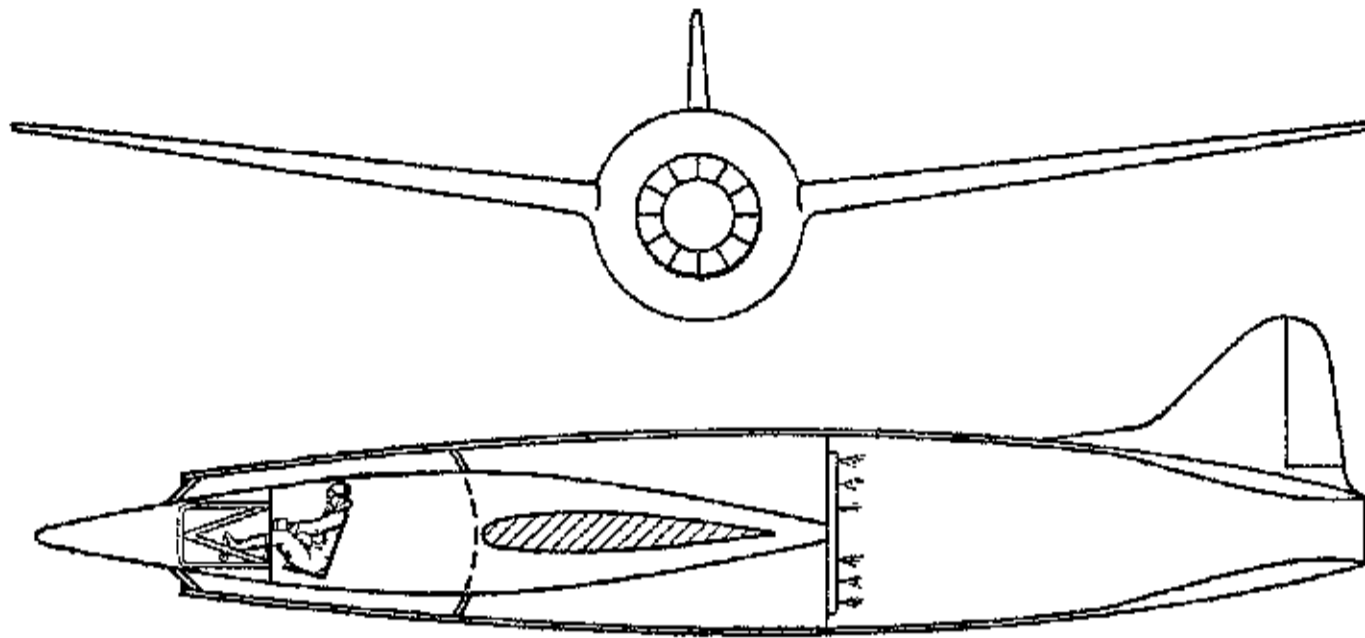
FIG. 1.   Ramjet engine applied to airplane propulsion as conceived by Leduc. (From *Gas Turbines and Jet Propulsion for Aircraft*, published by Aircraft Books, Inc , N. Y. C.)

means.   For illustrations showing the action of the ramjet the reader is referred to reference 2.   The origin of the ramjet is credited to Lorin of France in 1913.

(b) The Pulsejet or Intermittent-Firing Duct Engine.   This type of thermal jet engine, like the ramjet, requires no air compressor for its operation.   The forward end of the duct is equipped with one or more light shutters or valves that open inwardly against a spring pressure.   In flight, the air is forced into the device by ram pressure which forces the valves open.   Fuel is supplied continuously, and the fuel-air mixture is ignited initially by an electric spark.   The combustion pressure closes the valves, and the air admixed with combustion gases is discharged to the rear to form the fluid jet.   The ejection of the gases produces a suction causing the valves to reopen to start the next cycle.   The processes repeat themselves with a rapidity which depends on the natural frequency for the duct.   In the German V-1 winged missile, frequently called the *buzz bomb*, the firings occur at the rate of 40 per second.   Owing to the intermittent firing the propulsion thrust is not constant.   For a fuller description

of this device the reader is referred to reference 4. This device is illustrated in Fig. 2.

Pulsejet engine

Fuel injection jet

Electric spark ignites
fuel vapor

Air intake shutters

Rudder

Servo motors
controlled by gyro
move rudder
and elevators

Elevator

Gyro pilot controls bomb's
direction and height

Compressed air bottles
supply power for
servos and gyro pilot

Fuel tank

One ton explosive charge

Wing span: 16′
Length: 25′·4″
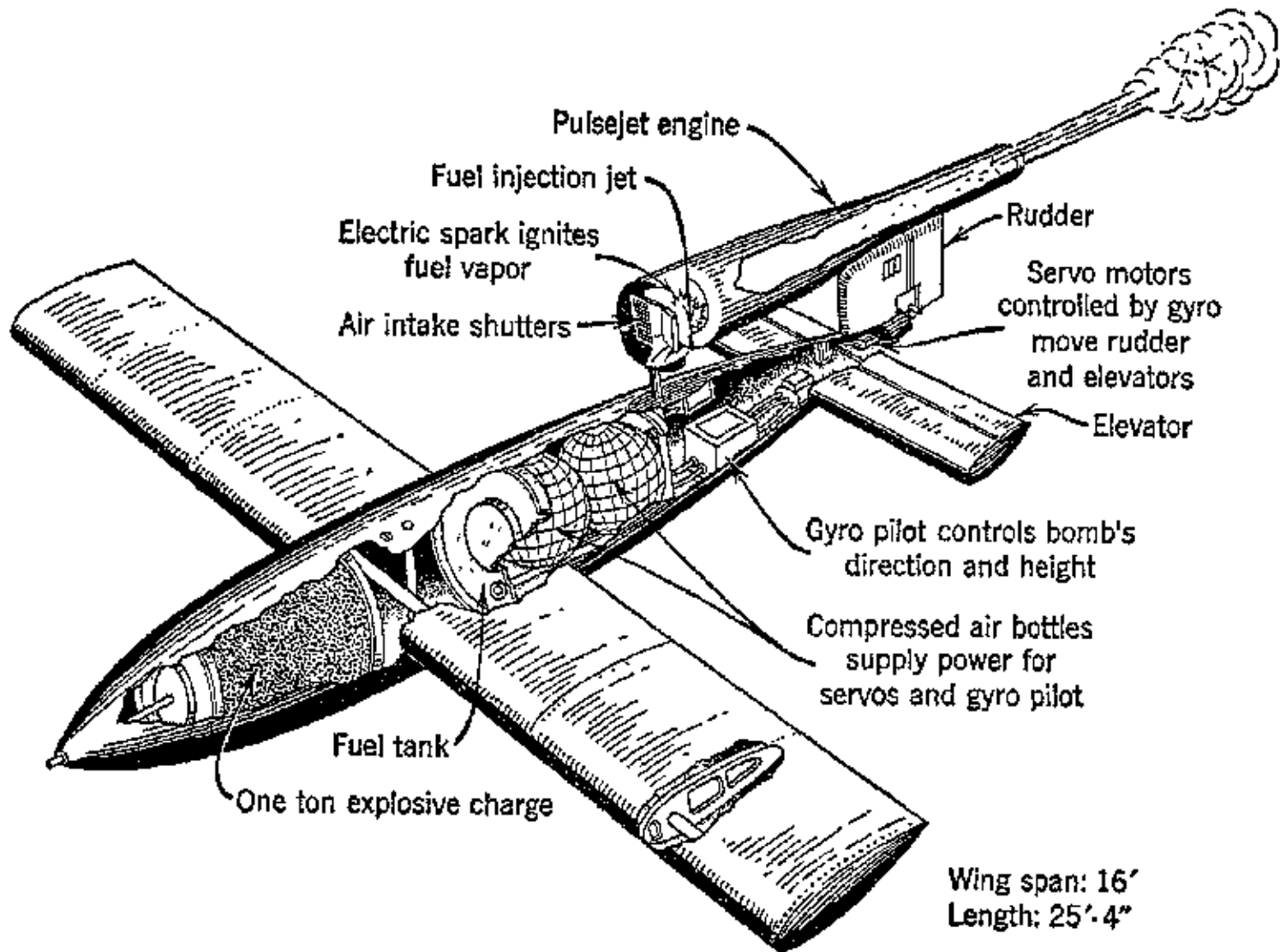
FIG. 2.   Principal elements of a pulsejet engine.

(c) **The Turbojet or Gas-Turbine Jet Engine.** This type of thermal jet engine has the advantage that its fuel consumption per pound of thrust is lower than that of the other two types. Furthermore, it does not depend upon the ram pressure of the entering air for

Four-stage
centrifugal
compressor

Air
chamber

Combustion
chamber

Fuel injector

Discharge nozzle
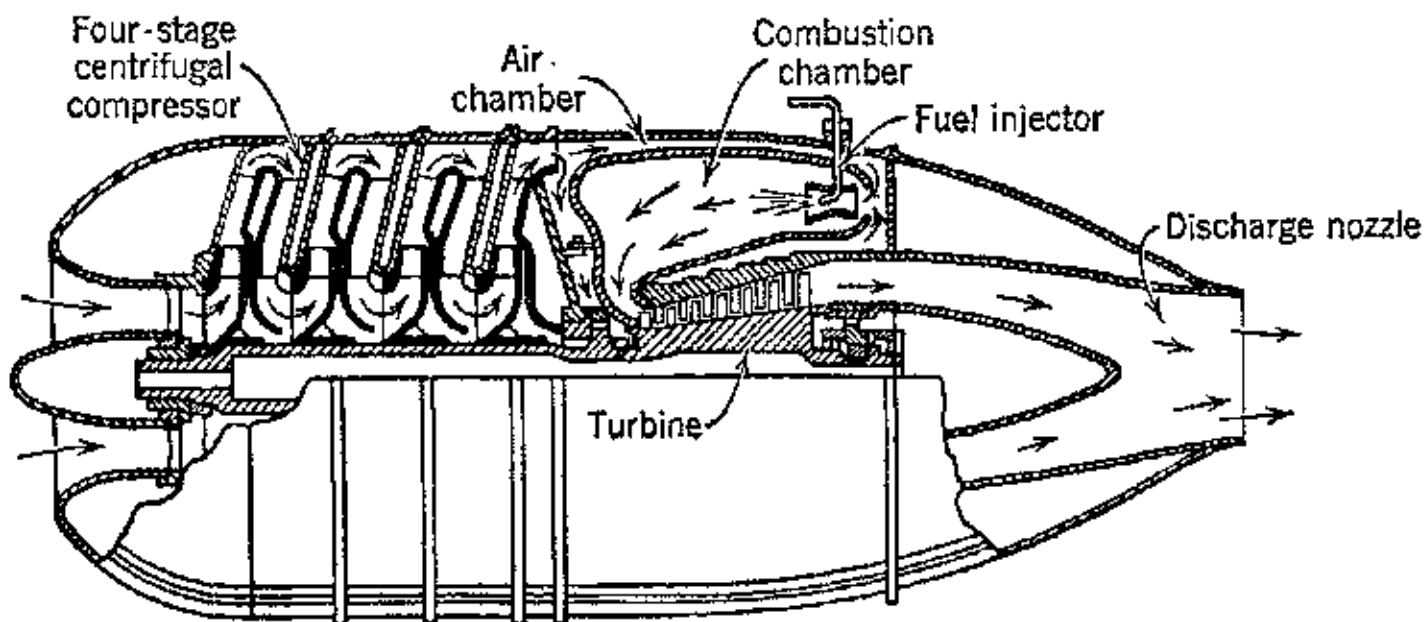
Turbine

FIG. 3.   Turbojet engine designed by A. Lysholm and sponsored by Milo Aktiebolaget of Stockholm, Sweden.   (From *Gas Turbines and Jet Propulsion for Aircraft*, published by Aircraft Books, Inc., N. Y. C.)

its operation, although the amount of ram pressure recovered affects its performance. In its essential features, it is a continuous-combustion gas turbine. The air entering the unit is compressed by some form of air compressor, heated by the combustion of a fuel, expands through a gas turbine, and then is discharged at high velocity through a nozzle at the rear of the unit. A form of turbojet engine, patented by the Swedish inventor A. Lysholm, is illustrated in Fig. 3.

A comparison of the general characteristics of the various types of propulsion systems as presented in reference 3, together with their probable ranges of operation, is summarized below.

Type of Propulsion Unit	Probable Range of Maximum Flight Speeds
Supercharged reciprocating engine with geared propeller and exhaust jet	150 to 450 mph
Gas turbine with geared propeller and exhaust jet	300 to 600 mph
Turbojet engine	400 to 700 mph
Pulsejet	1. 300 to 600 mph 2. For flying bombs
Ramjet	1. Above 500 mph 2. Long-range missiles
Rocket	1. Above 500 mph 2. For assisted takeoff 3. Long-range missiles

A similar comparison of the realm of usefulness of the above propulsion systems is presented in reference 5.

2. Brief Review of Turbojet Patent Literature

The patent literature discloses numerous arrangements for propelling an airplane by the reaction force of a fluid jet. On closer examination the apparent differences in the various schemes are seen to entail no essential difference in the basic operating principle. The differences are restricted to the methods employed by the various inventors either for compressing air or for driving the air-compression means. All of them utilize the same general features, which consist of compressing air, heating it, and ultimately discharging it through some form of nozzle in the direction opposite to that in which the airplane is to be moved.

The first airplane flight using jet propulsion exclusively was a Campini monoplane, known as the CC2, powered with a jet-propulsion system designed by Secondo Campini. This flight was made Aug. 27, 1940, and was of 10 minutes' duration.

An early Campini design for propelling aircraft at high altitudes at either subsonic or supersonic speeds is described in U. S. Patent

(1) Ovoid cabin	(4) Radial engine	(8) Discharge nozzle
(2) Enshrouding cylinder	(5) Rectifier-radiator	(9) Cone for varying nozzle orifice
(3) Two-stage centrifugal compressor	(6) Combustion space	(10) Controlled lateral orifices
	(7) Annular mixing channel	(11) Slidable shroud ring
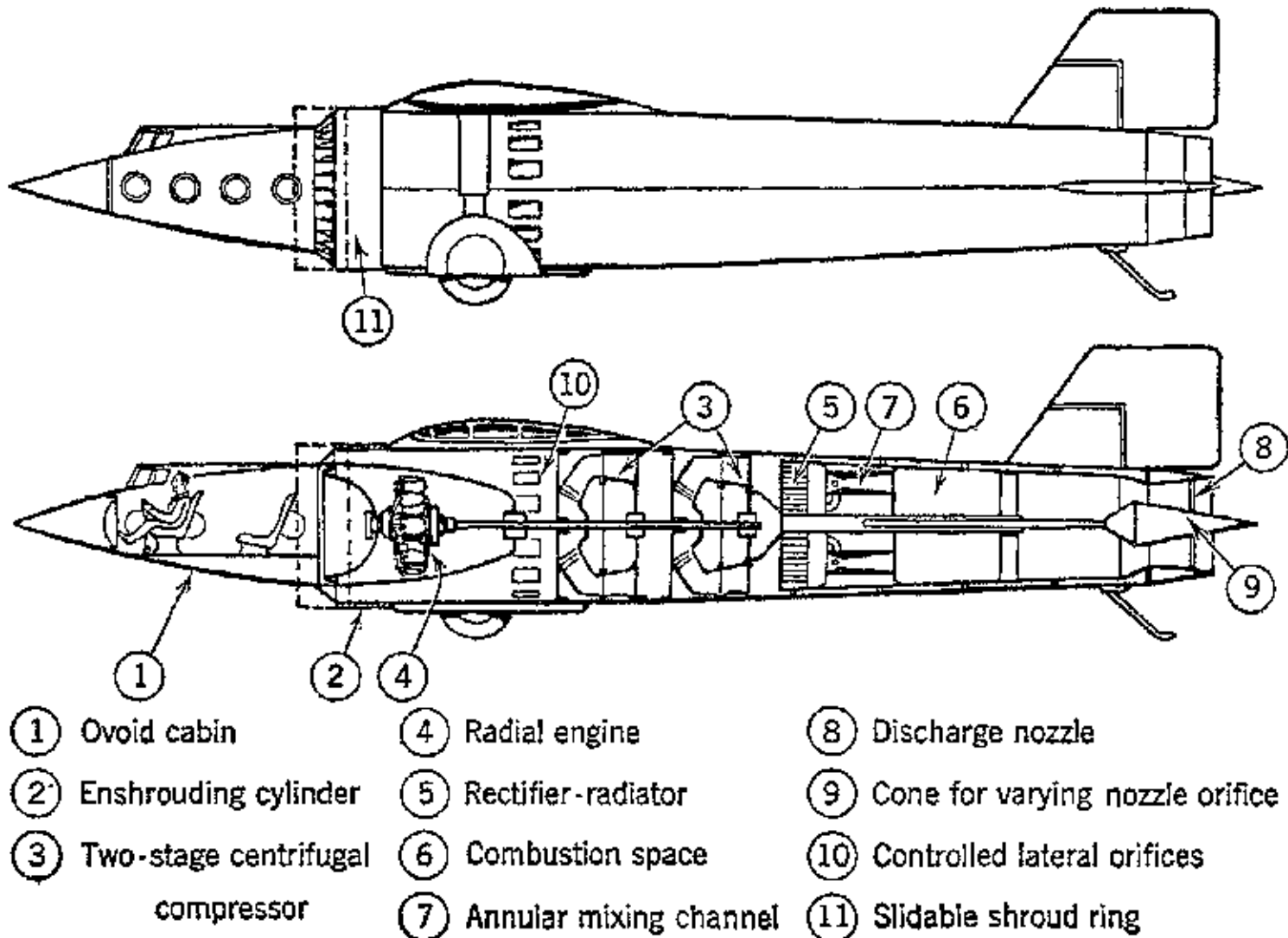
Fig. 4. Campini system of jet propulsion for aircraft. (From *Gas Turbines and Jet Propulsion for Aircraft*, published by Aircraft Books, Inc., N. Y. C.)

2,024,274, Dec. 17, 1935; it is illustrated in Fig. 4. In its essence the arrangement disclosed is as follows. Air enters at the front of the airplane and is compressed by a blower driven by a conventional aircraft engine. The compressed air is heated in a combustion chamber and then discharged to the rear of the airplane. For a more detailed description the reader is referred to the aforementioned patent or to reference 1.

One of the most active inventors in this field is F. Whittle of the R.A.F. The earliest disclosure filed by Whittle in 1930 described a jet-propulsion system comprising a multistage axial-radial flow compressor, multiple combustion chambers wherein fuel is burned to heat the compressed air, an impulse turbine with two rows of blades,

and a discharge nozzle of the De Laval type. This arrangement is illustrated in Fig. 5.

A later patent issued to Whittle is U. S. Patent 2,168,726, Aug. 8, 1939, illustrated in Fig. 6. The patent describes a type of thermal jet engine (turbojet engine) similar to that used on the first jet-propelled planes made by the British and that which was subsequently applied in this country in 1942 to one of the fighter craft manufactured by the Bell Aircraft Company.
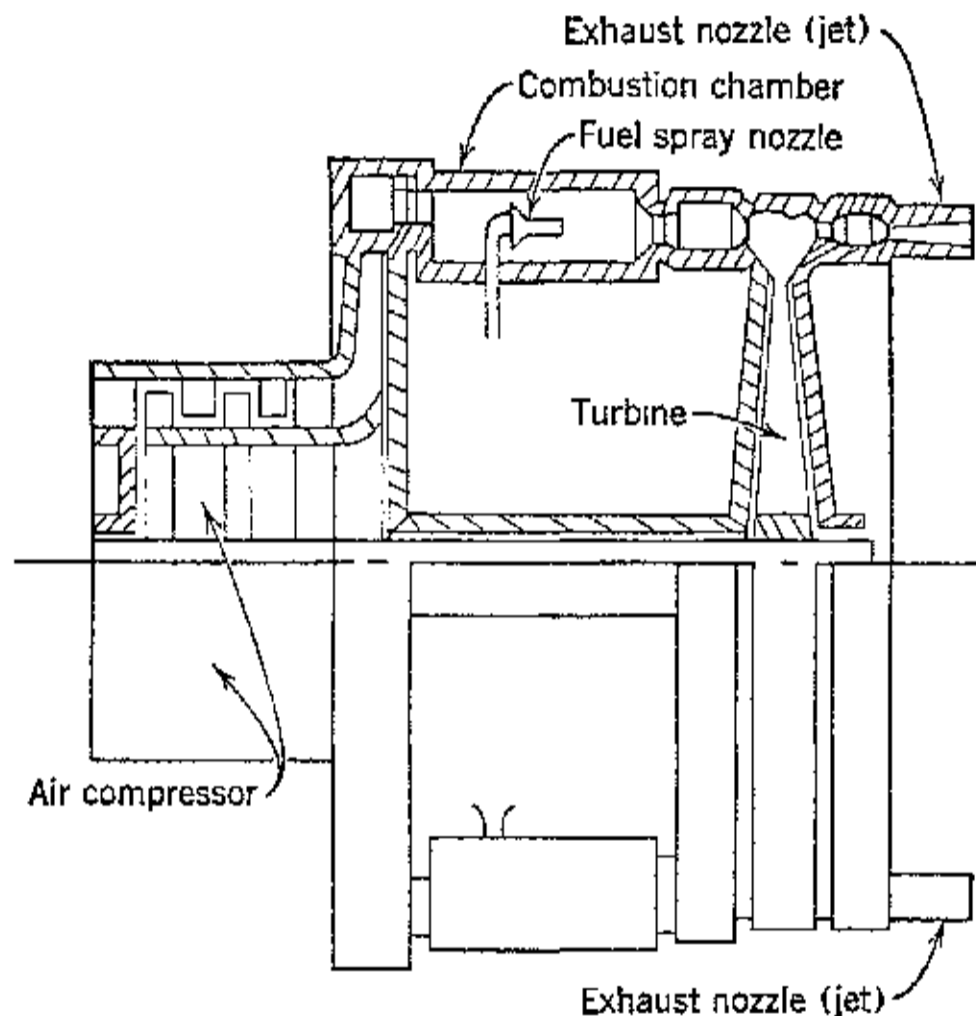
FIG. 5.   Early patent disclosure by F. Whittle.   (Reproduced from Sir A. H. Roy Fedden, *loc. cit.*)

The operating principle of the last-mentioned Whittle turbojet engine is briefly as follows. Air enters the jet system through a duct opening or scoops facing in the direction of travel. The air compressor, which is of the single-stage centrifugal type, is provided with two air intakes located on opposite sides of the impeller. The impeller rotates at such a speed that the air is discharged at the impeller tips with supersonic speed. In order to reduce the air velocity to subsonic speed before it reaches any stationary part and thereby reduce losses due to compression shock, the air is first discharged into a radial primary diffuser. From the primary diffuser the compressed air passes into a delivery scroll having an increasing cross-sectional area. The air then passes to a helical combustion

chamber which, owing to its tapered shape, acts as a secondary diffuser.   The discharge end of the combustion chamber connects to the annular passage located upstream to the blading of a single-stage impulse turbine.
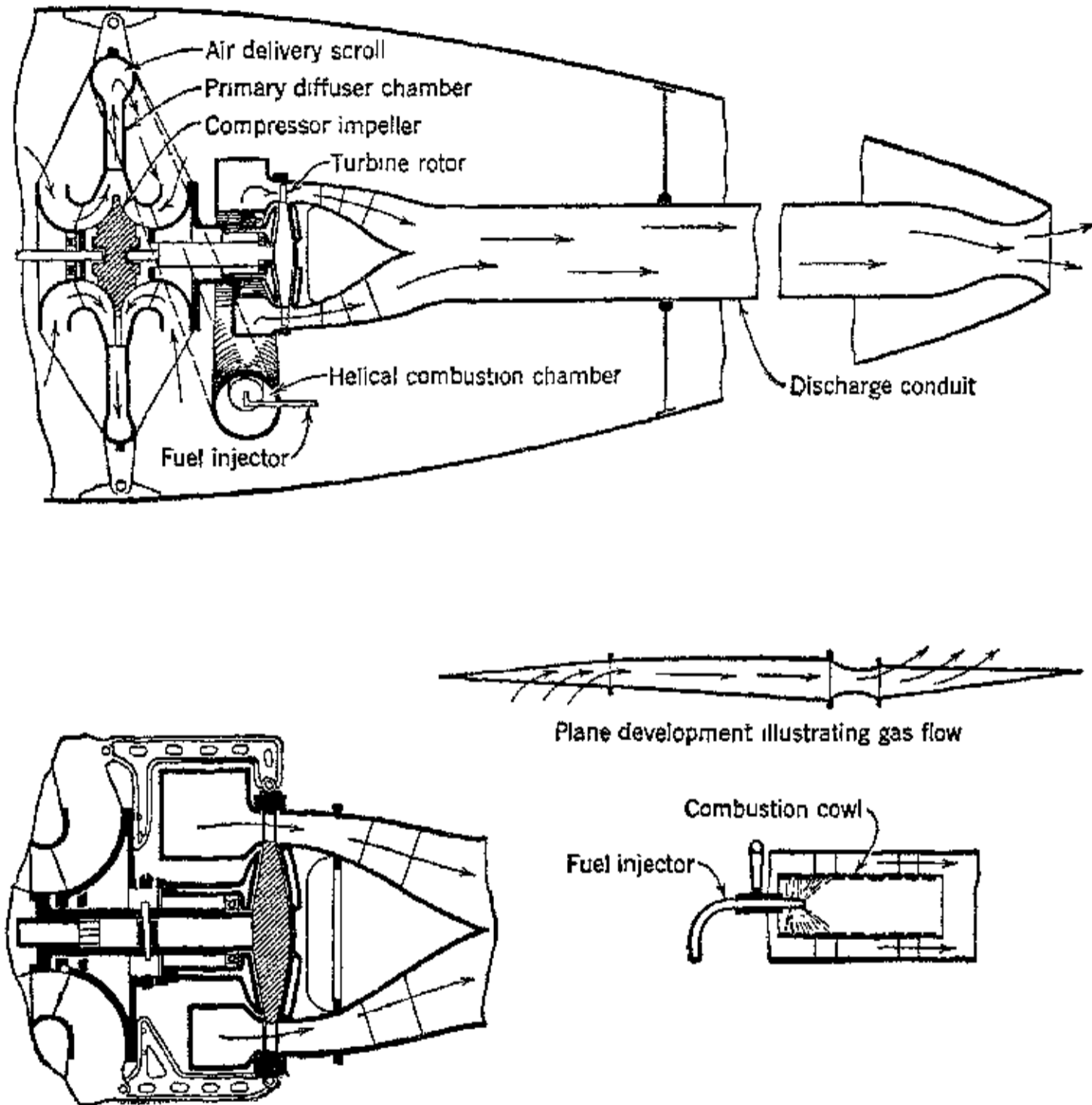
FIG. 6.   Disclosure by F. Whittle in 1939.   (From *Gas Turbines and Jet Propulsion for Aircraft*, published by Aircraft Books, Inc., N. Y. C.)

The air is heated in the combustion chamber by burning fuel therein.   The combustion chamber is equipped with a fuel nozzle which discharges into an inner cylindrical space of two concentrically disposed cylinders, the inner cylinder being shorter than the outer one.   The inner wall of the inner cylinder may be covered with a wire mesh or a perforated metal lining to furnish a slow-moving air layer for the purpose of insuring continuous combustion.   Only the portion of the total air flow that is required for combustion passes through the inner cylinder.   The balance passes through the annular

space between the two cylinders and mixes with the products of combustion in the region beyond the end of the inner cylinder. The entire body of air and combustion products intermingles to give a working fluid at high temperature.

The hot working fluid expands in the blades of the turbine rotor thereby furnishing the work for driving the compressor. The turbine exhaust gases pass through an annular duct formed between the main conduit and a cone mounted on the turbine casing. The main
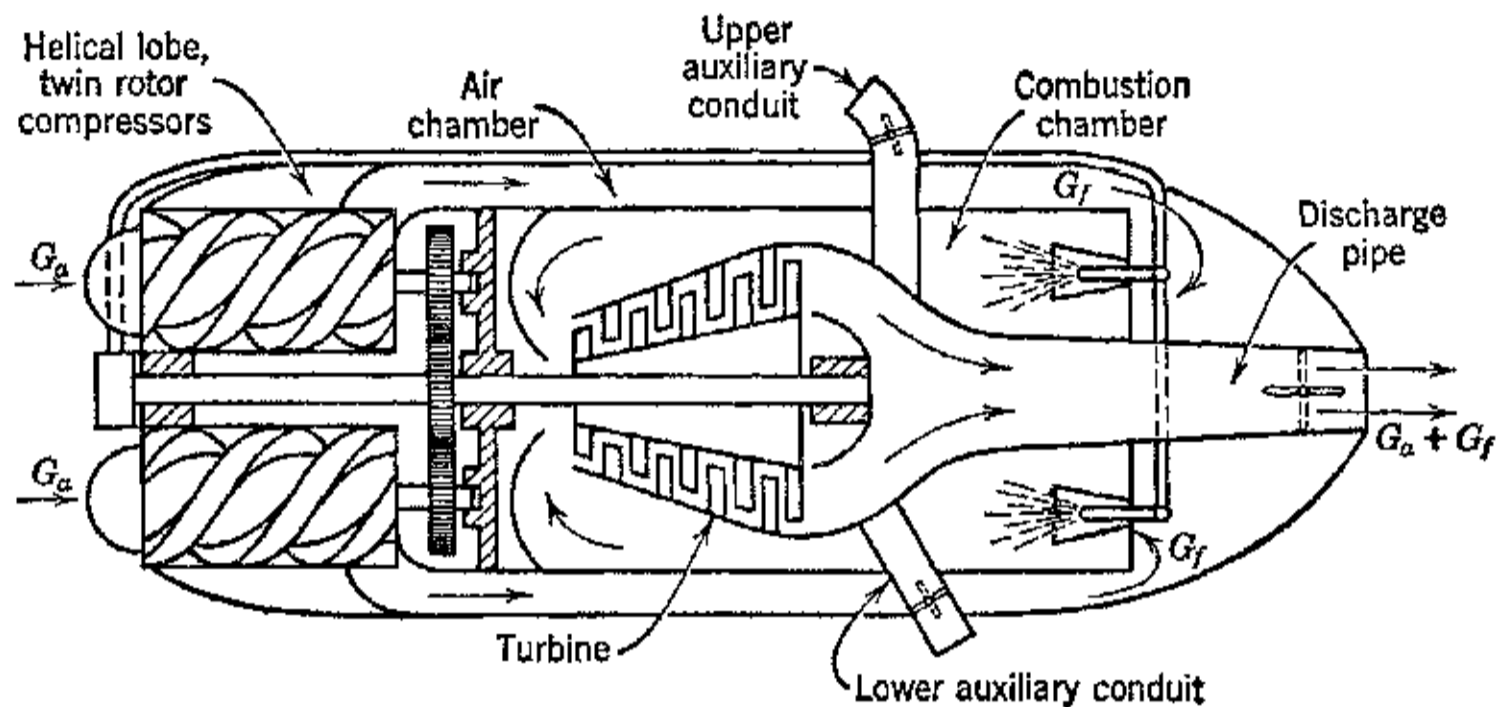
FIG. 7. Lysholm turbojet engine using positive displacement helical-lobe compressors. (From *Gas Turbines and Jet Propulsion for Aircraft*, published by Aircraft Books, Inc., N. Y. C.)

conduit, which is of circular cross section, then continues to the rear and is attached to the convergent-divergent nozzle forming the final member of the system.

In applications requiring two turbojet engines, they may be arranged so that the rotating elements rotate in opposite directions to reduce any tendency to produce gyroscopic action.

Another active inventor in the thermal jet propulsion field is the noted Swedish engineer Alf Lysholm. Several designs invented by him have been sponsored by Milo Aktiebolaget and by Aktiebolaget Ljungstroms Angturbin, both of Sweden. To date there have been no published reports indicating that any of the Lysholm designs have been reduced to practical application.

In his U. S. Patent 2,085,761, July 6, 1937, Lysholm describes a thermal jet engine comprising a four-stage centrifugal compressor, a single combustion chamber with multiple fuel injectors, a multi-stage reaction turbine, and a discharge nozzle. The components are arranged to give compactness, and the complete turbojet engine is intended for mounting in the wing of the airplane. For high-altitude

operation air is taken from the compressors for pressurizing the cabin and for heating it.

Figure 7 illustrates another Lysholm design, U. S. Patent 2,280,835, Aug. 28, 1942, which utilizes positive displacement compressors of the helical lobe type. An added feature is the means provided for bringing the thermal jet engine rapidly into operation. For a fuller description the reader is referred to the aforementioned patent.

Other jet-propulsion devices using a compressor are described in the following patents: U. S. Patent 2,256,198, Sept. 16, 1941, issued to Max Hahn; U. S. Patent 2,304,008, Dec. 1, 1942, issued to Max Muller.

The patent literature contains many systems for producing jet propulsion with heated air that do not require a compressor. The more interesting of these patents are listed below.

U. S. Patent 1,069,694, Aug. 12, 1913, issued to Hayot.
U. S. Patent 1,375,601, April 19, 1921, issued to Morize.
U. S. Patent 1,493,157, May 6, 1924, issued to Melot.
U. S. Patent 1,725,914, Aug. 27, 1929, issued to E. Hollowell.
U. S. Patent 1,888,749, Nov. 22, 1932, issued to K. M. Urquhart.
U. S. Patent 1,980,266, Nov. 13, 1934, issued to R. H. Goddard.
U. S. Patent 1,983,405, Dec. 4, 1934, issued to P. Schmidt.

Two interesting patents of jet propulsion are the autogiro design of J. G. Weir, U. S. Patent 1,897,092, Feb. 14, 1933, and the propeller patent granted to H. A. Duc, Jr., U. S. Patent 1,099,083, June 2, 1914.

Today the possibilities and potentialities of the turbojet engine are such as to indicate that with further development this engine can become a keen competitor of the conventional engine-propeller propulsion system for certain classes of service. At the present its main disadvantage is its high fuel consumption, but, as pointed out in the preceding chapter, this will undoubtedly be improved as machine efficiencies are raised and higher turbine inlet temperatures become permissible. Consequently, engineering development of more efficient machinery combined with progress in the field of high-temperature metals can exercise a great benefit in reducing the fuel consumption. In view of the low specific weight of the turbojet engine and the possibility of using cheaper fuels than high-octane gasoline, with further development this propulsion system will undoubtedly find a place in the commercial transport field.[6] Furthermore, with the jet method of propulsion it should be possible for airplane designers to design cleaner airplanes, a factor also having a bearing upon the problem of reducing fuel consumption.

Since the greatest activity at present is in thermal jet engines of the turbojet type, this chapter is devoted to the consideration of that type of thermal jet engine.

3. Thrust Equation for Thermal Jet Engine

The basic elements of a thermal jet engine and their arrangement are illustrated in Fig. 8.
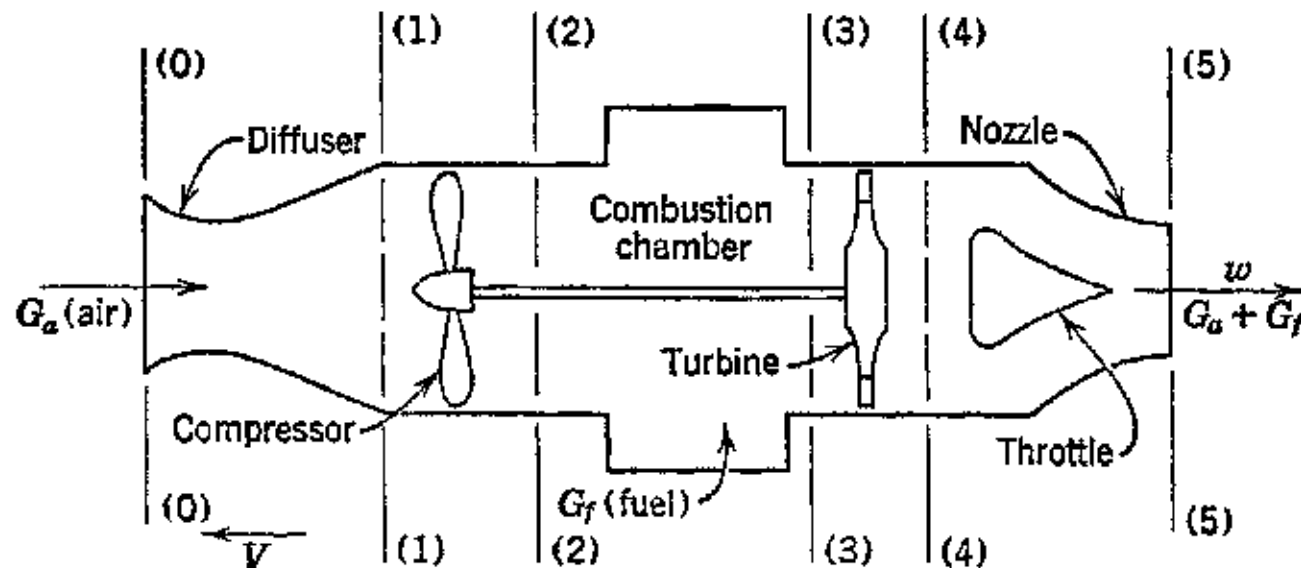
Fig. 8.   Elements of turbojet engine.

Atmospheric air enters the propulsion system at 0–0 and is compressed in the diffuser section 0–1 by the conversion of all or a portion of its velocity energy into pressure energy. The pressure ratio effected by the diffuser will depend upon the reduction in Mach number accomplished by it. This depends largely upon the length available for the diffusion process and the area ratio. The energy efficiency of the diffusion process will depend upon the smoothness of the walls of the diffuser and the angle of divergence. It should be noted that, in general, the guided flow of a fluid through a diverging passage is more likely to produce energy losses due to eddies and turbulence than guided flow through a convergent passage. To keep the energy losses at a minimum the conversion of the kinetic energy of the entering air into pressure energy must be gradual. This requires a small angle of divergence and consequently considerable length.

From the diffuser the air enters the compressor, wherein its pressure is raised by an amount governed by the pressure ratio of the compressor. The compressed air then flows into the combustion chamber where its temperature is raised by the combustion of fuel with a portion of the air. The highly heated gases then expand in the turbine which delivers exactly the amount of power that is needed to drive the air compressor.

The gases arrive at the turbine at a pressure slightly lower than the pressure of the air leaving the compressor, owing to the pressure

loss in the combustion chamber. This pressure loss must be kept small. Because of the high temperature of the gases, the expansion ratio for the turbine is smaller than the pressure ratio for the compressor. As a result the gases are discharged from the turbine at a pressure higher than the atmosphere. Consequently, the gases arriving at the entrance to the discharge nozzle are above the atmospheric back pressure and are at a relatively high temperature. These compressed hot gases expand in flowing through the nozzle and acquire a high exit velocity. The reaction of these fast-moving gases produces the thrust for propelling the airplane.

Since the turbojet engine has the same absolute velocity as the airplane to which it is attached, it is convenient to use the relative coordinate system. Thus it is assumed that the airplane is at rest and that the air approaches the intake system with a velocity equal in magnitude to the airplane velocity V.

Notation

a = acoustic velocity, fps.

A = area, ft^2.

$c = w - V$ absolute velocity of jet gases, fps.

$\bar{c}_{pt}$ = mean specific heat at constant pressure of the gases flowing through the turbine, Btu/lb F.

$\bar{c}_{pc}$ = mean specific heat at constant pressure of the air flowing through the air compressor, Btu/lb F.

D = diameter of exhaust nozzle, ft.

g = acceleration due to gravity, 32.174 ft/sec^2.

$G = G_a + G_f \approx G_a$ = weight rate of flow of propulsive fluid, lb/sec.

G_a = weight rate of flow of air, lb/sec.

G_f = weight rate of flow of fuel, lb/sec.

h = enthalpy of the working fluid at the state point indicated by the subscript, Btu/lb.

Δh_B = enthalpy added to each pound of air by the combustion of the fuel, Btu/lb.

H_c = calorific value of the fuel, Btu/lb.

J = mechanical equivalent of heat 778 ft-lb/Btu.

$k = c_p/c_v$ = specific heat ratio.

M = Mach number.

$\mathbf{M}$ = momentum, or rate of momentum, at section indicated by the subscript, slug-ft/sec.

p = pressure intensity at section indicated by subscript, psia.

$P = P_E - P_A$ = propulsion power, ft-lb/sec

$P_A = G_a V^2/2g$ = power of the entering air, ft-lb/sec.

$P_E = (G_a + G_f)w^2/2g$ = power of the gases leaving the turbo-jet engine in unit time, ft-lb/sec.

$P_L = G(w - V)^2/2g$ = leaving loss, ft-lb/sec.

$P_T = 3V$ = thrust power, ft-lb/sec.

$Q_i = G_f H_c$ = heat supplied the turbojet engine in the form of fuel, Btu/lb or Btu/sec as specified in text.

R = gas constant, ft-lb/lb F.

r_t = turbine pressure ratio.

r_c = compressor pressure ratio.

3 = thrust, lb.

3_0 = take-off thrust, lb.

$v = 1/\gamma$ = specific volume, ft^3/lb.

V = flight speed of airplane, fps.

w' = isentropic velocity of jet gases relative to exhaust nozzle, fps.

w = velocity of jet gases relative to the exhaust nozzle, fps.

Y see equation 45a.

Temperatures

T_0 = atmospheric temperature, R.

$T_1' = T_0\Phi$ = temperature of the air at the end of flow compression with 100 per cent ram, R.

T_1 = actual temperature of the air at the entrance to the air compressor, R.

$T_2' = T_1\theta$ = temperature of air at the end of isentropic compression in an ideal air compressor, R.

$T_2 = T_0\Phi[1 + (\theta - 1)/\eta_c]$ = actual temperature of air leaving the air compressor, R, (100 per cent ram).

$T_3 = \alpha T_0$ = temperature of working fluid leaving the combustion chamber, R.

$T_4' = [1 - \Phi(\theta - 1)/\alpha\eta_c\eta_t]T_0\alpha$ = temperature of gases after expansion in an ideal turbine, R, (100 per cent ram).

$T_4 = [1 - \Phi(\theta - 1)/\alpha\eta_c]T_0\alpha$ = temperature of gases after expansion in an actual turbine, R, (100 per cent ram).

$T_5' = T_4 T_6/T_4'$ = temperature of gases after expansion in an ideal nozzle, R, (100 per cent ram).

T_5 = (equation 49) temperature of gases after expansion in an actual nozzle, R, (100 per cent ram).

$T_6 = \alpha T_0(1/\theta\Phi)$ = temperature of gases after isentropic expansion from the turbine inlet temperature T_3 to the atmospheric pressure, R, (100 per cent ram).

Greek Symbols

$\alpha = T_3/T_0$ ratio of the temperature of the gases leaving the combustion chamber to the atmospheric temperature.

$\Phi = T_1'/T_0 = 1 + (k - 1)M^2/2$.

$\theta = T_2'/T_1 = (p_2/p_1)^{\frac{k-1}{k}}$.

$\gamma = $ specific weight, lb/ft^3.

$\rho = \gamma/g = $ density, $slug/ft^3$.

$\nu = V/w$ velocity ratio.

$\sigma = $ density ratio for atmospheric air (Table 1.6).

$\eta = P_T/JQ_i = $ plant or thermal efficiency.

$\eta_i = P/JQ_i = $ internal efficiency.

$\eta_a = $ compressor efficiency.

$\eta_B = $ combustion chamber efficiency.

$\eta_t = $ turbine efficiency.

$\eta_P = $ propulsion efficiency.

$\eta_r = $ ram efficiency.

$\eta_D = $ diffuser efficiency.

$\varphi = $ velocity coefficient $= w/w'$.

Referring to Fig. 8, the air crosses the entrance section *O-O* of the turbojet engine with the flow rate G_a and its momentum $\mathbf{M}_0$ rate is given by

$$\mathbf{M}_0 = \frac{G_a}{g} V \tag{1}$$

Similarly, the momentum of the gases crossing the exit section 5-5 in unit time is at the rate

$$\mathbf{M}_5 = (G_a + G_f) \frac{w}{g} \tag{2}$$

The net change in the linear momentum per unit time for the turbojet engine is given by

$$\mathbf{M}_5 - \mathbf{M}_0 = \frac{G_a}{g} (w - V) + \frac{G_f}{g} w \tag{3}$$

The net reaction force or thrust due to the above change in momentum is independent of all the forces and reactions taking place in the flow passage formed by the turbojet engine. Further, since this is the momentum change taking place in 1 sec, the reaction force or thrust is given by

$$\mathfrak{J} = \frac{G_a}{g} (w - V) + \frac{G_f}{g} w \tag{4}$$

In the last equation the relative exit velocity w is determined by the pressure ratio (or expansion ratio) for the nozzle, the gas constant for the fluid, its specific heat ratio, and the nozzle velocity coefficient; see Chapter 3.

Thus

$$w = 223.7\varphi\sqrt{h_4 - h_5'} \tag{5}$$

Since the air enters the thermal jet engine with the initial velocity V, the net change in its velocity is $(w - V)$. The fuel, however, enters the engine with no initial velocity, and it leaves with the velocity w. Hence the change in the velocity of the fuel is also w.

In general, the weight of the fuel consumed per second is approximately 2 per cent of the weight of air with which it is admixed. Consequently, no appreciable error is introduced if it is assumed that

$$G = G_a + G_f = G_a$$

The equation for the thrust developed by the turbojet engine based on the above assumption is

$$\mathfrak{I} = \frac{G}{g}(w - V) \tag{6}$$

This equation is identical with the thrust equation developed for the ideal propeller in Chapter 6. Equation 6 can be transformed to show the dependence of the thrust upon the velocity ratio ν. Thus

$$\mathfrak{I} = \frac{G}{g}w(1 - \nu) \tag{7}$$

or the thrust per pound of air flow per second is

$$\frac{\mathfrak{I}}{G} = \frac{w}{g}(1 - \nu) \tag{8}$$

Equation 8 indicates how the thrust developed, per pound of fluid flowing through the propulsion system per second, varies with the exit velocity w and the velocity ratio ν.

Figure 6·6 illustrates this relationship for several different values of the relative exit velocity w.

References to Chapters 2 and 6 will show that these equations are identical to those derived previously for hydraulic jet propulsion and the propeller. The basic characteristics of turbojet propulsion are, therefore, identical to those for hydraulic jet propulsion and propeller propulsion.

For a fixed velocity ratio the size of the required exit area increases as the speed of the airplane decreases. This indicates why the propeller with its ability to handle extremely large quantities of air at velocity ratios close to unity is better adapted to the propulsion of bodies at moderate and low speeds than the turbojet engine. This is particularly true since, as pointed out previously, operation close to unity velocity ratio gives high propulsion efficiency.

Figure 6·7 is a plot of the thrust per pound of air flow per second as a function of the velocity ratio for different flight speeds. On the same figure is plotted the ideal propulsion efficiency as a function of the velocity ratio.

EXAMPLE. An airplane is designed for a forward speed of 500 mph at 30,000-ft altitude. Its drag coefficient is 0.016, its weight 10,000 lb, and its wing area 200 sq ft. What is the approximate air consumption of its thermal jet engine in pounds per second per pound of thrust, if the jet velocity is 1500 fps?

Solution.

$$V = 500 \times \tfrac{88}{60} = 734 \text{ fps} \quad \text{and} \quad V^2 = 53.7 \times 10^4$$

$$\sigma = 0.374 \text{ (Table 1·6)}$$

$$\rho = 0.002378 \times 0.374 = 8.78 \times 10^{-4} \text{ slug/ft}^3$$

$$D = \text{drag} = \tfrac{1}{2}\rho V^2 S C_D = 3$$

$$= \tfrac{1}{2}(8.78 \times 10^{-4})(53.7 \times 10^4)(200)(1.6 \times 10^{-2}) = 755 \text{ lb}$$

$$G_a = \frac{755 \times g}{(1500 - 734)} = 31.4 \text{ lb/sec}$$

$$\nu = \frac{V}{w} = \frac{734}{1500} = 0.489$$

$$\frac{3}{G} = 0.03108w(1 - \nu)$$

$$= 0.03108 \times 1500(1 - 0.489) = 24.0 \text{ lb/lb of air per sec}$$

$$\frac{G}{3} = 0.04167 \text{ lb of air per sec/lb of thrust}$$

4. Propulsion Power and Propulsion Efficiency

By *propulsion power* is meant (as pointed out in Chapter 2) the total power supplied to a propulsion system. The portion of this power required to keep the airplane in motion is the *thrust power*, the product of the propulsion thrust and the flight speed. In the ideal case the difference between the propulsion and thrust powers constitutes the power loss associated with the propulsion system. The ratio

of the thrust power, the useful work of the system, to the propulsion power has been termed the *propulsion efficiency* and denoted by η_P.

The propulsion power for an engine-driven propeller is the brake horsepower of the engine. For a turbojet engine, the propulsion power is derived from the thermal energy of the fuel burned in the combustion chamber. This thermal energy, in the ideal case, is utilized only for increasing the kinetic energy of the working fluid flowing through the engine. The air enters the engine with the weight flow rate G_a and the relative intake velocity V. It is ejected from the exhaust nozzle with the relative exit velocity w. The corresponding absolute velocities for the air are zero at intake and $c = w - V$ at exit.

The kinetic energy associated with the air entering the system in unit time is given by

$$P_A = \frac{1}{2} \frac{G_a}{g} V^2 \tag{9}$$

Similarly, for the exit gases, which include the products of combustion of the fuel supplied at the rate G_f lb/sec, the kinetic energy per unit time is

$$P_E = \frac{1}{2} \frac{(G_a + G_f)}{g} w^2 \quad \text{ft-lb/sec} \tag{10}$$

The difference between P_E and P_A is the rate at which energy is supplied for propelling the airplane, which is the propulsion power P. Hence

$$P = P_E - P_A = \frac{1}{2} \frac{(G_a + G_f)}{g} w^2 - \frac{1}{2} \frac{G_a V^2}{g} \tag{11}$$

Since G_f is small compared to G_a, it can be assumed that $G = G_a \approx G_a + G_f$. Making this assumption, the expression for the propulsion power becomes

$$P = \frac{G}{2g} (w^2 - V^2) = \frac{G}{2g} w^2 (1 - \nu^2) \tag{12}$$

where, as before, $\nu = V/w$ is the velocity ratio.

In the ideal case the only energy loss accompanying the transformation of the propulsion power into thrust power is the leaving or exit loss P_L. Assuming G_f negligible,

$$P_L = \frac{G}{2g} c^2 = \frac{G}{2g} (w - V)^2 \tag{13}$$

In view of the assumption that the exit loss constitutes the only loss accompanying the conversion of the propulsion power P into the thrust power P_T it follows that, as in the case of hydraulic jet propulsion, the propulsion power is given by

$$P = P_T + P_L = \Im V + P_L \tag{14}$$

The ideal propulsion efficiency η_P is accordingly

$$\eta_P = \frac{\Im V}{P} = \frac{\Im V}{\Im V + P_L} \tag{15}$$

Equation 15 is equally valid for the ideal engine-driven propeller, hydraulic jet propulsion, and the thermal jet engine. On substituting for the propulsion thrust $\Im$ and the exit loss P_L, the propulsion efficiency equation becomes

$$\eta_P = \frac{2V[(G_a + G_f)w - G_a V]}{w^2(G_a + G_f) - V^2(G_a - G_f)} \tag{16}$$

Neglecting the effect of the fuel flow G_f,

$$\eta_P = \frac{2V}{w + V} = \frac{2V/w}{1 + V/w} = \frac{2\nu}{1 + \nu} \tag{17}$$

Equation 17 is identical with that previously derived for the propulsion efficiency of hydraulic jet propulsion, and the ideal propeller.

The ideal propulsion efficiency η_P for the turbojet engine as a function of the velocity ratio ν is presented in Fig. 6·7.

It should be noted that, like the hydraulic jet and the propeller, the turbojet engine delivers no thrust when the velocity ratio is unity. For these types of propulsion systems the relation between the thrust power P_T and the velocity ratio is

$$P_T = \Im V = \frac{G}{g} w^2(1 - \nu)\nu \tag{18}$$

Equation 18 was obtained for hydraulic jet propulsion in Chapter 2 and for propeller propulsion in Chapter 6. It typifies reaction systems operating by virtue of a difference in velocities. The velocity ratio corresponding to the maximum value of P_T has been shown to occur when $\nu = 0.5$, when the speed of the airplane is one-half the speed of the exhaust jet relative to the nozzle walls. The corresponding value of the propulsion efficiency (at $\nu = 0.5$) is $\eta_P = 0.667$. It is seen, therefore, that the velocity ratios corresponding

to the maximum thrust power and to the maximum propulsion efficiency are different.

Consequently, to obtain high propulsion efficiency together with a large thrust for an airplane designed for moderate speeds, it becomes necessary to induct large quantities of air into the engine. This can be accomplished only by providing large flow passages and large component machinery. Such an arrangement results in a bulky, heavy engine. For this reason the turbojet engine is inherently best suited for airplanes designed to travel at high speeds.

5. Propulsion Power and Discharge Area

A relationship can be derived relating the propulsion power P, the flight speed V, the density of the exit gases ρ, the diameter of the jet D, and the ideal propulsion efficiency η_P, as was done for the propeller in Chapter 6. The rate of flow of fluid through the exhaust nozzle, for which the diameter is D, is given by

$$G = \frac{\pi}{4} D^2 \gamma w \tag{19}$$

Substituting for G from equation 19 into equation 12 gives

$$P = \frac{\pi}{8} D^2 \rho w^3 (1 - \nu^2) = \frac{\pi}{8} D^2 \rho (w^3 - w V^2)$$

or

$$\frac{P}{D^2 \rho} = \frac{\pi}{8} (w^3 - w V^2)$$

Dividing both sides of the above by V^3 and letting $\nu = V/w$ gives

$$\frac{P}{D^2 \rho V^3} = \frac{\pi}{8} \left(\frac{1}{\nu^3} - \frac{1}{\nu} \right) \tag{20}$$

From equation 17, the propulsion efficiency equation, it is seen that

$$\frac{1}{\nu} = \frac{2 - \eta_P}{\eta_P} \tag{21}$$

Substituting from equation 21 into equation 20 gives

$$\frac{P}{D^2 \rho V^3} = \frac{\pi}{8} \left(\frac{8 - 12 \eta_P + 4 \eta_P^2}{\eta_P^3} \right) \tag{22}$$

Inverting this last equation and taking the cube root of each side gives

$$V \sqrt[3]{\frac{D^2 \rho}{P}} = \frac{1.364 \eta_P}{\sqrt[3]{8 - 12 \eta_P + 4 \eta_P^2}} \tag{23}$$

Figure 6·8 is a plot of the so-called propulsion parameter $V\sqrt[3]{D^2\rho/P}$ as a function of the ideal propulsion efficiency η_P. This curve is applicable to the ideal propeller as well as to the thermal jet engine. When applied to the propeller, D is its diameter, ρ is the atmospheric density, V is the airplane speed, and P is the power furnished by the engine.

The curve gives the maximum attainable propulsion efficiency for either type of propulsion system. It is seen that, to obtain high values of efficiency with low airplane speeds, D must be large, assuming the other factors constant. This operating condition is most readily met with propeller propulsion.

When flight speeds in excess of 500 mph are considered there arise problems connected with the engine size as well as those due the effect of compressibility of the air upon the propeller efficiency, for as shown in Chapter 5 the power requirements increase as the cube of the airplane speed. Thus if it takes 1200 hp to propel a given airplane at 360 mph at a given altitude, it would require an engine developing approximately 3200 hp to propel it at 500 mph, assuming that all other factors remained unchanged. If this power is to be furnished by a reciprocating engine the resulting power plant is complex and heavy, even if that amount of power could be furnished by a single engine. On the other hand, the thrust power for attaining a speed of 500 mph can be obtained from a turbojet engine of relatively light weight, with a jet diameter of 1 ft and an exhaust velocity of approximately 1500 fps.

The efficiency of an actual propeller will be approximately 0.85 per cent of the ideal propulsion efficiency, or 0.833. The reduction in propulsion efficiency is due to various losses neglected by the momentum theory, such as whirl energy imparted to the slipstream, non-uniformity of the thrust distribution over the blades, blade profile drag, and periodicity of the flow.

It was shown in the preceding that, to obtain the maximum propulsion power from a turbojet engine, the velocity ratio should be approximately 0.5, and for this condition the propulsion efficiency is 0.667. Assuming the operating data used for the propeller discussed in the preceding, and that the discharge temperature for the jet is 1200 R, so that $\rho = 0.00102$ slug/ft^3, then the propulsion efficiency is about 68 per cent of that obtainable with an ideal propeller.

6. Plant or Thermal Efficiency

This is the ratio of the useful work performed in propelling the airplane to the heat supplied the engine Q_i in the form of fuel.

Let η denote plant or thermal efficiency; then if H_c is the calorific value per unit weight of fuel

$$\eta = \frac{P_T}{JQ_i} = \frac{1}{Jg}\left[\frac{(G_a + G_f)w - G_aV}{G_fH_c}\right]V \tag{24}$$

Substituting for $G_fH_c = Q_i$ in terms of the enthalpies h_2 and h_3 at the entrance and exit sections of the combustion chamber respectively, then if η_B is the combustion chamber efficiency

$$\eta = \eta_B\frac{1}{Jg}\left[\frac{(G_a + G_f)w - G_aV}{(G_a + G_f)h_3 - G_ah_2}\right]V \tag{25}$$

If the influence of G_f is neglected, equation 25 reduces to

$$\eta = \eta_B\frac{1}{Jg}\left(\frac{w - V}{h_3 - h_2}\right)V \tag{26}$$

From equation 26 it is seen that the plant efficiency is zero when $V = w$ and also when $V = 0$. Consequently, between these two limiting values of V, assuming no change in the rate of fuel feed, there is a value of flight speed which yields the maximum value for thermal efficiency.

7. Internal Efficiency

This is a measure of the effectiveness with which the thermal energy supplied to the thermal jet engine is transformed into propulsion power.

The thermal energy furnished the propulsion system is

$$Q_i = G_fH_c \quad \text{Btu/sec} \tag{27}$$

The internal efficiency η_i is given by

$$\eta_i = \frac{P}{JQ_i} \tag{28}$$

Substituting for P from equation 11 and for Q_i from equation 27

$$\eta_i = \frac{P}{JG_fH_c} = \frac{1}{2gJG_fH_c}[(G_a + G_f)w^2 - G_aV^2] \tag{29}$$

The numerical value of the heat supplied is determined from the enthalpies at the exit and entrance to the combustion chamber. The

weight of fuel per pound of fuel-air mixture passing through the combustion chamber is, from Chapter 7, Section 4(*d*), given by

$$\frac{G_f}{G_a + G_f}$$

Hence the heat supplied to the combustion chamber per pound of mixture is

$$\frac{G_f H_c}{G_a + G_f}$$

Hence, if h_2 is the enthalpy of the air entering the combustion chamber, the enthalpy of the mixture leaving the combustion chamber, assuming no heat losses and constant pressure, is given by

$$h_3 = h_2 + \frac{G_f}{G_a + G_f} \times H_c$$

An indication of the air-fuel ratio ordinarily occurring is obtained from the following illustration. Assume that the pressure ratio of the compressor is 6 and its efficiency is 0.80, and consider sea-level conditions at the entrance section, subscript 1. Then from the air tables of Chapter 4, assuming $T_1 = 520$ R,

$$h_1 = 28.80 \text{ Btu/lb} \qquad p_{r1} = 2.506 \qquad \eta_c = 0.80$$

$$p_{r2} = 2.506 \times 6 = 15.036 \qquad T_{2s} = 864.2 \text{ R}$$

$$h_{2s} = 112.07 \quad \text{Btu/lb}$$

$$\frac{L_c'}{J} = 112.07 - 28.80 = 83.27 \quad \text{Btu/lb}$$

$$\Delta h_c = \frac{1}{\eta_c J} L_c = \frac{83.27}{0.8} = 104.09 \quad \text{Btu/lb}$$

$$h_2 = 104.09 + 28.80 = 132.89$$

$$T_2 = 948.5 \text{ R}$$

If the inlet temperature to the turbine is $T_3 = 1660$ R, each pound of air has the enthalpy $h_3 = 316.57$ Btu. Hence, the enthalpy added to each pound of air by the combustion of fuel denoted by Δh_B is

$$\Delta h_B = 316.57 - 132.89 = 183.68 \quad \text{Btu/lb of air}$$

Assuming that each pound of fuel has a calorific value of 18,500 Btu above the heat required to raise its temperature to combustion

conditions, then with $\eta_B = 0.98$ the weight of fuel added per pound of air is

$$\frac{183.68}{18,500} \times \frac{1}{\eta_B} = \frac{183.68}{18,500 \times 0.98} = 0.0102 \quad \text{lb fuel/lb of air}$$

This indicates that for each 100 lb of air passing through the combustion chamber approximately 1.0 lb of fuel will be added to it. Consequently, no appreciable error is introduced by the assumption that there is no increase in the weight of fluid at the combustion chamber and that the working substance entering the turbine is solely heated air. This assumption errs in the direction of conservatism.

Using this assumption, the heat supplied becomes

$$Q_i = \frac{G_f}{G_a} H_c = \frac{1}{\eta_B}(h_3 - h_2) \quad \text{Btu/lb of air}$$

and

$$\eta_i = \frac{\eta_B}{2gJ(h_3 - h_2)}(w^2 - V^2) = \frac{\eta_B(w^2 - V^2)}{50,000(h_3 - h_2)} \tag{30}$$

To obtain an indication of the effect of the speed of the airplane upon the internal efficiency, equation 30 is written

$$\eta_i = \frac{\eta_B w^2[1 - (V^2/w^2)]}{50,000(h_3 - h_2)} = \frac{\eta_B w^2(1 - \nu^2)}{50,000(h_3 - h_2)} \tag{31}$$

For a given operating temperature at the turbine, the enthalpy change $(h_3 - h_2)$ is constant. Hence when $V = w$ the internal efficiency is zero; this is readily appreciated, for under these conditions the thrust is zero and the kinetic energy added to the gas is zero. The air just passes through the system, and its velocity increase, relative to the airplane, is zero. On the other hand, if the velocity ratio is zero $(V = 0)$, then η_i depends entirely upon the magnitude of the jet velocity w. The internal efficiency will be high, but, since the airplane is not moving, no useful work is performed.

8. The Diffuser and Ram Pressure

In order to establish the conditions at the entrance to the air compressor, the temperature and pressure of the air leaving the diffuser must be determined. If the ram efficiency η_r or the diffuser efficiency η_D is known, then the pressure at the entrance to the compressor can be determined by the methods explained in Chapter 3, Section 29.

The function of the diffuser has been given detailed discussion in Chapter 3 and need not be repeated here. It should be noted that because of the losses in this piece of apparatus it is not possible to transform all the kinetic energy associated with the approaching air into pressure rise.

9. Thermodynamic Analysis on the Basis of the Perfect-Gas Laws

A good insight into the general characteristics of the thermal jet engine can be derived by applying the perfect-gas laws to the thermo-
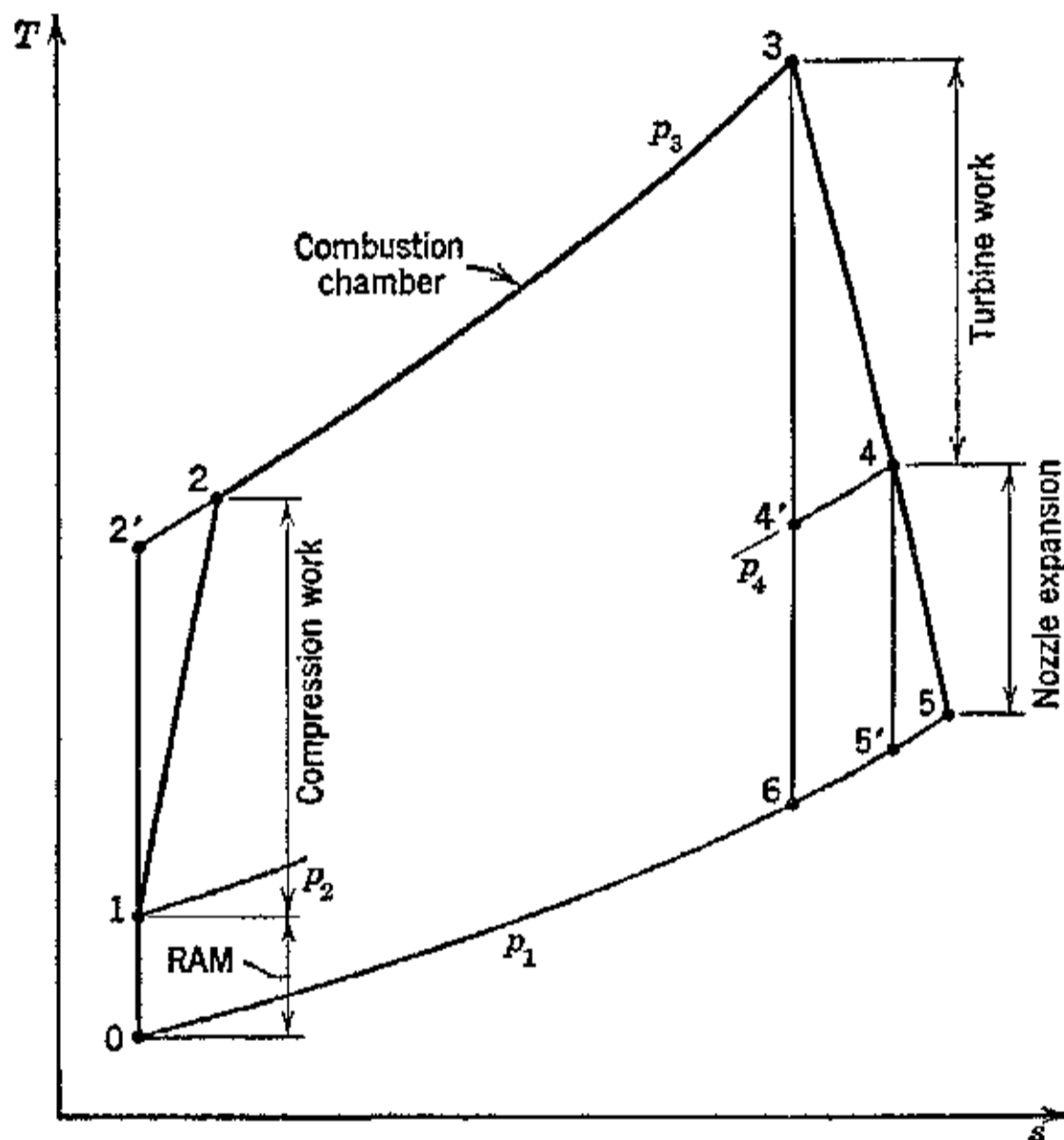
FIG. 9. Turbojet engine cycle on the T-s plane.

dynamic processes involved. The analysis which follows is based upon the following simplifying assumption: (a) there is full recovery of the dynamic pressure of the entering air (100 per cent ram); (b) there is no change in the mass rate of flow of fluid passing through the engine; (c) there is no change in the chemical composition of the working fluid, it being assumed to be air at all sections of the flow path; (d) the working fluid (air) behaves in accordance with the laws of perfect gases, so that the effect of temperature on the specific heat of the air may be neglected; (e) there are no pressure losses.

The inaccuracies introduced by the above assumptions are so small that for the practical purpose of obtaining a general insight into the behavior of the turbojet engine they are well justified. The advantage of this form of analysis is that general equations for the various performance characteristics can be derived.

Figure 9 illustrates the thermodynamic processes involved on the temperature-entropy (T-s) plane. The processes have been explained in the foregoing and are denoted on the diagram so that no further explanation is necessary.
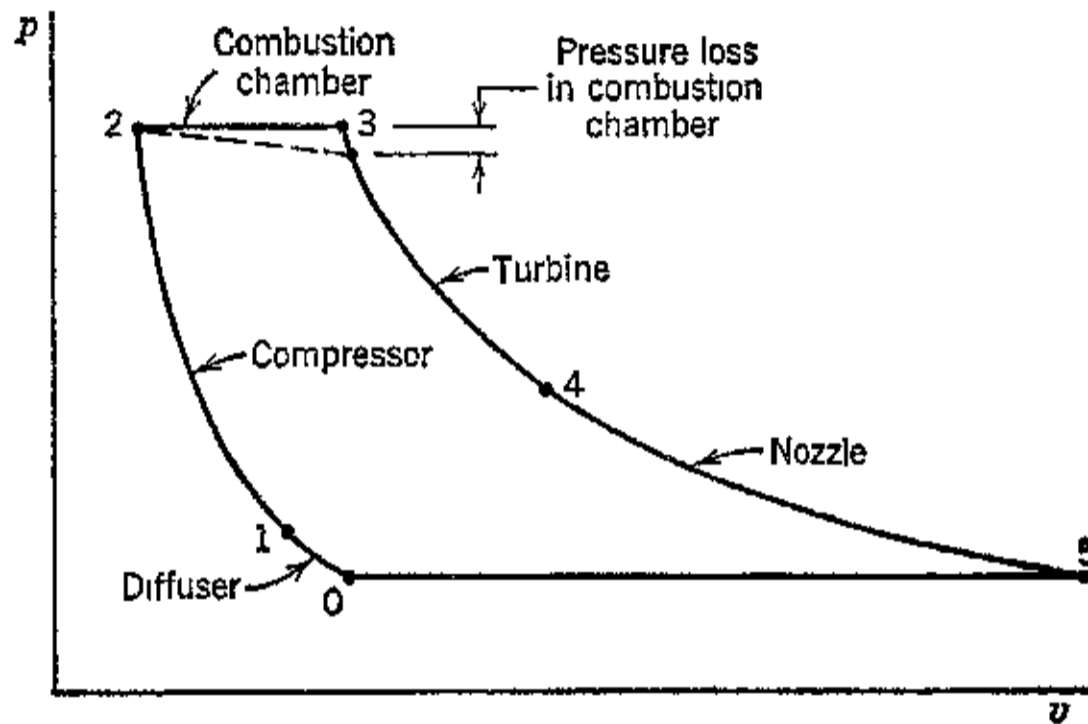
[FIG. 10.   Turbojet engine cycle on the p-v plane.

Figure 10 illustrates the turbojet engine cycle on the p-v plane. The pressure drop in the combustion chamber, indicated by the broken line, is neglected here.

The object of the analysis is to obtain equations for the temperatures at the state points indicated on the diagram in terms of the temperature of the incoming air and its Mach number.

The temperature of the air at the end of the isentropic compression in the diffuser (100 per cent ram) can be determined from equation 3·41 which for $k = 1.4$ becomes

$$\Phi = \frac{T_1'}{T_0} = 1 + \left(\frac{k-1}{2}\right) M_0^2 = 1 + 0.2 M_0^2 \tag{32}$$

Figures 3·3 and 3·4 present the ideal temperature-rise ratio Φ, and Fig. 3·5 the corresponding pressure-rise ratio p_1'/p_0, as functions of the Mach number of the entering air.

In this case $T_1 = T_1'$ and the temperature at the entrance to the compressor is

$$T_1 = T_0 \Phi \tag{33}$$

The temperature of the air is raised from T_1 to T_2. If the compression process were isentropic the compression temperature would be T_2' instead of T_2. The ratio T_2'/T_1 is denoted by θ as in Chapter 7. Thus

$$\theta = \frac{T_2'}{T_1} = \left(\frac{p_2}{p_1}\right)^{\frac{k-1}{k}} \qquad (34)$$

or

$$T_2' = T_1\theta \qquad (35)$$

Values of θ for different pressure ratios and values of k are presented in Table 7·1.

Since the compression process is not isentropic, the final air temperature T_2 is higher than T_2'. If the compressor efficiency is denoted by η_c, then

$$T_2 - T_1 = \frac{T_2' - T_1}{\eta_c} = T_1\left(\frac{\theta - 1}{\eta_c}\right)$$

so that

$$T_2 = T_0\Phi\left(1 + \frac{\theta - 1}{\eta_c}\right) \qquad (36)$$

In the combustion chamber the air temperature is raised from T_2 to T_3. It is convenient to express the temperature T_3 in terms of the atmospheric temperature T_0,

$$T_3 = \alpha T_0 \qquad (37)$$

Table 8·1 presents values of the coefficient α as a function of altitude for different values of T_3.

TABLE 8·1

VALUES OF $\alpha = T_3/T_0$ AS A FUNCTION OF ALTITUDE

Altitude	Values of T_3				
ft	1600 R	1700 R	1800 R	1900 R	2000 R
0	3.082	3.275	3.468	3.662	3.854
5,000	3.193	3.392	3.582	3.780	3.982
10,000	3.310	3.516	3.724	3.930	4.136
15,000	3.436	3.652	3.866	4.083	4.282
20,000	3.592	3.792	4.024	4.273	4.462
25,000	3.722	3.955	4.187	4.420	4.652
30,000	3.880	4.124	4.367	4.608	4.854
35,000	4.056	4.185	4.565	4.817	5.070
40,000	4.072	4.325	4.580	4.835	5.090

From the temperature-entropy diagram, Fig. 9, it is seen that, if the heated air expanded isentropically to the atmospheric pressure p_0, it would be in the state designated by the number 6. The part of the diagram 0-2′, 2′-3, 3-6, and 6-0 consists of two isobars and two isentropic processes. From elementary thermodynamics it follows that

$$T_3 T_0 = T_2' T_6$$

or

$$T_6 = \frac{T_3}{T_2'} T_0 = \alpha T_0 \frac{T_0}{T_1'\theta} = T_0 \alpha \left(\frac{1}{\Phi\theta}\right) \tag{38}$$

Table 8·2 presents values of the parameter $1/\Phi\theta$ as a function of the Mach number of the incoming air for different pressure ratios.

TABLE 8·2

VALUES OF PARAMETER $1/\Phi\theta$ FOR DIFFERENT PRESSURE RATIOS p_2/p_1 AS A FUNCTION OF MACH NUMBER

Mach No.	Pressure Ratio of Compressor p_2/p_1							
	1.5	2.0	2.5	3.0	3.5	4.0	5.0	6.0
0	0.8904	0.8204	0.7698	0.7304	0.6988	0.6725	0.6317	0.5995
0.1	.8890	.8191	.7683	.7299	.6980	.6712	.6308	.5987
0.2	.8825	.8138	.7635	.7247	.6930	.6678	.6268	.5950
0.3	.8750	.8059	.7560	.7177	.6868	.6609	.6205	.5893
0.4	.8630	.7946	.7465	.7078	.6796	.6521	.6125	.5813
0.5	.8480	.7815	.7332	.6960	.6658	.6408	.6018	.5714
0.6	.8309	.7655	.7186	.6815	.6520	.6275	.5895	.5593
0.7	.8107	.7474	.7012	.6656	.6367	.6130	.5755	.5462
0.8	.7893	.7273	.6827	.6472	.6198	.5964	.5632	.5319
0.9	.7664	.7060	.6631	.6285	.6019	.5792	.5440	.5117
1.0	.7362	.6832	.6419	.6085	.5828	.5606	.5267	.4999

The expansion of the gases in the turbine produces just enough work to drive the air compressor. Hence

$$\eta_t \bar{c}_{pt}(T_3 - T_4')\left(1 + \frac{G_f}{G_a}\right) = \frac{\bar{c}_{pc}}{\eta_c}(T_2' - T_1') \tag{39}$$

where $\bar{c}_{pt}$ = mean specific heat of the gases flowing through the turbine.

$\bar{c}_{pc}$ = mean specific heat of the air flowing through the compressor.

By virtue of assumptions (b), (c), and (d) it follows that equation 39 reduces to

$$\eta_t(T_3 - T_4') = \frac{1}{\eta_c}(T_2' - T_1) \tag{40}$$

Since the turbine work is exactly equal to the compressor work

$$T_3 - T_4 = T_2 - T_1 \tag{41}$$

From these last two expressions the equations for T_4' and T_4 are derived, by substituting from the preceding equations. Hence

$$T_4' = T_0\alpha\left[1 - \frac{\Phi(\theta-1)}{\eta_c\eta_t\alpha}\right] \tag{42}$$

and

$$T_4 = T_0\alpha\left[1 - \frac{\Phi(\theta-1)}{\eta_c\alpha}\right] \tag{43}$$

In order to establish the pressure at the entrance to the turbine, the pressure loss in the combustion chamber must be known or estimated. This loss must be kept low and is ordinarily only a few per cent of the pressure p_2. In this analysis, this pressure loss is neglected.

By the same thermodynamic principle used in deriving the expression for T_6 it follows that

$$T_5' = T_6\frac{T_4}{T_4'}$$

Substituting for T_6 from equation 38 and for T_4 and T_4' from above

$$T_5' = T_0\frac{\alpha}{\Phi\theta}\left[\frac{1 - \dfrac{\Phi(\theta-1)}{\eta_c\alpha}}{1 - \Phi\dfrac{(\theta-1)}{\eta_c\eta_t\alpha}}\right] \tag{44}$$

The temperature drop corresponding to an isentropic expansion in the nozzle is $T_4 - T_5'$. From equations 43 and 44

$$T_4 - T_5' = T_0\alpha\left\{\left[1 - \frac{\Phi(\theta-1)}{\eta_c\alpha}\right] - \frac{1}{\Phi\theta}\left[\frac{1 - \Phi\dfrac{(\theta-1)}{\eta_c\alpha}}{1 - \Phi\dfrac{(\theta-1)}{\eta_c\eta_t\alpha}}\right]\right\} \tag{45}$$

Let

$$Y = \left\{\left[1 - \Phi\frac{(\theta-1)}{\eta_c\alpha}\right] - \frac{1}{\Phi\theta}\left[\frac{1 - \Phi\dfrac{(\theta-1)}{\eta_c\alpha}}{1 - \Phi\dfrac{(\theta-1)}{\eta_c\eta_t\alpha}}\right]\right\} \tag{45a}$$

Then

$$T_4 - T_5' = T_0\alpha Y$$

Values of the parameter Y as a function of the Mach number, for the conditions $p_2/p_1 = 3.0$ and $\eta_c = \eta_t = 0.85$ are presented in Fig. 11.
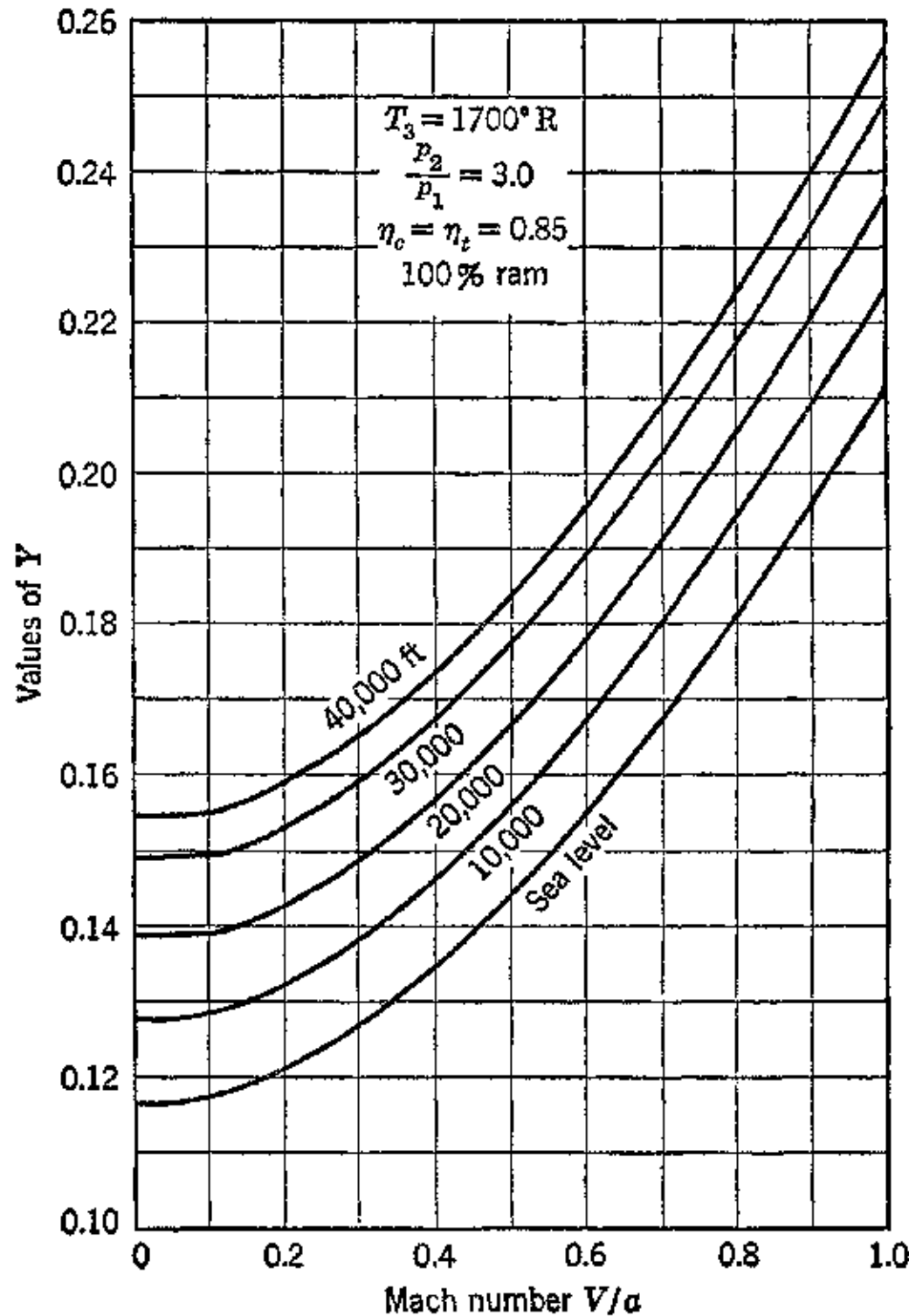
FIG 11. Values of parameter Y as a function of Mach number for different altitudes. (Reproduced from M. J. Zucrow, *Trans. A.S.M.E.*, May 1946.)

The value of the parameter Y depends upon the pressure ratio of the air compressor, the efficiencies of the compressor and turbine, the temperature of the air leaving the combustion chamber, the Mach number of the entering air, and the altitude of the system as expressed through $\alpha = T_3/T_0$.

Values of the parameters $\Phi(\theta - 1)/\eta_c\eta_t\alpha$ and $\Phi(\theta - 1)/\eta_c\alpha$ as functions of Mach number are plotted for different altitudes in Fig. 12 and 13 respectively. These curves are based on a pressure ratio $p_2/p_1 = 3.0$, $\eta_c = \eta_t = 0.85$, and $T_3 = 1700$ R.
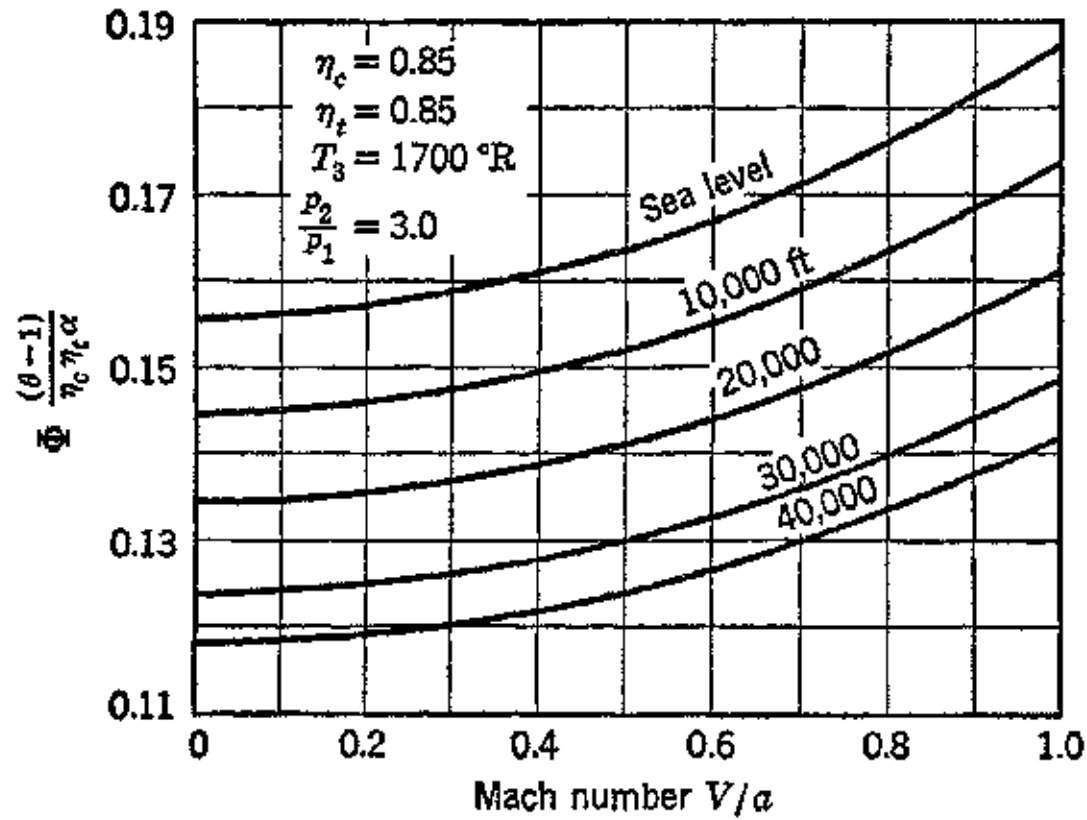
FIG. 12.   Values of the parameter $\Phi(\theta - 1)/\eta_c\eta_t\alpha$ as a function of Mach number for different altitudes.
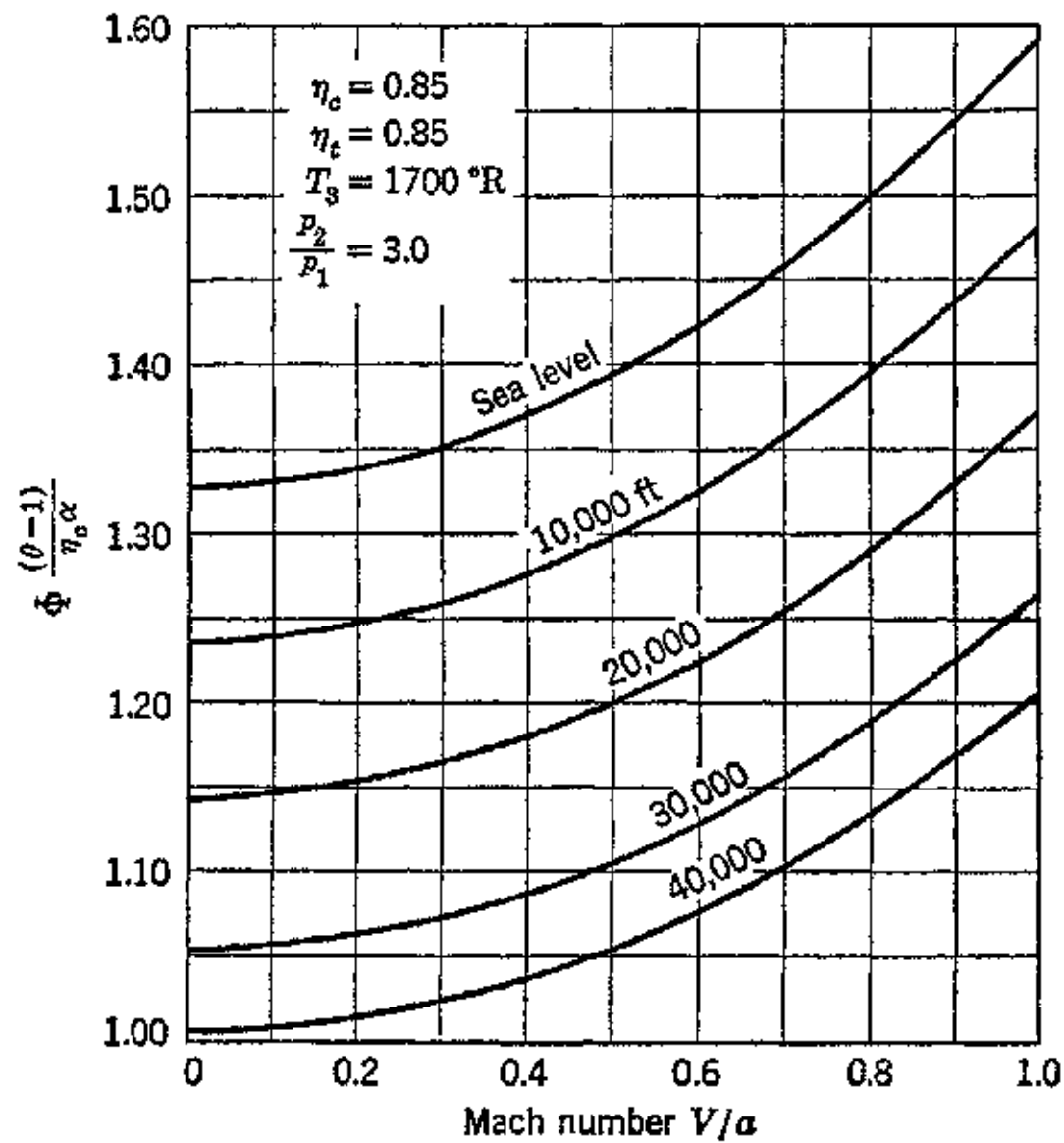
FIG. 13.   Values of the parameter $\Phi(\theta - 1)/\eta_c\alpha$ as a function of Mach number for different altitudes.

Values of the isentropic temperature drop $T_4 - T_5'$ for the conditions listed above are presented in Fig. 14.
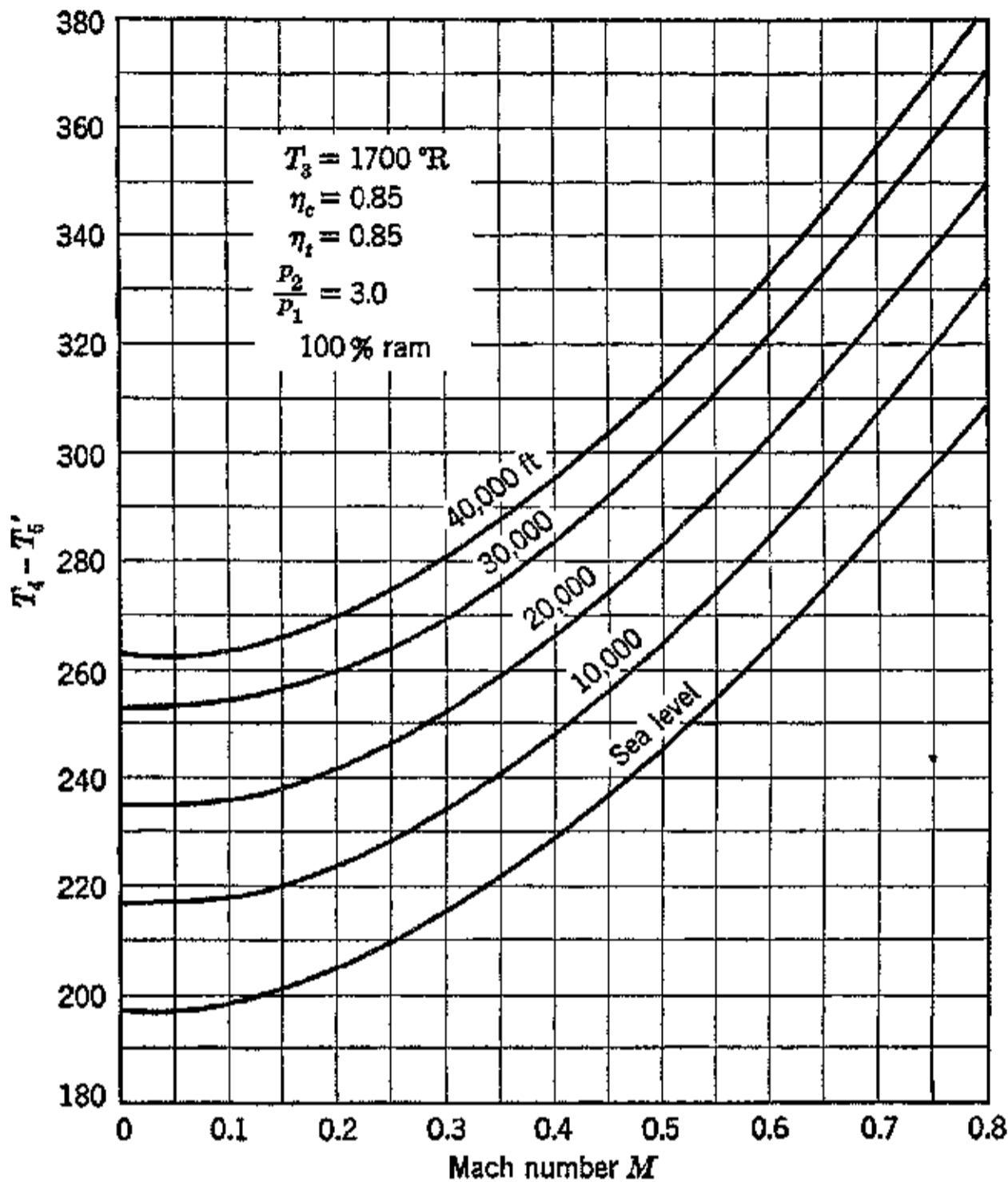
FIG. 14. Values of the isentropic temperature drop for the exhaust nozzle as a function of Mach number for different altitudes. (Reproduced from M. J. Zucrow, *loc. cit.*)

From the isentropic temperature drop $T_4 - T_5'$, the corresponding discharge velocity of the jet gases neglecting the approach velocity is readily calculated. Thus

$$w' = \sqrt{2gJc_pT_0\alpha Y} \tag{46}$$

or

$$w' = \sqrt{2gJc_p(T_4 - T_5')} = 223.7\sqrt{c_p(T_4 - T_5')} \tag{46a}$$

The last two equations give the isentropic exhaust velocity w' and are applicable to a perfect nozzle. For an actual nozzle the exhaust velocity is given by

$$w = \varphi w' = 223.7\varphi\sqrt{c_p(T_4 - T_5')} = 223.7\sqrt{c_p(T_4 - T_5)} \tag{47}$$

Figure 15 presents values of the isentropic exhaust velocity where $p_2/p_1 = 3.0$, $\eta_c = \eta_t = 0.85$, and $T_3 = 1700$ R. It is seen that at all the altitudes presented in the figure the exhaust velocity increases with the flight speed, because the ram effect increases the pressure at the entrance to the air compressor.
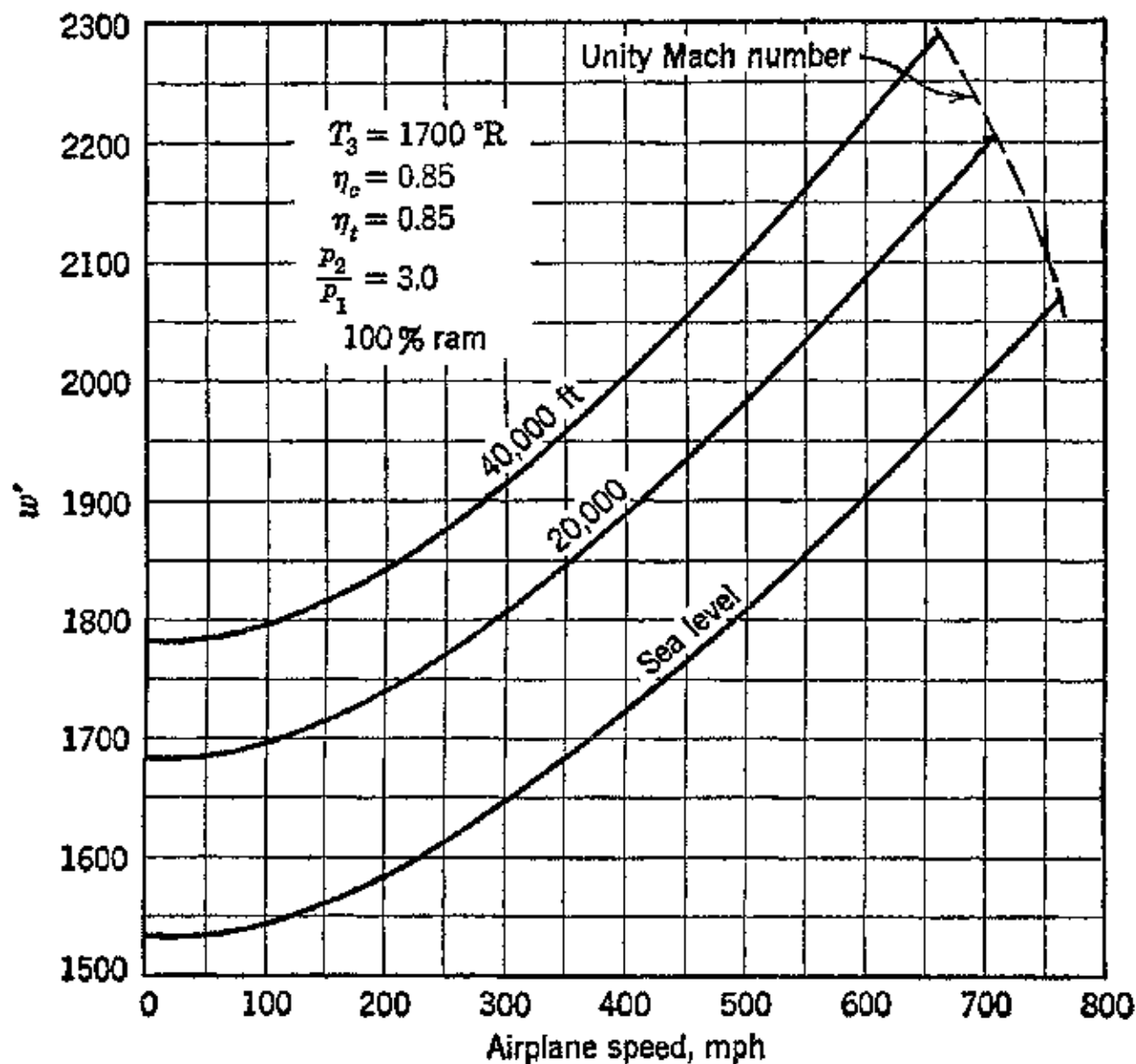
FIG. 15.   Isentropic jet velocity vs. Flight Speed for different altitudes.   (Reproduced from M. J. Zucrow, *loc. cit.*)

·From equation 47 it follows that the actual temperature drop in the nozzle $T_4 - T_5$ is given by

$$T_4 - T_5 = \varphi^2(T_4 - T_5') = \varphi^2 T_0 \alpha Y \tag{48}$$

Substituting for T_4 from equation 43

$$T_5 = T_0\alpha\left[1 - \Phi\frac{(\theta - 1)}{\eta_c\alpha} - \varphi^2 Y\right] \tag{49}$$

The equation for the isentropic exhaust velocity can be transformed to indicate the dependence of this velocity upon the acoustic velocity for the air entering the engine.   Thus, noting that

$Jc_pT_0 = kRT_0/(k - 1)$, where R is the gas constant for the atmospheric air, and that a = acoustic velocity = $\sqrt{gkRT_0}$, then, for $k = 1.4$, the exhaust velocity is

$$w' = a \sqrt{\frac{2}{k - 1}} \sqrt{\alpha Y} = 2.236a\sqrt{\alpha Y} \quad \text{fps} \qquad (50)$$

and

$$w = \varphi w' = 2.236a\varphi\sqrt{\alpha Y} \quad \text{fps} \qquad (51)$$

The exhaust velocity of the exhaust gases being known, the performance characteristics of the propulsion system can be readily determined.

EXAMPLE. An airplane powered by a turbojet engine has a flight speed of 600 mph at 30,000-ft altitude. The pressure ratio of the compressor is 3.0, and the gases enter the turbine at 1700 R. The nozzle coefficient is $\varphi = 0.95$. What is the exhaust velocity of the jet?

By equation 51

$$w = \varphi w' = 2.236 \times 0.95 \times a\sqrt{\alpha Y}$$

From Table 8·1

$$\alpha = \frac{T_3}{T_0} = 4.124$$

From Table 1·6

$$a = 997.9 \quad \text{fps}$$

so that $M = 880/997.9 = 0.882$. From Fig 11

$$Y = 0.230 \quad \alpha Y = 0.946 \quad \sqrt{\alpha Y} = 0.972$$

$$w = 2.236 \times 0.95 \times 997.9 \times 0.972 = 2060 \quad \text{fps}$$

10. Performance Characteristics of the Turbojet Engine

The performance characteristics of principal interest are the thrust and overall efficiency under different operating conditions. For simplicity it is assumed that the velocity coefficient of the nozzle is unity; so that $w = w'$.

The thrust developed is calculated by applying equation 6. Thus

$$\mathfrak{J} = \frac{G}{g} (w - V) = \frac{G}{g} \left[a \sqrt{\frac{2}{k - 1}} \sqrt{\alpha Y} - V \right] \quad \text{lb} \qquad (52)$$

It is convenient to express the thrust in terms of the area of the discharge nozzle A. This is accomplished in the following manner. Let γ_5 denote specific weight of exit gases, R the gas constant for

exit gases (assumed to be air), and p_0 the back pressure, assumed to be atmospheric. From equation 49

$$T_5 = T_0\alpha\left[1 - \Phi\frac{(\theta - 1)}{\eta_c\alpha} - \varphi^2 Y\right]$$

Further

$$\gamma_5 = \frac{p_0}{RT_5}$$

The weight rate of gas flow is given by

$$G = Aw\gamma_5 = \frac{\pi}{4}D^2 w\gamma_5 = Aw\frac{p_0}{RT_5} \tag{53}$$

Hence

$$\mathfrak{I} = \frac{Awp_0}{gRT_5}\left[a\sqrt{\frac{2}{k-1}}\sqrt{\alpha Y} - V\right] \tag{54}$$

At take-off, $V = 0$ and $\Phi = 1.0$, so that the *static thrust* is given by

$$\mathfrak{I}_0 = \frac{Ap_0}{gRT_5}w^2 = \frac{Ap_0}{gRT_5}a^2\frac{2}{k-1}\alpha Y \tag{55}$$

The *overall efficiency* of the system is the ratio of the thrust power $\mathfrak{I}V$ to the rate of fuel consumption in mechanical units. Thus, assuming $\eta_B = 1$,

$$\eta = \frac{\mathfrak{I}V}{GJc_p(T_3 - T_2)} \tag{56}$$

Or substituting for $\mathfrak{I} = (G/g)(w - V)$

$$\eta = \frac{V^2\left(\dfrac{w}{V} - 1\right)}{gJc_p(T_3 - T_2)}$$

Substituting for w, T_3, T_2, and $Jc_p = Rk/(k - 1)$

$$\eta = \frac{V^2\left(\dfrac{\varphi a\sqrt{2/(k-1)}\sqrt{\alpha Y}}{V} - 1\right)}{\dfrac{1}{k-1}gkRT_0\left[\alpha - \Phi\left(1 + \dfrac{\theta - 1}{\eta_c}\right)\right]}$$

Noting that $V/a = M$, and $gkRT_0 = a^2$, the efficiency equation becomes

$$\eta = \frac{M^2\left(\varphi\,\frac{1}{M}\sqrt{\frac{2}{k-1}}\,\sqrt{\alpha Y} - 1\right)}{\frac{1}{k-1}\left[\alpha - \Phi\left(1 + \frac{\theta-1}{\eta_c}\right)\right]}\tag{57}$$

Figure 16 illustrates how the weight rate of air flow through the system varies with Mach number, with the compressor running at constant speed.
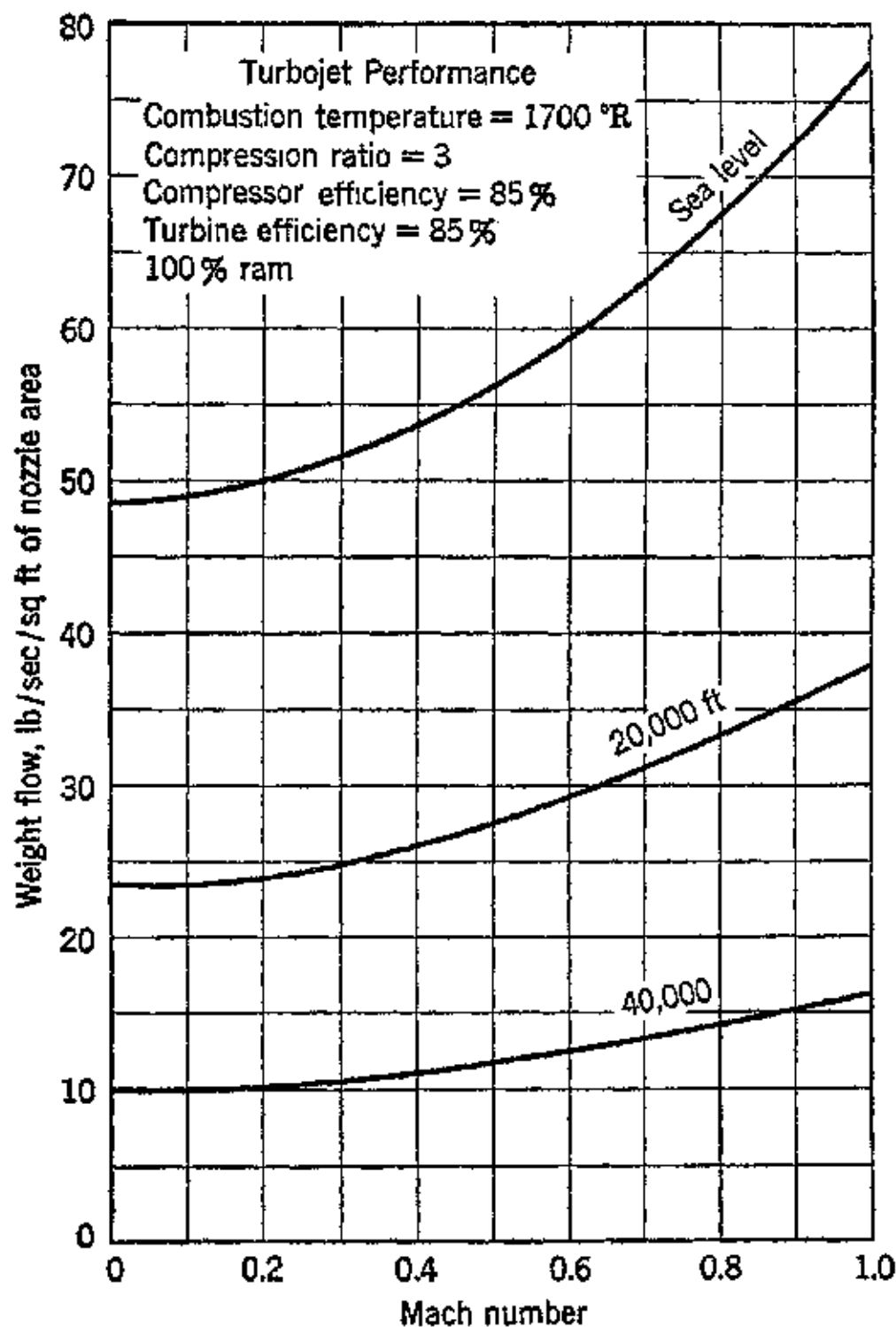
FIG. 16.   Weight rate of air flow vs. Mach number at different altitudes.   (Reproduced from M. J. Zucrow, *loc. cit.*)

Figure 17 shows the effect of true air speed on the thrust and the fuel consumption per pound of thrust; assuming that the fuel has a calorific value of 18,000 Btu/lb.   It is seen that the ratio of the static

thrust to flight thrust is considerably less than it is for a variable-pitch, constant-speed, engine-driven propeller. Owing to the ram effect, the thrust increases at higher air speeds after passing through a minimum point. The fuel consumption per pound of thrust in-
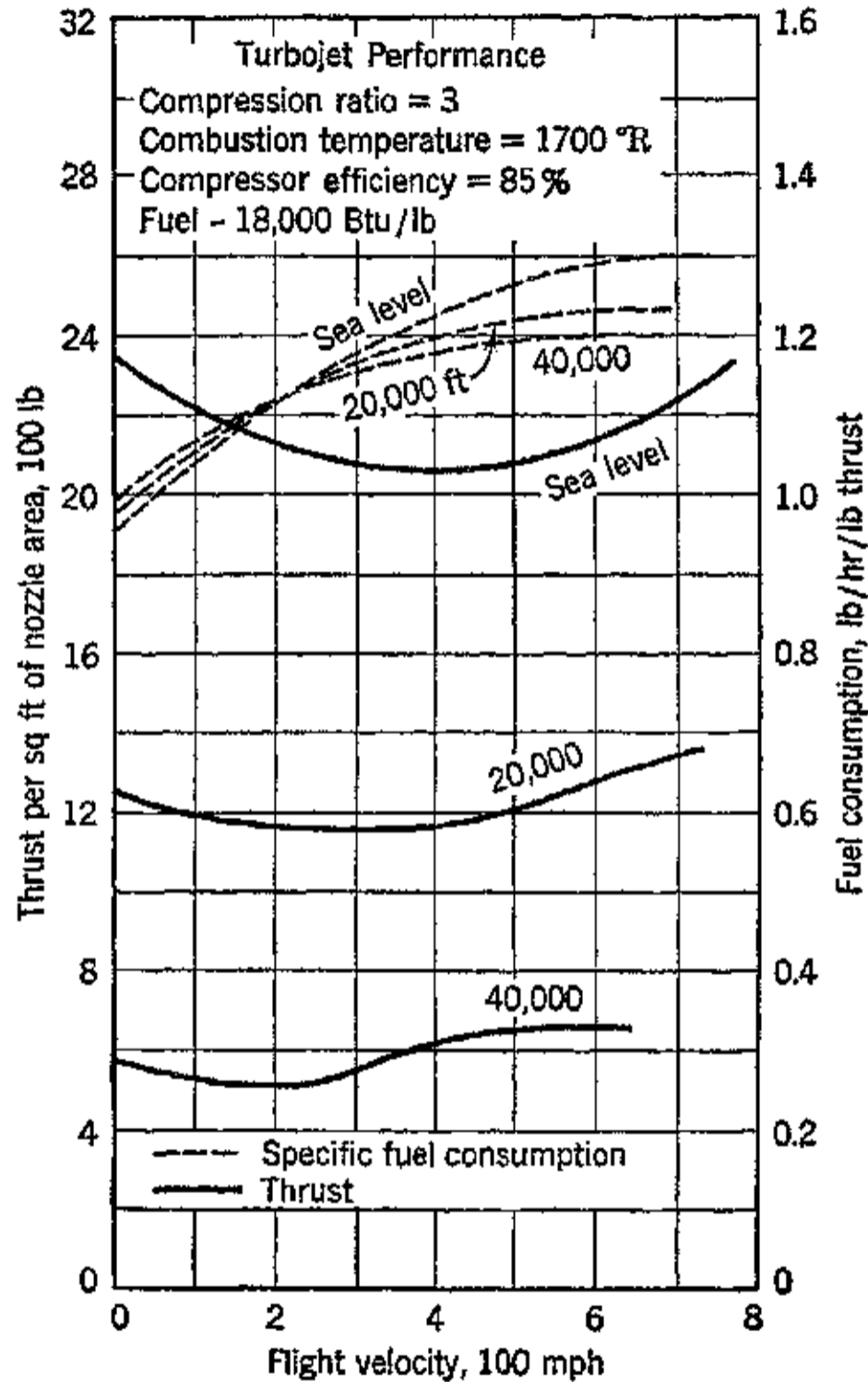
FIG. 17. Effect of true air speed on the thrust per square foot of nozzle area at different altitudes. (Reproduced from M. J. Zucrow, *loc. cit.*)

creases with flight velocity at all altitudes. Its rate of increase, however, diminishes with the altitude at speeds in excess of 250 mph. Figure 18 compares the thrust characteristics of the adjustable-pitch propeller with that of the turbojet engine. The basis of comparison is that both propulsion systems provide equal thrust at 375 mph.[10] Because of the small ratio of take-off thrust to flight thrust, the take-off characteristics of a turbojet-propelled plane will, in general, be inferior to that for a propeller-propelled plane.
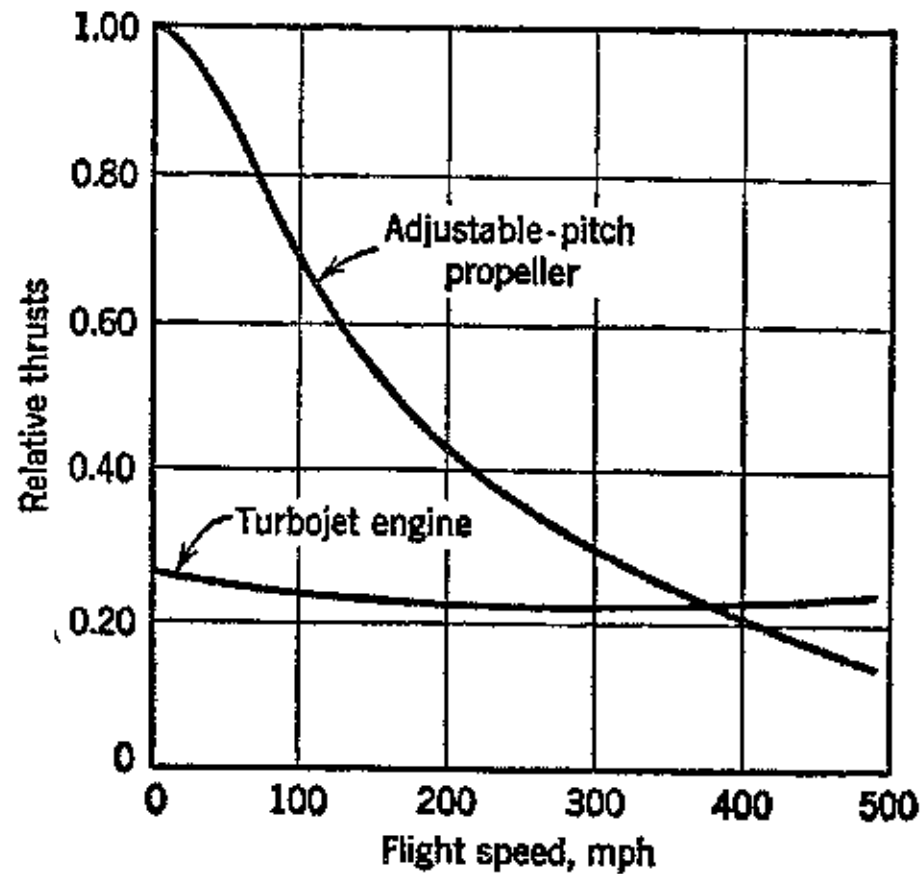
FIG. 18.   Comparison of the thrust characteristics of adjustable-pitch propeller and turbojet engine.   (Reproduced from F. W. Godsey and C. D. Flagle, *Westing-house Engineer*, June 1945.)
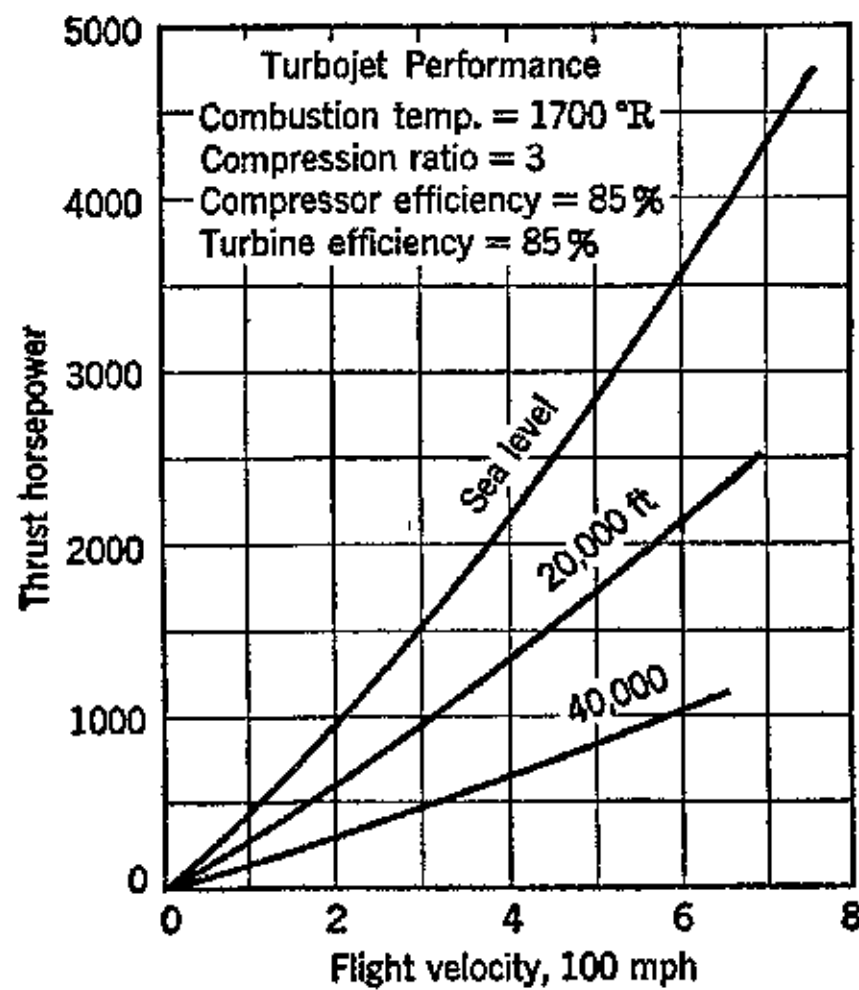
FIG. 19.   Thrust horsepower vs. flight velocity at different altitudes.   (Reproduced from M. J. Zucrow, *loc. cit.*)

Figure 19 illustrates the manner in which the *thrust horsepower* (*thp*) developed by the thermal jet engine varies with the flight speed and operating altitude. At high speeds the thrust horsepower developed per pound of fuel is not unreasonable.

Figure 20 presents performance characteristics calculated by Flagle and Godsey [10] for a fast high-altitude single-seater plane
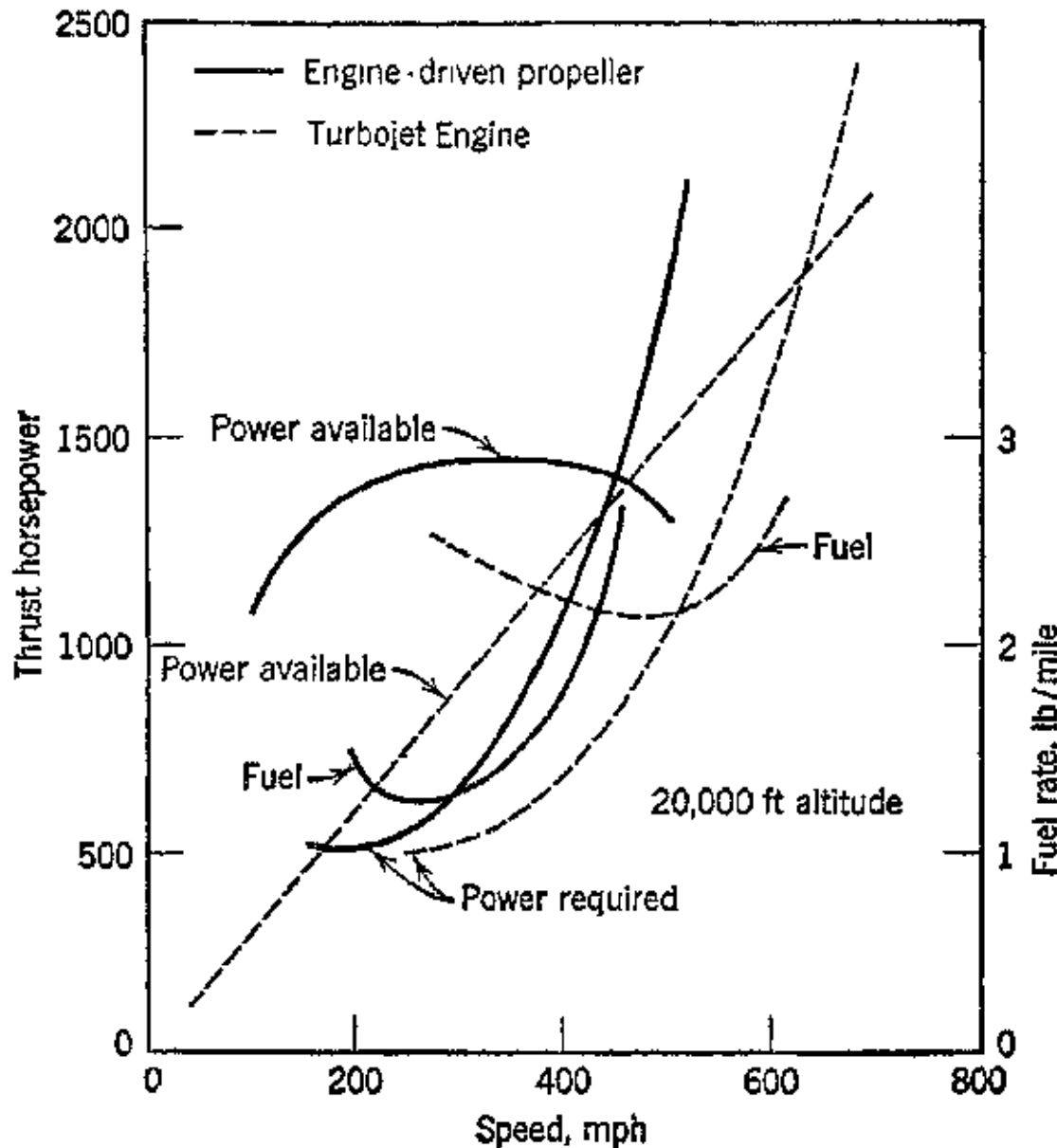
Fig. 20. Comparison of performance of engine-driven propeller and turbojet engine propulsion systems. (Reproduced from F. W. Godsey and C. D. Flagle, *loc. cit.*)

equipped with a reciprocating-engine-driven propeller and for a thermal-jet-propelled plane of equal gross weight and wing area. The calculations assumed the possible reduction in drag with jet propulsion to be 50 per cent of that for the reciprocating engine. The solid-line curves present the power required and power available for the engine-driven propeller plane, and the dotted lines present the same data for the jet-propelled airplane.

It is seen that, at the altitude of 20,000 ft, the maximum speed of the jet-propelled airplane is 600 mph against 460 mph for the conventional craft. The increase in speed of the jet-propelled plane

does not improve the cruising radius despite the allowance made in the calculations for increased fuel-carrying capacity. The lowest fuel rate for the conventional plane is 1 lb/mi (approximately) at 220 mph. The lowest fuel rate for the jet-propelled plane is 2.1
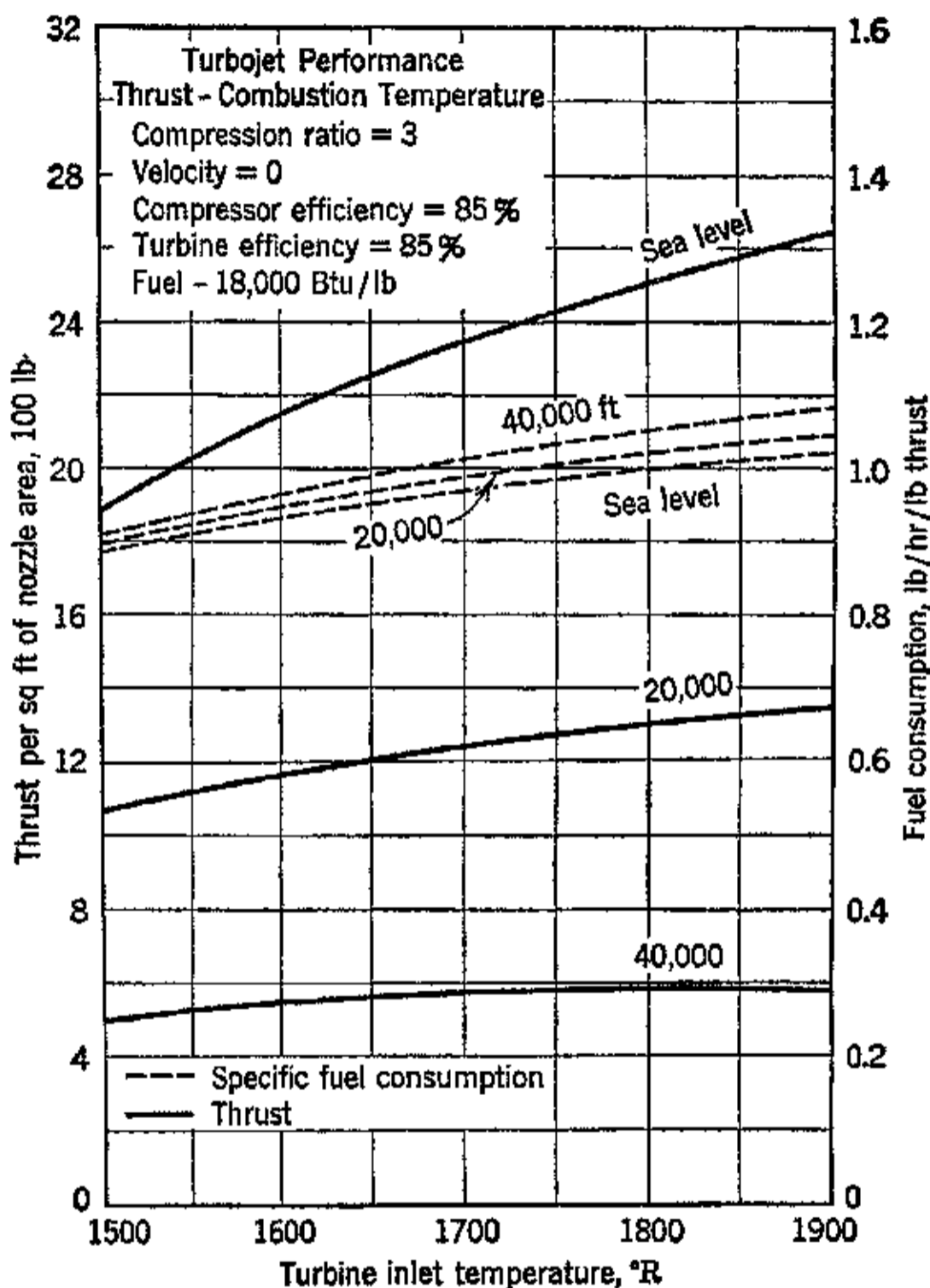
FIG. 21. Effect of turbine inlet temperature upon turbojet engine performance. (Reproduced from M. J. Zucrow, *loc. cit.*)

lb/mi at approximately 500 mph. This is beyond the operating speed of the conventional airplane.

Figure 21 illustrates the effect of increasing the air temperature leaving the combustion chamber upon the static thrust and fuel consumption per pound of thrust. It is seen that raising the temperature greatly increases the static thrust at sea level but the increased thrust is obtained at the expense of a slightly higher rate of fuel consumption per pound of thrust.

Figure 22 presents the static thrust and fuel consumption as functions of the pressure ratio for the air compressor, for a constant temperature at the entrance to the turbine. Increasing the pressure ratio is effective in increasing the thrust and decreasing the fuel consumption.
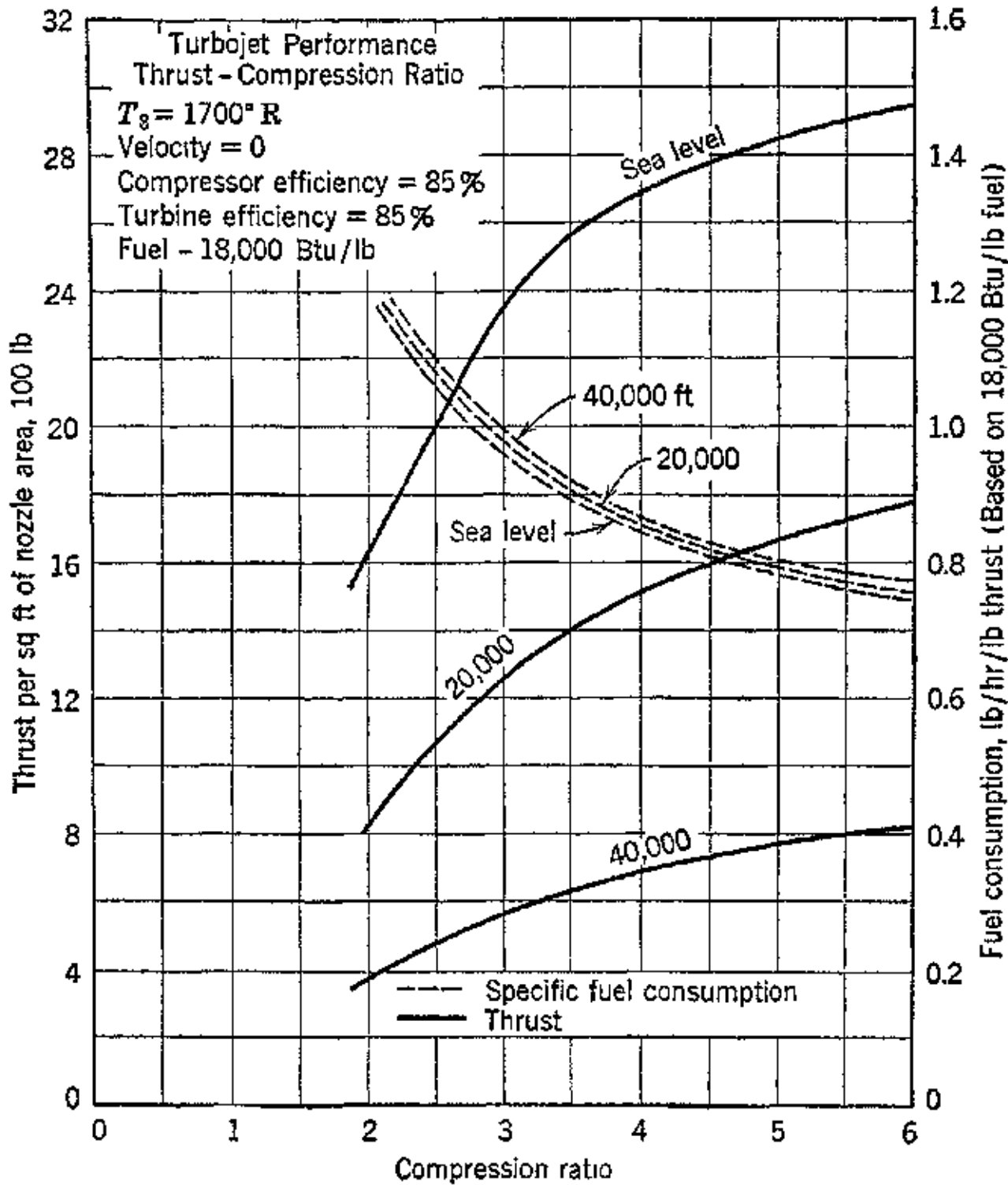
FIG. 22. Effect of cycle pressure ratio on turbojet engine performance. (Reproduced from M. J. Zucrow, *loc. cit.*)

With the assumed machine efficiencies $\eta_c = \eta_t = 0.85$, and a pressure of 3.0, the efficiency at 500 mph and 20,000-ft altitude is approximately 15 per cent. An engine-driven propeller with a propulsion efficiency of approximately 60 per cent would give the same overall efficiency. The overall efficiency, as a function of true air speed for different altitudes, is presented in Fig. 23.

Figure 24 illustrates the effect of the efficiency of the compressor upon the static thrust developed and the corresponding fuel consumption. It is seen that, with a turbine efficiency of 0.85 and a pressure ratio of 3.0, no thrust is developed if the compressor efficiency is less than 49 per cent. Increasing the efficiency of the compressor greatly reduces the fuel consumption and increases the thrust
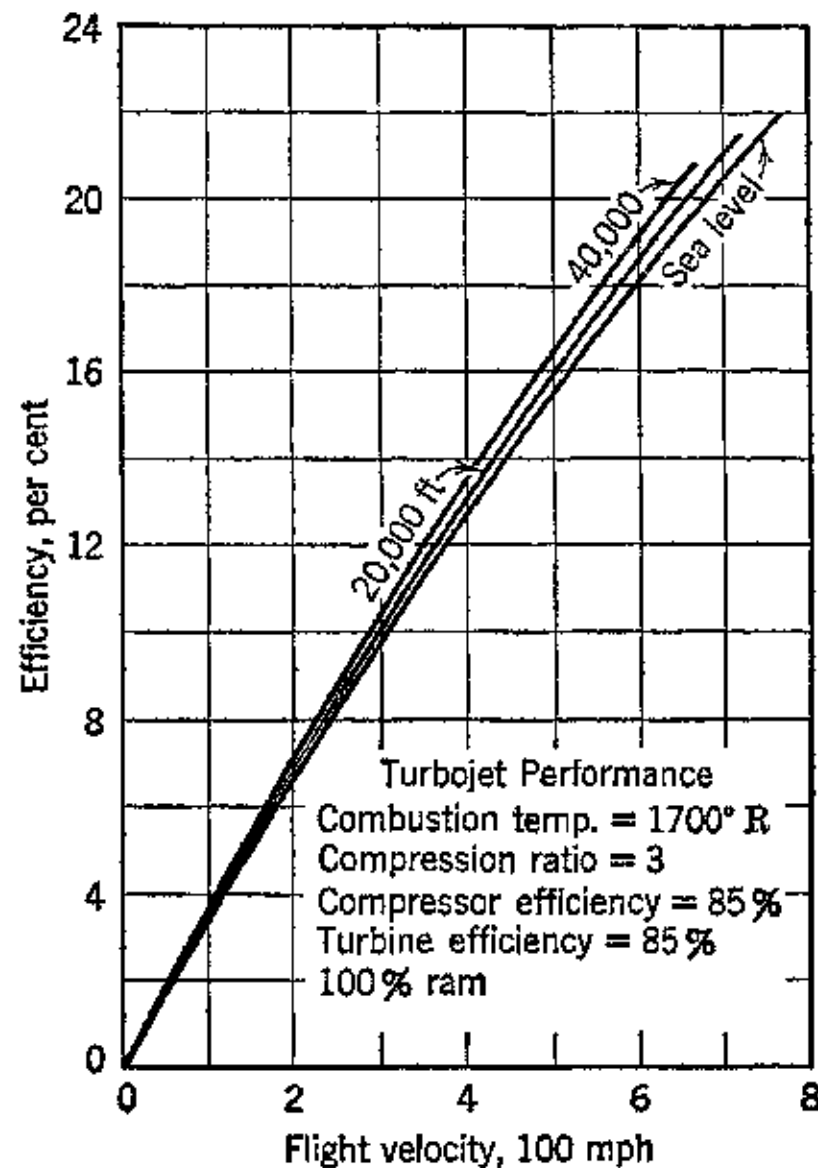
FIG. 23.   Efficiency as a function of flight velocity at different altitudes. (Reproduced from M. J. Zucrow, *loc. cit.*)

output. As a matter of fact, the efficiency of the system is improved by making the ratio of the compression work to the available energy of combustion as small as possible.

Figure 25 illustrates the total power requirements of a large transport airplane at 20,000-ft altitude.[10] Curve *A* is for a plane equipped with engine-driven propellers. Curve *B* applies to the same airplane equipped with gas-turbine-driven propellers. Curve *C* is for a jet-propelled transport having the same gross weight (120,000 lb), which includes the weights of the power plants plus the fuel weight.

The airplane corresponding to Curve *A* is equipped with four engines supercharged to 2000 hp at 20,000-ft altitude. The jet-propelled plane (Curve *C*) is equipped with four thermal jet engines

each delivering 6000 lb static thrust; this gives 24,000 lb thrust for take-off, which is comparable to the total static thrust for the four reciprocating engines. Two of the jet units are assumed to be turned off for cruising under 25,000-ft altitude. The power available for
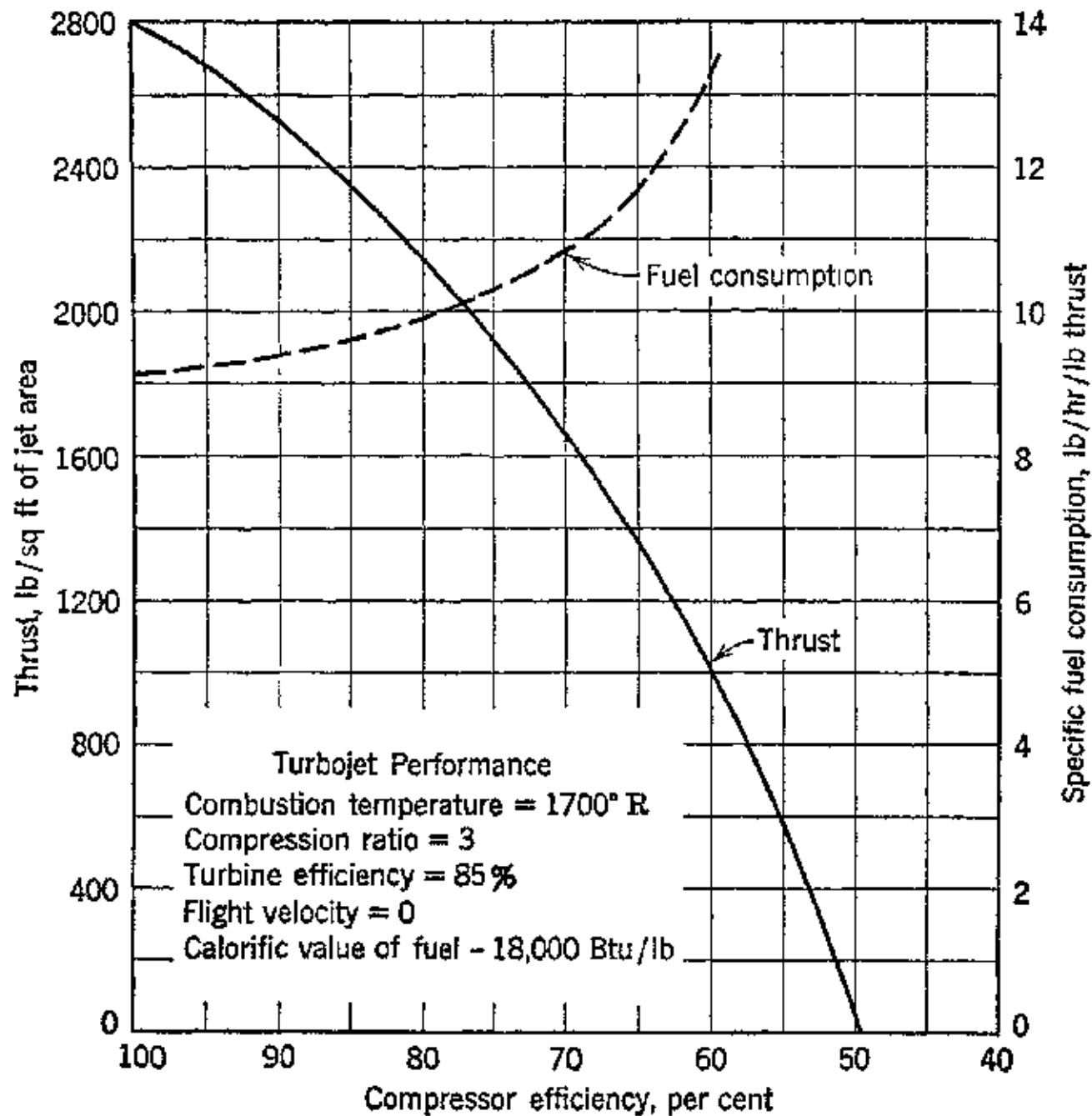
FIG. 24. Effect of compressor efficiency on turbojet engine performance. (Reproduced from M. J. Zucrow, *loc. cit.*)

propelling the airplane is illustrated for flight with either two or four of the turbojet engines being operated.

The gas-turbine-propeller propelled airplane (Curve *B*) is equipped with four gas turbines each delivering 3200 hp at take-off and 2000 hp at 20,000-ft altitude.

The general characteristics of the transport planes discussed above are compared graphically in Fig. 26. It is seen that the gas-turbine-propeller propelled airplane has characteristics superior to those of the engine-driven propeller plane on every basis of comparison except altitude ceiling, in which they are about equal.
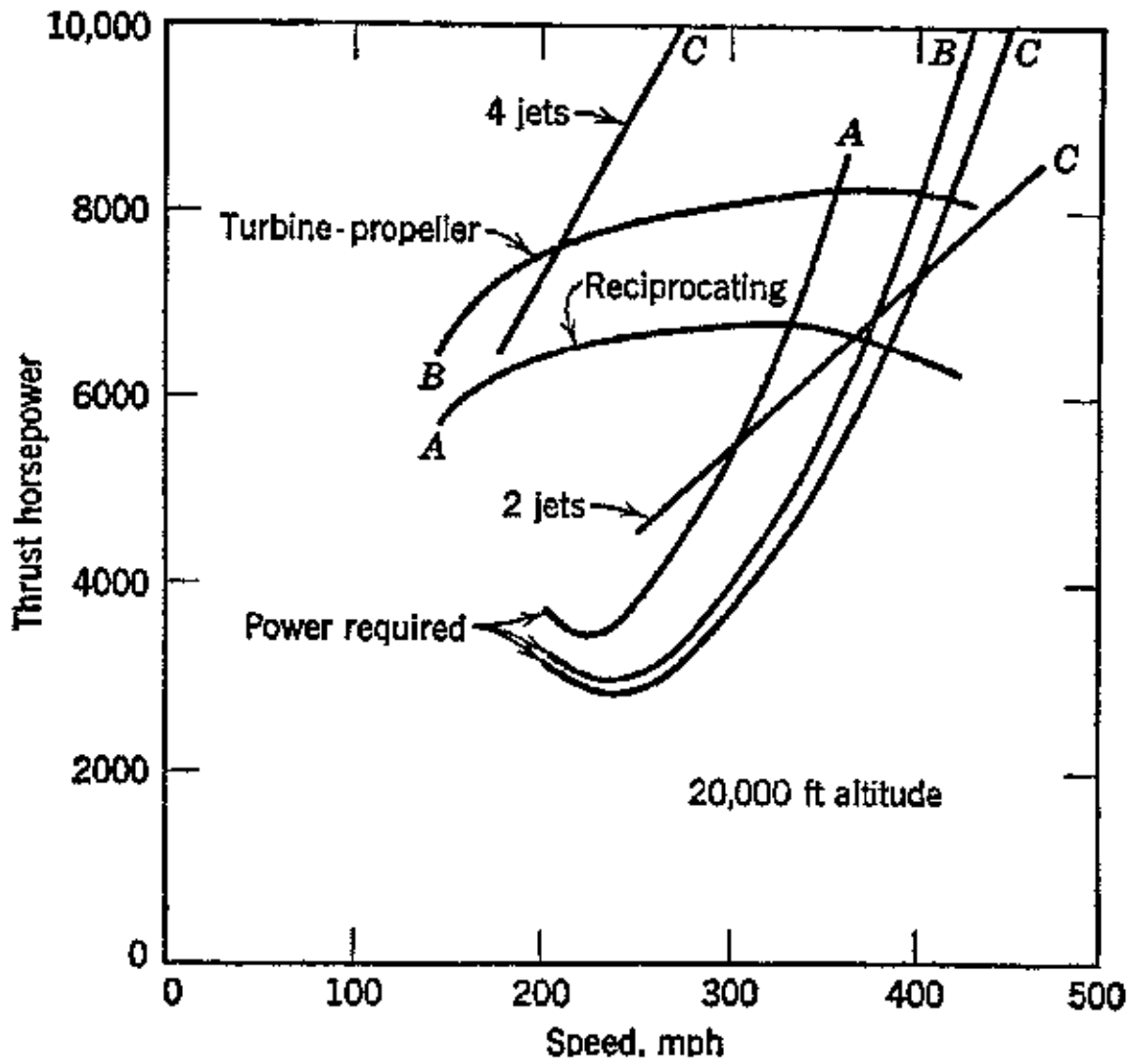
FIG. 25. Estimated total power requirements of a large transport airplane at 20,000-ft altitude with different propulsion systems. (Reproduced from F. W. Godsey and C. D. Flagle, *loc. cit.*)
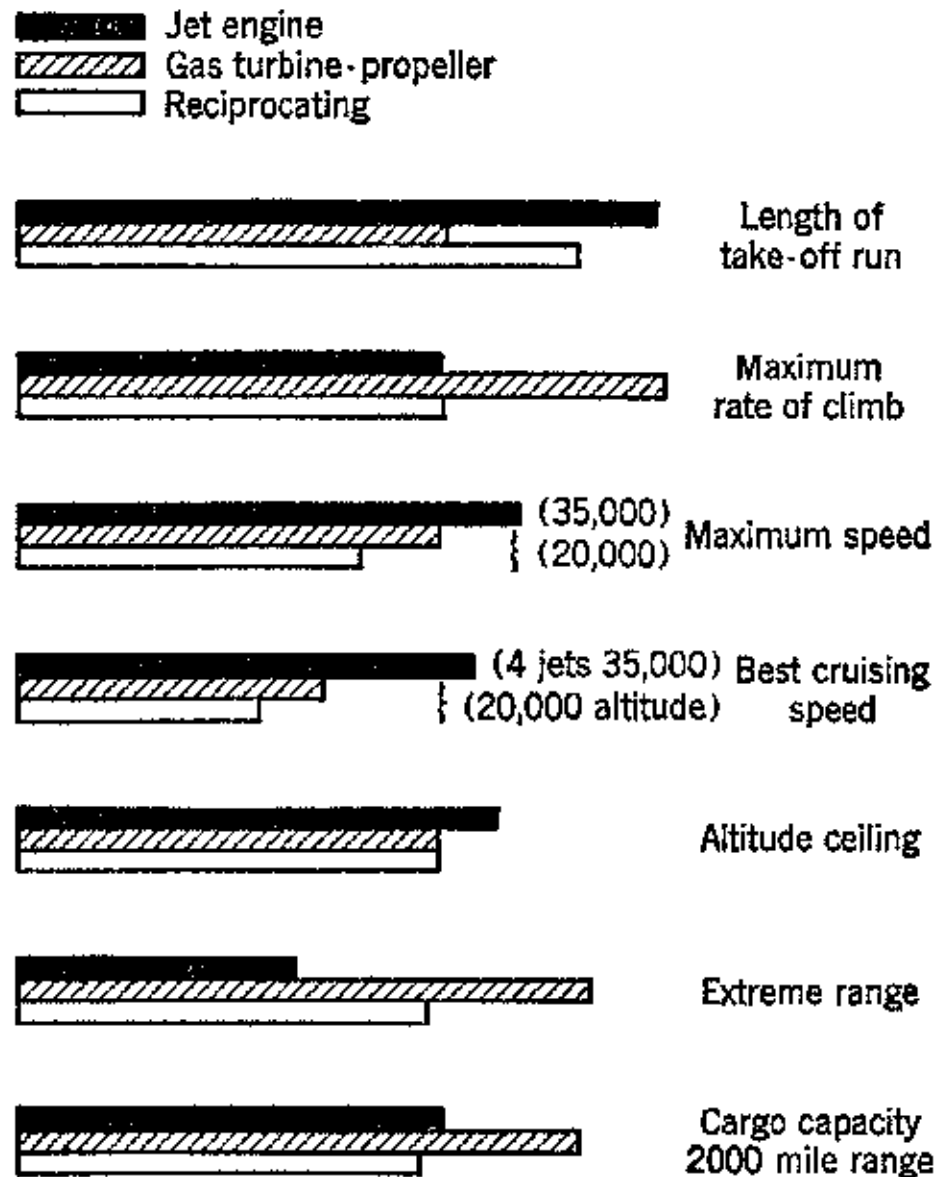
FIG. 26. Comparison of performance of a large transport plane with three different types of propulsion plants. (Reproduced from F. W. Godsey and C. D. Flagle.)

It is of interest to note that the jet-propelled airplane can make short flights with about 5 tons more payload than the conventional transport, and with about 3 tons more than the turboprop-propelled transport.[10]

11. Analysis Taking into Account the Variation in the Specific Heat with Temperature

This form of analysis can be carried out only by making step-by-step calculations for each element of the system. The methods of analysis have been discussed in Chapter 4 and will be illustrated by means of an example.

EXAMPLE. An airplane weighing 16,000 lb has a wing loading of 40 psf and a total drag coefficient $C_D = 0.012$. It is powered by a turbojet engine for which the machines have the following characteristics:

η_D = efficiency of diffuser = 0.95.
η_c = efficiency of compressor = 0.80.
η_t = efficiency of turbine = 0.85.
η_n = efficiency of nozzle = 0.96.
η_B = combustion efficiency = 0.98.
$T_3 = 1660$ R, $T_0 = 519$, $c_p = 0.243$, $k = 1.395$.
$r_c = 6.0$.

Calculate the thrust horsepower developed and the overall efficiency of the plant if the airplane travels at 420 mph at sea level, assuming that perfect-gas laws are applicable. Assume that the temperature of the air leaving the diffuser is 551 R and its pressure 17.89 psia.

$$V = 420 \times \frac{88}{60} = 615 \quad \text{fps} \qquad S = \frac{16,000}{40} = 400 \quad \text{ft}^2$$

Drag

$$D = \tfrac{1}{2}\rho V^2 C_D S = \tfrac{1}{2} \times 0.002378 \times 0.012 \times 400 \times 615^2$$

$$= 2150 \ \text{lb}$$

Thrust required is, therefore, equal to 2150 lb.
Diffuser. From data the temperature of the air entering the compressor is 551 R.
Compressor

$$\Delta h_c = \frac{1}{\eta_c} c_p T_1 Z_c; \quad \text{for } r = 6.0; \quad Z_c = 0.6604$$

Hence

$$\Delta h_c = \frac{1}{0.8} \times 0.243 \times 551 \times 0.6604 = 110.3 \quad \text{Btu/lb}$$

The temperature leaving the compressor is

$$T_2 = T_1 \left(1 + \frac{Z_c}{\eta_c}\right) = 551 \left(1 + \frac{0.6604}{0.8}\right) = 551 \times 1.826 = 1004 \ \text{R}$$

The pressure leaving the compressor is

$$p_2 = 6 \times p_1 = 6 \times 17.89 = 107.2 \quad \text{psia}$$

Combustion Chamber. Since the turbine inlet temperature is 1660 R, the heat added in the combustion chamber is

$$\Delta h_B = \frac{c_p}{\eta_B}(T_3 - T_2) = \frac{0.258}{0.98}(1660 - 1004) = 172.7 \quad \text{Btu/lb of air}$$

If the calorific value of the fuel is 18,500 Btu/lb, then the weight of fuel added per pound of air is

$$\frac{G_f}{G_a} = \frac{172.7}{18,500} = 0.00933 \quad \text{lb of fuel per lb of air}$$

Turbine. The turbine output is given by the equation

$$\Delta h_t = c_p T_3 \frac{Z_t}{1 + Z_t} \eta_t$$

The inlet temperature to the turbine is $T_3 = 1660$ R. It can be assumed as a first approximation that the temperature is that obtained by solving the relationship

$$\Delta h_t = \Delta h_c = c_p(T_3 - T_4) = 110.3 \quad \text{Btu/lb}$$

To obtain a closer first approximation to T_4, use an assumed value of c_p from Table 4·3 close to the range to be expected. Thus

Trial 1. Assume $(T_3 + T_4)/2 = 1400$. From the specific heat table, Chapter 4, $c_p = 0.2613$.

$$0.2613(1660 - T_4) = 110.3$$

$$434 - 0.2613 T_4 = 110.3$$

$$T_4 = \frac{434 - 110.3}{0.2613} = 1239 \text{ R}$$

Check. $(T_4 + T_3)/2 = 1450$.

Trial 2. Assume $(T_3 + T_4)/2 = 1450$ R, or average temperature is 990 F. From Chapter 4, $c_p = 0.264$.

$$1660 \times 0.264 - 0.264 T_4 = 110.3$$

$$T_4 = \frac{438 - 110.3}{0.264} = 1241 \text{ R} \quad \text{or} \quad \frac{T_4 + T_3}{2} = 1450 \text{ R}$$

Hence the value of c_p to be used is 0.264. The average temperature for the expansion is 1450 R. From Chapter 4, the average value of the specific heat ratio is $k = 1.352$. Using these values

$$\frac{k - 1}{k} = 0.2605$$

so that

$$\Delta h_t = (0.85)(0.264)(1660)\left(\frac{r^{0.2605} - 1}{r^{0.2605}}\right) = \Delta h_c = 110.3 \quad \text{Btu/lb}$$

$$372 r_t^{0.2605} - 438 = 110.3 r_t^{0.2605}$$

$$r_t = (1.422)^{3.84} = 3.86$$

Hence the pressure ratio of the turbine is 3.86, and its exhaust temperature T_4 = 1241 R. The pressure of the gases leaving is 107.2/3.86 = 27.75 psia.

Nozzle

Entrance conditions, T_4 = 1241 R, p_4 = 27.75 psia
Pressure ratio of nozzle, r_n = 27.75 ÷ 14.7 = 1.888
$\dfrac{1}{r_n}$ = 0.528, which is less than the critical ratio

The exhaust velocity is given by

$$w = 223.7\varphi\sqrt{c_p(T_4 - T_5')} = 223.7\varphi\sqrt{c_p\,T_4\frac{Z_n}{1+Z_n}}$$

or

$$T_4 - T_5' = T_4\frac{Z_n}{1+Z_n}$$

Substituting for $Z_n = r_n^{\frac{k-1}{k}} - 1$

$$T_5' = \frac{T_4}{Z_n + 1} = \frac{T_4}{r_n^{\frac{k-1}{k}}}$$

This equation is solved by trial and error, since k is unknown.

Trial 1. Assume $(T_4 + T_5')/2$ = 1150, k = 1.378 (Fig. 4·3), $(k-1)/k$ = 0.2745, and $r_n^{0.2745}$ = $(1.888)^{0.2745}$ = 1.190.

Hence

$$T_5' = \frac{1241}{1.190} = 1043 \text{ R}$$

Check. $(T_5' + T_4)/2$ = 1142; this is close enough for the purpose of illustration. Assume T_5' = 1048 R. Using the value of c_p corresponding to 1150 R, the exhaust velocity can now be calculated

$$w = 223.7 \times 0.98\sqrt{0.2532(1241 - 1048)} = 1535 \text{ fps}$$

Thrust. Neglecting the influence of G_f

$$\mathfrak{J} = \frac{G_a}{g}(w - V)$$

Hence the thrust per pound of air flow per second is given by

$$\frac{\mathfrak{J}}{G_a} = \frac{1}{32.2}(1535 - 615) = 28.6 \quad \text{lb thrust/lb air per sec}$$

The air flow required is

$$G_a = \frac{2150}{28.6} = 75.2 \quad \text{lb of air/sec}$$

The corresponding fuel flow is

$$G_f = 75.2 \times 0.00933 = 0.7 \quad \text{lb/sec} = 2520 \quad \text{lb/hr}$$

Thrust horsepower is

$$\frac{\mathfrak{J}V}{550} = \frac{2150 \times 615}{550} = 2405 \quad \text{thrust hp}$$

The plant efficiency is

$$\eta = \frac{2405 \times 2545}{2520 \times 18,500} = 0.131$$

ANALYSIS USING AIR TABLES OF CHAPTER 4

Diffuser

$$T_0 = 519; \qquad h_0 = 28.56; \qquad p_{r0} = 2.489$$

$$\Delta h' = V^2/50{,}000 = 615 \times 615/50{,}000 = 7.59$$

$$h_{1s} = 28.56 + 7.59 = 36.15 \quad \text{Btu/lb}; \qquad p_{r1_s} = 3.061$$

From page 352

$$p_1 = 17.89 \quad \text{psia} \quad \text{and} \quad T_1 = 551 \text{ R}$$

$$h_1 = 36.25 \quad \text{Btu/lb}$$

Compressor

$$T_1 = 551; \qquad h_1 = 36.25; \qquad p_{r1} = 3.060; \qquad p_{r2} = 6 \times 3.060 = 18.36$$

$$h_{2s} = 124.25; \qquad h_{2s} - h_1 = 124.25 - 36.25 = 88.0$$

$$\Delta h_c = 88.0/\eta_c = 88.0/0.8 = 110.0 \quad \text{Btu/lb}$$

$$h_2 = 110.0 + 36.25 = 146.25; \qquad T_2 = 1003 \text{ R}; \qquad p_{r2} = 25.68$$

$$p_2 = 6 \times 17.89 = 107.3 \quad \text{psia}$$

Combustion Chamber

$$h_2 = 146.25; \qquad T_2 = 1003 \text{ R}; \qquad p_{r2} = 25.68$$

$$T_3 = 1660 \text{ R}; \qquad h_3 = 316.57$$

$$h_3 - h_2 = 316.57 - 146.25 = 170.32 \quad \text{Btu/lb}$$

$$\frac{G_f}{G_a} = 170.32 \div 18{,}500 = 0.00921 \quad \text{lb fuel/lb air}$$

Turbine

$$h_3 = 316.57; \qquad p_{r3} = 171.56; \qquad T_3 = 1660 \text{ R}$$

$$h_{4s} = 316.57 - \frac{110.0}{\eta_t} = 316.57 - 129.41 = 187.16$$

$$p_{r4} = 44.57; \qquad r_t = 171.56 \div 44.57 = 3.85$$

$$p_4 = 107.3 \div 3.85 = 27.9 \quad \text{psia}$$

$$h_4 = 316.57 - 110.0 = 206.57 \quad \text{Btu/lb}$$

$$T_4 = 1241 \text{ R}$$

Nozzle

$$T_4 = 1241 \text{ R}; \qquad p_{r4} = 56.4; \qquad h_4 = 206.57$$

$$r_n = 27.9 \div 14.7 = 1.898$$

$$p_{r5} = 56.4 \div 1.898 = 29.72; \qquad h_{5s} = 156.51; \qquad \Delta h_n' = 50.06$$

$$\Delta h_n = 0.98 \times 50.06 = 49.06$$

$$w = 223.7\sqrt{49.06} = 1567 \quad \text{fps}$$

Thrust per Pound of Air Flow

$$\frac{3}{G_a} = \frac{1}{32.2}(1567 - 615) = 29.5 \quad \text{lb/lb of air/sec}$$

$$G_a = 2150 \div 29.5 = 72.9 \quad \text{lb of air per sec}$$

$$G_f = 0.00921 \times 72.9 = 0.671 \text{ lb/sec} = 2417 \quad \text{lb fuel/hr}$$

$$\text{Thrust horsepower} = \frac{3V}{550} = \frac{2150 \times 615}{550} = 2405 \quad \text{hp}$$

Plant Efficiency

$$\eta = \frac{2405 \times 2545}{2417 \times 18{,}500} = 0.136$$

Fuel per thrust horsepower-hour $= \frac{2417}{2405} = 1.005 \quad \text{lb/thrust hp-hr}$

Propulsion Efficiency

$$\eta_P = \frac{2V}{w + V} = \frac{2 \times 615}{1567 + 615} = 0.563$$

Internal Efficiency

$$\eta_i = \eta_B \frac{w(1 - v^2)}{50{,}000(h_3 - h_2)}$$

$$h_3 - h_2 = 170.32 \quad \text{Btu/lb}, \qquad v^2 = V^2/w^2 = 0.154$$

$$\eta_i = \frac{0.98 \times 1567 \times 1567 \times 0.846}{50{,}000 \times 170.32} = 0.236$$

12. Potentialities of the Turbojet Engine

At the present time the potentialities of the turbojet engine are being tested by all major countries. The applications have been to high-altitude, high-speed fighter aircraft. The current designs have shown that the turbojet engine offers the possibilities of a low-specific-weight, smooth-running, low-drag power plant. According to Sir A. H. Roy Fedden, "There seems to be no reason why the installed weight of the power unit (turbojet engine) should not be less than half that for an equivalent piston plant, and that is an important factor to be balanced against high fuel consumption."

In addition to its low specific weight the turbojet engine has the same mechanical advantages and the same general high temperature problems that were discussed in Chapter 7 in connection with the gas-turbine power plant.

At present both the axial-flow and the centrifugal types of air compressor are being used in the different turbojet engine designs. The centrifugal air compressor currently has the advantage, owing its high state of development and lighter weight. The demand for

higher pressure ratios and better compressor efficiencies justifies the prediction that the axial-flow compressor will eventually become a keen competitor. Light-weight, efficient axial-flow air compressors are being developed that have encouraging possibilities.

The turbojet engine has made it possible to attain flight speeds higher than those attainable with piston engine propeller propulsion. At present, because of its high rate of fuel consumption, the application of the turbojet engine has been restricted to short-endurance fighter aircraft. Since the trend in aviation has been to higher and higher speeds the turbojet type of thermal jet propulsion will undoubtedly be put to commercial use, even though its application may be limited to services where speed has economic value.

Too much emphasis has been given to the apparent limitations of this method of propulsion, particularly to its high fuel consumption. But these limitations appear to be related, to some extent at least, to the present state of the developments in the field of aerodynamics. Since thermal jet propulsion imposes less design restrictions upon the airplane designer, the commercial future of thermal jet propulsion is greatly dependent upon the ability of airplane designers to produce lower drag airplanes.

Perhaps the most attractive features of the turbojet engine, apart from its ability to provide propulsion at high speeds, are its simplicity and low weight. Furthermore, this power plant is relatively free from vibration, permits using cheaper fuels than high-octane gasoline, and should require less frequent major overhauls.

Another advantage which may be of significance is the simplification of cruise control offered by thermal jet propulsion, for, as pointed out by J. B. Rea,[9] "For a jet airplane, it will only be necessary to determine the speed and corresponding turbo-rpm for best range, for any density altitude and gross weight." Certain minor corrections will be necessary to take account of deviations from the normal atmosphere, as is customary with the conventional propulsion system. The flight testing of a jet-propelled airplane will be greatly simplified.

REFERENCES

1. G. Geoffrey Smith, *Gas Turbines and Jet Propulsion*, Dorset House, London, p. 44.
2. *Life Magazine*, Nov. 27, 1944.
3. "The Day Dawns for Jet Propulsion," *Westinghouse Engineer*, March, 1945, p. 51.
4. C. Giles, "The V-1 Robot Bomb," *Astronautics*, September, 1944.
5. *Douglas Air Review*, Douglas Aircraft Company, May, 1944.

6. E. P. Warner, "Postwar Transport Aircraft," *Aero. Eng. Review*, October, 1943.

7. M. J. Zucrow, "Jet Propulsion and Rockets for Assisted Take-Off," *Trans. A.S.M.E.*, May, 1946.

8. R. Eksergian, "On the Reactions of Fluid and Fluid Jets," *J. Franklin Inst.*, May, 1944.

9. J. B. Rea, "How Jet Propulsion Simplifies Cruise Control," *Aviation*, September, 1945, p. 184.

10. F. W. Godsey and C. D. Flagle, "The Place of the Gas Turbine in Aviation," *Westinghouse Engineer*, June, 1945.

11. Sir A. H. Roy Fedden, *Proc. Royal Aero. Soc.*, May 25, 1944.

BIBLIOGRAPHY

E. Buckingham, "Jet Propulsion for Airplanes," *N.A.C.A. Tech. Report* 159, March 23, 1922.

V. Dudaker, "Faster than Sound (the problem of supersonic flight)," *British Air Ministry Translation* 1426; from *Aeroplane, U.S.S.R.*, Vol. 18, M. 1, January, 1941, pp. 13–14.

E. Gambanuci, "An Elementary Theory of Thermal Jet Propulsion," *British Air Ministry Translation* 1483, from *L'Aerotecniea*, Vol. XXI, No. 12, December, 1941, pp. 774–797.

F. M. Rogalls, "Internal Flow Systems for Aircraft," *N.A.C.A. Tech. Report* 713, 1941.

G. B. Schubauer, "Jet Propulsion with Special Reference to Thrust Augmentors," *N.A.C.A. Tech. N.* 442, 1933.

"AAF and RAF Develop Jet Propulsion Planes," *Air Transport*, Vol. 2, February, 1944, p. 85.

S. Campini, "Analytic Theory of Campini Propulsion System," *N.A.C.A. Tech. Memo* 1010, March, 1942.

E. E. Miller, "And Now Jet Propelled Airplanes," *Aviation*, Vol. 43, February, 1944, pp. 116–117.

M. M. Munk, "Has Jet Propulsion Arrived?" *Aero Digest*, Vol. 44, Feb. 1, 1944, pp. 49–51.

"History of Jet Propulsion," *Engineer*, Vol. 177, Jan. 21, 1944, pp. 44–46; Jan. 28, pp. 64–66; Feb. 4, pp. 84–86.

"Jet Propelled Aircraft," *Engineer*, Vol. 176, Oct. 22, 1943, p. 326.

P. M. Heldt, "Jet Propulsion Developments," *Automotive and Aviation Industries*, Vol. 87, No. 6, Sept. 15, 1942, pp. 30–33.

E. J. Balban, "Nazi Jet-Bats Which Never Took Wing," *Aviation*, October, 1945, p. 172.

C. Giles, "Engine Exhaust Propulsion," *Astronautics*, October, 1942, pp. 11–12.

F. W. Lanchester, "Exhaust Efflux Propulsion," *Flight*, April 17, 1941, pp. 285–286.

"Whittle Systems of Jet Propulsion," *Automotive and Aviation Industries*, Jan. 15, 1944, pp. 42, 108.

AIR COMPRESSORS

The development of the gas-turbine power plant and of the turbojet engine is closely related to the developments in the fields of air-compression machinery. Three basic types of air compressors have been applied to these new power plants: (a) the centrifugal air compressor, (b) the axial-flow compressor, and (c) the positive displacement rotary compressor (Lysholm).

The centrifugal compressor has been used mainly for turbojet engines. The axial-flow compressor is used for turbojet engines and also for all types of gas-turbine power plants. The Lysholm compressor has so far been applied only to the marine gas-turbine field.

For aircraft propulsion engines the primary requirements imposed on the air-compression machinery are the same regardless of its operating principle. The requirements are low weight, small frontal area, high efficiency, large capacity per unit of frontal area, and reliability.

This chapter presents brief discussions of the characteristics of each of the aforementioned types of compressors. For convenience in treatment of the subject matter the chapter is divided into three self-contained parts: Part A discusses the centrifugal compressor; B, the axial-flow compressor; and C, the Lysholm compressor.

The section numbers are followed by the letter designating the part in which they are presented.

A. The Centrifugal Air Compressor

1A. Introduction

The centrifugal compressor was introduced by Professor Rateau and used in the Armengaud gas turbine discussed in Chapter 7. In recent years it has undergone intensive development to improve its efficiency and single-stage pressure ratio, and is used predominantly for supercharging both spark-ignition and compression-ignition engines. The turbojet engines developed by F. Whittle and the I-16

and I-40 turbojet engines built by the General Electric Company use centrifugal compressors. Figure 1, taken from reference 1, illustrates the arrangement of the components in a turbojet engine employing a centrifugal compressor.

In its basic design features the centrifugal compressor is similar to the centrifugal pump for liquids. Figure 2 is a cross-sectional diagram of a two-stage centrifugal compressor used for high-altitude supercharging. It consists of two impellers mounted on a single

(1) Accessories fairing	(6) Compressor casing	(11) Ignition plug	(16) Inner exhaust cone
(2) Accessories	(7) Impeller	(12) Combustion chamber	(17) Strut
(3) Accessory gear drive	(8) Balancing drum	(13) Turbine bearing	(18) Exhaust cone
(4) Front bearing	(9) Fuel manifold	(14) Turbine wheel	(19) Tailpipe
(5) Mounting trunnions	(10) Burner tip	(15) Turbine nozzle	(20) Final nozzle
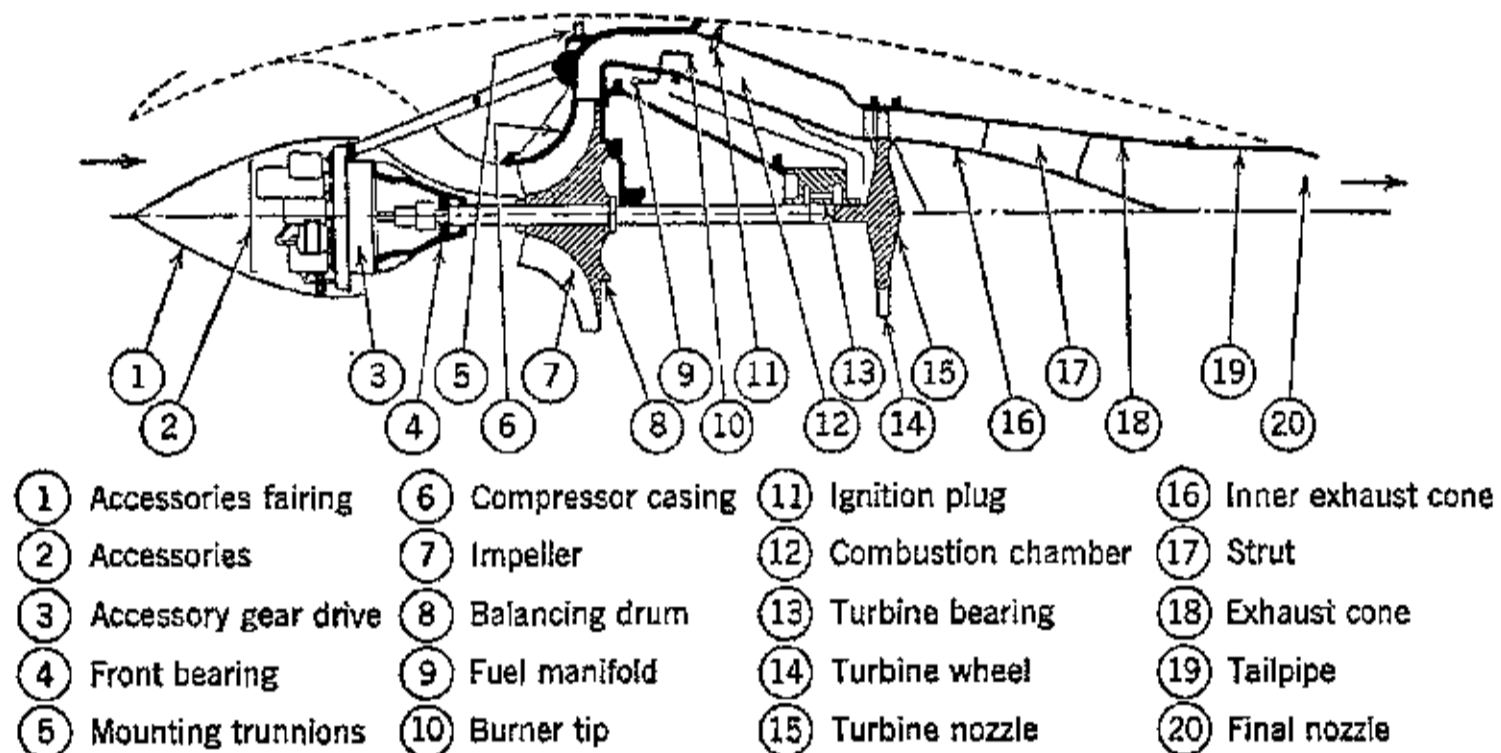
FIG. 1. Turbojet engine employing a centrifugal air compressor. (Reproduced from D. F. Warner and E. L. Auyer, *Mechanical Engineering*, November 1945.)

shaft. Each impeller is equipped with vanes for guiding the fluid flowing through it. The air usually enters the eye of the impeller in an axial or radial direction, and it may or may not have first passed through a set of stationary inlet vanes. Energy is transferred to the air by the rotating impeller, and the air leaves the impeller tip with a relatively high velocity and is delivered to a diffuser which transforms kinetic energy into pressure energy; the diffuser may or may not be equipped with guide vanes.

In its passage through the impeller the average direction of the motion of the air is changed through 90°. At the entrance section the absolute velocity of the air and the tangential velocity of the impeller are small, and both are increased materially at the exit or tip. As explained in Chapter 2, Section 8, the flow through the impeller passage is in the direction of increasing flow area, and there is a decrease in the relative velocity of the air from the entrance to the exit. This contributes to the conversion of kinetic energy into pressure.

The overall pressure rise developed by a centrifugal compressor depends upon the rotational speed of the impeller, the shape of its guide vanes, the tip diameter, the diffuser efficiency, and the number of stages. Because of the small specific weight of air, the impeller must rotate at high speeds to produce the requisite pressure rise.

The advantages of the centrifugal compressor stem from its being inherently a high-speed machine. They may be summarized as

Air discharge
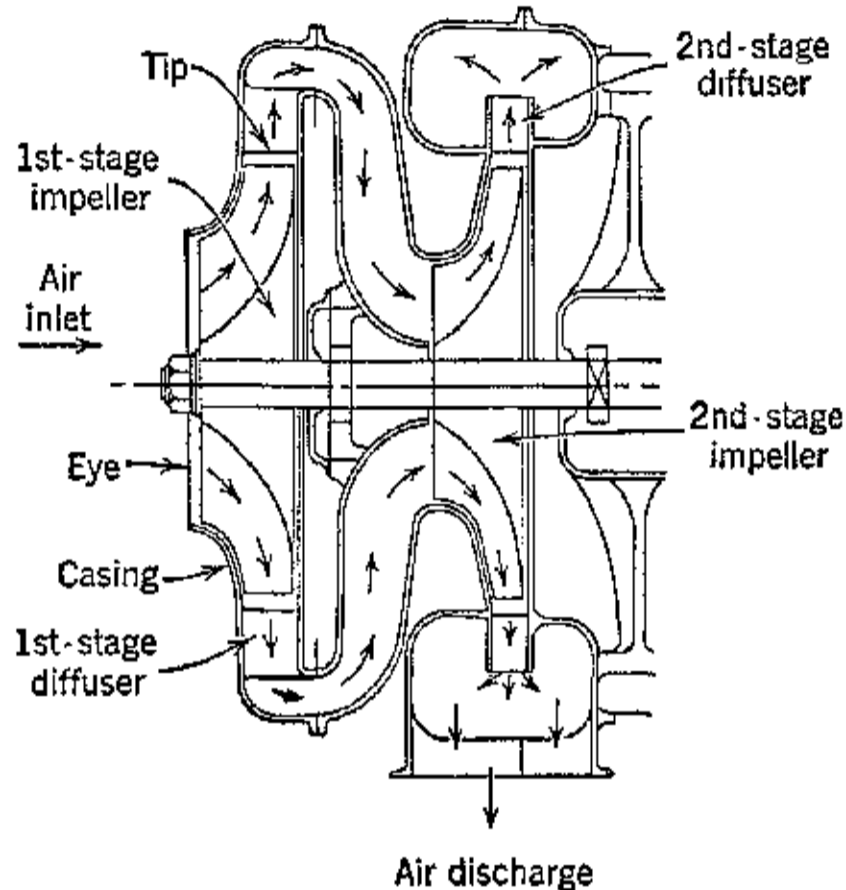
Fig. 2. Cross section through a two-stage centrifugal air compressor used for supercharging. (Reproduced from W. J. King, *J. Soc. Automotive Engineers*, Vol. 53, No. 12.)

follows. For a given capacity and pressure ratio, the compressor can be made small in size and weight. It can be coupled directly to a high-speed prime mover, such as a turbine. Its construction involves no internal rubbing parts; the only rubbing parts are the bearings, so that it is relatively free from mechanical difficulties. The bearings can be located outside the casing, thereby making their lubrication a simple matter. Since the motion is pure rotation the impellers can be balanced accurately and the machine made free from objectionable vibration.

A centrifugal air compressor is capable of moving large volumes of air at substantial pressure ratios for a single stage. The flow from the compressor outlet is quite steady so that no means are required for damping out pulsations. A centrifugal compressor can be operated at *shut-off head* without damage, and it can be regulated automatically by controls based on capacity, inlet pressure, or dis-

charge pressure. The efficiency of the centrifugal compressor can be maintained at reasonable values over a substantial range of air flow. There is, however, at each speed a certain flow below which the machine becomes unstable and the discharge becomes surging or pulsating.
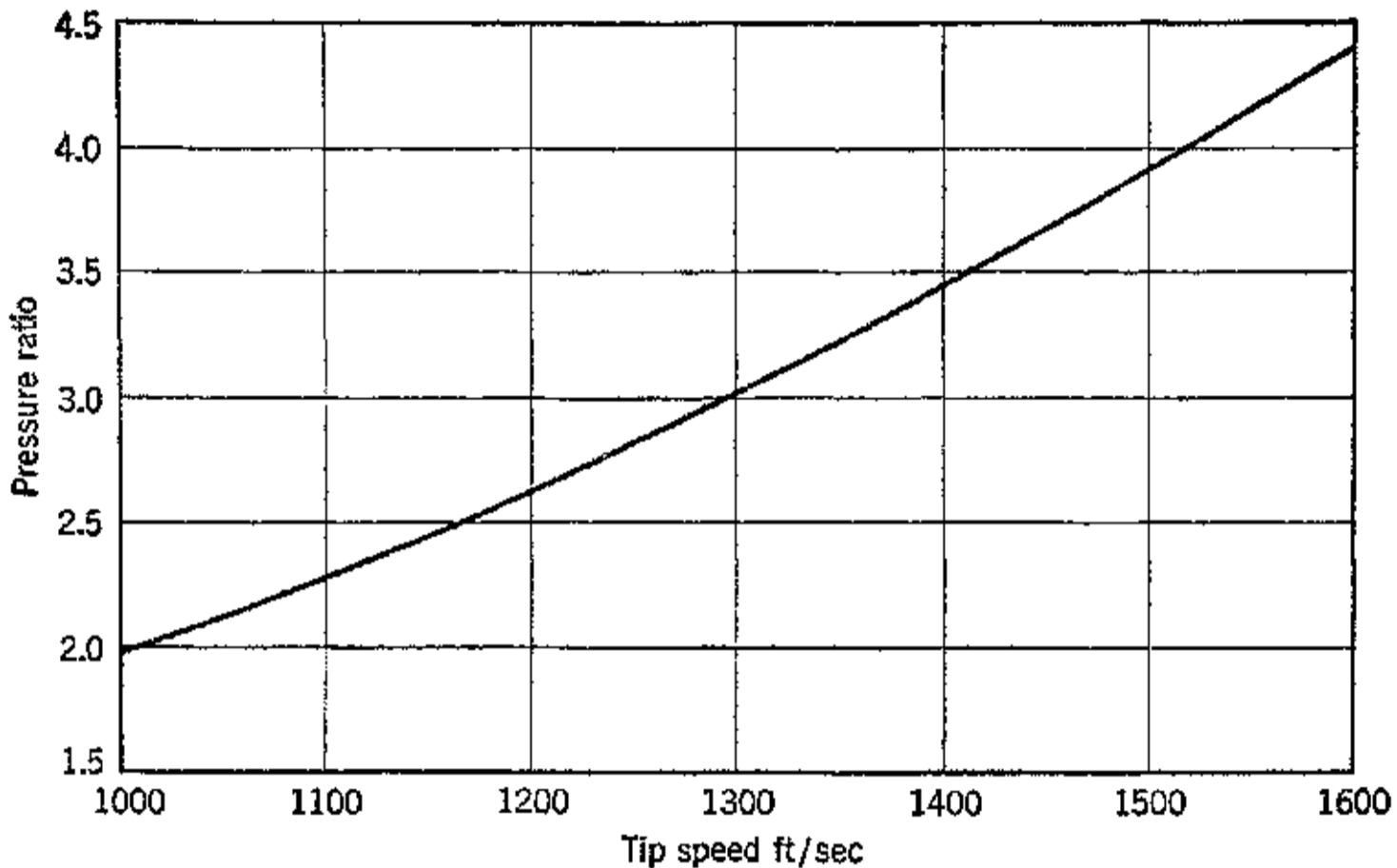
FIG. 3. Pressure ratio vs. tip speed for a centrifugal compressor. (Reproduced from W. R. Hawthorne, S.A.E., annual meeting, Detroit, Mich., Jan. 7–11, 1946.)

According to reference 12 the present state of the development of single-stage centrifugal compressors is in accordance with Table 9·1.

TABLE 9·1

PRESENT STATE OF DEVELOPMENT OF THE SINGLE-STAGE CENTRIFUGAL COMPRESSOR

Pressure Ratio r_c	Flow Parameter Q/ND^3	Compress Efficiency η_c
6 to 1	0.14 to 0.17	0.70 (minus)
4 to 1	0.14 to 0.17	0.75 to 0.80
2 to 1	0.16 to 0.35	0.75 to 0.80 (plus)

Figure 3 is a plot the pressure ratio versus tip speed characteristics obtained from the test of a single-stage air compressor for a turbojet engine.[13]

2A. Notation for Part A

A = area, ft^2.

A_e = area of annulus forming eye of impeller, ft^2.

b = width of impeller passage, ft.

c = absolute velocity of fluid at any point, fps.

c_u = tangential component of absolute velocity, fps.

c_a = axial component of absolute velocity, fps.

c_r = radial component of absolute velocity, fps.

D = tip diameter, ft or inches as specified in text.

eD = diameter of outer circle forming the eye of the impeller, ft.

hD = diameter of hub circle forming the eye of the impeller, ft.

G = weight flow rate in lb/sec or lb/min as specified in text.

g = acceleration due to gravity = 32.174 ft/sec^2.

H = measured static head, ft.

$H_{ti} = \dfrac{1}{g} (u_2 c_{2u} - u_1 c_{1u})$ = virtual head, ft.

$H_{ri} = \dfrac{1}{2g} [(u_2{}^2 - u_1{}^2) + (w_1{}^2 - w_2{}^2)]$ = ideal reaction effect, ft.

h = enthalpy, Btu/lb.

Δh = enthalpy change, Btu/lb.

J = mechanical equivalent of heat = 778 ft-lb/Btu.

$k = c_p/c_v$ = specific heat ratio.

L = energy transfer, ft-lb/lb.

L_t = energy transfer from fluid to rotor (turbine) in ft-lb or ft-lb/lb as specified in text.

L_c = work of compressors in ft-lb or ft-lb/lb as specified in text.

M_t = torque, ft-lb.

M = Mach number.

n = exponent in equation pv^n = constant.

N = rpm of impeller.

p = static pressure, psf.

$\Delta p_{ti} = \gamma H_{ti}$ = virtual pressure rise, psf.

$\Delta p_{ri} = \gamma H_{ri}$ = ideal reaction pressure rise, psf.

Q = heat added or removed, Btu/lb, or the volumetric flow rate in cfm, as specified in text.

$r = H_{ri}/H_{ti} = \Delta p_{ri}/\Delta p_{ti}$ = degree of reaction.

r_c = pressure ratio.

R = gas constant, ft-lb/lb F.

$R_1 = (eD - hD)/4 =$ radius at impeller entrance, ft.

$R_2 = D/2 =$ radius to impeller tip, ft.

$T =$ static temperature, R.

$T_t =$ total temperature = static temperature + temperature rise equivalent of the kinetic energy, R.

$u =$ tangential velocity $= \pi DN/720$ fps.

$v = 1/\gamma =$ specific volume, ft^3/lb.

$w =$ velocity relative to the impeller passage, fps.

$Z_c = (r_c^{\frac{k-1}{k}} - 1).$

$Z_{cn} = (r_c^{\frac{n-1}{n}} - 1).$

Greek Symbols

$\gamma =$ specific weight, lb/ft^3.

$\rho = \gamma/g =$ density, slug/ft^3.

$\eta =$ efficiency of a process.

$\eta_D =$ diffuser efficiency.

$\eta_h =$ hydraulic efficiency of impeller.

$\eta_M =$ mechanical efficiency.

$\eta_{ad} =$ adiabatic efficiency of compressor.

$\eta_c =$ overall efficiency of compressor.

$\eta_p =$ pressure energy coefficient for actual compressor.

$\nu_2 = c_{2u}/u_2 =$ velocity ratio.

$\psi_t =$ virtual or ideal pressure coefficient.

$\psi_{st} =$ static pressure coefficient.

$\psi_{dyn.} = \psi_t - \psi_{st} =$ dynamic pressure coefficient.

Angles

$\alpha_1 =$ angle between c_1 and u_1.

$\alpha_2 =$ angle between c_2 and u_2.

$\beta_1 =$ angle between w_1 and u_1.

$\beta_2 =$ angle between w_2 and u_2.

Subscripts

$0 =$ entrance to compressor.

$1 =$ entrance to impeller.

$2 =$ exit from impeller.

$3 =$ exit from diffuser.

$4 =$ exit from compressor.

i refers to an ideal compressor with an infinite number of blades.

3A. *Energy Transfer for Ideal Impeller with Infinite Number of Vanes*

The theory employed to obtain the energy-transfer relationships for the air flowing through the impeller is the Euler theorem of Chapter 2, Section 8. The basic assumptions underlying that theory have been discussed in Chapter 2 but are amplified here to show their relationships to the processes occurring in centrifugal compressors. The theory assumes the following.

(*a*) The flow conditions are steady, so that the flow of the fluid (air), the speed and torque of the impeller, and the energy transfer between it and the fluid are constant with time.

(*b*) The flow of fluid through the impeller is uniform; every filament of air enters and leaves the impeller with the same configuration.

(*c*) The blade thickness is infinitely small.

(*d*) The fluid enters the impeller centrally and in such a manner that its entrance to the blade passage is tangential; that is, the entrance is made without shock.

(*e*) The fluid leaves the passages formed by the impeller blades tangentially to the blade surfaces; that is, there is perfect guidance of the fluid at the exit.

(*f*) The impeller passages are completely filled with fluid at all times.

(*g*) The flow through the impeller passages is frictionless. ˙

The actual centrifugal compressor differs from this ideal machine in many respects, because of the presence of friction, turbulence, shock losses, imperfect guiding of the air, flow separation, and circulatory flow within the impeller passages. These factors are discussed in detail in references 3, 9, and 10 and need not be elaborated upon here.

The energy transferred by the impeller to the air manifests itself by a rise in the pressure, temperature, and velocity of the gas. Owing to the low specific weight of gases the effects of changes in elevation may be ignored. It was shown in Chapter 2, Section 8, that the energy transfer depends upon the entrance and exit whirls. For a compressor the exit whirl is the larger so that the energy transfer per pound of gas is given by equation 2·26*d* which is repeated here for convenience.

$$L_c = H_{ti} = \frac{1}{g}(u_2 c_{2u} - u_1 c_{1u}) \tag{1}$$

From equation 2·26*b* the energy transfer is also given by

$$L_c = H_{ti} = \frac{1}{2g}[(c_2{}^2 - c_1{}^2) + (u_2{}^2 - u_1{}^2) + (w_1{}^2 - w_2{}^2)] \tag{2}$$

Since it has been assumed that the blade passages are filled at all times, to satisfy the continuity equation the same weight of gas must in each second pass every concentric ring in the flow path. Hence if the flow rate is G lb/sec the total energy transfer is G times the values obtained from the preceding equations.

The physical significance of the terms in equation 2 have been discussed in Chapter 2, Section 8. It was pointed out that the term $\frac{1}{2}(c_2{}^2 - c_1{}^2)$ represents the change in the kinetic energy of the air because of the increase in its absolute velocity from c_1 at the entrance to c_2 at the exit. Any conversion of this kinetic energy into static pressure must take place beyond the impeller outlet, that is, in the diffuser. In the ideal case, assuming a diffuser efficiency $\eta_D = 1$, all this kinetic energy can be transformed into pressure rise. Unfortunately, as discussed in Chapter 3, diffusion processes are not highly efficient, and only a portion of the theoretically available pressure is recoverable. Because of the low efficiency of the diffusion process the kinetic energy term $(1/2g)(c_2{}^2 - c_1{}^2)$ should be kept as small a percentage of the energy transfer as possible. The magnitude of this term is dependent on the exit blade angle and is discussed in later sections.

It was shown in Chapter 2 that the energy transfer consists of a velocity head which is transformed into static pressure in the diffuser, and a static pressure rise or reaction effect accomplished wholly within the impeller. The ideal reaction effect, denoted by H_{ri}, is given by

$$H_{ri} = \frac{1}{2g}[(u_2{}^2 - u_1{}^2) + (w_1{}^2 - w_2{}^2)] \quad \text{ft} \tag{3}$$

Hence the head equivalent of the energy transfer, which will be termed the *virtual head* [9] and is denoted by H_{ti}, is given by

$$H_{ti} = H_{ri} + \frac{1}{2g}(c_2{}^2 - c_1{}^2) \quad \text{ft} \tag{4}$$

It follows from equation 4 that the virtual head has the following characteristics: (a) for an impeller rotating at a given speed, H_{ti} is independent of the specific weight of the gas; (b) for the same values of the tangential velocities u_1 and u_2 the ideal total head depends only upon the velocity components c_{1u} and c_{2u}; and (c) the virtual pressure rise $\Delta p_{ti} = \gamma H_{ti}$ can be calculated for any gas from the tests on the impeller conducted with only one gas.

Thus if $(p_{ti})_a$ is the ideal total pressure rise for air, then for any other gas the corresponding value of the ideal total pressure rise, denoted by $(p_{ti})_g$, is given by

$$\frac{(\Delta p_{ti})_g}{(\Delta p_{ti})_a} = \frac{\gamma_g}{\gamma_a} = \text{Specific gravity of gas} \tag{5}$$

It follows from equation 1 that, if the weight flow rate is G lb/sec, the ideal horsepower required to give the energy transfer is

$$(hp)_i = \frac{G}{550g}(u_2 c_{2u} - u_1 c_{1u}) \tag{6}$$

Owing to the imperfections of the theory the head developed by an actual compressor will be smaller and the power consumed larger. A detailed discussion of the main discrepancies is given in reference 9.

It was pointed out in Chapter 2 that one may conceive the flow through the impeller passage to consist of a circulatory flow superposed on a translatory flow. As a result the stream lines are crowded to one side of the passage and the pressure distribution is non-uniform. The net effect is to cause the fluid to leave the impeller at an angle less than the vane angle β_2 and to increase the angle α_2. At the inlet the tendency is to increase β_1, but on account of the closer spacing of the vanes the effect on the inlet velocity triangle is much smaller. The net effect of the finite number of blades is to reduce c_{2u} and increase c_{1u}.

Because of friction in the impeller passage there is a loss of head. This loss increases as the square of the relative velocity and with the wall surface in contact with the fluid.

Other sources of loss are shock due to entrance and exit velocity triangles departing from the design conditions, disk friction losses, leakage, mechanical friction in bearings and seals, and entrance losses due to prerotation of the fluid increasing the entrance whirl. The shock losses are practically proportional to $(Q - Q_d)^2$, where Q is the actual flow rate and Q_d is the design flow.

4A. Factors Affecting Degree of Reaction

If the inlet to the rotor has no guide vanes, the absolute velocity of the gas at the inlet is normal to an enveloping surface which includes the inlet tips of the vanes of the impeller. This is also an experimental fact according to reference 4. For an axial inlet, such as illustrated in Fig. 5, the absolute velocity at entrance is entirely

axial and there is no tangential component, so that $c_1 = c_{1a}$ and $c_{1u} = 0$. Further, if the inlet velocity is entirely radial at the inlet tips then $c_1 = c_{1r}$ and again $c_{1u} = 0$. The velocity diagrams for axial entrance and radial entrance are illustrated in Fig. 5.

Impeller with backward-curved vanes
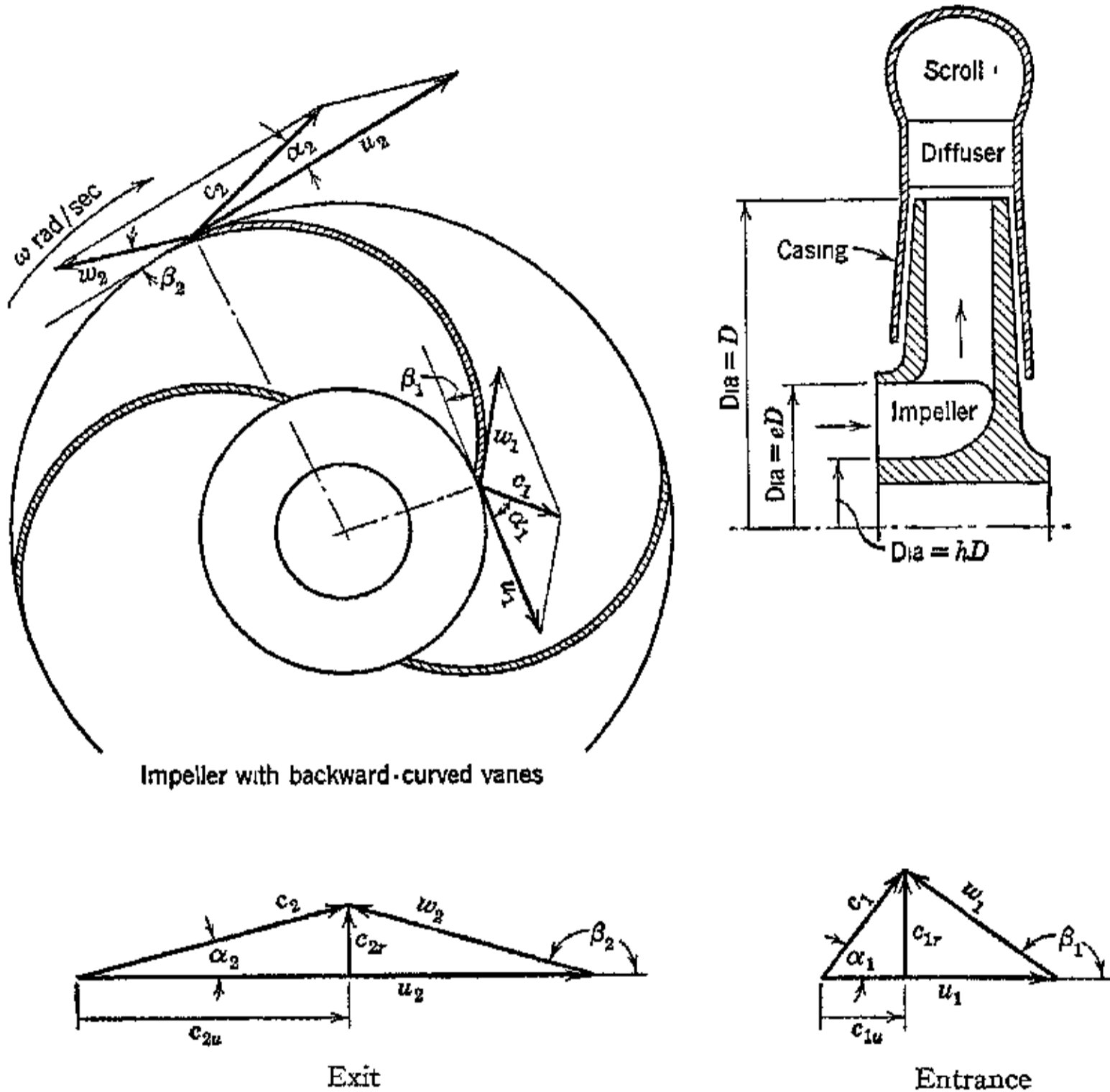
Exit   Entrance

FIG. 4.   Impeller with backward-curved blades with its entrance and exit velocity diagrams.

The energy transfer for either radial or axial entrance is, accordingly, for 1 lb of gas

$$L_c = \frac{u_2 c_{2u}}{g} \tag{7}$$

It is seen that the energy transfer is independent of the inlet velocities and the inlet diameter of the impeller.

The corresponding value of the virtual pressure rise is

$$\Delta p_{tt} = \frac{\gamma}{g} u_2 c_{2u} \tag{8}$$

Referring to Fig. 5 it is seen that

$$w_1{}^2 - u_1{}^2 = c_1{}^2 \tag{a}$$

Substituting the above into equation 3 gives the following expression for the ideal reaction effect in terms of pressure

$$\Delta p_{ri} = \frac{\gamma}{2g}(u_2{}^2 - w_2{}^2 + c_1{}^2) \tag{9}$$

Hence, the degree of reaction is

$$r = \frac{\Delta p_{ri}}{\Delta p_{tt}} = \frac{u_2{}^2 - w_2{}^2 + c_1{}^2}{2u_2 c_{2u}} \tag{10}$$

It can be shown [6] that equation 10 reduces to the expression

$$r = 1 - 0\ 5\nu_2 \tag{11}$$

where

$$\nu_2 = \frac{c_{2u}}{u_2} = \text{Velocity ratio} \tag{12}$$

Equation 11 shows that for either axial or radial entrance the degree of reaction depends directly upon the velocity ratio ν_2. Although ν_2 does not reveal it implicitly, the degree of reaction r depends upon the angles α_2 and β_2, since ν_2 is a function of these angles.   Refer to the velocity triangles of Fig. 4.   Thus by the law of sines
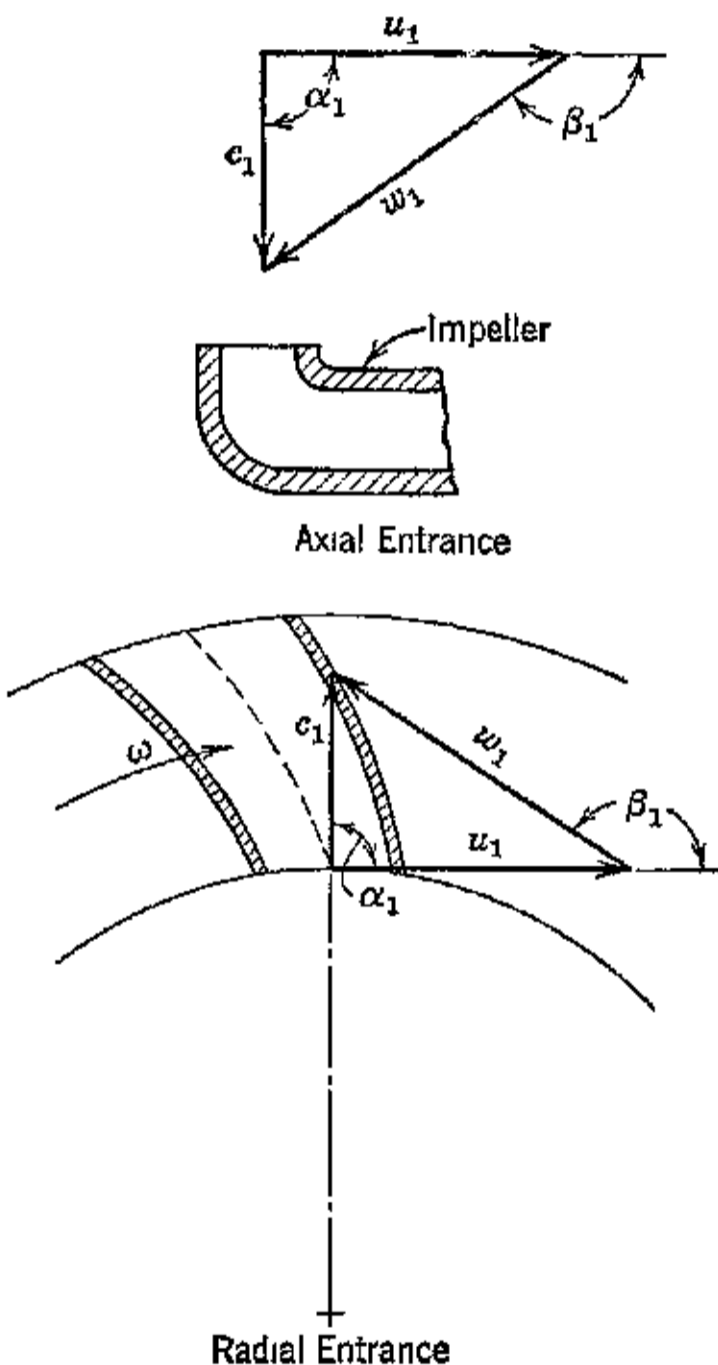
FIG. 5.   Velocity diagrams for axial or radial entrance to the impeller.

$$c_2 = u_2 \frac{\sin \beta_2}{\sin(\alpha_2 + \beta_2)} \tag{13}$$

Hence

$$c_{2u} = c_2 \cos \alpha_2$$

$$= u_2 \left[\frac{\sin \beta_2 \cos \alpha_2}{\sin(\alpha_2 + \beta_2)} \right] \tag{14}$$

Substituting for c_{2u} and u_2 from above into equation 12 gives the following expression for v_2

$$v_2 = \frac{\sin \beta_2 \cos \alpha_2}{\sin \alpha_2 \cos \beta_2 + \cos \alpha_2 \sin \beta_2} \tag{15}$$

Finally, dividing numerator and denominator by $\cos \alpha_2 \cos \beta_2$ gives

$$v_2 = \frac{\tan \beta_2}{\tan \alpha_2 + \tan \beta_2} \tag{16}$$

If the air enters the impeller radially, $\alpha_1 = 90°$. As the air comes in contact with the hub and the impeller, owing to its viscosity, it
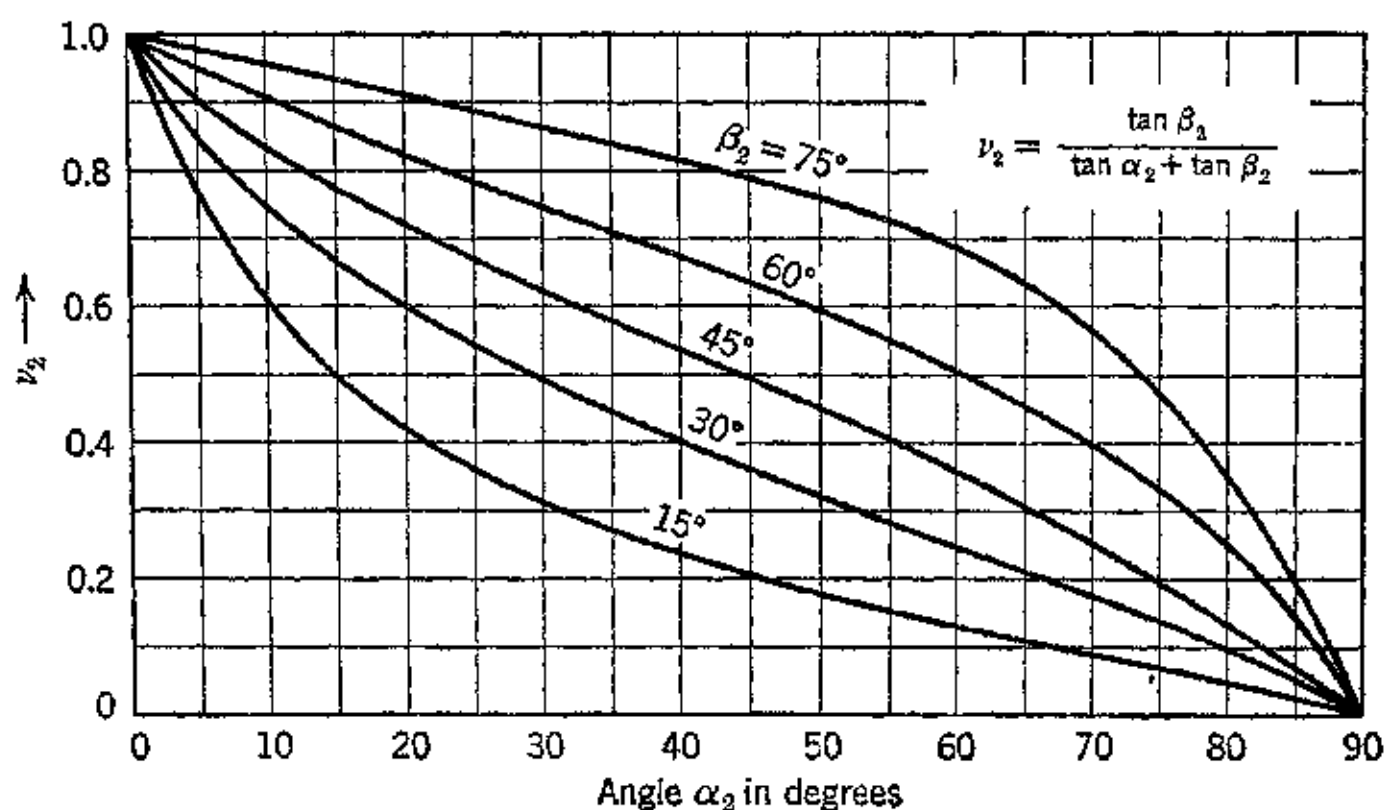
FIG. 6. Velocity ratio v_2 vs. exit angle α_2 for an ideal impeller with perfect guidance of the air.

tends to rotate with the impeller. This effect is called *prerotation*, and as already pointed out its effect is to decrease the virtual head since it increases the absolute-velocity component c_{1u}.

It is seen from equation 16 that v_2 depends only on β_2 and α_2. Figure 6 presents v_2 as a function of α_2 with β_2 as a parameter. This figure applies to either axial or radial entrance ($c_{1u} = 0$, so that $H_{ti} = u_2 c_{2u}/g$.

5A. Effect of Entrance Guide Vanes

The direction of the air at the impeller entrance and also at the tip affect the energy transferred to the air. In this section the effect of the inlet guide vane angle α_1 is investigated.

Rewriting the energy transfer equation in terms of the angles α and β, then for 1 lb of gas

$$L_c = \frac{1}{g}\left(u_2{}^2 + u_2 w_2 \cos \beta_2 - c_1 u_1 \cos \alpha_1\right) \tag{17}$$

If α_1 is smaller than 90°, which means that the inlet guides are pointed forward in the direction of rotation, then the larger the absolute velocity c_1 the smaller is the energy transfer. Furthermore, in an actual compressor the energy lost in friction will increase with c_1 and further reduce the energy transfer below the ideal value. For these reasons forward inlet guide vanes are rarely, if ever, used.

If α_1 is greater than 90°, inlet guide vanes turned backwards, then $\cos \alpha_1$ becomes negative and $(-c_1 u_1 \cos \alpha_1)$ positive. Hence with backward inlet guide vanes the energy transfer increases with the absolute velocity c_1. However, increasing c_1 also increases the relative velocity w_1, which reduces the reaction effect. Consequently, the kinetic energy entering the diffuser is increased and the reaction effect is decreased. The overall effect is to increase the quantity $(w_1{}^2 - c_1{}^2)$ and the net energy transfer. The latter increase, however, is not very large, especially if the impeller is of small diameter.

In an actual compressor the small increase in the energy transfer which accompanies the increasing of c_1 and w_1 also increases the friction and shock losses at the inlet to the impeller. For this, and for reasons of complexity in manufacture, the use of inlet guide vanes is not beneficial in all applications.

6A. Effect of Exit Angle

The effect of the exit angle β_2 can be determined from equation 17. The equation shows that the greatest rise in static pressure is pro-
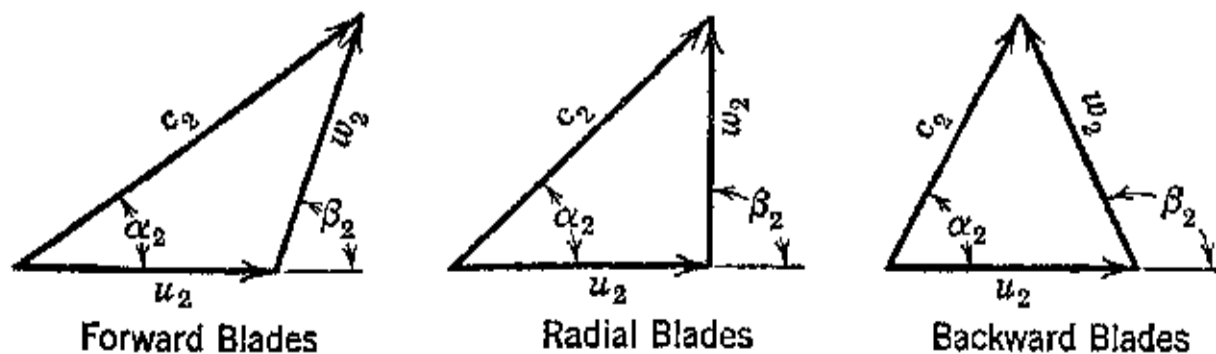
Fig. 7. Exit velocity diagrams for different types of blades.

duced if the exit angle β_2 is an acute angle, that is, with the blades turned forward. The exit velocity diagrams for different blade exit angles are illustrated in Fig. 7.

It follows from equation 17 that curving the blades forward increases the energy transfer, mainly as the result of raising the value for the exit absolute velocity c_2. Consequently more kinetic energy is supplied to the diffuser for conversion into pressure, and this is undesirable. Therefore the impellers for high-speed centrifugal compressors do not employ vanes which are turned forward.

If the blades are turned backward $\cos \beta_2$ is negative and both c_2 and the energy transfer are reduced. The virtual head is, therefore, smaller than it is with either forward-curved blades or radial outlet blades ($\beta_2 = 90°$). For low-pressure ratio applications, the backward-curved blades are advantageous because most of the energy transfer appears as reaction effect and only a small portion is in the form of velocity head to be converted into pressure by the diffuser. As a result this type of impeller gives high efficiency, but it delivers pressure ratios which are too low for application to turbojet engines or gas turbine-propeller engines.

7A. Effect of Velocity Ratio on Reaction Effect

It is convenient to study the reaction effect in terms of certain pressure coefficients.

Let ψ_t = virtual or ideal pressure coefficient.

ψ_{st} = static pressure coefficient.

$\psi_{dyn.} = \psi_t - \psi_{st}$ = dynamic pressure coefficient.

By definition

$$\psi_t = \frac{\Delta p_{ti}}{(\gamma u_2{}^2)/2g} = \frac{2gH_{ti}}{u_2{}^2} \tag{18}$$

and

$$\psi_{st} = \frac{\Delta p_{ri}}{(\gamma u_2{}^2)/2g} \tag{19}$$

Substituting for Δp_{ti} from equation 8 into equation 18,

$$\psi_t = 2\frac{c_{2u}}{u_2} = 2\nu_2 \tag{20}$$

Since $r = \Delta p_{ri}/\Delta p_{ti}$, it follows from equations 18 and 19 that

$$\psi_{st} = r\psi_t \tag{21}$$

The instantaneous values of ψ_t and ψ_{st} for different blade exit angles can be determined from the velocity triangles; this is done most conveniently by the graphical construction illustrated in Fig. 8.

The projection of the end point of c_2 upon u_2 determines c_{2u}, and for a fixed speed u_2 is constant.

Figure 8 shows that increasing the blade angle β_2 increases ψ_t but decreases $r = \psi_{st}/\psi_t$. Hence $\psi_{dyn.}$ is increased and the kinetic
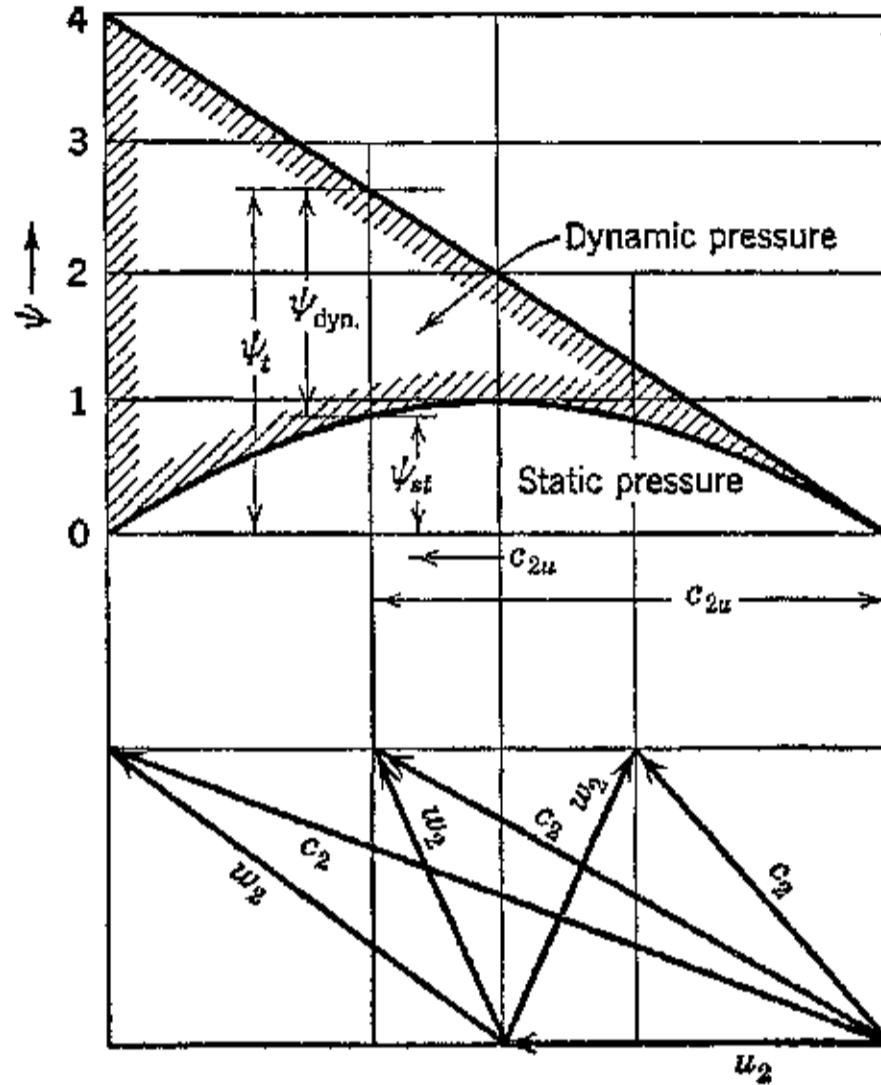
FIG. 8. Effect of exit angle β_2 upon the ideal pressure coefficients ψ_t, ψ_{st}, and ψ_{dyn}.

energy supplied to the diffuser is increased as previously pointed out. Since

$$\psi_t = 2v_2 = \frac{\psi_{st}}{r} \tag{22}$$

substituting for r from equation 11 and solving for ψ_{st} gives

$$\psi_{st} = 2v_2\left(1 - \frac{v_2}{2}\right) = v_2(2 - v_2) = 2v_2 - v_2{}^2 \tag{23}$$

Hence

$$\psi_{st} = 2\left(\frac{c_{2u}}{u_2}\right) - \left(\frac{c_{2u}}{u_2}\right)^2 \tag{24}$$

If ψ_{st} is plotted as a function of v_2 it is apparent from equation 24 that $\psi_{st} = 0$ when $v_2 = 0$ and $v_2 = 2$. Between these two limits there is a maximum value which can be determined by differentiating equation 24 with respect to v_2 and equating the result to zero. The

value of ν_2 which makes ψ_{st} a maximum is $\nu_2 = 1$. The maximum static pressure increase in the impeller is obtained, therefore, when $c_{2u} = u_2$. At $\nu_2 = 1.0$, the degree of reaction is $r = 0.5$ and $\Delta p_{st} = 0.5\Delta p_{ti}$. The condition $c_{2u} = u_2$ is fulfilled if the outlet portion of the impeller vane is made with the exit angle $\beta_2 = 90°$. The foregoing demonstrates that, if the impeller has radial ended blades, one half of the virtual pressure rise is in the form of static pressure and the other half is in the form of velocity pressure entering the diffuser.

When the velocity ratio $\nu_2 = 2$, then $c_{2u} = 2u_2$, and $\psi_t = 4$. This is the condition for maximum energy transfer, but from equation 24 it is seen to be also the condition for $\psi_{st} = 0$. In other words, all the energy transfer appears as an increase in the kinetic energy of the gas entering the diffuser. The impeller merely increases the velocity of the gas. The dynamic pressure coefficient then has its maximum value $\psi_{dyn.} = \psi_t - \psi_{st} = 4$.

For constant values of u_2 the components c_{2u} and c_{r2} depend for their values upon the blade exit angle β_2. It is evident from the above and from Section 6A that the angle β_2 exercises a decisive influence upon the degree of reaction.

The blades of the impeller may be one of the forms already discussed. The more common forms are either the backward-curved blades or the radial-ended type. The usual range of values for β_2 are from 45° to 90°. Most high-speed impellers, partly because of stress considerations, are equipped with radial-ended blades. These impellers rotate at high tip speeds up to 1500 fps. By employing an exit vane angle of 90° the bending stresses in the vane are largely eliminated.

In general, the radial-bladed impeller produces a larger pressure rise for a given peripheral speed than the backward-curved vane impeller. Furthermore, it is better suited for high tip speed service, is easier to build, and is sturdier. It is not as efficient as the backward-curved vane impeller, and its surge or pumping limit occurs at a higher value of its rated air capacity.[4]

8A. Flow Equation for Impeller

It was shown in Chapter 3, that for isentropic flow the continuity equation can be written in the form of equation 3·81 which is repeated here for convenience.

$$G = \frac{pA}{\sqrt{T_t}}\sqrt{M^2\frac{kg}{R}\left[1 + \left(\frac{k-1}{2}\right)M^2\right]} \qquad (25)$$

From equation 3·44 it follows that, in terms of the total pressure p_t and the total temperature T_t, the static pressure p is given by

$$p = p_t \Bigg/ \left(\frac{T_t}{T_1}\right)^{\frac{k}{k-1}} = p_t \left[\frac{1}{\left[1 + \left(\frac{k-1}{2}\right)M^2\right]^{\frac{2k}{k-1}}}\right]^{\frac{1}{2}} \qquad (26)$$

Substituting for p in equation 26 and rearranging, the flow equation becomes

$$\frac{G\sqrt{T_t}}{p_t A} = M \sqrt{\frac{kg}{R} \left[\frac{1}{\left[1 + \left(\frac{k-1}{2}\right)M^2\right]^{\frac{k+1}{k-1}}}\right]} \qquad (27)$$
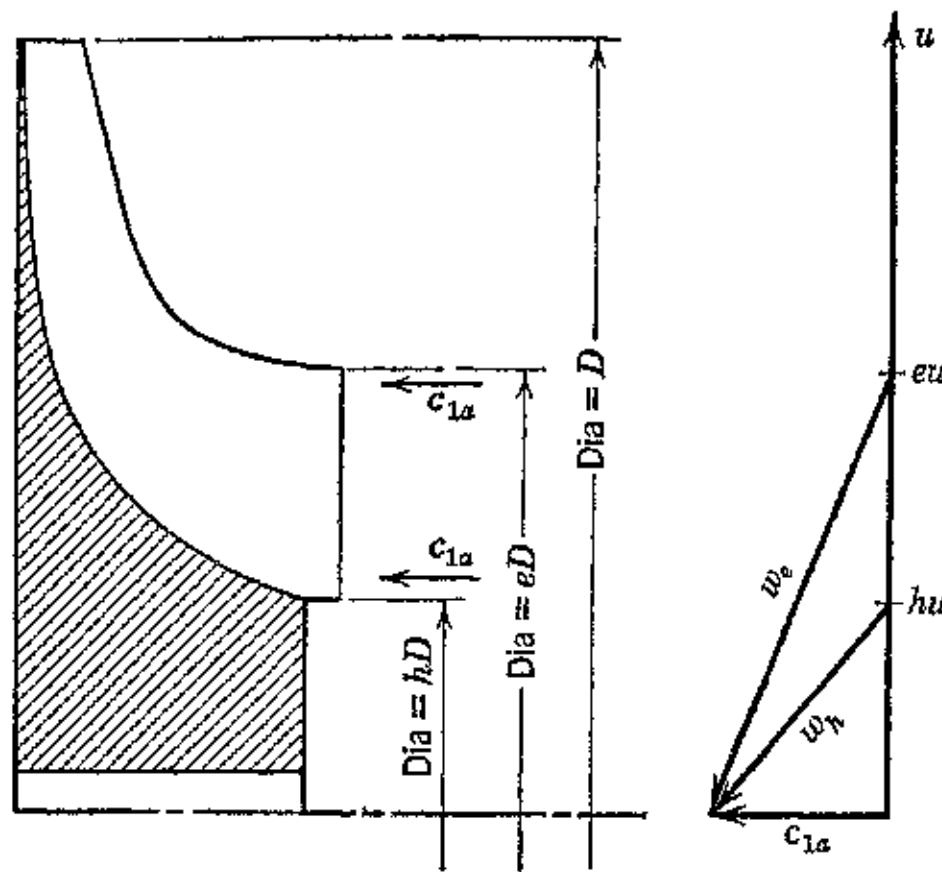
FIG. 9.　Entrance relative velocities at eye of impeller.

Equation 27 will be applied to the conditions at the inlet to the impeller using the method of reference 13. It is assumed that the velocity at the entrance is axial and uniform. Referring to Fig. 9 it is seen that the flow area at the inlet is given by

$$A = A_e = \frac{\pi}{4} D^2(e^2 - h^2) \qquad (28)$$

The velocity triangles at the entrance show that the relative velocity at entrance is greatest at the outer diameter of the eye; see Fig. 9. Hence, the largest relative velocity at the eye is

$$w_e^2 = c_{1a}^2 + e^2 u^2 \qquad (29)$$

where u is the tip speed of the impeller and c_a is the axial velocity at entrance. If M_a is the Mach number corresponding to c_a, then on substituting for $A = A_e$ from equation 28 into equation 27 the result is

$$\frac{G\sqrt{T_t}}{p_t \frac{\pi D^2}{4}(e^2 - h^2)} = M_a \sqrt{\frac{kg}{R}\left[\frac{1}{\left[1 + \left(\frac{k-1}{2}\right)M_a{}^2\right]^{\frac{k+1}{k-1}}}\right]} \qquad (30)$$

As pointed out in reference 13 it is convenient to correct the weight flow and tip speed u to the standard inlet conditions 520 R and 14.7 psia. Then

$$\frac{G_{\text{corr.}}\sqrt{520}}{14.7 \times 144} = \frac{G\sqrt{T_t}}{p_t} \qquad (31)$$

Let $U = u_{\text{corr.}}$; then

$$\frac{U}{\sqrt{520}} = \frac{u}{\sqrt{T_t}} \qquad (32)$$

For standard conditions the sonic velocity is given by

$$a_0 = \sqrt{gkR520} \qquad (33)$$

By rearranging equation 29, it can be shown [13] that

$$M_a{}^2 = \frac{M_e{}^2 - \left(\frac{eU}{a_0}\right)^2}{1 + \left(\frac{k-1}{2}\right)\left(\frac{eU}{a_0}\right)^2} \qquad (34)$$

where M_e is the Mach number corresponding to w_e.

Inserting the last four expressions into equation 30 and rearranging gives the following relationship [13]

$$\left(\frac{G_{\text{corr.}}}{D^2}\right)\left(\frac{e^2}{e^2 - h^2}\right)\left(\frac{U}{a_0}\right)^2$$

$$= \frac{4}{\pi}\left(\frac{2116.4}{\sqrt{520}}\right)\left(\frac{eU}{a_0}\right)^2 \sqrt{\frac{gk}{R}\frac{\left[M_e{}^2 - \left(\frac{eU}{a_0}\right)^2\right]\left[1 + \left(\frac{k-1}{2}\right)\left(\frac{eU}{a_0}\right)^2\right]^{\frac{2}{k-1}}}{\left[1 + \left(\frac{k-1}{2}\right)M_e{}^2\right]^{\frac{k+1}{k-1}}}}$$

$$(35)$$

Figure 10, taken from reference 13, presents the relationship expressed by equation 35 for several constant values of the Mach number M_e.

Figure 10 shows that the weight rate of flow through the impeller eye is proportional to D^2 where D is the tip diameter. For a constant value of M_e the weight of air increases with ratio of the eye
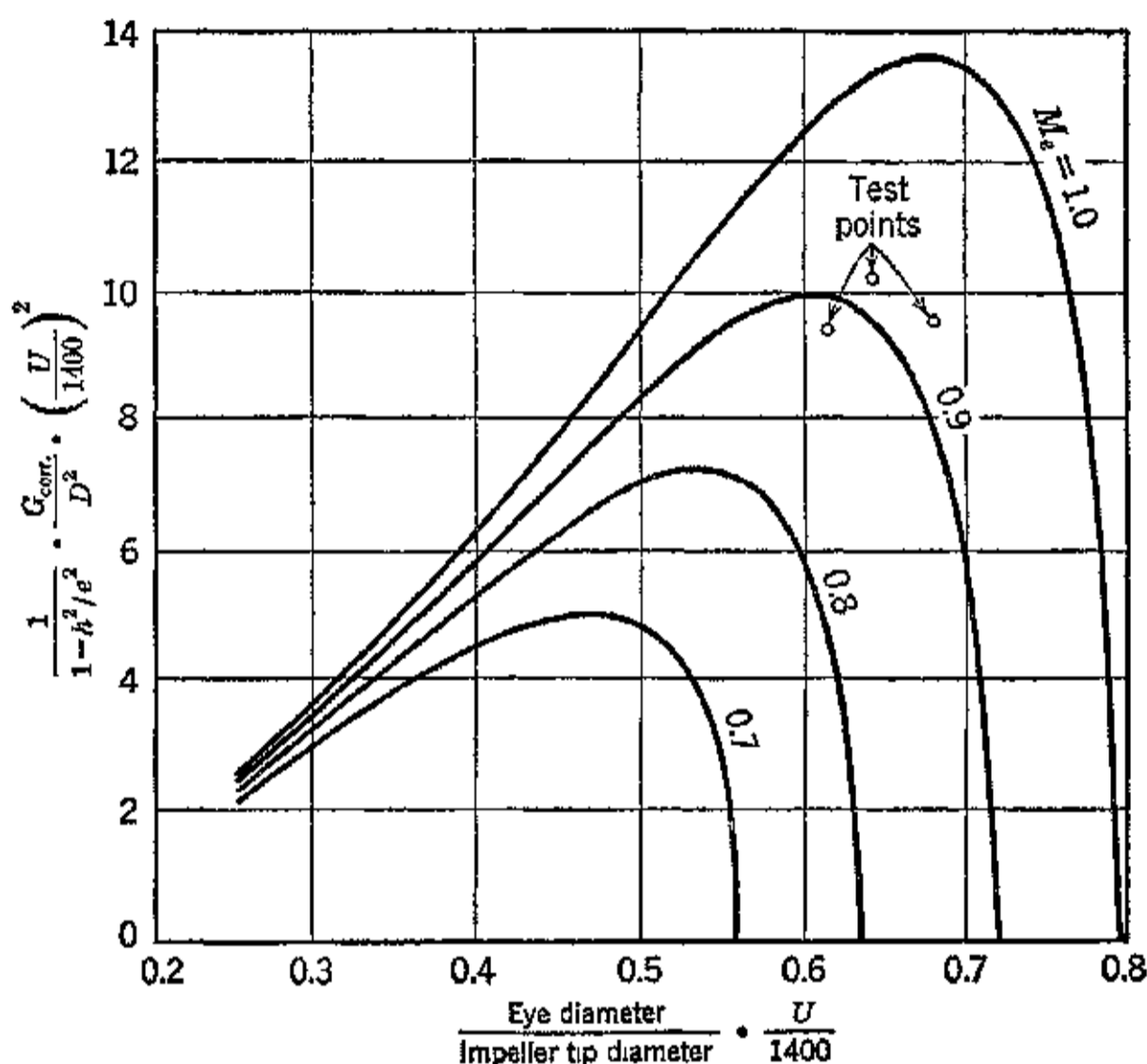
FIG. 10. Air induction capacity of impeller eye (factor 1400 is merely for obtaining a convenient scale). (Reproduced from W. R. Hawthorne, *loc. cit.*)

diameter to tip diameter up to a maximum value, the maximum value increasing with M_e. Beyond the maximum point the capacity decreases rapidly. According to reference 7 the diameter of the inlet should not exceed $0.65D$, and the Mach number M_e should not exceed 0.75 approximately. According to reference 13, however, if the inlet of the impeller vanes is designed with care and a large number of vanes are used there is no serious loss in efficiency with a Mach number of the order of 0.9. If the impeller is of the double-suction type the weight flow is twice that obtained from the curves of Fig. 10.

Since the weight rate of flow for a given corrected tip speed U depends on the Mach number M_e there is an optimum dimension for the eye of the impeller that gives the maximum weight rate of flow.

Figure 11, taken from reference 13, is based on the assumption that the optimum eye dimension is selected for each tip speed U, and a hub/tip diameter ratio of 0.3. The curves show that as the impeller tip speed is raised the maximum rate of flow decreases for any constant value of M_e. The curves apply to a single-suction impeller.
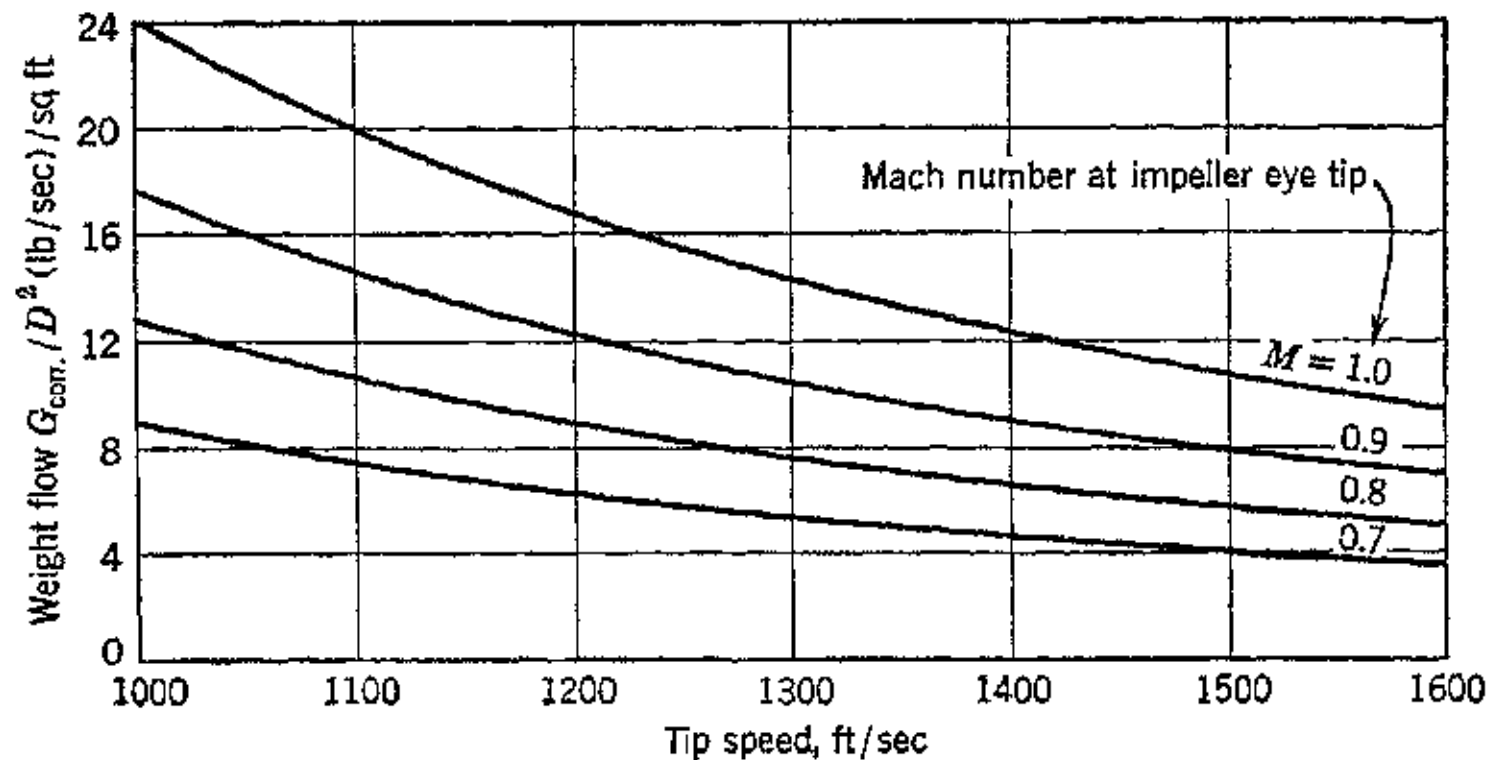
FIG. 11. Air induction capacity of impeller with optimum dimensions of intake. (Reproduced from W. R. Hawthorne, *loc. cit.*)

9A. Thermodynamic Relations

The energy equation written between any two points of the compressor, assuming adiabatic flow, is

$$c_p T_1 + \frac{c_1^2}{2gJ} + \frac{L}{J} = c_p T_2 + \frac{c_2^2}{2gJ} \tag{36}$$

Or in terms of the total temperature (see Chapter 3, Section 7)

$$L = Jc_p(T_{t2} - T_{t1}) = Jc_p \, \Delta T_t \tag{37}$$

In an actual machine some of the energy is dissipated in losses which appear as heat added to the fluid. If L_c and L_c' denote respectively the useful mechanical energy transferred to the fluid in the actual and isentropic cases, then for the isentropic case

$$L_c' = Jc_p \, \Delta T_t = Jc_p T_{t1} \left[\left(\frac{p_{t2}'}{p_{t1}} \right)^{\frac{k-1}{k}} - 1 \right] = Jc_p T_{t1} Z_c \tag{38}$$

In the actual case the final total pressure $p_{t2} < p_{t2}'$ but there is no change in the total temperature T_{t2}. If the compressed gas were expanded isentropically to the original total pressure p_{t1}, its final total temperature, denoted by T_{ts}, would be higher than the total

temperature T_{t1} from which the compression proceeded. The efficiency of the actual compression can be measured by comparing the aforementioned isentropic expansion with that for the isentropic compression process between T_{t1} and T_{t2}.

For the actual compression $pv^n = $ constant, but T_{t2} is the same for both the actual and isentropic processes,

$$\frac{T_{t2}}{T_{t1}} = \left(\frac{p_{t2}}{p_{t1}}\right)^{\frac{n-1}{n}} = \left(\frac{p_{t2}'}{p_{t1}}\right)^{\frac{k-1}{k}}$$

and for the isentropic compression work

$$L_c' = Jc_pT_{t1}\left[\left(\frac{p_{t2}}{p_{t1}}\right)^{\frac{n-1}{n}} - 1\right] = \frac{k}{k-1}RT_{t1}Z_{cn} \qquad (39)$$

For the actual process

$$L_c = \frac{n}{n-1}RT_{t1}Z_{cn} = \eta L_c' \qquad (40)$$

where η is defined by equation 3·73, and $n > k(n \approx 1.6$ for adiabatic flow).

The ratio

$$\eta = \frac{L_c}{L_c'} \qquad (41)$$

is called the *hydraulic efficiency* in the case of incompressible fluids and the *polytropic efficiency* for compressible fluids.

If the stations 1 and 2 are located where the velocities c_1 and c_2 are small, the total temperatures and pressures may be replaced by the local static temperatures and pressures.

10A. Compressor Performance Characteristics

The performance of a centrifugal air compressor is usually based upon static pressure and temperature measurements taken at the inlet and exit sections of the complete machine. This combines the losses in the inlet and exit flow passages with those in the impeller into a single energy loss for the complete air compressor. The performance calculations also neglect the velocity heads of the air in the inlet and exit piping. Neglect of the aforementioned velocity heads ordinarily introduces no significant error because of the low specific weight of the air.

(a) **Adiabatic Efficiency and Temperature Rise.** Let the subscripts 0 and 4 refer to the entrance and exit sections of the compressor respectively. Then the ratio of the input works, for the same pres-

sure ratio, for the ideal and actual compressor is called the *adiabatic efficiency*. Thus

$$\eta_{ad} = \frac{\Delta h_c'}{\Delta h_c} = \left(\frac{T_0}{T_4 - T_0}\right) Z_c \tag{42}$$

The product $T_0 Z$ is known as the *adiabatic temperature rise*.

(*b*) **Pressure Coefficient.** The actual static head developed by the compressor, which is denoted by H, is given by

$$H = J c_p \, \Delta T \approx \frac{p_4 - p_0}{\gamma_m} \tag{43}$$

where γ_m is the mean specific weight of the air between stations 0 and 4.

For an actual compressor an equation similar to equation 18 can be written. Thus denoting the actual pressure coefficient by η_p and substituting for u in terms of the impeller diameter D inches and its rpm N the static head H is given by

$$H = \eta_p \frac{u_2^2}{2g} = \frac{\eta_p}{2g} \left(\frac{\pi D N}{720}\right)^2 \tag{44}$$

From equation 44 the value of η_p can be calculated from a test of the compressor. If η_p is known then the impeller diameter D inches to produce a given static head H is calculated from

$$D = \frac{720}{\pi N} \sqrt{\frac{2gH}{\eta_p}} = \frac{1840}{N} \sqrt{\frac{H}{\eta_p}} \tag{45}$$

By equating equations 43 and 44 an expression for η_p is obtained in terms of the adiabatic temperature rise and the impeller tip speed. Thus

$$\eta_p = \frac{2gJc_p \, \Delta T}{u_2^2} \tag{46}$$

(*c*) **Adiabatic Horsepower.** If the weight of air inducted by the compressor is G lb/min and the air is compressed adiabatically from the pressure p_0 to p_4, the horsepower imparted to the fluid is the *adiabatic horsepower* hp_{ad} and is given by

$$\text{hp}_{ad} = c_p \frac{J T_0 Z_c G}{33,000} = 0.00573 G T_0 Z_c \tag{47}$$

(*d*) **Actual Temperature-Rise Horsepower.** This is the horsepower based on the actual temperature rise $T_4 - T_0$. Thus, let hp_{atr} denote this horsepower; then

$$\text{hp}_{atr} = 0.00573 G T_0 Z_{cn} \tag{48}$$

(e) **Overall Efficiency.** This is the ratio of the fluid horsepower hp_f = $GH/33,000$ to the brake horsepower supplied to the compressor.

$$\eta_c = \frac{GH}{550} \times \frac{1}{bhp} \qquad (49)$$

11A. General Performance Parameters

It can be shown by dimensional analysis that the pressure ratio developed by a centrifugal air compressor is a function of the following parameters [11]

$$r_c = \frac{p_4}{p_0} = f\left(R_e, K, \frac{u_2}{a_2}, \frac{Q}{ND^3}\right) \qquad (50)$$

where R_e = Reynolds number, K = adiabatic constant of compression. $\frac{Q}{ND^3}$ = flow factor, and $\frac{u_2}{a_2} = \frac{\text{Tip speed of impeller}}{\text{Local acoustic velocity}}$ = Mach number.

Tests of centrifugal air compressors have shown that, under the conditions of fully developed turbulence occurring in high-speed machines, the Reynolds number R_e has no measurable effect on the pressure ratio. Further, for the range of pressure ratios encountered K is practically constant.

Since it is difficult to measure the acoustic velocity at the impeller tip, the local Mach number is replaced by an equivalent Mach number based upon the acoustic velocity at the inlet. This modification has little effect upon the evaluation of compressor performance.

The pressure ratio equation can, therefore, be expressed by

$$r_c = f\left(\frac{Q}{ND^3}, \frac{u_2}{a_0}\right) \qquad (51)$$

For a given compressor the impeller diameter D is a constant. Further, the tip speed u_2 is proportional to N, the rpm. Also $a_0 = 1120\sqrt{T_0/520} = 49\sqrt{T_0}$ Hence, N can be substituted for u_2, and $\sqrt{T_0}$ for a_0. Equation 51 becomes

$$r_c = f\left(\frac{Q}{N}, \frac{N}{\sqrt{T_0}}\right) \qquad (52)$$

It follows from equation 52 that, for a compressor to give the same pressure ratios at different operating conditions, the parameters in the parentheses must remain unchanged in their values. Thus

$$\frac{Q_1}{N_1} = \frac{Q_2}{N_2} \text{ and } \frac{N_1}{\sqrt{T_{01}}} = \frac{N_2}{\sqrt{T_{02}}} \text{ so that}$$

$$\frac{Q_1}{Q_2} = \frac{N_1}{N_2} = \sqrt{\frac{T_{01}}{T_{02}}} \qquad (53)$$

It is seen that the inlet temperature affects the value of both Q/N and N/T_0. For this reason, as explained in the preceding section, the standard of comparison is made at a constant inlet temperature such as $t_0 = 60$ F (or $T_0 = 520$ R).
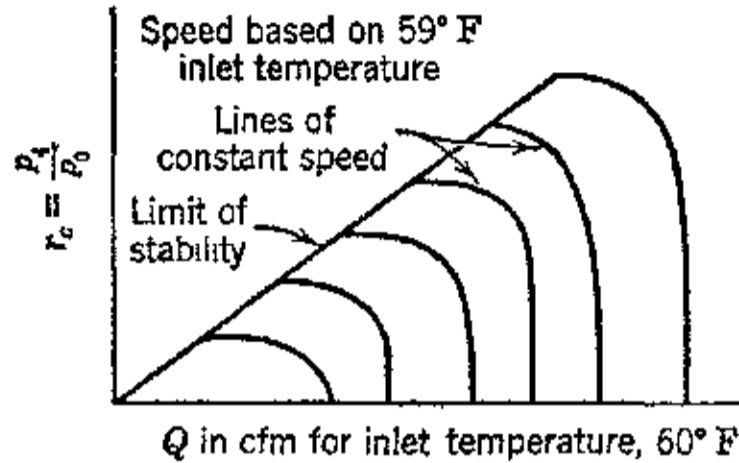
FIG. 12.   Pressure ratio vs. flow characteristic curves for a centrifugal compressor.

The performance characteristics of the compressor can be plotted as shown in Fig. 12. It is convenient also to plot lines of constant values of the temperature-rise factor $(T_4 - T_0)/T_0$ since they can be measured directly. The complete compressor characteristics are illustrated in Fig. 13.
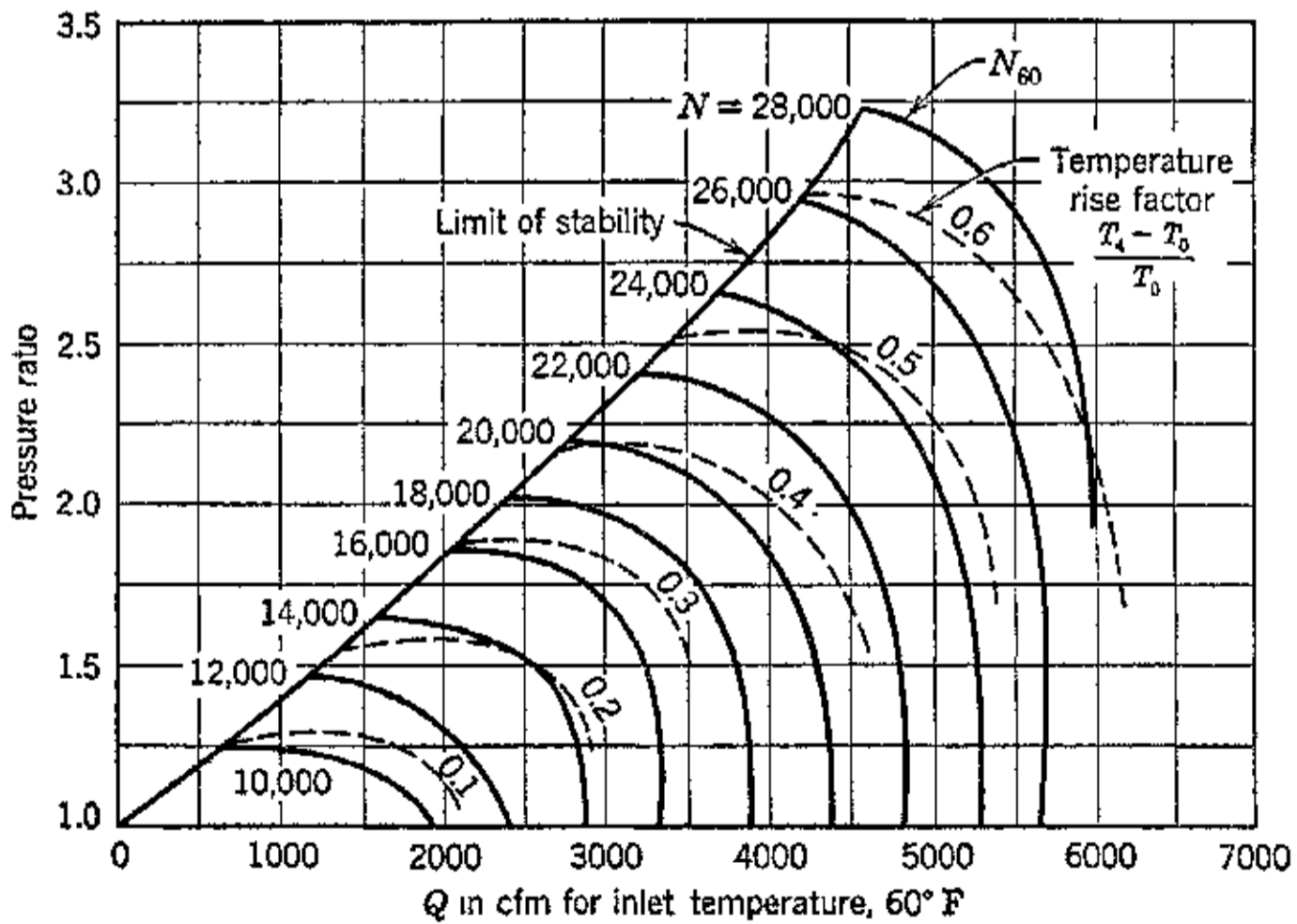
FIG. 13.   Centrifugal compressor performance chart.

EXAMPLE. A compressor has the characteristic curves presented in Fig. 13. It is to be used to supercharge an engine at 25,000-ft altitude. The delivery pressure is to be 28.5 in. of mercury absolute, and the air flow is 160 lb/min. Find: (a) inlet

air flow at 520 R; (b) rpm at altitude N_2; (c) discharge temperature T_4; (d) brake horsepower required at altitude.

Solution. From Table 1·6,

$$p_{02} = 11.1, \qquad T_{02} = 430 \text{ R}, \qquad \sigma = 0.4480, \qquad \gamma_{02} = 0.034 \text{ lb/ft}^3$$

Air flow. At 25,000 ft, $Q_2 = 160 \div 0.034 = 4700$ cfm.

(a) At 520 R, $Q_1 = 4700\sqrt{520 \div 430} = 5180$ cfm.

Pressure ratio r_{c2}. At 25,000 ft, $r_{c2} = 28.5 \div 11.1 = 2.56$.

From Fig. 13 the intersection of $r_{c2} = 2.56$ and $Q_1 = 5180$ cfm gives $N_1 = 26,300$ and $(T_4 - T_0)/T_0 = 0.548$.

(b) Rpm at altitude N_2. From equation 53

$$N_2 = N_1 \sqrt{\frac{T_{02}}{T_{01}}} = 26,300 \sqrt{\frac{430}{520}} = 23,700 \quad \text{rpm}$$

(c) Discharge temperature T_4.

$$\frac{T_4 - T_0}{T_0} = 0.548 \quad \text{(from Fig. 13)}$$

Hence

$$T_4 - T_0 = 0.548 \times 430 = 236 \text{ F}$$

$$T_4 = 430 + 236 = 666 \text{ R} = 206 \text{ F}$$

(d) Brake horsepower required.

$$\text{bhp} = 0.00572 G(T_4 - T_0) = 0.00572 \times 160 \times 236 = 216$$

12A. Effect of Changed Operating Conditions

The operating conditions to which the centrifugal compressor is applied are subject to variations, and its performance has to be predicted for the changed conditions. The developments of this section are based on reference 9 through the courtesy of the publisher.

(a) **Effect of Change in Impeller Speed.** Assuming that the ambient conditions at the compressor inlet are unchanged, the volumetric rate of air flow through the compressor Q varies directly with the impeller rpm N. Thus, if the impeller rpm changes from N_1 to N_2, then the peripheral velocity u of any point on the impeller changes in proportion to the rpm change, because $u = \pi N D/720$, where D is the impeller diameter in inches.

The change in rpm has no influence upon the inlet angles α_1 and β_1. Hence the velocity triangle for the inlet to the compressor changes so that the new triangle is similar to the original one. Let u_{11} be the tangential velocity at entrance corresponding to N_1, and u_{12} that corresponding to N_2; then

$$u_{12} = \frac{N_2}{N_1} u_{11}$$

All the sides of the velocity triangle are changed by the same ratio. The same considerations apply to the absolute entrance velocity c_1, which is a measure of the capacity of the air compressor. Thus

$$c_{12} = \frac{N_2}{N_1} c_{11}$$

Hence, the new air flow through the centrifugal compressor due to changing the speed from N_1 to N_2 is given by

$$Q_2 = \frac{N_2}{N_1} Q_1 \tag{54}$$

The effect of a change in impeller rpm upon the head is determined as follows. In general, the head can be expressed in terms of the actual pressure coefficient η_p by the equation

$$H = \eta_p \frac{c_{2u} u_2}{2g} \tag{54a}$$

In equation 54a the velocity vectors c_{2u} and u_2 are both directly proportional to the impeller rpm. Hence, since η_p may be assumed to be a constant,

$$\frac{H_2}{H_1} = \frac{N_2^2}{N_1^2} \tag{55}$$

Equation 55 can be expressed in terms of the pressure ratio developed by the compressor. Thus

$$H_1 \propto Z_{c1} \quad \text{and} \quad H_2 \propto Z_{c2}$$

so that

$$\frac{H_2}{H_1} = \frac{Z_{c2}}{Z_{c1}} = \frac{(r_c^{\frac{k-1}{k}} - 1)_2}{(r_c^{\frac{k-1}{k}} - 1)_1} = \frac{N_2^2}{N_1^2} \tag{56}$$

For a given single-stage compressor the efficiency does not change appreciably for a given value of air flow per revolution Q/N, since the magnitude of this parameter determines the ratios of the sides of the velocity triangles at the inlet and exit sections of the impeller. Consequently, for a small change in the speed of the impeller the efficiency can be assumed constant. The brake horsepower (bhp) to drive the compressor then depends only upon the product of the air flow Q and the actual head H. Hence from equations 54 and 55

$$\frac{bhp_2}{bhp_1} = \left(\frac{N_2}{N_1}\right)^3 \tag{57}$$

(b) **Effect of Changing Inlet Conditions.** Changing either the inlet pressure or the inlet temperature (or both of them) changes the specific weight γ_0 of the air flowing into the compressor.

If the impeller rpm is maintained constant, so that $N_2 = N_1 = N$, then from equation 54 the volumetric flow of air through the machine is constant, and $Q_2 = Q_1 = Q$. The weight flow of air G lb/min changes, however, because of the change in specific weight. Thus

$$G_2 = G_1 \frac{\gamma_{02}}{\gamma_{01}} \tag{58}$$

The volumetric flow Q against which the performance data are plotted is in reality a weight flow because it is based on $\gamma_0 =$ constant. Hence changing the value of γ_0 is equivalent to changing the value of Q for a fixed speed and fixed intake conditions. Changing γ_0 has the effect, therefore, of changing the value of the original reference volumetric air flow, which is denoted by Q_{r1}. The new reference volumetric air flow is given by

$$Q_{r2} = Q_{r1} \frac{\gamma_{02}}{\gamma_{01}} \tag{59}$$

Since only a change in the specific weight of the entering air is being considered, all other factors are constant. Hence the static head is unchanged. The discharge pressure is changed, however, since $\Delta p = \gamma H$. The change in γ_0 changes the horsepower required to drive the compressor because the horsepower is proportional to the product of the head and the weight flow G. Thus

$$bhp_2 = bhp_1 \left(\frac{\gamma_{02}}{\gamma_{01}} \right) \tag{60}$$

The actual volumetric flow of ambient free air Q is unaffected by a change in γ_0 since N is constant. This means that, for a fixed rpm, changing γ_0 does not alter the value of Q/N, and the efficiency η_c is unaffected. But

$$\gamma_0 = \frac{p_0}{RT_0}$$

Hence

$$\frac{\gamma_{02}}{\gamma_{01}} = \frac{p_{02}}{p_{01}} \cdot \frac{T_{01}}{T_{02}}$$

In general, the weight flow of air through a centrifugal compressor is given by

$$G_2 = G_1 \frac{N_2}{N_1} \cdot \frac{p_{02}}{p_{01}} \cdot \frac{T_{01}}{T_{02}} \tag{61}$$

Similarly the required brake horsepower is given by

$$bhp_2 = bhp_1 \cdot \frac{p_{02}}{p_{01}} \cdot \frac{T_{01}}{T_{02}} \cdot \left(\frac{N_2}{N_1}\right)^3 \tag{62}$$

or

$$bhp_2 = bhp_1 \cdot \frac{p_{02}}{p_{01}} \cdot \frac{Q_2}{Q_1} \cdot \frac{Z_{c2}}{Z_{c1}} \tag{63}$$

The pressure ratio can be determined from the general equation for Z_c and

$$Z_{c2} = Z_{c1} \left(\frac{N_2}{N_1}\right)^2 \frac{T_{01}}{T_{02}} \tag{64}$$

EXAMPLE. A centrifugal compressor delivers 2000 cfm of free air at a speed of 20,000 rpm. The initial conditions are $p_0 = 14.7$ and $t_0 = 68$ F. The pressure ratio is 2.0 and $\eta_c = 0.72$. Find the operating conditions at 18,000 rpm.
$N_1 = 20,000$, $p_0 = 14.7$, $t_0 = 68$, $p_4 = 29.4$ psia, $\eta_c = 0.72$, $Q_1 = 2000$
Initial Conditions.

$$p_0 = 14.7 \times 144 = 2117 \quad \text{psf} \qquad T_0 = 460 + 68 = 528 \text{ R}$$

$$v_0 = \frac{RT_0}{p_0} = \frac{53.35 \times 528}{2117} = 13.3 \quad \text{ft}^3/\text{lb}$$

$$G = \frac{2000}{13.3 \times 60} = 2.51 \quad \text{lb/sec}$$

Static head at design point

$$H_1 = \frac{RT_0(2^{0.283} - 1)}{0.283} = \frac{53.35 \times 528}{0.283} \times 0.21672 = 21,550 \quad \text{ft of air}$$

$$H_1 = \frac{p_0 v_0}{0.283} \times 0.21672 = \frac{2117 \times 13.3}{0.283} \times 0.21672 = 21,580 \quad \text{ft of air}$$

Air horsepower $= ahp = \dfrac{GH_1}{550} = \dfrac{2.51 \times 21,550}{550} = 115 \quad ahp$

Bhp required $= \dfrac{ahp}{\eta_c} = \dfrac{115}{0.72} = 159 \quad$ bhp

Effect of Speed Change.

$$\text{Speed ratio} = \frac{N_2}{N_1} = \frac{18}{20} = 0.9; \quad \left(\frac{N_2}{N_1}\right)^2 = 0.81; \quad \left(\frac{N_2}{N_1}\right)^3 = 0.729$$

Air flow, $Q_2 = 0.9 \times 2000 = 1800$ cfm.
Static head, $H_2 = (N_2/N_1)^2$. $H_1 = 0.81 \times 21,550 = 17,450$ ft of air.

Pressure ratio, $Z_{c2} = \dfrac{H_2}{RT_0/0.283} = \dfrac{17,450}{99,400} = 0.175.$

From Table 4-5, $(r_c)_2 = 1.953.$
Discharge pressure, $(p_4)_2 = 14.7 \times 1.953 = 28.8$ psia.
Brake horsepower $(bhp)_2 = (bhp)_1 \times (N_2/N_1)^3 = 159 \times 0.729 = 116$ bhp.
The efficiency of the compressor remains constant at $\eta_c = 0.72$.

B. The Axial-Flow Compressor

1B. Introduction

The axial-flow compressor is in its essential features a reaction turbine operated as an air pump. Figure 14 is a cross section of this type of compressor. It consists of a rotor equipped with several rows of airfoil-shaped blades and a stator with rows of stationary blades which are interposed between the rows of rotating blades. As the air flows through the rotating blades its static pressure and kinetic
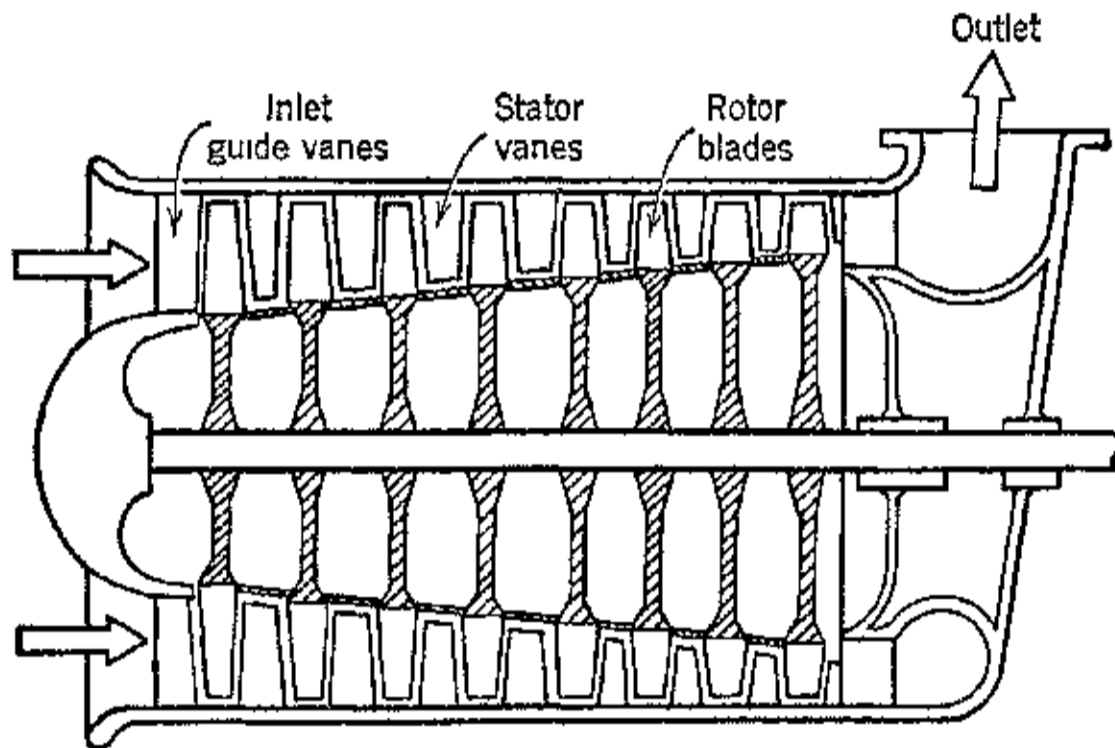
FIG. 14. Cross section through an axial-flow compressor. (Reproduced from W. J. King, *loc. cit.*)

energy are both increased. Each row of stationary blades acts both as a diffuser for converting the kinetic energy of the air leaving the preceding rotating row into pressure and as the nozzles for guiding the air into the next row of rotating blades. The flow path through an axial compressor is illustrated in Fig. 15.

The axial-flow compressor has attracted the attention of gas turbine and turbojet designers because its efficiency is generally higher than that of the centrifugal compressor. Another attractive feature is its ability to handle the same air flows with a much smaller frontal area. Its disadvantages are its greater length and its larger weight when compared with a centrifugal compressor furnishing the same pressure ratio. Because the pressure ratio per stage is approximately 1.2:1, several stages are needed to attain reasonable pressure ratios. Figure 16 illustrates the application of the axial-flow compressor to a gas turbine-propeller engine. The performance of an axial compressor stage is the result of the action of the stresses in the

fluid surrounding the blades upon the blade surfaces. These stresses are basically of two types: normal stress or pressure and tangential stress or shear. The pressure force is related to the main body of flow outside of the boundary layer, whereas the shear forces (skin
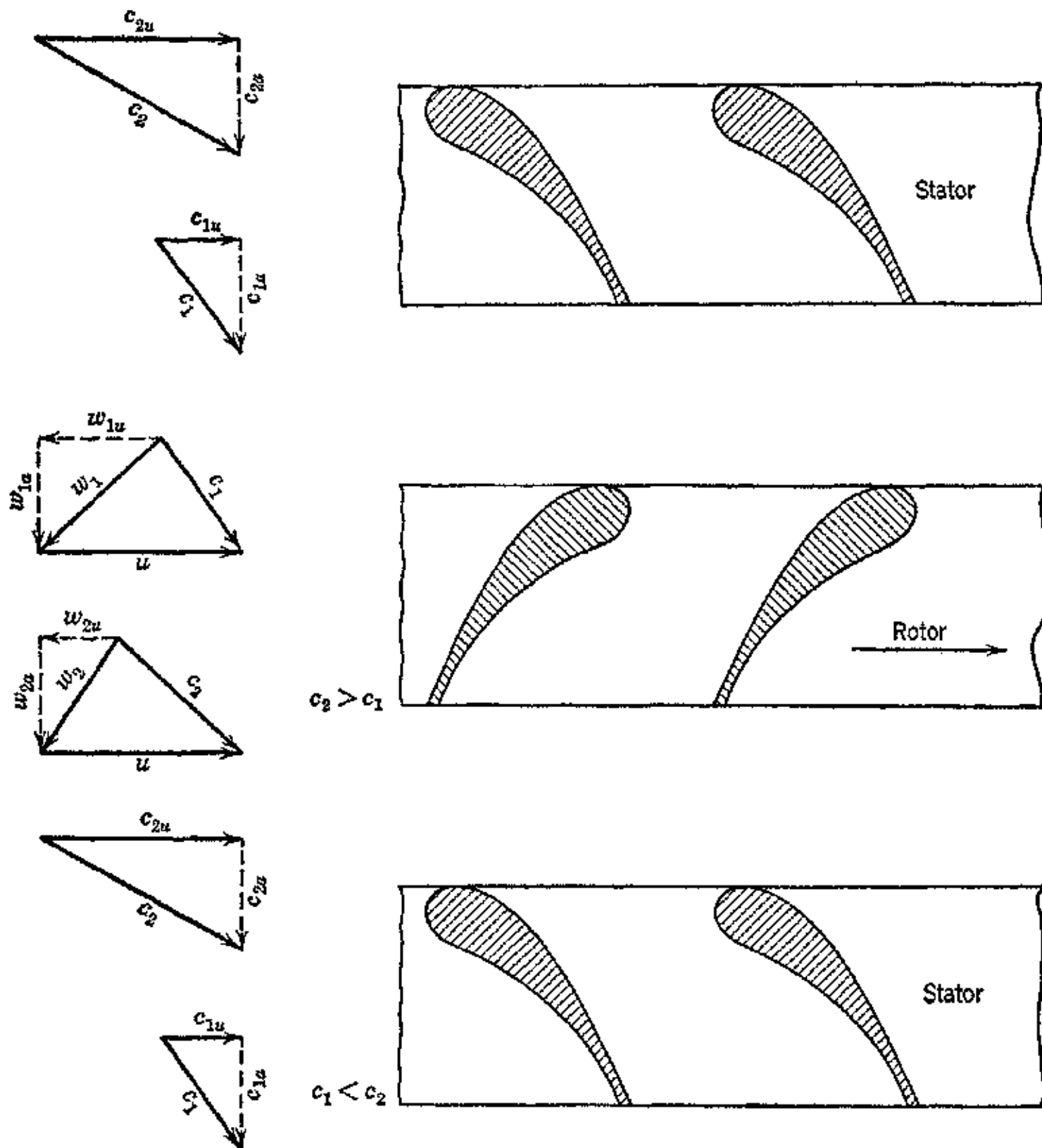
Fig. 15.   Velocity diagrams for an axial-flow compressor stage.

friction) arise from the viscosity effects of the flow within the boundary layer and, as pointed out in Chapter 1, are the source of the fluid friction losses. The shearing stresses are the ones that affect the stage efficiency.[20] An exact theory of the axial-flow compressor must be based on the accurate determination of the flow characteristics around each blade and the related forces. The aerodynamic problem

involved is the flow through lattices, and it must take into account the three-dimensional nature of the flow and the effects of viscosity and of compressibility. The theory is as yet incomplete, and the development of the most suitable profiles for the blades has to be based on experimental aerodynamic data.[20]

Although the more complex aerodynamic theories of the axial compressor are beyond the scope of this book, it is constructive to
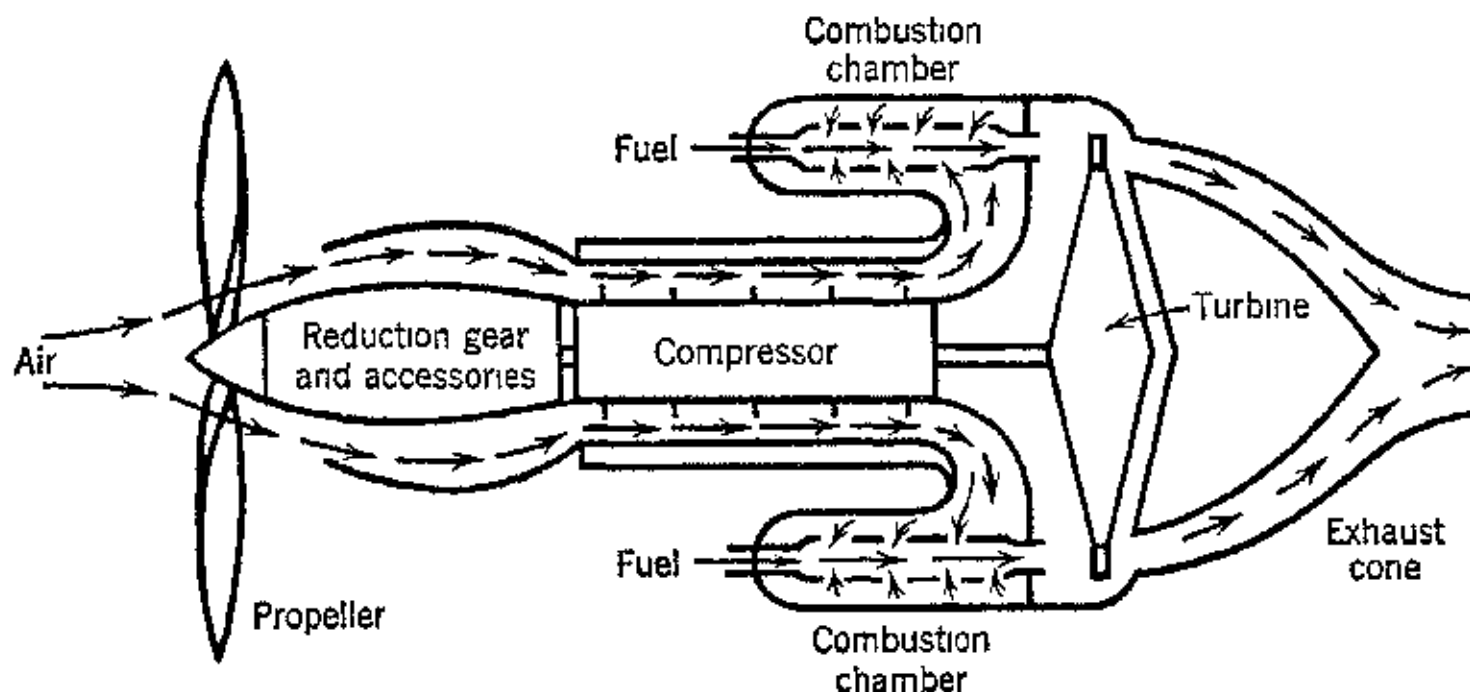
FIG. 16. Schematic arrangement of a gas turbine-propeller engine (turboprop engine) employing an axial-flow compressor. (Reproduced from *Western Flying*, December 1945.)

consider certain aspects of the simpler two-dimensional theory based on the incompressibility of the fluid. The basic ideas have already been discussed in Chapter 2, Section 8, and in Chapter 6, Section 7.

2B. Notation for Part B

b = chord length.

b/t = solidity ratio.

c = absolute velocity.

C_D = drag coefficient.

C_L = lift coefficient.

D = drag component of resultant force.

dT = tangential force on blade element = $\rho c_a \Gamma_z \, dr$.

dS = normal force in blade element = $\rho w_m \Gamma_z \, dr$.

dR = resultant force on blade element = $dL/\cos \epsilon$.

Δp_i = ideal pressure rise = $\rho \Gamma_z w_{mu}/t$.

Δp_i = $p_2' - p_1$ = ideal pressure rise.

Δp = actual pressure rise = $dS/t \cdot dr$.

dL = lift force acting on blade element = $\tfrac{1}{2} C_L \rho w_m^2 b \, dr$.

dD = drag force acting on blade element = $\frac{1}{2}C_D\rho w_m{}^2 b\, dr$.

$\Delta c_u = (c_{1u} - c_{2u})$.

p = static pressure.

p_2' = ideal final pressure.

R = resultant force per unit radial length of blade.

r = radius.

$t = 2\pi r/z$ = pitch.

u = peripheral velocity.

w = relative velocity.

X = force component per unit length of blade in direction of axis of cascade.

Y = force component per unit length of blade perpendicular to lattice axis.

z = number of blades.

Subscripts

1　inlet condition.

2　outlet conditions.

u　in direction of tangential velocity.

a　in axial direction.

z　a single blade.

m　mean geometric value.

Greek Symbols

β = angle between w and u.

β_p = angle of profile section.

β_m = effective pitch angle.

ρ = density.

γ = specific weight.

ϕ = angle between chord and lattice axis.

δ = angle of attack = $\phi - \beta_m$.

$\epsilon = C_D/C_L$.

Γ_z = circulation for a single blade = $t(c_{1u} - c_{2u})$

　　　= $t(w_{1u} - w_{2u})$.

η_b = blading efficiency = $\Delta p/\Delta p_i$.

3B. Two-Dimensional Incompressible Flow through a Rotating Blade Lattice

Figure 17 illustrates the basic dimensions of an arbitrary blade of a lattice set at the pitch angle ϕ with respect to the axis of the lattice. Consider an element of the blade of length dr located at the distance r from the axis of rotation, as illustrated in Fig. 18. If

the bounding cylindrical surfaces passing through all the blades are developed into two parallel planes the lattice illustrated in Fig. 19 is obtained, the length of each blade perpendicular to the plane of the paper being dr. The distance between neighboring blades, called the pitch t, is given by

$$t = \frac{2\pi r}{z} \qquad (65)$$

FIG. 17.   Basic dimensions of an arbitrary blade of a lattice

If b is the chord length of the blade, the *solidity ratio* for the lattice is $b/t = bz/2\pi r$.

The aerodynamic forces acting on the blades arise from the change in momentum of the air flowing through the blade passages as demonstrated in Chapter 2, Section 8.   From Fig. 15 it is seen that the air leaves the stator with the absolute velocity c_1, and owing to energy imparted to it by the rotor, the air leaves the rotor with the larger absolute velocity c_2.   Since it is assumed that the density of the air ρ remains constant, from continuity, $c_{1a} = c_{2a} = w_{1a} = w_{2a} = c_a$.   Because of the constancy of the axial-flow component, as pointed out in Chapter 2, Section 10, there is no change in momentum in the axial direction; there is, however, a change in momentum in the tangential direction, i.e., in the direction of the lattice axis.   Let x and y denote the directions parallel and perpendicular to the lattice axis and dT and dS the forces acting in

FIG. 18.   An element of a blade at an arbitrary distance from the axis of rotation.

x and y directions respectively.   These forces acting on the blade element are illustrated in Fig. 20.

The force dT corresponds to dQ in Fig. 6·11 and is the force re-

quired to overcome the resistance to motion of the blade element. The force dS is the pressure force arising from the change in the kinetic energy of the air passing through the passage of area $t\ dr$.

It follows immediately from the results derived in Chapter 2, Section 10, that the magnitude of the force dT is obtained from equation 2 60 by multiplying that equation by the blade length dr.
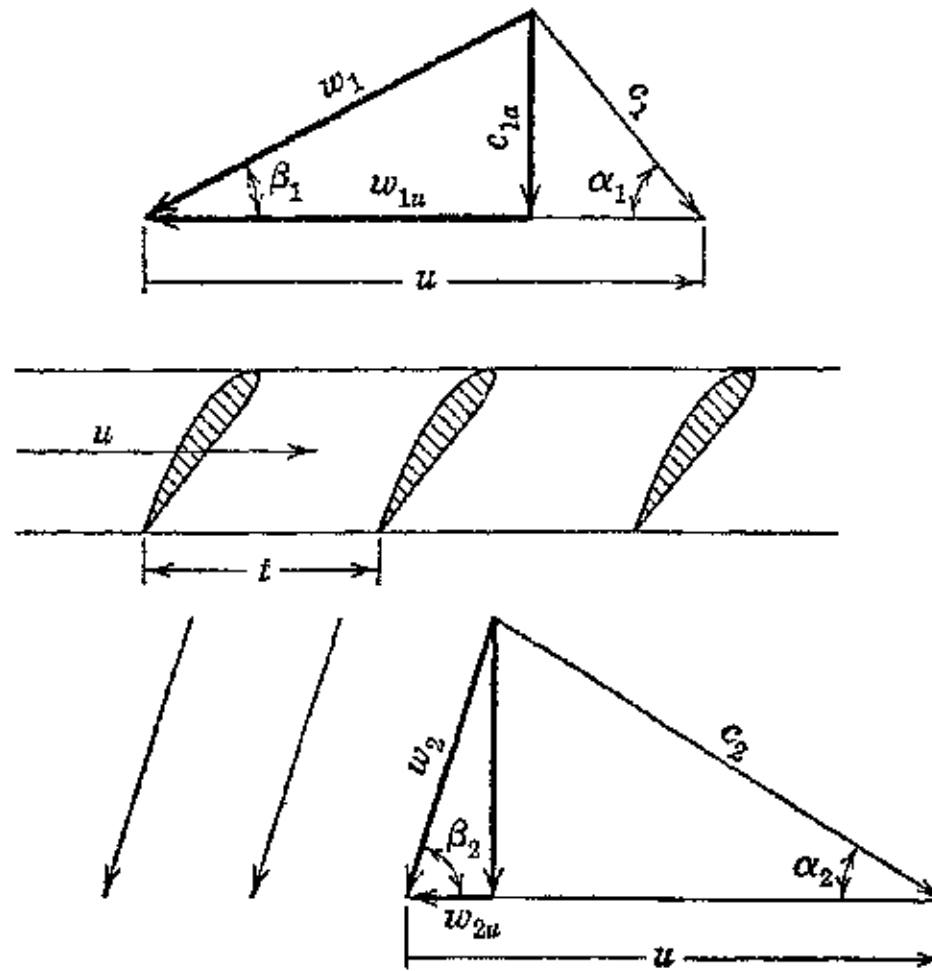
FIG. 19   Development of the blade lattice in the parallel planes.

Similarly, the force dS is obtained by multiplying equation $2 \cdot 59$ by dr Hence

$$dT = \rho c_a t\ dr(w_{1u} - w_{2u}) \tag{66}$$

and

$$dS = \rho t\ dr \frac{(w_{1u} + w_{2u})}{2} (w_{1u} - w_{2u}) \tag{67}$$

These forces can be expressed in terms of the peripheral components of the absolute velocities c_1 and c_2 by noting that $c_{1u} = w_{1u} - u$ and $c_{2u} = w_{2u} - u$, so that

$$w_{1u} - w_{2u} = c_{1u} - c_{2u} \tag{68}$$

For a unit length of blade, it follows from equation $2 \cdot 61$, that the product $t(w_{1u} - w_{2u})$ is the circulation around the blade and is denoted by Γ_z, then

$$dT = \rho c_a \Gamma_z \cdot dr \tag{69}$$
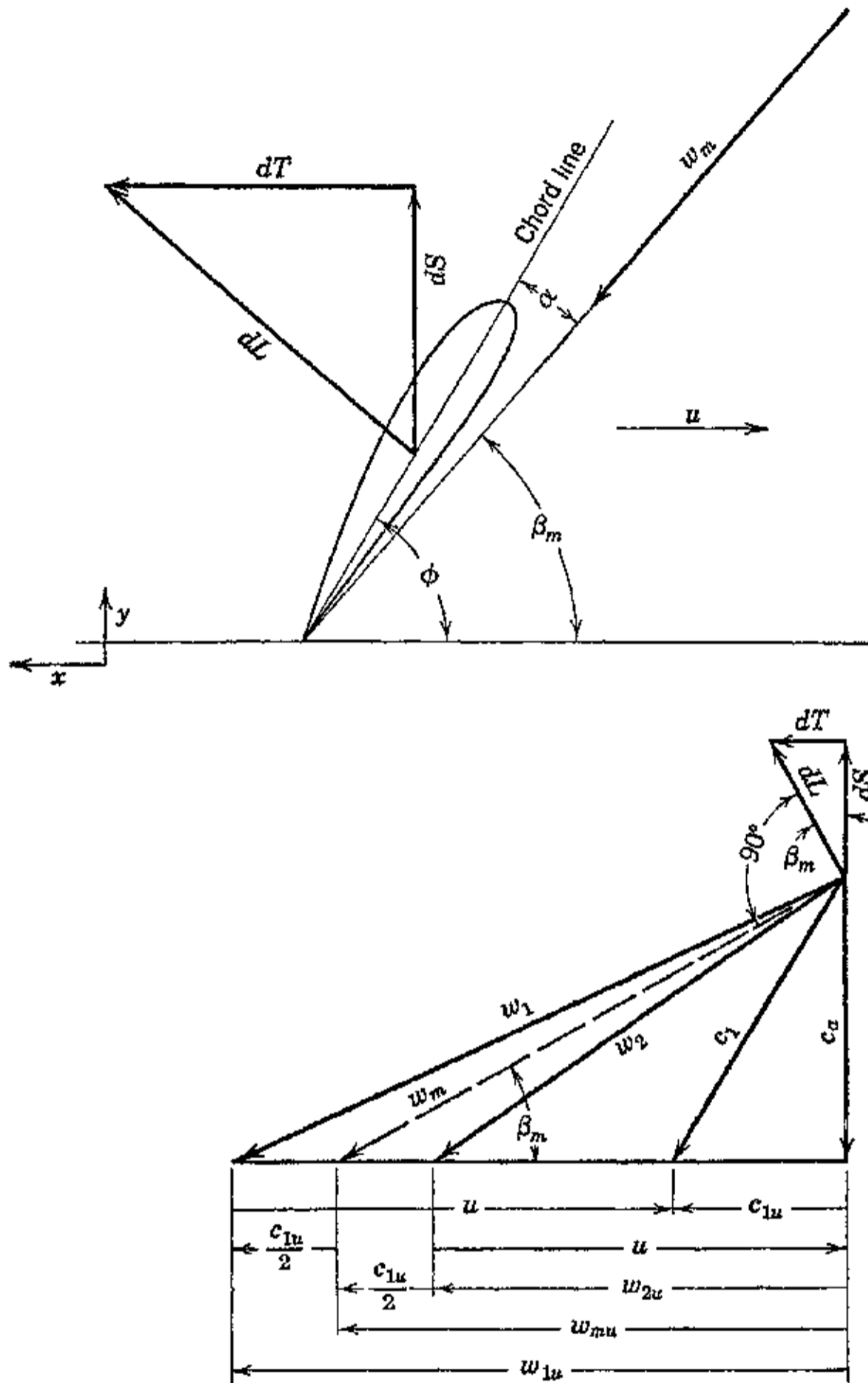
FIG. 20. Force and velocity diagrams for a blade element.

and

$$dS = \rho \frac{(w_{1u} + w_{2u})}{2} \Gamma_z \cdot dr \tag{70}$$

where

$$\Gamma_z = t(w_{1u} - w_{2u}) = t(c_{1u} - c_{2u})$$

Equations 69 and 67 show that the tangential force dT is proportional to the axial velocity component c_a, and that the pressure force

dS is proportional to $\frac{1}{2}(w_{1u} + w_{2u})$. The resultant force, denoted by dL, is perpendicular to the geometrical mean velocity w_m, which is the geometrical sum of $\frac{1}{2}(w_{1u} + w_{2u})$, and c_a as illustrated in Fig. 20 The geometric mean relative velocity w_m characterizes the direction of the flow toward the blade lattice.[20] The angle β_m which w_m makes with the x direction is (see Fig. 20) given by

$$\beta_m = \tan^{-1}\frac{c_a}{w_{mu}} \qquad (71)$$

where

$$w_{mu} = \frac{w_{1u} + w_{2u}}{2} = \left(u + \frac{c_{1u}}{2}\right) \qquad (72)$$

The magnitude of the resultant force is the vector sum of dT and dS and is given by

$$dL = \rho w_m t\, dr(w_{1u} - w_{2u})$$

or

$$dL = \rho w_m \Gamma_z\, dr \qquad (73)$$

If p_2' is the final pressure in the ideal case, the normal force expressed in terms of the ideal pressure change across the lattice is

$$dS = (p_2' - p_1)t\, dr \qquad (74)$$

From Fig 20 it is seen that $dS = dL \cos \beta_m$. Substituting this last expression into equation 74 and solving for $\Delta p_i = (p_2' - p_1)$

$$(p_2' - p_1)t\, dr = dL \cos \beta_m = \rho w_m \Gamma_z dr \cos \beta_m \qquad (75)$$

From Fig. 20 it is seen that

$$w_m \cos \beta_m = u + \frac{c_{1u}}{2} \qquad (76)$$

Hence equation 75 becomes

$$\Delta p_i = p_2' - p_1 = \rho\frac{\Gamma_z}{t}\left(u + \frac{c_{1u}}{2}\right) = \rho\frac{\Gamma_z}{t}w_{mu} \qquad (77)$$

Equation 77 gives the increase in static pressure due to the energy transfer.

It was shown in Chapters 5 and 6 that because of the viscosity of the air there are surface friction and eddies which cause the blade element to experience a drag force dD in addition to the lift force dL. The accompanying energy losses depend upon the magnitude of the relative velocity and the blade profile. As for the propeller discussed

in Chapter 6, Section 7, the efficiency of the entire blade is calculated from the efficiencies of the individual blade elements at each radius r. The overall efficiency is then the mean value obtained by integrating the efficiency curve plotted as a function of the radius
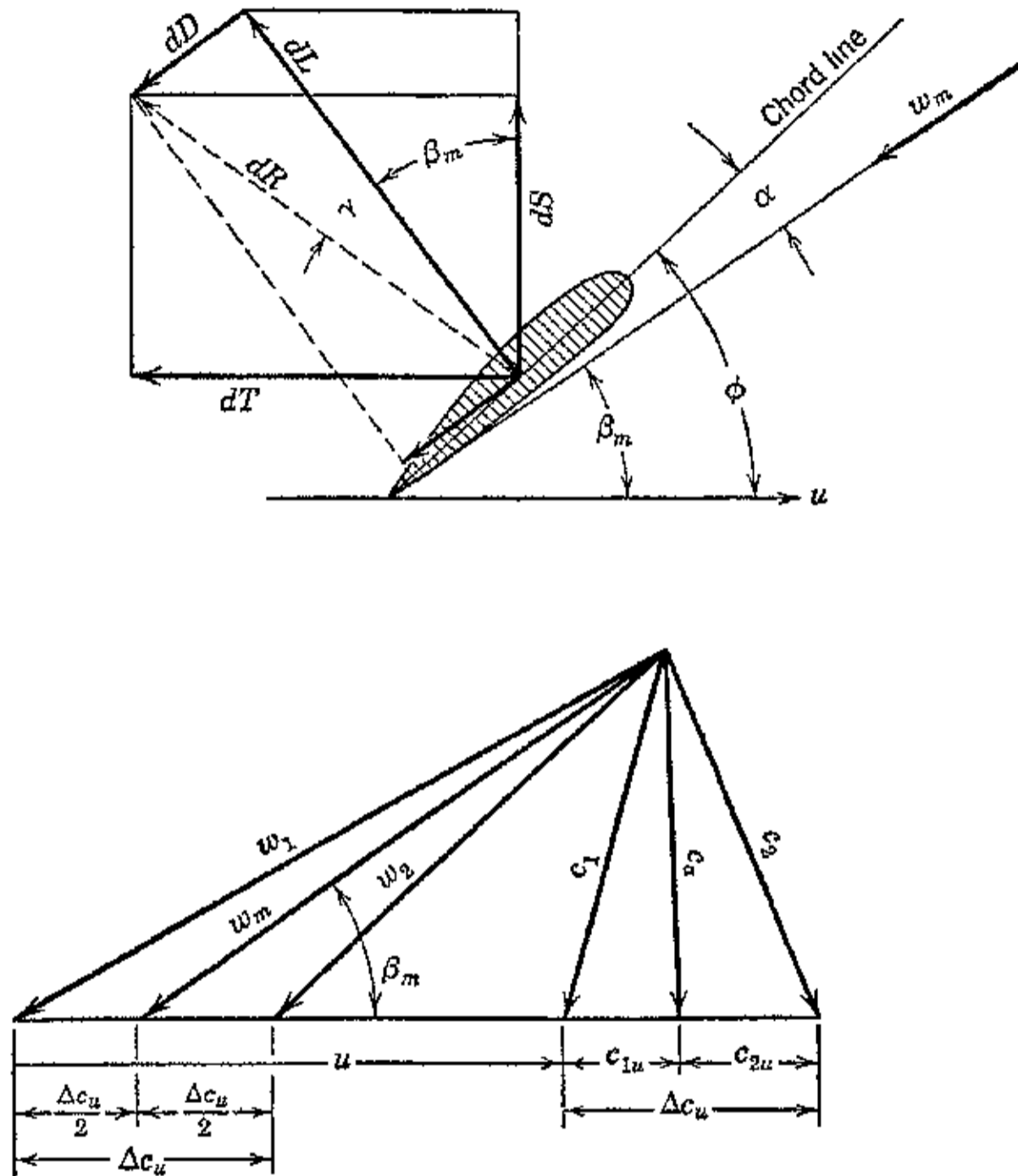
FIG. 21. Lift and drag forces acting on a blade element.

The blade element theory discussed in Chapter 6, Section 7, is applicable to the element of Fig. 21. Consequently, the results of Chapter 6, Section 7, can be applied directly. The lift force is given by equation 6·31 and the drag force by equation 6·32. Thus, if C_L and C_D are the lift and drag coefficients for the blade element, then

$$dL = \tfrac{1}{2}C_L\rho w_m{}^2 b \cdot dr \tag{78}$$

and

$$dD = \tfrac{1}{2}C_D\rho w_m{}^2 b \; dr \tag{79}$$

Figure 21 illustrates the resolution of the forces acting on the blade element   The ratio $\epsilon = C_D/C_L$ = reciprocal of lift/drag ratio for

the blade profile is a characteristic of the aerodynamic performance of the blade profile. The resultant force on the blade element dR in terms of the lift is given by equation 6·34, thus

$$dR = \frac{dL}{\cos \gamma} \tag{80}$$

In terms of the normal force dS it follows from geometry or from equation 6·34

$$dR = \frac{dS}{\cos (\beta_m + \gamma)} \tag{81}$$

In terms of the tangential force, dR is given by

$$dR = \frac{dT}{\sin (\beta_m + \gamma)} \tag{82}$$

Hence from equations 80 and 81

$$dS = dR \cos (\beta_m + \gamma) = \frac{dL \cos (\beta_m + \gamma)}{\cos \gamma} \tag{83}$$

Expanding the cosine term and noting that $dD/dL = \tan \epsilon$ gives

$$dS = dL \cos \beta_m - dD \sin \beta_m \tag{84}$$

The actual pressure rise is accordingly

$$\Delta p = \frac{dS}{t \, dr} \tag{85}$$

Substituting for dL and dD in terms of their coefficients and substituting for dS from equation 84, the pressure-rise equation becomes

$$\Delta p = \frac{1}{2} \rho w_m{}^2 \cos \beta_m \cdot \frac{b}{t} \cdot C_L(1 - \epsilon \tan \beta_m) \tag{86}$$

The ideal pressure rise is given by the change in the kinetic energy of the air. Thus, since the air enters with the velocity c_1 and leaves with the velocity c_2, the ideal pressure rise Δp_i is

$$\Delta p_i = \tfrac{1}{2}\rho(w_1{}^2 - w_2{}^2) \tag{87}$$

From Fig. 21, $w_1{}^2 = w_a{}^2 + w_{1u}{}^2$ and $w_2{}^2 = w_a{}^2 + w_{2u}{}^2$, so that

$$\Delta p_i = \rho(w_{1u} - w_{2u}) \frac{(w_{1u} + w_{2u})}{2} = \rho(w_{1u} - w_{2u})w_{mu}$$

But

$$w_{mu} = c_a \cot \beta_m \qquad (88)$$

Hence

$$\Delta p_i = \rho c_a (w_{1u} - w_{2u}) \cot \beta_m \qquad (89)$$

But $\Delta p_i \cdot t \; dr$ is the force acting in the direction of dT and must be equal to the rate of change in momentum in that direction. The change in momentum is given by

$$\rho c_a t \; dr(w_{1u} - w_{2u})$$

The corresponding force is

$$dL \sin \beta_m + dD \cos \beta_m$$

Hence

$$\rho c_a (w_{1u} - w_{2u}) = \frac{1}{t \; dr} (dL \sin \beta_m + dD \cos \beta_m) \qquad (90)$$

Substituting for dL and dD in terms of their respective coefficients C_L and C_D, from equations 78 and 79, respectively, gives

$$\rho c_a (w_{1u} - w_{2u}) = \frac{1}{2} \rho w_m^2 \sin \beta_m \cdot \frac{b}{t} C_L (1 + \epsilon \cot \beta_m) \qquad (91)$$

Substituting this last expression into equation 89,

$$\Delta p_i = \frac{1}{2} \rho w_m^2 \cos \beta_m \cdot \frac{b}{t} C_L (1 + \epsilon \cot \beta_m) \qquad (92)$$

The ratio $\Delta p / \Delta p_i$ is defined as the blading efficiency and denoted by η_b. Hence from equations 86 and 92

$$\eta_b = \frac{1 - \epsilon \tan \beta_m}{1 + \epsilon \cot \beta_m} \qquad (93)$$

If equation 93 is differentiated with respect to β_m, assuming that ϵ is constant, and the result is equated to zero it is seen that the blade element has its maximum efficiency when β is close to 45°. This same result was obtained for the propeller blade element in Chapter 6, Section 7.

4B. *The Multistage Axial Compressor*

A multistage compressor is formed by combining several alternating rows of rotating and stationary blades. Since the blading efficiency has its maximum value when w_m is at 45° to the lattice axis, a stage arranged to give this result for both the stator and rotor

blades gives symmetrical velocity diagrams and is called a symmetrical stage. A multistage compressor is usually built of symmetrical stages having identical blade profiles. For such a stage $w_1 = c_2$ and $w_2 = c_1$.

The pressure rise for the stage, neglecting radial flow, is determined by the Euler theorem of Chapter 2, assuming that $u_1 = u_2 = u$. Hence, the centrifugal force term $(u_2{}^2 - u_1{}^2) = 0$ and

$$\Delta p = \tfrac{1}{2}\rho[(w_1{}^2 - w_2{}^2) + (c_2{}^2 - c_1{}^2)] \tag{94}$$

In the axial compressor the reaction effect is given by $\tfrac{1}{2}\rho(w_1{}^2 - w_2{}^2)$ and is smaller than it is for the centrifugal type. The term $\tfrac{1}{2}\rho(c_2{}^2 - c_1{}^2)$ is the kinetic energy to be transformed into pressure in the stator blades, which functions as a diffuser.

Equation 94, as shown in Part A of this chapter, can also be written in the form

$$\Delta p = \tfrac{1}{2}\rho u(c_{1u} - c_{2u}) = \tfrac{1}{2}\rho u \Delta c_u \tag{95}$$

The change in whirl Δc_u in the usual construction is much smaller than it is for the centrifugal compressor, with the result that the pressure rise per stage is lower. The whirl can be increased in any rotating machine only by increasing the deflection of the fluid passing through it. Thus, if the stator blades are curved so that the air leaves in the axial direction $(c_1 = c_{1a})$, then $c_{1u} = 0$. Further, if the rotor blades are curved, as pointed out in reference 8, so that $w_2 = w_{2a} = c_{2a}$, then the exit velocity c_2 is equal to u, since $c_2 = w_2 + u$, and $c_{2u} = u$. Then the energy transfer is u^2/g, which is the same as for a centrifugal compressor.

The factors affecting the boost per stage are the effect of the angle of attack $\alpha = \phi - \beta_m$ on the lift and drag coefficients and the

FIG. 22. Performance characteristics of a six-stage axial-flow compressor. (Reproduced from *N.A.C.A.T.M.* 1073.)

compressibility effects due to the local acoustic velocity being reached at the blade tips. If the air is deflected too greatly, losses due to flow separation, eddies, and the like are introduced.

It was pointed out in the preceding section that β_m should be close to 45°. Further, the pressure distribution along the blade should be kept uniform. Since the pressure distribution depends directly upon $u \Delta c_u$ the blading should be designed to keep this product constant along the blade length. Because u is smaller at the root than it is
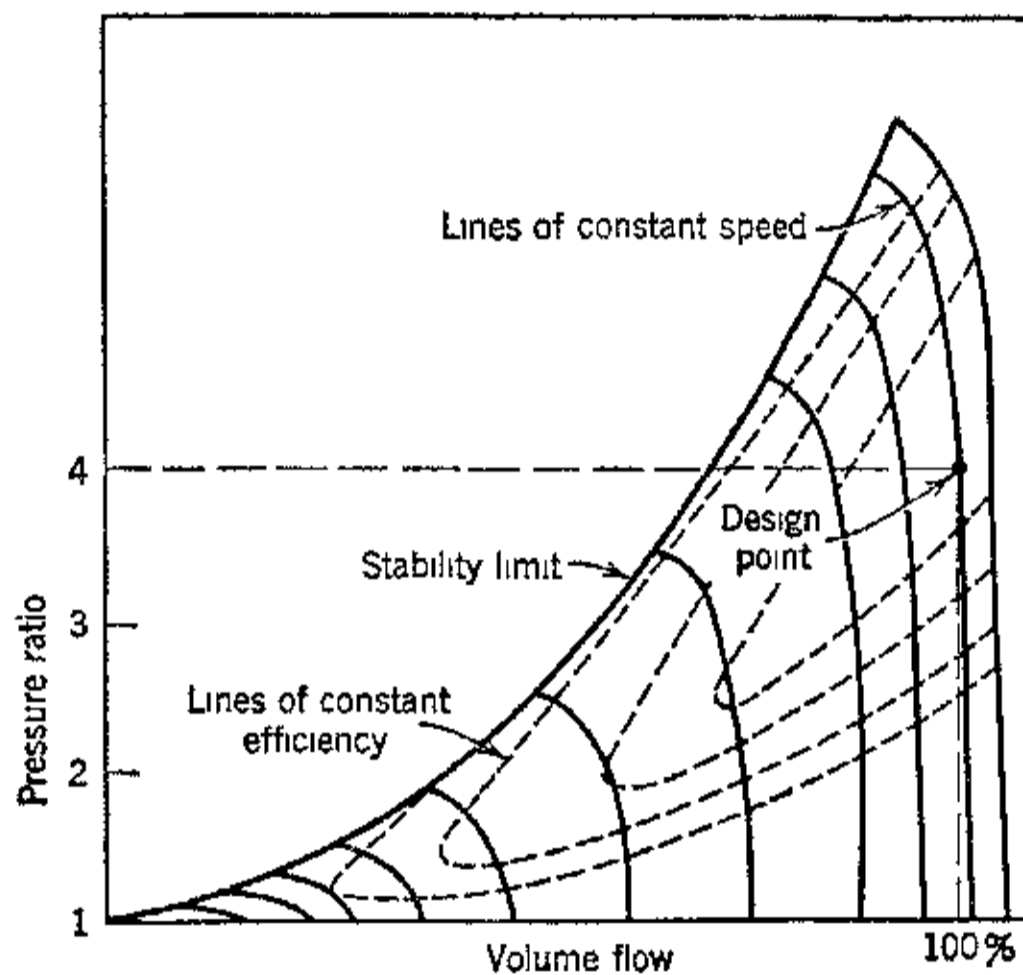
FIG. 23. Typical axial-flow-compressor performance chart. (Reproduced from J. K. Salisbury, *Mechanical Engineering*, June 1944.)

at the tip, Δc_u should be inversely proportional to the radius to each element of the blade. Since c_a is substantially constant along the blade, w_m does not make the angle $\beta_m = 45°$ at each blade point.

If the rotor speed is constant and the flow is decreased from the design value, the axial velocity c_a is reduced and the angle of attack of the air is increased. It will be recalled from Chapters 5 and 6 that increasing the angle of attack increases both the lift and drag coefficients. Increasing the angle of attack too much causes the blades to become "stalled"; the lift coefficient decreases rapidly while the the drag coefficient increases, as illustrated for an airfoil in Fig. 6·12. The stall phenomenon leads to rather peaked efficiency curves as a function of flow rate at any given speed. The same remarks are applicable to the pressure ratio delivered, since this ratio depends upon the same factors. Figure 22, taken from reference 14, presents

the performance characteristics of a six-stage axial compressor for
supercharging.   A typical axial-flow-compressor performance chart,
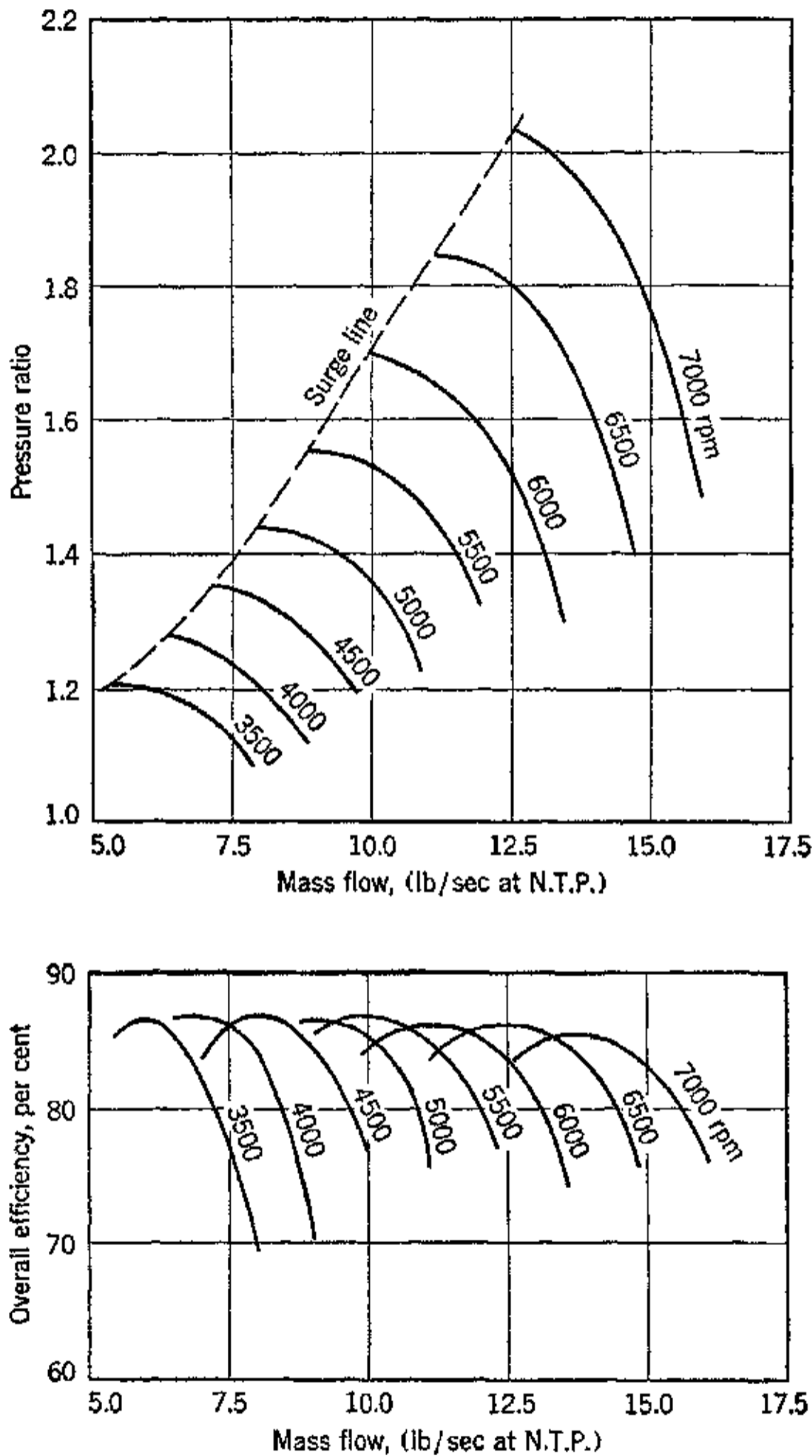
Test data for the British B-11 axial-flow compressor.

FIG. 24.   Reproduced from H. Roxbee Cox, *J. Aero. Sci.*, February 1946.

taken from reference 19, is illustrated in Fig. 23, and Fig. 24 presents
the actual performance characteristics of the British B-10 axial com-
pressor.[21]

C. The Lysholm Compressor

1C. Introduction

This compressor was invented by Alf Lysholm, Chief Engineer, Aktiebolaget, Angturbin, Sweden. Its American development is due to the Elliott Company, Jeannette, Pennsylvania, and the drawings presented here were furnished through the courtesy of that company.

The principal objective of this development was to produce an air compressor of high efficiency which is not subject to the stability limitations of either the centrifugal or axial-flow types. The material presented here is taken from references 22, 23, and 24.

2C. Description of Lysholm Compressor

Figure 25 is a sectional view through one of the 10,000-cfm Elliott-Lysholm compressors used in the Elliott gas turbine for marine propulsion. For a description of this turbine consult the references presented at the end of Chapter 7.

The geometry of the rotors is illustrated in Fig. 26. The helical lobes of the male and female rotors are so designed that their coaction compresses the air between a pair of lobes as it is transported diagonally from the inlet to the exit port. The cooperating parts do not touch but are separated by a small clearance. Each charge of air confined between a pair of lobes is separated from the preceding and succeeding charges so that different pressures exist in adjacent charges. This is the distinguishing feature of this compressor according to its inventor. It produces the type of compression obtained in a reciprocating compressor, the compression of successive trapped charges. This feature results in substantially high adiabatic efficiencies over a wide range of pressure ratios for a fixed rotation speed. The effect of speed is related mainly to its influence upon the rate of leakage through the clearances. Consequently, the volumetric efficiency of the compressor at a fixed speed decreases with increased pressure ratios, owing to the higher pressures causing leakage flow through the clearances, and increases at a fixed pressure ratio with increase in the speed of rotation. To keep the internal leakage at a minimum the mechanical clearances between the rotor profiles, the rotors, and the casing must be small.

Another factor affecting the performance is the "ramming" effect of the air entering the inlet port. In the air induction process the rotor lobes are moving apart, thereby increasing the space between them until a maximum volume for the particular design is formed by the rotor and casing surfaces. Compression then begins. The
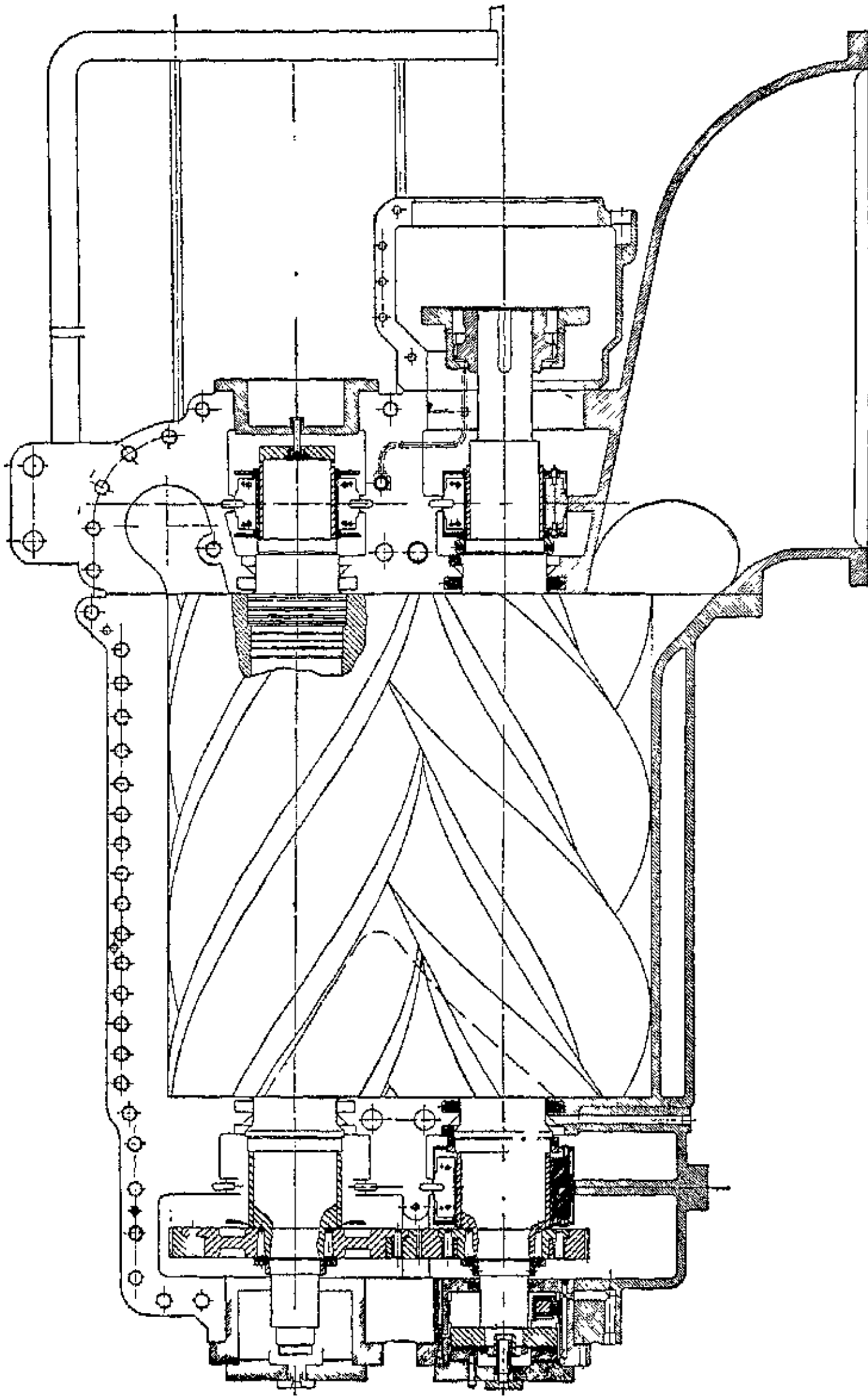
FIG 25   Cross section through a Lysholm compressor   (Courtesy, Elliott Company, Jeannette, Pa)

rotors in compressing the charge tend to push some of it out through the inlet port, but because of the high axial velocity of the air an "inertia" supercharging occurs and the air entrapped by the rotors is at a somewhat higher pressure than the inlet pressure. This ram-
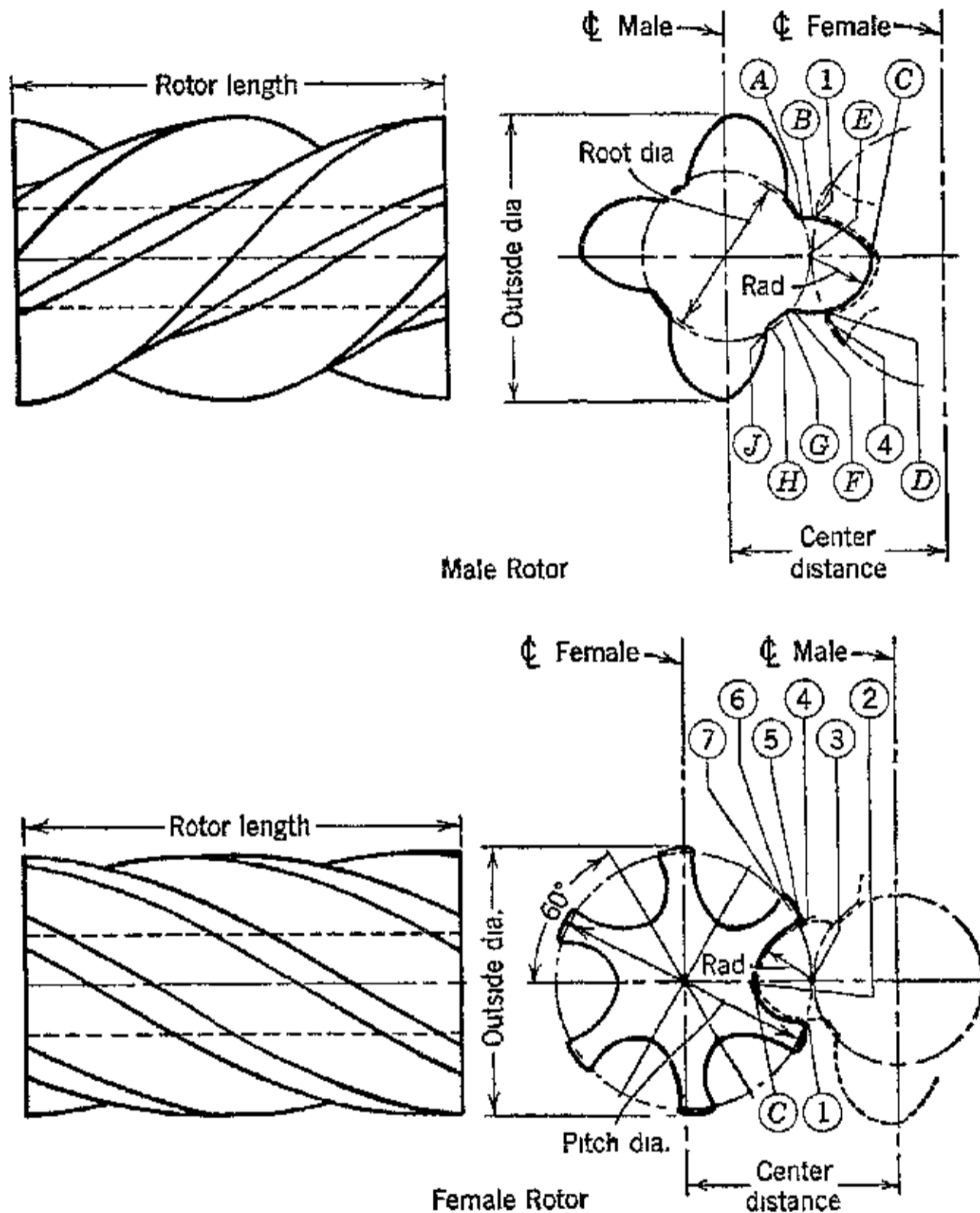
FIG. 26.   Male and female rotor lobe forms of a Lysholm compressor   (Courtesy, Elliott Company, Jeannette, Pa)

ming effect is influential in raising the volumetric efficiency of the compressor. The inlet port must be designed correctly to take advantage of this phenomenon.

In addition to the losses due to leakage, fluid friction, and induction there are the losses due to bearing, gear, and seal friction. These losses are largely a function of the speed of operation.

The combined effects of the fluid losses and the mechanical losses affect the performance characteristics of the compressor. The fluid-

leakage losses increase in their absolute value with the pressure ratio, but on a percentage basis they decrease with the speed. The mechan-
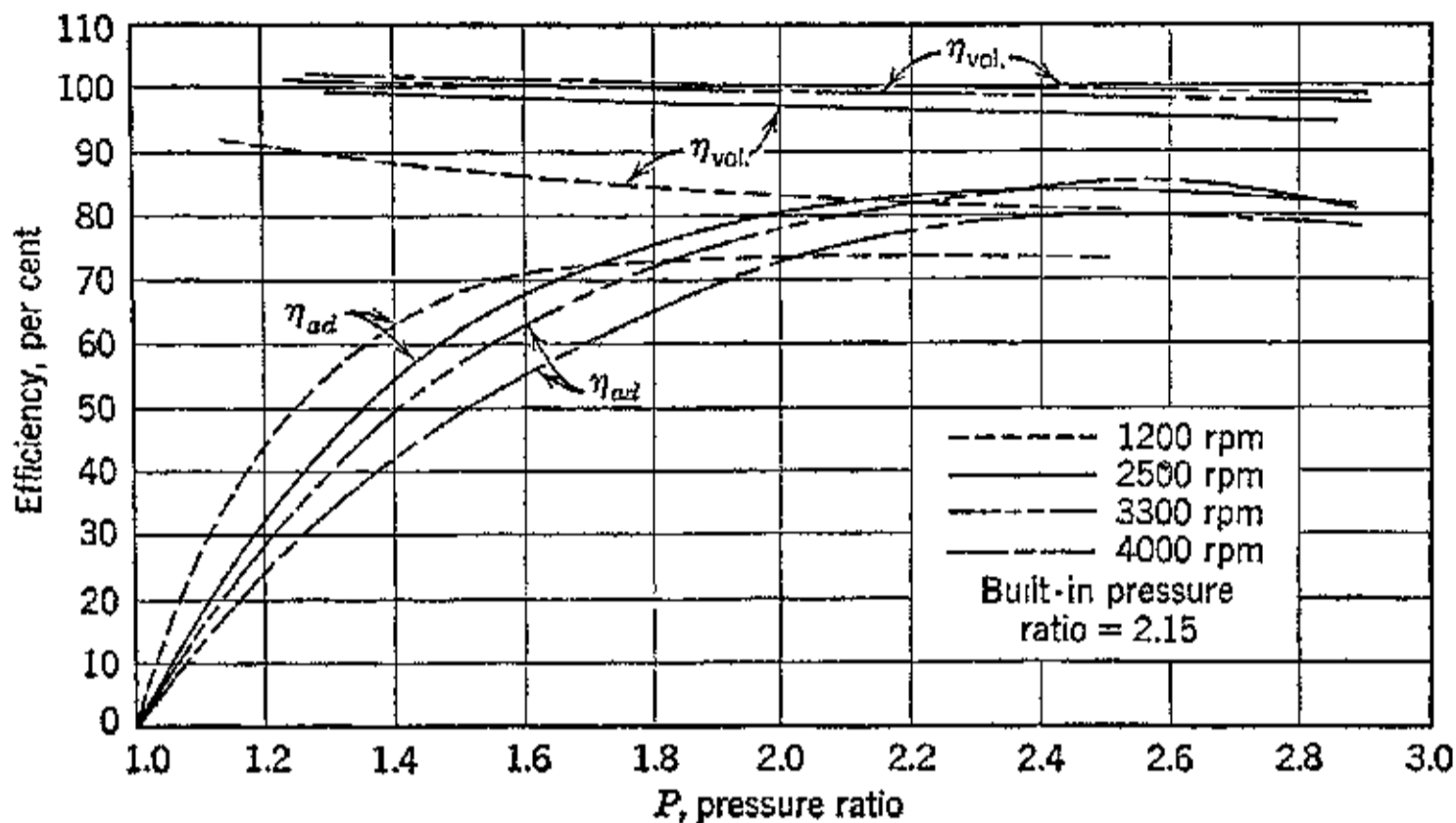
Fig. 27. Efficiency vs. pressure ratio for a Lysholm compressor with 2.15 built-in pressure ratio. (Courtesy, Elliott Company, Jeannette, Pa.)

ical and fluid-friction losses, however, increase with the speed and on a percentage basis decrease with increasing pressure ratio. The resultant effect of the losses is to give the overlapping performance
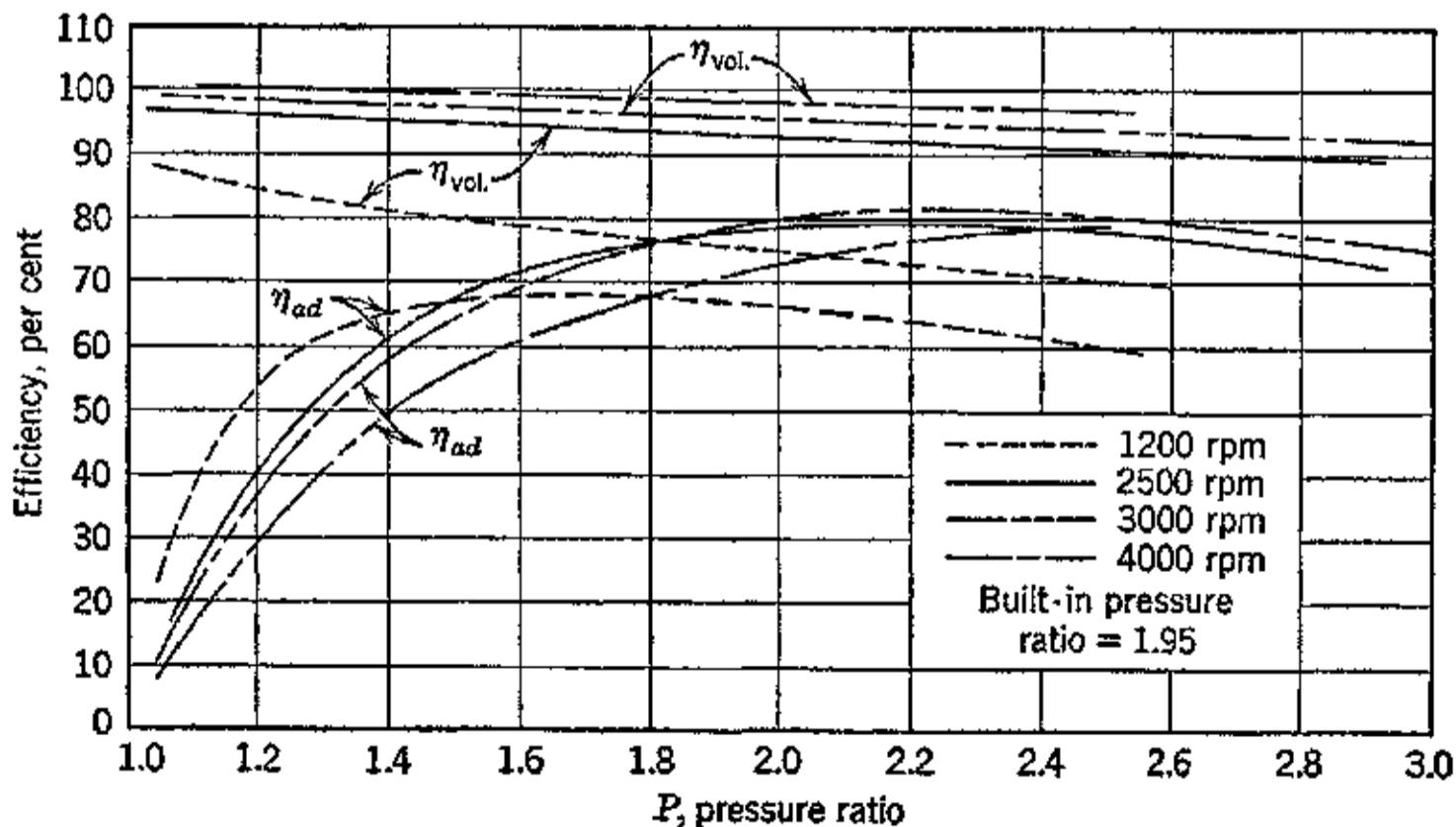
Fig. 28. Efficiency vs. pressure ratio for a Lysholm compressor with 1.95 built-in pressure ratio. (Courtesy, Elliott Company, Jeannette, Pa.)

characteristics illustrated in Figs. 27 and 28. These figures are for two compressors of the same capacity but having "built-in" pressure ratios of 2.15 and 1.95 respectively.

REFERENCES

1. D. F. WARNER and E. L. AUYER, "Contemporary Jet-Propulsion Gas Turbines for Aircraft," *Mech. Eng.*, November, 1945, pp. 707–714.

2. P. R. SIDLER, *Trans. A.S.M.E.*, July, 1944, p. 367.

3. E. W. F. FELLER, *Air Compressors*, McGraw-Hill Book Co., New York, 1944.

4. S. A. MOSS, C. W. SMITH, and W. R. FOOTE, 'Energy Transfer between a Fluid and a Rotor for Pump and Turbine Machinery," *Trans. A.S.M.E.* August, 1942, pp. 567–597.

5. R. EKSERGIAN, *Trans. A.S.M.E.*, August 1942, p. 590.

6. ECK-KEARTON, *Turbo-gebläse und Kompressoren*, Julius Springer, Berlin.

7. K. CAMPBELL and J. E. TALBERT, "Some Advantages and Limitations of Centrifugal and Axial Aircraft Compressors," *J.S.A.E.*, October, 1945, pp. 607–620.

8. W. J. KING, "Axial vs. Centrifugal Superchargers," *J.S.A.E.*, December, 1945, pp. 736–741.

9. A. H. CHURCH, *Centrifugal Pumps and Blowers*, John Wiley & Sons, New York, 1944.

10. A. STODOLA (L. LOEWENSTEIN), *Steam and Gas Turbines*, McGraw-Hill Book Co., New York, Vol. 2, 1927.

11. B. E. DEL MAR, "Presentation of Centrifugal-Compressor Performance in Terms of Nondimensional Relationships," *Trans. A.S.M.E.*, August, 1936, pp. 483–490.

12. R. S. HALL, "Aircraft Gas Turbines with Centrifugal Compressors," S.A.E. National Aeronautic Meeting, New York, April 3–5, 1946.

13. W. R. HAWTHORNE, "Factors Affecting the Design of Jet Turbines," S.A.E. Annual Meeting, Detroit, Mich., Jan. 7–11, 1946.

14. A. BETZ, "Axial Superchargers," *N.A.C.A. Tech. Memo* 1073, 1944.

15. E. STRUVE, "Theoretical Determination of Axial Fan Performance," *N.A.C.A. Tech. Memo* 1042, 1943.

16. P. RUDEN, "Investigation of Single-Stage Axial Fans," *N.A.C.A. Tech. Memo* 1062, 1944.

17. A. BETZ, "Diagrams for Calculation of Airfoil Lattices," *N.A.C.A. Tech. Memo* 1022, 1942.

18. C. KELLER and L. S. MARKS, *The Theory and Performance of Axial Flow Fans*, McGraw-Hill Book Co., New York, 1937.

19. J. K. SALISBURY, "The Basic Gas Turbine Plant and Some of Its Variants," *Mech. Eng.*, June, 1944, pp. 373–383.

20. J. R. WESKE, "Investigation of Blade Characteristics," *Trans. A.S.M.E.*, July, 1944, pp. 413–420.

21. H. ROXBEE COX, "British Aircraft Gas Turbines," J. *Aero. Sci.*, February, 1946, pp. 53–87.

22. A. LYSHOLM, R. B. SMITH, and W. A. WILSON, "The Elliott-Lysholm Supercharger," S.A.E. Annual Meeting, Detroit, Mich., Jan. 11–15, 1943.

23. W. A. WILSON and J. W. CROCKER, "Fundamentals of the Elliott Lysholm Compressor," A.S.M.E. Annual Meeting, New York, Nov. 26–29, 1945.

24. A. LYSHOLM, "A New Rotary Compressor," *Inst. Mech. Eng. J. and Proc.*, Vol. 150, No. 1, November, 1943, p. 11.

TURBINE CHARACTERISTICS

1. Introduction

The turbine is a major component common to the gas turbine-propeller engine, discussed in Chapter 7, and to the thermal jet engine, discussed in Chapter 8. In the gas turbine-propeller engine the turbine must develop the shaft power for driving the air compressor, propeller, and the auxiliaries. In the thermal jet engine, however, it is required to furnish only sufficient power to drive the air compressor and the auxiliaries. It should be noted that, in general, gas turbine-propeller engines are designed to deliver auxiliary jet thrust from the exhaust gases in addition to the propeller thrust, the usual proportions being 80 per cent propeller thrust and 20 per cent auxiliary jet thrust.

The general characteristics of turbines are well understood, and a wealth of information concerning them has been gathered during the past decades. Particularly helpful to the development of turbines which operate with highly heated gases are the experiences gathered in the development of turbo-superchargers and also steam turbines for high-pressure and high-temperature applications. In many respects the turbine for gas turbine-propeller engines or turbojet engines is quite similar to the conventional steam turbine, the major difference being in the metallurgy, the means provided for cooling the bearings and highly stressed parts, and in the constructional features to safeguard against thermal distortion. The basic theory underlying their design and the evaluation of their operating characteristics is identical with that for steam turbines and is discussed in detail in the works of A. Stodola[16] and G. Flügel.[11] The major difference is that the gas laws can be applied, with account taken of the variation in specific heat, in computing the enthalpy changes. Furthermore, the problem of moisture condensation in the low-pressure stages of the turbine is absent.

2. Principal Types of Turbines

As explained in Chapter 2, Section 8, turbines may be segregated into two broad classes: axial-flow and radial-flow machines. In this country, except for hydraulic machinery, which does not enter into the discussions, axial-flow turbines are used exclusively. The discussions of this chapter are, therefore, restricted to that class of turbine.

Axial-flow turbines are segregated into two basic types: *impulse turbines* and *reaction turbines*. In a pure impulse turbine the total isentropic heat drop experienced by the fluid flowing through a stage, and also the stage pressure drop, occurs in one or more stationary nozzles that discharge into the blades attached to the rotor. A portion of the thermal energy of the fluid is transformed into kinetic energy by virtue of its expansion in the nozzles. Further, the fluid is deflected as it flows through the blades, and the accompanying change in momentum produces the force, termed the impulse force, for rotating the turbine wheel (rotor). Theoretically, no change in pressure is experienced by the fluid as it flows through the blades, the pressure at the exit section of a blade passage being equal to that at the inlet section. Pure impulse stages, therefore, are also called *equal-pressure stages;* a stage consists of one set of stationary nozzles and one set of coacting moving blades, or it is the space between two planes perpendicular to the shaft and located at the entrance sections of two consecutive rows of nozzles. The selection of the pressure drop for the nozzle is determined by the allowable peripheral velocity for the moving blades. An impulse stage consisting of one set of nozzles, or a single nozzle, discharging into a single moving row of blades is called a *Rateau stage*. As will be seen later, the ratio of the peripheral or tangential speed of the blades to the spouting velocity of the jet, called the *velocity ratio*, has a decisive influence on the efficiency of the turbine.

It is frequently necessary to utilize such a large pressure drop in the stationary nozzles of an impulse turbine that the tangential velocity of the blades would exceed the permissible value if operated at the velocity ratio for maximum efficiency with a single row of blades. In such cases a *double-velocity impulse stage*, called a *Curtis stage*, is used. The Curtis stage consists of a single row of stationary nozzles followed by a wheel equipped with two rows of blades. The blades are so spaced that an intermediate stationary row of blades can be inserted between them. For a Curtis stage to operate as a pure impulse machine, there can be no change in the pressure of the fluid as it flows through the blade rows. The stationary intermediate

blades serve merely as a guide passage for deflecting the fluid into the second row of moving blades. In practice both the Rateau and Curtis stages are designed to operate with a slight degree of reaction because a slight reaction benefits the efficiency of the blades. Impulse turbines operate with either partial or full admission depending upon the weight of fluid flowing through the turbine and the required flow area.

The *reaction stage* differs from the Rateau and the Curtis stage in that the enthalpy drop per stage is divided between the stationary row of blades and the moving ones. Consequently, the fluid flowing through the moving blades is not only deflected, as in impulse turbines, but in addition the fluid is expanded. The conversion of thermal energy into mechanical energy in the moving blade row causes the moving blade row to experience a reaction force, because of the increased velocity of the fluid, in addition to the impulse force resulting from deflecting it. The degree of reaction, denoted by r, is defined by the ratio

$$ r = \frac{H_r}{H_s + H_r} = \frac{H_r}{H} \tag{1} $$

where H_s = isentropic heat drop for stationary blade row, Btu/lb.

H_r = isentropic heat drop for rotating blade row, Btu/lb.

$H = H_s + H_r$ = available energy for the stage, Btu/lb.

If the blades of the stationary and moving rows have identical cross sections, called the blade section, then the expansion process, in the ideal case at least, is the same in each row of blades. A reaction stage of this type is said to have symmetrical blading and to operate with 50 per cent reaction ($r = 0.5$). In such a turbine stage the enthalpy changes in each row are equal. Consequently, the velocity triangles for an ideal 50 per cent reaction stage are similar for the stationary and moving blade rows.

Reaction stages operate with full admission. Consequently, the rotors of small power output reaction turbines have to be of small diameter in order to obtain reasonable blade heights for the low rates of fluid flow involved. In general, the total enthalpy drop for a reaction stage is much smaller than it is for an impulse stage of like output operating with partial admission. Because of the small enthalpy drop in each row of blades, the reaction turbine blade rows operate with less than the critical pressure ratio. A critical pressure drop may occur, however, in the low-pressure stages of reaction steam turbines.

The manner in which the pressure of the working fluid varies as it flows through a Rateau, a Curtis, and a reaction stage is illustrated schematically in Fig. 1.

The turbines for turbojet engines have been mainly single-stage
Rateau machines because of their lower weight. For turboprop
engines and stationary or for marine plants either multistage reaction
turbines [15] or multistage impulse machines and their combination are
applicable.

(a) Pressure distribution Rateau stage

(b) Curtis two-row stage
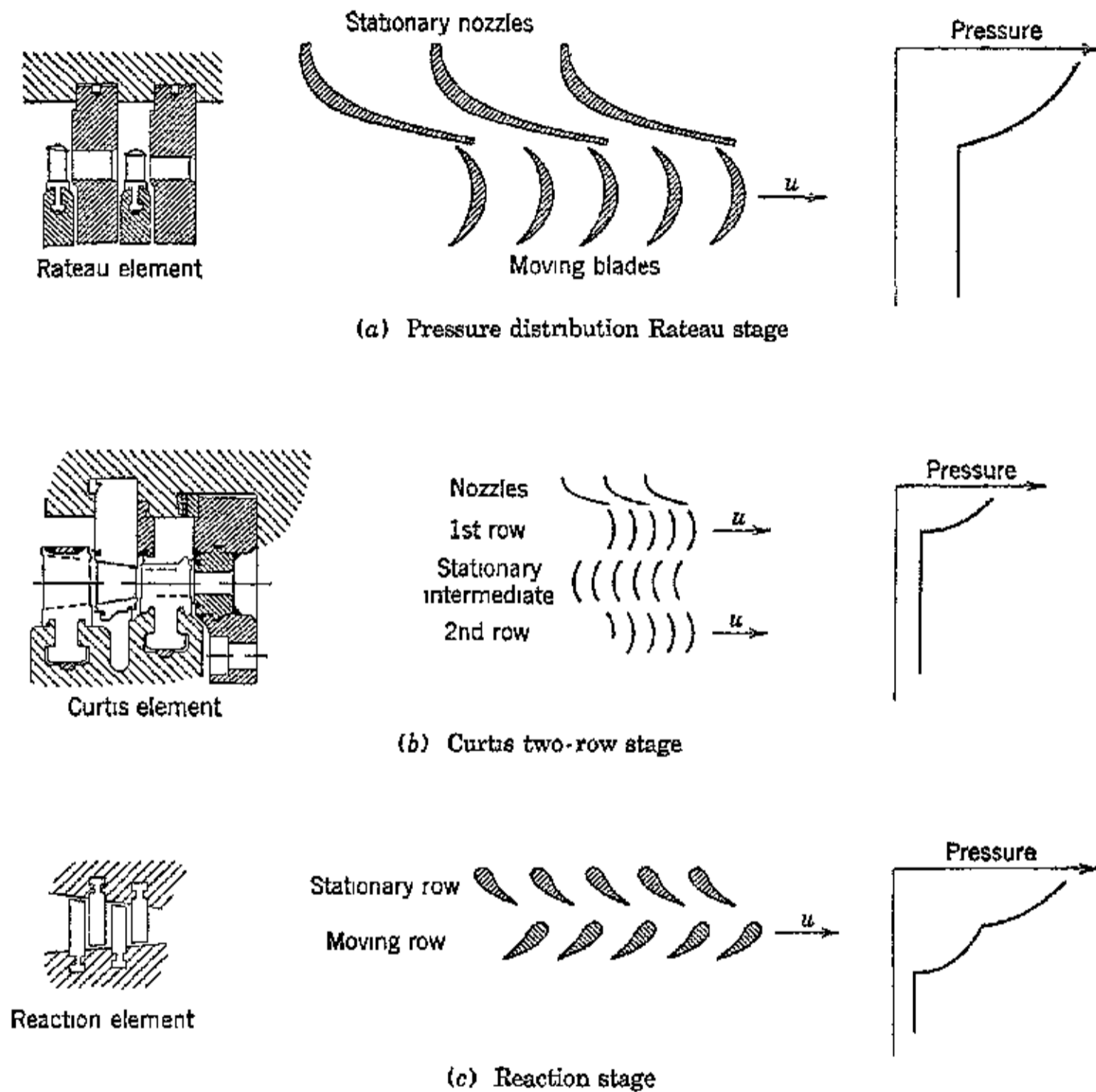
(c) Reaction stage

FIG. 1.   Blade arrangement and pressure changes in Rateau, Curtis, and reaction
stages.

3. Basic Requirements

The basic requirements for the turbine are the same for either type
of engine. Although the remarks which follow apply specifically to
the turbine for a turbojet engine, it should be understood that they
apply equally well to the turbines for turboprop engines. The prin-
cipal requirements are: (a) light weight; (b) small frontal area;
(c) high efficiency; (d) ability to operate for sustained periods at
high temperature; and (e) reliability and serviceability.

Light weight is secured by operating the turbine rotor with the highest permissible rim speed, using small-diameter rotors. Since the stresses in a given turbine disk increase approximately as the square of the rim speed, the maximum rim speed is limited by strength considerations, which are governed by the stress characteristics of the disk and blade materials at the operating temperature. Although low rim speeds are desirable from a stress standpoint, there is a lower limit to the rim speed imposed by the dictates of high efficiency which, in general, improves with rim speed. According to reference 3 the lower limit of the rim speed in feet per second, which is dictated by flow conditions, must be larger than $100\sqrt{\Delta T/4.5}$, where ΔT is the temperature drop through the turbine in degrees Fahrenheit. Since the turbine efficiency improves, in general, with increasing rim speed and permits using lower bucket temperatures for the same power output, the choice of rim speed is a compromise between allowable stress and turbine efficiency. The rim speeds of most turbojet turbines range from 820 to 1000 fps.

The general design of the turbine passages is based primarily on considerations which are mainly fluid dynamical. The flow conditions must be so designed that, for the required thrust output and mass flow of gas, the acoustic velocity (unity Mach number) is not reached at the outlet from the buckets (or in the ducting downstream leading the exhaust gases away from the turbine, or in the exhaust nozzle), for, as pointed out in Chapter 3, choking of the flow occurs if the Mach number in these flow passages attains the value unity. The critical Mach number is based on the axial velocity of the gas in the exit annulus from the turbine.[3] The possibility of attaining unity Mach number in the outlet from the turbine buckets is a consideration to be investigated in Rateau stage turbines, for the reasons presented in Section 2.

Disk and rim failures in turbojet turbines did occur in the early development stages of this propulsion engine. They have now been overcome by the application of such methods as improved gas seals, the incorporation of methods for cooling the disk, and improved metallurgy. As pointed out by reference 4, one of the major factors has been a better understanding of the metallurgical problem. Research has shown that if the disk operates with high temperatures or steep temperature gradients it is likely to develop plastic deformation. If this occurs the stress distribution can no longer be based on conventional elastic theory, and when the disk cools off after operating it is subjected to large residual stresses. As a consequence of the residual stresses there is a change in the natural vibration frequencies,

which are functions of the stress conditions.[4] Furthermore, successive periods of plastic strain, cooling, and then heating again modify the stress-strain characteristics of the disk material and may lead to changes in its crystal structure. By applying the remedies mentioned above these difficulties can be avoided.

In turbojet engines employing a centrifugal compressor, the turbine imposes no problem in the securing of small frontal area. The frontal area of the turbine is much smaller than that of the compressor and combustion chamber assembly and has little influence upon the overall size in that type of application. Where the turbine drives an axial-flow compressor the frontal areas of the turbine and compressor become more nearly equal, as can be seen from the published illustrations of the German BMW 003 and the Westinghouse 19-B Yankee Turbojet.[7, 8]

The turbine blades may be either solid or hollow, the type of construction being influenced by the material selected for their manufacture. The hollow blade offers the advantages of being adapted to cooling by flowing cold air through its interior and of reducing weight.[7] The walls of the blade are usually tapered so that the outer extremity, where the stress vanishes, is quite thin. As pointed out in reference 6 the greatest benefit derived from cooling is at the root of the blade where the stresses are high; the outer edge, because of its small stress, may be allowed to run hot. In most designs the blades are twisted to maintain a favorable angle of attack for the fluid throughout its length (see Chapter 6). In the early development of the turbojet, blading failures did occur, but according to reference 4, which discusses British experience, they are now a rarity. The difficulties were overcome by increased accuracy in the manufacture of the blades, avoidance of small radii at root junctions, better analysis of vibration problems, and improved metallurgy.

Since improving turbine efficiency and output are related to ability to operate with higher temperatures, developments aimed at raising the permissible operating temperature of the turbine are of great importance. Some of these have been mentioned in Chapter 7. One promising approach is the application of ceramic coatings on the turbine blades to take the impact of the hot gases. The problem here is to develop a ceramic coating of high melting point which will bond to the metal and will have a coefficient of expansion close enough to that of the metal to prevent the coating from cracking or flaking off. Another approach proposes to let cooling liquid flow through a passage in the root of the blades.[10]

Tables 10·1 and 10·2, taken from reference 9, present data on

TABLE 10·1

DESIGN DATA OF BMW 003 SERIES TURBOJETS

Model	Static Thrust lb	Specific Fuel Consumption lb/lb-hr	Engine Speed rpm	Weight lb	Air Flow lb/sec	Pressure Ratio	Stages of Compression	Compressor Tip Speed ft/sec	Turbine Stages	Turbine Tip Speed ft/sec
003A0	1,000 *	2.2 *		1,650						
003A1	1,764	1.47	9,500	1,345						
003A2	1,764	1.47	9,500	1,345	41.9	3.09	7	896	1	1,024
003B1	1,980	1.40	9,500	1,650			7		1	
003C	1,984	1.30	9,800	1,345 *	44.1	3.42	7	935	1	1,056
003D	2,646	1.10	10,000	1,366 *	55.1	4.91	8	961	2	1,089
003E1										
003E2										
003R	1,764	1.47	9,500	1,576						

* Information doubtful.

German practice in the development of turbojet engines. For detailed information on British practice the reader is referred to references 3, 4, and 5.

TABLE 10·2

COMPARISON OF BMW 003 AND JUMO 004 PRODUCTION TURBOJETS

Model		BMW 109-003A-2	JUMO 109-004B-4
Static thrust	lb	1764	1984
Specific fuel consumption	lb/lb-hr	1.47	1.48
Turbine speed	rpm	9500	8700
Weight	lb	1345	1543
Specific weight	lb/lb thrust	0.76	0.78
Length	in.	143	163
Diameter	in.	27.2	28.7
Air flow	lb/sec	41.9	46.3
Compressor tip diameter	in.	21.65	21.46 (stage 1)
Compressor diameter ratio		0.725	0.645
No. compression stages		7	8
Turbine tip diameter	in.	24.70	27.48
Turbine diameter ratio		0.71	0.68
Burner temperature	°F	1382	1390
No. of burners		16	6
Combustion chambers		1 annular	6 individual

4. Notation

a = area of blade cross section in.^{2}

a = acoustic velocity, fps.

A = flow area in general, or flow area denoted by subscript, ft^2.

b = width of blade, in.

c = absolute velocity, fps.

$c_0 = \sqrt{2gJH}$ = isentropic velocity, fps.

c_1 = absolute velocity of jet leaving nozzles or stationary blades, fps.

c_{1u} = tangential component of c_1, fps.

c_2 = absolute velocity of fluid leaving moving blades, fps.

c_{2u} = tangential component of c_2, fps.

c_{2v} = carry-over velocity from preceding stage, fps.

$\Delta c_u = c_{1u} - c_{2u}$ = whirl velocity, fps.

D = diameter of wheel, units specified in text.

D_p = pitch diameter, units specified in text.

e_0 = carry-over function corresponding to design flow, G_0.

e_1 = carry-over function corresponding to new flow G_1.

e = admission fraction or carry-over function as specified in text.

f_c = centrifugal force acting on a blade, lb.

F = force, lb.

F_u = force acting in direction of tangential velocity u, lb.

g = acceleration due to gravity.

G = weight rate of flow, lb/sec.

G_0 = design weight rate of flow, lb/sec.

G_1 = weight rate of flow for a condition other than the design value, lb/sec.

h = enthalpy of fluid, Btu/lb.

h_0 = enthalpy of fluid at entrance to a row of stationary blades or nozzles, Btu/lb.

h_1 = enthalpy at the entrance to a moving row of blades, Btu/lb.

h_2 = enthalpy at the exit from a moving row of blades, Btu/lb.

Δh = enthalpy change with friction, Btu/lb.

$\Delta h'$ = isentropic enthalpy change, Btu/lb.

H = available energy for a stage or a complete turbine as specified in text, Btu/lb.

H_r = available energy for a moving row of blades, Btu/lb.

H_s = available energy for a stationary row of blades (or nozzles), Btu/lb.

H_w = internal output of a stage or turbine, the work done on the rotor periphery, Btu/lb.

H' = total energy supplied stage or turbine, Btu/lb.

J = mechanical equivalent of heat = 778 ft-lb/Btu.

k = c_p/c_v = specific heat ratio.

l = length of blade, in.

l_1 = length of blade at entrance, in.

l_2 = length of blade at exit, in.

L = energy transfer or external work, ft-lb/lb.

L_t = energy transferred from a fluid to a rotor, ft-lb/lb.

L_r = rotation loss, ft-lb/lb or kw as specified in text.

$\mathbf{M}$ = momentum, slug-ft/sec.

M = mass, slug.

m = G/g = mass rate of flow, slug/sec.

n = exponent in pv^n = constant, or rpm, as specified in text.

p = pressure, psfa.

p_0 = pressure at entrance to nozzles or stationary blades, psfa.

p_1 = pressure at exit from nozzles or stationary blades, psfa.

p_2 = pressure at exit from moving blades, psf.

p_{2v} = exit pressure of preceding stage.

P = power denoted by subscript, ft-lb/sec.

P_z = power developed at periphery of rotor, ft-lb/sec.

P_s = stage power output, ft-lb/sec.

$r = H_r/H$ = degree of reaction.

$\mathcal{R}$ = energy expended in overcoming friction, ft-lb/lb.

R = gas constant or resultant force in lb as specified in text.

R_1 = radius to entrance of flow passage, ft.

R_2 = radius to exit from flow passage, ft.

$\mathcal{R}_s$ = friction and thermal losses in stationary blades or nozzles, ft-lb/lb.

$\mathcal{R}_r$ = friction and thermal losses in moving blades, ft-lb/lb.

u = tangential velocity, fps.

$v = 1/\gamma$ = specific volume, ft³/lb.

w = relative velocity of fluid with respect to moving blades, fps.

z = number of blade passages.

Greek Symbols

α = angle between the direction of the absolute velocity of the fluid c and the direction of the peripheral velocity u.

β = angle between the direction of the relative velocity of the fluid w and the peripheral velocity u.

ω = angular velocity.

$\nu_0 = u/c_0$ = isentropic velocity ratio.

$\nu = u/c$ = velocity ratio.

φ_1 = velocity coefficient for stationary blades or nozzles.

φ_{2v} = carry-over coefficient for stationary blades or nozzles.

ψ_1 = carry-over coefficient for moving blades.

ψ_2 = velocity coefficient for moving blades.

$\psi = \psi_1\psi_2$ = blading coefficient for moving blades.

$\epsilon = \nu \cos \alpha_1 - \nu^2$ = diagram factor.

λ = loss coefficient for residual energy, or gauging of reaction blades, as specified in text.

λ_v = loss coefficient for carry-over energy.

$\rho = \gamma/g$ = density.

σ = stress.

η = efficiency.

γ = specific weight

Subscripts

0   at entrance to nozzle, or isentropic, as specified in text.

1   at entrance to flow passage.

2   at exit from flow passage.

2v   from preceding stage.

> a axial.
> b blading.
> i internal (at wheel periphery) or ideal as indicated in text.
> n nozzle.
> nb nozzle and blading.
> s stage.
> t turbine.
> u peripheral.

Superscript

Prime denotes isentropic process.

A general thermodynamic treatment can be applied to both impulse and reaction stages by considering an intermediate stage of a multistage reaction turbine; the intermediate stage typifies the general case of a turbine stage. In such a stage the stationary blade row is the counterpart of the nozzle of an impulse stage.

5. Energy Transfer Equations for Turbine

Figure 2 represents the flow passage formed by an arbitrary selected pair of moving blades attached to a turbine rotor. These may be either impulse or reaction blades. The fluid enters the passage with the absolute velocity c_1 and after being deflected by the blades leaves with the absolute velocity c_2. The pressure of the fluid and also its specific weight may change as a consequence of the flow through the passage, which is accompanied by a transfer of energy from the fluid to the rotor. The relationships derived in Chapter 2, Section 8, for the transfer of energy from a fluid to a rotor are applicable if it is assumed that (1) the flow is steady and is uniform at the entrance and exit sections of the passage (see Chapter 3); (2) the rotor to which the blades are attached rotates with a uniform angular velocity; (3) the losses due to fluid by-passing the blading and to friction of the fluid on the sides of the rotor may be neglected.

FIG. 2. Conditions at entrance and exit for a moving blade passage.

The significance of the first two assumptions has been pointed out in Chapter 2 and will not be repeated here.   In axial-flow turbines the inlet and exit reference stations are assumed to lie on the pitch circle for the rotor.

The performance of a turbine stage is due to the interaction of the fluid and the blade surfaces. As pointed out in reference 15 it is related to the stress in the fluid working on these surfaces. From Chapters 5 and 6 it is apparent that each blade acts as an airfoil immersed in a flowing fluid, with the consequence that it experiences lift and drag forces. The drag will consist of the pressure drag and the skin friction due to shearing stresses in the boundary layer. The torque component of the resultant of the lift and drag forces, as in the blade element of an axial-flow compressor, contributes to the peripheral force for rotating the turbine wheel. Owing to the interference effects of neighboring blades and the radial flow component it is difficult to analyze turbine performance by the application of airfoil theory. Consequently the momentum theory discussed in Chapter 2 is most generally used in obtaining the turbine characteristics.

In an actual blade passage the velocity and pressure distributions are not uniform and are usually different from those existing over the entrance and exit sections.[12] Because of the complex flow conditions within the passage the average relative velocity of the fluid leaving the passage generally deviates in its direction from that corresponding to the geometric blade angle. The departure from the geometric blade angle, termed *slip*, is aggravated as the number of blades is decreased. In theory, if the rotor is equipped with an infinite number of blades of infinitesimal thickness the slip would be zero and the theory exact.[14]

The disk friction and blade windage losses, the losses resulting from fluid by-passing the blade passage, and the gland leakage losses can be

Entrance velocity diagram   Exit velocity diagram

FIG. 3.   Entrance and exit velocity diagrams for a moving blade passage of an axial-flow turbine.

taken into consideration by properly modifying the final equations for the power developed by the rotor. The equations derived in this chapter are, therefore, applicable to the fluid which actually flows through the blade passages.

Figure 3 presents the general velocity diagrams for a fluid entering and leaving a moving blade passage. The angle β_1 is that between
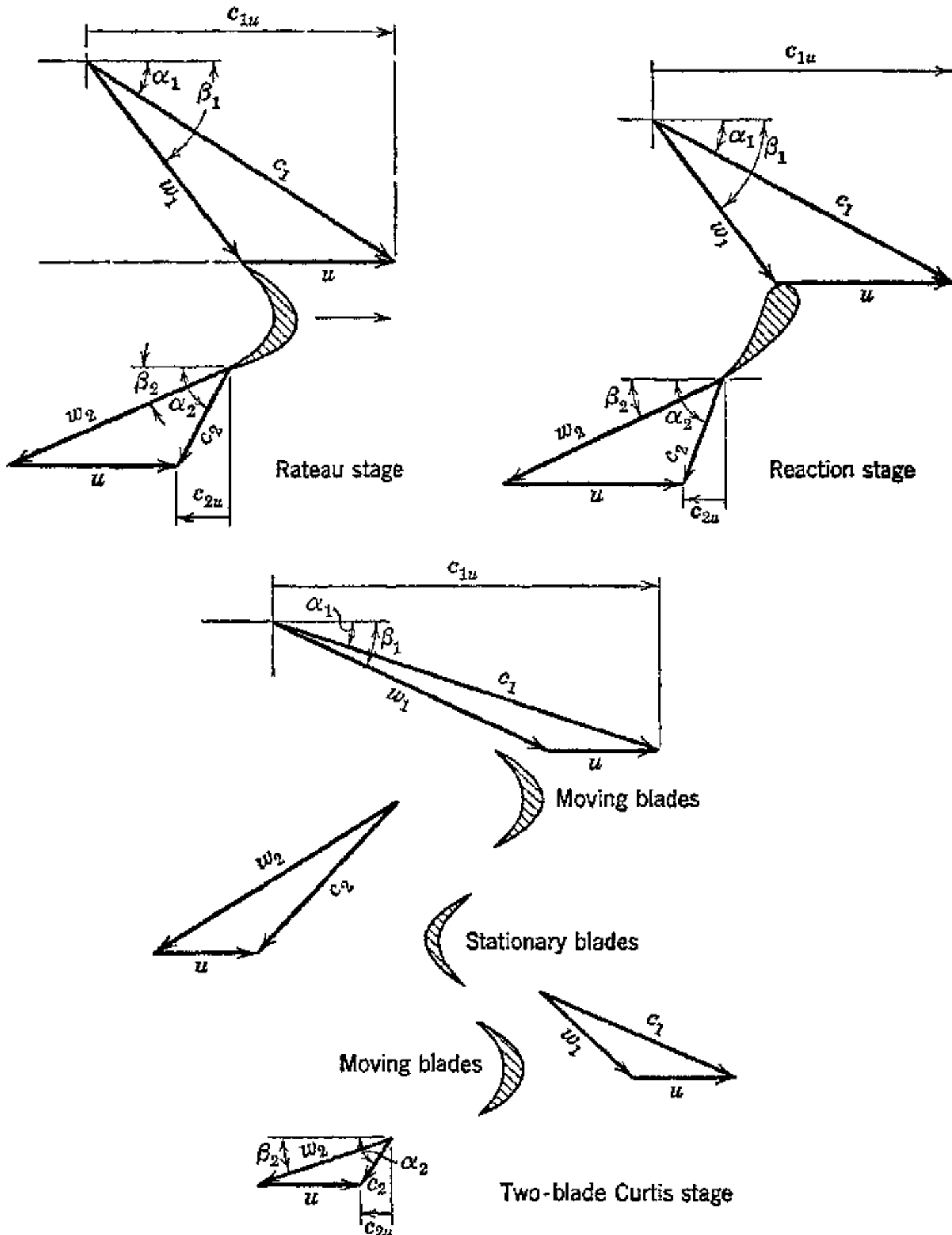
FIG. 4. Velocity diagrams for impulse and reaction stages.

the relative velocity w_1 and peripheral velocity u. Similarly the angle β_2 is that between the relative velocity w_2 and the tangential velocity. As pointed out in Chapter 2, Section 8, these angles are not in a strict sense the geometric angles of the blading but may be

regarded as being the blade angles required to give the fluid shockless entrance and the minimum exit loss. The velocity diagrams for the Rateau, Curtis, and reaction stages are illustrated in Fig. 4.

The relationships between the vectors of the velocity diagrams have been developed in Chapter 2, Section 8.

Since the exit whirl is less than the entrance whirl, the torque exerted on the rotor per pound of fluid per second is

$$\Phi_t = \frac{1}{g}(R_1 c_{1u} - R_2 c_{2u}) \tag{2}$$

and the energy transfer is given by

$$L_t = \frac{1}{2g}[(c_1{}^2 - c_2{}^2) + (u_1{}^2 - u_2{}^2) + (w_2{}^2 - w_1{}^2)] \quad \text{ft-lb/lb} \tag{3a}$$

Equation 3a can be expressed in terms of the angles α_1 and β_2, thus

$$L_t = \frac{1}{g}[u_1 c_1 \cos \alpha_1 - u_2{}^2 + u_2 w_2 \cos \beta_2] \quad \text{ft-lb/lb} \tag{3b}$$

For an axial-flow machine, it can be assumed that the fluid leaves and enters at the same radius, $u = u_1 = u_2$ and $R = R_1 = R_2$, so that the torque and energy transfer equations per pound of fluid become

$$\Phi_t = \frac{R}{g}(c_{1u} - c_{2u}) = \frac{R}{g}\Delta c_u \tag{4}$$

and

$$L_t = \frac{1}{2g}[(c_1{}^2 - c_2{}^2) + (w_2{}^2 - w_1{}^2)] = \frac{u}{g}\Delta c_u \tag{5}$$

where $\Delta c_u = c_{1u} - c_{2u}$. In terms of the angles α_1, β_1, and β_2

$$L_t = \frac{u}{g}(c_1 \cos \alpha_1 + w_2 \cos \beta_2 - u) = \frac{u}{g}(w_1 \cos \beta_1 + w_2 \cos \beta_2) \tag{6}$$

It is seen from equation 6 that to obtain the maximum energy transfer the exit velocity c_2 should be as small as possible, unless the kinetic energy associated with it can be used effectively in the next stage of the turbine. When c_2 is the absolute exit velocity for the last stage of a multistage machine or for a single-stage machine, its equivalent in kinetic energy is termed the *leaving loss*.

It is apparent from equation 6 that the nozzle angle α_1 should be as small as possible to obtain the greatest energy transfer.

6. Power Output

If the fluid flows through the blade passages of the turbine rotor at the rate of G lb/sec, the power developed at the periphery of the turbine wheel is given by

$$P_i = \frac{G}{g} u(c_{1u} - c_{2u}) = \frac{G}{g} u \, \Delta c_u \qquad (7)$$

The power output denoted by P_i is that done on the blading of the rotor and may be termed the *internal power output.* The *stage output* is less than this power because not all the energy transferred to the rotor is available at the turbine shaft, and there are losses due to fluid leakage and to fluid by-passing the blades. Some energy is also consumed in overcoming the *rotation loss* of the stage. Thus, if the rotation loss in horsepower is denoted by hp_r, the stage power output in horsepower is

$$hp_s = \frac{G}{550g} (u \, \Delta c_u) - hp_r \qquad (8)$$

The rotation loss comprises the losses due to disk friction hp_{df} and the blade windage loss hp_{bw} due to operation with partial admission. The rotation loss in horsepower can be calculated from Kerr's formula

$$hp_r = \{K_1 D + nK_2(1 - e)l^{1.5}\} \left(\frac{u}{100}\right)^3 \frac{D_p}{v} \qquad (9)$$

where D_p = mean diameter of pitch circle, ft.
  l = effective blade height, in.
  u = mean tangential velocity of blades, fps.
  v = specific volume of fluid surrounding rotor, ft³/lb.
  K_1 = 0.0607; K_2 = 0.458.
  e = admission fraction, nozzle arc to total circumference.
  n = 1 for wheels with 1 row of blades.
    = 1.2 for wheels with 2 rows of blades.

7. Analysis of the Fluid Flow Path

The thermodynamic processes for an impulse and a reaction stage can be generalized. The physical arrangements under consideration are illustrated schematically in Fig. 5. If an expansion takes place from an initial pressure p_0 to the back pressure p_2, the pressure p_0 is that upstream to the nozzle for a Rateau stage, whereas for a reaction stage it is the pressure upstream to the stationary blading. The

pressure p_1 refers to pressure at the entrance to the moving blades of a reaction stage; in a pure impulse stage, $p_1 = p_2$.

From the foregoing it follows that the pressure drop in the stationary blade row of a reaction stage is the difference $p_0 - p_1$.

In subsequent discussions the terms nozzle and stationary blades will be used interchangeably. A nozzle is any stationary passage wherein the working fluid expands before flowing through the blades attached to the turbine rotor. To calculate the relationships for determining the performance of a turbine stage the state of the

Impulse stage
$$H_s = h_0 - h_1 = h_0 - h_2$$
$$H_r = 0$$

Reaction stage
$$H_s = h_0 - h_1$$
$$H_r = h_1 - h_2$$
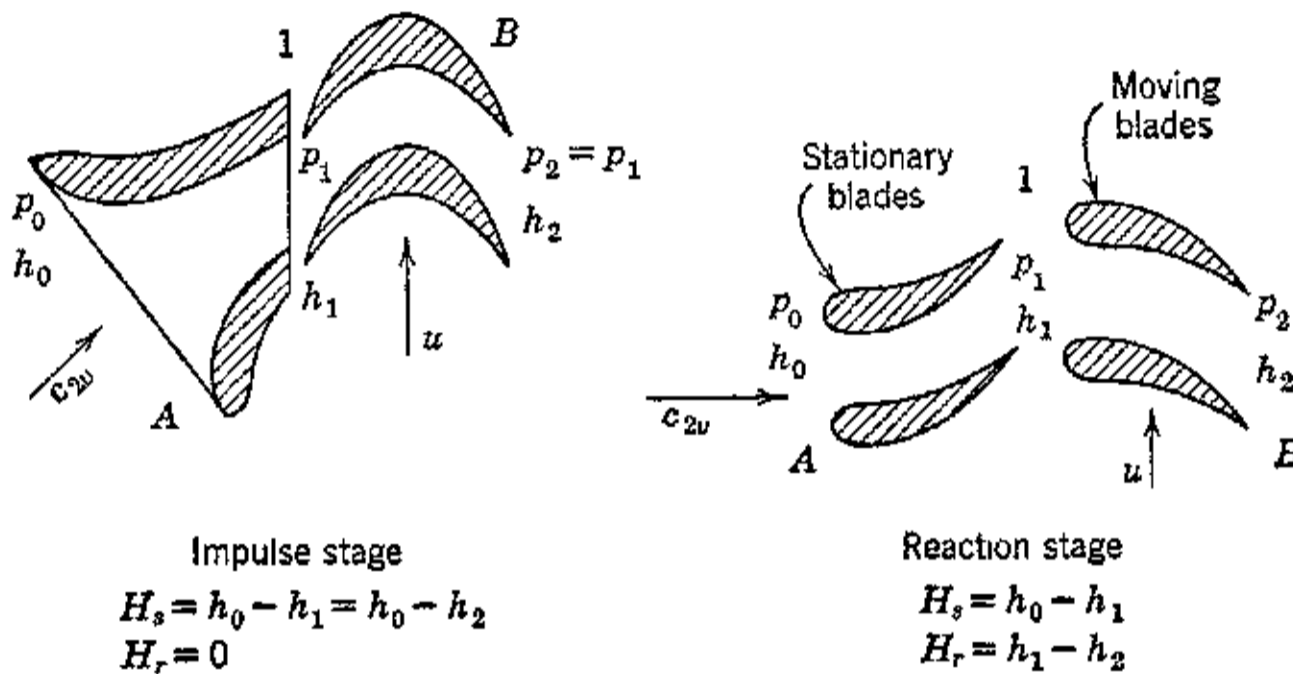
Fig. 5. Flow conditions for impulse and reaction stages.

working fluid at each significant point in its flow path must be determined. For determining the state points it is convenient to represent the flow process on the enthalpy-entropy h-s plane, as illustrated in Fig. 6.

In Fig. 6 the state point A corresponds to the state of the fluid at its entrance to the nozzles. The enthalpy of the fluid at A is h_0 Btu/lb. The fluid may arrive at the nozzle entrance with the approach velocity c_{2v} called the *carry-over velocity*. In the first stage of a multistage turbine, impulse or reaction, the carry-over velocity c_{2v} is so small that it may be neglected, and the fluid may be assumed to start from rest. In an intermediate stage of a multistage turbine the exit velocity c_2 of the fluid leaving the moving blades of the preceding stage, if properly guided, can be utilized in the nozzles or stationary blades. Consequently, the fluid at B corresponds to the state at the exit of a moving row of blades; its corresponding enthalpy is h_2, and its velocity is c_2.

The flow process in the nozzles is accompanied by both frictional and thermal energy losses. These losses, expressed in heat units, are

denoted by $\mathcal{R}/J$. The fluid is discharged from the nozzles with its kinetic energy increased, and at the entrance section of the moving blades its relative velocity is w_1. The kinetic energy corresponding to w_1 is available for energy transfer in the moving blade row. This kinetic energy can be represented on the h-s plane as an isentropic increase in the enthalpy of the fluid above that corresponding to static conditions at the pressure p_1.
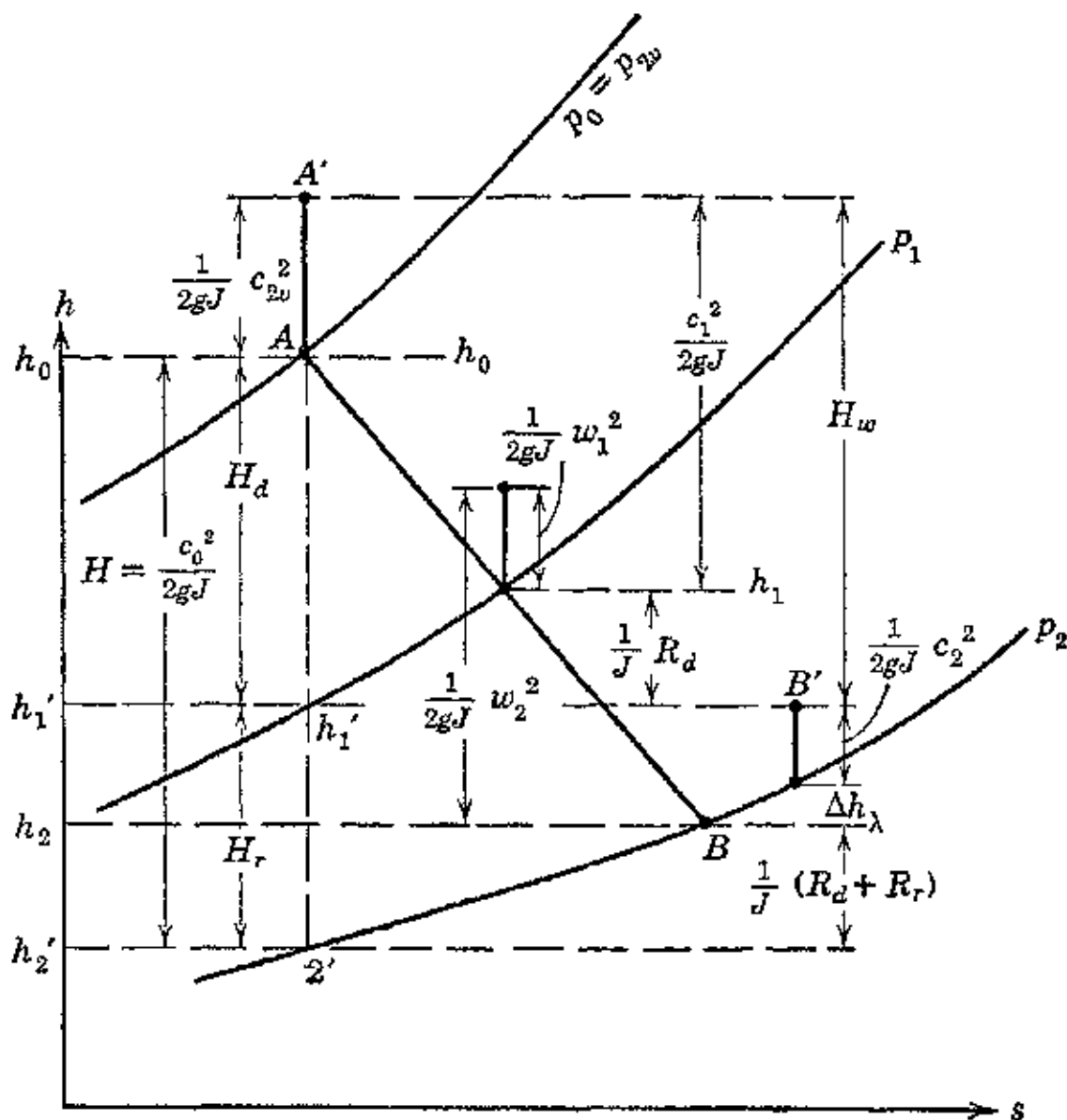
FIG. 6. Representation on the h-s plane of expansion of the working fluid in an intermediate stage of a group of stages.

The frictional and thermal energy losses in the moving row of blades are denoted by $\mathcal{R}/J$ Btu/lb. In addition to the aforementioned losses there are others due to disk friction and windage. These produce a heating of the fluid and a corresponding increase in its final enthalpy denoted by Δh_λ Btu/lb.

The effect of the carry-over velocity c_{2v} is taken into account in the same way as the effect of the relative velocity w_1. The velocity corresponds to an isentropic change in enthalpy from a fictitious state A' to the actual initial state A. This enthalpy change, measured in Btu per pound, is $c_{2v}{}^2/2gJ$.

The absolute exit velocity of the fluid leaving the moving row of blades is c_2 and is identical with the approach velocity c_{2v} for the next row of stationary blades in a multistage turbine. If the stage under consideration is assumed to be the last stage of the turbine the kinetic energy corresponding to c_2 is lost.

Referring to Fig. 6, it is seen that the enthalpy of the fluid corresponding to the back pressure p_2 for the stage is given by

$$h_2 = h_0 - H + \frac{1}{J}(\mathcal{R}_d + \mathcal{R}_r)$$

The fluid approaching the stationary blades with the velocity c_{2v} has the kinetic energy $\frac{1}{2g} c_{2v}^2$ ft-lb/lb. Consequently, the final enthalpy h_2 can be stated in terms of the velocities. Thus

$$h_2 = h_0 - \frac{1}{2gJ}(c_1^2 + w_2^2 - c_{2v}^2 - w_1^2)$$

The enthalpy of the fluid immediately upstream to the moving blades is h_1 Btu/lb.

$$h_1 = h_0 - H_d + \frac{1}{J}\mathcal{R}_d = h_0 - \frac{1}{2gJ}(c_1^2 - c_{2v}^2) \tag{10}$$

The velocity corresponding to the conversion of the available energy H into kinetic energy by an isentropic expansion is denoted by c_0, where

$$c_0 = \sqrt{2gJH} \tag{11}$$

The velocity c_0 is called the *isentropic velocity*.

8. Flow through Turbine Blades

Consider an arbitrary pair of moving blades, as illustrated in Fig. 2. The entrance conditions will be denoted by the subscript 1 and the exit conditions by the subscript 2. The blades move with the tangential velocity u and deliver to the turbine shaft L_t ft-lb/lb of working fluid. The flow process may be assumed to be adiabatic. Hence, the energy equation for the flow through the passage formed by the blades is

$$0 = J(h_1 - h_2) + \frac{c_1^2 - c_2^2}{2g} - L_t$$

It has been shown that the energy transferred to the rotor by the 1 lb of fluid is given by

$$L_t = \frac{u}{g} \Delta c_u = \frac{u}{g}(c_{1u} - c_{2u}) \tag{12}$$

It should be realized that c_{1u} and c_{2u}, being velocity components, are vector quantities. Hence, expressing these velocity components in terms of their absolute magnitudes,

$$L_t = \frac{u}{g} \Delta c_u = \frac{u}{g}(c_1 \cos \alpha_1 + c_2 \cos \alpha_2)$$

$$= \frac{u}{g}(c_1 \cos \alpha_1 - u + w_2 \cos \beta_2) \tag{13}$$

If the blade passage is for an axial-flow turbine, the only type considered here, the energy transfer is

$$L_t = \frac{w_2^2 - w_1^2}{2g} - \frac{c_2^2 - c_1^2}{2g} \tag{14}$$

The energy equation for the rotating blade passage can be written in terms of the enthalpy change. Thus

$$0 = J \int_1^2 dh + \frac{1}{2g}(w_2^2 - w_1^2) \tag{15}$$

The flow is adiabatic but accompanied by friction. Hence, if dE_F is the work expended in overcoming friction, then

$$J \int_1^2 dh = - \int_1^2 v \, dp + \int_1^2 dE_F \tag{16}$$

For this process the available energy H is given by

$$H = h_1 - h_2' = - \int_1^2 \frac{v}{J} dp \tag{17}$$

For convenience let the available energy in mechanical units be defined by

$$JH = \frac{c_0^2}{2g} \tag{18}$$

Combining equations 16, 17, and 18 gives

$$H = \frac{c_0{}^2}{2g} = h_1 - h_2' = -\int_1^2 \frac{v}{J}\, dp = \frac{w_2{}^2 - w_1{}^2}{2gJ} + \int_1^2 \frac{dE_F}{J} \quad (19)$$

It is convenient to conceive the losses in the blade passage as being composed of two distinct parts, regardless of their character: those associated with the energy of the fluid at the entrance to the passage, and those occurring within the passage itself. The aforementioned losses can be expressed in terms of the kinetic energies associated with the fluid at entrance and at exit sections of the passage by the introduction of appropriate loss coefficients.

Let $\rho_{R1} \dfrac{w_1{}^2}{2g}$ = energy loss at the entrance to passage.

$\rho_{R2} \dfrac{w_2{}^2}{2g}$ = energy loss in the passage itself.

The total loss of energy for the flow passage is given by the term $\displaystyle\int_1^2 dE_F$. Hence

$$\int_1^2 dE_F = \rho_{R1} \frac{w_1{}^2}{2g} + \rho_{R2} \frac{w_2{}^2}{2g} \quad (20)$$

Substituting the above expression for $\displaystyle\int_1^2 dE_F$ into equation (19)

$$\frac{c_0{}^2}{2g} = JH = \frac{w_2{}^2 - w_1{}^2}{2gJ} + \rho_{R1} \frac{w_1{}^2}{2g} + \rho_{R2} \frac{w_2{}^2}{2g} \quad (21)$$

or

$$\frac{c_0{}^2}{2g} = \frac{w_2{}^2}{2g}(1 + \rho_{R2}) + \frac{w_1{}^2}{2g}(\rho_{R1} - 1) \quad (22)$$

so that

$$w_2{}^2(1 + \rho_{R2}) = c_0{}^2 + w_1{}^2(1 - \rho_{R1}) \quad (23)$$

or

$$w_2{}^2 = \frac{1}{1 + \rho_{R2}}[c_0{}^2 + (1 - \rho_{R1})w_1{}^2] \quad (24)$$

To simplify equation 24 it is convenient to introduce the *blading coefficients*, ψ_1 and ψ_2, which are defined by

$$\psi_1{}^2 = 1 - \rho_{R1} \quad (a)$$

and

$$\psi_2{}^2 = \frac{1}{1 + \rho_{R2}} \quad (b)$$

Substituting from equations (a) and (b) into equation 24 gives

$$w_2 = \psi_2 \sqrt{c_0{}^2 + \psi_1{}^2 w_1{}^2} \qquad (25)$$

A similar expression can be derived for the discharge velocity from a stationary blade passage. In this case, however, the work delivered externally is zero.

Let c_{2v} = the discharge absolute velocity from the preceding rotating blade passage, called the carry-over velocity, fps.

$$\varphi_1{}^2 = \frac{1}{1 + \rho_{s1}} = \text{stationary blade velocity coefficient.}$$

$$\varphi_{2v}{}^2 = 1 - \rho_{s2} = \text{stationary blade carry-over coefficient.}$$

Hence for the stationary blades

$$c_1 = \varphi_1 \sqrt{c_0{}^2 + \varphi_{2v}{}^2 c_{2v}{}^2} \qquad (26)$$

The foregoing equations for w_2 and c_1 present the exit velocities from the rotating blades and the stationary blades as functions of the available energy $H = c_0{}^2/2gJ$ for the passage and two blading coefficients. The introduction of two coefficients may appear to be arbitrary and a needless complication of the equations, but further consideration of the flow problem will reveal the usefulness of these expressions.

The discharge velocity from a blade passage will depend on the available energy H, on the kinetic energy made available to the passage, and possibly on the ratio of the exit and entrance velocities. In the interests of a rational analysis of the losses in the flow passage at least two coefficients are required.

For the present state of knowledge of the problem of flow through blades, it is sufficient if a distinction can be made between the characteristics of the losses occurring between the exit of one row of blades and the entrance to the next, and those in the flow passage itself. The first-mentioned loss is characterized by the values of the coefficients φ_{2v} and ψ_1. Thus these coefficients determine the efficiency with which the energy from one passage is "carried over" to the next. This energy is for brevity called the "carry-over," and the coefficient φ_{2v} or ψ_1 determines the effectiveness in making the carry-over available for useful work in the subsequent blade passage. The efficiency with which the carry-over actually supplied the blade passage, and the efficiency of utilization of the available energy H, may be conceived to be measured by φ_1 and ψ_2.

To illustrate, consider first the nozzle of an impulse turbine stage. Here the carry-over to the nozzle is zero; what little approach velocity

there is in the approach piping can be assumed to be converted into useful work without loss. For this type of nozzle, the coefficient $\phi_{2v} = 1.0$, and the nozzle discharge velocity may be represented by

$$c_1 = \varphi_1 \sqrt{c_0{}^2 + \varphi_{2v}{}^2 c_{2v}{}^2} = \varphi \sqrt{c_0{}^2 + c_{2v}{}^2} \qquad (27)$$

Thus one coefficient may be used for describing the performance of an impulse turbine nozzle.

When turbine blades are tested statically, and the apparatus arranged so that the fluid enters the blading without shock, the conditions are similar to those of an impulse element nozzle. In this case only φ_1 is measured, and its magnitude determines the characteristic loss for the blade passage.

In a pure impulse blade the enthalpy change from entrance to exit is zero, consequently $c_0{}^2 = 0$, and the discharge velocity is

$$w_2 = \psi_1 \psi_2 w_1 = \psi w_1 \qquad (28)$$

Thus, though there are special solutions to the velocity equations for certain cases, the real advantage of expressing them in the form used is that they are perfectly general. They can be applied with equal facility to the Rateau, impulse, and reaction stages, or to nozzle flow.

9. The Single-Stage Rateau Turbine

In a single-stage Rateau turbine, owing to losses in the blading, the exit relative velocity is smaller than the entrance value, and the approach velocity for the nozzles is zero. The exit relative velocity w_2 is from equation 28

Fig. 7. Flow conditions for impulse blades.

$$w_2 = \psi w_1 \qquad (29)$$

The coefficient ψ is termed the *blading coefficient*. Substituting for w_2 from equation 29 into equation 13

$$L_t = \frac{u}{g} (c_1 \cos \alpha_1 + \psi w_1 \cos \beta_2 - u) \qquad (30)$$

Equation 30 shows that in the interest of a large energy transfer to the rotor the nozzle angle α_1 should be as small as possible. Fairly small angles are practicable, and in actual turbines the values of α_1 range between $12°$ and $15°$.

Expressing w_1 in terms of α_1, u, and β_1

$$w_1 = \frac{c_1 \cos \alpha_1 - u}{\cos \beta_1} \tag{31}$$

Substituting the above into equation 30 gives the following equation for the energy transfer

$$L_t = \frac{u}{g}\left[c_1 \cos \alpha_1 - u + \psi(c_1 \cos \alpha_1 - u)\frac{\cos \beta_2}{\cos \beta_1}\right] \tag{32}$$

Rearranging

$$L_t = \frac{u}{g}(c_1 \cos \alpha_1 - u)\left(1 + \psi \frac{\cos \beta_2}{\cos \beta_1}\right) \tag{33}$$

Rearranging and introducing the velocity ratio $\nu_1 = u/c_1$

$$L_t = \frac{u^2}{g}\left(\frac{\cos \alpha_1}{\nu} - 1\right)\left(1 + \psi \frac{\cos \beta_2}{\cos \beta_1}\right) \tag{34}$$

(a) **Blading Efficiency.** The ratio of the energy transfer L_t to the kinetic energy of the jet is denoted by η_b and is termed the *blading efficiency.* Dividing equation 34 by the jet kinetic energy $c_1^2/2g$

$$\eta_b = 2\left(1 + \psi \frac{\cos \beta_2}{\cos \beta_1}\right)(\nu_1 \cos \alpha_1 - \nu_1^2) \tag{35}$$

The above is the equation of a parabola. It is seen that the blading efficiency η_b depends on the blade angles β_1 and β_2, and on the velocity ratio ν_1. If α_1, ψ, and the ratio $\cos \beta_2/\cos \beta_1$ are held constant, then η_b is a function ν_1 alone. The value of ν_1 which gives the maximum value for η_b is obtained by differentiating equation 35 and setting the result equal to zero.

$$\frac{d\eta_b}{d\nu_1} = 2\left(1 - \psi \frac{\cos \beta_2}{\cos \beta_1}\right)(\cos \alpha_1 - 2\nu_1) = 0 \tag{36}$$

Hence

$$\cos \alpha_1 = 2\nu_1 \tag{37}$$

and the value of ν_1 for $(\eta_b)_{\text{max.}}$ is

$$\nu_1 = \frac{\cos \alpha_1}{2} \tag{38}$$

Substituting the above value of ν_1 into equation 35 gives the following equation for the maximum blading efficiency $(\eta_b)_{max}$.

$$(\eta_b)_{max.} = \left(1 + \psi \frac{\cos \beta_2}{\cos \beta_1}\right) \frac{\cos^2 \alpha_1}{2} \qquad (39)$$

It is apparent from equation 35 that the energy transfer depends upon the velocity ratio and the angles β_1 and β_2. In a single-stage Rateau turbine of conventional design the blading is unsymmetrical; the exit angle is usually smaller than the entrance angle. This construction improves the efficiency.

The inlet angle β_1 is usually made from 28° to 32°, and the exit angle β_2 ranges from 19° to 23°. The smaller exit angles are used with the narrower blade sections, and the smaller entrance angles with the wider sections.

Usually the difference between the blading angles is so small that w_1 and w_2 can be assumed to make the same angle with u. If it is assumed that $\beta_1 = \beta_2 = \beta$, then the maximum energy transfer results when

$$\nu_1 = \frac{u}{c_1} = \frac{\cos \alpha_1}{2} \qquad (40)$$

and the maximum efficiency of the blading is

$$(\eta_b)_{max.} = (1 + \psi) \frac{\cos^2 \alpha_1}{2} \qquad (41)$$

The entrance and exit velocity diagrams for an impulse blade passage, with flow losses, are illustrated in Fig. 7.

(b) **Nozzle and Blading Efficiency.** This efficiency takes into account that the jet velocity of the gases leaving the nozzle c_1 is smaller than the ideal value c_0. If η_n is the efficiency of the nozzle and η_{nb} the nozzle and blading efficiency then in general

$$\eta_{nb} = \eta_n \eta_b = \eta_i \qquad (42)$$

The nozzle efficiency is defined, in general, as the ratio of the increase in the kinetic energy of the fluid produced by the nozzle, to the available energy for the stage. In a Rateau stage the approach velocity for the fluid entering the nozzle may be neglected, and if φ_1 is the velocity coefficient for the nozzle then as shown in Chapter 3, Section 13, $\eta_n = \varphi_1^2$, and $c_1 = \varphi_1 c_0$.

Multiplying equation 35 by $\varphi_1{}^2 = \eta_n$, noting that $c_0 = c_1/\varphi_1$, and letting $\nu_0 = u/c_0 = $ *isentropic velocity ratio*, then

$$\eta_i = \eta_{nb} = \eta_n\eta_b = 2\nu_0\left(1 + \psi\frac{\cos\beta_2}{\cos\beta_1}\right)(\varphi_1\cos\alpha_1 - \nu_0) \quad (43)$$

It is seen from equation 43 that the nozzle and blading efficiency, which will be called the *internal efficiency* η_i, is a function of ν_0, ψ_2, φ_1 and the ratio $\cos\beta_2/\cos\beta_1$. The entrance angle β_1 is selected to give shockless entrance of the fluid at the most important operating condition. The exit angle β_2 is based on the continuity requirements for the blade passage. It is preferable to make β_2 somewhat smaller than that obtained by applying the continuity equation to the exit area of the blade passage. The effect of reducing the value of β_2 is to cause the blades to operate with a slight reaction, which is beneficial from the standpoint of blade efficiency, as explained in Section 15.

For equiangular blades equation 43 reduces to

$$\eta_i = \eta_{nb} = 2\nu_0(1 + \psi)(\varphi_1\cos\alpha_1 - \nu_0) \quad (44)$$

The usefulness of equations 43 and 44 is somewhat limited since their application requires that ψ and φ_1 be known functions of ν_0. Furthermore, an actual Rateau stage usually operates with a small amount of reaction. Because of the foregoing $\eta_i = \eta_{nb}$ is determined experimentally, and the energy transfer to the rotor is calculated from the available energy H for the stage.

$$L_t = \eta_{nb}JH = \eta_iJH \quad (45)$$

For a given turbine all the terms except ν_0 may be considered to be constants. Hence equation 44 can be written in the form

$$\eta_i = C_1\nu_0 - C_2\nu_0{}^2 \quad (46)$$

where C_1 and C_2 are constants.

This last expression is the equation of a parabola. Hence the internal efficiency is a parabolic function of the isentropic velocity ratio.

In some cases it is of more advantage to plot the efficiency as a function of the reciprocal of the isentropic velocity ratio, called the velocity number.

Referring to equation 44, it is seen that increasing α_1 and decreasing the ratio $\cos\beta_2/\cos\beta_1$ reduces the efficiency. However, very small values of α_1 should not be used, because then the long inclined

cut-off of the nozzle produces an increase in its surface friction decreasing the value of the loss coefficient φ_1 and the efficiency.

Although the preceding was derived for an impulse stage the parabolic law applies also to the internal efficiency of a reaction stage as a function of $\nu_0 = u/c_0$.

According to reference 11 the *highest efficiency* values for impulse stages are attained when $1/\nu_0 = 2.1$, corresponding to which $(\eta_i)_{max.} = 0.80$ to 0.84. In a symmetrical reaction stage ($r = 0.5$) the highest efficiency is attained when $1/\nu_0 = 1.55$, for which $(\eta_i)_{max.} = 0.80$ to 0.88.

It can be said, in general, that the stage efficiency attains its maximum value if the fluid is discharged perpendicularly to the wheel, that is, when the value of c_2 is a minimum, and the exit fluid contains a minimum of energy. However, this rule should not be taken too absolutely because several other factors are influential.

10. The Reaction Stage

The blade profiles employed in reaction turbines are different from impulse blading. The exit angle of the reaction blade is smaller, in the neighborhood of 15°, and the trailing edge is made as thin as practicable. In recent years there has been a development of the shape of the reaction blade, concerned mainly with the profile for the inlet edge.

The older reaction blade sections had a sharp, hooked inlet edge quite similar to that of impulse blades. In modern designs the hooked inlet has been replaced by a blunt, rounded entrance similar to the leading edge of an airfoil. This blading is what might be termed airfoil blading. For this type of blading it is difficult to define the inlet angle accurately, but, in general, it is such that the inlet relative velocity makes an angle of 80° to 90° with the tangential velocity. The efficiency of the rounded entrance blading is higher than that of the earlier types, and shockless entrance of the fluid can be obtained over a wider range of velocity ratios.

Consider an intermediate stage of a reaction turbine, and assume that the blades of the stationary blade row have identical sections. Similarly, assume that the blades in the moving row have identical sections, but not necessarily the same sections as the stationary blades. The fluid enters each stationary blade row except the first with a kinetic energy corresponding to the exit velocity c_2 for the preceding row of moving blades. The exit velocity for a preceding row of moving blades c_2 will be denoted by c_{2v}, where c_{2v} is the *carry-over velocity* and is equal to c_2. It has been mentioned, see Chap-

ter 3, that the kinetic energy associated with c_{2v} is not wholly available because of inlet losses in the stationary blades. The actual carry-over energy available to the stage is $\phi_{2v}{}^2 c_{2v}{}^2/2gJ$ Btu/lb, where $\phi_{2v} < 1$ is the carry-over coefficient. Hence, the kinetic energy gained in the stationary blades is $(c_1{}^2 - \phi_{2v}{}^2 c_{2v}{}^2)/2gJ$ Btu/lb. Let the isentropic velocity c_0, corresponding to the available energy for the stage $H = H_s + H_r$, be defined by

$$c_0{}^2 = 2gJH \tag{47}$$

Since $\varphi_{2v}{}^2 c_{2v}{}^2$ represents the carry-over actually used in the stationary blades, the gain in kinetic energy is at the expense of the enthalpy decrease in the blade row. Let ϕ_1 denote the nozzle coefficient for the stationary blades; then the energy equation is

$$\frac{c_1{}^2}{2gJ} - \frac{\varphi_{2v}{}^2 c_{2v}{}^2}{2gJ} = \phi_1{}^2(1 - r)H \tag{48}$$

For the rotating blades the exit relative velocity w_2 is accordingly defined by

$$w_2{}^2 = \psi_2{}^2 r c_0{}^2 + \psi_1{}^2 w_1{}^2 \tag{49}$$

where ψ_1 and ψ_2 are loss coefficients for the rotating blades.

The change in the whirl velocities is from Fig 7

$$\Delta c_u = (c_{1u} - c_{2u}) = c_1 \cos \alpha_1 - u + w_2 \cos \beta_2 \tag{50}$$

The energy transfer from the fluid to the rotor per pound of fluid is as before

$$L_t = \frac{u}{g} \Delta c_u \tag{51}$$

Substituting for Δc_u from equation 50

$$L_t = \frac{u}{g} (c_1 \cos \alpha_1 - u + w_2 \cos \beta_2) \tag{52}$$

Letting $\nu_1 = u/c_1$ and $\nu_2 = u/w_2$,

$$L_t = \frac{1}{g} (c_1{}^2 \nu_1 \cos \alpha_1 - c_1{}^2 \nu_1{}^2 + w_2{}^2 \nu_2 \cos \beta_2) \tag{53}$$

The nozzle and blading efficiency is

$$\eta_{nb} = \eta_t = \frac{L_t/J}{H_s + H_r} \tag{54}$$

Owing to leakage of fluid through the clearances between the rotating blades and the cylinder, and between the stationary blades and the rotor, the actual efficiency of the stage is reduced. The foregoing equations apply only to the fluid which actually flows through the blades.

11. Symmetrical Reaction Stage

An ideal reaction stage with identical blade sections for the blades in the stationary and moving rows has equal enthalpy drops in the two rows. Consequently the entrance and exit velocity triangles for the moving blades are identical. If ϕ_1 is the loss coefficient, and H the available energy for the stage, then the enthalpy drop in each row is $\phi_1^2 H/2$.

In a symmetrical reaction stage, also called a 50 per cent reaction stage,

$$c_1 = w_2 \qquad w_1 = c_2 \qquad \alpha_1 = \beta_2 \qquad \alpha_2 = \beta_1$$

$$\phi_1 = \psi_2 \quad \text{and} \quad \varphi_{2v} = \psi_1 \tag{55}$$

Hence, substituting for $w_2 = c_1$ and $\beta_2 = \alpha_1$ in equation 52 gives the following expression for the energy transferred to useful work

$$L_t = \frac{u}{g}(2c_1 \cos \alpha_1 - u) \quad \text{ft-lb/lb} \tag{56}$$

In terms of the velocity ratio $\nu_1 = u/c_1 = u/w_2$,

$$L_t = \frac{c_1^2}{g}(2\nu_1 \cos \alpha_1 - \nu_1^2) \tag{57}$$

The nozzle and blading efficiency η_i is accordingly

$$\eta_i = \frac{c_1^2}{gJH}(2\nu_1 \cos \alpha_1 - \nu_1^2) \tag{58}$$

From equations 47 and 48, noting that for the symmetrical reaction stage $r = 0.5$,

$$\phi_1^2 J \frac{H}{2} = \frac{c_1^2}{2g} - \phi_{2v}^2 \frac{c_{2v}^2}{2g} \tag{59}$$

so that

$$JH = \frac{c_1^2}{g\phi_1^2}\left(1 - \phi_{2v}^2 \frac{c_{2v}^2}{c_1^2}\right) \tag{60}$$

Substituting for JH in equation 58 from equation 60,

$$\eta_i = \phi_1^2 \frac{2\nu_1 \cos \alpha_1 - \nu_1^2}{1 - \phi_{2v}^2(c_{2v}^2/c_1^2)} \tag{61}$$

Since $c_2 = c_{2v}$, it follows from the velocity triangles for a symmetrical stage that (see Fig. 7)

$$c_{2v}{}^2 = c_2{}^2 = w_2{}^2 + u^2 - 2uw_2 \cos \beta_2 \qquad (a)$$

but for the symmetrical stage $w_2 = c_1$ and $\beta_2 = \alpha_1$. Hence

$$c_{2v}{}^2 = c_1{}^2 + u^2 - 2uc_1 \cos \alpha_1 \qquad (b)$$

and

$$\frac{c_{2v}{}^2}{c_1{}^2} = 1 + \nu_1{}^2 - 2\nu_1 \cos \alpha_1$$

$$= 1 - (2\nu_1 \cos \alpha_1 - \nu_1{}^2) \qquad (62)$$

Introducing the *diagram factor* ϵ, which is defined by

$$\epsilon = 2\nu_1 \cos \alpha_1 - \nu_1{}^2 \qquad (63)$$

The equation for the nozzle and blading efficiency can be written in the form

$$\eta_i = \phi_1{}^2 \frac{\epsilon}{1 - \phi_{2v}{}^2(1 - \epsilon)} \qquad (64)$$

It is seen from equation 64 that η_i for a symmetrical stage depends upon the diagram factor and the blading coefficients. Since the diagram factor is a function of the velocity ratio $\nu_1 = u/c_1$ and of the angle α_1, these factors influence the efficiency. If for a given stage α_1, ϕ_1, and φ_{2v} are assumed to be substantially constant, which is approximately correct, then the efficiency is a function only of the velocity ratio ν_1.

Equation 64 can be written in the form

$$\eta_i = \frac{\phi_1{}^2}{\dfrac{1 - \varphi_{2v}{}^2}{\epsilon} + \varphi_{2v}{}^2} \qquad (65)$$

Since ϕ_1 and φ_{2v} may be assumed to be constant for a given stage, the maximum value of $\eta_i = (\eta_i)_{max.}$ occurs when $\epsilon = \epsilon_{max.}$. Differentiating equation 65 with respect to ν_1, and setting the result equal to zero, gives the value of ν_1 corresponding to $\epsilon_{max.}$ and $(\eta_i)_{max.}$.

$$\frac{d\epsilon}{d\nu_1} = 2 \cos \alpha_1 - 2\nu_1 = 0$$

and the value of ν_1 corresponding to $\epsilon_{max.}$ is

$$\nu_1 = \cos \alpha_1 \qquad (66)$$

The corresponding values of $\epsilon_{max.}$ and $(\eta_i)_{max.}$ are

$$\epsilon_{max.} = 2 \cos^2 \alpha_1 - \cos^2 \alpha_1 = \cos^2 \alpha_1 \tag{67}$$

and

$$(\eta_i)_{max.} = \phi_1{}^2 \frac{\cos^2 \alpha_1}{1 - \varphi_{2v}{}^2(1 - \cos^2 \alpha_1)} \tag{68}$$

The actual efficiency of the stage will be smaller than that given by equation 68 because of leakage of fluid through the clearances between the moving blade tips and the casing, and the stationary blade tips and the rotor. In addition there are the losses due to disk friction, gland leakage, and bearing friction.

12. Enthalpy Drop for Impulse and Reaction Stages

It has been demonstrated in the preceding sections that the velocity ratio for best efficiency is $\nu_1 = \cos \alpha_1/2$ for the Rateau stage and $\nu_1 = \cos \alpha_1$ for the ideal reaction stage. It can be shown by similar methods that the optimum velocity ratio for an ideal Curtis stage is $\nu_1 = \cos \alpha_1/4$. Figure 8 presents the internal efficiency η_i as a function of the velocity ratio for the Rateau, Curtis, and reaction stages.
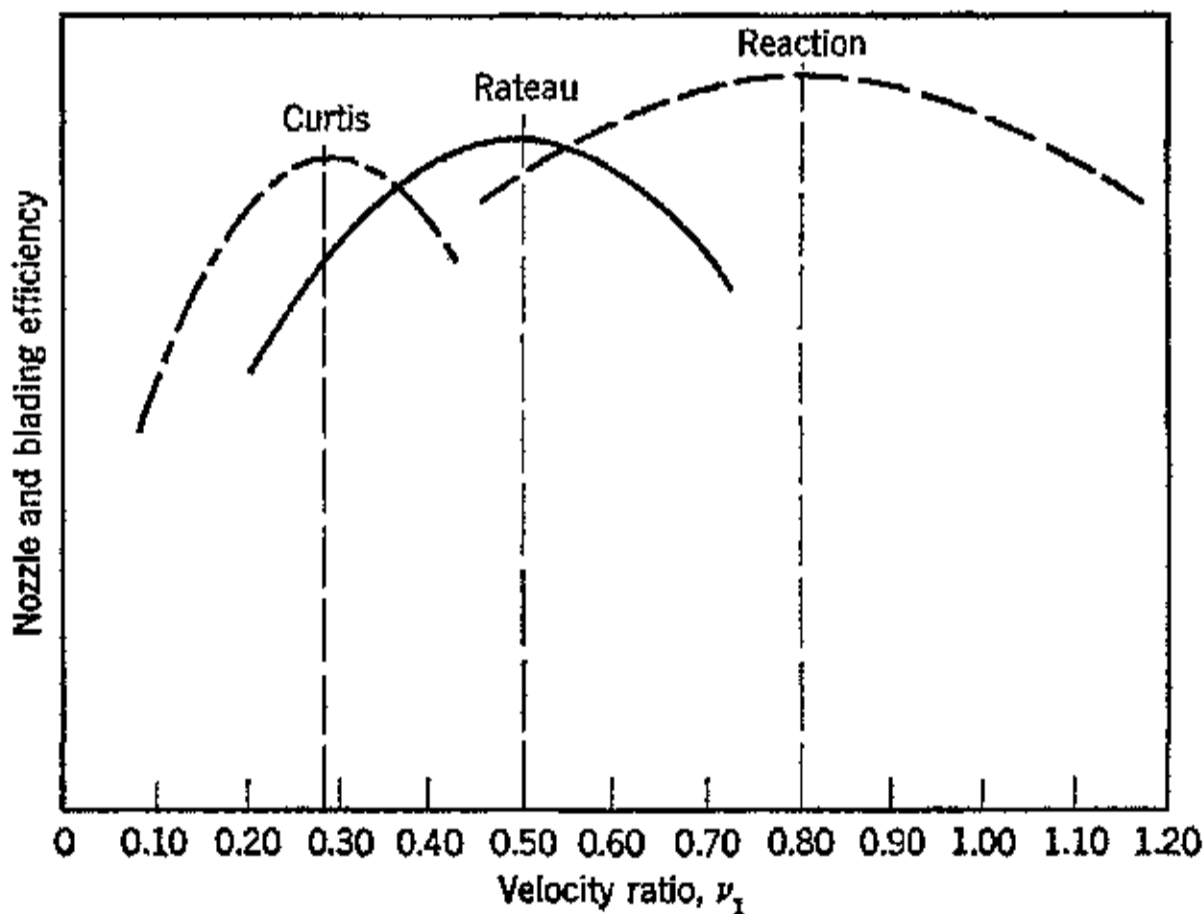
Fig. 8. Comparison of nozzle and blading efficiencies of Rateau, Curtis, and reaction stages.

As pointed out in the preceding, the efficiencies presented in Fig. 8 are not the overall efficiencies for the stage, because the only losses considered in the foregoing were those associated with the transformation of thermal energy into kinetic energy in the nozzle or stationary

blades and accompanying the energy transfer to the rotor. To calculate the overall efficiency of the stage, called the stage efficiency η_s, the effects of disk friction, blade windage, reheat, leakage, blade losses, etc., must be taken into account.

From the optimum velocity ratio for the three types of stages the heat-absorbing capacity of each stage is readily determined. The enthalpy drop corresponding to the fluid velocity c is $\Delta h = c^2/50,000$ Btu/lb.

Assuming that the peripheral velocity of a given turbine stage is limited by stress considerations to 500 fps, the enthalpy drop for each of the three stages is determined as follows.

(*a*) **Rateau Stage.** For maximum efficiency, assuming $\nu_1 = 0.48$,

$$c_1 = \frac{u}{\nu_1} = \frac{500}{0.48} = 1042 \quad \text{fps}$$

$$\Delta h_s = \frac{c^2}{50,000} = \frac{(1042)^2}{50,000} = 21.7 \quad \text{Btu/lb (per stage)}$$

(*b*) **Curtis Stage.** For maximum efficiency, assuming $\nu_1 = 0.28$,

$$c_1 = \frac{u}{\nu_1} = \frac{500}{0.28} = 1785 \quad \text{fps}$$

$$\Delta h_s = \frac{(1785)^2}{50,000} = 64 \quad \text{Btu/lb (per stage)}$$

(*c*) **Reaction Stage.** For maximum efficiency, assuming $\nu_1 = 0.85$,

$$c_1 = \frac{500}{0.85} = 590 \quad \text{fps}$$

$$\Delta h_r = \frac{(590)^2}{50,000} = 6.95 \quad \text{Btu/lb (per row)}$$

for the stage $\Delta h_s = 2\Delta h_r = 13.90$ Btu/lb.

The enthalpy drop per stage can be expressed in terms of the wheel diameter D in inches and n the rpm. Thus

$$\Delta h_s = \frac{c_1^2}{50,000} = \left(\frac{u}{\nu_1}\right)^2\left(\frac{1}{50,000}\right) = \left(\frac{\pi D n}{720\nu_1}\right)^2\left(\frac{1}{50,000}\right) \tag{69}$$

From the above it is apparent that the enthalpy drop varies as the square of the turbine wheel diameter. Consequently, in the interest of reducing the number of stages the wheel diameter must be large, but if the diameter is increased the fluid velocity must be raised in the same proportion to maintain a constant velocity ratio. For a full admission turbine the nozzle discharge area is proportional

to the product of the wheel diameter and the nozzle height. Similarly the blade height varies inversely as the square of the wheel diameter. If the wheel diameter is too large the nozzle and blade proportions will be such that efficiency is impaired. In impulse turbines, this consideration can be overcome by using partial admission, thereby making it possible to utilize practical dimensions for the nozzle and blade heights.

It should be noted that the fluid-friction losses increase as the square of the fluid velocity, whereas the leakage losses, due to flow around the blading and through the clearances between the stationary and moving members of the machine, increase with the pressure drop across the blading. Consequently, the fluid friction losses are likely to be smaller in a reaction stage than in an impulse stage, but the leakage losses tend to be smaller in an impulse stage. The leakage losses are a function of the bucket flow area and the area of the clearance space.

For aircraft gas turbines or turbojet engines the single-stage Rateau turbine when applicable has the advantage of low weight and permits operation at a somewhat higher temperature at the entrance to the nozzles. The expansion of the gases in the nozzles reduces their temperature before they enter the blading, so that only stationary elements are exposed to the highest temperatures. This tends to compensate for the lower efficiency of the single-stage machine.

13. Blading Coefficients

It has been shown that the absolute velocity for the fluid leaving the stationary blade row (or nozzles) c_1 is given by equation 48, and the relative velocity for the fluid leaving the moving blades w_2 is given by equation 49. These equations apply to the fluid which actually flows through the blade passages. The final results can be corrected for the leakage losses.

For a constant-pressure stage (impulse stage) the reaction is zero. Substituting $r = 0$ in equations 25 and 26 gives the following equations for the absolute velocity of the fluid leaving the nozzles c_1, and for w_2, then,

$$c_1 = \varphi_1 \sqrt{c_0{}^2 + \varphi_{2v}{}^2 c_{2v}{}^2} \tag{70}$$

and

$$w_2 = \psi_2 \sqrt{\psi_1{}^2 w_1{}^2} = \psi_2 \psi_1 w_1 \tag{71}$$

Let

$$\psi = \psi_1 \psi_2 \tag{72}$$

Then

$$w_2 = \psi w_1 \tag{73}$$

With good average dimensions, that is, blades having lengths of 1.5 in. to 2 in. and small clearances and shrouds, the blading coefficients will have the following values:[11] $\varphi_1 = \psi_2 = 0\ 95$; $\psi_1 = 0\ 95 - 0.08r$; $\psi_1 = \varphi_{2v} = 0\ 8$ for the intermediate stages of impulse turbines with $r = 0$ to $r = 0\ 5$; and $\psi_1 = \varphi_{2v} = 0.9$ for the intermediate stages of reaction turbines with $r = 0\ 5$.

According to G. Flugel (*Die Dampfturbinen*, pp. 73 and 74), the coefficients attain the following values under the most favorable conditions: $\varphi_1 = \psi_2 = 0\ 97$ and $\varphi_2 = \varphi_{2v} = \psi_1 = 0.95$. Many experiments have been conducted, with both stationary and rotating blades, to determine the effect of fluid velocity upon φ and ψ. The results, however, are still too inconclusive to support any generalizations. For further discussion of this see references 11 and 14.

14. Stage Efficiency Equation

It has been shown that the internal efficiency of a turbine stage η_i is defined, in general, by

$$\eta_i = \frac{\text{Work done in the stage}}{\text{Energy supplied to the stage}} \tag{74}$$

Equation 74 is also applicable to a complete multistage machine The internal efficiency for a multistage turbine will be denoted by η_{it} to distinguish it from the efficiency of a single stage η_i. Hence, for either a multistage or a single-stage turbine, the following general equation can be written:

$$\eta_i = \eta_{it} = \frac{L_t}{JH'} \tag{75}$$

In equation 75 the term L_t, or its equivalent H_w, is the internal output of either a single-stage or a complete turbine. Similarly H' is the energy supplied to either a single-stage or a complete turbine. In practice H_w is determined from the output measured with some form of dynamometer by correcting the measured output for losses. The energy supplied is calculated from measurements of the state properties of the fluid entering and leaving the stage or the turbine as the case may be.

In a multistage turbine the carry-over energy can be utilized in all stages except the last one. In the ideal turbine all the carry-over energy is utilized, but in an actual one only a portion of the carry-over energy does useful work   Hence, the usable carry-over energy is $\lambda_v c_{2v}^2/2gJ$, where λ_v is the carry-over coefficient for an *ideal* stage.

Similarly the usable exit energy can be expressed $\lambda c_2{}^2/2gJ$, where λ is the *residual energy coefficient* for an ideal stage   Hence, the total useful energy supplied to any arbitrary stage of an ideal multistage turbine, which is denoted by H', is given by

$$H' = H + \lambda_v \frac{1}{2gJ} c_{2v}{}^2 - \lambda \frac{1}{2gJ} c_2{}^2 \tag{76}$$

In the ideal case the energy coefficients λ_v and λ can have either of two values: unity when the carry-over energy is fully utilized, and zero when it cannot be utilized.   Hence, equation 76 gives the total useful energy furnished to any arbitrary selected stage.   The stage internal output H_w is given by

$$H_w = \frac{1}{J} L_t = \frac{u}{gJ} \Delta c_u \tag{77}$$

The general form of the efficiency equation is

$$\eta_t = \frac{H_w}{H'} = \frac{(u/gJ)\, \Delta c_u}{H + (1/2gJ)(\lambda_v c_{2v}{}^2 - \lambda c_2{}^2)} \tag{78}$$

If the losses due to friction, etc. are neglected

$$H_w = h_0 - h_2 + \frac{1}{2gJ}(\varphi_{2v}{}^2 c_{2v}{}^2 - c_2{}^2) \tag{79}$$

Hence, equation 78 can be written in the form

$$\eta_t = \frac{h_0 - h_2 + (1/2gJ)(\varphi_{2v}{}^2 c_{2v}{}^2 - c_2{}^2)}{H + (1/2gJ)(\lambda_v c_{2v}{}^2 - \lambda c_2{}^2)} \tag{80}$$

Equation 80 is applicable to either a reaction or an impulse stage, and to any arbitrary selected stage of a multistage machine.

Case A. Single-Stage Impulse Turbine. In this case the approach velocity of the fluid entering the nozzles c_{2v} is so small that it may be assumed that $c_{2v} = 0$ Furthermore, the residual energy $c_2{}^2/2gJ$ Btu/lb cannot be utilized. Hence, $\lambda_v = \lambda = 0$, and the efficiency equation becomes

$$\eta_{ts} = \frac{(h_0 - h_2) - (1/2gJ)c_2{}^2}{H} \tag{81}$$

The efficiency has been denoted by η_{ts} to indicate that it is the internal efficiency of a single-stage machine   The energy relationships

for a single-stage impulse turbine are illustrated graphically in Fig. 9.
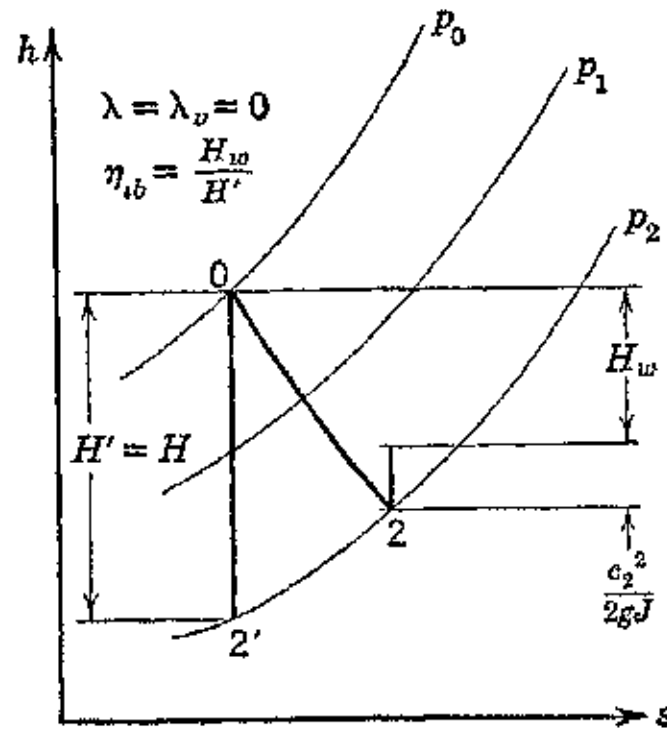
FIG. 9.   Representation of stage expansion with negligible velocity of approach.

Case B.   First Stage in a Group of Stages.   In this case, too, the approach velocity for the nozzles c_{2v} is negligible.   The residual energy $c_2{}^2/2gJ$ is made available, however, for utilization in the next stage.   Hence $\lambda_v = 0$, and $\lambda = 1$, so that the stage efficiency is given by

$$\eta_{i1} = \frac{h_0 - h_2 - (c_2{}^2/2gJ)}{H - (c_2{}^2/2gJ)} \tag{82}$$

The internal efficiency is denoted by η_{i1} to indicate that it applies to the first stage of a multistage machine.   The energy conditions are illustrated in Fig. 10.
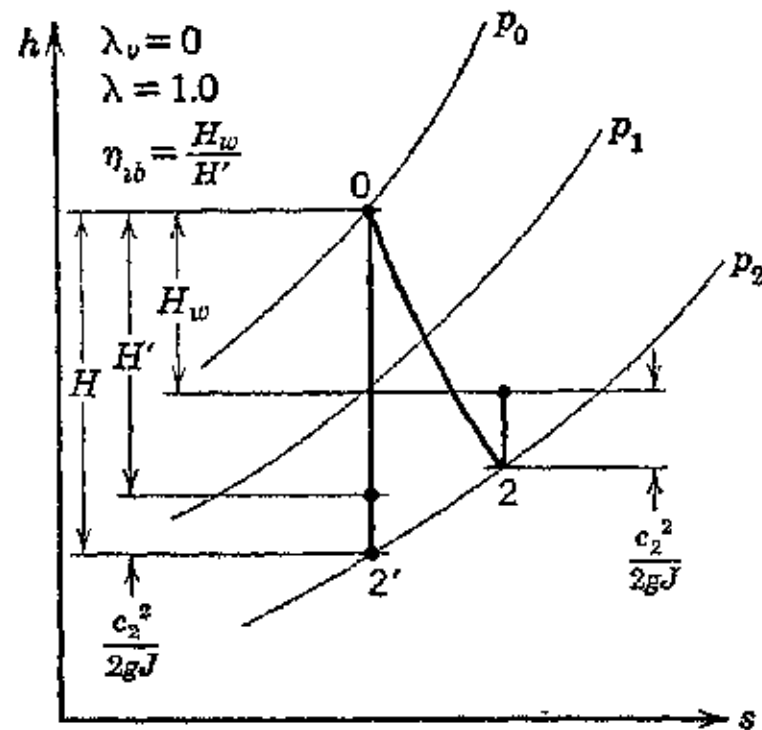
FIG. 10.   Representation on the h-s plane of the first stage expansion for a group of stages.

Case C. Last Stage of a Group. In this case the carry-over energy is available to the stage and $\lambda_v = 1$. The residual energy $c_2^2/2gJ$ cannot be utilized; it is the leaving loss, so that $\lambda = 0$. The efficiency equation becomes

$$\eta_{il} = \frac{h_0 - h_2 + (1/2gJ)(\varphi_{2v}^2 c_{2v}^2 - c_2^2)}{H + (c_{2v}^2/2gJ)} \tag{83}$$

This case is illustrated in Fig. 11.
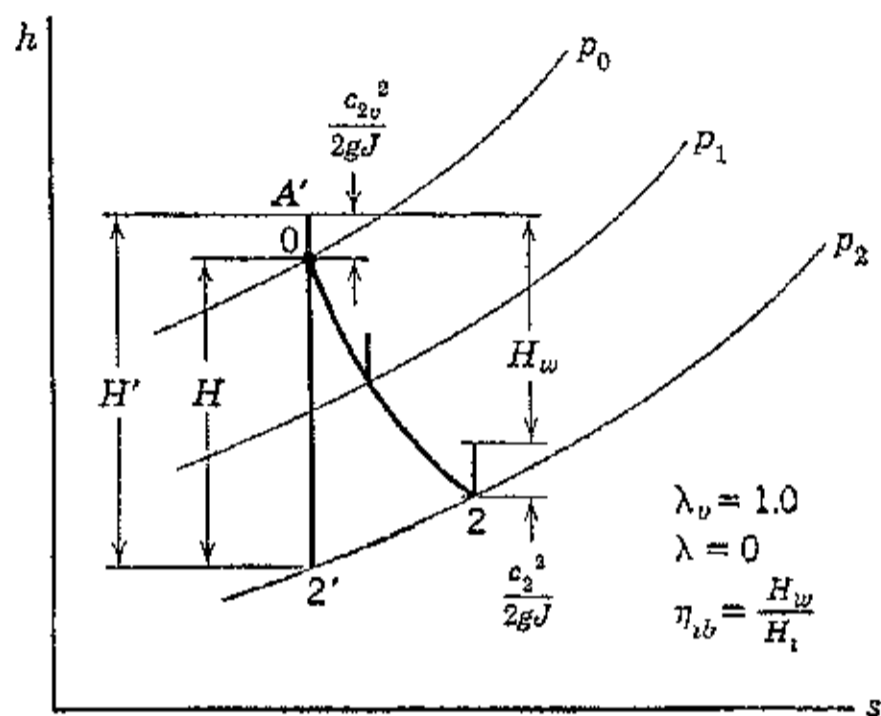
FIG. 11. Representation on the *h-s* plane of the last stage expansion for a group of stages.

Case D. Intermediate Stage of a Group. Both the carry-over and residual kinetic energies are utilizable, so that $\lambda_v = \lambda = 1$. Furthermore, the approach velocity c_{2v} is not very much different from the exit velocity c_2. Assuming that $c_{2v} = c_2$,

$$\eta_i = \frac{h_0 - h_2}{H} \tag{84}$$

This is the general case for the reaction stage illustrated in Fig. 6.

15. Effect of Reaction in Impulse Blading

The equations of Section 10 will be now applied to a single-stage Rateau turbine, and it will be assumed that the rotating blading operates with some degree of reaction. The degree of reaction is governed by the ratio of the exit area of the nozzle to the exit area of the moving-blade passages.

The approach velocity in the nozzle chamber c_{2v} is so small compared to the velocity of the jet leaving the nozzle that it may be

neglected. Hence, the jet velocity for the impulse turbine is given by equation 48, which reduces to

$$c_1 = \varphi_1 \sqrt{(1 - r)c_0{}^2} \tag{85}$$

If the rotating blades operate with reaction, the relative velocity w_2 is given by equation 49, so that

$$w_2 = \psi_2 \sqrt{rc_0{}^2 + \psi_1{}^2 w_1{}^2} \tag{86}$$

The values of the coefficients ψ_1 and ψ_2 depend on the design of the blading, and for a given design their values are fixed. The effect of reaction will be investigated upon the aforementioned basis.

It was shown in Section 13 that, if the blading operates without reaction, equations 72 and 73 give the relationship between the velocities and the blading coefficients. The efficiency of the blade passage η_b is the ratio of the energies leaving and entering it and is given by

$$\eta_b = \frac{w_2{}^2}{w_1{}^2} = \frac{\psi_2{}^2 \psi_1{}^2 w_1{}^2}{w_1{}^2} = \psi_1{}^2 \psi_2{}^2 = \psi^2 \tag{87}$$

If the blading operates with considerable reaction so that r is close to unity, it follows from equation 86 that, since w_1 is small compared to c_0, the exit relative velocity is approximately

$$w_2 \approx \psi_2 c_0 \sqrt{r} \approx \psi_2 c_0 \tag{88}$$

For $w_2 = \psi_2 c_0$ the efficiency is

$$\eta \approx \frac{w_2{}^2}{c_0{}^2} \approx \psi_2{}^2 \tag{89}$$

Since ψ_1 and ψ_2 are fractions

$$\psi_1{}^2 \psi_2{}^2 = \psi^2 < \psi_2{}^2 \tag{90}$$

Comparing the two efficiency equations 87 and 89 with equation 90 it is apparent that if the rotating blades operate with some reaction there is an improvement in the blade efficiency. This is borne out in practice.

The efficiency of reaction blades lies between the extremes of equations 87 and 89 since the efficiency of reaction blades is dependent upon the effectiveness with which the carry-over energy from the preceding stage is utilized. A properly shaped reaction blade may be expected to have a lower efficiency than a nozzle but a higher efficiency than that for impulse blades.

16. Flow Area and Blade Height

The flow areas for the nozzles and rotating blades are determined by applying the continuity equation to the area under consideration.

The function of the nozzle is to increase the velocity of the fluid stream and give it a definite direction of flow. When the turbine is designed for full admission, the cross sections of the discharge area are rectangular and the walls between the individual nozzles are made quite thin. Figure 12 illustrates the geometry of such a nozzle for an impulse turbine. In reaction turbines the stationary blades perform the functions of the nozzles.
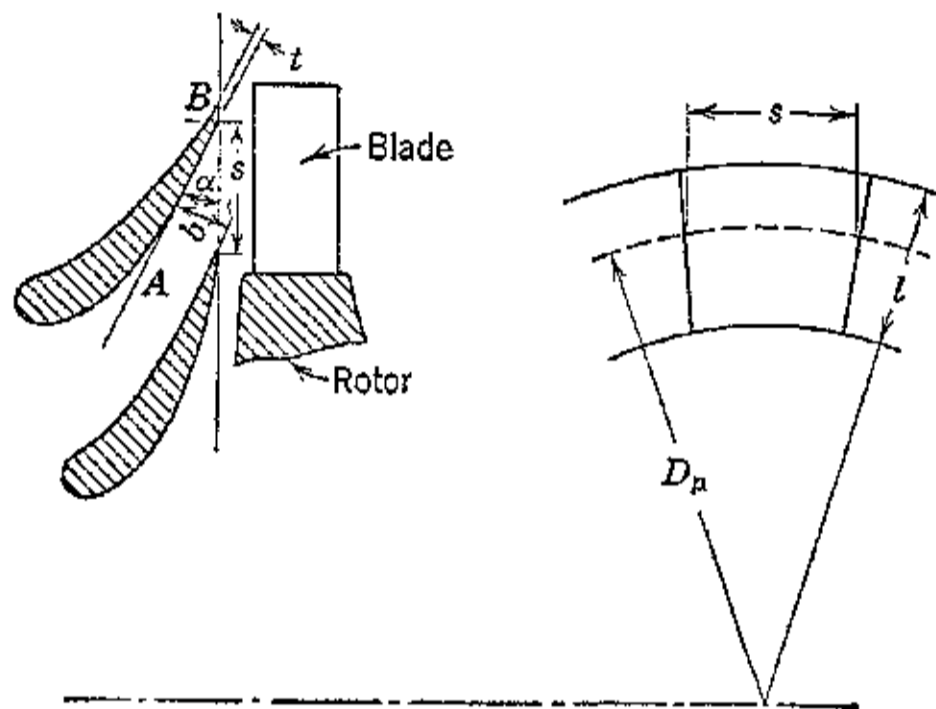
FIG. 12. Cross section through an impulse turbine nozzle.

In an impulse-turbine nozzle the walls forming the flow path usually have a flat surface corresponding to AB in Fig. 12. The angle made by this surface with the plane perpendicular to the axis of rotation, denoted by α in the figure, is termed the *nozzle angle*. The angle of the velocity of the fluid stream is usually slightly different from the nozzle angle.

The effective flow area for one nozzle passage is in general

$$A = bl \tag{91}$$

where b is the mean width of the passage and l its height. If S is the mean pitch for the passage, t the edge thickness of the passage wall, and α the nozzle angle, then from Fig. 12

$$A = bl = (S \sin \alpha - t)l = \delta l S \sin \alpha \tag{92}$$

where δ is the edge thickness factor and is given by

$$\delta = \frac{S \sin \alpha - t}{S \sin \alpha} \tag{93}$$

If the turbine operates with full admission, the number of nozzles required is $z = \pi D_p/S$, where D_p is the diameter of the pitch circle. The total nozzle area for full admission, z nozzles, is

$$A_z = \pi D_p l \delta \sin \alpha \tag{94}$$

The ratio of the actual nozzle flow area to the annulus $\pi D_p l$ is the admission factor e.

For reaction blading it is difficult to define the nozzle angle, as explained earlier. The setting of the blades is defined by a factor called the *gauging* which is denoted by λ. The area of a single flow passage is

$$A = \lambda S l \tag{95}$$

Since the reaction stage operates with full admission the complete flow area for a stage is given by

$$A_z = \lambda \pi D_p l \tag{96}$$

The gauging usually has a value ranging from 0.30 to 0.40. Hence, for a row of stationary reaction blades,

$$G = \lambda \pi D_p l c_1 \gamma_1 \tag{97}$$

and for a row of rotating reaction blades,

$$G = \lambda \pi D_p l w_2 \gamma_2 \tag{98}$$

If D_p and l are in inches, then for the stationary blades

$$l_s = \frac{144 G v_1}{\lambda \pi D_p c_1} \tag{99}$$

where v_1 is the specific volume at the blade exit.

Similarly for the rotating blades

$$l_r = \frac{144 G v_2}{\lambda \pi D_p w_2} \tag{100}$$

It is convenient to express the blade length in terms of the velocity ratio and wheel speed. Thus consider the rotating row and let $\nu_2 = u/w_2$; then

$$l_r = \frac{144 G v_2 \nu_2}{\lambda \pi D_p u} \tag{101}$$

Let $R_A = l_r/b$ be the aspect ratio of the blading, and ω the rotative speed in radians per second; then

$$l_r = bR_A = \frac{144 G v_2 \nu_2}{\lambda \pi D_p{}^2 (\omega/24)} \tag{102}$$

The weight rate of flow through the blading is accordingly

$$G = \frac{\lambda \pi D_p ub R_A}{144 v_2 \nu_2} \quad \text{lb/sec} \tag{103}$$

17. Effect of Changing Operating Conditions

A turbine is designed basically for a single set of operating conditions, such as flow and pressure ratio. When the flow conditions differ from the design values the pressure ratio must adjust itself to the new flow.

Case A. Critical Velocity in Passages. It follows from Chapter 3 that, where the velocity in the narrowest passage is equal to the critical velocity, the maximum flow in pounds per second is given by equation 3·122, which can be written in the form

$$G_{\text{max}} = C_D A_m \sqrt{2g \left(\frac{k}{k+1}\right) m^{2/k}} \sqrt{\frac{p_1}{v_1}} \quad \text{lb/sec} \tag{104}$$

where A_m = minimum flow area.

m = critical pressure ratio.

C_D = discharge coefficient.

or

$$G_{\text{max.}} = C_D A_m \sqrt{\frac{2g}{R} \left(\frac{k}{k+1}\right) m^{2/k}} \left(\frac{p_1}{\sqrt{T_1}}\right) \tag{105}$$

If the subscript 1 refers to the new operating condition and the subscript 0 to the design condition, then, assuming C_D constant, the relationship between the weight flow and the upstream pressure to the turbine stage under critical flow conditions is given by

$$\frac{G_1}{G_0} = \frac{p_{11}}{p_{10}} \sqrt{\frac{T_{10}}{T_{11}}} = \sqrt{\frac{p_{11}}{p_{10}} \cdot \frac{v_{10}}{v_{11}}} \tag{106}$$

This equation is applicable to a single stage of the turbine or several stages in series, and it assumes that there is no change in the flow-path cross sections with change in operating conditions. Obviously, this equation is inapplicable to stages where a regulating valve controls the flow-passage area.

A small change in the temperature of the working fluid has a minor effect upon the weight flow because its absolute temperature enters the equation to the one-half power. Consequently, the weight flow depends primarily upon the admission pressure p_1 and is practically proportional to it.

EXAMPLE. A De Laval nozzle is designed for initial conditions of $p_1 = 200$ psia and $T_1 = 1600$ R. The initial conditions are changed to 100 psia and 1400 R. What will be the ratio of the new flow to the design flow?

$$p_{10} = 200 \qquad T_{10} = 1600 \text{ R} \quad \text{flow is critical}$$

$$p_{11} = 100 \qquad T_{11} = 1400 \text{ R} \quad \text{flow is critical}$$

$$\frac{G_1}{G_0} = \frac{p_{11}}{p_{10}} \sqrt{\frac{T_{10}}{T_{11}}} = \frac{100}{200} \sqrt{\frac{1600}{1400}} = 0.5 \times 1.065 = 0.533$$

Case B. Subcritical Velocities. This condition applies principally to reaction turbines. Assume that the flow area is A and the clearance losses are too small to influence the problem. Then the continuity equation for any reaction blading row is

$$G = \frac{A C_D}{v} \sqrt{c_0{}^2 + c_{2v}{}^2} = \frac{A C_D}{v} c_0 \sqrt{1 + e} \tag{107}$$

In equation 107 the factor e is defined by the relationship

$$e = \frac{c_{2v}{}^2}{c_0{}^2} = \frac{(1 - \epsilon_0)\varphi^2}{1 - \varphi^2(1 - \epsilon_0)} \tag{108}$$

where as before ϵ_0 is the diagram factor and is defined here by

$$\epsilon_0 = 2\nu_0 \cos \alpha_1 - \nu_0{}^2 \tag{109}$$

Squaring both sides of equation 107, rearranging, expressing G in terms of the flow for perfect gases, and noting that $c_0{}^2/2gJ = \Delta h_0'$, then

$$\frac{G^2 v^2}{A^2 C_D{}^2} \cdot \frac{1}{1 + e} \cdot \frac{1}{2vJ} = \Delta h_0' \tag{110}$$

For brevity let

$$\Delta\Phi = \frac{1}{(1 + e)A^2 C_D{}^2} \cdot \frac{1}{2gJ} \tag{111}$$

Then, assuming C_D constant, for a given set of blading equation 110 becomes

$$G^2 v^2 (\Delta\Phi) = \Delta h_0' \tag{112}$$

For a turbine containing several stages, the last expression can be written in differential form, thus

$$G^2 v^2 \, d\Phi = -dh = \frac{v}{J} dp \tag{113}$$

the negative sign denoting that the enthalpy decreases as the fluid expands through the turbine.

For a polytropic expansion having an efficiency η_t, the characteristic equation is $pv^n = $ constant, and from equation 3·71 the relation between η_t, k, and n is, for small pressure ratios,

$$\frac{1}{n} = 1 - \eta_t \left(\frac{k-1}{k}\right) \tag{114}$$

Integrating equation 113 and assuming the expansion to be polytropic

$$G^2 \int d\Phi = \frac{1}{Jn} \left(\frac{p_1}{v_1}\right) \left[1 - \left(\frac{p_2}{p_1}\right)^n\right] \tag{115}$$

where n is defined by equation 114 and

$$\int d\Phi = \sum_0^z \left(\frac{1}{1+e}\right) \left(\frac{1}{A^2 C_D^2}\right) \left(\frac{1}{2gJ}\right) \tag{116}$$

If the blades are nearly similar and there are z rows of blades, then

$$\int d\Phi = \left(\frac{z}{2gJ}\right) \left(\frac{1}{A^2 C_D^2}\right) \left(\frac{1}{1+e}\right) \tag{117}$$

The value of e is determined from the average value of v_0 for the complete turbine.

Comparing two different flows for the turbine

$$\frac{G_1^2}{G_0^2} \cdot \left(\frac{1+e_0}{1+e_1}\right) = \frac{p_{11} v_{10}}{v_{11} p_{10}} \frac{\left[1 - \left(\frac{p_{21}}{p_{11}}\right)^n\right]}{\left[1 - \left(\frac{p_{20}}{p_{10}}\right)^n\right]} \tag{118}$$

where $p_{10} = $ initial pressure corresponding to the weight flow G_0.
$p_{11} = $ initial pressure corresponding to flow G_1.
$v_{10} = $ initial specific volume corresponding to flow G_0.
$v_{11} = $ initial specific volume corresponding to flow G_1.
$p_{20} = $ back pressure corresponding to G_0.
$p_{21} = $ back pressure corresponding to G_1.
$e_0 = $ carry-over function corresponding to flow G_0.
$e_1 = $ the value of e_0 corresponding to flow G_1.

Equation 118 can be expressed in terms of pressures and temperatures, thus

$$\frac{G_1}{G_0} = \sqrt{\frac{1+e_1}{1+e_0}} \sqrt{\frac{T_0}{T_1}} \sqrt{\frac{p_{11}^2 \left[1 - \left(\frac{p_{21}}{p_{11}}\right)^n\right]}{p_{10}^2 \left[1 - \left(\frac{p_{20}}{p_{10}}\right)^n\right]}} \tag{119}$$

The quantity $(1 + e_1)/(1 + e_0)$ is a speed correction factor which enters because of the variation in the amount of carry-over energy between the stages, with changes in speed.

For approximation purposes it can be assumed that $n = 2$. Further, the speed correction factor $\sqrt{(1 + e_1)/(1 + e_0)}$ can be assumed to be unity.

For approximate purposes the flow relationship becomes

$$\frac{G_1}{G_0} = \sqrt{\frac{T_0}{T_1}} \sqrt{\frac{p_{11}^2}{p_{10}^2} \frac{\left[1 - \left(\frac{p_{21}}{p_{11}}\right)^2\right]}{\left[1 - \left(\frac{p_{20}}{p_{10}}\right)^2\right]}} \tag{120}$$

or finally

$$\frac{G_1}{G_0} = \sqrt{\frac{T_0}{T_1}} \sqrt{\frac{p_{11}^2 - p_{21}^2}{p_{10}^2 - p_{20}^2}} \tag{121}$$

18. Wheel Diameter and Blade Stress

The wheel diameter can be related to the blade stress in the following manner. Let

M = mass of one blade, slug.
a = area of blade section, in.^{2}
D = diameter to center of gravity of blade, in.
u = peripheral speed of blade, fps.
f_c = centrifugal force acting on one blade, lb.
σ = blade stress, psi.
ν = velocity ratio u/c_1 or u/w_2.
ω = angular velocity of blade, rad/sec.
ρ = density of blade material, slug/in.^{3}
v = specific volume, ft^3/lb.
λ = gauging.

Then the centrifugal force due to the inertia of one blade at radius $D/2$ in. is given by

$$f_c = M \frac{u^2}{D/24} = 24M \frac{u^2}{D} \quad \text{lb} \tag{122}$$

The stress on the blade is given by

$$\sigma = \frac{f_c}{a} = \frac{24}{a} M \frac{u^2}{D} \quad \text{psi} \tag{123}$$

The mass of a blade of length l, assuming constant cross-sectional area throughout its length, is given by

$$M = \rho a l \tag{124}$$

Hence, substituting for l in terms of the blade width b and its aspect ratio R_A, equation 123, becomes

$$\sigma = 24\rho l \frac{u^2}{D} = 24\rho R_A \frac{u^2}{D} b \tag{125}$$

Solving for the aspect ratio

$$R_A = \frac{\sigma D}{24\rho b u^2} = \frac{24\sigma}{\rho b \omega^2 D} \tag{126}$$

Hence from equation 125 the blade length is given by

$$l = b R_A = \frac{144 G v \nu}{\lambda \pi D^2 (\omega/24)} = \frac{24\sigma}{\rho \omega^2 D}$$

or

$$144 G v \nu \rho \omega = \lambda \pi \sigma D \tag{127}$$

Hence, the wheel diameter is given by

$$D = \frac{144\rho\omega v \nu G}{\pi \sigma \lambda} \quad \text{in.} \tag{128}$$

EXAMPLE. Inlet conditions to a gas turbine wheel are

$G = 30$ lb/sec.   Inlet temperature $T_1 = 1660$ R.
$\nu = 0.85$.
$\omega = 380$ rad/sec.   Inlet pressure $p_1 = 90$ psia.
$\lambda = 0.35$.
$\sigma = 4000$ psi   (design stress).
$\rho = 8.8 \times 10^{-3}$ slug/in.^{3} (alloy steel).
b = blade width = $\frac{3}{4}$ in.

Find the wheel diameter and blade height.

$$v = \frac{RT}{p} = \frac{53.3 \times 1660}{90 \times 144} = 6.82 \quad \text{ft}^3/\text{lb}$$

Using equation 128

$$D = \frac{(144)(8.8 \times 10^{-3})(380)(0.85)(6.82)(30)}{(\pi)(4000)(0.35)} = 19.0 \quad \text{in.}$$

Using equation 126

$$R_A = \frac{24 \times 4000}{(8.8 \times 10^{-3})(0.75)(380)^2(19)} = 5.32$$

Hence

$$l = b R_A = 0.75 \times 5.32 = 3.98 \quad \text{in.} \quad \text{(say, 4 in.)}$$

$$\text{Wheel diameter} = 19.0 - 4.0 = 15.0 \quad \text{in.}$$

REFERENCES

1. H. J. CLYMAN, "Jet Propulsion and Gas Turbines in Aviation," *S.A.E.J.*, Vol. 54, No. 3, March, 1946, p. 26.
2. C. W. TERRY, "Vistas Wide, Complex for Jet Propulsion Use," *S.A.E.J.*, Vol. 54, No. 2, February, 1946, p. 28.
3. W. R. HAWTHORNE, "Factors Affecting the Design of Jet Turbines," S.A.E. Annual Meeting, Detroit, Mich., Jan. 7–11, 1946.
4. H. ROXBEE COX, "British Aircraft Gas Turbines," *J. Aero. Sci.*, February, 1946, pp. 53–87.
5. J. FOSTER, JR., "Comprehensive Chronology of British Turbojet Developments," *Aviation*, April, 1946, pp. 78–81.
6. N. C. PRICE, "Mechanical Design Considerations Influencing Blading Performance in Aircraft Gas Turbine Power Plants," S.A.E. Annual Meeting, Detroit, Mich., Jan. 7–11, 1946.
7. R. C. SCHULTE, "Design Analysis of BMW 003 Turbojet," *Aviation*, March, 1946, pp. 55–68.
8. J. FOSTER, "Design Analysis of Westinghouse 19-B Yankee Turbojet," *Aviation*, January, 1946, pp. 60–68.
9. W. G. LUNDQUIST and R. W. COLE, "Performance Characteristics of the BMW 003 Turbojet Engine and a Comparison with the JUMO 004," S.A.E. National Aeronautic Meeting, New York, April 3–5, 1946.
10. W. F. DURAND, "Jet Propulsion," *Mechanical Engineering*, March, 1946, pp. 191–193.
11. G. FLÜGEL, *Die Dampfturbinen*, Julius Springer, Berlin.
12. W. SPANNHAKE, *Centrifugal Pumps, Turbines, and Propellers*, authorized translation by JOHN B. DRISKO, Technology Press, Massachusetts Institute of Technology, Cambridge, 1934.
13. W. R. NEW, "An Investigation of Energy Losses in Steam-Turbine Elements by Impact Static Test with Air at Subacoustic Velocities," *Trans. A.S.M.E.*, August, 1940, pp. 489–502.
14. S. A. MOSS and C. W. SMITH, "Energy Transfer between a Fluid and a Rotor for Pump and Turbine Machinery," *Trans. A.S.M.E.*, August 1942, pp. 567–597.
15. J. R. WESKE, "Investigation of Blade Characteristics," *Trans. A.S.M.E.*, July, 1944, pp. 413–420.
16. A. STODOLA (L. LOWENSTEIN), *Steam and Gas Turbines*, McGraw Hill Book Co., New York, 1927, Vols. 1 and 2.
17. J. KEENAN, *Thermodynamics*, John Wiley & Sons, New York, 1941.
18. W. KERR, "The Steam Friction of Turbine Wheels," *Engineering* (London), 1913, Vol. 96, p. 268.

THE COMBUSTION CHAMBER

1. Introduction

The function of the combustion chamber is the same in either the gas-turbine power plant or the turbojet engine. It is the component wherein fuel is introduced and burned to raise the temperature of the working fluid to the desired value. The fuel is burned in a primary air stream, where the air-fuel ratio is close enough to the stoichiometric ratio to initiate combustion, and finally the products of complete combustion are cooled by mixing them with the balance of the air flow; there is, therefore, the problem of securing an intimate mixture of the cool and hot stream in addition to the combustion problem. Since the maximum allowable temperature of the final mixture is dictated by the permissible operating temperature for the turbine blading it is important that the final mixture be of uniform temperature throughout.

The principal requirements for the combustion chamber are: (a) low weight and small frontal area; (b) low pressure loss; (c) stable and efficient combustion over the operating flight altitudes and speeds; (d) reliability, serviceability, and reasonable life; and (e) thorough mixing of the hot and cold fluid streams to give a uniform temperature distribution throughout the final mixture arriving at the inlet to the turbine.

Since some of these requirements call for conflicting design features the final design is a compromise to obtain the most satisfactory overall result. To illustrate, it has been pointed out in Chapter 7 that low pressure loss is extremely desirable from the point of view of plant efficiency. To secure the lowest pressure loss the ducts should be large and the velocities small. This, however, is in direct conflict with the requirements of low weight, low frontal area, and thorough mixing. Furthermore, since all the processes involve such phenomena as turbulence, chemical reaction rates, and energy transfer which have not been harmonized into a single coordinated theory of combustion, the design of combustion chambers has to be based on experimental data. Nevertheless, many of the individual processes in-

volved are well understood from research in other fields, and the available knowledge is helpful in guiding experimental work and in making preliminary judgments. These will be discussed briefly.

2. Combustion Process

The combustion problem differs from that encountered in stationary plants and internal-combustion engines in that the fuel must be burned in a rapidly moving body of air, and the overall air-fuel ratio greatly exceeds the stoichiometric ratio. In general, the fuels employed are liquid hydrocarbons. It is worth mentioning here that considerable experimentation is being conducted both here and abroad with coal-burning combustion chambers for use in stationary gas-turbine plants and locomotive gas turbines. The reported results appear encouraging.[1] For the purposes at hand, the discussions which follow are limited to combustion chambers for liquid hydrocarbon fuels.

The fuel may be introduced into the combustion chamber in the form of a fine spray, it may be vaporized outside the combustion chamber, or it may be vaporized inside the combustion chamber. Investigations by the British indicate that external vaporization has not been as satisfactory as liquid-spray injection.[2,3] Internal vaporization when properly developed has given good results. Irrespective of the means employed for introducing the fuel the objectives sought are identical: to prepare the fuel so that it will unite readily with the oxygen in the air and ignite rapidly.

The problem of burning atomized liquid fuel has received considerable study in its applications to stationary oil burners and quite intensive study in its application to internal-combustion engines. Since the observations made in these two fields give an insight into the problems encountered in burning liquid fuels in turbojet-engine combustion chambers they will be reviewed briefly.

It was pointed out by H. Ricardo [4] that there are three distinct stages in the combustion of a liquid fuel in a diesel engine. These three stages are related to three distinct processes which must take place from the instant a fuel droplet finds itself in the combustion air and finally bursts into flame. The first stage is a slow vaporization of the fuel particle accompanied by a catalytic oxidation at low temperature; the second is a slow oxidation of the fuel vapor; and the third is the ignition of the fuel and combustion.

The time required to complete the first process is a function of the fineness of atomization of the fuel, its boiling point, the predominating temperature, and the turbulence in the combustion chamber.

The fact that this low-temperature vaporization process can and actually does take place in diesel engines and the factors influencing it are reported in reference 5 and discussed in reference 6.

During the second process the hydrocarbon fuel goes through a series of reactions which produce partly oxidized compounds such as aldehydes. Then the third process occurs, which is the thermal decomposition of the fuel, followed by the combustion of the partly oxidized products.[7, 8]

Of the three processes, the slow oxidization in the vapor phase appears to be the most important since it is related directly to what is termed "ignition lag." This process is speeded up if the temperature is increased or if ignition promoters are added to the fuel to assist in the formation of compounds which reduce the time for slow oxidation. If the time that the fuel stays in the combustion chamber is insufficient to permit the combustion process to complete itself no ignition will take place. Consequently, the maximum velocity of the air flowing through the combustion chamber is limited by the aforementioned considerations.

As far as injection of the liquid fuel is concerned, the appropriate injection pressures and the design of the atomizing nozzles do not appear to be radically different from those for stationary oil burner practice. The importance of thorough atomization is apparent from the preceding because of its bearing on fuel vaporization and the slow oxidation stage which takes place in the vapor phase. Increasing the ease of vaporization promotes the attainment of the vapor phase and subsequent ignition. It should be realized, however, that complete vaporization of the fuel before ignition is unnecessary and actually has not been satisfactory in practice. Sufficient vaporization is necessary, however, to promote the combustion processes. Thereafter the heat developed during combustion completes the vaporization of the fuel by radiation and conduction.

According to reference 9 extremely fine atomization of the fuel does not appear to be necessary to secure good combustion. Nevertheless, there is reason to believe that the requirements for thorough mixing of the fuel and air are of great importance, and the accomplishment of that objective is assisted by fine atomization. The smaller the fuel particles, the easier it is for the air to carry them. The mixing, however, cannot be accomplished by atomization alone. It requires, in addition, that the air movement be sufficiently turbulent. Turbulence can be achieved by so designing the flow passages that the Reynolds number of the flowing air will be large enough to give fully developed turbulent motion. The amount of turbulence

must, however, be limited to conform with the pressure loss that can be tolerated. Consequently, one of the major problems in the design of the combustion chamber is to produce the maximum turbulence with the minimum pressure drop. This problem has to be worked out experimentally for each physical arrangement.

The process of securing a thorough mixing of the cold air with the hot products of combustion must be given careful consideration. This is one of the major problems with internal vaporizing systems. Otherwise, gases which are too hot, and even flame, may enter the turbine and cause damage. The objectives should be to secure thorough mixing in the shortest length; otherwise the length and weight of the combustion chamber may be excessive. The best arrangement of parts to accomplish the above will depend on the geometry of the combustion chamber and its general design features. The final arrangement has to be determined empirically.

Figure 1 illustrates schematically the basic construction of the tubular type of combustion chamber used in certain turbojet engines.
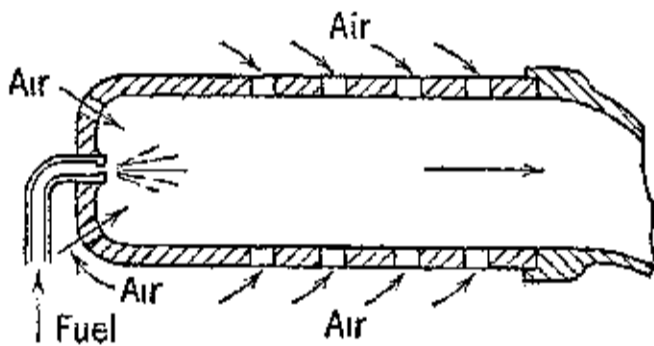
FIG. 1. General operating principle of the tubular combustion chamber.

It consists of a tube with a fuel injection nozzle at one end and a series of air admission holes disposed along its length. The fuel-air mixture ratio is richer at the injection end, and the fuel spray continues to burn as it moves through the chamber until it has encountered sufficient air to give complete combustion. According to F. C. Mock [9] the velocity of the fuel leaving the nozzle is of the order of 100 fps and that of the air at full load is about 120 fps. The length of the flame body appears to be a function of the fuel-air ratio and is practically independent of the rate of fuel feed. The richer the mixture, the larger the flame body. Since the combustion chamber is ordinarily designed to give a definite maximum body of flame under steady operation at full power, and since the maximum outlet temperature is limited, the flame body decreases in size with the leaner fuel-air mixtures at decreased loads.

Problems, therefore, arise in maintaining stable combustion under all operating conditions. There are two important limiting mixture ratios: (1) the leanest or flame extinction limit, and (2) the richest or ignition limit. If the fuel-air ratio is leaner than the first limit, flame propagation ceases; if it is richer than the second, combustion cannot be initiated. Measurements in an experimental combustion

chamber indicate that the flame-extinction limit is leaner than the ignition limit and that the absolute pressure has no influence on either limit.[18]   These tests also indicated that increasing the temperature improves the ignition limit, while improving the atomization aids the flame-extinction limit.   Attention must be given, therefore, in the development of a combustion chamber to the problem of securing stable combustion over the entire range of operation and quick ignition.   These problems are more difficult to solve in this liquid-fuel application than for stationary oil-burning installations because of the high air velocities and the absence of radiation surfaces.
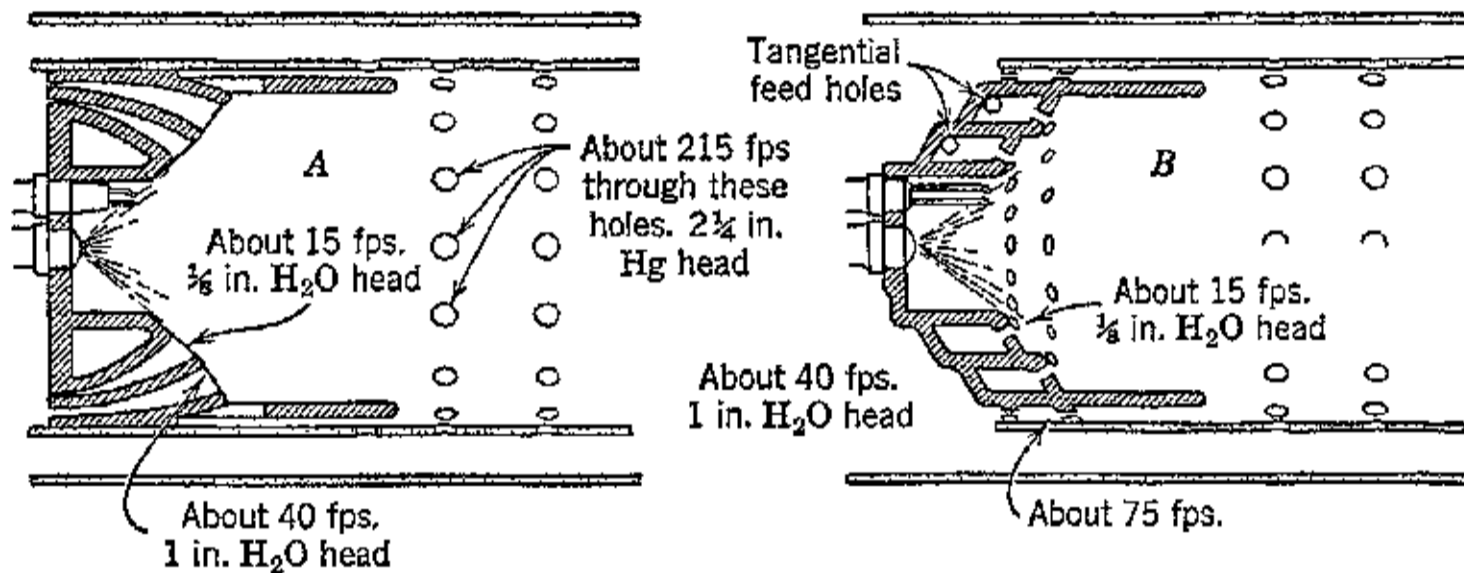
Fig. 2.   Examples of graduated air velocity combustion chambers.   (Reproduced from F. C. Mock, *Jour. S.A.E.*, May 1946.)

The developments in this connection have been described by F. C. Mock,[9] and they appear to be based on controlling the turbulence of the air fed to the flame as it progresses through the combustion chamber.   The tests described indicate that any means which shelters the conical fuel spray in the initial ignition stages from the high-velocity air currents improves the stability of combustion under idling conditions and aids the starting of ignition.   There are several approaches to securing the desired graduated turbulence required for attaining the foregoing objectives.   Two methods described by Mr. F. C. Mock are illustrated in Fig. 2.   The objectives of these two arrangements are to produce a shielded central stable flame which is fed by relatively gentle reverse air currents, and thereafter to feed the supplemental air to the flame with increasing velocities as it progresses down the chamber until combustion is completed.

A factor bearing upon the ignition problem appears to be the position of the fuel spray cone with reference to the spark plug.*   The results obtained from the tests of a single burner [9] at different air-

---

* The use of torch igniters, combination of spark plug and its own injection system, is becoming the practice in British designs.

flow rates with fixed spark-plug position are illustrated in Fig. 3.
It is seen that ignition conditions were most favorable when the spray
cone was slightly outside the spark-plug gap; when the spray cone
was in the region of the spark-plug points there was no stable ignition.
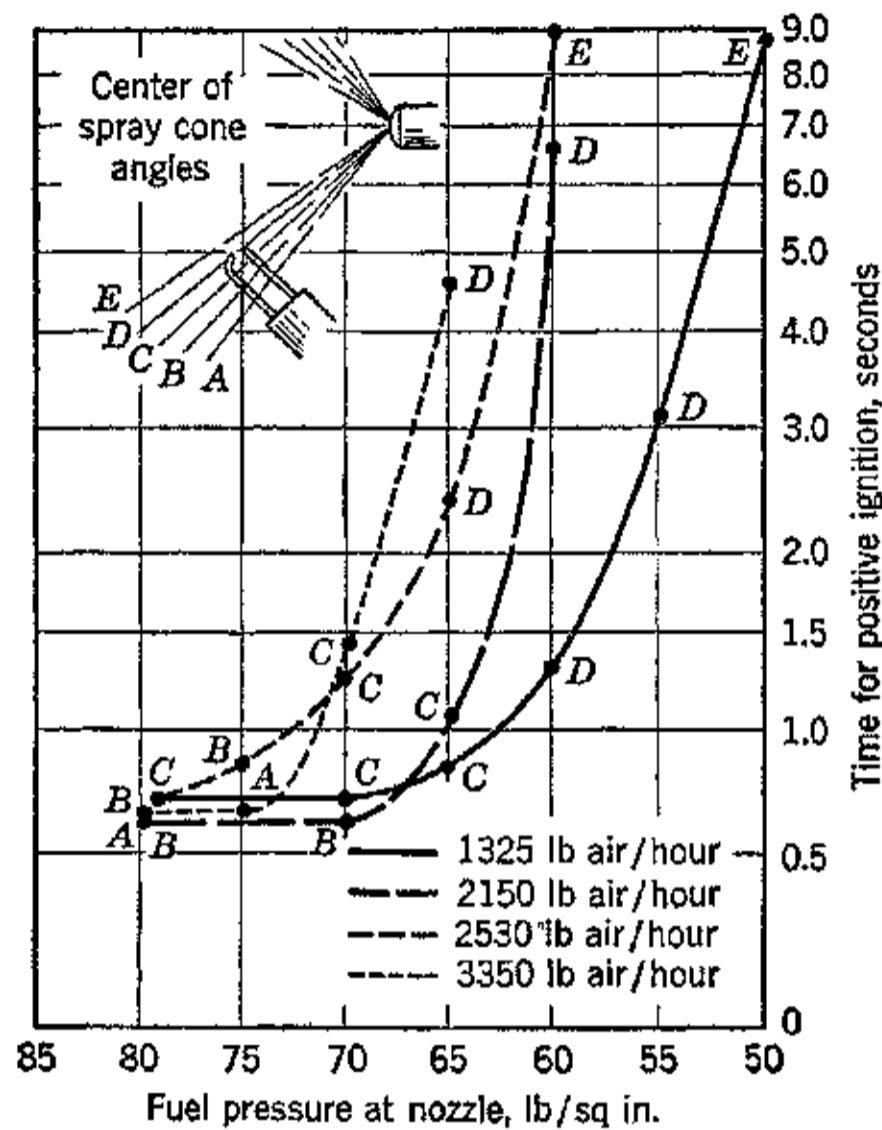
FIG. 3.   Tests of factors affecting ease of ignition.   (Reproduced from F. C. Mock, *loc. cit.*)

3. Flow Phenomena

The flow conditions for the combustion chamber can be illustrated
by considering the duct of constant cross-sectional area illustrated
in Fig. 4.   For simplicity the velocity w is assumed to be uniform
throughout the entire cross section and the coordinates p, γ, and T,
are constant.   Further, let c_p be constant, so that $k = c_p/c_v$ is also
constant.   For a constant-weight flow of mixture, G_m lb/sec, the con-
tinuity equation (see Chapter 3) is

$$G_m = \frac{Aw}{v} = \text{Constant} \tag{1}$$

Hence, since G_m and A are constant

$$\frac{dw}{w} - \frac{dv}{v} = 0 \tag{2}$$

The momentum of the fluid entering the element at the left is $(G_m/g)w$. Similarly the momentum of the fluid leaving the right-hand face is $(G_m/g)(w + dw)$. Hence, substituting for G_m from equation 1, the change in momentum is $A(\gamma/g)w\,dw = A\rho w\,dw$. The net external force, neglecting wall friction, is $-A\,dp$. Hence

$$-dp = \frac{\gamma}{g}w\,dw = \frac{1}{vg}w\,dw \tag{3}$$
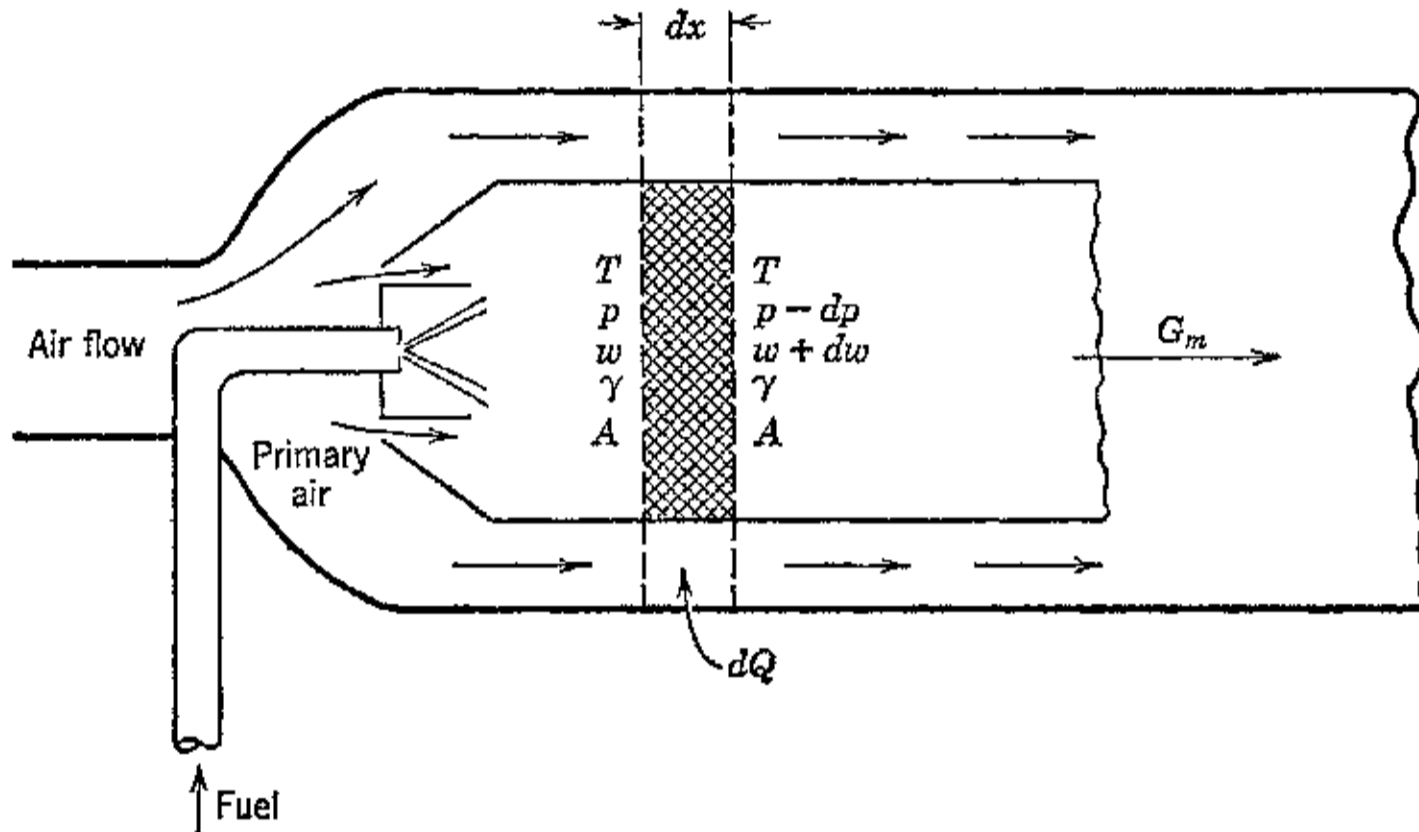
FIG. 4.   Flow with heat transfer in a constant-area duct.

Since the gas does no external work, and assuming no elevation change, it follows from Chapter 3 that the energy equation is

$$J\,dQ = dh + \frac{w}{g}dw = d\left(h + \frac{w^2}{2g}\right) \tag{4}$$

If it is assumed that the mixture is homogeneous and follows the laws of perfect gases, then substituting for h in equation 4 from equation $1\cdot57$ gives

$$J\,dQ = d\left(\frac{w^2}{2g} + \frac{k}{k-1}pv\right)$$

$$= \frac{w}{g}dw + \frac{k}{k-1}p\,dv + \frac{k}{k-1}v\,dp$$

Substituting for dp and dv from equations 2 and 3

$$J\,dQ = \frac{w}{g}dw + \frac{gkpv}{(k-1)g}\frac{dw}{w} - \frac{k}{k-1}v\frac{1}{vg}w\,dw$$

Hence

$$\frac{g}{w} J \, dQ = dw \left(1 + \frac{1}{(k-1)M^2} - \frac{k}{k-1} \right)$$

where, as before, M is the Mach number.

Rearranging and solving for $J \, dQ$ gives the following

$$J \, dQ = \frac{1 - M^2}{(k-1)M^2} \cdot \frac{w}{g} dw \qquad (5)$$

The effect of adding heat to the working fluid is to increase its specific volume. Since the weight rate of flow is presumed constant as indicated by equation 1, the fluid velocity is increased by the heat addition, and with it the local Mach number. Since the air enters the combustion chamber with subsonic velocity, its Mach number can increase only until the local acoustic velocity ($M = 1$) is reached at the outlet of the combustion chamber. This signifies that the maximum amount of heat that can be added is that required to accelerate the heated gases to the local sonic velocity. According to reference 10 this so-called *rich mixture* or *choking limit* has never been attained in turbojet combustion chambers because of the limitations imposed on pressure loss. It can be reached, however, in the case of tail pipe burning where fuel is burned upstream to the exhaust nozzle to increase thrust.

4. Pressure Loss in Combustion Chamber

The total loss in static pressure by the gases flowing through the combustion chamber consists of the pressure drop due to friction Δp_F and the differential pressure $(p_1 - p_2)$ required to accelerate the fluid from its entering velocity to the exit velocity. From Chapter 3, the total pressure-change equation for a fluid is

$$dp = -\rho f \frac{w^2}{2m} dx - \rho w \, dw \qquad (6)$$

where $\rho = \gamma/g$ = density of fluid in slugs per cubic foot.

The friction loss is readily calculated from the gas velocity, friction coefficient, diameter, and length. The discussion which follows is concerned with evaluating the differential pressure $(p_1 - p_2)$. This is most conveniently accomplished by applying the analysis used in reference 11.

The pressure loss of a gas flowing with heat transfer and no friction is given by

$$dp = -\rho w \, dw \qquad (7)$$

Since the cross-sectional area of the combustion chamber is constant ρw = constant. Hence, integrating equation 7,

$$\int_1^2 dp = -\rho w \int_{w_1}^{w_2} dw$$

or

$$p_2 - p_1 = -\rho_2 w_2{}^2 + \rho_1 w_1{}^2 \tag{8}$$

Substituting for $\rho = p/gRT$, from the characteristic equation, and introducing the Mach number $M^2 = w^2/gkRT$, equation 8 becomes

$$p_2 - p_1 = -kp_2 M_2{}^2 + kp_1 M_1{}^2 \tag{9}$$

Rearranging and solving for the pressure loss ratio

$$\frac{p_1}{p_2} = \frac{(1 + kM_2{}^2)}{(1 + kM_1{}^2)} \tag{10}$$

Equation 10 relates the pressures and Mach numbers for flow with heat transfer and constant flow area, and is the equation of a Rayleigh line.[10, 11]

It was shown in Chapter 3 that, in flow in a passage of constant cross-sectional area A, since $G = \dfrac{pA}{RT} w$ for a perfect gas,

$$\frac{w}{T} = \frac{RG}{pA} \tag{11}$$

The values of w and T can be obtained from Chapter 3; the appropriate equations are repeated here for convenience; thus

$$w = \sqrt{\frac{kgRT_t M^2}{1 + \left(\dfrac{k-1}{2}\right) M^2}} \tag{12}$$

and

$$T = \frac{T_t}{1 + \left(\dfrac{k-1}{2}\right) M^2} \tag{13}$$

where T_t is the stagnation temperature.

Substituting equations 12 and 13 into equation 11 yields

$$\frac{RG}{A} = p \sqrt{\frac{kgRM^2 \left\{ 1 + \left(\dfrac{k-1}{2}\right) M^2 \right\}}{T_t}} = \text{Constant} \tag{14}$$

Hence

$$p_1 \sqrt{\frac{kgRM_1{}^2\left[1 + \left(\frac{k-1}{2}\right)M_1{}^2\right]}{T_{t1}}}$$

$$= p_2 \sqrt{\frac{kgRM_2{}^2\left[1 + \left(\frac{k-1}{2}\right)M_2{}^2\right]}{T_{t2}}} \qquad (15)$$

Combining equations 15 and 10

$$\frac{M_2 \sqrt{1 + \left(\frac{k-1}{2}\right)M_2{}^2}}{1 + kM_2{}^2} = \frac{M_1 \sqrt{1 + \left(\frac{k-1}{2}\right)M_1{}^2}}{1 + kM_1{}^2} \sqrt{\frac{T_{t2}}{T_{t1}}} \qquad (16)$$

Equation 16 relates the entering and exit Mach numbers for flow in a constant-area duct with heat transfer and no friction. Since
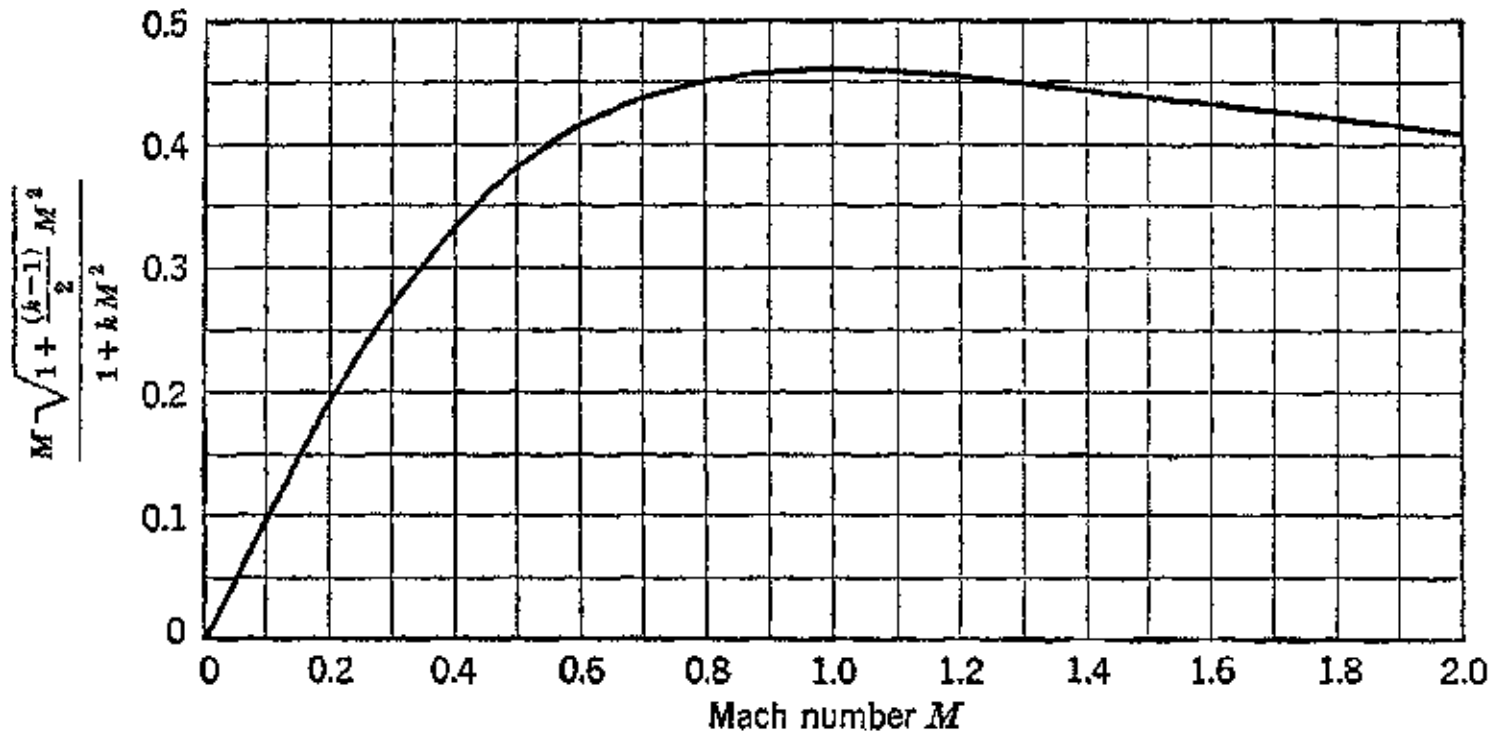
FIG. 5. Mach number relationships for heating of a fluid flowing in a constant-area duct with no friction.

the initial Mach number is known and the desired stagnation temperature ratio is readily calculated, the final Mach number is readily determined from Fig. 5; the curve is based on $k = 1.38$, which is reasonably close for the gases flowing through the combustion chamber. Once the final Mach number has been determined the pressure ratio required to accelerate the gases is determined from equation 10.

If the entering velocity is subsonic, heating causes acceleration of the gases. On the other hand, if the entering velocity is supersonic,

as in supersonic ramjets, heating causes deceleration of the gases; that is, the gases must actually be cooled in order to be accelerated. This indicates why sonic velocity at the exit of the combustion chamber has not been attained or exceeded. If there is a maximum allowable temperature to be reached in the combustion chamber, then
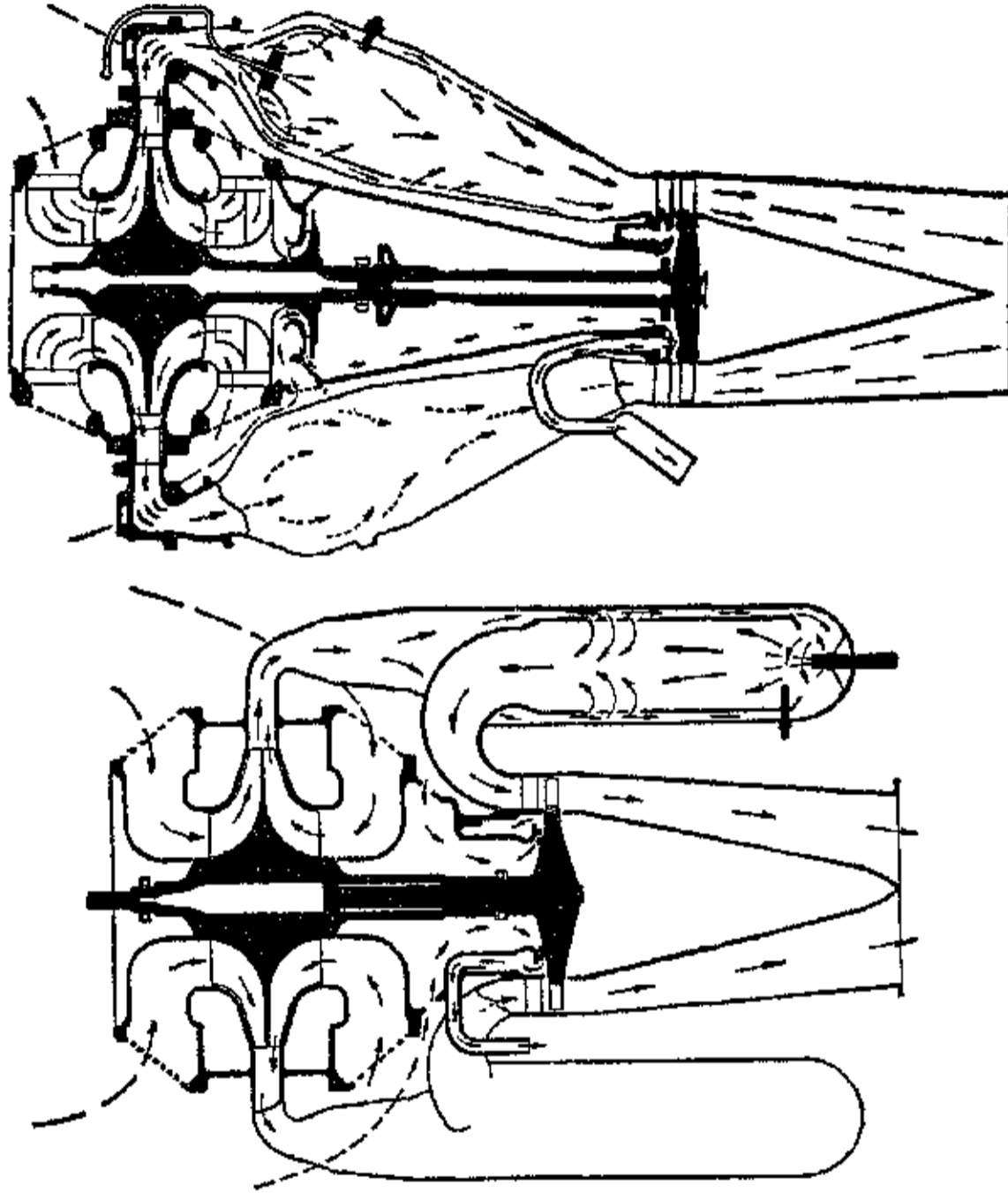
FIG. 6. Comparison of "return-flow" and "straight-through" combustion systems on double-sided impeller engines. (Reproduced from H. R. Cox., *J. Inst. Aero Sci.*, February 1946.)

a maximum temperature may be reached at some location upstream to the exit section and thereafter the velocity decreases from the acoustic value so that its final Mach number is less than unity.

The total pressure loss in the combustion chamber is, of course, the sum of the losses $\Delta p_F + (p_1 - p_2)$.

In comparing the pressure-loss performance of combustion chambers, it is convenient to express the pressure loss in terms of the percentage of the total pressure at the entrance to the combustion chamber.

5. Combustion-Chamber Arrangements and Operating Characteristics

The general practice is to employ several combustion chambers of cylindrical shape symmetrically disposed around the turbine inlet. For turbojet engines the length/diameter ratios vary from 2.25 to 5.0, and the heat releases obtained range from 1.5 to 4.0×10^6 Btu/ft^3/hr.[10] In general the constructions which have been used may be segregated into three basic types: (a) the return-flow combustion system, (b) the straight-through combustion system, and (c) the annular combustion chamber. Types (a) and (b) are illustrated in Fig. 6 taken from reference 2. The advantages and disadvantages of systems (a) and (b) as analyzed by reference 10 are presented in Table 11·1. It appears that the straight-through system when properly developed should have one important advantage, that is, it can be designed to operate with a smaller pressure drop for the same overall diameter.

TABLE 11·1

COMPARISON OF RETURN-FLOW AND STRAIGHT-THROUGH COMBUSTION SYSTEMS

(H.R. Cox, *J. Inst. Aero. Sci.*, February, 1946)

Return-Flow Combustion System			Straight-Through Combustion System
1.	+	−	Requires a longer shaft, involving a third bearing and a flexible coupling.
2. Permits automatic compensation of expansion without special joints.	+	−	Requires expansion joints to allow differential expansion.
3. Is such that the turbine stator and rotor blades are shielded from direct high-temperature radiation from the flame.	+	−	Subjects turbine stator and rotor blades to direct high-temperature radiation from the flame with possibly higher metal temperatures.
4. Involves two 180° bends in the path of the gas.	−	+	Involves no bends and so has the lower pressure loss.
5.	−	+	Allows the greater cross-sectional area for combustion within a given overall diameter.
6.	−	+	Is simpler to manufacture.
7. Allows easier location and inspection of burners and easier assembly and removal of combustion chambers.	+	−	
8.	−	+	Should provide the more even air distribution.

REFERENCES

1. *Mech. Eng.*, April, 1946, p. 387.
2. H. Roxbee Cox, "British Aircraft Gas Turbines," *J. Aero. Sci.*, February, 1946, pp. 53–87.
3. W. F. Durand, "Jet Propulsion," *Mech. Eng.*, March, 1946, pp. 191–193.
4. H. Ricardo, *The High Speed Internal Combustion Engine*, D. Van Nostrand Co., New York, 1931, Chapter XIII, pp. 397–415.
5. A. M. Rothrock and C. D. Waldron, *National Advisory Committee for Aeronautics, Report* 545, 1935.
6. C. B. Dicksee, *The High Compression-Ignition Engine*, Interscience Publishers, New York, 1940, Chapter VI.
7. G. D. Boerlage and J. J. Broeze, *Ind. Eng. Chem.*, Vol. 28, 1936, pp. 1229–1234.
8. M. A. Elliott and L. B. Berger, "Combustion in Diesel Engines," *Ind. Eng. Chem.*, September, 1942, pp. 1065–1071.
9. F. C. Mock, "Engineering Development of the Jet Engine and Gas Turbine Burner," S.A.E. Annual Meeting, Detroit, Mich., Jan. 7–11, 1946.
10. W. R. Hawthorne, "Factors Affecting the Design of Jet Turbines," S.A.E. Annual Meeting, Detroit, Mich., Jan. 7–11, 1946.
11. N. P. Bailey, "Thermodynamics of Air at High Velocities," *J. Aero. Sci.*, July, 1944, pp. 227–239.
12. J. Keenan, *Thermodynamics*, John Wiley & Sons, New York, 1941, pp. 334–336.
13. D. G. Samaras, *J. S.A.E.*, May, 1946, p. 227.

THE ROCKET MOTOR

1. Introduction

The first use of rockets cannot be stated with certainty. An old, well-illustrated Chinese manuscript describes the *fire arrow* used by the Chinese against the Mongols in the battle of Pien-King, A.D. 1232. The rockets were attached to conventional arrows to increase their range. It seems probable, however, that the rocket principle was known to the Greeks several centuries earlier. Marcus Graecus in his *Liber ignium*, probably written in the eighth century, discusses *flying fire* and the directions for making it.[1]

Since its earliest beginnings the application of the rocket has oscillated between its wartime use as a weapon and its peacetime application to devices for signaling or pyrotechnic displays. The use of the rocket as a weapon was practically eliminated, however, during the latter part of the nineteenth century by the advances made in the development of artillery with its greater accuracy and increased range. In World War I, the rocket was employed but little as an offensive weapon. In World War II, however, it reappeared as a major offensive weapon employed by all the warring powers, and also as a possible means for propelling aircraft.[26]

The underlying developments which have brought the rocket to its present prominence must be credited to the imagination and efforts of such pioneers as Ziolkovsky (1903) and Alexander Rynin in Russia; H. Oberth, Max Valier, Fritz von Opel, E. Sänger, and others in Germany; Robert Esnault Pelterie in France; and the late Dr. R. H. Goddard in the United States. These men saw in the rocket its great possibilities as a means for attaining *extreme altitudes* and for *space travel*. Despite many discouragements and even ridicule they persisted in their efforts to demonstrate to the scientific world that the rocket principle had the potentialities for attaining the aforementioned objectives.

In the above connection the work of Dr. Goddard was pre-eminent. Although the basic idea of utilizing the rocket principle to attain

extreme altitudes was conceived in the middle of the eighteenth century, Dr. Goddard conducted the first scientific experiments, and his report, published by the Smithsonian Institution in 1919, was the first scientific publication on this subject.[2] It was followed a few years later by noteworthy publications of others. Thus the classic treatise by H. Oberth [3] was published in 1923. This was followed by the work of Dr. W. Hohman,[4] the book by Max Valier [5] in 1925, and the papers of Robert Esnault Pelterie. The excellent book by Dr. Eugen Sänger [6] appeared in 1933.

The particular advantages of the rocket are: (1) its thrust is practically independent of its environment; (2) it requires no atmospheric oxygen for its operation; and (3) it can function in a vacuum. Further, it appears to be the simplest means for converting the thermochemical energy of a propellant combination (fuel plus oxidizer) into the kinetic energy associated with a jet of flowing gases. It will be seen later in this chapter, however, that the efficiency of the rocket type of jet propulsion, on an energy basis, is satisfactory only at extremely high flight speeds, considerably above the speed of sound. Consequently, as a sole source of propulsion for aircraft its propellant consumption is so enormous that endurance of the rocket airplane is limited to flights of a few minutes' duration. The rocket should not be regarded as a competitor of existing means for propelling aircraft but as a device which has the potentialities of attaining objectives unattainable with other propulsion means.

World War II saw the development and use of a variety of rocket weapons. The incentives for their development were their small weight compared to artillery pieces for large-caliber projectiles, the freedom of the rocket launcher from recoil, and the need for equipping infantrymen and aircraft with light-weight large-caliber weapons. Of particular fame are the American, Launcher, Rocket, AT, M-1, commonly known as the *bazooka*, and the Russian *Katusha* which was employed with particular effectiveness in the defenses of Leningrad, Moscow, and Stalingrad. (These are described in reference 7 and in several popular magazines.) Furthermore, the possibilities of the rocket as a propulsion plant for long-range pilotless missiles have been demonstrated by the German V-2 rocket-propelled missile. The Germans also developed a fast intercepter airplane, the ME-163, which employed a liquid-propellant rocket power plant for propelling it.[27] In this country, until recently the application of rocket propulsion to aircraft has been limited to its use as an auxiliary to the airscrew for assisting in the take-off of aircraft, principally for flying

boats.[13]   The British and the Germans have also employed rockets for assisted take-off purposes.

Despite its apparent simplicity, the development of a reliable rocket jet-propulsion system encounters several perplexing problems.   The rocket system must be light in weight, and the rocket motor must be capable of sustained operation in contact with gases at temperature above 5000 F and at appreciable pressures.   The problem of materials is consequently a major one.   Furthermore, owing to the enormous energy releases involved, problems of ignition, smooth start-up, thrust control, cooling, etc., arise.

A major obstacle confronting the workers in this field is the development of better propellant combinations for liquid-rocket motors. This remark is directed particularly to oxidizers.   The selection of propellants is governed by such factors as the maximum energy per minimum total weight (propellants plus containing vessels) and convenience factors such as safety in handling, dependability, corrosive tendencies, cost, availability, and storage problems.   Furthermore, the effective exhaust velocity of the ejected gases must be as high as possible in order to reduce the propellant consumption.   E. Sänger has listed several promising fuels and oxidizing agents, among them liquid hydrogen and liquid ozone.   Practical considerations, however, react against the use of liquid ozone, and Sänger conducted most of his experiments with gasoline and liquid oxygen.   This particular propellant combination has been used by a great many experimenters, but several others have also been tried.   In general, it can be stated that there is a wide variety of fuels that are satisfactory for rocket purposes, but the choice of oxidizers is at present distinctly limited.

For short-duration purposes solid-propellant rockets have been used exclusively.   They have been of two basic types: (1) *unrestricted-burning* types for projectiles and launching rockets; and (2) *restricted-burning* types for the assisted take-off of aircraft and for propelling missiles.   In the unrestricted-burning rocket all surfaces of the propellant grain except the ends are ignited; in restricted-burning rockets only one surface of the propellant is permitted to burn.   Several types of solid propellants have been used.   For unrestricted-burning charges they have been largely modified double-base powders; for restricted charges the propellant is usually a thorough mixture of a solid fuel matrix and a solid oxidizer.   Unrestricted-burning grains made from the type of propellant employing a resinous base fuel have been employed for large-thrust (over 50,000 lb), short-duration (2 sec or less) launching rockets for guided missiles.

For more complete information regarding the historical development of the rocket from its earliest beginnings to modern times the reader is referred to references 1, 7, 8, and 9.

This chapter discusses the more important principles underlying the operation of the rocket motor. The derivations of many of the equations have been presented in Chapter 3, and frequent reference will be made to that chapter.

2. General Principles

The propelling action of a rocket motor is derived from the generation of large quantities of gases by the chemical reaction of suitable propellants within the rocket motor.
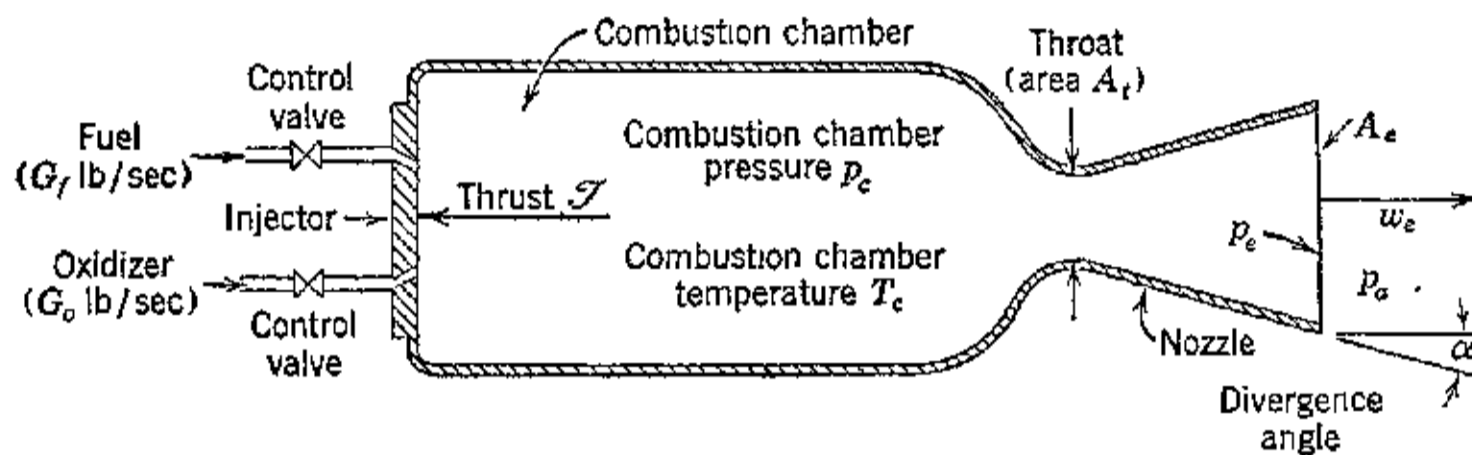
Fig. 1. Principal elements of a bipropellant uncooled rocket motor.

Figure 1 illustrates the principal elements of a bipropellant liquid-rocket motor. It comprises a combustion chamber, a De Laval type of exhaust nozzle, an injection system, and propellant control valves. The propellant gases are produced in the combustion chamber at pressures governed by the chemical characteristics of the propellants, their rate of consumption, and the cross-sectional area of the nozzle throat. The gases are ejected into the atmosphere through the nozzle with supersonic velocity. The function of the nozzle is to convert the pressure of the propellant gases into kinetic energy. The reaction to the discharge of the propellant gases constitutes the thrust developed by the rocket motor.

As pointed out in Section 1, the propellants employed in a rocket motor may be a solid, two liquids (fuel plus oxidizer), or materials containing an adequate supply of available oxygen in their chemical composition (monopropellants). Solid propellants are used for rockets which are to operate for relatively brief periods, up to possibly 45 sec. Their main application is to projectiles, guided missiles, and the assisted take-off aircraft. The shorter-duration units, less

than 3 sec, utilize unrestricted-burning charges, and the larger-duration units employ restricted-burning charges.

Figure 2 illustrates one method for constructing a restricted-burning solid-propellant rocket motor.[18] To obtain the desired action, the propellant (fuel plus oxidizer) characteristics must be such that the propellant burns at a uniform rate at substantially constant pressure in layers perpendicular to the motor axis; that is, the burning is restricted so that it takes place in only one direction. One method for accomplishing this is to bond the propellant charge and the steel wall of the motor chamber with a special flexible sealing
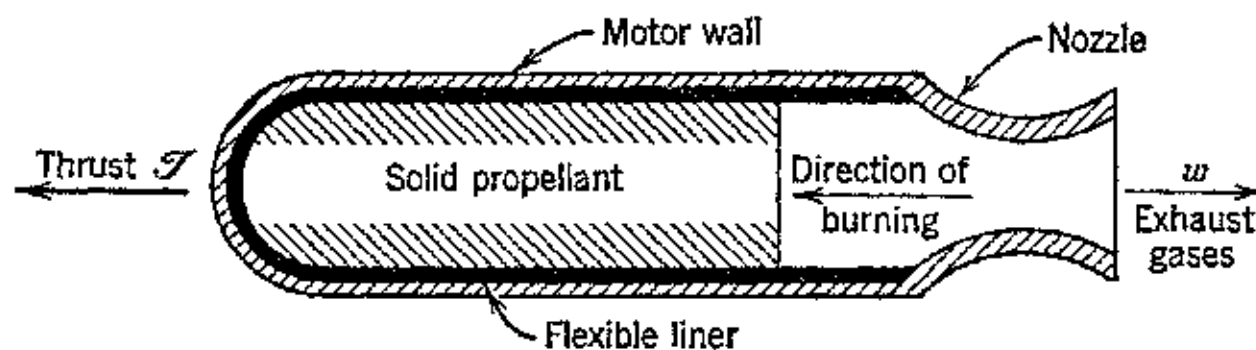
FIG. 2. One type of restricted-burning solid-propellant rocket motor. (Reproduced from M. J. Zucrow, *Jour. S.A.E.*, July 1946.)

material, or liner, which allows the propellant stick the freedom of motion it requires for adapting its shape to the deformations produced by the gas pressure, thermal expansion differences, and internal stresses. The liner material is selected upon the basis of its adherence to the propellant, non-burning characteristics, and elastic properties.

Figure 3 illustrates the essential components for a bipropellant liquid-rocket jet-propulsion system. The propellants are removed from the supply tanks at the rate of G lb/sec; the rate of fuel flow is G_f lb/sec, plus the rate of oxidizer flow G_0 lb/sec. At section 1 the pressure of the propellants is raised by some suitable pressurizing means, and at section 2 the propellants are forced into the combustion chamber against the combustion-chamber pressure. The pressurizing means may be an inert gas held in a separate container at high pressure or some form of pumping plant operated by a gas turbine which obtains its working fluid from the reaction of rocket propellants.[17]

A liquid-rocket jet-propulsion system can be started and stopped at will by the remote operation of the propellant control valves. This cannot be done with solid-propellant systems; once they have been started they can be stopped at will but not restarted.
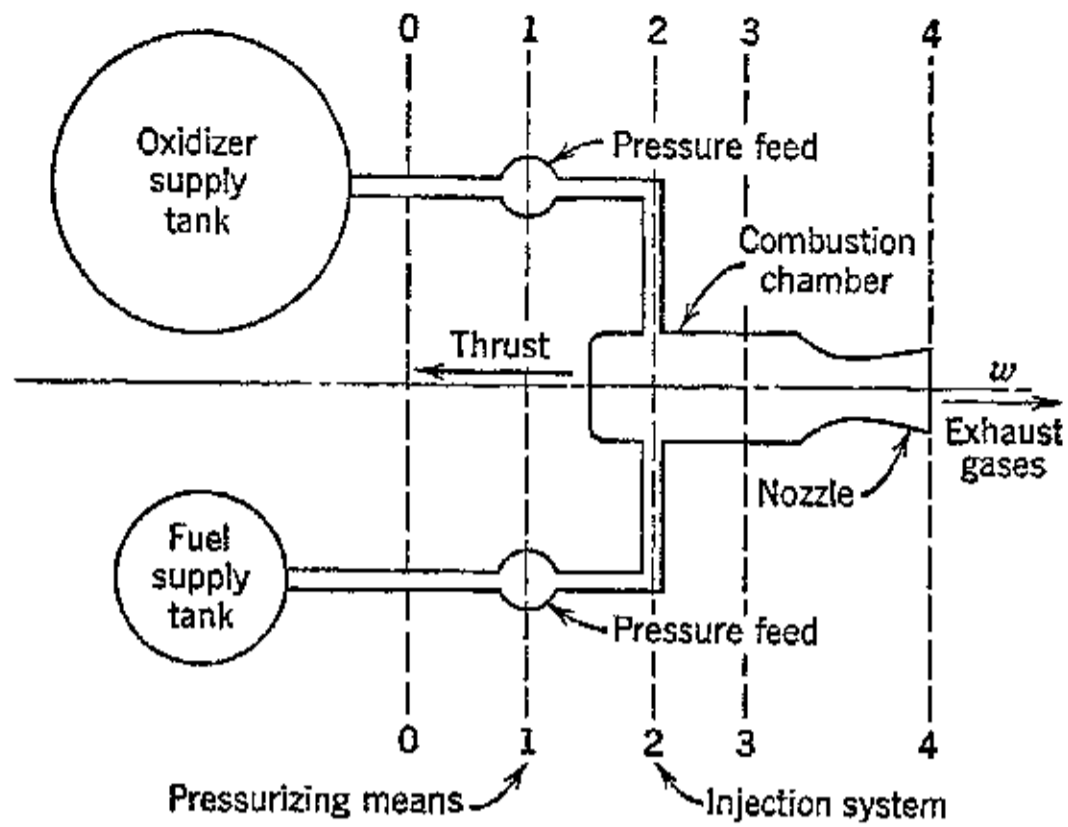
FIG. 3. Elements of liquid-propellant rocket jet propulsion system.
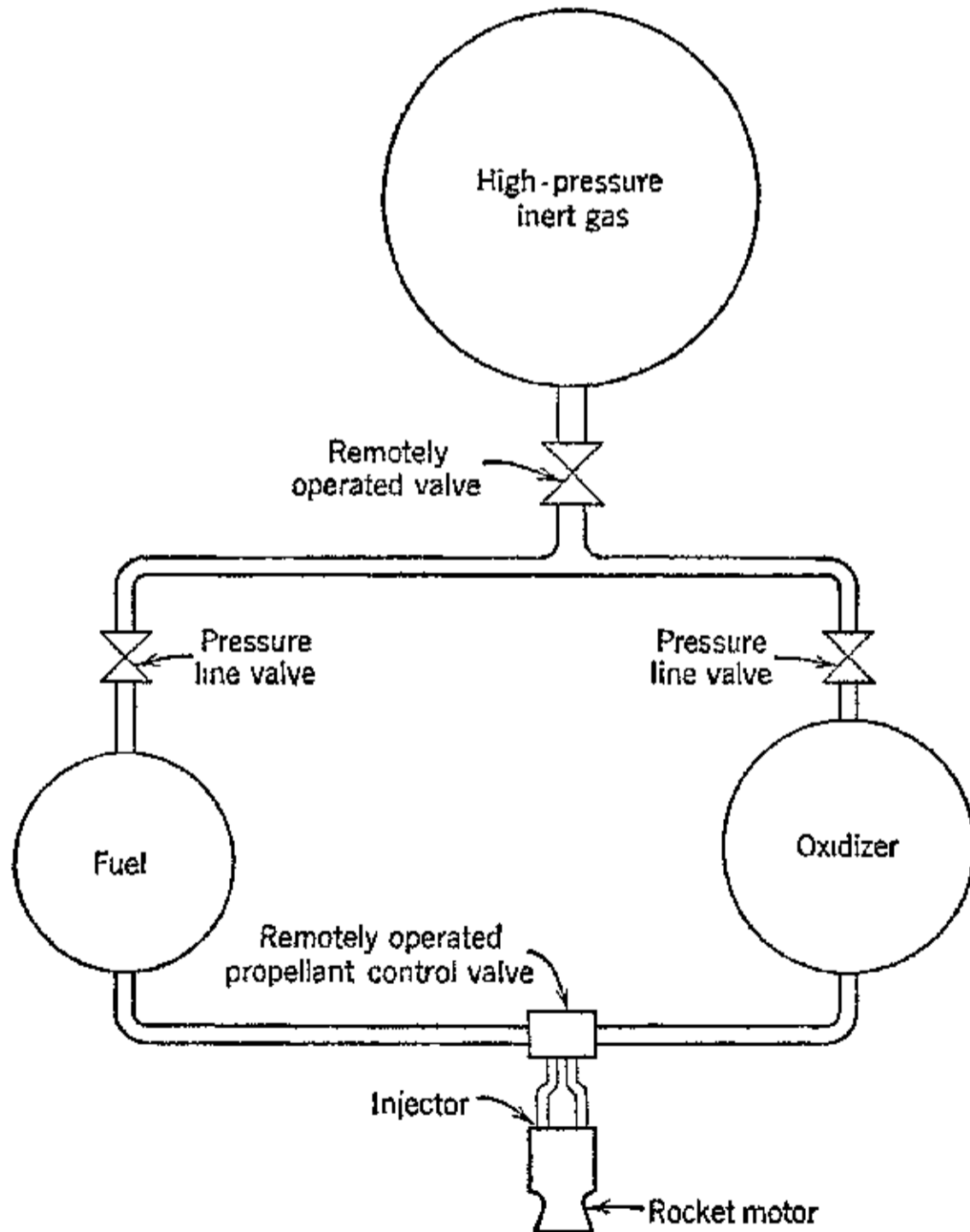
FIG. 4. Bipropellant rocket jet propulsion system employing a high-pressure inert gas to pressurize the propellants.

469

The injection system through which the liquid propellants flow into the combustion chamber is usually designed to atomize the propellants as they enter or as several pairs of the two liquid streams impinge upon each other. To start the operation of the rocket motor
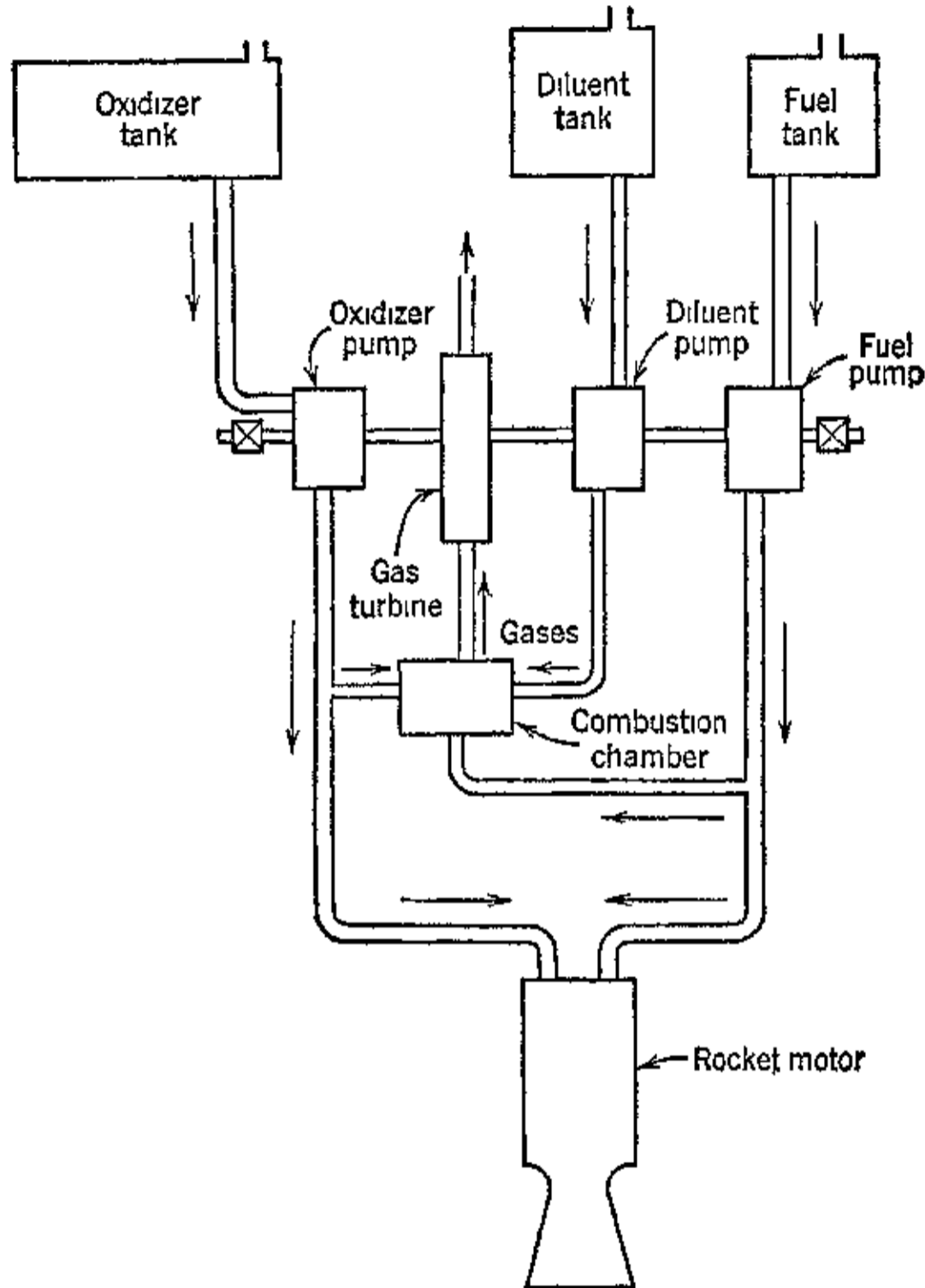
FIG. 5. Elements of turbo-rocket power plant.

an electric igniter may be necessary with some propellants, but propellants which ignite spontaneously on contact with each other are most frequently employed and are preferable.

Figure 4 illustrates schematically the essential components of a rocket jet-propulsion system employing an inert gas under pressure for feeding the propellants to the rocket motor. The system consists of the oxidizer and fuel tanks, the propellant control valves, the rocket motor, and the high-pressure inert-gas storage tank. This type of system is satisfactory for operating durations up to possibly

45 sec. For longer operating periods the tank weights become excessive. Developments have been conducted to eliminate the inert high-pressure gas and employ gases generated by reacting the propellants for pressurizing. In such a system the propellant tanks must be able to withstand the expulsion pressure that is required.

The limitations imposed by gas pressurizing, either stored inert gas or gases generated by reacting propellants, stimulated the development of pumping systems for feeding propellants to the rocket motor. Figure 5 illustrates the principal elements of such a system. It should be realized, however, that the design features of an actual pumping plant are governed by the specific propellants employed and the number of rocket motors to be fed.

Modern pumping systems utilize a gas turbine to drive the propellant pumps; but reciprocating engine-driven pumping systems have been investigated experimentally. The high-pressure high-temperature gases for driving the turbine are produced in a gas generator by reacting suitable propellants. These need not be the same propellants that are fed to the rocket motors. If the temperature of the combustion-chamber gases is excessive a diluent is mixed with them in the gas generator to reduce the gas temperature to a safe value. Usually the diluent is a mixture of water and alcohol.

Turbine-driven pumping units of this type have been built for the acid-aniline propellant system, the liquid oxygen-methyl alcohol system, the hydrogen peroxide-hydrazine methyl alcohol system, and the nitromethane monopropellant system.

The best-known gas turbine-driven pumping units are the one in the German V-2 missile, and the Walter rocket power plant used for propelling the ME-163 airplane. In the V-2 unit the gases for the turbine are produced by reacting concentrated hydrogen peroxide

TABLE 12·1

WEIGHT BREAKDOWN, WALTER POWER PLANT 109–509A-1

Motor	80.96 lb
Propellant control valves	31.9
Steam generator	36.96
Framework	71.72
Pumps and turbine	57.2
Piping	32 56
Motor gear box	42.46
Electrical apparatus	13.86
Control levers	0.88
Total	368.5 lb

TABLE 12·2

VALUES OF FUNCTIONS OF k

k	$\dfrac{1}{k}$	$\sqrt{k}$	$\dfrac{1}{k-1}$	$\dfrac{k}{k-1}$	$\sqrt{\dfrac{k}{k-1}}$	$\dfrac{2gk}{k-1}$	$\sqrt{\dfrac{2gk}{k-1}}$	$\dfrac{k}{k+1}$	$\sqrt{\dfrac{k}{k+1}}$	$\dfrac{k-1}{k}$
1.10	0.9091	1.049	10.00	11.00	3.317	707.83	26.61	0.5238	0.7237	0.0909
1.15	.8696	1.072	6.667	7.667	2.769	493.36	22.21	.5349	.7314	.1304
1.20	.8333	1.095	5.000	6.000	2.449	386.09	19.65	.5455	.7385	.1667
1.21	.8265	1.100	4.762	5.762	2.400	370.77	19.26	.5475	.7399	.1736
1.22	.8197	1.105	4.545	5.545	2.355	365.81	18.89	.5495	.7413	.1803
1.23	.8130	1.109	4.348	5.348	2.313	344.13	18.55	.5516	.7427	.1870
1.24	.8065	1.114	4.167	5.167	2.273	332.49	18.23	.5536	.7440	.1936
1.25	.8000	1.118	4.000	5.000	2.236	321.74	17.94	.5556	.7454	.2000
1.26	.7937	1.123	3.846	4.846	2.201	311.83	17.66	.5575	.7467	.2064
1.27	.7874	1.127	3.704	4.704	2.169	302.69	17.40	.5595	.7480	.2126
1.28	.7813	1.131	3.571	4.571	2.138	294.13	17.15	.5614	.7493	.2188
1.29	.7752	1.136	3.448	4.448	2.109	286.22	16.92	.5633	.7505	.2248
1.30	.7692	1.140	3.333	4.333	2.082	278.82	16.70	.5652	.7518	.2308
1.31	.7634	1.145	3.226	4.226	2.056	271.93	16.49	.5671	.7531	.2366
1.32	.7576	1.149	3.125	4.125	2.031	265.44	16.29	.5690	.7543	.2424
1.33	.7519	1.153	3.030	4.030	2.007	259.32	16.10	.5708	.7555	.2481
1.34	.7463	1.158	2.941	3.941	1.985	253.60	15.92	.5726	.7567	.2537
1.35	.7407	1.162	2.857	3.857	1.964	248.19	15.75	.5745	.7579	.2593
1.36	.7353	1.166	2.778	3.778	1.944	243.11	15.59	.5763	.7591	.2647
1.37	.7299	1.170	2.703	3.703	1.924	238.28	15.44	.5781	.7603	.2701
1.38	.7246	1.175	2.632	3.632	1.906	233.71	15.29	.5798	.7614	.2754
1.39	.7194	1.179	2.564	3.564	1.888	229.34	15.14	.5816	.7626	.2806
1.40	.7143	1.183	2.500	3.500	1.871	225.22	15.01	.5833	.7638	.2857
1.45	.6897	1.204	2.222	3.222	1.795	207.33	14.40	.5918	.7693	.3103
1.50	.6667	1.224	2.000	3.000	1.732	193.04	13.89	.6000	.7746	.3333
1.55	.6452	1.245	1.818	2.818	1.679	181.33	13.47	.6078	.7796	.3548
1.60	.6250	1.265	1.667	2.667	1.633	171.62	13.10	.6154	.7845	.3750
1.65	.6061	1.285	1.539	2.539	1.593	163.38	12.78	.6226	.7891	.3939
1.67	.5988	1.293	1.493	2.493	1.579	160.42	12.67	.6255	.7909	.4012

k	$\frac{k+1}{k-1}$	$\sqrt{\frac{k+1}{k-1}}$	$\left(\frac{k+1}{2}\right)^{\frac{1}{k-1}}$	$\frac{2}{k+1}$	$\sqrt{\frac{2}{k+1}}$	$\left(\frac{2}{k+1}\right)^{\frac{k+1}{2(k-1)}}$	$\Omega*$	$\left(\frac{2}{k+1}\right)^{\frac{k}{k-1}}$	$\frac{2}{k}$	$\frac{1}{\sqrt{k}}$
1.10	21.000	4.583	1.629	0.9524	0.9759	0.5991	0.6284	0.5847	1.818	0.9535
1.15	14.333	3.786	1.620	.9302	.9645	.5955	.6386	.5744	1.739	.9325
1.20	11.000	3.317	1.611	.9091	.9535	.5920	.6485	.5645	1.667	.9121
1.21	10.524	3.244	1.609	.9050	.9513	.5913	.6505	.5626	1.653	.9091
1.22	10.091	3.177	1.608	.9009	.9492	.5906	.6524	.5607	1.639	.9054
1.23	9.696	3.114	1.606	.8969	.9470	.5900	.6543	.5588	1.626	.9017
1.24	9.333	3.055	1.604	.8929	.9449	.5893	.6562	.5569	1.613	.8980
1.25	9.000	3.000	1.602	.8889	.9428	.5886	.6581	.5549	1.600	.8944
1.26	8.692	2.948	1.600	.8850	.9407	.5879	.6599	.5532	1.587	.8909
1.27	8.407	2.899	1.598	.8811	.9387	.5872	.6618	.5513	1.575	.8874
1.28	8.143	2.854	1.596	.8772	.9366	.5866	.6636	.5494	1.563	.8839
1.29	7.897	2.810	1.595	.8734	.9346	.5859	.6655	.5475	1.550	.8805
1.30	7.667	2.769	1.594	.8696	.9325	.5852	.6673	.5457	1.538	.8771
1.31	7.452	2.730	1.592	.8658	.9305	.5846	.6691	.5439	1.527	.8737
1.32	7.250	2.693	1.591	.8621	.9285	.5839	.6709	.5422	1.515	.8704
1.33	7.061	2.657	1.589	.8584	.9265	.5832	.6726	.5405	1.504	.8671
1.34	6.882	2.623	1.587	.8547	.9245	.5826	.6744	.5386	1.493	.8639
1.35	6.714	2.591	1.585	.8511	.9226	.5819	.6761	.5369	1.481	.8607
1.36	6.556	2.560	1.584	.8475	.9206	.5813	.6779	.5352	1.471	.8575
1.37	6.405	2.531	1.582	.8439	.9186	.5806	.6797	.5334	1.460	.8544
1.38	6.263	2.503	1.580	.8403	.9167	.5800	.6813	.5315	1.449	.8513
1.39	6.128	2.475	1.579	.8368	.9148	.5793	.6830	.5299	1.439	.8482
1.40	6.000	2.449	1.577	.8333	.9129	.5787	.6847	.5283	1.429	.8452
1.45	5.444	2.333	1.569	.8163	.9035	.5755	.6930	.5200	1.379	.8305
1.50	5.000	2.236	1.563	.8000	.8944	.5724	.7011	.5120	1.333	.8165
1.55	4.636	2.153	1.556	.7843	.8856	.5694	.7089	.5043	1.290	.8032
1.60	4.333	2.082	1.549	.7692	.8770	.5664	.7165	.4968	1.250	.7906
1.65	4.077	2.019	1.542	.7547	.8687	.5635	.7238	.4895	1.212	.7785
1.67	3.985	1.996	1.539	.7491	.8655	.5623	.7266	.4867	1.198	.7738

$*\,\Omega = \sqrt{k}\left(\frac{2}{k+1}\right)^{\frac{k+1}{2(k-1)}}$

with a solution of calcium permanganate. These two chemicals are fed to the gas generator under pressure supplied by nitrogen bottles. The advantage of this reaction is that the gases produced, mainly steam, are at the low temperature of 790 F so that no diluent is required. The pressure of the gases entering the single-stage partial admission turbine is approximately 350 psia. The turbine rotates at 4000 rpm and develops 500 to 600 hp. The operating-chamber pressure for the rocket motor was 300 psia, and the temperature of the chamber gases approximately 5400 R.

The Walter power rocket plant, Model 109-509A-1, used concentrated hydrogen peroxide and a solid catalyst, consisting of stones impregnated with calcium or sodium permanganate, to produce the gases for operating the turbine; the turbine operated at 16,500 rpm. This was the first successful rocket power plant used as the sole propulsion means of a piloted airplane. The weight distribution of this power plant, which developed approximately 3300 lb thrust, is presented in Table 12·1. It is of interest to note in passing that ratio of the landing weight (4620 lb) to the take-off weight (9020 lb) for the ME-163 airplane is 0.51.

The liquid rocket jet-propulsion system can be operated for extended periods limited only by the capacity of the propellant supply tanks.

The operating pressures of liquid-propellant rocket motors are lower than those employed with solid-propellant units. Depending upon the propellants employed, the chamber pressure will range from 300 to 750 psia for liquid rocket motors, and from 1500 to 3000 psia for solid-propellant rocket motors.

For the more common propellants the specific heat ratio k has values ranging from 1.20 to 1.30; Table 12·2 presents various function of k. In the reaction of an excess of liquid hydrogen with liquid

TABLE 12·3

VALUES OF THE SPECIFIC-HEAT RATIO FOR THE COMBUSTION PRODUCTS OF OXYGEN-HYDROGEN MIXTURES

(According to H. Oberth)

O/H Ratio by Weight	Value of $k = c_p/c_v$	O/H Ratio by Weight	Value of $k = c_p/c_v$
0.8	1.400	1.5	1.388
0.9	1.398	1.6	1.386
1.0	1.396	1.7	1.385
1.1	1.394	1.8	1.384
1.2	1.393	1.9	1.383
1.3	1.391	5.33	1.33
1.4	1.389		

TABLE 12·4

$$\text{Values of } \sqrt{\frac{Z}{1+Z}} = \sqrt{1 - \left(\frac{p_e}{p_c}\right)^{\frac{k-1}{k}}}$$

p_c/p_e	Values of k									
	1.20	1.21	1.22	1.23	1.24	1.25	1.26	1.27	1.28	1.29
1	0.000	0.000	0.000	0.000	0.000	0.000	0.000	0.000	0.000	0.000
2	.330	.337	.343	.349	.354	.360	.365	.370	.375	.380
3	.409	.417	.424	.431	.438	.444	.450	.456	.462	.468
4	.454	.462	.470	.478	.485	.492	.499	.505	.511	.517
5	.485	.494	.502	.510	.517	.525	.532	.538	.545	.551
6	.508	.517	.525	.534	.541	.549	.556	.563	.569	.576
7	.526	.535	.544	.552	.560	.568	.575	.582	.589	.595
8	.541	.550	.559	.568	.576	.583	.591	.598	.605	.611
9	.554	.563	.572	.580	.589	.596	.604	.611	.618	.624
10	.565	.574	.583	.591	.600	.607	.615	.622	.629	.636
15	.603	.612	.622	.630	.639	.647	.654	.662	.669	.675
20	.627	.637	.646	.655	.663	.671	.679	.686	.693	.700
25	.644	.654	.664	.672	.681	.689	.697	.704	.711	.718
30	.658	.668	.677	.686	.694	.702	.710	.717	.724	.731
35	.669	.679	.688	.697	.705	.713	.721	.728	.735	.742
40	.678	.688	.697	.706	.714	.722	.730	.737	.744	.751
45	.685	.695	.705	.714	.722	.730	.738	.745	.752	.758
50	.692	.702	.711	.720	.729	.737	.744	.751	.758	.765
60	.703	.713	.723	.731	.740	.748	.755	.762	.769	.776
70	.712	.722	.732	.740	.749	.757	.764	.771	.778	.784
80	.720	.730	.739	.748	.756	.764	.771	.779	.785	.792
90	.726	.736	.746	.754	.763	.770	.778	.785	.791	.798
100	.732	.742	.751	.760	.768	.776	.783	.790	.797	.803
120	.741	.751	.760	.769	.777	.785	.792	.799	.806	.812
140	.749	.759	.768	.777	.785	.792	.800	.806	.813	.819
160	.756	.765	.774	.783	.791	.799	.806	.812	.819	.825
180	.761	.771	.780	.788	.796	.804	.811	.818	.824	.830
200	.766	.775	.784	.793	.801	.808	.815	.822	.828	.834
400	.795	.804	.813	.821	.828	.836	.842	.849	.855	.860

oxygen, the variation in k is from 1.3 to 1.4. With this propellant combination the combustion gases consist of superheated steam and hydrogen. Calculations, by H. Oberth, as reported by E. Sänger, of the values of k for different ratios of oxygen to hydrogen are presented in Table 12·3.

TABLE 12·5

VALUES OF $\left(\dfrac{p_c}{p_e}\right)^{\frac{1}{k}}$

p_c/p_e	Values of k									
	1.10	1.15	1.20	1.21	1.22	1.23	1.24	1.25	1.26	1.27
1	1.000	1.000	1.000	1.000	1.000	1.000	1.000	1.000	1.000	1.000
2	1.879	1.827	1.782	1.773	1.765	1.757	1.749	1.741	1.734	1.726
3	2.715	2.600	2.498	2.479	2.461	2.443	2.426	2.408	2.392	2.375
4	3.505	3.339	3.175	3.145	3.115	3.086	3.059	3.032	3.005	2.979
5	4.320	4.053	3.824	3.782	3.740	3.701	3.662	3.624	3.587	3.552
6	5.100	4.750	4.447	4.396	4.344	4.292	4.242	4.194	4.146	4.100
7	5.861	5.431	5.058	4.993	4.929	4.865	4.804	4.743	4.685	4.628
8	6.620	6.100	5.650	5.577	5.493	5.423	5.349	5.279	5.209	5.141
9	7.370	6.757	6.240	6.146	6.052	5.968	5.882	5.800	5.719	5.640
10	8.120	7.416	6.820	6.705	6.602	6.501	6.404	6.310	6.218	6.129
11	8.845	8.045	7.376	7.256	7.138	7.025	6.915	6.810	6.707	6.607
12	9.574	8.678	7.931	7.797	7.667	7.540	7.419	7.301	7.187	7.076
13	10.30	9.303	8.478	8.340	8.185	8.046	7.912	7.782	7.652	7.535
14	11.01	9.923	9.018	8.856	8.698	8.546	8.400	8.258	8.120	7.989
15	11.73	10.54	9.551	9.376	9.204	9.040	8.881	8.728	8.578	8.435
16	12.44	11.14	10.08	9.888	9.704	9.526	9.355	9.190	9.028	8.874
17	13.14	11.75	10.60	10.40	10.12	10.01	9.823	9.645	9.474	9.308
18	13.84	12.35	11.12	10.90	10.69	10.49	10.29	10.10	9.914	9.738
19	14.54	12.94	11.63	11.40	11.17	10.98	10.75	10.54	10.35	10.16
20	15.23	13.53	12.14	11.89	11.65	11.42	11.20	10.98	10.78	10.58
21	15.92	14.12	12.64	12.38	12.13	11.88	11.65	11.42	11.21	10.99
22	16.61	14.70	13.14	12.86	12.60	12.34	12.09	11.86	11.62	11.40
23	17.30	15.28	13.64	13.35	13.06	12.80	12.53	12.29	12.04	11.81
24	17.97	15.85	14.13	13.83	13.53	13.25	12.98	12.71	12.46	12.21
25	18.66	16.43	14.62	14.30	13.99	13.69	13.41	13.13	12.86	12.61
26	19.34	17.00	15.10	14.77	14.45	14.14	13.84	13.55	13.27	13.01
27	20.01	17.57	15.59	15.24	14.90	14.58	14.27	13.97	13.68	13.40
28	20.68	18.13	16.07	15.70	15.35	15.02	14.69	14.35	14.08	13.79
29	21.35	18.70	16.55	16.17	15.80	15.45	15.11	14.79	14.47	14.17
30	22.02	19.25	17.02	16.62	16.24	15.88	15.53	15.20	14.87	14.56
32	23.35	20.36	17.96	17.54	17.13	16.74	16.36	16.00	15.65	15.31
34	24.68	21.47	18.89	18.44	18.00	17.58	17.18	16.80	16 43	16.07
36	25.99	22.56	19.81	19.33	18.86	18.42	17.99	17.58	17.19	16.80
38	27.30	23.64	20.72	20.21	19.72	19.25	18.79	18.36	17.94	17.54

Table 12·4 presents values of the parameter $\sqrt{Z/(1 + Z)}$ for different pressure ratios, and Table 12·5 presents values of $(p_c/p_e)^{\frac{1}{k}}$ for different values of k.

TABLE 12·5 (*Continued*)

$$\text{Values of } \left(\frac{p_c}{p_e}\right)^{\frac{1}{k}}$$

p_c/p_e	Values of k									
	1.28	1.29	1.30	1.35	1.40	1.45	1.50	1.55	1.60	1.65
1	1.000	1.000	1.000	1.000	1.000	1.000	1.000	1.000	1.000	1.000
2	1.719	1.711	1.705	1.671	1.641	1.613	1.587	1.564	1.542	1.522
3	2.359	2.343	2.330	2.256	2.193	2.133	2.080	2.031	1.987	1.946
4	2.954	2.929	2.907	2.793	2.692	2.601	2.510	2.446	2.378	2.317
5	3.517	3.482	3.449	3.295	3.156	3.034	2.924	2.825	2.734	2.652
6	4.055	4.012	3.970	3.771	3.598	3.441	3.302	3.178	3.065	2.962
7	4.573	4.520	4.467	4.227	4.012	3.826	3.659	3.509	3.374	3.252
8	5.076	5.013	4.950	4.666	4.415	4.196	4.000	3.825	3.668	3.526
9	5.565	5.491	5.420	5.091	4.800	4.551	4.326	4.126	3.948	3.787
10	6.046	5.960	5.885	5.504	5.188	4.894	4.642	4.418	4.217	4.037
11	6.510	6.416	6.325	5.907	5.544	5.226	4.946	4.698	4.476	4.278
12	6.969	6.864	6.763	6.301	5.900	5.550	5.242	4.968	4.726	4.509
13	7.417	7.303	7.193	6.685	6.247	5.864	5.529	5.232	4.968	4.732
14	7.860	7.735	7.614	7.063	6.587	6.171	5.807	5.488	5.206	4.950
15	8.294	8.160	8.030	7.433	6.919	6.473	6.082	5.738	5.434	5.162
16	8.724	8.578	8.438	7.797	7.246	6.767	6.349	5.982	5.657	5.367
17	9.147	8.990	8.841	8.154	7.566	7.057	6.611	6.220	5.875	5.567
18	9.565	9.400	9.238	8.509	7.882	7.340	6.868	6.454	6.089	5.765
19	9.979	9.802	9.631	8.857	8.192	7.619	7.120	6.684	6.299	5.958
20	10.39	10.20	10.02	9.198	8.498	7.893	7.367	6.908	6.503	6.144
21	10.79	10.59	10.40	9.538	8.798	8.163	7.611	7.129	6.705	6.329
22	11.19	10.98	10.78	9.871	9.097	8.430	7.851	7.346	6.903	6.510
23	11.58	11.37	11.16	10.20	9.389	8.692	8.088	7.560	7.097	6.688
24	11.95	11.75	11.53	10.53	9.680	8.951	8.321	7.771	7.289	6.863
25	12.36	12.12	11.89	10.85	9.965	9.205	8.549	7.977	7.476	7.033
26	12.75	12.50	12.26	11.17	10.25	9.459	8.777	8.182	7.663	7.205
27	13.13	12.87	12.62	11.49	10.53	9.709	9.001	8.385	7.845	7.370
28	13.59	13.24	12.98	11.80	10.81	9.955	9.222	8.583	8.026	7.535
29	13.88	13.60	13.33	12.11	11.08	10.20	9.439	8.780	8.204	7.697
30	14.26	13.96	13.68	12.42	11.35	10.43	9.655	8.973	8.380	7.856
32	14.99	14.68	14.38	13.03	11.89	10.92	10.08	9.355	8.724	8.170
34	15.72	15.39	15.06	13.63	12.42	11.38	10.50	9.739	9.062	8.476
36	16.44	16.09	15.74	14.22	12.93	11.84	10.90	10.09	9.390	8.774
38	17.15	16.78	16.41	14.80	13.44	12.29	11.30	10.45	9.713	9.067

TABLE 12·5 (*Continued*)

$$\text{VALUES OF } \left(\frac{p_c}{p_e}\right)^{\frac{1}{k}}$$

	Values of k									
p_c/p_e	1.10	1.15	1.20	1.21	1.22	1.23	1.24	1.25	1.26	1.27
40	28.60	24.72	21.63	21.09	20.57	20.07	19.59	19.13	18.69	18.26
42	29.90	25.79	22.53	21.95	21.40	20.88	20.37	19.89	19.45	18.97
44	31.19	26.86	23.42	22.82	22.24	21.68	21.16	20.64	20.15	19.68
46	32.48	27.92	24.30	23.67	23.07	22.48	21.93	21.39	20.88	20.39
48	33.76	28.97	25.12	24.51	23.88	23.27	22.69	22.13	21.59	21.08
50	35.03	30.02	26.05	25.36	24.69	24.06	23.45	22.87	22.31	21.76
55	38.21	32.62	28.21	27.43	26.70	26.00	25.32	24.68	24.06	23.46
60	41.35	35.18	30.33	29.49	28.68	27.91	27.16	26.46	25.78	25.13
65	44.47	37.71	32.42	31.50	30.62	29.78	28.97	28.21	27.47	26.76
70	47.57	40.22	34.48	33.49	32.54	31.63	30.76	29.93	29.13	28.37
75	50.65	42.71	36.52	35.46	34.43	33.46	32.52	31.63	30.77	29.96
80	53.71	45.17	38.54	37.39	36.30	35.26	34.26	33.31	32.39	31.51
85	56.76	47.61	40.53	39.31	38.15	37.03	35.97	34.95	33.98	33.05
90	59.78	50.04	42.51	41.21	39.97	38.80	37.66	36.59	35.56	34.57
95	62.79	52.45	44.47	43.10	41.79	40.54	39.35	38.21	37.12	36.08
100	65.80	54.84	46.42	44.97	43.58	42.27	41.01	39.81	38.67	37.57
110	71.75	59.59	50.25	48.65	47.14	45.67	44.29	42.96	41.70	40.49
120	77.66	64.27	54.04	52.28	50.61	49.02	47.51	46.06	44.69	43.37
130	83.50	68.90	57.75	55.85	54.04	52.31	50.67	49.10	47.61	46.19
140	89.33	73.48	61.43	59.38	57.42	55.56	53.79	52.11	50.50	48.96
150	95.11	78.02	65.07	62.86	60.77	58.77	56.88	55.06	53.35	51.70
160	100.90	82.52	68.66	66.31	64.06	61.94	59.91	57.98	56.14	54.39
170	106.57	86.99	72.23	69.71	67.33	65.06	62.90	60.86	58.91	57.05
180	112.27	91.45	75.75	73.10	70.57	68.17	65.88	63.72	61.65	59.68
190	117.93	95.84	79.25	76.43	73.76	71.23	68.82	66.54	64.35	62.28
200	123.55	100.20	82.70	79.73	76.93	74.26	71.72	69.31	67.01	64.83
250	151.32	121.86	99.59	95.88	92.34	89.02	85.86	82.85	80.00	77.29
300	178.60	142.57	115.94	111.48	107.25	103.26	99.47	95.87	92.46	89.21
350	205.48	163.02	131.84	126.63	121.70	117.05	112.86	108.47	104.50	100.75
400	232.02	183.08	147.37	141.42	135.80	130.48	125.45	120.69	116.18	111.92
450	258.24	202.82	162.55	155.86	149.53	143.57	137.93	132.59	127.56	122.78
500	284.13	222.29	177.48	170.07	163.03	156.43	150.18	144.27	138.70	133.40
600	335.48	260.51	206.60	197.69	189.31	181.41	173.99	166.95	160.30	154.02
700	385.86	297.86	234.90	224.56	214.82	205.61	196.97	188.82	181.13	173.89

TABLE 12·5 *(Continued)*

VALUES OF $\left(\dfrac{p_c}{p_e}\right)^{\frac{1}{k}}$

p_c/p_e	Values of k									
	1.28	1.29	1.30	1.35	1.40	1.45	1.50	1.55	1.60	1.65
40	17.85	17.46	17.07	15.37	13.94	12.73	11.70	10.80	10.03	9.353
42	18.54	18.12	17.73	15.94	14.43	13.16	12.08	11.15	10.34	9.633
44	19.23	18.79	18.37	16.50	14.92	13.60	12.47	11 49	10.65	9.909
46	19.91	19.45	19.01	17.05	15.41	14.02	12 84	11.82	10.96	10.18
48	20.58	20.10	19.64	17.59	15.88	14.43	13.21	12.15	11.24	10.45
50	21.25	20.75	20.27	18.13	16.35	14.85	13 57	12.48	11.53	10.71
55	22.89	22.34	21.82	19.46	17.50	15.86	14.46	13.27	12.24	11.34
60	24.50	23.90	23.32	20.76	18.63	16.84	15.33	14 04	12.92	11.96
65	26.08	25.43	24.80	22.02	19.72	17.80	16.17	14.78	13.59	12.55
70	27.64	26.93	26.26	23.26	20.79	18.73	16.99	15.50	14.23	13.13
75	29.17	28.42	27.69	24.49	21.85	19.64	17.79	16.21	14.86	13.63
80	30.68	29.87	29.10	25.69	22.82	20.53	18.57	16.90	15.47	14.23
85	32.16	31.31	30.49	26.86	23.83	21.41	19.33	17.57	16.07	14.77
90	33.63	32.73	31.86	28.02	24.88	22.27	20.08	18.23	16.65	15.29
95	35.08	34.13	33.22	29.17	25.86	23.12	20.82	18.87	17.22	15.80 '
100	36.52	35.52	34.55	30.31	26.83	23.95	21.54	19.51	17.78	16.30
110	39.34	38.24	37.18	32.52	28.71	25.58	22.96	20.75	18.87	17.27
120	42.11	40.91	39.75	34.68	30.56	27.16	24.33	21.95	19.93	18.20
130	44.82	43.52	42.28	36.80	32.35	28.70	25.66	23.11	20.95	19.11
140	47.49	46.09	44.75	38.88	34.11	30.20	26.96	24.24	21.95	19.98
150	50.16	48.63	47.20	40.92	35.84	31.68	28.23	25.35	22.91	20.84
160	52.72	51.12	49.60	42.92	37.53	33.12	29.47	26.43	23.85	21.67
170	55.28	53.57	51.96	44.89	39.19	34.53	30.69	27.48	24.77	22.48
180	57.81	56.01	54.31	46.83	40.82	35.92	31.88	28.51	25.68	23.37
190	60.30	58.41	56.62	48.76	42.43	37.29	33.05	29.53	26.56	24.05
200	62.77	60.77	58.89	50.63	44.01	38.63	34.20	30.52	27.42	24.80
250	74.71	72.26	69.90	59.73	51.62	45.05	39.68	35.24	31.53	28.40
300	86.15	83.23	80.43	68.36	58.79	51.09	44.81	39.64	35.33	31.71
350	97.18	93.79	90.58	76.65	65.64	56.83	49.66	43.79	38.91	34.82
400	107.87	104.03	100.37	84.62	72.22	62.31	54.29	47.73	42.30	37.76
450	118.25	113.96	109.88	92.33	78.55	67.58	58.73	51.49	45.53	40.55
500	128.35	123.67	119.18	99.83	84.69	72.68	63.00	55.11	48.63	43.23
600	148.06	142.45	137.12	114.27	96.48	82.42	71.14	62.00	54.50	49.41
700	167.01	160.52	154.37	128.08	107.70	91.65	78.84	68.47	60.00	53.00

3. Notation

a = acceleration, ft/sec^2.

a = acoustic velocity, fps.

A_e = area of nozzle exit section, sq in.

A_t = area of nozzle throat section, sq in.

c = absolute velocity, fps.

C_D = discharge coefficient or drag coefficient as specified in text.

$C_G = G/A_t p_c$ = weight flow coefficient.

$C_T = 3/A_t p_c$ = thrust coefficient.

D = drag, lb.

E_p = thermochemical energy of propellant mixture, Btu/lb.

g = acceleration due to gravity = 32.174 ft/sec^2.

$G = xgm_P$ = weight rate of propellant consumption, lb/sec.

G_f = weight rate of fuel flow, lb/sec.

G_0 = weight rate of oxidizer flow, lb/sec.

H_c = calorific value of fuel, Btu/lb.

h = altitude attained by rocket system at any time t during the power flight, ft.

h_p = altitude attained by rocket at the end of the power flight, ft.

h_C = altitude traversed by the rocket during coasting after the propellants have been consumed, ft.

$h_T = h_p + h_C$ = total altitude attained, ft.

J = 778 ft-lb/Btu = mechanical equivalent of heat.

$k = c_p/c_v$ = specific heat ratio.

L = external work, ft-lb/lb.

m_P = propellant mass at beginning of powered flight ($t = 0$), slugs.

m = mass of rocket system exclusive of propellants in slugs, mass in general, or molecular weight, as indicated in text.

$M_0 = m + m_P$ = mass of rocket system at the beginning of the powered flight ($t = 0$), slugs.

M = instantaneous mass of rocket system (including the propellants) during the powered flight, slugs.

M = Mach number.

$\mathbf{M}$ = momentum, slug ft/sec.

p_a = pressure intensity of atmosphere surrounding rocket motor, psia.

p_e = pressure intensity acting on exit area of rocket motor nozzle, psia.

p_c = pressure intensity of the gases in the rocket motor combustion chamber, psia.

P = propulsion power, ft-lb/sec.

$P_T = 5V$ = thrust power, ft-lb/sec.

$P_L = Gc^2/2g$ = leaving loss, ft-lb/sec.

$r = G_0/G_f$ = mixture ratio.

s = distance, ft.

t = time, sec.

t_p = duration of powered flight, sec.

$\mathfrak{I}$ = thrust, lb.

T_c = temperature of gases in combustion chamber, R.

T_t = temperature of gases in nozzle throat section, R.

T_e = temperature of gases in nozzle exit section, R.

$v = 1/\gamma$ = specific volume, ft^3/lb.

w = effective exhaust velocity or relative velocity as indicated in text, fps.

w_t = velocity of gases in throat section, fps.

w_e = velocity of gases in exit section, fps.

$w_u = \sqrt{2gJE_P}$ = ultimate velocity, fps.

W_P = total weight of propellants consumed, lb.

$w_P = gm_P$ = initial propellant weight, lb.

x = fraction of initial propellant mass m_P consumed in unit time.

$$Z = (p_c/p_o)^{\frac{k-1}{k}} - 1.$$

$$Z/(1 + Z) = 1 - (p_o/p_o)^{\frac{k-1}{k}}$$

Greek Symbols

α = divergence angle of nozzle exit.

$\lambda = 1/2 + 1/2 \cos \alpha$ = correction factor for divergence of nozzle exit.

$\gamma = 1/v$ = specific weight, lb/ft^3.

$\rho = \gamma/g$ = density, slugs.

η_i = internal efficiency.

η_P = propulsion efficiency.

$$\Omega = \sqrt{k} \left(\frac{2}{k + 1} \right)^{\frac{k+1}{2(k-1)}}$$

φ = velocity coefficient.

4. Thermodynamic Relationships Based on Perfect Gas Laws

For most rocket motors operating under steady-state conditions the equations presented in Chapters 1 and 3 are applicable without serious error. For convenience some of the equations derived in those chapters are presented below.

Assuming that the critical pressure ratio for the nozzle is exceeded, the state magnitudes p_t, T_t, and v_t for the gases in the throat section, expressed in terms of the conditions in the combustion chamber (denoted by the subscript c), are given by

$$p_t = \left(\frac{2}{k+1}\right)^{\frac{k}{k-1}} p_c \tag{1}$$

$$T_t = \left(\frac{2}{k+1}\right) T_c \tag{2}$$

and

$$v_t = \left(\frac{p_c}{p_t}\right)^{\frac{1}{k}} v_c \tag{3}$$

The velocity of the gases in the throat section is the local sonic velocity a_t. Its magnitude is calculated from

$$w_t = a_t = \sqrt{gkRT_t} = \sqrt{\frac{2gkRT_c}{k+1}} = 315\ 3 \sqrt{\left(\frac{k}{k+1}\right)\left(\frac{T_c}{m}\right)} \tag{4}$$

If the throat pressure p_t is plotted as a function of the chamber pressure p_c, the result is a straight line with the slope $\left(\frac{2}{k+1}\right)^{\frac{1}{k-1}}$ The critical pressure is a function only of the specific-heat ratio, which depends basically upon the composition of the propellant gases It was shown in Chapter 3 that when the ratio p_c/p_a, where p_a is the external or back pressure, exceeds the critical ratio the velocity in the throat is independent of the chamber pressure and the rocket motor operates with *complete nozzling*.

From Chapter 3, the critical pressure ratio is

$$\left(\frac{p_c}{p_a}\right)_{cr} = \left(\frac{k+1}{2}\right)^{\frac{k}{k-1}} \tag{5}$$

Although the critical pressure ratio depends solely upon the value of k, it is not greatly affected by the possible range of k values which may be encountered with rocket propellants. The lowest value of k to be expected is approximately 1.2; the maximum attainable value (helium) is 1.67. The critical pressure ratios corresponding to the above values of k are 1 77 and 2 12 respectively. This means that at sea level the rocket motor will operate with complete nozzling as

long as the chamber pressure exceeds 32 psia. Since the chamber pressure p_c for a rocket motor greatly exceeds this value, a rocket motor always operates with complete nozzling

EXAMPLE Calculate the throat velocity and throat temperature for a rocket motor nozzle for which $T_c = 5520$ R, $m = 25\ 4$, $p_c = 300$ psia, $p_a = 14.4$ psia, $k = 1\ 25$.

Solution. From Table 12 2

$$\left(\frac{2}{k+1}\right)^{\frac{k}{k-1}} = 0\ 5549$$

Hence $300 \times 0\ 5549 = 166\ 5$ psia is the critical value for the atmospheric pressure Since $14\ 4 < 166\ 5$, equation 4 applies

$$\sqrt{\frac{T_c}{m}} = 14\ 8, \qquad \sqrt{\frac{k}{k+1}} = 0\ 7454$$

$$w_t = 315\ 3 \times 0\ 7454 \times 14\ 8 = 3480 \quad \text{fps}$$

From equation 2

$$T_t = \frac{2}{1.25 + 1}\,T_c = 0.889 \times 5520 = 4910\ \text{R}$$

5. Conditions at Any Section of Nozzle

The conditions at any section x in the divergent portion of the rocket motor nozzle, assuming perfect gases and no discontinuities in the flow, are related to the throat conditions by the following equations

$$\frac{w_x}{w_t} = \sqrt{\frac{k+1}{k-1}\left[1 - \left(\frac{2}{k+1}\right)\left(\frac{p_x}{p_t}\right)^{\frac{k-1}{k}}\right]} \tag{6}$$

$$\frac{T_x}{T_t} = \left(\frac{p_x}{p_t}\right)^{\frac{k-1}{k}} \tag{7}$$

$$\frac{v_x}{v_t} = \frac{\gamma_t}{\gamma_x} = \left(\frac{p_t}{p_x}\right)^{\frac{1}{k}} \tag{8}$$

$$\frac{A_x}{A_t} = \left(\frac{p_t}{p_x}\right)^{\frac{1}{k}}\frac{w_t}{w_x} \tag{9}$$

From equation 6 it is seen that the pressure ratio for $w_x = 0$ is given by

$$\frac{p_x}{p_t} = \left(\frac{k+1}{2}\right)^{\frac{k}{k-1}} \tag{10}$$

which is identical with that for the critical pressure ratio for sonic
velocity in the throat.

6. *Nozzle Area Ratio*

The rocket motor gives its maximum performance when the nozzle
is designed so that the gases are expanded completely to the pre-
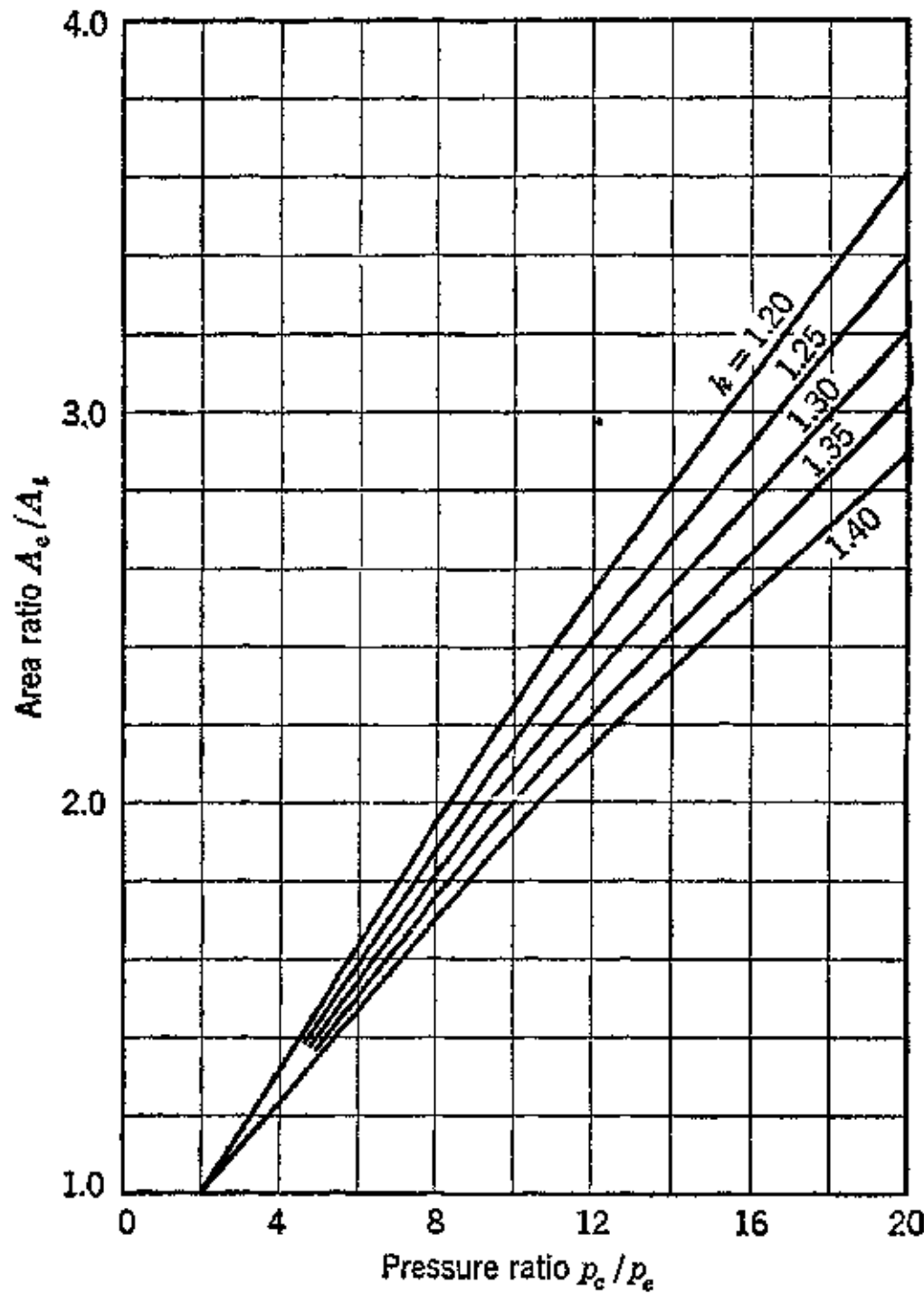
FIG. 6.   Area ratio of exhaust nozzle vs. pressure ratio for different specific-heat
ratios.

dominating back pressure, that is, when $p_e = p_a$. Consequently,
the area ratio A_e/A_t for the rocket nozzle is of significance.   It was
shown in Chapter 3, in the discussion of the De Laval nozzle, that
the area ratio for complete expansion is given by

$$\frac{A_t}{A_e} = \left(\frac{k+1}{2}\right)^{\frac{1}{k-1}}\left(\frac{p_e}{p_c}\right)^{\frac{1}{k}}\sqrt{\frac{k+1}{k-1}\left[1-\left(\frac{p_e}{p_c}\right)^{\frac{k-1}{k}}\right]} \qquad (11)$$
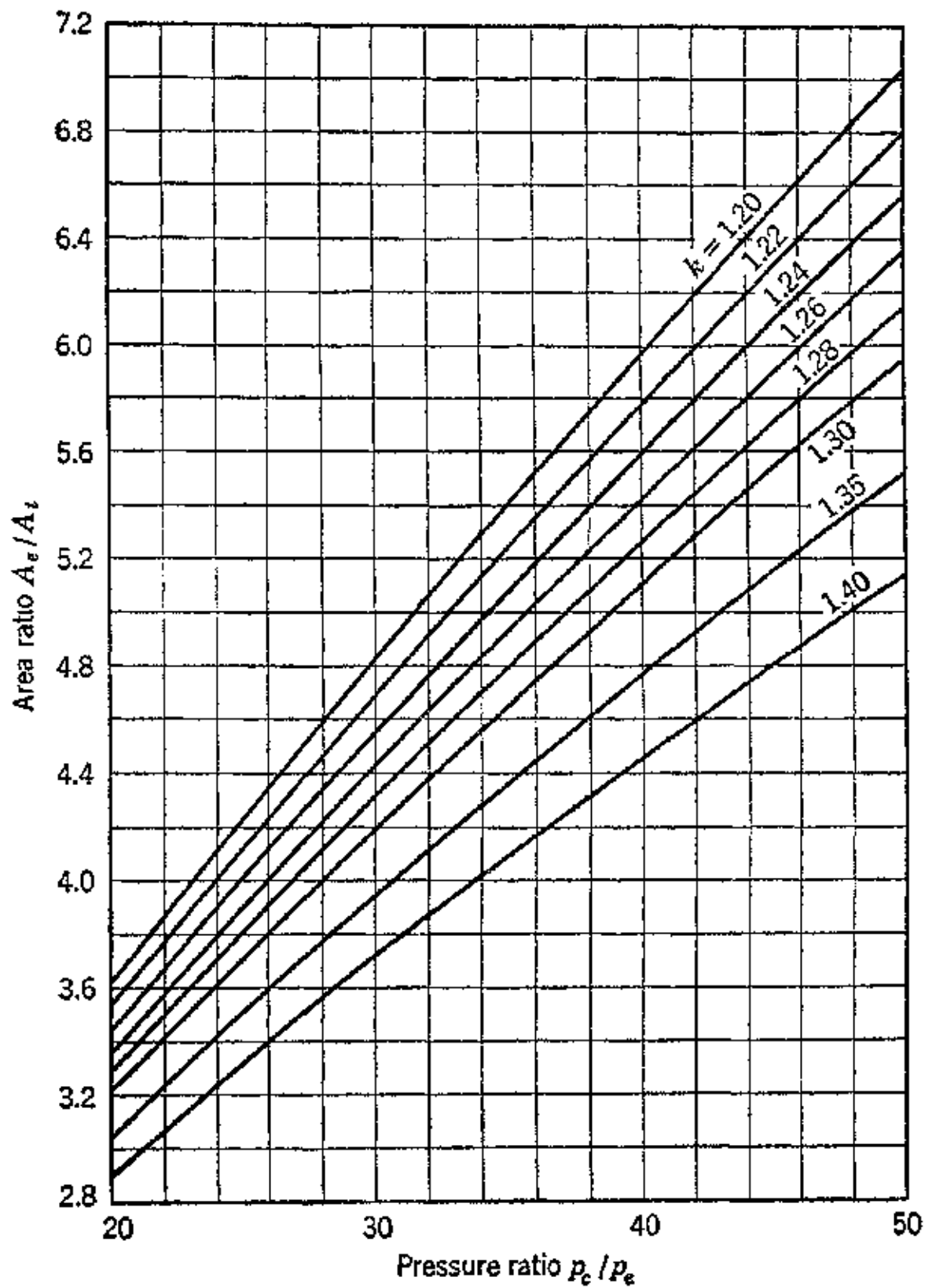
FIG. 7.   Area ratio of exhaust nozzle vs. pressure ratio for different specific-heat ratios.

It is convenient for calculation purposes to express the last equation in either of the following forms

$$\frac{A_e}{A_t} = \frac{[2/(k+1)]^{\frac{1}{k-1}}(p_c/p_e)^{\frac{1}{k}}}{\sqrt{\left(\dfrac{k+1}{k-1}\right)\left[1 - \left(\dfrac{p_c}{p_e}\right)^{\frac{1-k}{k}}\right]}} \tag{12}$$

or

$$\frac{A_e}{A_t} = \frac{(p_c/p_e)^{\frac{1}{k}}}{\left(\dfrac{k+1}{2}\right)^{\frac{1}{k-1}}\sqrt{\dfrac{k+1}{k-1}}\sqrt{\dfrac{Z}{1+Z}}} \tag{13}$$

The advantage of the last equation is that the values of the functions given in Tables 12·2 and 12·3 can be used to simplify the calculation of A_e/A_t. However, for most applications Figs. 6, 7, and 8 give the values A_e/A_t directly with sufficient accuracy. To each
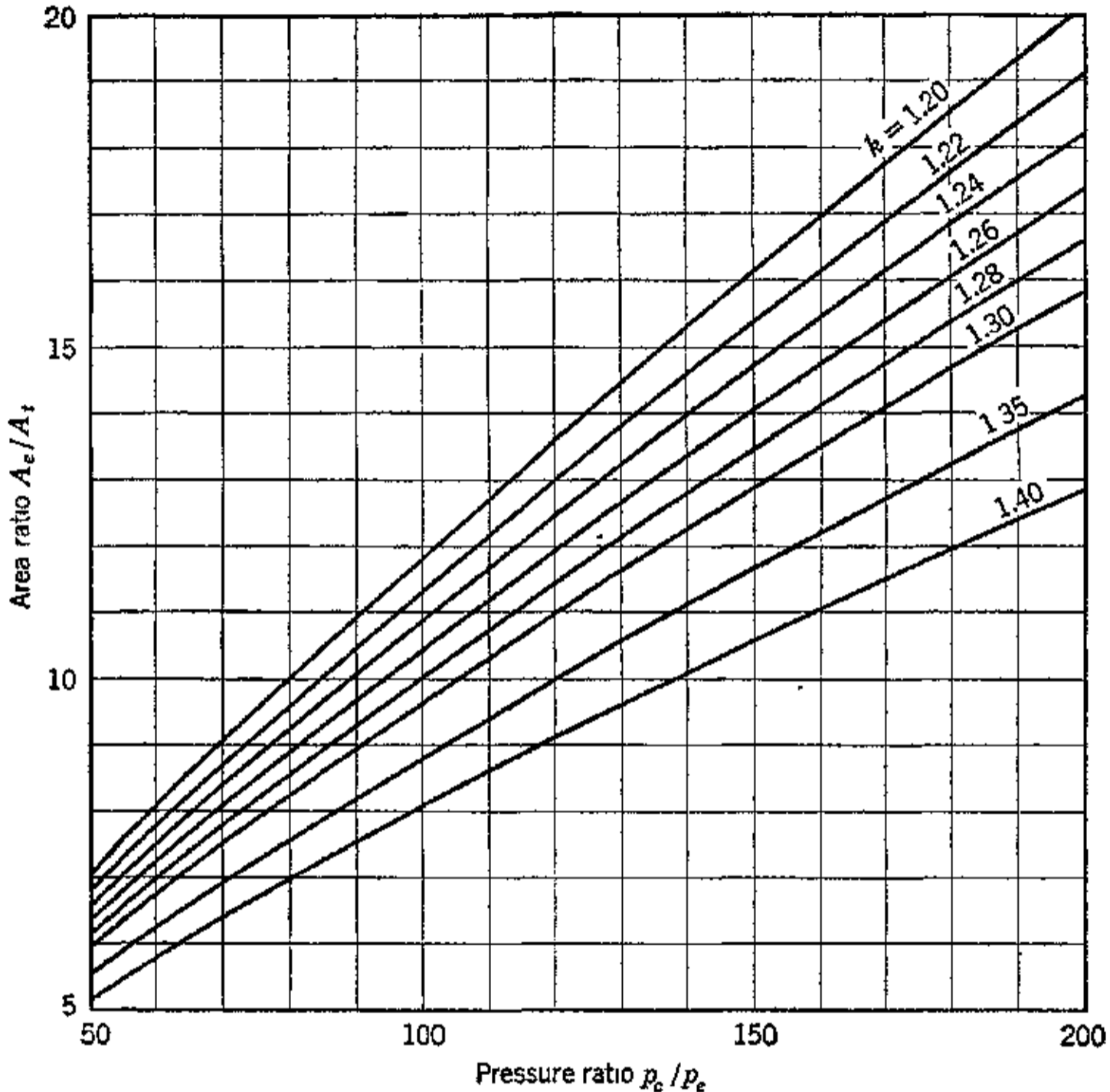
FIG. 8.   Area ratio of exhaust nozzle vs. pressure ratio for different specific-heat ratios.

value of the pressure ratio p_c/p_e there is one corresponding value of the nozzle area ratio A_e/A_t that makes the nozzle exit pressure equal to the external pressure. This area ratio is termed *optimum area ratio*.

EXAMPLE.   The nozzle for a rocket motor is to be designed so that the exit pressure is 2 psi lower than the atmospheric pressure, 14.5 psia. The chamber pressure is 300 psia, and $k = 1.25$. Calculate the nozzle area ratio.

Solution. From Table 12·2

$$\left(\frac{k+1}{2}\right)^{\frac{1}{k-1}} = 1.602$$

$$\sqrt{\frac{k+1}{k-1}} = 3.000$$

$$p_e = p_a - 2.0 = 14.5 - 2 0 = 12.5$$

$$\frac{p_c}{p_e} = \frac{300}{12.5} = 24.0$$

$$\left(\frac{p_c}{p_e}\right)^{\frac{1}{k}} = 24^{\frac{1}{1 \cdot 25}} = 12.71$$

From Table 12·4

$$\sqrt{\frac{Z}{1+Z}} = 0.6856$$

Hence

$$\frac{A_e}{A_t} = \frac{12.71}{1.602 \times 3.000 \times 0.6856} = 3.86$$

Check from Fig. 6

$$\frac{A_e}{A_t} = 3.86$$

7. Exit Velocity of Gases

The linear velocity of the propellant gases crossing the exit section of the nozzle, measured with respect to the rocket motor, is called the *exit velocity*. From Chapter 3, assuming one-dimensional gas dynamics and that the velocity of the gases approaching the exhaust nozzle is negligible gives for the *ideal exit velocity*

$$w_e' = \sqrt{2g\frac{k}{k-1}RT_c\left[1 - \left(\frac{p_e}{p_c}\right)^{\frac{k-1}{k}}\right]} \tag{14}$$

Equation 14 may be written in the form

$$w_e' = \sqrt{2g\frac{k}{k-1}RT_c}\sqrt{\frac{Z}{1+Z}} \tag{15}$$

substituting $R = 1545/m$ gives

$$w_e' = 315.3\sqrt{\frac{T_c}{m}}\sqrt{\frac{k}{k-1}}\sqrt{\frac{Z}{1+Z}} \tag{16}$$
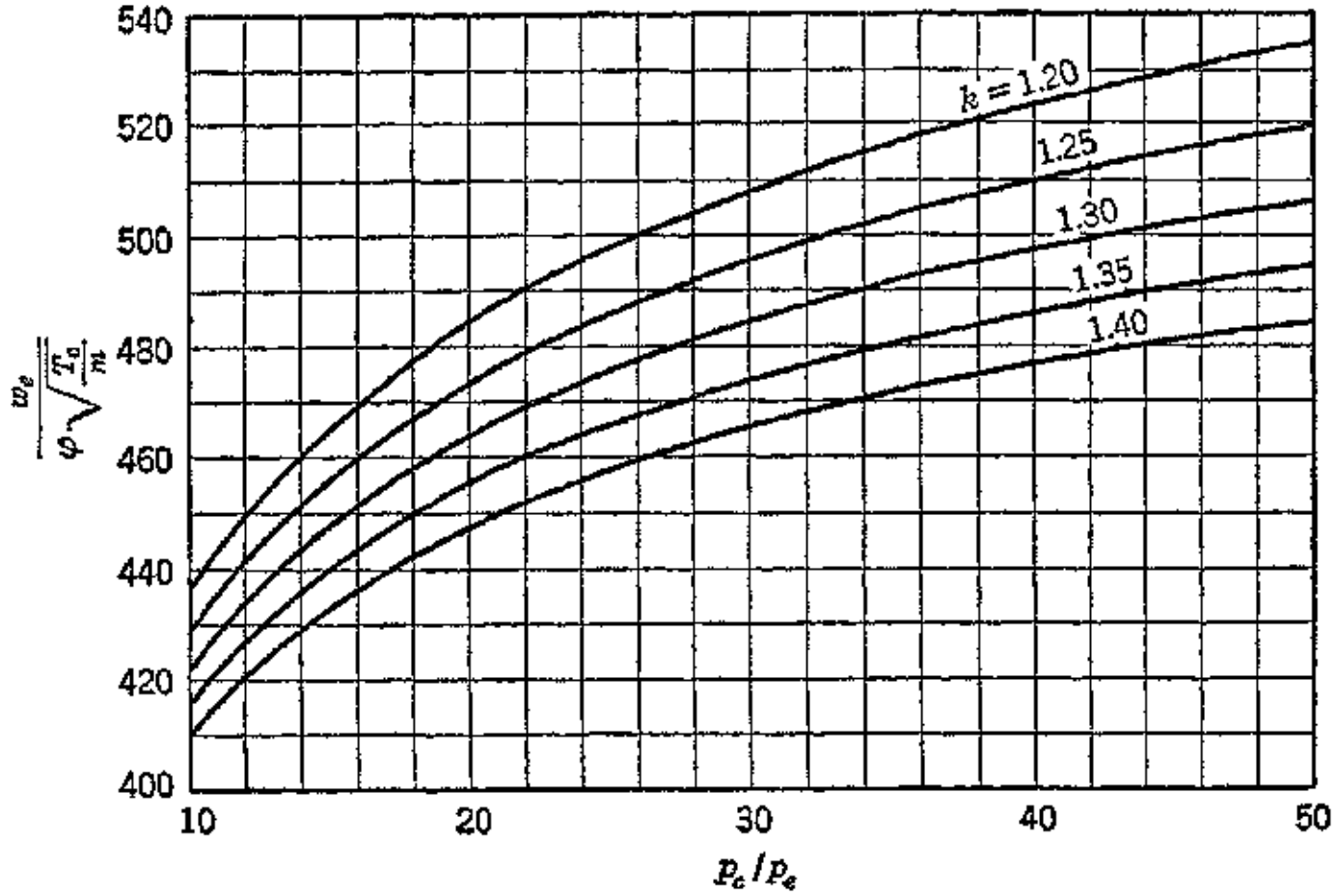
Fig. 9. Velocity parameter $w_e/\varphi\sqrt{T_c/m}$ as a function of pressure ratio for different values of the specific-heat ratio.
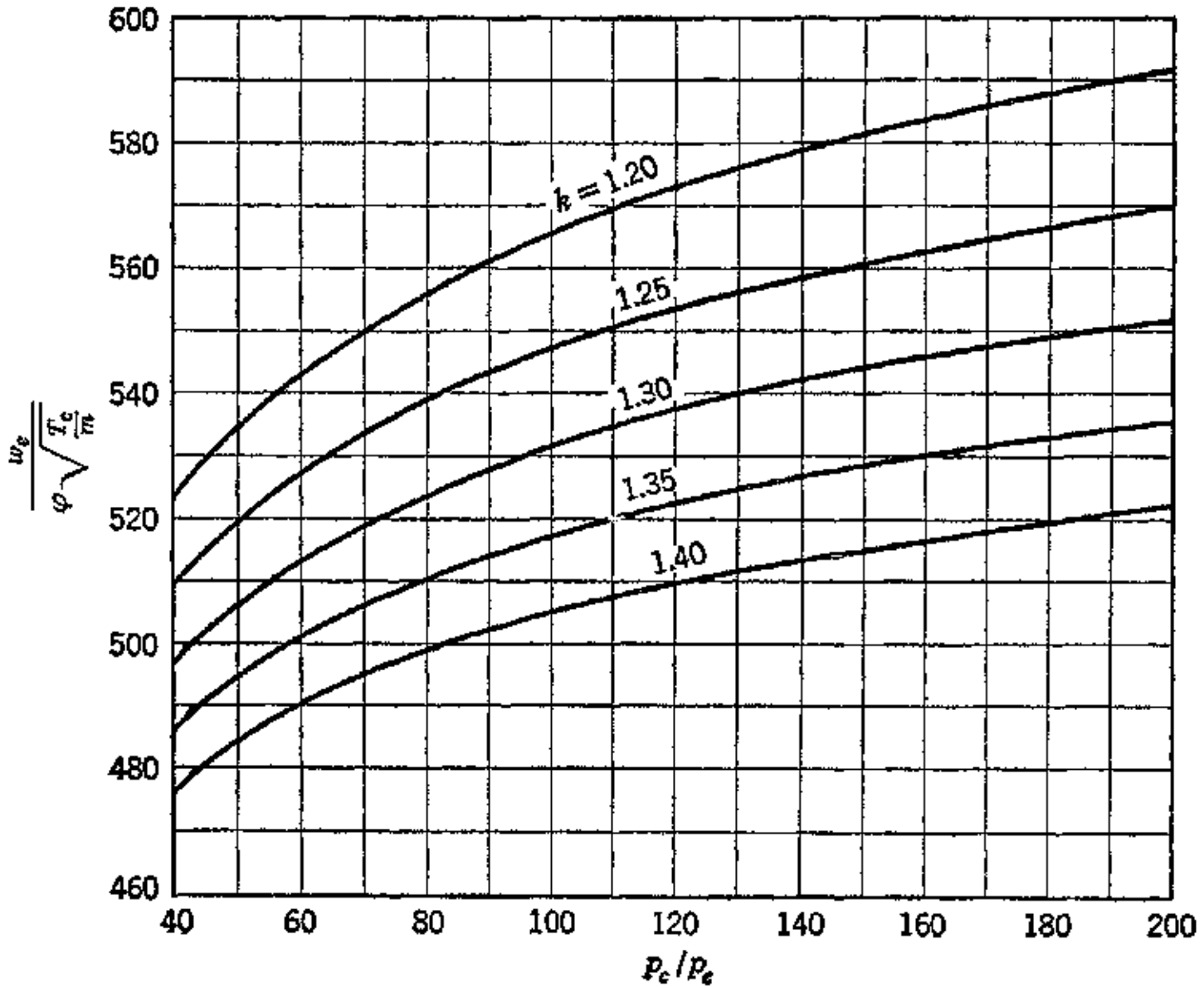
Fig. 10. Velocity parameter $w_e/\varphi\sqrt{T_c/m}$ as a function of pressure ratio for different values of the specific-heat ratio.

Equation 16 is used for estimating w_e' when T_c and m have been calculated by thermodynamic methods.

Friction, turbulence, and the fact that the approach velocity is not zero cause the actual exit velocity to be smaller than the ideal exit velocity. Introducing the velocity coefficient $\varphi < 1$, then

$$w_e = \varphi w_e' \tag{17}$$

The value of φ is usually between 0.9 and 1.0; its exact value is obtainable only by test. When no test data are available, the value $\varphi = 0.95$ is recommended.

Calculation of w_e is reduced by using Figs. 9 and 10.

EXAMPLE. A liquid-propellant rocket motor operates with 300 psia chamber pressure. The propellants are such that $T_c = 5520$ R, $m = 25.4$, and $k = 1.25$. The nozzle is designed so that the exit pressure is equal to the local atmospheric pressure of 14.4 psia. Calculate the exit velocity.

Solution.

$$\sqrt{\frac{T_c}{m}} = 14.8$$

$$\frac{p_c}{p_e} = \frac{300}{14.4} = 20.8$$

From Fig. 9 for $p_c/p_e = 20.8$ and $k = 1.25$

$$\frac{w_e}{\varphi\sqrt{T_c/m}} = 475$$

Hence

$$w_e = 475 \times 0.95 \times 14.8$$

$$= 6680 \quad \text{fps}$$

It is preferable to estimate $\sqrt{T_c/m}$ from experimental data rather than from thermodynamic calculations.

The following equation relates the exit and throat velocities.

$$\frac{w_e'}{w_t} = \sqrt{\frac{k+1}{k-1}\left[1 - \left(\frac{p_c}{p_e}\right)^{\frac{1-k}{k}}\right]} = \sqrt{\frac{k+1}{k-1}}\sqrt{\frac{Z}{1+Z}} \tag{18}$$

8. Weight Flow and Weight Flow Coefficient

The weight rate of flow of propellant gases G lb per sec, called the rate of propellant consumption, is the same as that for the De Laval nozzle discussed in Chapter 3. Let C_D be an empirical correction factor called the discharge coefficient; then

$$G = \frac{A_t p_c C_D}{\sqrt{RT_c}} \sqrt{\frac{2gk}{k-1}} \left(\frac{p_e}{p_c}\right)^{\frac{1}{k}} \sqrt{1 - \left(\frac{p_e}{p_c}\right)^{\frac{k-1}{k}}} \qquad (19)$$

or

$$G = 0.2041 \ C_D \ \frac{A_t p_c}{\sqrt{T_c/m}} \sqrt{\frac{k}{k-1}} \left(\frac{p_e}{p_c}\right)^{\frac{1}{k}} \sqrt{\frac{Z}{1+Z}} \qquad (20)$$

Since rocket motors always operate with the exit pressure less than the critical pressure, the weight flow equation reduces to

$$G = C_D \frac{A_t p_c}{\sqrt{RT_c}} \sqrt{g} \ \sqrt{k} \left(\frac{2}{k+1}\right)^{\frac{k+1}{2(k-1)}} \qquad (21)$$

For convenience let

$$\Omega = \sqrt{k} \left(\frac{2}{k+1}\right)^{\frac{k+1}{2(k-1)}} \qquad (22)$$

Then

$$G = C_D \frac{A_t p_c}{\sqrt{RT_c}} \sqrt{g} \ \Omega \qquad (23)$$

or

$$G = 0.1443 \frac{C_D A_t p_c}{\sqrt{T_c/m}} \Omega \qquad (24)$$

Values of Ω as a function of k are presented in Table 12·2. Equation 24 shows that, for a given propellant combination and a fixed temperature for the combustion-chamber gases, the rate of propellant consumption is directly proportional to $A_t p_c$. It is convenient, therefore, to express G in terms of $A_t p_c$ and a coefficient C_G called the *weight flow coefficient*.

$$G = C_G A_t p_c \qquad (25)$$

Hence the weight flow coefficient in terms of calculated thermodynamic data is given by

$$C_G = 0.1443 \frac{C_D}{\sqrt{T_c/m}} \Omega \qquad (26)$$

The weight flow coefficient C_G is readily calculated from test data.

$$C_G = \frac{G}{A_t p_c} \qquad (27)$$

When no test data are available C_G can be estimated by using calculated values of the thermodynamic data T_c, m, and k and equation 26.

The experimental values of the weight flow coefficient C_G can be used to obtain a satisfactory estimate of the parameter $\sqrt{T_c/m}$. Since any reasonable error in estimating the value of k has little influence on the results, $\sqrt{T_c/m}$ can be obtained from

$$\sqrt{\frac{T_c}{m}} = 0.1443 \frac{\Omega C_D}{C_G} \tag{28}$$

where C_G is calculated from equation 27 and G, A_t, and p_c are values obtained by test.

EXAMPLE. A propellant is to be operated at 300 psia chamber pressure. The molecular weight of the combustion gases is 26, and $T_c = 4000$ R. If $k = 1.25$, and $C_D = 0.95$, what throat diameter is required to give a flow of 5 lb/sec?
Solution.
From Table 12·2, $\Omega = 0.6581$.

$$\sqrt{\frac{T_c}{m}} = \sqrt{\frac{4000}{26}} = 12.3$$

From equation 24,

$$C_G = \frac{0.95 \times 0.1443 \times 0.6581}{12.3} = 0.00733$$

From equation 25,

$$A_t = \frac{5}{0.00733 \times 300} = 2.27 \text{ sq in.}$$

$$d^2 = \frac{2.27}{0.7854} = 2.89$$

$$d = 1.70 \text{ in.}$$

9. Thrust of Rocket Motor

Refer to Fig. 1. The thrust developed by the rocket motor is the resultant of the pressure forces acting upon its inner and outer surfaces. Hence, the thrust, denoted by $\mathfrak{I}$, is given by the surface integral

$$\mathfrak{I} = \int p \, dA_x \tag{28a}$$

where dA_x is the component of the motor wall area acting in the direction of the thrust.

The above integral actually consists of two parts: one representing the integration of the pressure over the inner wall of the motor, and

the other the integration over the external surface.[11]   Hence

$$\Im = \int_{\text{out}} p \, dA_x + \int_{\text{in}} p \, dA_x \tag{29}$$

The first integral is evaluated readily. The pressure acting on the outer surface is that of the surrounding atmosphere p_a, which may be assumed constant. If the outer bounding surface were a completely closed metallic surface, so that there were no nozzle exit, then the first integral would have the value zero. Because of the exit opening, area A_e, the integral differs from zero by the pressure $A_e p_a$ lb; this force acts in the opposite direction to the thrust developed by the motor. Hence

$$\int_{\text{out}} p \, dA_x = -A_e p_a \tag{30}$$

To evaluate the second integral of equation 29 it is necessary to apply the momentum principles, discussed in Chapter 2, to the flow of gases through the motor. The gases are bounded at the inner wall and by the exit surface A_e. The gas pressure acting on A_e is denoted by p_e, which is not necessarily the same as the external pressure (atmospheric) p_a. Hence the x component of the integral for the inner surface is

$$\int_{\text{in}} p \, dA_x - \int_e p_e \, dA_x \tag{31}$$

The resultant momentum of the gases in the direction of thrust is that associated with gases crossing the exit surface A_e, and is given by the integral

$$\mathbf{M}_x = \int \rho w_x{}^2 \, dA_x$$

From the momentum principle

$$\int_e \rho w_x{}^2 \, dA_x = \int_{\text{in}} p \, dA_x - \int_e p_e \, dA_x$$

or

$$\int_{\text{in}} p \, dA_x = \int_e p_e \, dA_x + \int_e \rho w_x{}^2 \, dA_x \tag{32}$$

Substituting equations 32 and 30 into equation 29 gives

$$\Im = \int_e p_e \, dA_x + \int_e \rho w_x{}^2 \, dA_x - A_e p_a \tag{33}$$

Under the *steady-state* conditions assumed in the discussions of this chapter, the pressure, density, and velocity of the gases are constant. Let G denote the weight flow rate in pounds per second; then the thrust is given by

$$\mathfrak{I} = A_e p_e - A_e p_a + \frac{G}{g} w_{xe} = A_e(p_e - p_a) + \frac{G}{g} w_{xe} \qquad (34)$$

In the above equation w_{xe} is the average value of the x component of the gases crossing A_e.

Let w_e denote the exit velocity of the rocket gases, assumed to be constant, and let $w_{xe} = \lambda w_e$. Then equation 34 becomes

$$\mathfrak{I} = (p_e - p_a)A_e + \lambda \frac{G}{g} w_e \qquad (35)$$

The coefficient λ is the correction factor for the divergence angle α of the exit conical section of the nozzle. According to reference 11, if α is the divergence angle of the nozzle wall then

$$\lambda = \frac{1 - \cos 2\alpha}{4(1 - \cos \alpha)} = \frac{1}{2} + \frac{1}{2}\alpha \qquad (36)$$

Figure 11 is a plot of the coefficient λ as a function of α.
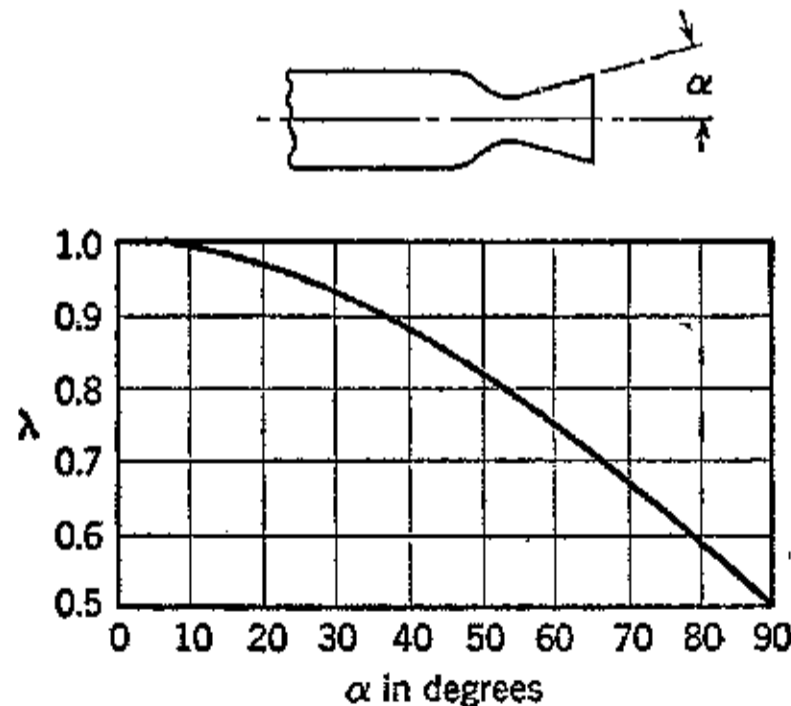
FIG. 11.   Divergence angle correction factor λ as a function of the divergence angle. (Based on F. J. Malina, *J. Franklin Inst.*, October 1940.)

Equation 35 indicates the manner in which the atmospheric pressure affects the thrust developed by the rocket motor: the higher the atmospheric pressure, assuming all other factors unchanged, the smaller the value of the term $(p_e - p_a)A_e$ and correspondingly the thrust. The maximum thrust would be developed when $p_a = 0$.

Hence, *the rocket motor develops its maximum thrust when it is operated in a vacuum.*

The magnitude of the pressure term $(p_e - p_a)A_e$ can be reduced by increasing the exit area until complete expansion to the atmosphere back pressure is obtained. As discussed in Chapter 3, there is only one area ratio A_e/A_t that satisfies this condition. Increasing A_e beyond that value makes $(p_e - p_a)A_e$ negative so that the thrust is decreased. The effect of changing the area ratio A_e/A_t is discussed in detail in Section 10.

Equation 36 shows that the thrust developed by a constant-pressure rocket motor consists of two parts: the *pressure thrust* $(p_e - p_a)A_e$, and the *velocity thrust* $\lambda(G/g)w_e$. Only the velocity thrust is affected by the angle of divergence of the nozzle exit section, and, as illustrated in Fig. 11, for the divergences commonly used (15° or less) the coefficient λ is practically unity.

Substituting for G in terms of Ω from equations 22 and 23

$$\mathfrak{I} = \lambda C_D \Omega w_e \frac{p_c A_t}{\sqrt{gRT_c}} + (p_e - p_a)A_e \tag{37}$$

and in terms of C_G

$$\mathfrak{I} = \lambda C_G \frac{w_e}{g} p_c A_t + (p_e - p_a) A_e \tag{38}$$

Equation 38 may be used for estimating the exit velocity w_e. Since the main use of the exit velocity is to calculate thrust of the rocket motor, it is generally better to estimate w_e from

$$w_e = \frac{[\mathfrak{I} - (p_e - p_a)A_e]}{\lambda G/g} \tag{39}$$

This equation is not used frequently in experimental work. Nevertheless, it offers certain advantages in reducing data to a comparable basis by eliminating variations in nozzle design.

EXAMPLE. A solid-propellant rocket motor operates at 2000 psia chamber pressure. The experimental weight flow coefficient is 0.00872, and k is 1.28. If the exit pressure is 14.4 psia and $\alpha = 15°$, what is the exit velocity?

Solution. From Table 12·2 for $k = 1.28$

$$\Omega = 0.6636$$

Hence

$$\sqrt{\frac{T_c}{m}} = 0.1443 \times \frac{0.6636}{0.00872} = 11.0$$

$$\frac{p_c}{p_e} = \frac{2000}{14.4} = 139$$

From Fig. 10 for $p_c/p_e = 139$ and $k = 1.28$

$$\frac{w_e}{\varphi\sqrt{T_c/m}} = 543$$

$$w_e = 543 \times 1.00 \times 11.0$$

$$= 5970 \quad \text{fps}$$

Solution. From Fig. 11, for $\alpha = 15°$,

$$\lambda = 0.983$$

Equation 39

$$w_e = \frac{1000 - (12.0 - 14.4) \times 6}{0.983 \times 5.5/32.174}$$

$$= 6030 \quad \text{fps}$$

10. Effect of Area Ratio on Thrust

Consider a rocket motor operating with a constant chamber pressure, and suppose that it is possible gradually to increase the exit area A_e while maintaining the same divergence angle for the downstream cone. Since the nozzle operates with the critical pressure ratio in the throat and supersonic velocities in the exit cone, the conditions in the throat section are unaffected by the increase in the area of the exit section.

The velocity of the gases crossing A_e is increased by the increased expansion. The ratio of the exit velocity w_e to the throat velocity w_t is obtained from equation 18. The relationship between the ratio of the exit pressure to the nozzle throat pressure p_e/p_t is given by equation 10.

Figure 12 presents w_e and p_e plotted as functions of the area ratio A_e/A_t for a given rocket motor. It is seen that, as A_e is first increased, p_e and w_e increase at a much more rapid rate. As a result, although the pressure term $(p_e - p_a)A_e$ is reduced, the increase in the exhaust velocity is such that the thrust is increased. The increase in thrust continues with the increase in area ratio A_e/A_t until the exit pressure p_e becomes equal to the atmospheric pressure p_a. When this occurs the pressure term $(p_e - p_a)A_e$ reduces to zero. The gases are completely expanded to the atmospheric back pressure and attain the velocity corresponding to expansion from the combustion-chamber pressure to the atmospheric pressure. At this point the area ratio is defined by equation 12 and the exhaust velocity by equations 16 and 17.

Until the condition $p_e = p_a$ is reached a portion of the energy of the gases is not converted into kinetic energy and is lost as far as

thrust development is concerned. The nozzle functions with *under-expansion* as explained in Chapter 3.

If the area ratio A_e/A_t is increased beyond the value required to make $p_e = p_a$, then the exit pressure of the gases falls below the atmospheric pressure. The pressure term $(p_e - p_a)A_e$ becomes
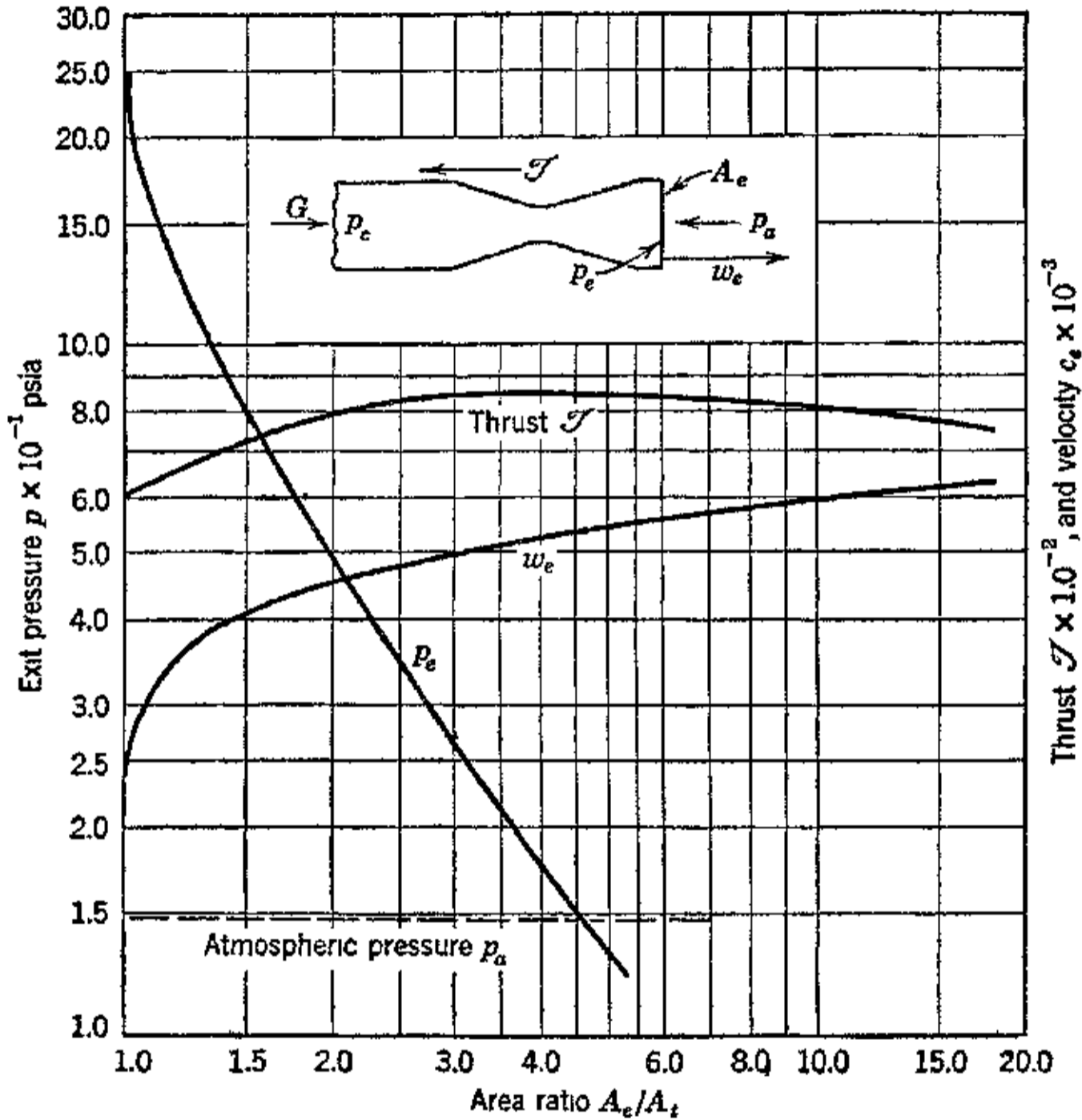
FIG. 12.   Effect of area ratio on the thrust developed by a constant-pressure rocket motor.   (Reproduced from M. J. Zucrow, *Jour. S.A.E.*, July 1946.)

negative, and, since the exit velocity is practically unaffected, see Fig. 12, the thrust is reduced. The nozzle operates with over-expansion. If the overexpansion is large enough, shock waves may be formed in the nozzle exit cone, and before the overexpanded condition is reached the jet may separate from the nozzle wall.

11. Thrust Coefficient (C_T)

In testing a rocket motor, the combustion-chamber pressure p_c and the throat area A_t of the nozzle are two magnitudes that can be

measured accurately. It is convenient, therefore, to relate the thrust to these two variables. Let

$$\mathfrak{I} = C_T p_c A_t \tag{40}$$

where C_T is called the thrust coefficient. Equating equations 37 and 40 and solving for C_T

$$C_T = \lambda C_D \Omega \frac{w_e}{\sqrt{gRT_c}} + \left(\frac{p_e}{p_c} - \frac{p_a}{p_c}\right)\frac{A_e}{A_t} \tag{41}$$

Substituting for w_e from Section 7

$$C_T = \lambda C_D \varphi \Omega \sqrt{\frac{2k}{k-1}} \sqrt{\frac{Z}{1+Z}} + \left(\frac{p_e}{p_c} - \frac{p_a}{p_c}\right)\frac{A_e}{A_t} \tag{42}$$

Equation 42 shows that the thrust coefficient C_T is independent of the gas temperature or molecular weight and depends only upon k, p_c, p_a, and A_e/A_t.

Where the nozzle is designed for the optimum area ratio, so that $p_e = p_a$, then

$$C_T = \lambda C_D \varphi \Omega \sqrt{\frac{2k}{k-1}} \sqrt{\frac{Z}{1+Z}} \tag{43}$$

The thrust coefficient may be determined from equation 42 or more readily from a chart such as Fig. 13, which was calculated by Mr. R. D. Geckler for $\lambda = 0.9830$ ($\alpha = 15°$) and for $C_D = \varphi = 1.0$.
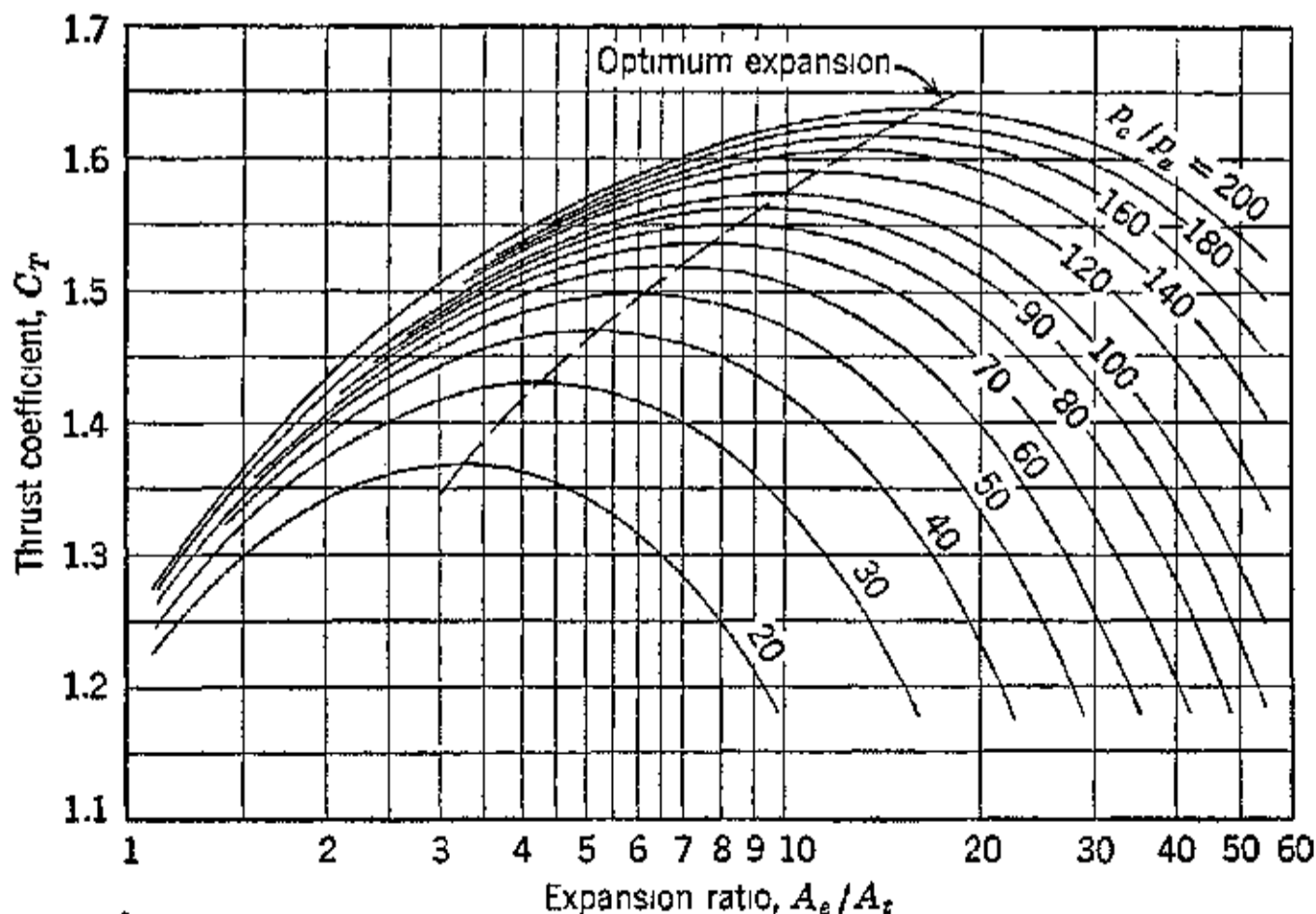
FIG. 13. Calculated thrust coefficient vs. expansion ratio for different pressure ratios (based on $k = 1.28$, $\lambda = 0.9830$, $C_D = \varphi = 1.0$).

Equation 40 is one of the basic design formulas for rocket motors. The value of C_T as a function of the combustion-chamber pressure is determined experimentally for the particular propellants to be employed. This is readily accomplished since the thrust, chamber pressure, and throat area can be measured accurately. The curve of C_T vs. p_c gives the data for establishing the basic dimensions of the nozzle for any specified thrust or operating chamber pressure.

EXAMPLE. A rocket motor operates with a chamber pressure of 364 psia. The atmospheric pressure is 14.7 psia, and the area ratio for the nozzle is 3.0. Calculate the thrust coefficient if $k = 1.28$ and the exit half-angle of the nozzle is 15°.
   Solution. For $\alpha = 15°$, $\lambda = 0.9830$. From Fig. 6, $A_e/A_t = 3.0$, $p_c/p_e = 20$. Hence

$$p_e = \frac{364}{20} = 18.2 \quad \text{psia}$$

and

$$\left(\frac{p_e}{p_c} - \frac{p_a}{p_c}\right)\frac{A_e}{A_t} = \frac{18.2 - 14.7}{364} \times 3$$

$$= 0.029$$

From Table 12·2,

$$\sqrt{\frac{2k}{k-1}} = 1.414 \times 2.138 = 3.02; \quad \Omega = 0.6636$$

From Table 12·4,

$$\sqrt{\frac{Z}{1+Z}} = 0.6933$$

Assume $C_D = 0.95$, and $\varphi = 0.98$. By equation 42

$$C_T = 1.268 + 0.029 = 1.297$$

12. Effective Exhaust Velocity (w)

In the test of a rocket motor the variables—the thrust $\mathfrak{I}$, the total propellant consumption $G \Delta t$ pounds, and the duration Δt seconds—are measured. It is convenient, therefore, to express the thrust by the equation.

$$\mathfrak{I} = \frac{G}{g} w \tag{44}$$

where w is called the effective exhaust velocity.
   It follows from equations 38 and 44 that

$$w = \lambda w_e + \frac{g}{G}(p_e - p_a)A_e \tag{45}$$

Consequently, if the thermodynamic properties of the combustion gases are known, so that w_e can be calculated, the effective exhaust velocity can be determined by calculation. Otherwise w is determined by a test wherein the total propellants $W_P = G \, \Delta t$ consumed in Δt seconds is measured. The tests also give a thrust-duration curve such as that illustrated in Fig. 14. From the test data $G = W_P/\Delta t$ and

$$w = \mathfrak{J} \, \Delta t \, \frac{g}{W_P} \tag{46}$$

The product $\mathfrak{J} \, \Delta t$ is the integral of the thrust vs. duration curve (Fig. 14) and is called the impulse I in pound-seconds. Hence, if the impulse produced by the consumption of W_P lb of propellant is I, then

$$w = \frac{g}{W_P} I \quad \text{fps} \tag{46a}$$

The effective exhaust velocity is one of the most important criteria of rocket-motor performance. The objectives of research and development are to increase its value continually.
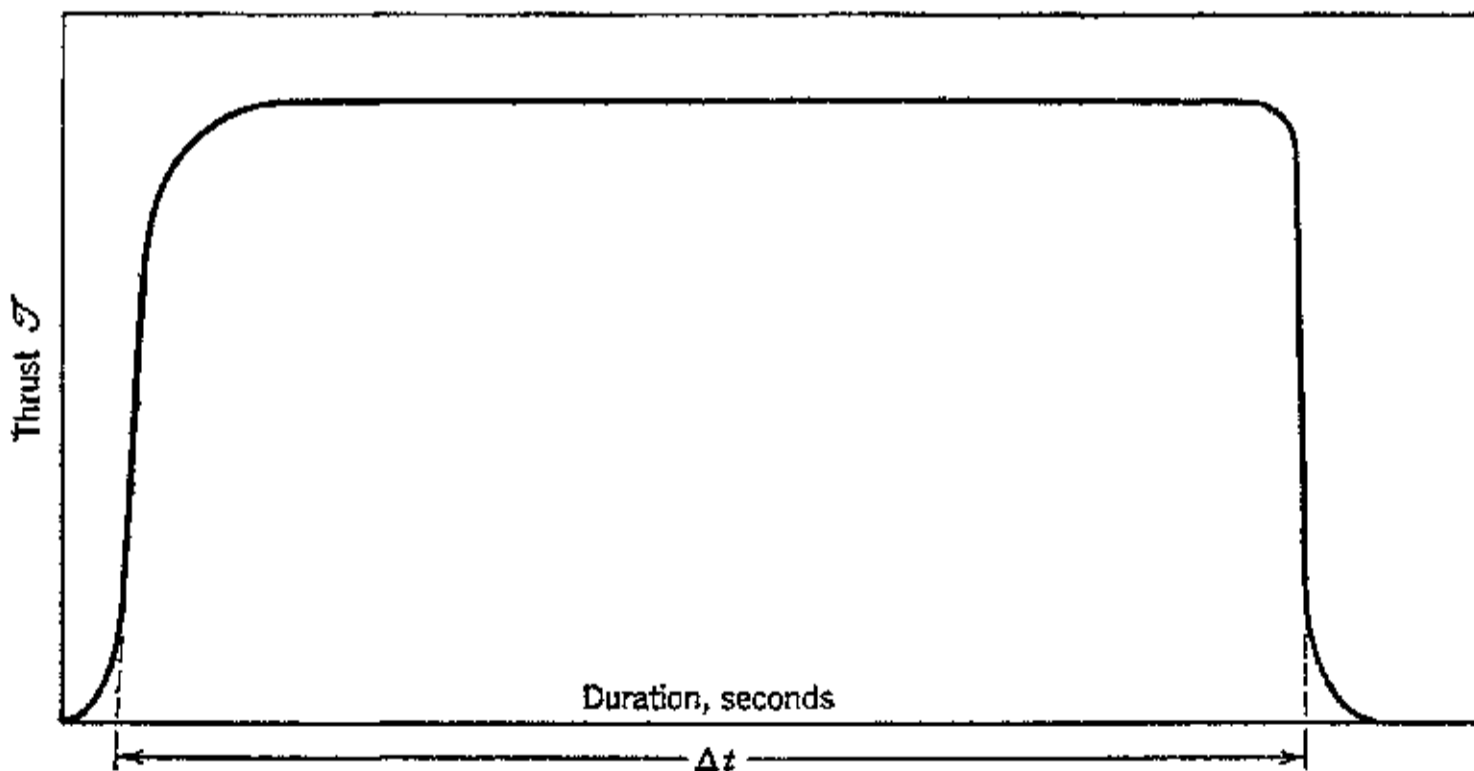
FIG. 14.   Illustration of thrust-duration curve for a constant-pressure rocket motor.

For given propellants the magnitude of the effective exhaust velocity is affected mainly by the conditions within the rocket motor. It is practically independent of the surrounding atmosphere. This is to be expected from the basic phenomena associated with the supersonic flow of gases, according to which the pressure distribution in the nozzle cannot be affected by conditions beyond its exit.

If the area ratio for the nozzle is selected so that the gases are expanded to the atmospheric pressure when they reach the exit section A_e, then $p_e = p_a$. The thrust equation accordingly becomes

$$\mathfrak{J} = \lambda w_e \frac{G}{g} \tag{46b}$$

and for $\lambda = 1$

$$\mathfrak{J} = \frac{G}{g} w_e = \frac{G}{g} w \tag{46c}$$

In this case the effective exhaust velocity is identical with the exit velocity.

For a given rocket motor the thrust will vary as the back pressure is changed. Consequently, if the motor is to operate at different altitudes, the area ratio must be selected so that it is the best compromise for the operating conditions. Usually, the nozzle is designed so that it will operate with a slight underexpansion at the most significant operating altitude. The effect of altitude on the performance of two different motors designed to operate with different degrees of underexpansion at sea level is illustrated in Fig. 15.

For the optimum area ratio the effective exhaust velocity in terms of the thermodynamic properties of the propellant gases and their expansion ratio is given by

$$w = \varphi \sqrt{2g \frac{k}{k-1} R T_c \left[1 - \left(\frac{p_e}{p_c}\right)^{\frac{k-1}{k}} \right]} \tag{47}$$

The above equation shows that the effective exhaust velocity increases directly as the square root of the product of the combustion-chamber temperature T_c and the gas constant R. It also increases with the expansion ratio and with a decrease in the specific-heat ratio for the gases. The two last-mentioned factors exert only a minor influence, so that for practical purposes it can be assumed that the effective exhaust velocity is proportional to $\sqrt{T_c R}$. Since the gas constant $R = 1545/m$, where m is the molecular weight of the gases, it follows directly that the effective exhaust velocity is proportional to $\sqrt{T_c/m}$.

Figure 16 illustrates the manner in which the combustion-chamber temperature and pressure affect the effective exhaust velocity. The curves were calculated on the basis that the molecular weight is constant and $k = 1.2$.
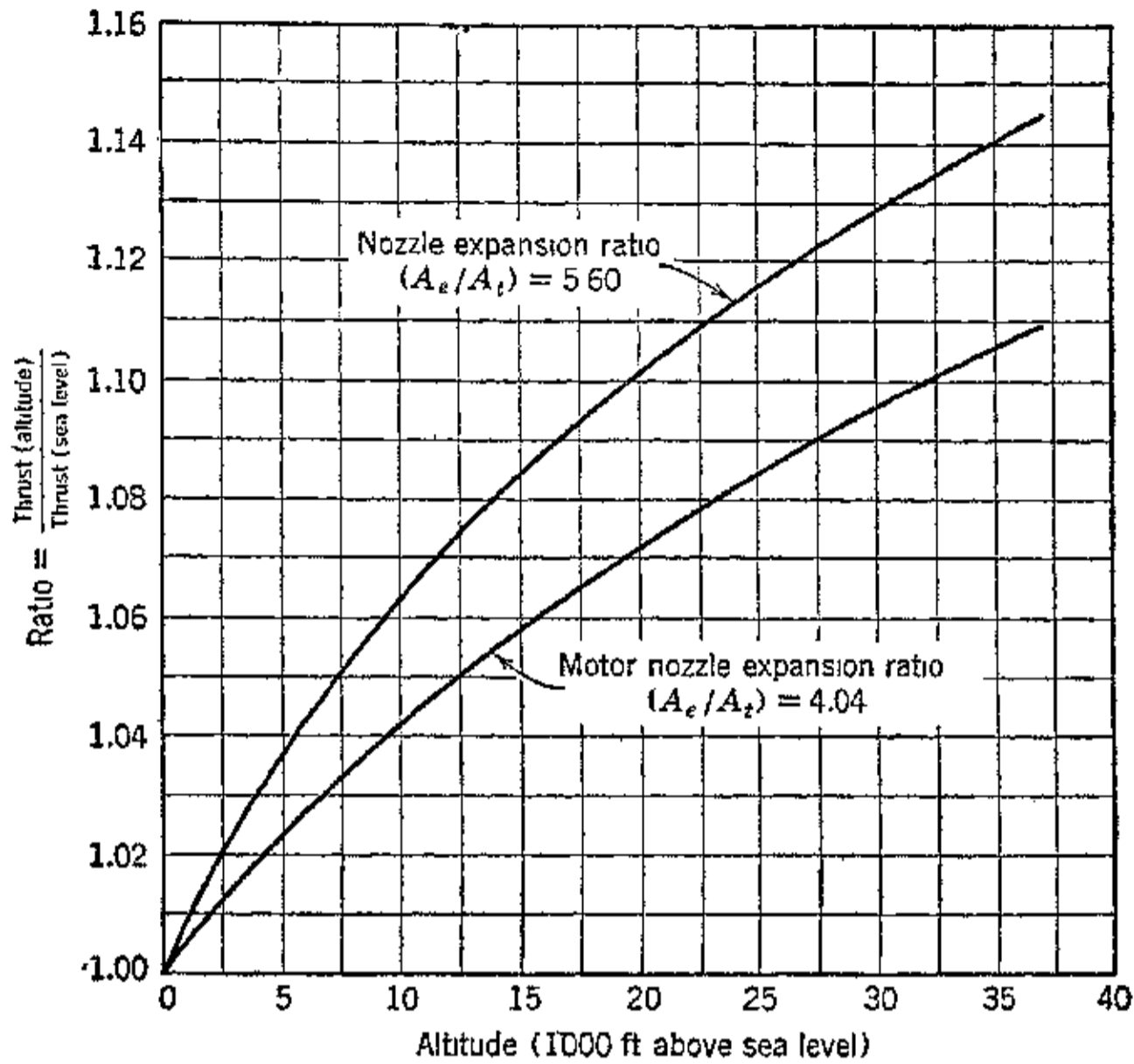
FIG. 15.   Thrust vs. altitude curves for two different rocket motors.   (Reproduced from M. J. Zucrow, *loc. cit.*)
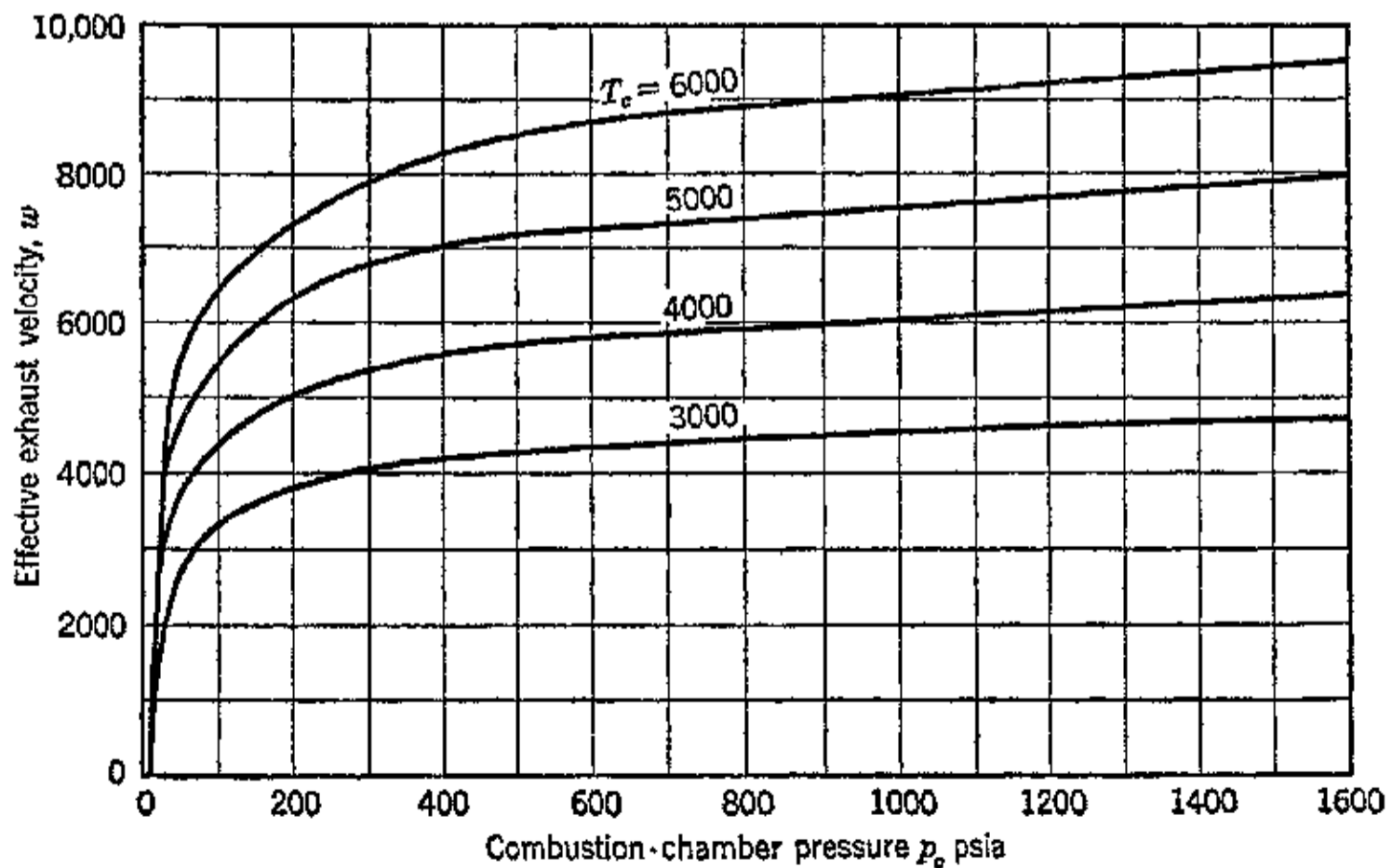
FIG. 16.   Effect of chamber temperature and expansion ratio on effective exhaust velocity (constant value of $k = 1.2$).   (Reproduced from M. J. Zucrow, *loc. cit.*)

For the gases generated by the propellants currently being used the values of R can be assumed to vary from 60 to 80. The combustion-chamber temperature will range from 3500 R to 6000 R.

EXAMPLE. A rocket motor using liquid propellants is operated at 300 psia chamber pressure. The nozzle is designed for the optimum area ratio for the sea-level atmospheric pressure of 14 7 psia; the throat diameter is 2 in., and the divergence angle is 15°. Calculate the effective exhaust velocity and thrust at sea level and at 20,000 ft altitude. Assume $k = 1.25$, $\sqrt{T_c/m} = 14.8$, and $C_D = 0.95$.

Solution. From Table 12·2, $\Omega = 0.6581$. Hence from equation 26

$$C_G = \frac{0.95 \times 0.1443 \times 0.6581}{14.8} = 0.0061$$

From equation 25

$$G = 0.00610 \times (2)^2 \times 0.7854 \times 300$$

$$= 5.75 \quad \text{lb/sec}$$

This rate is independent of the atmospheric pressure. From Fig. 9 the exit velocity is obtained as follows: $(p_c/p_e) = 300/14.7 = 20.4$. Hence

$$\frac{w_e}{\varphi \sqrt{T_c/m}} = 475$$

$$w_e = 0.95 \times 14.8 \times 475 = 6680 \quad \text{ft/sec}$$

The effective exhaust velocity is obtained from equation 45. From Fig. 11

$$\lambda = 0.9830 \text{ for } \alpha = 15°$$

$$w = 0.9830 \times 6680 + \frac{g}{G}(p_e - p_a)A_e$$

At sea level the last term is zero, and

$$w = 6560 \quad \text{fps}$$

At 20,000 ft, $p_a = 6.73$ psia and the last term becomes

$$\frac{g}{5.75}(14\ 7 - 6.73)A_e$$

A_e is determined from Fig. 7 as 11 sq in. Hence

$$w = 6560 + \frac{32.174}{5.75}(8.0)11$$

$$= 6560 + 486$$

$$= 7046 \quad \text{fps}$$

At sea level:

$$\mathfrak{F} = \frac{5.75}{32.174} \times 6560$$

$$= 1175 \quad \text{lb}$$

At 20,000 ft:

$$\mathfrak{F} = \frac{5.75}{32.174} \times 7046$$

$$= 1260 \quad \text{lb}$$

13. Specific Impulse (I_{sp})

The performance of a liquid-propellant rocket motor is quite generally stated in terms of its effective exhaust velocity. Solid-propellant rocket-motor performance is expressed more frequently in terms of the impulse delivered per unit weight of propellant consumption. This is termed the *specific impulse* of the propellants. Thus,

$$I_{sp} = \frac{I}{W_P} \tag{48}$$

The use of this criterion is becoming more prevalent in all fields of rocketry.

The specific impulse is a thermodynamic property of the propellant gases, and its magnitude for a given expansion ratio is independent of the motor design. For a given propellant the specific impulse depends only upon the nozzle expansion ratio.

The relationship between the effective exhaust velocity and the specific impulse is obtained as follows:

From equation 44 the effective exhaust velocity is

$$w = \Im\frac{g}{G} \tag{49}$$

Comparing equations 48 and 49 it is seen that

$$I_{sp} = \frac{w}{g} \tag{50}$$

In other words the effective exhaust velocity is g times the specific impulse.

From equations 49 and 50

$$\Im = GI_{sp} = \frac{W_P}{\Delta t} \cdot I_{sp} \tag{51}$$

Comparison of equations 25, 40, and 51 furnishes the following relationship.

$$I_{sp} = \frac{C_T}{C_G} \tag{52}$$

The I_{sp} of the propellants can be calculated from thermodynamic values of T_c and m by substituting for C_G

$$I_{sp} = 6.93 \frac{C_T\sqrt{\dfrac{T_c}{m}}}{C_D\Omega} \tag{53}$$

The values of C_T can be taken directly from charts or can be calculated from equation 42.

If the rocket-motor nozzle has the optimum area ratio, then substituting for w from equation 47 gives

$$I_{sp} = \frac{w}{g} = 6.93\varphi \sqrt{\frac{T_c}{m}} \sqrt{\frac{2k}{k-1}\left[1 - \left(\frac{p_e}{p_c}\right)^{\frac{k-1}{k}}\right]} \qquad (54)$$

This last equation shows that the specific impulse depends primarily upon the square root of the ratio of the temperature of the
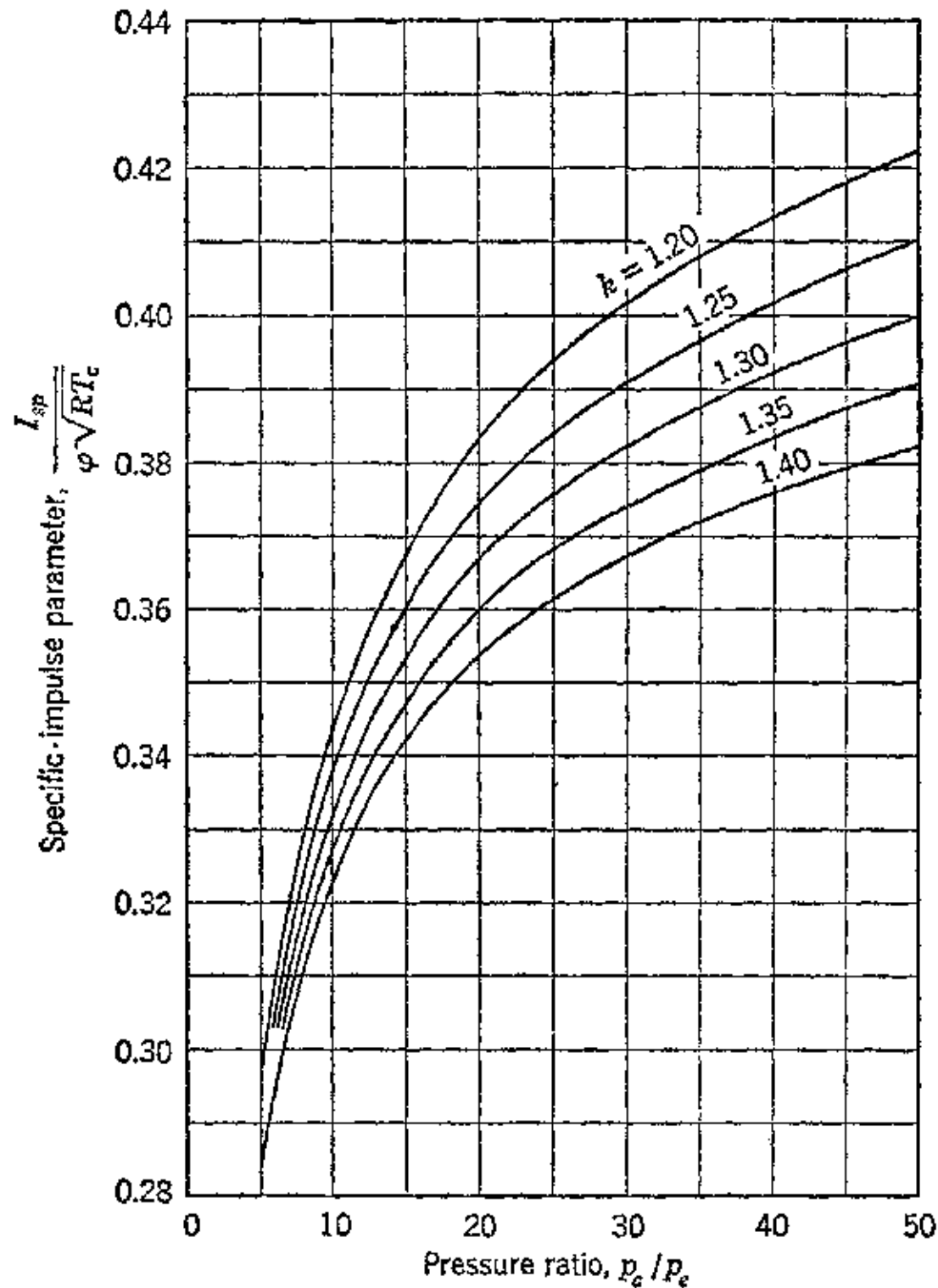
Fig. 17. Specific impulse parameter $I_{sp}/\varphi\sqrt{RT_c}$ as a function of pressure ratio for different values of specific-heat ratio.

gases in the combustion chamber to their molecular weight; this follows from the preceding discussion of the equation for the effective exhaust velocity.

The maximum temperature in the combustion chamber is limited by dissociation reactions and from a practical standpoint by the materials available for constructing rocket motors. Consequently, the possibility of increasing the specific impulse by raising the combustion-chamber temperature is limited until new methods for protecting the combustion chamber and nozzle walls are developed.

The possibility of increasing the specific impulse by reducing the molecular weight of the gases by using fuels rich in hydrogen also suffers from certain restrictions. Fuels rich in hydrogen have low specific weight, so that the average specific weight for the propellants is reduced. This makes it necessary to use supply tanks having large volumes, thereby increasing the overall weight of the jet-propulsion system. Therefore an additional guide to the selection of a propellant combination, all other things being equal, is the product: specific impulse $\times$ specific weight. If stepped rockets are considered, where the empty propellant tanks are discarded from the rocket system as they are emptied, then the specific impulse is the unique criterion.

Figure 17 plots the dimensionless ratio $I_{sp}/\varphi\sqrt{RT_c}$ as a function of the pressure ratio. This ratio is sometimes called the *reduced specific impulse;* its value depends only upon the specific-heat ratio for the combustion-chamber gases.

14. Specific Propellant Consumption

The propellant consumption of a rocket motor is usually stated in terms of the required flow rate of propellants to produce 1 lb-sec impulse. Let G_{sp} denote the specific propellant consumption (fuel + oxidizer), and G the rate of propellant flow. For a given thrust $\mathfrak{I}$, it follows from equation 49 that

$$G = \frac{\mathfrak{I}g}{w} \quad \text{lb/sec}$$

But $G_{sp} = G/\mathfrak{I} = 1/I_{sp}$; hence

$$G_{sp} = \frac{g}{w} \tag{55}$$

Thus, if the effective exhaust velocity of a rocket motor is 6200 fps, its specific propellant consumption is $G_{sp} = 32.174/6200 = 0.0052$ lb/lb-sec.

The specific propellant consumption, being the reciprocal of the specific impulse, is affected by the same factors.

15. Characteristic Velocity (c*)

A useful criterion of rocket-propellant performance is the so-called *characteristic velocity* c^* defined by

$$c^* = \frac{w}{C_T} \tag{56}$$

Substituting for w and C_T gives

$$c^* = \frac{p_c A_t g \, \Delta t}{W_P} = \frac{g \cdot p_c \cdot A_t}{G} \tag{57}$$

This is the equation used for determining c^* in experimental work, and it is evident that the value of c^* is independent of thrust $\mathfrak{I}$, and no measurement of $\mathfrak{I}$ is required for calculating the value of c^*.

Since $G = C_G p_c A_t$, it follows that

$$c^* = \frac{g}{C_G} \tag{58}$$

The characteristic velocity and the weight flow coefficient are evidently equivalent, and it is a matter of choice which parameter is actually used to express the performance of a propellant. Generally, c^* is more common in studying liquid propellants and C_G is used almost exclusively in studying solid propellants.

Substituting for C_G in equation 58 gives

$$c^* = \frac{\sqrt{RT_c}}{C_D \Omega} g \tag{59}$$

Substituting for $R = 1544/m$

$$c^* = \frac{223.0 \sqrt{T_c/m}}{C_D \Omega} \tag{60}$$

This equation is useful for computing the temperature of the gas in the combustion chamber.

Substituting for w and for C_T in equation 56 and assuming $\varphi = 1$ for convenience gives the following equation for c^*.

$$c^* = \frac{\sqrt{2g\left(\frac{k}{k-1}\right)RT_c}}{2\sqrt{\frac{k^2}{k^2-1}\left(\frac{2}{k+1}\right)^{\frac{2}{k-1}}}} = \frac{\sqrt{gkRT_c}}{\sqrt{2\left(\frac{2}{k+1}\right)^{\frac{2}{k-1}}\left(\frac{k^2}{k+1}\right)}} \tag{61}$$

The numerator is the acoustic velocity corresponding to conditions in the combustion chamber a_c. Hence

$$c^* = \frac{a_c}{\sqrt{2\left(\dfrac{2}{k+1}\right)^{\frac{2}{k-1}}\left(\dfrac{k^2}{k+1}\right)}} \qquad (62)$$

It is seen from equation 62 that the characteristic velocity c^* depends only upon the operating mixture ratio (oxidizer/fuel) and the combustion-chamber pressure and/or temperature.

For a given ratio of oxidizer to fuel the effect of pressure on the combustion-chamber temperature is slight. This is particularly true for compounded solid propellants and not significantly incorrect for liquid propellants where the temperatures reached do not give appreciable dissociation. Consequently, it can be assumed without serious error that c^* is independent of the chamber pressure for a fixed mixture ratio.

In the experimental testing of rocket motors the value of c^* is calculated from equation 57 and the measurements of the total propellants consumed W_P, the duration of the run Δt, the combustion-chamber pressure p_c, and the area of the nozzle throat section A_t.

16. Combustion in the Rocket Motor

The energy developed in the rocket motor for propulsion purposes is derived from the thermochemical energy of the propellants. Their chemical reaction (combustion) is exothermic and is accompanied by the evolution of large quantities of gases at high temperature. Since the fuels employed are predominantly hydrocarbons the products of the reaction usually contain CO_2, CO, and H_2O as principal constituents. Both the temperature attained by the reaction and the composition of the reaction products are influenced to some extent by the mixture ratio (oxidizer weight/fuel weight) and by the phenomenon of dissociation. The conditions for chemical equilibrium between the reaction products determine the final gas composition. [13,14,15]

Because of the high temperature reached, the chemical reaction of the propellants does not go to completion. Thus some of the CO_2 present dissociates into $CO_2 = CO + \frac{1}{2}O_2$, the water vapor into $H_2O = H_2 + \frac{1}{2}O_2$. If the temperature is allowed to become sufficiently high the dissociation results in the further breakdown of these products. Thus at 4500 F, approximately, the water vapor

dissociates into H + OH, and at 7200 F it dissociates into H + H + O. At temperatures above 9000 F no molecular components are present in the reaction products.[16]

As a consequence of the dissociation phenomena the maximum temperature which can be reached by the combustion gases is limited. The amount of dissociation occurring will depend mainly upon the predominating temperature and pressure. In general, it can be said that the higher the temperature the greater the dissociation, and the higher the pressure the less the dissociation. This is apparent from Table 12·6, which presents dissociation data for CO_2 and H_2O.

TABLE 12·6

DISSOCIATION OF H_2O AND CO_2 IN PER CENT

(Marks' *Handbook;* data of Tizard and Pye, *Automobile Engineer*, 1921)

Temper-ature °F	Pressure in Atmosphere							
	H_2O				CO_2			
	0.1	1.0	10	100	0.1	1.0	10	100
2730	0.043	0.02	0.009	0 004	0.104	0.048	0.0224	0.01
3630	1.25	0.58	0.27	0.125	4.35	2.05	0.96	0.445
4530	8.84	4.21	1.98	0.927	33.5	17.6	8.63	4.09
5430	28.4	14.4	7.04	3.33	77.1	54.8	32.2	16.9

From a practical standpoint, however, any phenomenon which aids in limiting the maximum temperature in the combustion chamber without affecting the performance too adversely is beneficial because of the limitations imposed by the materials and cooling methods currently available for constructing rocket motors.

Dissociation may be conceived as a decomposition of the formed chemical compounds resulting from exposing them to high temperatures. Because of this phenomenon not all the thermochemical energy of the propellants is available to the rocket motor for transformation into kinetic energy. Consequently, the effective exhaust velocity attained will be lower than the theoretical value based on the thermochemical energy content of the propellants. In addition to the unavoidable loss resulting from dissociation there are other losses due to such effects as radiation, fluid friction in piping and nozzle, and imperfect combustion due to some of the propellants being inadequately mixed.

The effect of the pressure in the combustion chamber upon the completeness of reaction is governed by the subsequent reactions which can take place between the products of combustion. When the

subsequent reaction is such that the volume of the reactants is larger than that obtainable from their complete reaction, increasing the combustion-chamber pressure favors driving such a chemical reaction to completion. If the completed chemical reaction does not produce a change in volume, pressure has no effect on the reaction. On the other hand, if the completed reaction will produce an increase in volume, increasing the pressure hinders the progress of that chemical reaction.[17] Consequently, the chamber pressure exerts an influence upon the final gas composition. Its effect on dissociation is to reduce this tendency. In general, a high chamber pressure favors improved performance, but the rate of improvement decreases for values of p_c larger than 300 psia.

Table 12·7 presents pertinent thermochemical data on liquid fuels which may find usefulness in liquid bipropellant systems.

TABLE 12·7

THERMOCHEMICAL DATA ON LIQUID FUELS

Calculated from data in (1) *Chem. Eng. Handbook*, pp. 272–311; (2) Hougen and Watson, *Industrial Chemical Calculations*, pp. 168–170; (3) Robinson, *Thermodynamics of Firearms*, pp. 46–51.

Fuel	Chemical Formula	Molecular Weight	Heat of Combustion * (Btu/lb)	Heat of Formation (Btu/lb)
Carbon disulfide	CS_2	76.13	5,960	−519
Methanol	CH_3OH	32.07	9,078	3,462
Acetylene	C_2H_2	26.04	20,770	−4,015
Ethanol	C_2H_5OH	46.07	11,930	2,619
Gasoline	C_8H_{18}	114 23	19,245	
Ethylene (gas)	C_2H_4	28.05	20,300	. . . .
Hydrogen	H_2	2.016	51,608	0
Methane	CH_4	16.04	21,529	2,000
Hydrocarbon oils	C_nH_{2n+2}	.	22,000 (approx.)	. . . . . .
Propane	C_3H_8	44.09	19,940	
Benzene	C_6H_6	78.11	17,190	−300

* A method for calculating the heats of combustion of compounds, developed by Kharasch and Sher, is reported in *Bureau of Standards Journal of Research*, Vol. 2, pp. 359–430, 1929. If the structural formula of a compound is known, its heat of combustion may be calculated by this method with an accuracy that is within 1 per cent of the experimentally determined value. Values in the table are lower heating values.

17. Cooling of Rocket Motor

The adequacy of a rocket motor depends almost entirely upon its ability to perform without damage at high temperatures for the

operating duration, and the number of runs, to which it is subjected. Of the total heat liberated by the reaction of the propellants approximately 5 per cent is transferred to the motor and nozzle walls; this amounts to 120 to 200 Btu/sec. There are at present four major methods for protecting the motor walls from this transferred heat: (1) the motor walls and nozzle can be constructed of suitable materials, heavy enough to absorb the heat during the operating period; (2) one of the propellants in its passage to the injection system can be circulated around the heat-absorbing surfaces to keep them cool—this is the regenerative cooling system and decreases the heat losses; (3) high-temperature-resistant materials (refractories) can be used for lining the heated surfaces; and (4) film cooling can be applied.

Method 1 employs the principle of supplying a heat reservoir capable of receiving the total quantity of heat to be absorbed without raising the metal temperatures to dangerous values. The most suitable materials for this type of cooling are those for which the product (specific heat $\times$ thermal conductivity $\times$ density) has high values. The best material from this standpoint is copper. The foregoing criterion is not, however, a unique guide to motor construction, since considerations of strength and weight are frequently of greater importance. In any case, as the required operating duration for an uncooled motor is raised, the requisite motor weight becomes excessive for practical use. Consequently, this type of motor construction is adaptable only to rocket motors which are to be operated for short durations and may be operated with high fuel oxidizer ratios to reduce the operating temperature. Satisfactory motors of this type have been built for durations up to 35 sec. They weigh more than rocket motors of equal thrust output that employ regenerative cooling.

Method 2, regenerative cooling, appears currently to be a sound approach to the solution of the heat problem. It has the advantage that, once the cooling system has been developed correctly, the motor can be operated for long durations (several minutes at a time) without damage. Furthermore, these motors can be made extremely light in weight, the thrust-weight ratio increasing markedly with the larger thrusts. A large number of successful motors of this type have been built.

Little advance has been made using method 3, but it seems probable that good results will be obtained by combining it with method 2.

Method 4, film cooling, appears to offer the ultimate in permitting high temperatures to prevail in the combustion chamber. It is based on forming, over the inside walls of the chamber and nozzle, a com-

plete film of liquid which by its evaporation keeps these surfaces cool. The effectiveness of this form of cooling can be judged by the results obtained in the German V-2 rocket motor which used a crude version of this form of cooling. By permitting approximately 7 per cent of the total fuel (alcohol) consumption to enter the nozzle surfaces to give a form of film cooling, temperatures of 5400 R could be withstood without damage in a motor having a thin carbon-steel inner wall. True film cooling as discussed above is still in the development stage.

18. Propulsion Efficiency

Consider a rocket-jet-propelled body moving at the constant flight speed V prior to the exhaustion of its propellant supply. Assuming steady conditions, the rate of propellant consumption $G = G_o + G_f$ lb/sec and the effective exhaust velocity w fps are constants. Under these conditions the thrust of the rocket motor $\mathfrak{I} = \dfrac{G}{g} w$ remains constant.

The useful work or thrust power P_T is accordingly

$$P_T = \mathfrak{I}V = \frac{G}{g} wV \tag{63}$$

Let $c = w - V$ denote the absolute exit velocity of the propellant gases; then the leaving loss P_L is

$$P_L = \frac{G}{2g} c^2 = \frac{G}{2g} (w - V)^2 \tag{64}$$

The propulsion power P is given by

$$P = P_T + P_L = \frac{G}{2g} (w^2 + V^2) \tag{65}$$

The instantaneous propulsion efficiency η_P is accordingly

$$\eta_P = \frac{\mathfrak{I}V}{P} = \frac{2(V/w)}{(V/w)^2 + 1} \tag{66}$$

Letting $\nu = V/w =$ velocity ratio

$$\eta_P = \frac{2\nu}{\nu^2 + 1} \tag{67}$$

The propulsion efficiency of the rocket motor at any instant is seen to be zero when the rocket-jet-propelled system is at rest; $w = 0$.

As the flight speed of the system is increased, so that w increases, the propulsion efficiency increases until the velocity of the body is identical with the effective exhaust velocity of the gases; $w = 1$. For the last condition the leaving loss is zero and the ejected gases have transformed all their kinetic energy to propulsion work. If the flight speed can be increased so that v becomes greater than unity, the thrust power is likewise greater. This increase in the useful output is attained, however, at the expense of the kinetic energy asso-
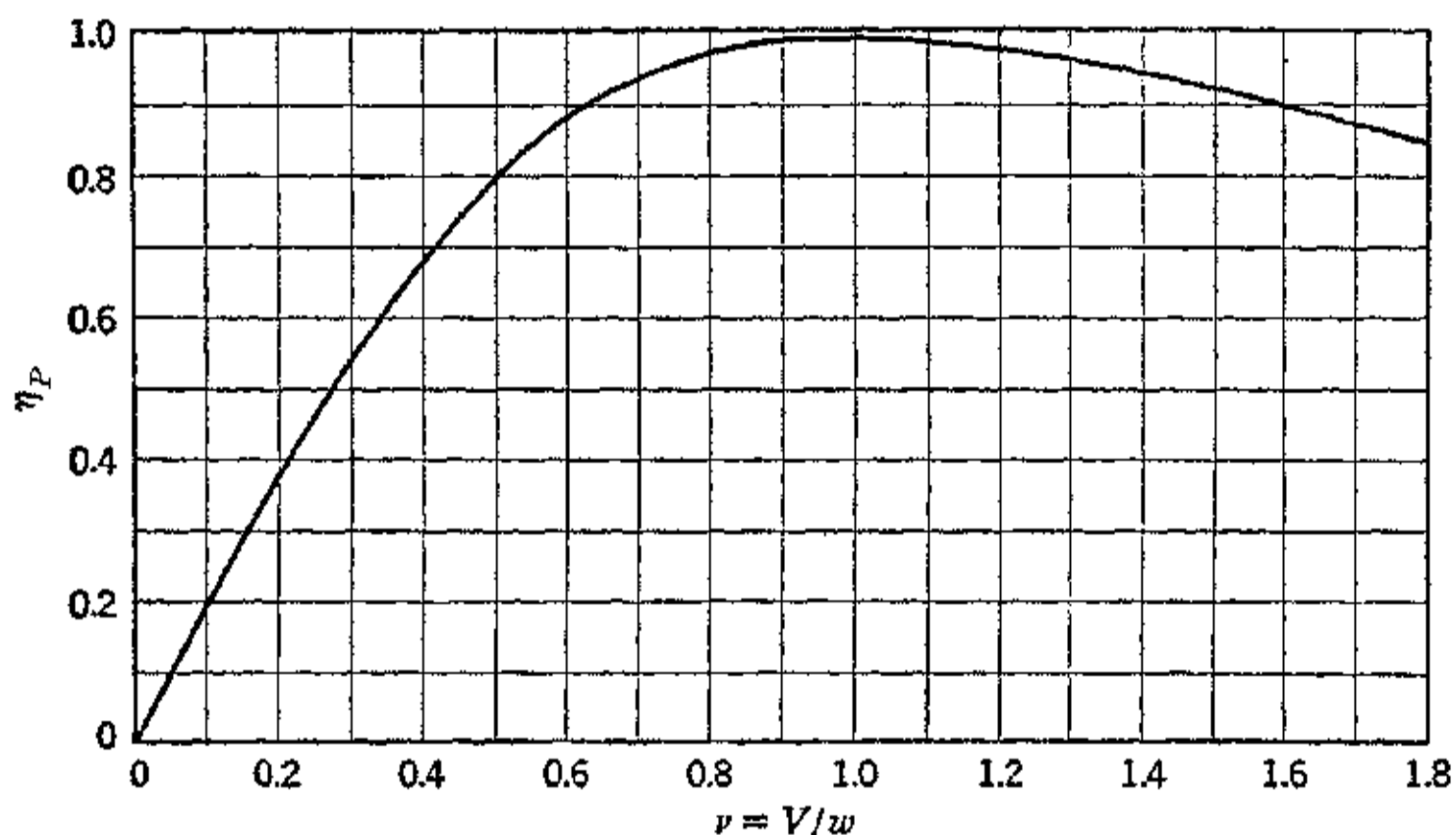
FIG. 18. Propulsion efficiency vs. velocity ratio for a constant-pressure rocket system. (Reproduced from M. J. Zucrow, *loc. cit.*)

ciated with the moving propellants. The result is a decrease in the instantaneous propulsion efficiency, because not all the energy of the ejected gases is converted into energy of motion.

Figure 18 presents the instantaneous propulsion efficiency of the rocket jet as a function of the velocity ratio.

The action of the rocket jet differs from that of either the propeller or thermal jet in that the thrust depends only upon the effective exhaust velocity. For the other two propulsion systems the thrust depends upon a difference in velocities. The magnitude of the rocket motor thrust is independent of its motion, assuming all other conditions unchanged. The magnitude of its propulsion efficiency, however, is dependent upon both the flight speed V and the effective exhaust velocity w. The effect of the exhaust velocity and the flight speed is illustrated in Fig. 19.

Because the thrust of the rocket depends only upon the effective exhaust velocity, operation at unity velocity ratio or higher is a

possibility. However, operation at close to unity velocity ratio is obtainable only if the flight speed is extremely high. Referring to
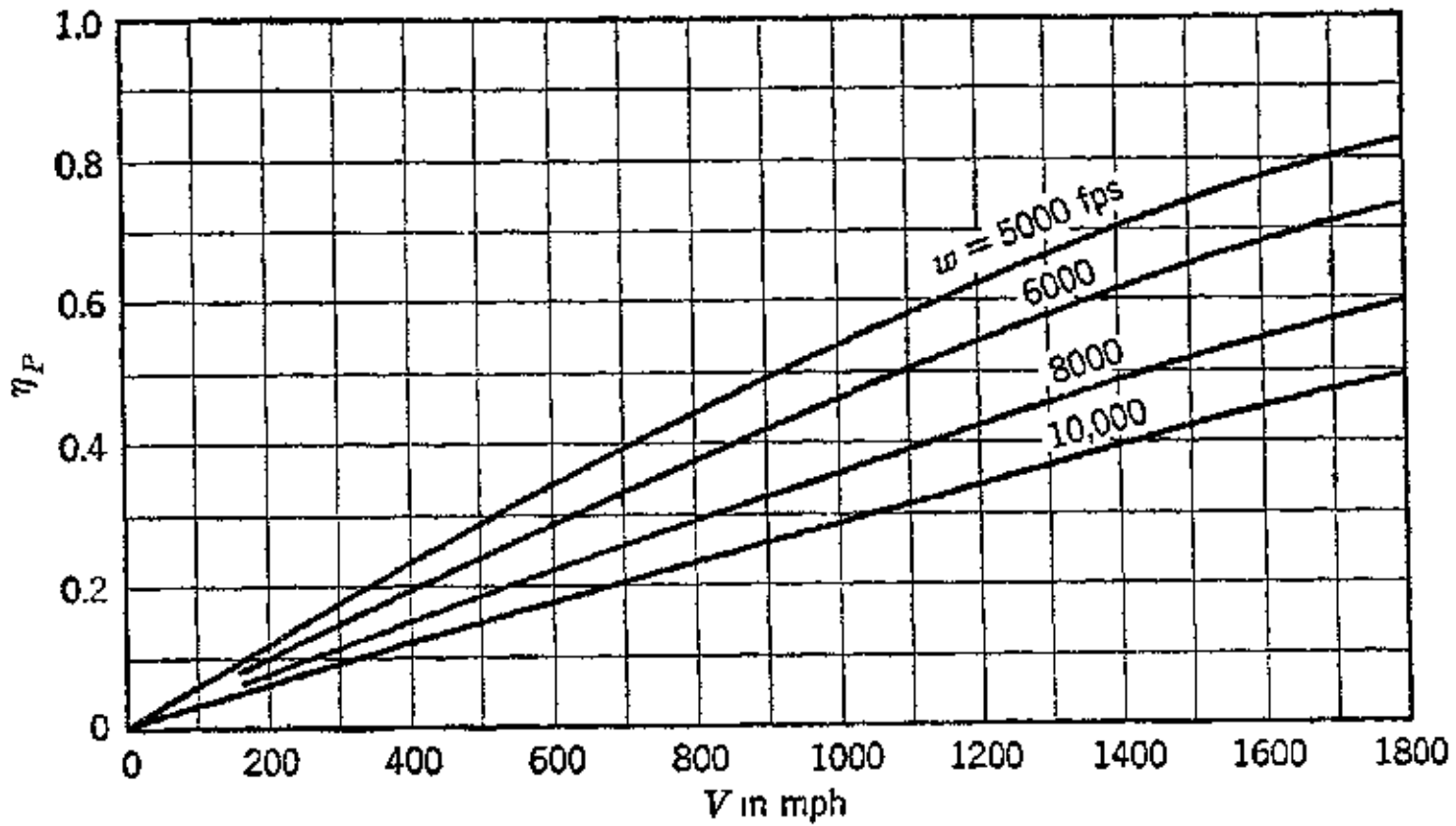
FIG. 19. Propulsion efficiency of rocket system as a function of true air speed for different values of the effective exhaust velocity. (Reproduced from M. J. Zucrow, *loc. cit.*)

Fig. 19 it is apparent that the rocket jet is an inefficient propulsion device at speeds comparable to those currently being attained by the speediest fighter aircraft.
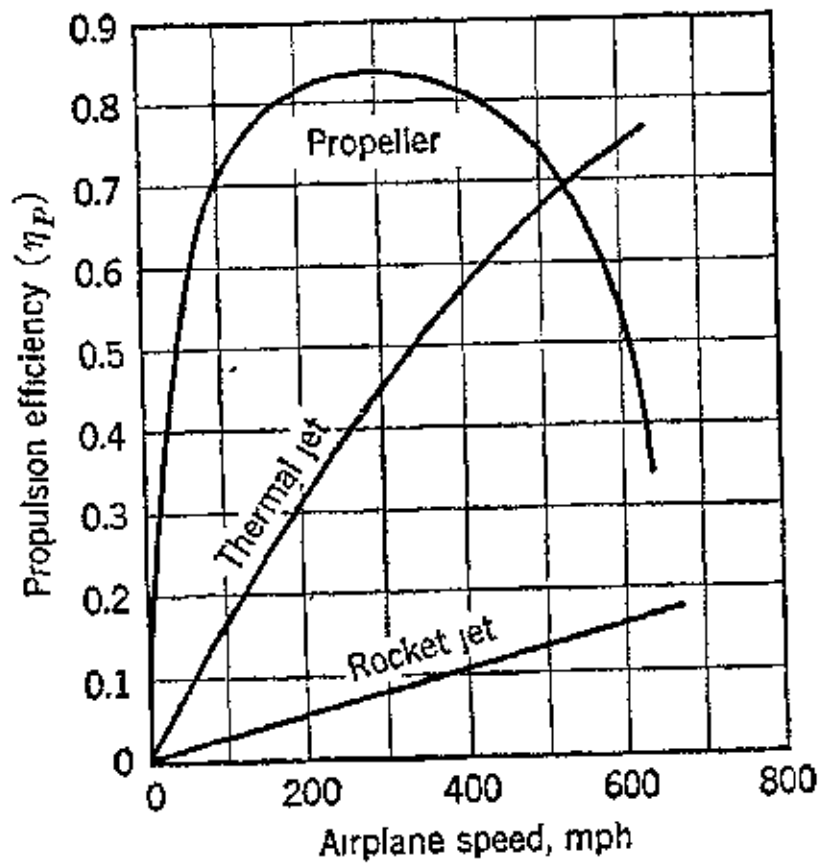
FIG. 20. Comparison of propulsion efficiencies of propeller, thermal jet, and rocket jet at 20,000 ft altitude. (Reproduced from Sir A. H. Roy Fedden, *Proc. Royal Aero. Soc.*, May 25, 1944.)

Figure 20 compares the calculated instantaneous propulsion efficiencies of the propeller, thermal jet, and rocket jet at 20,000 ft altitude (Sir A. H. Roy Fedden, *Proc. Royal Aero. Soc.*, May 25, 1944).

The principal thrust and power relationships for the propeller, thermal-jet, and rocket-jet propulsion are assembled for convenience in Table 12·8.

TABLE 12·8

THRUST AND POWER RELATIONSHIPS

Item	Propeller and Thermal Jet	Rocket Jet	Units
Thrust $\mathfrak{J}$	$\mathfrak{J} = \dfrac{G}{g}(w - V) = \dfrac{G}{g}w(1 - \nu)$ $\dfrac{\mathfrak{J}}{G} = \dfrac{w}{g}(1 - \nu)$	$\mathfrak{J} = \dfrac{G}{g}w$ $\dfrac{\mathfrak{J}}{G} = \dfrac{w}{g}$	lb $\dfrac{\text{lb}}{\text{lb/sec}}$
Exit loss P_L	$P_L = \dfrac{G}{2g}c^2 = \dfrac{G}{2g}(w - V)^2$	$P_L = \dfrac{G}{2g}c^2$ $P_L = \dfrac{G}{2g}(w - V)^2$	$\dfrac{\text{ft-lb}}{\text{sec}}$
Thrust power P_T	$P_T = TV = \dfrac{G}{g}w^2(1 - \nu)\nu$	$P_T = \mathfrak{J}V = \dfrac{G}{g}wV$ $= \dfrac{G}{g}w^2\nu$	$\dfrac{\text{ft-lb}}{\text{sec}}$
Propulsion power P	$P = P_T + P_L = \mathfrak{J}V + P_L$ $= \dfrac{G}{2g}(w^2 - V^2) = \dfrac{G}{2g}w^2(1 - \nu^2)$	$P = \mathfrak{J}V + P_L$	$\dfrac{\text{ft-lb}}{\text{sec}}$
Ideal propulsion efficiency ηP	$\eta P = \dfrac{2\nu}{1 + \nu}$	$\eta P = \dfrac{2\nu}{1 + \nu^2}$	. . . . .

$\nu = V/w$
G = fluid flow rate, lb/sec
V = true air speed, fps
w = relative exit velocity of propulsion fluid or effective exhaust velocity, fps

For a purely rocket-propelled body, the main object is usually to attain as high a flight speed as possible. Consequently, the flight speed V is not constant and at any instant the efficiency of propellant

utilization depends, as is shown in a later section, on the ratio of the instantaneous mass of the system to its initial mass when $V = 0$. Consequently, the propulsion efficiency varies throughout the *powered flight*, that is, while the propellants are being consumed.

19. Ideal Velocity of Rocket System

The *ideal velocity* is the speed the rocket system would attain if it moved in a frictionless medium without doing work against gravity. Although the results for the above ideal conditions cannot be applied directly, they do give an insight into the effect of certain characteristics of the rocket system upon the maximum attainable flight speed and upon the efficiency of rocket jet propulsion.

Assume that the rocket motor operates under steady conditions, so that the chamber pressure and the effective exhaust velocity do not change with time. For the notation used in this section, see Section 3.

At the beginning of the powered flight (when $t = 0$), the mass of the rocket system is $M_0 = m + m_P$ slugs, where m_P is the initial propellant mass at $t = 0$. Let x be the fraction of the total propellant mass consumed in unit time; then at any instant t during the powered flight the mass of the rocket system is given by

$$M = M_0 - xm_Pt \quad \text{slugs} \tag{68}$$

The rate of decrease in the mass of the system is $-dM/dt$ and is equal to the rate of propellant consumption. Hence

$$-\frac{dM}{dt} = xm_P \tag{69}$$

The thrust $\mathfrak{J}$ developed by the rocket motor accelerates the system at the rate dV/dt. The thrust is given by

$$\mathfrak{J} = xm_Pw = -w\frac{dM}{dt} \tag{70}$$

the negative sign denoting that the mass of the system is decreasing. Hence, since the increase in momentum of the system must equal the momentum change for the gases,

$$M\,dV = -dM \cdot w \tag{71}$$

or

$$M\,dV + w\,dM = 0 \tag{72}$$

Hence

$$dV = -w\frac{dM}{M} \tag{73}$$

Integrating and noting that when $t = 0$, $V = 0$, $M = M_0$, and at the end of the powered flight $t = t_p$, $V = V$, and $M = M_0 - m_P$, then

$$V = w \log_e \frac{M_0}{M_0 - m_P} \qquad (74)$$

Since $M_0 = m + m_P$, where m is the mass of the system exclusive of propellants, the ideal velocity V becomes

$$V = w \log_e \left(1 + \frac{m_P}{m}\right) = w \log_e \frac{M_0}{m} \qquad (75)$$

The ratio m_P/m is called the *mass ratio* and is a criterion of the design of the rocket system. The effect of the mass ratio on the ideal velocity, for different effective exhaust velocities, is shown in Table 12·9.

TABLE 12·9

EFFECT OF MASS RATIO AND EFFECTIVE EXHAUST VELOCITY ON IDEAL VELOCITY

Mass Ratio m_P/m	$w = 5000$ fps	$w = 6000$ fps	$w = 7000$ fps	$w = 8000$ fps	$w = 9000$ fps	$w = 10,000$ fps
0.2	910	1,090	1,275	1,460	1,640	1,820
0.4	1,680	2,020	2,350	2,690	3,030	3,370
0.6	2,350	2,820	3,290	3,750	4,220	4,700
0.8	2,940	3,530	4,120	4,700	5,300	5,880
1.0	3,470	4,150	4,850	5,550	6,230	6,930
1.2	3,940	4,740	5,520	6,310	7,100	7,890
1.5	4,580	5,500	6,410	7,320	8,230	9,160
2.0	5,490	6,590	7,690	8,770	9,890	10,990
2.5	6,260	7,530	8,770	10,200	11,260	12,530
3.0	6,930	8,400	9,700	11,050	12,460	13,860
4.0	8,050	9,650	11,250	12,850	14,450	16,090
5.0	8,960	10,740	12,520	14,330	16,100	17,920
10.0	11,990	13,800	16,100	18,400	20,700	23,400
20.0	15,230	18,250	21,300	24,400	27,400	30,450

It is seen from Table 12·9 that, for any given effective exhaust velocity, the mass ratio must be of the order of 2, if the ideal velocity is to be nearly equal to the effective exhaust velocity. The tabulated values neglect the influence of the air resistance, so that the mass ratio actually required will be much larger. To illustrate, the German V-2 missile weighed approximately 24,000 lb. Of this 18,000 lb were propellants and the balance war head, casing, and control mechanism. The effective exhaust velocity is estimated to have been 6400 fps, and the duration 71 sec. The maximum velocity attained was close to 6000 fps (4000 mph approximately). The trajectory and flight

characteristics for this missile according to references 7 and 19 are as follows:

Initial acceleration	$1g$
Duration of powered flight	71 sec
Velocity at end of powered flight	5300 fps
Height at end of powered flight	22 mi
Maximum height reached	68 mi
Velocity at top of trajectory	3900 fps
Time to reach top of trajectory	193 sec
Horizontal distance traversed	200 mi

The effect of the mass ratio on the overall efficiency of the rocket jet-propulsion method can be obtained by means of the following argument taken from reference 21.

In the ideal case the work done by the reaction force of the rocket jet is

$$L = \int_0^t \mathfrak{J} \cdot V \, dt = x m_P w \int_0^t V \, dt \tag{76}$$

But, from equation 75, $V = w \log_e (M_0/m)$. Hence, noting that $m = M_0 - x m_P t$, the work done is given by

$$L = x m_P w^2 \int_0^t \left[\log_e M_0 - \left\{ \log_e M_0 + \log_e \left(1 - \frac{x m_P t}{M_0} \right) \right\} \right] dt \tag{77}$$

Expanding the last term into a series [23]

$$\log_e \left(1 - \frac{x m_P t}{M_0} \right) = - \frac{x m_P t}{M_0} - \frac{1}{2} \left(\frac{x m_P t}{M_0} \right)^2 - \frac{1}{3} \left(\frac{x m_P t}{M_0} \right)^3 \cdots \tag{77a}$$

Hence

$$L = x m_P w^2 \int_{t=0}^{t=t_P} \left[\frac{x m_P t}{M_0} + \frac{1}{2} \left(\frac{x m_P t}{M_0} \right)^2 + \frac{1}{3} \left(\frac{x m_P t}{M_0} \right)^3 + \cdots \right] dt \tag{78}$$

Integrating between the limits $t = 0$ and $t = t_P$

$$L = \left[\frac{x^2 m_P^2 t_P^2}{2 M_0} + \frac{x^3 m_P^3 t_P^3}{6 M_0^2} + \frac{x^4 m_P^4 t_P^4}{12 M_0^3} + \cdots \right] w^2 \tag{79}$$

But the duration of the powered flight t_P is given by

$$t_P = \frac{1}{x} \tag{80}$$

Hence the work done during the powered flight is

$$L = \left[\frac{m_P^2}{2 M_0} + \frac{m_P^3}{6 M_0^2} + \frac{m_P^4}{12 M_0^3} + \cdots \right] w^2 \tag{81}$$

The overall efficiency of the rocket is given by the ratio of the work done L to the thermal energy of the propellants consumed $JE_PG_P = JE_Pgm_P$.

$$\eta = \frac{L}{JgE_Pm_P} \tag{82}$$

Let E_P denote the thermochemical energy of the propellants in Btu per pound, and let η_i denote the internal efficiency. Hence

$$\eta_i = \frac{w^2}{2gJE_P} \tag{83}$$

so that $JE_Pg = w^2/2\eta_i$. Substituting this last expression into equation 82 gives

$$\eta = \frac{2\eta_i L}{m_P w^2} \tag{84}$$

Substituting for L from equation 81 the result is

$$\eta = \eta_i \left[\frac{m_P}{M_0} + \frac{m_P{}^2}{3M_0{}^2} + \frac{m_P{}^3}{6M_0{}^3} + \cdots \right] \tag{85}$$

Since η_i can be assumed constant throughout the flight for reasons already discussed, it follows that the overall efficiency η depends upon the mass ratio m_P/M_0, and in the case where there is no frictional resistance to flight it is of the same order of magnitude as the mass ratio. When the body encounters resistance the efficiency will be reduced, because of the effects of gravity and of the air resistance. These will not affect the thrust of the motor, which, except for the small effects produced by altitude changes, can be assumed to be constant. There are propellants and jet-propulsion systems available that justify the assumption that the burning rate can be maintained constant.

20. Vertical Flight with No Air Resistance

This analysis, based on references 20 and 21, should be considered to give the optimum performance of the rocket motor in attaining extreme altitudes. It will be assumed that the rocket motor operates under steady-state conditions so that its thrust and effective exhaust velocity are constants.[20, 21]

The equation of motion for the rocket system *including air resistance or drag D*, during the *powered flight*, while the total propellant supply has not been consumed, is given by

$$\mathfrak{J} - Mg - D = Ma = \frac{dV}{dt} = \frac{d^2h}{dt^2} \quad \text{lb} \tag{86}$$

The assumed constant thrust is given by equation 70. Hence the acceleration a of the rocket system at any instant during the powered flight is given by

$$a = \frac{xm_P}{M} w - g - \frac{D}{M} \quad \text{ft/sec}^2 \qquad (87)$$

Owing to the constant rate of propellant consumption, the mass of the rocket system at any instant during the powered flight is given by

$$M = M_0 - xm_P t \quad \text{slug} \qquad (88)$$

Substituting for M from equation 88 gives the following equation for the acceleration.

$$a = \frac{xm_P w}{M_0 - xm_P t} - g - \frac{D}{M_0 xm_P t} \quad \text{ft/sec}^2 \qquad (89)$$

At the beginning of the powered flight the following conditions obtain.

$$t = 0, \quad M = M_0, \quad V = 0, \quad D = 0, \quad \text{and} \quad a = a_0 \qquad (90)$$

Hence, the initial acceleration at the time $t = 0$ is given by

$$a = a_0 = \frac{xm_P w}{M_0} - g$$

So that

$$xm_P = \frac{(a_0 + g)M_0}{w} = \frac{G}{g} \quad \text{slug/sec} \qquad (91)$$

Substituting for xm_P into equation 89, the acceleration equation becomes

$$a = \frac{a_0 + g}{1 - \frac{(a_0 + g)t}{w}} - g - \frac{D}{M_0}\left(\frac{1}{1 - \frac{(a_0 + g)t}{w}}\right) \qquad (92)$$

The drag D is a function of the flight speed V, the air density ρ, the largest cross-sectional area S, and the drag coefficient C_D, as explained in Chapter 5. Thus, letting σ denote the density ratio and ρ_0 the sea-level density,

$$D = \tfrac{1}{2}\rho_0 \sigma V^2 C_D S \qquad (93)$$

If it is assumed that there is no air resistance, then $D = 0$ and equation 92 becomes

$$a = \frac{dV}{dt} = \frac{a_0 + g}{1 - \frac{(a_0 + g)t}{w}} - g \quad \text{(No drag)} \qquad (94)$$

The velocity at any instant is obtained by integrating equation 94

$$V = \frac{dh}{dt} = -w \log_e \left[1 - \frac{(a_0 + g)t}{w} \right] - gt + V_0 \qquad (95)$$

where V_0 is the initial velocity of the rocket system.

The height reached by the rocket system at any instant during the powered flight is obtained by integrating equation 95. Thus

$$h = \left(\frac{w^2}{a_0 + g} - wt \right) \log_e \left(1 - \frac{(a_0 + g)t}{w} \right) + wt - \frac{1}{2} gt^2 + V_0 t + h_0$$

$$(96)$$

The maximum velocity of the rocket system is attained when the acceleration is zero. This occurs at the instant when all the propellants are consumed. The time when this occurs, called the *duration of powered flight*, is denoted by t_P. From equation 88 the following equation results when $t = t_P$.

$$M = M_0 - x m_P t_P \qquad (97)$$

But from equation 91

$$x m_P = \frac{M_0}{w} (a_0 + g)$$

Hence

$$m_P = \frac{M_0}{w} (a_0 + g) t_P$$

So that the duration of powered flight is given by

$$t_P = \frac{m_P}{M_0} \left(\frac{w}{a_0 + g} \right) \qquad (98)$$

Substituting for $t = t_P$ in equation 95 gives the maximum velocity $V_{\text{max.}}$. Thus

$$V_{\text{max.}} = -w \left[\frac{g(m_P/M_0)}{a_0 + g} + \log_e \left(1 - \frac{m_P}{M_0} \right) \right] \qquad (99)$$

The height reached by coasting after the propellants are consumed is denoted by h_C, where

$$h_C = \frac{V_{\text{max.}}^2}{2g} \quad \text{ft} \qquad (100)$$

The maximum height attained is the sum of the height reached during the powered flight and that attained by coasting; it is denoted

by $h_{\max.}$. Hence, if h_P is the height reached during the powered flight, then

$$h_{\max.} = h_P + h_C \tag{101}$$

The magnitude of h_P is obtained by substituting for $t = t_P$ from equation 98 into equation 96. Combining the result with equation 100 gives an expression for the maximum altitude. Thus

$$h_{\max} = \frac{w^2}{g} \left\{ \frac{\left[\log_e \left(1 - \frac{m_P}{M_0} \right) \right]^2}{2} + \frac{\left[\frac{m_P}{M_0} + \log_e \left(1 - \frac{m_P}{M_0} \right) \right]}{(a_0/g) + 1} \right\} \tag{102}$$
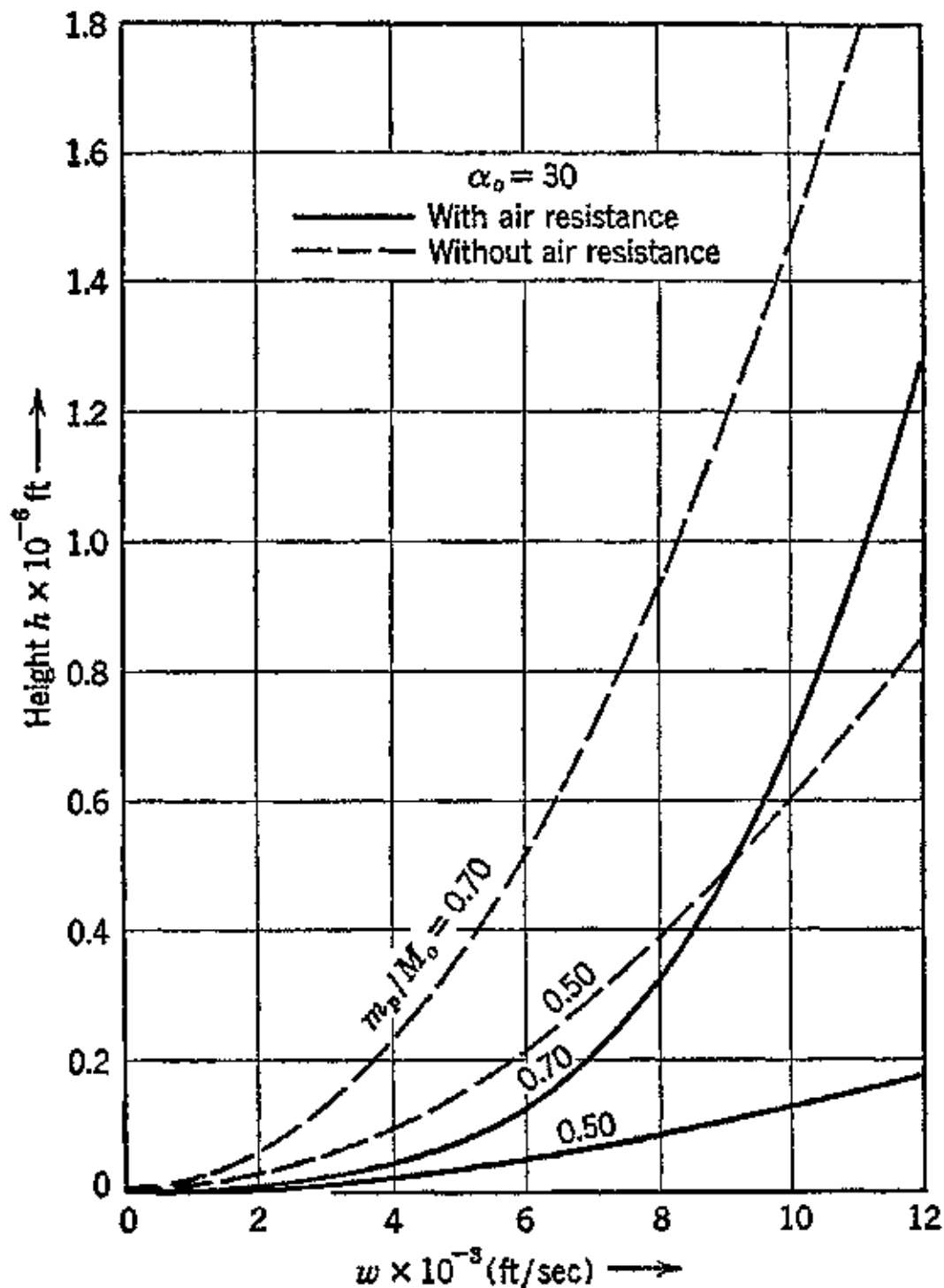
FIG. 21. Altitude attained as a function of effective exhaust velocity, with and without air resistance. (Based on F. J. Malina and A. M. O. Smith, *J. Inst. Aero. Sci.*, March 1938.)

It is seen from equation 102 that the maximum height reached by the rocket system depends upon the following parameters: a_0

m_P/M_0, and w.   Figure 21 taken from reference 20 illustrates the effect of these parameters on the maximum height attained with no air resistance.   It is seen that the ratio m_P/M_0 has a great influence on the maximum height.   The initial acceleration a_0 is very important until it has the value $a_0 = 6g$.

The effect of air resistance is to decrease the maximum height attained, as is illustrated in Fig. 21, which presents the calculated results of Malina and Smith for the cases with and without air resistance, and an initial acceleration $a_0 = 30g$.   The air resistance was assumed to be in accordance with the drag coefficient (C_D) curve, Fig. 22.   A high speed of flight through the lower reaches of
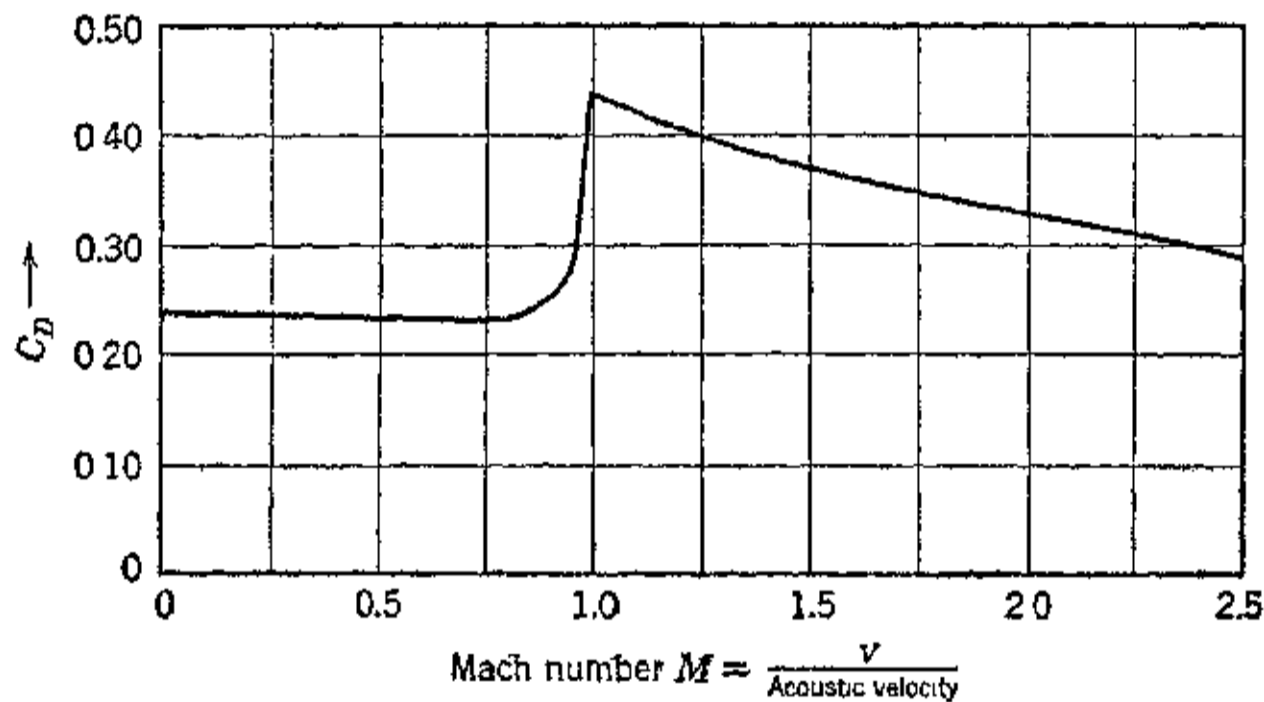
FIG. 22.   Drag coefficient vs. Mach number.   (Reproduced from F. J. Malina and A. M. O. Smith, *loc. cit.*)

the atmosphere where the air density is high results in a rapid consumption of the propellants.   Consequently, a great advantage is secured by launching the rocket system from an initial altitude. The calculations indicate that a sounding rocket having an effective exhaust velocity $w = 10,000$ fps and launched from a station at 10,000-ft altitude, to avoid the high drag of the lower atmosphere, will reach a height of 170 mi.

21. Application of Rockets to Assisted Take-Off of Aircraft

In this country the main application of rockets to aircraft, apart from their use as weapons, has been to reduce the take-off distance and/or time of engine-driven propeller-propelled aircraft.   The majority of applications during the war were to flying boats where the added thrust of the jato units (jet assisted take-off) made it possible to take off under conditions such that without them success-

ful take-off would have been problematical. This increased the usefulness of these aircraft for rescue work in forward combat areas. Jato units have also been applied to both carrier and land-based aircraft. As was to be expected, reduction in both take-off distance and time resulted from their use. For an analysis of the take-off problem for seaplanes and flying boats, see reference 22.

The estimated reduction in the take-off distance for the DC-3 airplane, if operated under C.A.A. take-off regulations, with a 1000-lb jato unit for 14 sec, is from 4600 ft to 3250 ft at sea level and from 5800 to 3850 ft at 6000-ft elevation. These are the distances required to clear a 50-ft obstacle.

Two types of units have been applied: those employing liquid propellants, and those employing a solid propellant. To the writer's knowledge, the solid-propellant units have found the greater favor, owing to the ease of their installation and the fewer logistic problems introduced by their use.

A liquid-propellant rocket system is ordinarily controlled from a single electric switch operated by the pilot. The switch actuates an electric control valve, thereby causing an inert pressurizing gas to communicate with the propellant tanks. The pressurizing gas passes through a regulating valve which maintains the gas pressure on each propellant tank at a constant value. This gas is also utilized for actuating the propellant flow-control valves located upstream relative to the injector which introduces the propellants into the motor. No ignition system is employed, since the propellants used with this unit react spontaneously upon contact with each other.

Liquid-propellant jato units have been constructed either so that they can be mounted as fixed installations in the aircraft or so that they can be dropped by parachute after use. Reliable liquid-propellant rocket motors have been developed that have operated without difficulty for continuous periods of several minutes. These motors are light in weight and are cooled by circulating one of the propellants around the combustion chamber and nozzle. For example, a rocket motor of this type developing 1500 to 2000 lb thrust can be built to weigh less than 45 lb.

22. Propellants for Rocket Motors

The ideal rocket propellant is one which satisfies the following principal requirements: (1) the calorific value per pound of propellant should be as high as possible; (2) the density should be high to keep the space requirements for containers at a low value; (3) the propellant should be easily stored and require no special handling equip-

ment; (4) its corrosiveness should be low; (5) its toxicity should be low; (6) its performance should not be affected too greatly by ambient temperatures; (7) its ignition should be smooth and reliable; (8) it should be stable chemically and not deterioriate appreciably over reasonable storage periods; and (9) if a liquid, its viscosity change with temperature should be low so that the pumping work at low operating temperatures will not be excessive.

These requirements are not satisfied completely by any of the rocket propellants known to the author.

In general, rocket propellants may be divided into four principal groups: (a) monopropellants; (b) compounded propellants; (c) fuels; (d) oxidizers.

(a) **Monopropellants.** A monopropellant is a substance that requires no auxiliary material (oxidizer) for bringing about the release of its thermochemical energy. To this class of materials belong such explosives as nitroglycerin $C_3H_5(ONO_2)_3$, picric acid $C_6H_2(NO_2)_3OH$ and its derivatives, trinitrotoluene $C_6H_2(CH_3)(NO_2)_3$, ethylene glycol dinitrate $C_2H_4(ONO_2)_2$, nitromethane CH_3NO_2, and others. For thermochemical data on explosives and possible monopropellants the reader is referred to reference 15.

For a liquid to be a satisfactory monopropellant for a liquid-propellant rocket motor it must satisfy the practical considerations discussed in Section 1. It must be stable under all conditions but must decompose completely once it has been introduced into the combustion chamber. These two requirements are, in general, conflicting ones and greatly restrict the choice of materials for possible liquid monopropellants.

For solid-propellant rocket motors for short-duration burning, especially of the unrestricted type, monopropellants are used extensively. In these rocket motors the decomposition is started by the energy supply released by the igniter—usually black powder or a similar material.

To this same class of materials might be added such future sources of energy as that produced by the association of monotomic hydrogen and by atomic energy. The exceedingly high energy releases to be expected from atomic disintegration will require extremely high flight velocities to obtain a significant propulsion efficiency. The association of atomic hydrogen to molecular hydrogen releases 52,500 kcal/kg according to Bichofsky-Copeland, *Journal American Chemical Society*, Vol. 50, p. 315, 1928. This would give a theoretical effective exhaust velocity of 20,000 meters/sec, which is not too large for obtaining a fair propulsion efficiency. The solution of the

problem of utilizing this source of energy would be of tremendous importance to rocket jet propulsion.

(b) **Compounded Propellants.** These are mechanical mixtures of a fuel and an oxidizing agent. This type of propellant is used for launching rockets and also for relatively long-duration solid-propellant rocket motors such as those for the assisted take-off of airplanes. The fuel is generally a hydrocarbon and the oxidizer, an inorganic compound. The homogeneity of the mixture is secured by various means, depending upon the physical characteristics desired in the propellant.

(c) **Fuels.** These are materials which cannot liberate their thermochemical energy unless reacted with some auxiliary material, usually an oxidizer. The energy release is then an exothermic oxidation process.

There are a number of materials which can serve as a liquid rocket motor fuel. In the main they are hydrocarbons or hydrocarbon derivatives. Those having the lowest carbon to hydrogen ratio (C/H) liberate the maximum energy per pound of fuel. Since fuels are always used with an oxidizer it is the energy liberation per pound of propellant (oxidizer + fuel) that is of importance. Furthermore, the less oxidizer required the smaller is the space requirement for that auxiliary liquid.

(d) **Oxidizers.** For compounded solid propellants inorganic oxidizers are generally used. These oxidizers, see Table 12·10, contain a large proportion of non-useful materials in their compositions.

TABLE 12·10

OXIDIZERS FOR ROCKET MOTORS

(Sänger, *Raketenflugtechnik*, p. 58)

Name	Chemical Formula	Per Cent Oxygen by Weight
Potassium perchlorate	$KClO_4$	46.2
Potassium nitrate	KNO_3	48.5
Perchloric acid	$HClO_4$	64.0
Nitrogen pentoxide	N_2O_5	74.2
Nitric acid	HNO_3	76.3
Hydrogen peroxide (conc.)	H_2O_2	94.2 × conc.
Liquid ozone	O_3	100
Liquid oxygen	O_2	100

For liquid bipropellant rocket motors the liquid oxidizer should contain a large percentage of oxygen. Of course, liquid oxygen and

liquid ozone are the best from this point of view.   During World War II the Germans developed a hydrogen peroxide of high concentration, reported to be 82 per cent.*   Another oxidizer which has been tested extensively is concentrated nitric acid, and the reaction between aniline and nitric acid has been investigated for some time.

It should be noted that in any rocket jet-propulsion system it is the oxidizer that determines the principal characteristics of the system and largely controls the design.   None of the principal oxidizers—liquid oxygen, nitric acid, or hydrogen peroxide—satisfies all the requirements for an ideal oxidizer.   All of them introduce practical problems, as will be seen later.   It is because of these deficiencies that the search for better oxidizers is being prosecuted by all research groups.

Each of the three oxidizers discussed above has been investigated with a variety of fuels.   The principal oxidizer-fuel combinations are presented in Table 12·11.

TABLE 12·11

LIQUID BIPROPELLANT SYSTEMS

Liquid Oxygen (O_2)	Nitric Acid (HNO_3)	Hydrogen Peroxide (H_2O_2)
Liquid hydrogen (H_2)	Aniline ($C_6H_5NH_2$)	Ethanol (C_2H_5OH)
Gasoline (C_8H_{18})	Furfuryl alcohol ($C_4H_3OCH_2OH$)	Methanol (CH_3OH)
Ethanol (C_2H_5OH)	Monoethylaniline ($C_2H_5C_6H_4NH_2$)	Hydrazine (N_2H_4)
Methanol (CH_3OH)		
		Ethylene diamine ($C_2H_4N_2H_4$)
Hydrazine (N_2H_4)		
Liquid ammonia (NH_3)		

Calculated values of the thermodynamic properties of the combustion gases for the liquid oxygen-liquid hydrogen, liquid oxygen-gasoline, liquid oxygen-hydrazine, and nitric acid-aniline systems are presented in Figs. 23, 24, 25, and 26 respectively.   The author is indebted to his former colleague Mr. W. Murray for his assistance in preparing the aforementioned figures.

Except for the liquid oxygen-liquid hydrogen combination the theoretical specific impulses obtainable from the propellants listed in Table 12·11 range from 200 to 260, at approximately 300 psia combustion-chamber pressure, the highest values being for those using

* The Buffalo Electrochemical Company has 90 per cent hydrogen peroxide in regular production.

liquid oxygen. The density specific impulses (specific impulse × specific gravity) range from 250 to 300, the nitric acid and hydrogen peroxide combinations giving the highest values. It is interesting to note that the liquid hydrogen-liquid oxygen combination which gives a specific impulse of 353 lb/(lb/sec) has a density impulse of less than
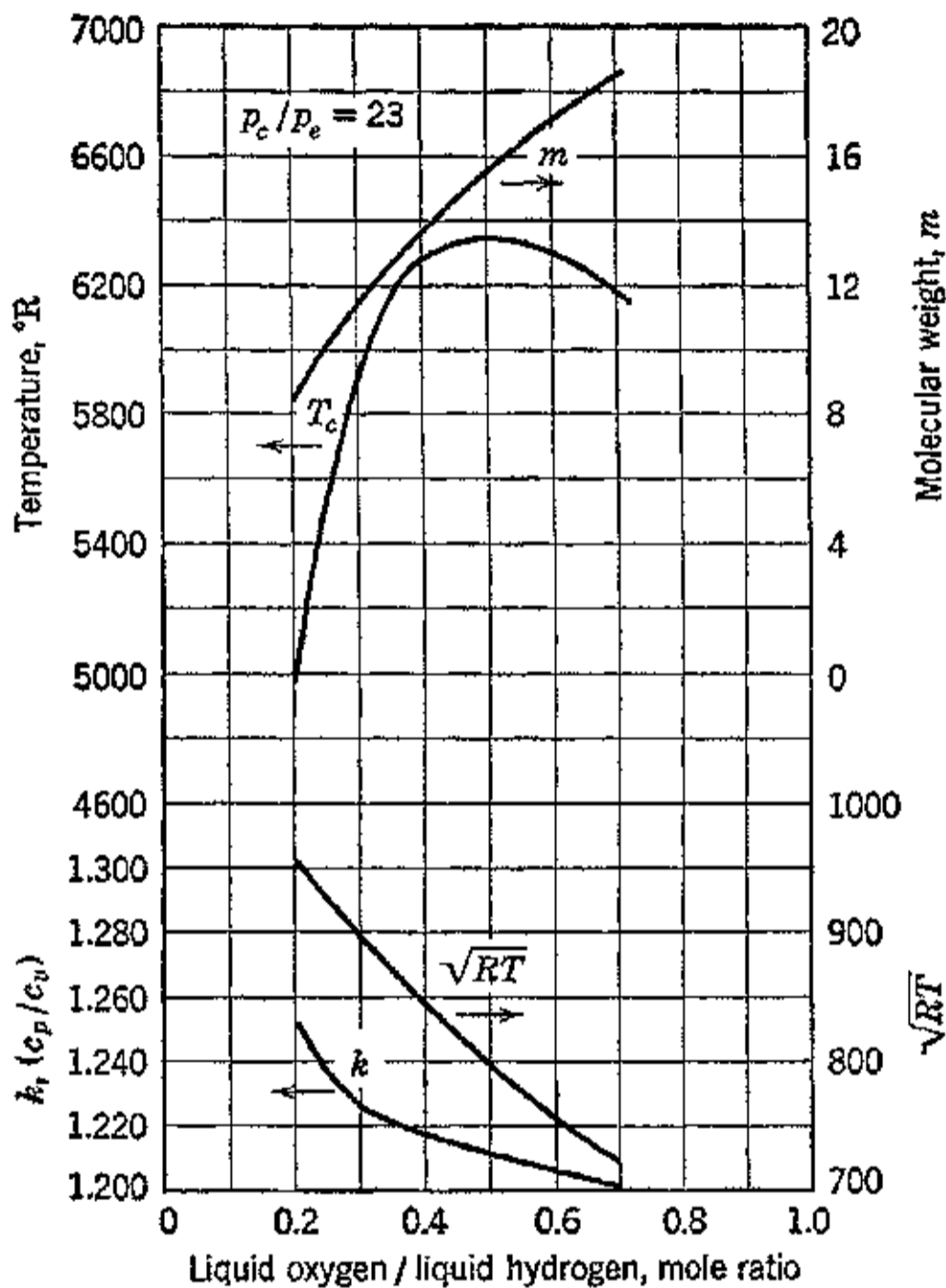
FIG. 23. Calculated thermodynamic characteristics of the liquid oxygen-liquid hydrogen bipropellant system.

100 lb/(lb/sec), the lowest of all the propellants listed. In general, the range of density impulses for the propellants listed in Table 12·11 is not large enough to favor any particular combination from a performance standpoint. Consequently, the choice is usually based upon the physical and chemical properties of the materials and the familiarity with their handling problems.

As mentioned above, liquid oxygen was used in the earliest experiments with rocket motors, and many successful motors of all sizes have been developed. For example, the German V-2 missile used this oxidizer. Those familiar with its handling problems are advo-

cates of its use, despite its disadvantages from other points of view, such as storage problems due to its low boiling point (-270 F), its high vapor pressure at ambient temperature which complicates its pumping problems, and its danger to personnel if not handled with care.

Nitric acid was investigated extensively during the war, and so were its modifications, such as red fuming nitric acid containing up
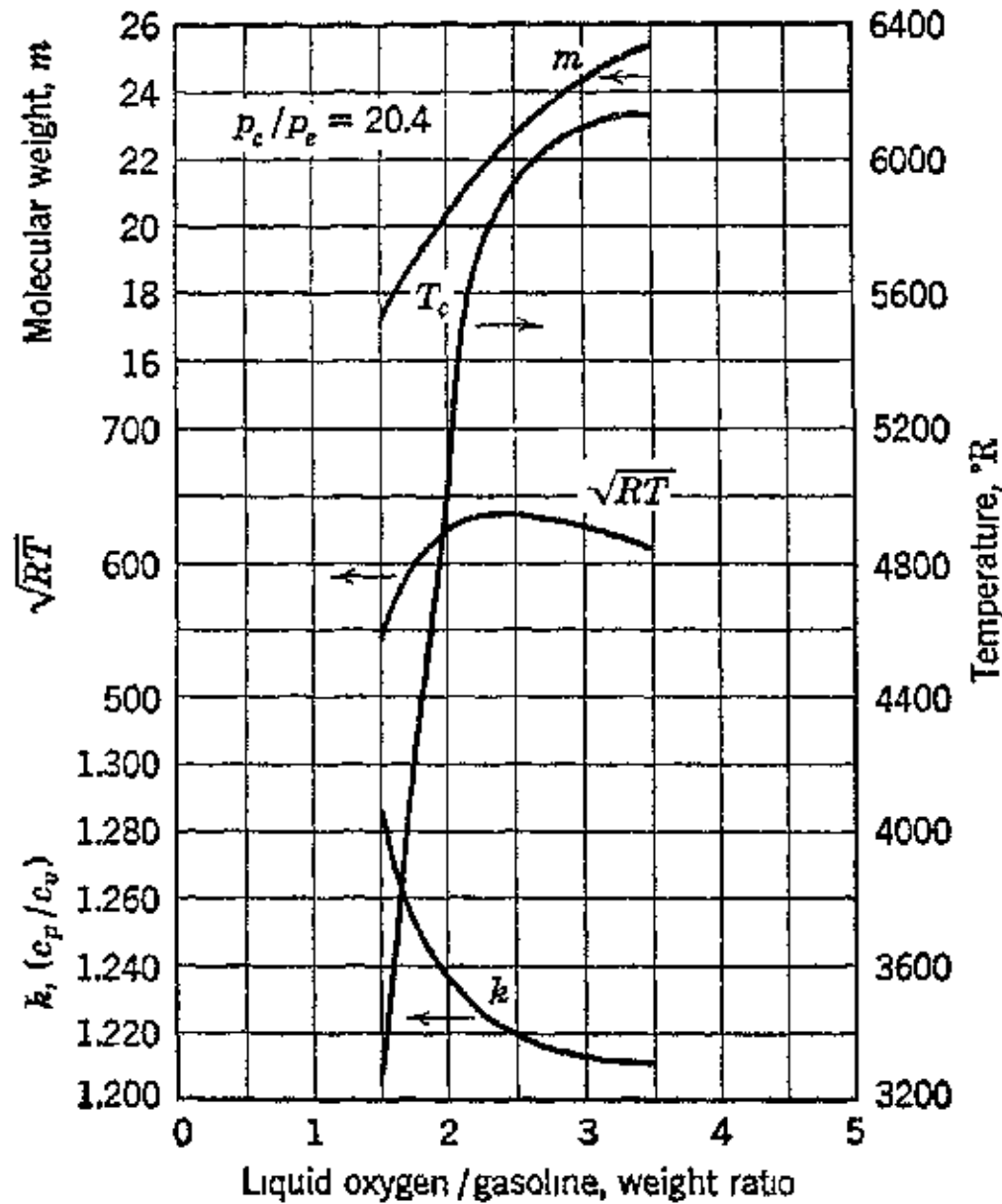
FIG. 24. Calculated thermodynamic characteristics of the liquid oxygen-gasoline bipropellant system.

to 13 per cent nitric oxide, white fuming nitric acid, and mixed acid—a mixture of nitric acid with sulfuric acid containing sulfur trioxide. Techniques for handling it without danger to personnel have been worked out, and consequently this oxidizer has its advocates.

Nitric acid is less hazardous as far as temperature effect or storage is concerned than either liquid oxygen or hydrogen peroxide. Its extreme corrosiveness requires that all containers for it be of stainless steel, and it introduces problems of materials for valve seats, packing, etc. Most of these, however, have been solved to the point where reliable units using nitric acid are possible.

Concentrated hydrogen peroxide, in concentration of 80 to 90 per cent, has been used on a large scale by the Germans. The power plant for the German rocket jet-propelled intercepter airplane designated as the ME-163 used concentrated hydrogen peroxide as the oxidizer and a mixture of hydrazine hydrate plus methyl alcohol as
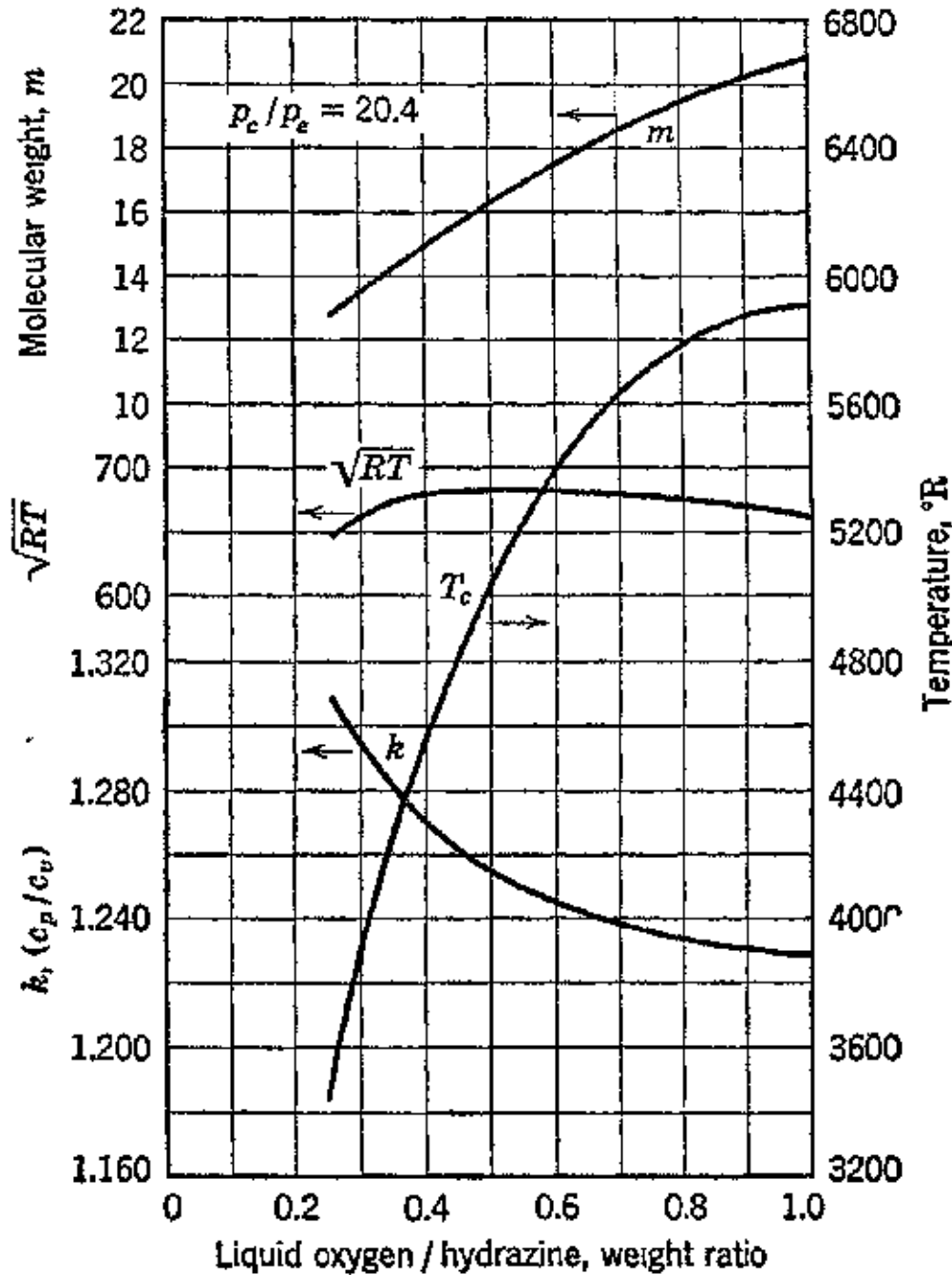
FIG. 25.   Calculated thermodynamic characteristics for the liquid oxygen-hydrazine bipropellant system.

the fuel.[26]   The experience with concentrated hydrogen peroxide in this country is quite limited.   Data on its properties have been pub-published.[28]   Its more widespread use will naturally be hampered by the lack of complete operating data and familiarity with its properties.   The author's experience with this oxidizer has been favorable, and he feels its application will increase despite the fact that its handling and storage may involve certain dangers unless precautionary methods are instituted.

The aforementioned oxidizers have an undesirable property in common.   All are corrosive to some degree and introduce problems

of material selection. The most corrosive ones also make it necessary to replace certain parts at frequent intervals and to service the equipment at regular periods. These problems, however, are not insurmountable, and they serve as the stimulus for investigating other possible propellants.
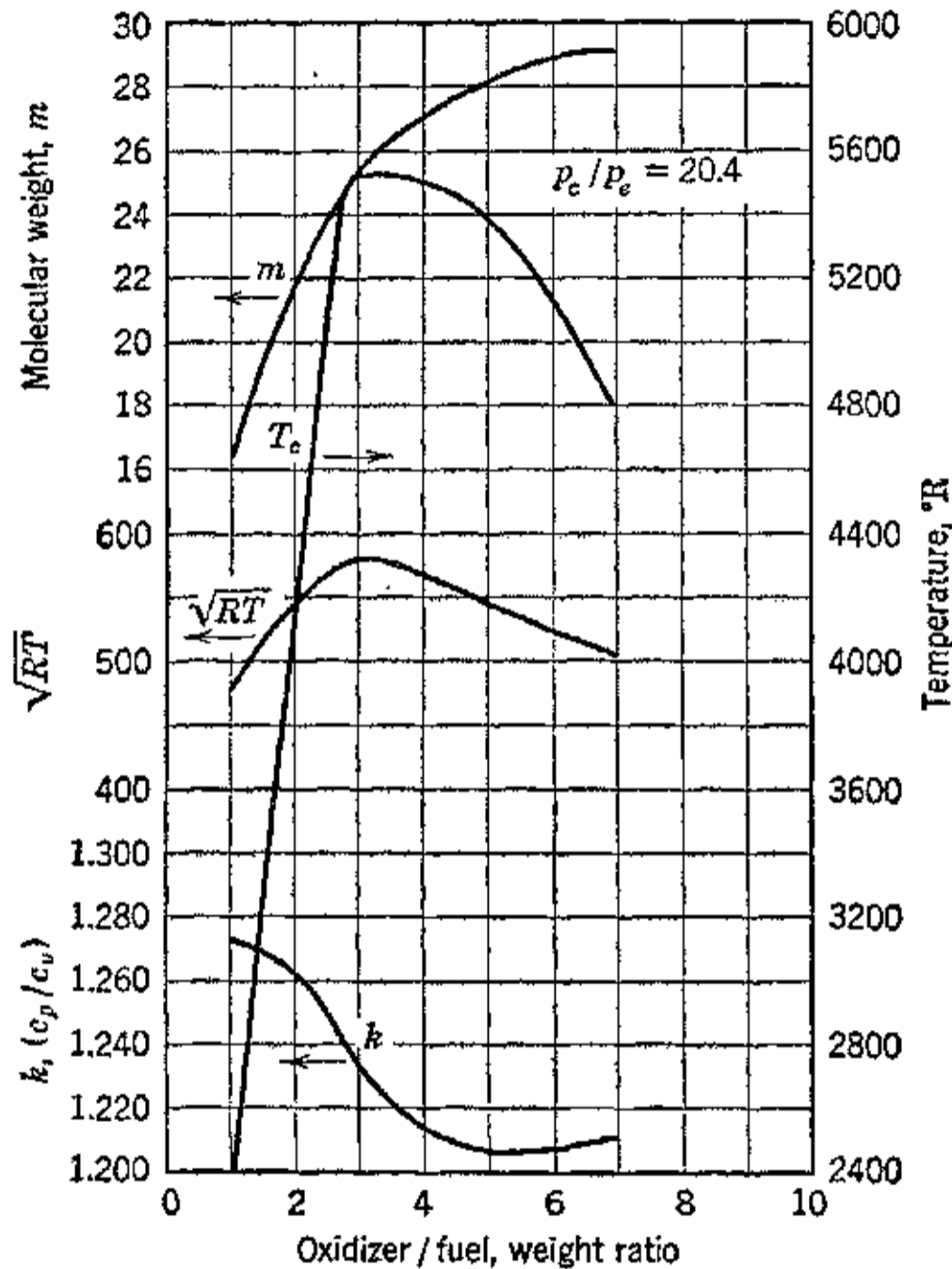
FIG. 26. Calculated thermodynamic characteristics for the red fuming nitric acid (0.15 weight fraction N_2O_4)-aniline bipropellant system.

23. Conclusions

The rocket motor has been developed to the stage where it can be applied as the power plant for short-duration high-speed military aircraft,[26] such as the German ME-163. Its usefulness as the propulsion system for long-range missiles, such as the German V-2, has been established, and no doubt it will find application in the future development of pilotless aircraft for high-altitude high-speed flight. Other applications where its advantages may be of value are for torpedo drive, hydrobombs, sounding rockets, and the assisted take-off of aircraft.[17]

The high-temperature-, high-pressure-gas-generating capabilities of the rocket system should also find fields of application. To give a few examples: the gases generated by reacting rocket propellants can be utilized as the working fluid for operating auxiliary turbines for the short periods required for starting rotating machinery. It can be said that, for any service where a temporary source of high-pressure gases can be employed for useful purposes, the possibilities of satisfying this requirement with a rocket system are worthy of investigation.

In conclusion it can be said that as far as airplane propulsion is concerned the rocket cannot compete commercially with conventional propulsion systems. Nevertheless, the rocket jet and also the thermal jet engine have now demonstrated their abilities to attain extremely high speeds of flight unattainable with propeller propulsion.

REFERENCES

1. WILLEY LEY, *Rockets*, Viking Press.
2. R. H. GODDARD, *A Method of Reaching Extreme Altitudes*, Smithsonian Institution, 1919.
3. H. OBERTH, *Die Rakete zu den Planetenraumen*, R. Oldenbourg, Munich, 1923.
4. W. HOHMAN, *Die Erreichbarkeit der Himmelskörper*, R. Oldenbourg, 1925.
5. MAX VALIER, *Die Raketenfahrt*, R. Oldenbourg, 1925.
6. E. SÄNGER, *Die Raketenflugtechnik*, R. Oldenbourg, 1933.
7. H. S. ZIM, *Rockets and Jets*, Harcourt, Brace and Co.
8. C. P. LENT, *Rocket Research*, Pen-ink Publishing Co.
9. *Encyclopædia Britannica*, "Rockets."
10. E. SÄNGER, *Flug*, Sonderheft, 1934.
11. F. J. MALINA, "Characteristics of Rocket Motor Unit Based on Theory of Perfect Gases," *J. Franklin Inst.*, Vol. 230, No. 4, October, 1940.
12. C. CRANZ, *Lehrbuch der Ballistik*, Springer, Vol. 2, p. 416, 1927.
13. B. F. DODGE, *Chemical Engineering Thermodynamics*, McGraw-Hill Book Co.
14. R. J. WENNER, *Thermochemical Calculations*, McGraw-Hill Book Co.
15. C. S. ROBINSON, *The Thermodynamics of Firearms*, McGraw-Hill Book Co.
16. I. LANGMUIR, "The Dissociation of Hydrogen into Atoms," *J. Am. Chem. Soc.*, Vol. 37.
17. M. J. ZUCROW, "The Rocket Power Plant," *Jour. S.A.E.*, July, 1946.
18. M. J. ZUCROW, "Jet Propulsion and Rockets for Assisted Take-Off," *Trans. A.S.M.E.*, April, 1946.
19. *Life Magazine*, Dec. 25, 1944.
20. F. J. MALINA and A. M. O. SMITH, "Flight Analysis of the Sounding Rocket," *J. Inst. Aero. Sci.*, March, 1938, p. 199.
21. R. EKSERGIAN, "On the Reactions of Fluids and Jets," *J. Franklin Inst.*, May, 1944.
22. E. G. STOUT, "Take-off Analysis for Flying Boats and Seaplanes," *Aviation*, 1945.

23. L. S. MARKS, *Mechanical Engineers' Handbook*, McGraw-Hill Book Co., New York, 1941, p. 160.
24. C. F. BRINSMADE, thesis for M.S. degree, M.I.T., 1942.
25. E. SÄNGER, *Flug*, Sonderheft, 1934; also *N.A.C.A. Tech. Memo* 1066.
26. R. HEALEY, "How Nazis' Walter Engine Pioneered Manned Rocket Craft," *Aviation*, January, 1946, p. 77.
27. M. SUMMERFIELD, "The Rocket's Future Influence on Transport Designs," January, 1946, p. 73.
28. F. BELLINGER, H. B. FRIEDMAN, W. H. BAUER, et al., "Chemical Propellants," *Ind. Eng. Chem.*, Vol. 38, Nos. 2, 3, and 6, 1946.

SOME ASPECTS OF HIGH-TEMPERATURE METALLURGY

by C. T. Evans, Jr.,* and M. J. Zucrow

1. Introduction

It has been pointed out in the preceding chapters that the future of the gas-turbine and of jet-propulsion engines is closely related to metallurgical developments. Recent years have seen a feverish search for new alloys capable of withstanding high dynamic stresses at elevated temperatures. The initial incentive for the effort was created by the demands related to the development and application of the turbo-supercharger to the spark- and the compression-ignition internal-combustion engines. Added impetus resulted immediately from the introduction of the gas-turbine and jet-propulsion power plants, which have created a demand for even better alloys.

At this time efforts to develop better alloys for service at elevated temperatures are being exerted on a vastly expanded scale. Various government and private organizations are cooperating; extensive research programs have been sponsored, largely by government agencies, and the wealth of information that has been assembled is being thoroughly coordinated. The progress has surpassed the expectations of the most optimistic, and many improved alloys have become available.

In addition, the significant properties of many of the older compositions have been determined, and, although the newer alloys are generally more attractive, availability and economic and fabrication considerations may often still indicate choice of the older materials. Cooling schemes and heat-exchanger arrangements may also be employed by the designer to reduce metal working temperatures to the ranges which can be served by less highly alloyed compositions.

The properties of the older materials have been treated extensively by one of the authors in reference 4.

Many factors are involved in the selection and specification of alloys most suitable for the component parts of high-temperature machinery. Inasmuch as the problems are largely metallurgical, a brief review of the metallurgical principles involved is presented in this chapter.

The authors acknowledge with thanks the valuable suggestions received from their former and present colleagues, including the technical staff of the Universal-Cyclops Steel Corporation, and Mr. J. Riordan, Metallurgist, Aerojet Engineering Corporation.

2. Division of Metallurgical Fields

The study of metals may be divided into (a) ferrous and (b) non-ferrous metallurgy. *Ferrous* metallurgy comprises the study of the physical, chemical, and thermal properties of the element iron and of alloys containing iron as a major constituent. *Non-ferrous* metallurgy is concerned with the physical, chemical, and thermal properties of metals other than iron and alloys not containing iron as the major constituent.

The alloys employed for service at elevated temperatures belong in general to the field of ferrous metallurgy. The exceptions are nickel-base and cobalt-base alloys. Their physical natures, however, are such that they can be best studied from the viewpoint of ferrous metallurgy. The discussion which follows is, therefore, limited to the principles of ferrous metallurgy.

3. Basic Structure of Metals and Alloys

All material substances are composed of atoms. In metals and alloys the atoms are disposed so that they present a definite orderly arrangement of crystals. Monatomic metals, such as iron and cobalt, have three basic types of crystal structure. Arranged in the order of increasing atomic density, these are: (a) the body-centered cubic lattice; (b) the face-centered cubic lattice; and (c) the hexagonal close-packed lattice.

The body-centered cubic lattice has two atoms per cubic cell. The face-centered cubic lattice possesses four atoms per cubic cell. The basic cell of the hexagonal lattice contains two atoms and is the prism possessing an equiangular triangle.[2]

Common metals classified in accordance with the three simple structures discussed above are listed in Table 13·1.

TABLE 13-1

METALS POSSESSING THE THREE SIMPLE METALLIC LATTICES

(F. Seitz, *The Physics of Metals*, McGraw-Hill)

Body-Centered Cubic	Face-Centered Cubic	Hexagonal Close-packed
Lithium (Li)	Copper (Cu)	Beryllium (Be)
Sodium (Na)	Silver (Ag)	Magnesium (Mg)
Potassium (K)	Gold (Au)	Zinc (Zn)
Vanadium (V)	Aluminum (Al)	Cadmium (Cd)
Tantalum (Ta)	Thorium (Th)	Thallium (Tl)
α Chromium (Cr)	Lead (Pb)	Titanium (Ti)
Molybdenum (Mo)	γ Iron (Fe)	Zirconium (Zr)
Tungsten (W)	α Cobalt (Co)	Hafnium (Hf)
α Iron (Fe)	Nickel (Ni)	Chromium (Cr)
β Iron (Fe)	Rhodium (Rh)	Cobalt (Co)
δ Iron (Fe)	Palladium (Pd)	Ruthenium (Ru)
	Iridium (Ir)	Osmium (Os)
	Platinum (Pt)	

An extensive tabulation of the crystal structures of various elements and compounds is presented in reference 2.

Most pure metals maintain the same atomic arrangement up to the melting point. Reference to Table 13-1 indicates that this is not true of iron. Iron undergoes a change in atomic structure at two definite temperatures, known as the temperatures of *allotropic* or *polymorphic* transformations.

4. Allotropic Modifications of Iron

In its normal state, pure iron is extremely ductile and possesses magnetic properties, and in that state it is called *alpha* (α) *ferrite*, or *alpha iron*. The atomic structure of alpha iron belongs to the general class of body-centered cubic lattice.

Alpha iron is capable of dissolving a few hundredths of 1 per cent of carbon, thus forming a *solid solution;* a solid solution may be regarded as a homogeneous union of two or more substances, in indefinite proportions, that persists in the solid state. The union of the substances in a solid solution is so complete that the individual substances cannot be distinguished under the microscope. It should be noted that this is a physical union entirely and there is no chemical combination; the carbon merely dissolves in the iron, like sugar in water. The solid solution of carbon in alpha iron is called *ferrite*. The temperature range over which ferrite can exist in pure iron

extends from approximately 910 C (1665 F) down to room temperature and lower.

When alpha iron, that is, pure iron, is heated to a temperature somewhat higher than 1400 F, it loses most of its magnetic properties and in that condition is known as *beta* (β) *iron*. Further heating of the beta iron produces another allotropic form known as *gamma* (γ) *iron*.

Gamma iron is non-magnetic, and its structure is the face-centered cubic arrangement. In this condition the iron is capable of dissolving up to 1.7 per cent of carbon. The resulting solid solution is termed *austenite*. Since austenite is a constituent that forms at high temperatures, it can be decomposed quite readily upon cooling the alloy and subsequently tempering the structure.

The various decomposition products of austenite are called "martensite," "troosite," "sorbite," or "pearlite." Martensite is the first decomposition product formed and the hardest. Its presence is favored by rapid cooling and low tempering. On the other hand, pearlite is the softest decomposition product and is formed on slow cooling.

"Isothermal quenching," as developed by Bain, Davenport, and others, involves quenching to the tempering heat, instead of room temperature, and holding for various periods. Intermediate austenite transformation products are formed, called "bainite," which have an unusual combination of strength and toughness.

Another allotropic form of iron, known as *delta* (δ) *iron*, exists at temperatures above 1400 C (2550 F). The crystalline structure of delta iron is similar to that of alpha iron; that is, it belongs to the body-centered cubic arrangement of atoms. Because of the similarity in crystal structure and in other properties, delta and alpha iron are commonly believed to be identical phases.

When iron and carbon are present together, a certain amount of the carbon may unite chemically with the iron to form a carbide, Fe_3C, called *cementite* (Cm). All the carbon and iron in excess of that entering into the formation of cementite remains free and uncombined.

5. Critical Points

The temperature at which one crystalline form of iron changes into another, or at which an allotropic change occurs, is called a *critical point*, and the critical points which have been discussed are given definite designations. Thus:

A_4 point. The temperature at which *delta iron changes to gamma iron;* in pure iron it occurs at slightly above 1400 C (2500 F).

A_3 point. The temperature at which *gamma iron changes to alpha iron;* it occurs in pure iron when cooling (or reverse when heating) through the temperature 910 C (1665 F). In iron-carbon alloys, *increasing the carbon content lowers the A_3 point.*

A_2 point. This is the *Curie or magnetic change point* which is at 770 C (1410 F); on being heated through this point magnetic alpha iron shows a marked decrease in ferromagnetism but no change in crystal structure.

A_1 point. In iron-carbon alloys this represents the *eutectoid point,* or the point of solid phase equilibrium where austenite begins to decompose.

The above designations for describing iron-carbon alloys are also used for describing more complex systems containing other constituents. Thus, the austenite of the so-called 18-8 alloys is not a solid solution of carbon in gamma iron, but a solid solution of carbon, gamma iron, chromium, and nickel.

6. Methods of Testing for High-Temperature Properties

The determination of the suitability of an alloy for a particular high-temperature application requires the consideration of the following primary factors: (1) temperature range to be expected; (2) type and magnitude of load or stress; (3) allowable strain or deformation; (4) time or desired service life.

In designing machinery the interest is principally in *dynamic* loading properties rather than static loading. To obtain the desired information, test data covering the following information are needed.

(a) Stress to rupture.
(b) Creep.
(c) Creep relaxation.
(d) Oxidation and/or corrosion.
(e) Effect of temperature fluctuations.
(f) Effect of stress fluctuations.
(g) Fatigue.
(h) Damping capacity.
(i) Effect of stress concentrations.
(j) Change of ductility with time, temperature, stress, and rate of strain.

(k) Change of shock (impact) resistance with time, temperature, and stress.
(l) Thermal expansion.
(m) Thermal conductivity.
(n) Density.
(o) Changes in microstructure
(p) Changes in hardness.
(q) Hot hardness.
(r) Short-time tensile, impact, and modulus of elasticity.

It should be noted that the main factors—temperature, stress, strain, and time—must be considered simultaneously.

The more important tests include creep, stress-to-rupture, fatigue, modulus of elasticity, oxidation and/or corrosion. On the other hand, the short-time tensile test and hot hardness test have shown themselves to be unreliable for evaluating the long-time service capabilities of an alloy at elevated temperatures.

Creep. Creep tests consist of subjecting a specimen to a constant stress, at a constant temperature, and plotting the resulting strain as a function of testing time.

During a creep test, three stages are observed as illustrated in Fig. 1: (1) a combination of elastic and plastic deformation with a
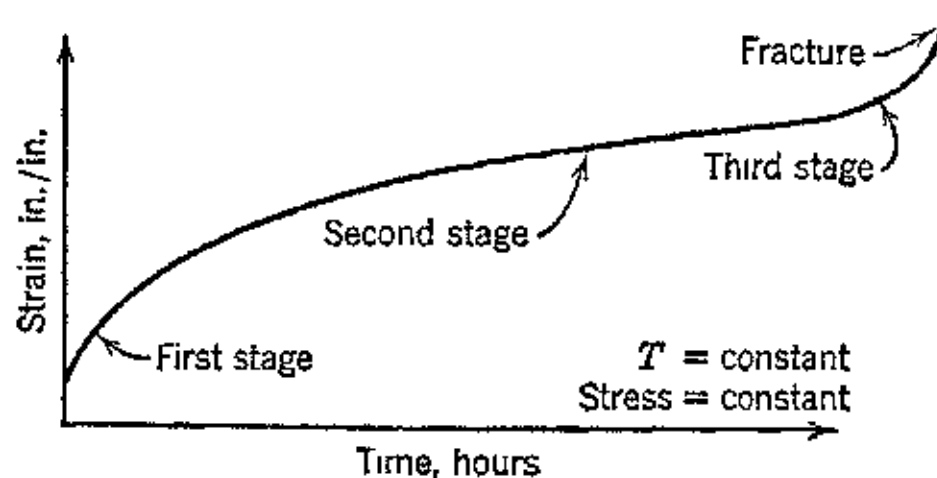
FIG. 1.   Typical creep test curve.

decreasing rate of elongation; (2) the rate of elongation remains constant—if the slope of the second stage is zero, the load is insufficient to cause creep; (3) the rate of elongation increases rapidly until fracture occurs.

The stresses used for making creep tests are quite low. Most creep tests do not stretch the specimen beyond the continuous-flow or second stage. When the stresses are increased to produce fracture within a reasonably short period of time (2000 hours or less), the test comes within the category of the stress-to-rupture test.

Stress-to-Rupture. A set of specimens is held at a given temperature with static breaking loads of decreasing magnitude, the purpose being to obtain data for a plot of stress vs. rupture in hours. This test is illustrated in Fig. 2. The loads used in stress-to-rupture tests are usually selected so that the specimen is fractured in 2000 hr or less. Ordinarily, the loads are selected to give three or four points up to 1000 hr. Any changes in ductility and impact resistance with time can be determined from the ruptured specimens. Usually periodic strain measurements are made on the specimens subjected to the smaller loads, for the purpose of obtaining accelerated creep data.

When the stress-to-rupture time relationship is plotted on log-log coordinate paper, a more or less straight line is obtained. This plot will have changes in its slope only if some structural or surface instability of the alloy occurs. Such instability may or may not be serious.
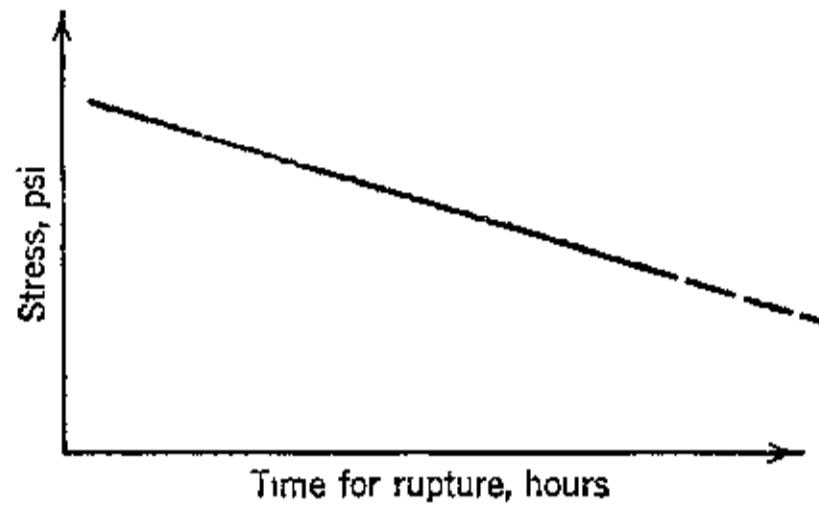
Fig. 2.   Typical stress-to-rupture plot.

Creep Relaxation. This test yields data directly applicable to the suitability of a material for high-temperature bolts. A plot of strain against time is constructed in which a single specimen of the alloy at a given temperature receives a series of loads which are decreased every time a predetermined constant strain is reached. This strain corresponds to the initial bolting stress to which the stud will be "pulled up" at room temperature. Figure 3 illustrates the plot.
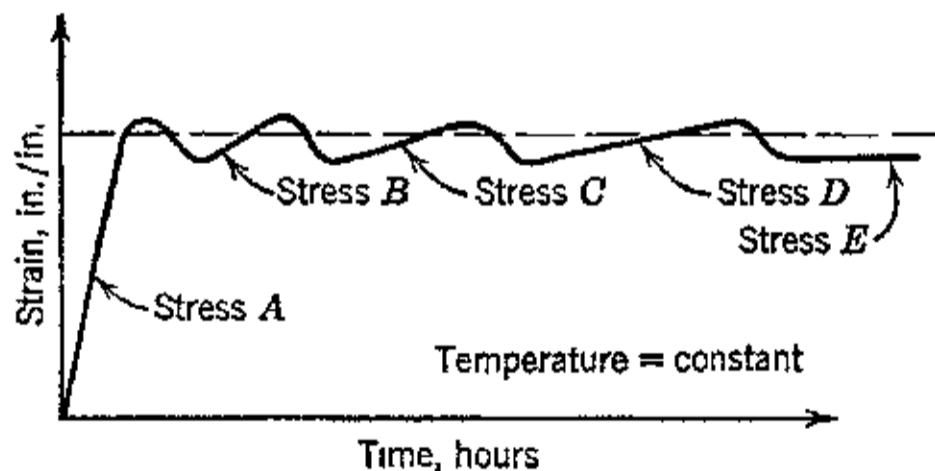
Fig. 3.   Typical creep-relaxation plot.

The purpose of this test is to obtain data from which can be calculated the residual or relaxation elastic stress which will remain in the bolt at any temperature after a given time.

Damping Capacity. This property appears to be an inherent characteristic of each material, and it is sometimes referred to as the *logarithmic decrement*. In plain language, it is the ability of an alloy to damp out vibration by virtue of its internal molecular friction.

Since alternate pulsations, particularly those associated with partial admission turbines, can build up to very high vibrating stresses, the ability of a material to *damp out* quickly would seem to be of considerable importance.

There are several ways of measuring this property, the most popular utilizing a simple tuning fork. The change in modulus with temperature can be determined in this same test.

Oxidation and/or Corrosion. These tests are made by subjecting specimens to the same oxidizing and/or corroding conditions that exist in actual service. At various intervals the specimens are examined to determine what losses, if any, have occurred in weight as the result of oxidation and/or corrosion. Metallographic sections should also be prepared to determine whether intergranular penetration has taken place.

7. Alloying Iron for High-Temperature Service

For applications where the temperatures exceed 1000 F the heat-treatable carbon or low-alloy steels can be immediately dismissed from consideration. None of these steels possesses the necessary strength at temperatures exceeding 1000 F. Furthermore, experience has demonstrated that, for satisfactory long-time oxidation and/or corrosion resistance at those temperatures, the steel must contain a minimum of 12 per cent chromium.

Data indicate that one significant or critical temperature, as far as the *hot strength* of an alloy is concerned, is the lowest temperature of recrystallization (the *equicohesive point*). At temperatures below that value, materials appear to be capable of withstanding appreciable stresses. At temperatures above the equicohesive point measurable and continuous creep is obtained even with the smallest loads.

Since austentic structures have high equicohesive points, it is apparent why austenitic alloys (or alloys composed principally of a solid solution of the same general type as austenite) are employed almost universally for high-temperature service. As pointed out, the gamma iron has a higher recrystallization temperature and a lower recrystallization velocity and, therefore, a greater resistance to change of shape than alpha iron.

From the foregoing, two important axioms pertaining to alloys for high-temperature use become apparent: (1) the alloy must have a chromium content of at least 12 per cent to resist oxidation and/or corrosion; (2) the alloy should be austenitic in structure to possess strength at high temperature.

It is evident why chromium plays an important part in the de-

velopment of high-temperature alloys. Chromium, however, when added to iron is a *ferrite* former. We find that an alloy containing more than 13 per cent chromium cannot be entirely austentic at any temperature, but with less than 13 per cent chromium content the alloy becomes entirely austenitic only when its temperature is raised above 1600 F. The alloy upon being heated through 1600 F undergoes a phase change. The chromium-ferrite transforms to chromium-austenite, and the reverse takes place upon cooling. To eliminate the occurrence of this phase change, the chromium content must exceed 16 per cent. The single phase present then is the alpha solid solution (ferrite). It should be realized that ferrite, in addition to having a relatively low recrystallization temperature, is also subject to embrittlement after having been heated at a high temperature. It can be concluded, therefore, that, for most high-temperature services, the alloy should *not* consist of iron alloyed with chromium alone.

It becomes necessary to use a third alloying element, which when added to chromium-iron alloys containing more than 12 per cent chromium will render the gamma phase, or austenite, stable at all temperatures up to the melting point of the alloy. Such an element is nickel. When 8 to 12 per cent nickel is added to the alloy, it will render alloys containing from 16 to 20 per cent chromium austenitic at all temperatures. From a strict physiochemical standpoint, the austenite so formed is not stable at low temperatures. However, because of sluggishness of the transformation from austenite to ferrite in these alloys, the austenite formed by adding from 8 to 12 per cent nickel may be regarded as being stable even at low temperatures.

The foregoing briefly describes the basis underlying the development of the 18-8 alloys (18 per cent chromium and 8 per cent nickel). In the past, the simple 18-8 alloys as well as the 25-12, 25-20, and 15-35 alloys were used for most high-temperature applications; 25-20 is still used for many such applications where the critical factor is high-temperature oxidation and/or corrosion resistance and not strength. Thus, it is a satisfactory material for lining such parts as combustion chambers. For a long time the aforementioned alloys were superior to any other known alloys, but more recent metallurgical developments have outmoded them.

Although the 18-8 alloy, as such, is not regularly used for dynamic load applications, many of its metallurgical features are common to the recently developed so-called superalloys. For this reason it is instructive to consider the metallurgy of the 18-8 alloy.

8. *Metallurgy of 18-8 Alloy*

The predominating phase in the 18-8 alloy is the gamma solid solution. This phase is so opposed to transformation that low-carbon alloys of this type remain wholly austenitic even upon very slow cooling. Thus, for all practical purposes, the 18-8 alloy may be regarded as an austenitic material, since it is austenitic after all commercial treatments.

In a true physiochemical sense, however, the 18-8 alloy is not in a state of equilibrium. Experiments have demonstrated that the same reaction characteristic of the iron-carbon or iron-chromium alloys, namely, the transformation of gamma to alpha, does assert itself in this alloy.

The metastability of the austenite in the 18-8 alloy, with the accompanying gradual change in its properties as it transforms (as at times happens in service), is determined by testing for magnetic properties, electrical conductivity, or even by microscopic observations. The two methods generally employed are as follows: (1) reheating for a long time within a certain temperature range; and (2) cold working at room or slightly elevated temperature.

The physiochemical processes which may occur with the first method are complex and beyond the scope of this discussion. The fact, however, that magnetic chromium-nickel-ferrite can be produced by merely cold working non-magnetic chromium-nickel-austenite indicates that the austenitic condition is not the stable phase. If the cold-worked alloy is reheated to 500 to 600 C (930 to 1110 F), a rapid precipitation of carbides occurs. The presence of carbides is determined by the effect of corrosive agents upon the cold-worked and reheated alloy. The carbides precipitate along the slip planes produced by the cold work, provided that the alloy contains sufficient carbon.

The second method of indicating the metastability of the austenite in 18-8 steel is to reheat it to a certain temperature, maintain the temperature for a prolonged period, cool, and then determine whether there is a change in its physical characteristics. If this procedure is utilized, a definite and appreciable amount of a magnetic phase appears, accompanied by embrittlement. This phenomenon has been found to be a process of precipitation from the solid solution, generally termed *precipitation hardening*. In industrial precipitation hardening of alloys designed primarily for this characteristic, the procedure is first to heat the alloy to a high enough temperature to insure complete solubility of the element or elements in the matrix. The resulting solid solution is retained in the supersaturated state

by means of quenching. The excess constituent is subsequently precipitated by reheating the alloy to a certain low temperature.

Also, in commercial precipitation hardening, the precipitated constituent is *regularly distributed throughout the grains.* The matrix within which the precipitation occurs does not undergo any phase change, the phenomenon of precipitation being entirely a matter of solid solubility. In austenitic chromium-nickel steels, on the other hand, the carbides precipitate predominantly at the grain boundaries, and, in addition, ferrite is found to be present around the precipitated boundary carbides.

The above phenomena, the formation of boundary carbides and the formation of ferrite around these precipitated carbides, are matters of concern whenever austenitic materials are used for high-temperature service   The boundary carbides lower the chromium content of the metal in their immediate vicinity to a value below that necessary for oxidation and/or corrosion resistance. A vulnerable path is formed along the grain boundaries where damaging oxidation and/or corrosion may take place.

It should be mentioned, however, that the presence of ferrite increases the hot ductility of the material under load. It is often a vital problem to determine how much ductility under load is really required, but the ability to deform, or redistribute stresses, inevitably increases the factor of safety in a given construction. Since most high-temperature materials without ferrite tend to lose their ductility under load quite rapidly, the presence of ferrite may sometimes be beneficial. In most alloys, however, ferrite appears to hinder actual *resistance* to deformation.

To "stabilize" the alloy and prevent the formation of damaging boundary chromium carbides, two methods are employed (frequently simultaneously): (1) severely cold working the alloy, thus providing sufficient slip planes upon which precipitation can occur to prevent large concentrations of chromium carbides at the grain boundaries; (2) adding alloying agents such as titanium, columbium, tungsten, and molybdenum which have a greater affinity for carbon than does chromium. These elements form their respective carbides and leave the chromium in solid solution to exert its maximum effect on oxidation and/or corrosion resistance.

The deleterious formation of ferrite at the grain boundaries may also be eliminated by greater additions of austenite-forming elements such as nickel or manganese or by increasing the carbon content. At high temperatures, the effects of carbon and nickel on high-chromium alloys are remarkably similar; the carbon, however, is

some 30 or 40 times as effective as nickel in stabilizing austenite. Carbon, besides inhibiting the formation of high-temperature ferrite, is also effective in diminishing the amount of ferrite produced by cold work.

9. Sigma Phase

Although a detailed treatment is beyond the scope of this review, it should be mentioned that still another phenomenon, known as *sigma phase*, can complicate the metallurgy of the chromium-nickel heat-resisting alloys. This phenomenon occurs under conditions similar to the carbide precipitation—ferrite formation previously described by heating in the temperature range of 650 C–900 C (1202 F–1652 F). In fact, it is difficult to differentiate metallographically between chromium-rich ferrite and sigma phase. Sigma, however, is non-magnetic, and X-ray diffraction evidence definitely points to its being a separate and distinct phase. At room temperature, sigma phase is brittle and very hard.

Sigma formation is accompanied by severe loss of room-temperature corrosion resistance and increased notch sensitivity, as measured by the impact test. Very little is known about its effect on high-temperature creep and stress-to-rupture characteristics. There is evidence that alloys high in sigma have less resistance to deformation but tend to retain higher ductility after long times at temperature under stress. This last characteristic is the reverse of what might be predicted from the characteristics of the alloys after cooling to room temperature and is a good example of the complete necessity for prolonged high-temperature tests in the evaluation of materials for high-temperature service.

Although the tendency has been to avoid using alloys high in sigma, one of the outstanding special valve steels (28 per cent Cr, 5 per cent Ni, 3 per cent Mo) is almost entirely sigma as treated for heavy duty in trucks, busses, and aircraft. There is evidence that some of the newer and more successful compositions for gas-turbine service are also high in sigma.

Sigma is not found in ordinary 18-8 but tends to form in nearly all modifications of 18-8, such as 25-20, 25-12, 18-8 plus molybdenum, and 18-8 plus columbium. Chromium appears to be the basis of sigma formation, and any alloying elements in addition to chromium which tend to form ferrite also tend to form sigma phase. Since virtually all other alloying elements (such as nickel and nitrogen) also tend to form sigma over certain ranges, it is easy to see why the presence of this constituent is quite common. When nickel is in

substantial excess over chromium, as in the 15 per cent chromium 35 per cent nickel alloys so widely used in cast furnace parts, sigma phase does not form.

An extensive study of sigma phase in heat-resisting alloys is recorded in reference 5.

10. Super High-Temperature Alloys

It has been stated that the 18-8, 25-12, and 25-20 chromium-nickel-austenitic steels are not being generally used today for high-temperature applications where the main requirement is high strength. The newer alloys are of the general austenitic type, but other alloying elements are added in varying amounts to improve the basic iron, chromium, nickel, austenitic matrix. These other elements are manganese, silicon, tungsten, molybdenum, columbium, titanium, aluminum, cobalt, nitrogen, and carbon.

Manganese, nitrogen, copper, nickel, and carbon are known as austenite-forming elements. In other words, when added in any amounts to iron, they tend to promote the formation of the gamma iron. With the exception of carbon, if added in sufficient quantities they completely suppress the alpha form of iron and make gamma iron the stable phase at all temperatures.

Silicon, chromium, tungsten, molybdenum, columbium, titanium, and aluminum are called ferrite-forming or gamma-loop-forming elements. These elements suppress the gamma form of iron by raising the temperature of the critical point A_3 and lowering the A_4 point to form the so-called gamma loops. Outside of the loop the alloy exists in the alpha (ferrite) form up to the melting range. These elements also form carbides when carbon is present in sufficient amounts.

Cobalt is an element quite similar to iron and nickel. Like iron it has high- and low-temperature allotropic forms. Its high-temperature form (above 790 F) is the same as that for iron, the face-centered cubic. However, its low-temperature allotropic form is hexagonal-close-packed, while the low-temperature form for iron is body-centered cubic. The high-temperature form of cobalt is also superior in hot strength to that of iron, at least over certain temperature ranges. Like iron, cobalt forms solid solutions with such alloying elements as chromium, nickel, and tungsten. The solid solutions of cobalt differ from those with iron, chromium, and other ferrite formers in that these elements do not seem to form gamma loops with cobalt. The sluggishness of the transformation of the high-temperature form, face-centered cubic, to the low-temperature form, hex-

agonal-close-packed, is much greater in cobalt than in the comparable transformation in iron.

The ultimate aim of alloying additions to high-temperature alloys is, first, to stiffen up the matrix itself, and second, to place certain "keys" or "stops" in the body of the matrix in order to inhibit its plastic flow at high temperatures. It is believed that most of the alloying elements mentioned above act in both ways to improve the high-temperature strength. However, it is generally assumed that the solid-solution alloys of nickel, cobalt, and manganese act primarily to stiffen the matrix, whereas the primary function of the other elements is to form carbides and/or nitrides which have a keying action. It is also true that alloying elements generally elevate the lowest temperature of recrystallization. In addition, we must keep in mind the many possibilities for intermetallic compounds.

A word about impurities: zinc, lead, tin, antimony, silver, and other elements which may form low-melting eutectics should be strictly avoided in heat-resisting alloys.

11. Factors Affecting "Hot Strength"

It has been demonstrated that the *hot strength* of an alloy is a more sensitive property than the room-temperature physical characteristics to changes in the material itself. The major factors in influencing the hot strength are:

(*a*) **Composition.** This has been discussed previously. One final admonition is necessary, however. It should be emphasized that a continual increase in the amount of a strengthening element does not necessarily result in a continual increase in hot strength. In fact, many results indicate that, for any combination of alloying elements, certain definite proportions of each must be present for the maximum hot strength.

(*b*) **Method of Melting.** (1) Electric furnace alloys are superior to open-hearth alloys. Induction electric alloys are the best of the electric furnace alloys. (2) "Killed" or deoxidized alloys are superior to non-deoxidized alloys.

(*c*) **Effect of Grain Size.** At temperatures below about 650 C (1202 F) fine-grained materials possess the maximum hot strength. At higher temperatures coarse-grained materials are superior. One explanation for these findings is believed to be that at the lower temperatures the grain boundaries are stronger than the crystals and, therefore, the deformation occurs largely within the grains. At the higher temperatures, on the other hand, the crystals themselves are the stronger and the deformation occurs at the boundaries. The

relative amounts of the weaker and stronger portions present will, therefore, influence the strength as determined by test. This probably explains why wrought alloys (grain size small) are superior in the lower range of temperatures, and cast alloys (grain size large) have better creep resistance in the higher temperature ranges.

Like most generalities, however, this rule breaks down under certain conditions, particularly where high-temperature fatigue may be a limiting factor. Wrought materials, with inherently finer grain structure, appear to have better fatigue endurance than the alloys in cast form, even at very high temperatures.

(*d*) **Recrystallization Temperature.** This has been discussed previously. (See Section 7.)

(*e*) **Heat Treatment.** Though conventional hardening heat treatments are not applicable to these alloys, they are susceptible to certain "solution" and "precipitation" heat treatments. These treatments consist of soaking these alloys at some sufficiently high temperature to place all the carbides, and other intermetallic compounds, in solution. This is followed by a rapid quench in order to retain these constituents in metastable solution. The compounds thus held in solution are projected out in the body of the matrix by "precipitation" or "aging" treatment. At least a portion of the precipitation treatment is usually first carried out at a temperature from 50 to 100 F in excess of the expected service temperature of the alloy. This treatment insures that precipitation will not occur in service, since such reactions are ordinarily accompanied by distortion. However, in many of the strongest materials precipitation effects are coincident with service temperatures and may never be considered complete.

(*f*) **Processing.** The manner in which an alloy is fabricated can profoundly influence its high-temperature properties. Actually, this factor can overshadow all other variables, including major changes in composition. Some basic differences between cast and wrought products have been mentioned above. Within the wrought classification, whether an alloy is cold worked, warm worked, hot worked, solution treated, aged, or given any combination of these processes may make a difference of several hundred per cent in creep and stress-to-rupture properties over certain temperature ranges.

Generally speaking, cold work or warm work is helpful in giving high values of stress to rupture up to 1000 hr. One difficulty with this method of processing is that it is impractical in large sections, and different section sizes tend to give widely varying results unless percentage reductions are carefully regulated. Solution treatments

and aging are beneficial to long-time creep and stress-to-rupture properties. Both types of treatment tend to reduce retention of ductility under load at temperature, so that closely controlled hot work plus stress relief, or modified aging, may be the best compromise. Likewise, in cast alloys, the multitude of casting variables must be under close control if optimum properties are to be achieved and met consistently.

12. High-Temperature Design Data

Figures 4, 5, and 6 show the mean high-temperature properties of 100-hr and 1000-hr stress-to-rupture and stress for secondary creep rate of 0.10 per cent per 1000 hr (1 per cent per 10,000 hr) vs. temperature for eight of the prominent older materials; they also give some indications of the improvements which have been obtained with four classes of the recently developed alloys. For security reasons, the names and exact compositions of the new materials cannot be divulged. However, a rough indication of their alloy constituents is given in Table 13·2.

TABLE 13·2

MATERIAL	APPROXIMATE COMPOSITION	REMARKS
SAE 1015	0.15 C	For comparative purposes only. Unsatisfactory oxidation resistance above 1000 F.
5% Cr and Mo (AISI 502)	0.12 C, 5 Cr, 0.55 Mo	Most widely used oil refinery material. Unsatisfactory for long-time oxidation resistance above 1150 F.
12% Cr (AISI 410)	0.10 C, 12.5 Cr	Highly successful in steam turbine blading through 975 F. Resistant to oxidation through 1250 F.
28% Cr (AISI 446)	0.12 C, 26 Cr, 0.125 N	Highly resistant to oxidizing conditions through 2000 F.
18–8 (low C) (AISI 304)	0.06 C, 18 Cr, 9 Ni	Widely used for miscellaneous statically stressed parts. With columbium or titanium additions, widely used in exhaust manifolds. Oxidation resistant through 1650 F.
18–8 Mo (AISI 316)	0.07 C, 18 Cr, 13 Ni, 2.5 Mo	Strongest simple 18–8 modification. Successfully applied in supercharger nozzleboxes. Oxidation resistant through 1650 F.

TABLE 13·2 (*Continued*)

MATERIAL	APPROXIMATE COMPOSITION	REMARKS
25–20 (AISI 310)	0.12 C, 1.75 Si, 24.5 Cr, 20.5 Ni	Successfully applied in combustion chambers. Oxidation resistant through 2000 F.
Inconel	0.08 C, 13 Cr, 79.5 Ni, 6.5 Fe	Satisfactory for exhaust manifolds, combustion chambers. Oxidation resistant through 2000 F.
Alloy A	18–8 modified with W, Mo, Cb, and Ti	For rotating parts in Allis Chalmers Houdry gas turbines (920 F, 17,000 psi maximum stress); Elliott diesel engine superchargers (1020 F, 25,000 psi maximum stress); Elliott 2500-hp marine prime-mover gas turbine (1200 F, 8000 psi maximum stress). Obtains properties by hot working and partial aging.
Class B	1. Same as Alloy A with higher C and Mo. 2. Same as Alloy A with higher C and Mo; Ti replaced with Cb and part of Ni replaced with Mn 3. Same as 18–8 Mo with higher Ni than Cr, higher Mo, and N addition. 4. Same as Inconel with substantial T and/or Cb addition	The Inconel modification obtains its properties by heat treatment. The other alloys in this class obtain their high short-time-rupture properties by carefully controlled warm working.
Class C	Higher Ni, Mo, W, and Cb additions than Class B and usually with part of the Fe replaced by Co. N added or high C contents.	Obtain properties by solution treatment and aging for higher part of temperature range and by hot work or solution treatment and aging in lower part of temperature range.
Class D	"Stellite" (Co, Cr, W) type cast alloys with Mo substituted for or in addition to W. Part of the Co can be replaced with Ni.	Have good resistance to deformation "as cast," but can be improved by solution treating and/or aging.
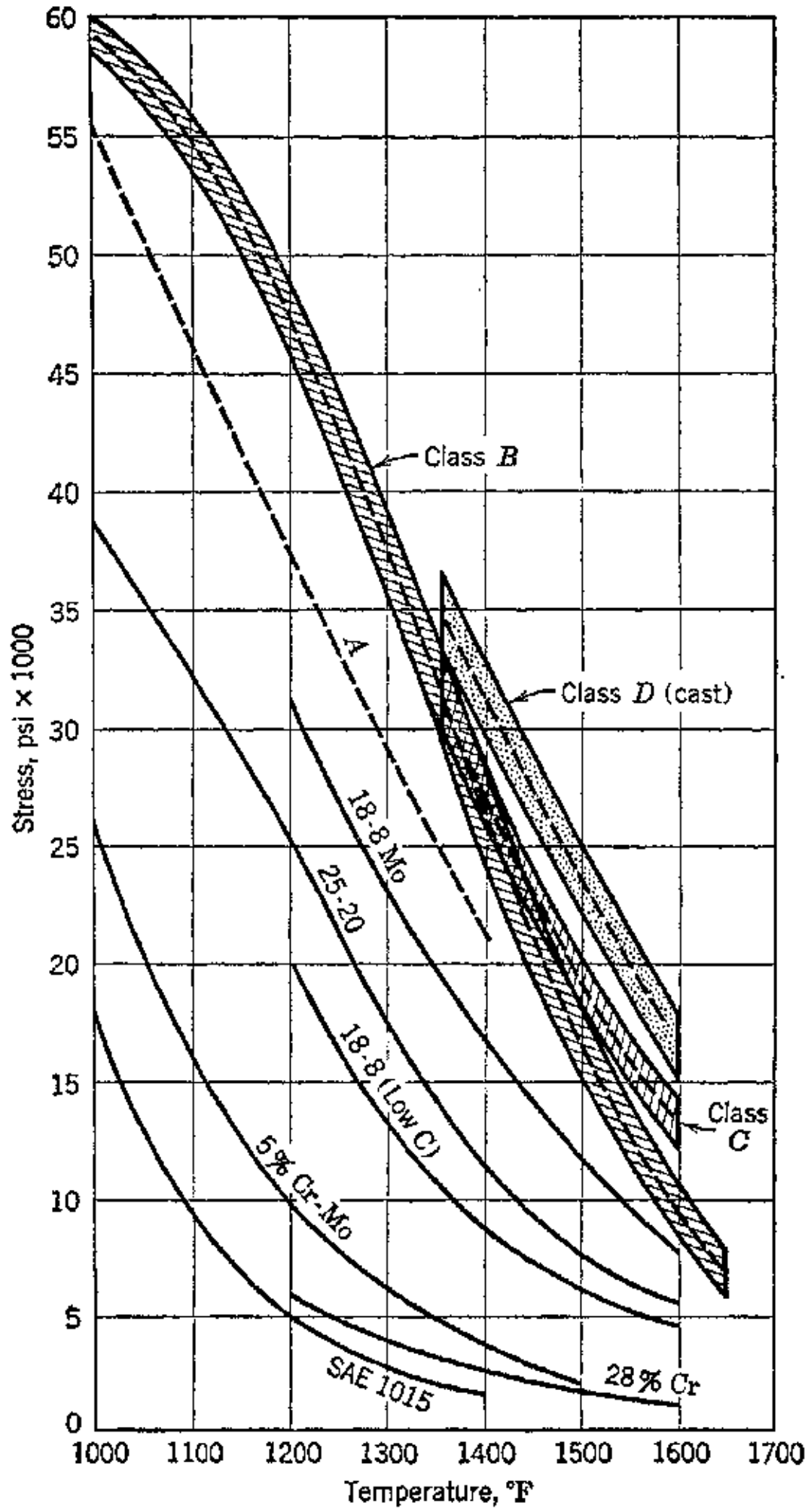
FIG. 4.   One hundred hour stress-to-rupture vs. temperature.
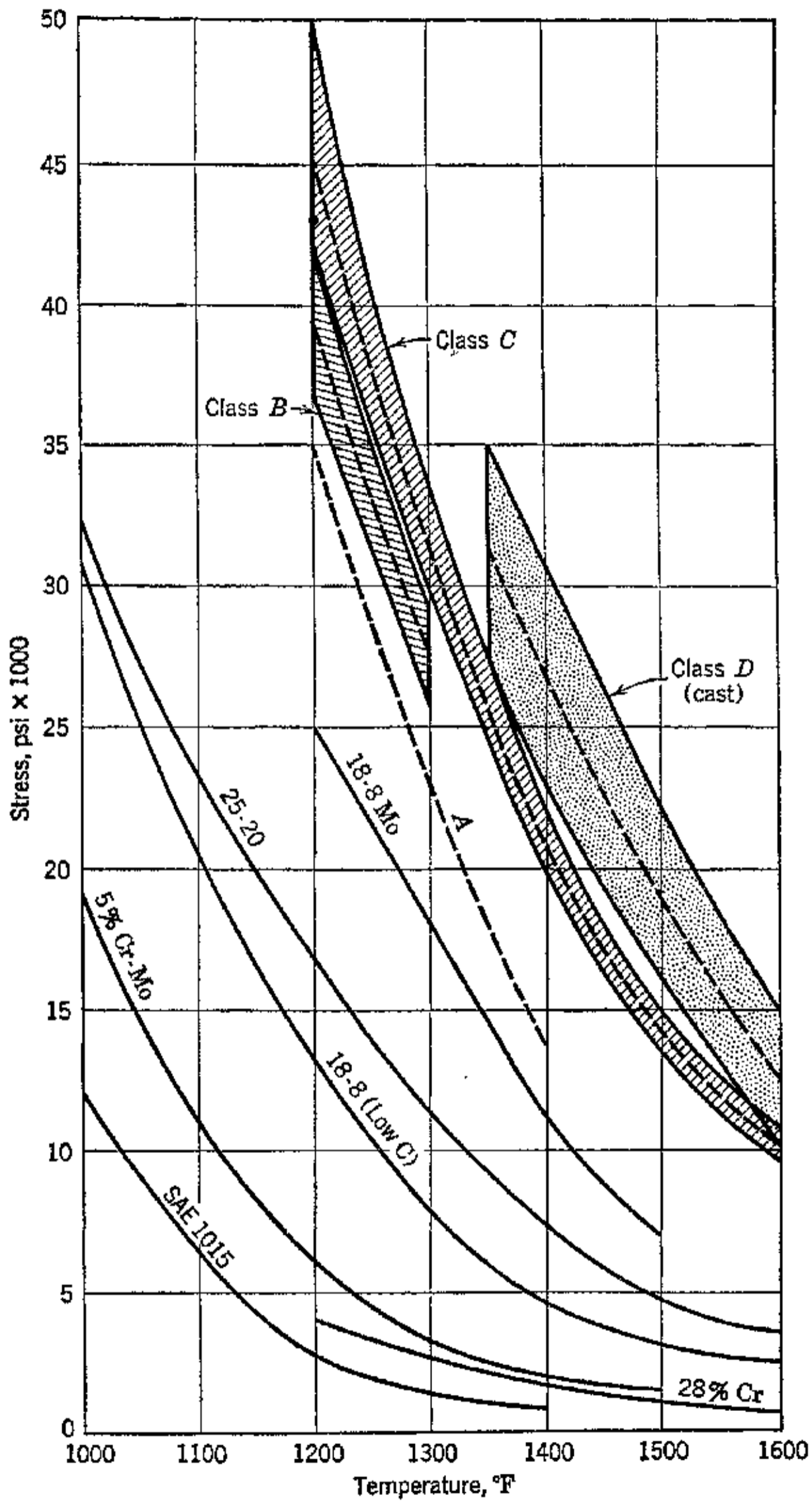
Fig. 5.   One thousand hour stress-to-rupture vs. temperature.
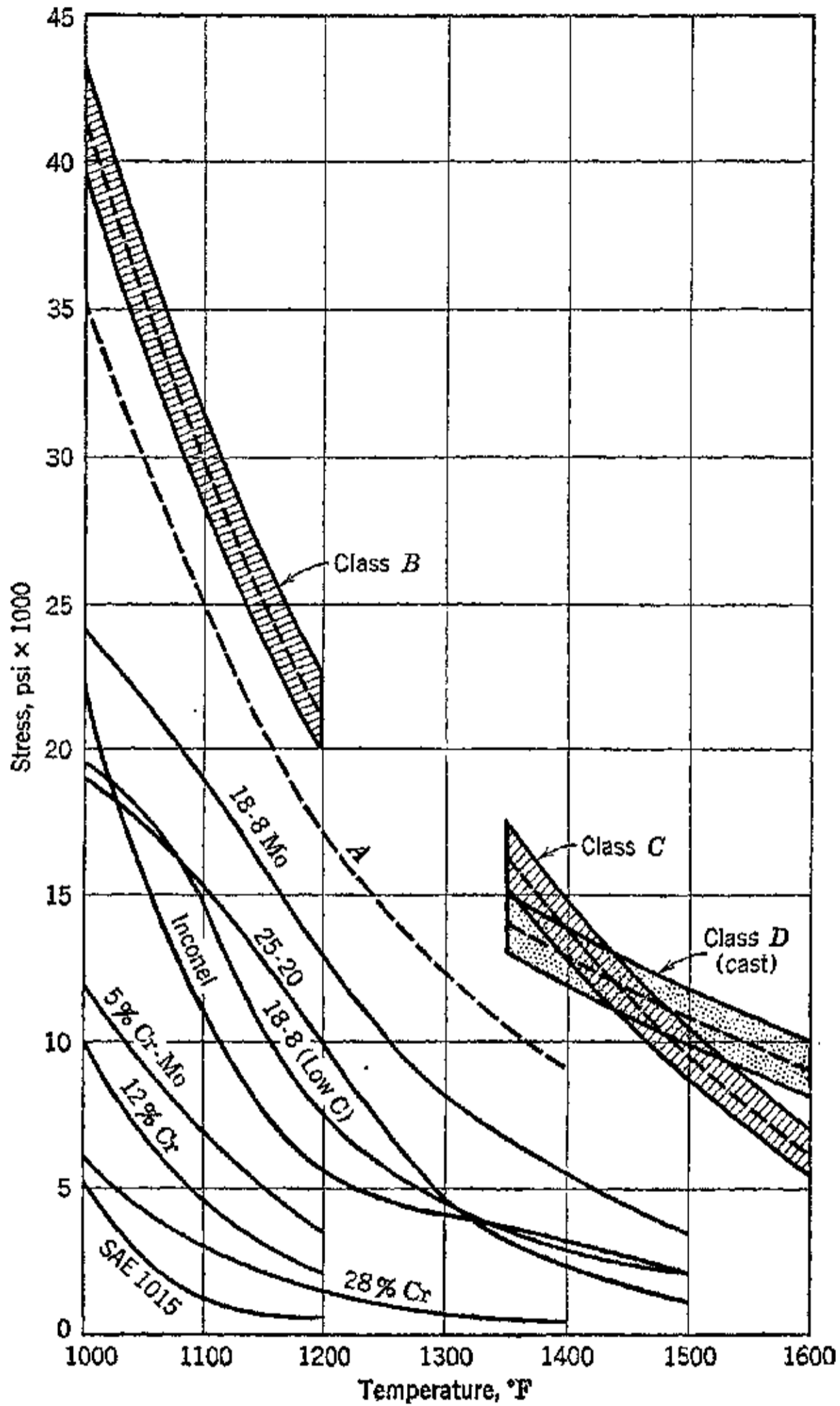
FIG. 6.   Stress for secondary creep rate of 0.10 per cent per 1000 hours (1 per cent per 10,000 hours) vs. temperature.

13. Selection of Alloy

The selection of the most appropriate alloy for a specific service requires a rigid analysis of the requirements of the particular application. It will be seen from Figures 4, 5, and 6 that none of the known alloys is a "cure all." Even the more outstanding compositions can be considered superior to other alloys only over a relatively narrow temperature range. Also, at a given temperature, one alloy may be superior for high stress service and a totally different analysis may be outstanding for service where the stress can be kept low. Likewise, the time element is of extreme importance; thus a material suitable for 100-hr service life may be totally unsuitable for 1000-, 10,000-, or 100,000-hr service life. Figures 4, 5, and 6 present curves which are of primary interest to designers of equipment where relatively short life is required, such as in jet propulsion. In considering the materials for service in stationary or marine gas turbines for 10-yr life, lower creep rates and fatigue data would have to be examined.

In the selection of an alloy for a specific application, it is also well to determine the availability of the alloy. All these alloys contain large percentages of strategic materials, though some contain more than others. Thus, a lower-strategic-content alloy should be used if, for the particular application, it is equal in properties to a more highly alloyed material. Cost may also be a limiting factor.

Of critical importance is the question of procurement of a particular alloy in the form desired. As these materials have high hot strengths, it is easily understandable that they are difficult to work even in the high-temperature ranges. Working these alloys in normal hot-working ranges is roughly the same as working low-alloy steels absolutely cold. Indeed, many of the newer alloys are so difficult to work that they are usable only in the cast form.

In any event, the selection of an alloy should be based on a careful analysis of *all* the limiting conditions and upon tests which duplicate the service conditions as precisely as is practicable.

REFERENCES

1. L. CAMMEN, *Principles of Metallurgy of Ferrous Metals*, A.S.M.E., New York.
2. C. S. BARRETT, *Structure of Metals*, McGraw-Hill Book Co., 1943.
3. C. T. EVANS, JR., "High Temperature Alloys for Dynamic Loading," *Iron Age*, June, 1944.
4. C. T. EVANS, JR., "Wrought Heat Resisting Alloys for Gas Turbine Service," *Metal Progress*, November, 1945.
5. F. B. FOLEY, "The Sigma Phase," *Alloy Casting Institute Bulletin*, July, 1945.

Index